Aurora Mascolo

University of Salerno - Department of Civil Engineering

Development of advanced tools for modelling, prediction and mapping of environmental noise and sound perception

PhD course in "Risk and Sustainability in Civil, Architectural and Environmental Engineering Systems"
XXXVIII cycle

A.A. 2025/2026

PhD Supervisor
Prof. Claudio Guarnaccia · *University of Salerno* · Italy

PhD Coordinator
Prof. Fernando Fraternali · *University of Salerno* · Italy

External Reviewers
Prof. Joaquim M. G. Macedo · *University of Aveiro* · Portugal
Prof. Laura E. Mauriz · *University of León* · Spain

Examination Committee
Prof. Francesco Aletta · *University College London* · United Kingdom
Prof. Giacomo Viccione · *University of Salerno* · Italy
Prof. Giovanni Zambon · *University of Milano-Bicocca* · Italy

Copyright
© 2026 Aurora Mascolo. All rights reserved.
aurora.mascolo@gmail.com

Colophon
This document was typeset with the help of KOMA-Script and LaTeX using the kaobook class. The initial source code used to create this document is available at https://github.com/fmarotta/kaobook.

Devi fare ciò
che ti fa stare bene.

Preface

The world is never truly silent. It is woven from sound; a constant and complex acoustic tapestry that envelops us from birth. Sound is a far more than a passive background: it colours every experience, shapes every emotion, directing and influencing attention and concentration, determining emotional states and the sense of place. It is a subtle yet potent architect of our reality. The resonant quiet of a cathedral inspires introspection, the rhythmic cacophony of a city street propels us forward, and the familiar timbre of a loved one's voice provides comfort. Sound colours memories and informs the present moment, acting as an invisible but powerful medium through which the world is perceived and experienced.

Yet, in the symphony of the contemporary world, a single voice, a single instrument has grown to dominate the composition, playing too loudly, drowning out the others, often becoming a source of dissonance rather than harmony. For the majority of the global population, indeed, the inescapable soundtrack of daily life is composed by the ceaseless motion of road traffic.

Such a pervasive hum, punctuated by the crescendo of engines and the percussive rhythm of tyres on pavement, has become the default acoustic setting for our cities and towns: a pervasive presence that we have learned to endure, but whose effects cannot be overstated, as it represents the most widespread and impactful source of environmental noise exposure, with crucial implications for public health, cognitive functions and overall quality of life for humanity.

This is precisely *why* we study it.

The challenge of road traffic noise is not just one of volume, but of character and consequence. To mitigate its negative impacts on public health, we must first be able to describe, predict, and understand it. This has led to a rich field of research dedicated to modelling and predicting its intensity and impacts, aiming to create tools for urban planners, engineers, and policymakers.

Historically, this has driven lot of research efforts on quantifying its physical energy, yielding valuable models based on metrics like the A-weighted equivalent sound pressure level ($L_{A,eq}$). However, these metrics often fail to capture the rich complexity of the human perceptual experience. They cannot fully explain why two soundscapes with identical energy levels may evoke vastly different subjective responses, one being tolerable, the other intensely annoying.

The crucial gap lies not in measuring the *quantity* of noise, but in understanding its *quality*.

This dissertation embarks on a journey to contribute to this critical field, trying to bridge this chasm between physical measurements and human perception. The inquiry starts with a comprehensive review of the existing literature, charting the evolution of road traffic noise modelling from historical and statistic model to dynamic ones.

Building upon this foundation, the core of this work is dedicated to the development and validation of a novel road traffic noise model that could better embrace the complexity of the major cause of noise exposure. Instead of using a macroscopic or a statistic approach, as commonly suggested by national standards, a microscopic model has been built. Each vehicle is treated as an individual sound source, a distinct voice in the chorus of the traffic phenomenon. However, the model's realism is rooted in its stochastic nature. The speed of each vehicle is not a fixed, predetermined or even averaged value, but rather a variable drawn from a probability distribution which reflects the collective behavior of the traffic flow. Each vehicle, is thus assigned with a randomly selected speed, allowing us to reconstruct not only an average noise level, but the vibrant, fluctuating and unpredictable character of real-world traffic.

This granularity of analysis extends not only to the vehicles' behavior, but also to their exact position in space. The resolution of the model has been even increased to account for the specific lane each vehicle occupies on a multi-lane road. While conventional models often treat the road as a single, idealised line, the approach to be presented recognises it for what it is: a composite of distinct lanes. Positioning each vehicle in its specific lane is not a mere technicality; it is fundamental to reconstructing a realistic listening experience. The subtle differences in propagation distance are precisely what create the dynamics, the movement, and the spatial

depth of the traffic soundscape, transforming it from a flat sound into a three-dimensional acoustic scene. In this way, the approach to be presented aims to capture not just the volume, but the very texture and variability of the traffic soundscape, embracing the randomness that deterministic models often overlook.

The value of a model, however, extends beyond its success as a tool for scientific inquiry. Its ultimate worth is proven by its practical utility in addressing tangible, real-world challenges. One of the most complex challenges may be the acoustic assessment of infrastructure that does not yet exist, for which direct traffic data is, by definition, missing. To bridge this gap, the research will explore the integration of such noise model with time series analysis. The core idea is to "feed" predictive models with data collected from existing infrastructures that are structurally similar to learn their temporal traffic patterns. These models can learn and replicate the temporal patterns of traffic, with its daily and weekly fluctuations: their output then becomes the dynamic, realistic input for microscopic noise models. This integrated approach has been successfully tested and validated, demonstrating its effectiveness in generating realistic traffic data. While its direct application to hypothetical design scenarios is beyond the scope of this specific work, a powerful and robust methodology will be presented. Its practical implications extend beyond pure research, laying a solid foundation for future applications in the field of proactive acoustic design.

However, the journey does not end with the physical modelling of sound.

To truly grasp the human experience of acoustic environments, the focus must shift from the singular instrument to embrace the complexity of the entire orchestra. Urban environments are intricate acoustic ecosystems, where road traffic is but one voice in a vibrant, often cacophonous, chorus. Different sources possess unique acoustic signatures, and their constant interplay creates a rich, perceptual tapestry that cannot be understood by studying its threads in isolation. This realisation propelled the investigation toward a broader, more ambitious question: is it possible to decipher the acoustic DNA of an urban area without placing a microphone on every corner? Can the noise levels a person is exposed to be predicted, simply by understanding the acoustic fingerprints of the area in which they are?

The goal is to build a framework capable of inferring the acoustic character of an unmeasured area by observing a similar one, thus transforming scattered data points into a holistic understanding of the urban soundscape. This may be achieved by training a model to recognise the deep connection between the acoustic reality and the underlying urban form, as well as the city's temporal rhythms. The idea is to understand how the soundscape breathes and transforms with the passing of hours, the cycle of seasons, and even the whims of the weather.

Nevertheless, a fundamental premise needs to be addressed: the subjective experience of sound is not dictated by its energy alone. A single decibel value cannot capture the profound difference between the monotonous hum of distant traffic and the sharp, intermittent sounds of a nearby park with chipping birds. It is the character of the sound, its texture, its rhythm, its spatial dynamics, that truly shapes the human response. Because the level alone is not enough, the sophisticated physical characterisation becomes not an end in itself, but a necessary foundation.

Thus, the investigation pivots from the physical to the perceptual, a transition that, for me, represents the heart of this entire work. It is a personal attempt to contribute in bridging the vast gap between the objective and measureable to the subjective world that is actually experienced. To do so, weaving together the disparate threads of engineering, physics, and psychology, a challenge I undertook from the conviction that no single discipline holds the key. The results, I hope, is a more nuanced framework for assessing environmental noise. But beyond the framework itself, my aspiration is that this research contributes to a more human-centered approach to urban design: to help see a different point of view from the physical approach, which is one of perception, leading to engineering environments that are not only quieter, but are sonically richer, healthier, and ultimately more attuned to the profound subtleties of human experience.

Aurora Mascolo

Acknowledgements

It's hard to wrap my mind around what has been a long journey and to open my heart and disclose my feelings in a few words, so you will excuse me if I will take longer than what it's actually expected for an acknowledgment section. I want to be sure to thank everyone who has been part of this experience, and to do so in a way that reflects the importance of their contribution to my life and to this work.

First and foremost, I would like to express my deepest gratitude to my supervisor, Prof. Claudio Guarnaccia, for his invaluable guidance and support throughout these years. You have not only been a mentor but also a source of inspiration. Your insights and encouragement have been crucial in navigating the challenges of research and in shaping the direction of this thesis. I am truly grateful for the opportunities you have provided me to grow as a researcher and for your unwavering belief in my potential (I do not forget how you told me you were my biggest supporter) and I do appreciate the countless hours spent together discussing ideas, refining my work, and pushing me to think critically. I have learnt so much from you, my teaching skills have been shaped by your example, and I hope to be able to pass on the knowledge and the passion for research that you have instilled in me to the people I will have the chance to work with in the future. You were not only my supervisor, but also a friend, and I will always cherish the moments shared in the lab, as the party you organized before I left for Nantes (i.e., my first ever surprise party) and during our travels to conferences. I feel like I cannot resume my gratitude in a few words, so I will just say, breaking my tradition of calling you by your title: thank you for everything, Claudio.

I am also incredibly grateful to my colleagues and research buddies who shared the highs and lows of this journey with me. To live the research life it's not possible in isolation, and I have been fortunate to be surrounded by a supportive and collaborative community. In particular, I want to thank Domenico for the endless discussions, the launch breaks that kept me sane and far from the desk for a little while, and the countless talks about life and research while coming back home at the end of the day. Your friendship and support have been invaluable, starting almost together a new adventure for both of us in the University, feels like we have been through a lot together, and I am grateful for every moment shared.

A significant role in this journey has been played by Antonio: you have been an invaluable source of support and encouragement. I truly consider your friendship as precious, and I am grateful for the inspiration that your passion and dedication to research provides me. Whenever I wrote you to ask for help, you were always there, and I really appreciate it.

A mention also goes to Prof. Michele Grimaldi, whose expertise and insights have been instrumental in shaping the direction of part of this research. I am grateful for the time spent together, for the stimulating discussions, and for the valuable feedback that has helped me to refine my work.

To the rest of the LAFIN team, which is ever changing and growing, thank to all of you for the friendships that I will carry with me in my heart. I want to thank also the students undergoing their Bachelor and Master thesis in the lab, who I had the immense pleasure to supervise: thanks for trusting me, for your enthusiasm and for the great work we have done together. Being able to share my knowledge (which in my eyes still seems to be so limited) and experience with you has been one of the most rewarding aspects of this journey, and I am proud of what we have accomplished together.

As an undeniable part of my research experience and unlimited source of inspiration, I want to thank Prof. Francesco Aletta. Hearing your speak in the first workshop I attended in the University Of Salerno, back in Octber 2018, was a revelation for me. It was the first time I heard about soundscape studies, and I was immediately fascinated by the idea of studying the acoustic environment from a human-centered perspective. Being a Civil Engineering student, it was a serious challenge to jump on a subjective and qualitative approach when you are used and you are strictly trained to be objective and quantitative, and I remember how skeptical people were when I started to talk about soundscape studies and about the idea of using a qualitative approach to study the acoustic environment. However, your work and your passion have always been that inspiring that since that October 2018 I wanted to be part of it. I am grateful for the opportunity to have met you and to have had the chance to discuss with you about soundscape studies, it's a great honor for me to have you as a member of the committee of this thesis. It feels like the end of a circle.

My thanks also go to the colleagues and friends I met during my research stays abroad, in particular to the team of the UMRAE lab in Nantes, with whom I had the pleasure to collaborate and share ideas during my stay in France. Reflecting upon myself, I feel like I grew so much during that period, both professionally and personally, and that I have been lucky to have had the chance to experience a different and so stimulating research environment and to meet such wonderful people. I will never forget the moments shared with you, from the work in the lab to the walks together to the canteen. Judicaël, Pierre, Arnaud, Gwendall, Nicolas, Aman, Julien, Benoit, Bill, Jonathan, Leonardo, Maguette, Rim, Yu, Robin, Nara, Sacha: thanks to all of you. A special thanks to Claudia and Valentin, who endured my presence in their office for the whole period, sharing tiramisù recipes and deep life stories. I am grateful for having met you, you have been a great example of how to be a good researcher and a good person, and I hope we will have the chance to meet again in the future.

My deepest thanks also extend to Prof. Joaquim M. G. Macedo and Prof. Laura E. Mauriz for their invaluable feedback on this thesis. Your insights and suggestions have been instrumental in refining the quality of this work, and I am deeply grateful for the time and effort you have dedicated to reviewing my thesis. I am honored to have had the opportunity to meet you and to be able to discuss with you about my research, receiving your positive feedback and your encouragement has been a great motivation for me, and I will always be thankful for your support.

A special thanks also goes to the members of the PhD Examination Committee, Prof. Francesco Aletta, Prof. Giacomo Viccione and Prof. Giovanni Zambon. I am deeply honored to have you as members of the committee, and I am grateful for the time and effort you have dedicated to my research.

A sincere and heartfelt thank you goes to Silvano and Filippo, without you this thesis would not have been possible. You helped me navigate the research process, providing me with the tools and the knowledge necessary to conduct my studies. I am indebted to you for your support during these years.

Finally, I want to thank the PhD Coordinator, Prof. Fernando Fraternali, and all the professors of the Department of Civil Engineering of the University of Salerno who I met on my journey, from the first day of my Bachelor degree to the last day of my PhD. I am grateful for the knowledge you have shared with me, for the opportunities you have given me to grow and to learn, and for the support you have provided me throughout these years. University is not only a place of learning, but also a community, and I am proud to have been part of such a vibrant and supportive academic environment. A special mention, to Prof. Giacomo Viccione, whose warm smile and handshake always made me feel welcome and seen.

To all of you, a sincere thank you for being part of this journey, for each word of encouragement, for each piece of advice, for each moment and laugh shared. I hope to have the chance to meet you again, to continue our discussions, to share new ideas and to learn from you. **Thank you.** Hoping to not forget anyone, please accept my apologies, but I will switch to my native language for the more personal acknowledgments.



Molte sono state le volte in cui il mio pensiero ha indugiato sulla possibilità di mettere un punto a questo percorso. Quando anche il più piccolo evento del tutto quotidiano ti ricorda che le speranze nel futuro desiderato sono così poche, che sembrano soltanto un infinitesimo di ordine inferiore rispetto invece alla possibilità di stare solo...perdendo tempo, inizi a chiederti se tutto abbia senso. Ma, alla fine, cosa significa perdere tempo? Quando dopo tre anni non sai qual è il tuo posto nel mondo, hai veramente perso tempo? Procedere in questo percorso in un periodo storico terribile come quello in cui stiamo vivendo geopoliticamente e dal punto di vista ambientale, climatico e sociale, è stata una sfida enorme. La sorda consapevolezza di vivere in un mondo che sta andando a rotoli, in cui l'apertura dei social per una pausa dalla scrittura di un paper o durante l'esecuzione di un codice può farti imbattere in immagini devastanti che marcheranno il tuo cervello a fuoco... mi ha fatto sembrare tutto così tante volte distopico, da essere quasi inutile. Diverse volte, nel pullman che mi portava all'università, la mia mente ha vagato tra i pensieri più disparati, e spesso disperati. Uno sguardo puntato dritto davanti a me, cercando di scorgere il giorno che probabilmente stiamo vivendo se state leggendo questo paragrafo per la prima volta, la conclusione di un percorso, di sforzi e fatica. Un riconoscimento di tanta passione, di tanto lavoro. Una soddisfazione, per quanto apra porte sul futuro alquanto incerte. Un silenzioso *"Ce la puoi fare"* che dicevo a me stessa, prefigurandomi il momento in cui, finalmente, avrei potuto dire a me stessa *"Ce l'hai fatta"*. Eppure, un altro sguardo si perdeva tra pensieri ben più cupi, ai bombardamenti, alle immagini di una guerra che abbiamo

visto chissà quante volte da farci diventare quasi insensibili, come se stessimo vedendo un film, piuttosto che la realtà più sconcertante e oscena. Sto andando all'Università, sto facendo ricerca, sto scrivendo una tesi, sto seguendo dei tesisti, sto facendo lezione a degli aspiranti ingegneri, eppure, quei bombardamenti ora... potrebbero star colpendo chi aveva il mio stesso sogno, solo qualche migliaio di chilometri da me? E sono caduta più volte in delle spirali che mi portavano a chiedermi solo "Ha senso tutto questo?". Ha senso fare ricerca, ha senso temere per un futuro incerto, che miei coetanei con assoluta certezza non avranno mai più, solo per la sfortuna di essere nati dal lato sbagliato di linee immaginarie?

In alcuni periodi in questo percorso, mi sono sentita come se stessi vivendo in una bolla, in un mondo a parte, forse in una vita nemmeno mia, in cui tutto ciò che esisteva era la ricerca, o il paper da sottomettere, o il paper da correggere, o il codice da eseguire, o la tesi da scrivere, o la lezione da preparare. Li ho vissuti con il pilota automatico, come da ubriachi, quando vuoi solo tornare a casa e dormire. Alle volte mi chiedo dove abbia trovato la forza di non fermarmi, quando non riuscivo a vedere la fine del tunnel, quando non riuscivo a vedere la luce, quando non riuscivo a vedere un futuro. Quando non riuscivo a vedere un senso. Non vi mentirò, nonostante le tante soddisfazioni, è stato un percorso difficile e trovo emotivamente drenante scrivere queste sentite parole di ringraziamento, e al contempo sento di dovervi esternare il mio più sentito e sincero affetto e la mia più profonda gratitudine, perché senza di voi, forse non ce l'avrei fatta.

Questa tesi non esisterebbe senza te, Mamma. Temo di donarti in questo testo parole che esprimo poche volte, ma che sento viscerali dentro di me. Sei la mia forza, la mia ancora, il mio porto sicuro. Ci sei sempre, quando rido, quando piango disperatamente, quando mi sento persa, quando voglio parlarti, quando non voglio parlarti. Sei la prima persona a cui penso quando ho una novità da condividere, un inciucio o un successo da festeggiare. Quando le domande sulla vita e la confusione è tanta, so che posso parlarne con te. Ed è sufficiente. Le nostre chiacchierate, di ritorno dall'Università, senza nemmeno spostare lo zaino dal tavolo, sono state una delle principali fonti di ristoro e rifugio in questi anni. Non so come ringraziarti della fortuna che sento di averti come madre, e al contempo non so come aiutarti a vedere quanto sei stata e sei la madre migliore che potessi (e potessimo) avere.

Papà, non c'è mai stato un giorno in cui non abbia saputo di poter contare su di te. La tua presenza costante e il tuo supporto incondizionato sono stati sempre una sicurezza. Laddove potessi aver paura di cadere, sapevo che tu saresti stato lì con mamma a sostenermi come quando da piccola mi portavi in montagna, e su qualche scarpata un po' più impervia mi sostenevi tendendomi la mano e quando invece mi sentivo sicura, mi lasciavi camminare da sola, ma sempre con la consapevolezza che se avessi avuto bisogno di te, saresti stato lì pronto a sostenermi. Non posso che ringraziarti, per essere stato sempre una presenza solida e per avermi incoraggiato a continuare con un percorso a cui avevi capito che tenevo tanto.

Mary. Senza di te perdo qualsiasi connotazione. Cos'è una sorella minore senza una sorella maggiore? Spero di essere tua sorella in qualsiasi linea spazio-temporale possa mai esistere, perché esserlo in una sola vita non mi sembra abbastanza. Spero che l'universo possa essermi così benevolo da darmi sempre te come sorella. La mia infanzia ha come soundscape l'eco delle nostre risate, dei nostri giochi, delle nostre canzoni. E anche in questo percorso, seppur maledettamente distanti, sei stata sempre al mio fianco, una voce che voglio sentire dopo una giornata di lavoro, per raccontarti le mie avventure, per condividere con te i miei successi, per sfogarmi quando le cose non andavano come speravo. Non siamo mai state uguali, siamo sempre state molto diverse. Ma forse è quello il punto? Siamo un'anima divisa in due, io ho qualcosa di te e tu hai qualcosa di me. Sei con me in ogni cosa che faccio; non posso ringraziarti abbastanza per essere mia sorella.

Alessio, il mio percorso di dottorato è scandito dai ricordi di momenti condivisi con te, di risate, di chiacchierate, di cene, di viaggi, di avventure, ma soprattutto di tanto, tanto amore. In questi anni sei passato da essere un conoscente, a un amico, al mio tutto. Eppure, indipendentemente da come io ti avrei definito in ciascun momento, tu sei stato costantemente al mio fianco, a sostenermi, a incoraggiarmi, a farmi sentire importante, a farmi sentire amata. Sei presente fin dai dolcini con cui festeggiamo in lab la mia laurea magistrale e la mia immatricolazione al dottorato, e ora fino alla chiusura di questo percorso. Nei momenti in cui mi sentivo più persa, più stanca, più arresa, le tue parole e la tua presenza, il tuo caldo abbraccio e il tuo sguardo rassicurante, mi hanno fatto andare avanti. Credi in me più di quanto io creda in me stessa, e questo è un dono per cui non potrò ringraziarti mai abbastanza. Se credo un po' nel futuro, è solo perché in quel futuro ci vedo anche te. Spero di poterti restituire tutto l'amore e il supporto che mi hai dato in questi anni. Mi hai insegnato che posso farcela, e che seppur io tenda a partire dal presupposto che tutto vada male... può anche andare bene. Ti amo. Grazie.

A tutti i miei amici, che sono stati una parte integrante di questo percorso, che mi hanno sostenuto, incoraggiato, ascoltato, amato. Grazie per essere stati al mio fianco, per aver condiviso con me le gioie e le difficoltà di questo percorso, per avermi fatto sentire meno sola nei momenti di difficoltà subendosi tanti tanti minuti di messaggi vocali (Lina, Robi, Giovi, parlo di voi) o chiamate discord (Claudia), o semplicemente per avermi fatta sentire amata. Una menzione speciale a Fabrizio e Anna Maria, mi conoscete da tanto tempo e siete stati testimoni di tante fasi importanti della mia vita, siete una presenza costante e importante, sono profondamente grata della vostra amicizia. A voi tutti, vi voglio bene e vi ringrazio dal profondo del cuore per essere parte della mia vita e di questo viaggio.

Higher and higher you chase it, it's deep in your bones, go and take it. This is your moment, now is your time, so prove yourself and rise.

Contents

Preface v

Acknowledgements vii

Contents xi

List of Figures xiii

List of Tables xvii

Glossary of Formulae and Indicators xix

1 Introduction 1
- 1.1 Background . . . 1
  - 1.1.1 Environmental Noise: an Evolving Challenge . . . 1
  - 1.1.2 Environmental Noise: When Sound Becomes Pollution . . . 3
  - 1.1.3 Environmental Noise: When Sound Becomes Resource . . . 5
- 1.2 Aims and Objectives . . . 7
  - 1.2.1 Advancing Urban Noise Source Modelling . . . 7
  - 1.2.2 Expanding the Scope and Integrating Perception . . . 8
- 1.3 Research Questions . . . 8
- 1.4 Structure of the thesis . . . 9

2 A Review of Road Traffic Noise Prediction Models 11
- 2.1 The Rationale for Assessing Road Traffic Noise . . . 11
- 2.2 The Road Traffic Noise Modelling Chain . . . 12
- 2.3 The Evolution of Road Traffic Noise Models (RTNMs) . . . 14
  - 2.3.1 Historical Statistical Models . . . 15
  - 2.3.2 General Equation of the Early Models . . . 18
  - 2.3.3 Overview of National RTNMs . . . 19
  - 2.3.4 Machine Learning Models . . . 23
- 2.4 Noise Emission Models (NEMs): a Comprehensive Overview . . . 24
  - 2.4.1 Microscopic Approach: Single Vehicle Noise Emission Models . . . 25
  - 2.4.2 Micro to macro transition: from single vehicle to traffic flow emission . . . 33
- 2.5 Propagation and assessment at the receiver . . . 34
  - 2.5.1 Propagation models . . . 35
- 2.6 Assessment at the Receiver . . . 36
  - 2.6.1 Common Regulation Indicators . . . 36
  - 2.6.2 Exposure and Effects on Human Health (DALYs) . . . 37
  - 2.6.3 External Costs of Transportation . . . 40
- 2.7 Final Remarks . . . 42

3 Road Traffic Noise modelling: a Stochastic and Microscopic Approach 45
- 3.1 The Fundamentals of the Stochastic and Microscopic Approach: Model Architecture and Core Logic . . . 46
- 3.2 Spatial Analysis: Application of the Stochastic Model Using Variable Level of Aggregation of Traffic Flows . . . 51
  - 3.2.1 Spatial Disaggregation of Traffic Flows . . . 52
  - 3.2.2 Mathematical Formulation of the Lane-Specific Stochastic Model . . . 53
- 3.3 Temporal Analysis: Combination of the Stochastic Approach with Time Series Forecasting . 54
  - 3.3.1 First Step: Time-series Forecasting of Traffic Inputs . . . 55

3.3.2 Second Step: Integration of the Stochastic Model with Time-Series Forecasting 57
3.4 Case Study: The Long-Term Monitoring Station (LTMS) Dataset 58
3.4.1 Raw Data Access and Microscopic Resolution 61
3.5 Dataset Exploration: Models Implementation and Validation 61
3.5.1 Baseline Stochastic Model Implementation and Validation 62
3.5.2 Spatial Application of the Stochastic Model Using Variable Level of Aggregation of Traffic Flows: Implementation and Validation 75
3.5.3 Hybrid Time-Series Forecasting Implementation and Validation 84
3.6 Final Remarks 104

4 Beyond Physical Indicators: the Soundscape Approach to Map the Intangible 107
4.1 Changing the Paradigm: from Physical Metrics to Perceptual Experience Assessment 108
4.1.1 The Mismatch Between Physical Metrics and Human Experience 108
4.1.2 Theoretical Reorientation: from Pathogenic to Salutogenic 109
4.2 The Ontology of Soundscape: from its Definition to ISO Standards 110
4.2.1 Definitions of Soundscape: What is the Soundscape? - ISO 12913-1: 2014 110
4.2.2 The Measurement of Soundscape Perception: How and What to Measure? - ISO 12913-2:2018 and ISO 12913-3:2019 112
4.2.3 Current Developments in Soundscape Standardisation - ISO 12913-4 116
4.2.4 Soundscape Design Interventions in Urban Environments 117
4.3 The University Campus as a Soundscape Laboratory 118
4.4 Case Study: The Fisciano Campus of the University of Salerno 121
4.5 Material and Methods: Analyse the Campus Soundscape and Map its Pleasantness 123
4.5.1 Campus Soundscape Analysis via Standardised Soundwalks 123
4.5.2 Campus Soundscape Assessment via Crowdsourcing Science 125
4.5.3 Pleasantness Mapping via Inverse Distance Weighting (IDW) Interpolation 127
4.6 Soundscape Dataset Description and Analysis 130
4.6.1 Sound Sources Predominance Analysis 130
4.6.2 Point-specific Circumplex Analysis 133
4.7 Mapping Pleasantness of the Campus Soundscape: Results and Discussion 140
4.7.1 Pleasantness Mapping Interpolation Results 140
4.7.2 Spatial Analysis of Pleasantness Maps: The Influence of Predominant Sound Sources 146
4.7.3 Temporal Analysis of Pleasantness Maps: The Evolution of Soundscape over Time . 151
4.8 Final Remarks 155

5 Conclusions 157
5.1 Synthesis of the Research: Key Findings and Contributions 157
5.2 Implications for Theory and Practice 158
5.3 Limitations of the Study 159
5.4 Future Research Directions 161

Appendix 163

A Questionnaire used during the soundwalk activities 165

B Maps of Pleasantness During the Years 167

C Appended Papers 171

Bibliography 287

List of Figures

2.1 Schematic representation of the general modelling chain for Road Traffic Noise Models (RTNMs). 13

3.1 Flowchart of the proposed road traffic noise model. The dotted line represents a loop to be repeated for each vehicle considered. . . . 47
3.2 Graphical representation of the time-varying distance between the moving source (vehicle) and the fixed receiver. . . . 49
3.3 Schematic representation of the three spatial modelling levels with different level of disaggregation. 53
3.4 Schematic representation of the hybrid approach integrating time-series predictions with the stochastic microscopic noise model. . . . 58
3.5 Location of Saint-Berthevin: (a) overview within the Pays de la Loire region in France; (b) close-up of the municipality. (Maps available from: OpenStreetMap®). . . . 59
3.6 Schematic representation of acoustic and meteorological sensor positions [209]. . . . 60
3.7 Boxplot of light (N_L) and heavy-duty (N_H) vehicle flow. . . . 63
3.8 Boxplot of light (v_L) and heavy-duty (v_H) vehicle mean speed. . . . 64
3.9 Boxplot of the measured equivalent continuous sound level ($L_{A,eq,15min,meas}$). . . . 64
3.10 Matrix of scatter plots relating all model input variables to each other and their respective Spearman's correlation coefficients. . . . 65
3.11 Violin plots comparing the distributions of measured (green) and simulated (orange) equivalent continuous sound levels ($L_{A,eq,15min}$). . . . 66
3.12 Histograms comparing the distributions of measured (green) and simulated (orange) equivalent continuous sound levels ($L_{A,eq,15min}$). . . . 67
3.13 Scatter plot of simulated data ($L_{A,eq,15min,sim}$) versus the corresponding measurements ($L_{A,eq,15min,meas}$). 68
3.14 Distribution of error values. . . . 69
3.15 Measured and simulated equivalent continuous sound levels as a function of light vehicle flow (N_L). . . . 70
3.16 Correlation heatmap of the $L_{A,eq,15min,sim}$ and the model errors with $L_{A,eq,15min,meas}$ and model main parameters. . . . 72
3.17 Errors plot versus, from left to right, the $L_{A,eq,15min,meas}$, the variables of the model, and the $L_{A,eq,15min,sim}$. . . . 72
3.18 Distribution of $L_{A,eq,15min,meas}$ (in green) compared with the distribution of $L_{A,eq,15min,sim}$ computed with CNOSSOS-EU model (in blue) and the proposed stochastic model (in orange). . . . 73
3.19 Distribution of the stochastic model error values (in green) overlapped with the distribution of CNOSSOS-EU model error values (in blue). . . . 74
3.20 Light vehicles flows plotted versus the ID of the quarter-hour, over the 28 days under analysis. 76
3.21 Heavy vehicles flows plotted versus the ID of the quarter-hour, over the 28 days under analysis. 76
3.22 Boxplots of light (L) and heavy (H) vehicles flows, divided by lane, over the 28 days under analysis. 78
3.23 Boxplots of light (L) and heavy (H) vehicles mean speeds, divided by lane, over the 28 days under analysis. . . . 78
3.24 Cross-sectional schematic of the case study road segment showing the calculated source-to-receiver distances for the three modelling schemes: single source (d_0, cyan), two sources (d_{12}, d_{34}, green), and four sources (d_1 to d_4, red). The receiver is located 5 m from the roadside at a height of 5 m. Absolute geometric dimensions are indicated in meters. . . . 80
3.25 Boxplot of measured and simulated sound pressure levels (L_{Aeq}) for the three spatial modelling schemes: single source (1S), two sources (2S), and four sources (4S). . . . 82
3.26 Pairs panel of the main input parameters and the error values for the 4-Sources model. Scatter plots are shown below the diagonal, histograms on the diagonal, and Pearson correlation coefficients above the diagonal. . . . 84
3.27 Boxplots of light (N_L) and heavy (N_H) vehicle flows, for the calibration and validation sets of the hybrid model. . . . 87

3.28 Boxplots of light (v_L) and heavy (v_H) vehicles speeds, for the calibration and validation sets of the hybrid model. . . . 87
3.29 Boxplots of equivalent continuous sound level ($L_{A,eq,1h}$), for the calibration and validation sets of the hybrid model. . . . 88
3.30 Time series and decomposition of the light vehicle flows (N_L). The original time series, the trend component, the seasonal component, and the residuals are represented. . . . 90
3.31 Autocorrelation (ACF) and partial autocorrelation (PACF) of the light vehicle flows (N_L). . . . 90
3.32 Time series and decomposition of the heavy vehicle flows (N_H). The original time series, the trend component, the seasonal component, and the residuals are represented. . . . 91
3.33 Autocorrelation (ACF) and partial autocorrelation (PACF) of the heavy vehicle flows (N_H). . . . 91
3.34 Time series and decomposition of the light vehicle speeds (v_L). The original time series, the trend component, the seasonal component, and the residuals are represented. . . . 92
3.35 Autocorrelation (ACF) and partial autocorrelation (PACF) of the light vehicle speeds (v_L). . . . 92
3.36 Time series and decomposition of the heavy vehicle speeds (v_H). The original time series, the trend component, the seasonal component, and the residuals are represented. . . . 93
3.37 Autocorrelation (ACF) and partial autocorrelation (PACF) of the heavy vehicle speeds (v_H). . . . 93
3.38 Overlapping time series of measured (blue) and predicted (red) values from June 28th to August 1st, 2004 for light vehicle flows (N_L). . . . 94
3.39 Overlapping time series of measured (blue) and predicted (red) values from June 28th to August 1st, 2004 for heavy vehicle flows (N_H). . . . 95
3.40 Overlapping time series of measured (blue) and predicted (red) values from June 28th to August 1st, 2004 for light vehicle speeds (v_L). . . . 95
3.41 Overlapping time series of measured (blue) and predicted (red) values from June 26th to August 1st, 2004 for heavy vehicle speeds (v_H). . . . 96
3.42 Overlapping time series of measured (blue) and predicted (red) $L_{A,eq,1h}$ values from July26^{th} to August 1st, 2004. . . . 97
3.43 Boxplots of measured (blue) and simulated (red) $L_{A,eq,1h}$ values from July 26th to August 1st, 2004. 98
3.44 Scatter plot of simulated noise level versus the corresponding measurements. . . . 99
3.45 Error histogram of the hybrid model. . . . 100
3.46 Error over time of the hybrid model. . . . 101
3.47 Overlapping time series of measured (blue), hybrid model predicted (red), and fully stochastic model predicted (green) $L_{A,eq,1h}$ values from July 26th to August 1st, 2004. . . . 102

4.1 Circumplex model of soundscape perception based on Pleasantness and Eventfulness dimensions as represented in ISO 12913-3:2019 [229]. . . . 113
4.2 Location of the Fisciano campus of the University of Salerno (Italy). Red line in the left plot is the campus border, while the right plot shows a zoomed-out view of the campus area in the Campania region. . . . 122
4.3 Map of the Fisciano campus . . . 124
4.5 Screenshot of the NoiseCapture app during a measurement session. . . . 126
4.4 Routes followed during the NoiseCapture parties organized within the Fisciano campus of the University of Salerno. . . . 126
4.6 Flowchart resuming the steps followed for the spatial analysis of the pleasantness maps. . . . 129
4.7 Predominant perceived sound sources detected during the soundwalk activity in the six selected points (2019 soundwalk). . . . 131
4.8 Predominant perceived sound sources detected during the soundwalk activity in the six selected points (2024 soundwalk). . . . 131
4.9 Global circumplex analysis of the soundscape perceptual attributes for the six selected points (2019 soundwalk). . . . 132
4.10 Global circumplex analysis of the soundscape perceptual attributes for the six selected points (2024 soundwalk). . . . 132
4.11 Point 1 circumplex (2024 soundwalk). . . . 133
4.12 Point 2 circumplex (2019 soundwalk). . . . 133
4.13 Point 2 circumplex (2024 soundwalk). . . . 134

4.14 Point 3 circumplex (2019 soundwalk). 134
4.15 Point 3 circumplex (2024 soundwalk). 135
4.16 Point 4 circumplex (2024 soundwalk). 135
4.17 Point 5 circumplex (2019 soundwalk). 136
4.18 Point 5 circumplex (2024 soundwalk). 136
4.19 Point 6 circumplex (2024 soundwalk). 137
4.20 Point 7 circumplex (2019 soundwalk). 137
4.21 Point 7 circumplex (2024 soundwalk). 138
4.22 Point 8 circumplex (2019 soundwalk). 138
4.23 Point 8 circumplex (2024 soundwalk). 139
4.24 Point 9 circumplex (2019 soundwalk). 139
4.25 Point 9 circumplex (2024 soundwalk). 139
4.26 Pleasantness map of the Fisciano campus generated using IDW interpolation with a 50-meter search radius. 141
4.27 Comparison of mean pleasantness measured with the two methods during the soundwalk and simulated with the IDW interpolation of the NoiseCapture parties data at each of the six soundwalk points. 142
4.28 Sensitivity analysis of the mean pleasantness values at the six soundwalk points by varying the search radius from 50 to 300 meters. 144
4.29 Variation of pleasantness error at each soundwalk point as the search radius changes. 145
4.30 IDW interpolated map of pleasantness across the Fisciano Campus with a search radius of 100 meters. The measurement points refer to the 2019 soundwalk activity. 147
4.31 Land use and facility map of the Fisciano Campus. 147
4.32 Overlapping of the pleasantness IDW map with the land use and facility map of the Fisciano Campus. 148
4.33 Mean pleasantness values in each polygon of the facilities and land use map of the Fisciano Campus. 149
4.34 Mean percentages of each sound source predominance in the selected points of the Fisciano Campus. 150

B.1 Pleasantness map of the 2019 edition of the NoiseCapture party. 168
B.2 Pleasantness map of the 2022i edition of the NoiseCapture party. 168
B.3 Pleasantness map of the 2022ii edition of the NoiseCapture party. 169
B.4 Pleasantness map of the 2023 edition of the NoiseCapture party. 169
B.5 Pleasantness map of the 2024 edition of the NoiseCapture party. 170

List of Tables

3.1 A selection of lines from the dataset used for the baseline stochastic model implementation. . . 62
3.2 Summary statistics of the main variables within the dataset used for the baseline stochastic model implementation. . . 63
3.3 Quartiles of measured and simulated equivalent continuous sound levels. . . 67
3.4 Summary statistics of measured and simulated equivalent continuous sound levels. . . 67
3.5 Errors significant quartiles. . . 69
3.6 Errors summary statistics. . . 69
3.7 Details of the selected error outliers. . . 71
3.8 Summary error metrics of the stochastic model. . . 72
3.9 Comparison between error metrics of the CNOSSOS-EU model and the proposed stochastic model. 73
3.10 Source-to-receiver distances defined for the three spatial modelling schemes. . . 80
3.11 Mean values and standard deviations of the distributions of parameters for each lane, for both reference databases. Raw databases (before any filtering) include 2688 entries (28 days) while filtered databases (filtering on quarters-hour that include the measured Leq) have 443 entries. . 81
3.12 Main descriptive statistics of measured and simulated equivalent levels ($L_{A,eq,15min}$) for the three modelling schemes. . . 82
3.13 Main descriptive statistics of the error distributions obtained with the three modelling schemes. 83
3.14 A selection of lines from the dataset used for the hybrid model implementation. . . 86
3.15 Summary statistics of the main variables within the dataset used for the hybrid model implementation. . . 86
3.16 Variance explained by seasonal components for different periods (24-168h). . . 89
3.17 Selected SARIMA models for each time series. . . 94
3.18 Residuals metrics for the selected models (Calibrated dataset). . . 97
3.19 Residuals metrics for the selected models (Validation dataset). . . 97
3.20 $L_{A,eq,1h,meas}$ and $L_{A,eq,1h,sim}$ significant quartiles. . . 99
3.21 $L_{A,eq,1h,meas}$ and $L_{A,eq,1h,sim}$ main statistics. . . 99
3.22 Errors significant quartiles. . . 100
3.23 Errors main statistics. . . 100
3.24 Summary error metrics of the hybrid model. . . 102
3.25 Summary error metrics of the compared model. . . 104

4.1 Characteristics of the four diagonal soundscape attributes in the Pleasantness-Eventfulness circumplex. . . 114
4.2 Soundwalk stepover points characteristics with corresponding IDs from 2019 and 2024 soundwalk. Points order is the same as in Figure 4.3. . . 124
4.3 NoiseCapture parties and soundwalks activities characteristics within the Fisciano campus of the University of Salerno. . . 127
4.4 Mean pleasantness measured with the soundwalk methods and simulated with IDW mapping. 142
4.5 IDW pleasantness ([%]) in the six considered points with different search radius values. . . 144
4.6 Difference [%] between IDW simulated values and soundwalk measurement, i.e., pleasantness error. . . 144
4.7 Summary of pleasantness values in %, measured during the soundwalk activity, obtained by IDW interpolation map and averaged in the polygon retrieved from the land use map. . . 151
4.8 Comparison of pleasantness as measured through soundwalk activity and computed through IDW interpolation with 2024 data and with the total cleaned dataset with different search radius *r*. 153
4.9 Comparison of pleasantness computed through IDW interpolation with different datasets and search radius *r=100m*, and measured during soundwalks. . . 154

B.1 Comparison of pleasantness computed through IDW interpolation with different datasets and measured during soundwalks. 167

Glossary of Formulae and Indicators

Descriptive Statistical Indicators

The following indicators are used to characterise the distribution and central tendency of the acoustic datasets.

- **Mean (μ)**: The arithmetic average of the data points.
- **Median ($\tilde{x}$)**: The middle value separating the higher half from the lower half of the data sample (corresponding to the 50th percentile).
- **Standard Deviation (σ)**: A measure of the amount of variation or dispersion of a set of values.

$$\sigma = \sqrt{\frac{1}{n-1}\sum_{i=1}^{n}(x_i - \mu)^2} \tag{1}$$

- **Quartiles (Q_1, Q_3)**: The values that divide the dataset into four equal parts. Q_1 (First Quartile) represents the 25th percentile, while Q_3 (Third Quartile) represents the 75th percentile.
- **Interquartile Range (IQR)**: A measure of statistical dispersion representing the range of the middle 50% of the data.

$$IQR = Q_3 - Q_1 \tag{2}$$

- **Skewness (γ_1)**: A measure of the asymmetry of the probability distribution about its mean.

$$\gamma_1 = E\left[\left(\frac{X - \mu}{\sigma}\right)^3\right] \tag{3}$$

- **Kurtosis (γ_2)**: A measure of the "tailedness" of the probability distribution.

$$\gamma_2 = E\left[\left(\frac{X - \mu}{\sigma}\right)^4\right] \tag{4}$$

Statistical Error Metrics

To evaluate the accuracy of the predictive models and the deviation between measured and calculated values, the following error metrics are defined. Let y_i be the observed value and $\hat{y}_i$ be the predicted value for n observations.

- **Mean Error (ME)**: The average of all the errors in a set.

$$ME = \frac{1}{n}\sum_{i=1}^{n}(y_i - \hat{y}_i) \tag{5}$$

- **Mean Absolute Error (MAE)**: The average of the absolute differences between predictions and actual observations.

$$MAE = \frac{1}{n}\sum_{i=1}^{n}|y_i - \hat{y}_i| \tag{6}$$

- **Mean Percentage Error (MPE)**: The average of percentage errors by which forecasts of a model differ from actual values.

$$MPE = \sum_{i=1}^{n}\frac{y_i - \hat{y}_i}{y_i} \tag{7}$$

- **Mean Absolute Percentage Error (MAPE)**: A measure of prediction accuracy of a forecasting method in statistics.

$$MAPE = \sum_{i=1}^{n} \left| \frac{y_i - \hat{y}_i}{y_i} \right| \tag{8}$$

- **Mean Squared Error (MSE)**: The average of the squares of the errors.

$$MSE = \frac{1}{n} \sum_{i=1}^{n} (y_i - \hat{y}_i)^2 \tag{9}$$

- **Root Mean Squared Error (RMSE)**: The square root of the average of squared differences between prediction and actual observation.

$$RMSE = \sqrt{\frac{1}{n} \sum_{i=1}^{n} (y_i - \hat{y}_i)^2} \tag{10}$$

- **Coefficient of Variation of the RMSE (CV(RMSE))**: A normalised measure of the RMSE, often used to compare models with different scales.

$$CV(RMSE) = \frac{RMSE}{\bar{y}} \tag{11}$$

where $\bar{y}$ is the mean of the observed values.

Acoustic Indicators

This Section provides the definitions and mathematical formulations of the primary acoustic indicators used throughout this thesis. Unless otherwise specified, all logarithmic indicators are expressed in decibels (dB), and frequency weighting follows the A-weighting curve (L_A), consistent with human auditory perception.

- **Equivalent Continuous Sound Level ($L_{eq,T}$)**: The steady-state sound pressure level that, over a given time period T, contains the same total energy as the actual time-varying sound pressure level.

$$L_{eq,T} = 10 \log_{10} \left[\frac{1}{T} \int_0^T \frac{p^2(t)}{p_0^2} dt \right] \quad [dB] \tag{12}$$

where:

  - T is the integration time interval $[s]$;
  - $p(t)$ is the instantaneous sound pressure $[Pa]$;
  - p_0 is the reference sound pressure ($20 \mu Pa$).

- **Sound Exposure Level (SEL)**: The constant sound level which, if maintained for a period of 1 second, would contain the same amount of energy as the actual noise event.

$$SEL = 10 \log_{10} \left[\frac{1}{T_0} \int_{t_1}^{t_2} \frac{p^2(t)}{p_0^2} dt \right] \quad [dB] \tag{13}$$

where:

  - T_0 is the reference duration of 1 second;
  - $t_2 - t_1$ is the duration of the specific noise event.

According to the European Environmental Noise Directive (2002/49/EC), the following indicators are used for assessment and mapping:

- **Day-time Level (L_{day})**: The equivalent continuous sound level over the day period. It typically covers a 12-hour duration.

$$L_{day} = 10 \log_{10} \left[\frac{1}{T_d} \int_{T_d} \frac{p_A^2(t)}{p_0^2} dt \right] \quad [dB(A)] \tag{14}$$

  where T_d is the daytime interval (usually 07:00–19:00).
- **Evening-time Level ($L_{evening}$)**: The equivalent continuous sound level over the evening period, typically 4 hours.

$$L_{evening} = 10 \log_{10} \left[\frac{1}{T_e} \int_{T_e} \frac{p_A^2(t)}{p_0^2} dt \right] \quad [dB(A)] \tag{15}$$

  where T_e is the evening interval (usually 19:00–23:00).
- **Night-time Level (L_{night})**: The equivalent continuous sound level over the night period, typically 8 hours.

$$L_{night} = 10 \log_{10} \left[\frac{1}{T_n} \int_{T_n} \frac{p_A^2(t)}{p_0^2} dt \right] \quad [dB(A)] \tag{16}$$

  where T_n is the night interval (usually 23:00–07:00).
- **Day, Evening, and Night Levels ($L_{day}, L_{evening}, L_{night}$)**: These represent the A-weighted long-term average sound levels determined over all the day, evening, and night periods of a year, respectively.
  - L_{day}: calculated over a 12-hour period (e.g., 07:00–19:00).
  - $L_{evening}$: calculated over a 4-hour period (e.g., 19:00–23:00).
  - L_{night}: calculated over an 8-hour period (e.g., 23:00–07:00).
- **Day-Evening-Night Level (L_{den})**: The overall descriptor for the 24-hour period, which includes penalties for the evening and night periods to account for increased noise sensitivity.

$$L_{den} = 10 \log_{10} \frac{1}{24} \left(12 \cdot 10^{\frac{L_{day}}{10}} + 4 \cdot 10^{\frac{L_{evening}+5}{10}} + 8 \cdot 10^{\frac{L_{night}+10}{10}} \right) \quad [dB] \tag{17}$$

Introduction 1

1.1 Background 1
1.2 Aims and Objectives . . . 7
1.3 Research Questions . . . 8
1.4 Structure of the thesis . . 9

1.1 Background

The human experience is inextricably woven into the acoustic tapestry in which it is immersed. Sound is not merely a passive backdrop to our lives; it is an active, dynamic force that shapes our perceptions, emotions, and interactions with the world around us. From the soothing rustle of leaves to the cacophony of urban traffic, sound defines the character of our environments and profoundly influences daily lives and well-being. It is a subtle yet potent architect of reality, shaping emotional states, influencing attention and concentration, and defining the character of place. The resonant quiet of a cathedral inspires introspection, the rhythmic cacophony of a city street propels us forward, and the familiar timbre of a loved one's voice provides comfort. Sound colours memories and informs the present moment, acting as an invisible but powerful medium through which the world is perceived and experienced.

In the contemporary world, however, this intricate symphony is increasingly dominated by the pervasive dissonance of environmental noise, particularly the ceaseless motion of road traffic. To contextualise the modern struggle for acoustic quality, it is essential to trace the evolution of sound from its historical role as a localised urban nuisance to its current status as a global public health priority and, ultimately, to its emerging recognition as a vital resource for human well-being.

This Chapter establishes the historical and conceptual framework of the research, tracing the evolving relationship between human society and its acoustic environment. By examining the transition of noise from a localised urban nuisance to a pervasive global health hazard, and eventually to its contemporary recognition as a potential restorative resource, the following Subsections provide the necessary context for the modelling and perceptual methodologies developed throughout this Thesis. Beyond this foundational background, the Chapter articulates the core aims and objectives of the study, centering on the convergence of physical acoustics and human perception, before providing a structural roadmap for the entire investigative journey.

1.1.1 Environmental Noise: an Evolving Challenge

The challenge of managing unwanted sound in human settlements is not a uniquely modern issue. Concerns over the detrimental effects of noise on the quality of life are indeed deeply rooted in the history of urbanization. Cultural and legal efforts to mitigate the impacts of noise date back millennia, reflecting a long-standing recognition of its potential to disrupt daily life.

Lex Iulia Municipalis, written in the 45 BCE and attributed to Julius Caesar, included provisions to limit noise from workshops and taverns during certain hours to protect residents' peace [1–3].[1]

The Roman poet Giovenale, in his Satire III, lamented the cacophony of urban life, highlighting the struggle for tranquillity amidst the clamor

1: The use of carts and wagons in the city was prohibited during nighttime due to the loud *strepitus rotarum*, e.g., the clatter of wheels, which disturbed the sleep of many citizens.

of the city. The poet remarked on the high cost for dwelling in places of tranquillity, where the creaking of carts along tortuous roads and the distant clamor of enclosed herds would not intrude upon the serenity of daily life [4, 5].[2]

This lament for urban chaos[3] reflected a deeply held cultural appreciation for its antithesis: rural peace[4]. This ideal found its most strong expression in the pastoral tradition, which explicitly defined tranquillity through its natural *soundscape*. Virgil's Eclogues, for instance, are saturated with the acoustic imagery of this restorative areas, where the cooing of doves and the gentle hum of bees formed the very audible texture of a quiet and relaxed life lived in harmony with nature [6, 7].[5]

For the poet and philosopher Lucretius, moreover, natural sounds were an integral prerequisite for achieving the philosophical state of *ataraxia*, a serene detachment realised through the rational disengagement from the anxieties and ambitions of the urban life [8, 9].

Evidently, the quest for urban quietude is not a modern preoccupation; it is, rather, a historical constant that underscores the persistent tension between the necessities of urban functionality and the human need for repose. Centuries later, indeed, some medieval European cities adopted several other measures to mitigate urban noise. In England, for example, it was common practice to cover that cobblestone streets outside the house of a sick or dying person with straw to muffle the disruptive sounds [10, 11].

Beyond secular authorities, starting in the thirteenth century, a significant and innovative wave of noise regulation emerged from within the liturgical and canonical traditions of the Catholic Church, even if not always effectively enforced and often specifically aiming at the conduct of the clergy, for example prohibiting loud hunting excursions[6], playing music in the streets at night[7], and similar disruptive activities [14].

Bishops independently experimented with noise regulation many times over, with different local goals but converging concerns over uncontrolled, unwanted and annoying sounds. For example, any disruptive noise during the celebration of the Mass was strictly forbidden.[8] These early instances highlight a recurring theme in urban life: the tension between the inevitable sounds of human activity and the enduring need for tranquillity.

While these historical antecedents establish noise as a long-standing problem, the 20th century witnessed even a more profound transformation in both the scale and the severity of the problem. The rapid population growth, together with the urbanization, and the exponential technological development gave rise to an acoustic environment of unprecedented intensity [15]. The sounds of industry, transportation, and consumer products became ubiquitous, escalating from a localised annoyance to a pervasive environmental stressor.[9] This shift culminated in the formal recognition of noise as a significant public health hazard by the United States government in 1968, when noise was acknowledged not only as "undesirable" sounds, but also as potentially "*harmful*" [19].

This acknowledgment was echoed at the international scale when a World Health Organization (WHO) working group concluded in 1971 that noise constituted a major threat to human well-being [20]. This growing awareness, propelled by the broader environmental movement of the era, catalyzed a brief but vigorous period of legislative action in the United States. The cornerstone of this effort was the Noise Control Act of 1972, a landmark piece of legislation in noise pollution control.[10]

2: *"nam quae meritoria somnum admittunt? magnis opibus dormitur in urbe. inde caput morbi. raedarum transitus arto uicorum in flexu et stantis conuicia mandrae eripient somnum Druso uitulisque marinis."* - Juvenalis, Satire III, 234-238 [4].

3: *"Negotium"*.

4: *"Otium"*.

5: *"Fortunate senex, hic, inter flumina nota et fontis sacros, frigus captabis opacum! hinc tibi, quae semper, vicino ab limite, saepes Hyblaeis apibus florem depasta salicti saepe levi somnum suadebit inire susurro; hinc alta sub rupe canet frondator ad auras; nec tamen interea raucae, tua cura, palumbes, nec gemere aëria cessabit turtur ab ulmo."* - Virgil, Eclogus, 52-58 [6, 7].

6: *"Et ne ludos taxillorum et monstra larvarum, hastiludia seu tormenta, clamosas venaciones, negociaciones inhonestas emendo vel vendendo causa lucri exerceant, penitus inhibemus"* - Kammin, 1352 [12].

7: *"Item statuimus, quod neque Canonici, neque Clerici vagentur nocturno tempore per plateas, psallentes, et si aliquos transire oporteat ex legitima et justa causa, hoc faciant sine clamore, et sine cantu, sine citharis, sine tympanis, et sine quolibet strepitu, vel chorea"* - Cologne, 1281 [13].

8: *"Cum igitur Missa in aliqua ecclesia nostrae provinciae in nota celebratur, debent omnes, maxime sacerdotes et clerici in ecclesia ipsa, quantum possunt, assistere celebranti, ac omnis clamor, strepitus et tumultus, in eadem ecclesia conquiescere."* - Bologna, 1317 [14].

9: New York City's 1930 for example, responded to the overwhelming noise generated by the city's increasing traffic and industrial activities by using both noise measurements and questionnaires to ask citizens which noises were bothering them during the night [16–18].

10: *"The policy of the United States to promote an environment for all Americans free from noise that jeopardises their health or welfare"*. - Noise Control Act, 1972 [21, 22].

Through the Office of Noise Abatement and Control, indeed, noise emission standards for a wide array of sources were set, including motor vehicles, aircraft, industrial machinery, and common consumer products. However, such ordinances at a local level have been proven insufficient to address a pervasive environmental problem like transportation noise, which transcends municipal boundaries [22].

As a result, noise pollution still persists as a major, under-addressed public health threat. Today, more than 100 million Americans are considered to be at risk from harmful noise exposure [23], while in Europe, where regulatory efforts have been more sustained through the years, noise pollution ranks second only to air pollution as the most harmful environmental exposure to public health [24].

For this reason, in terms of modern regulations, the European Union has pursued a very systematic and harmonised approach. The keystone of this effort is the Environmental Noise Directive (2002/49/EC) [25], which mandates that member states produce strategic noise maps to assess population exposure and develop action plans to prevent and reduce environmental noise where necessary. This framework signals a broader paradigm shift from the previous one, a simple source-specific emission limits, to a more holistic management of the acoustic environment, emphasising assessment, planning, and public information. Nevertheless, the persistent gap between regulatory intent and public health outcomes makes a thorough understanding of the specific impacts of noise pollution more critical than ever [26].

1.1.2 Environmental Noise: When Sound Becomes Pollution

The persistent, high global prevalence of noise pollution clearly demonstrates that existing policies discussed earlier, have been insufficient to resolve the issue. Thereafter, fully understanding the scope of this modern public health challenge requires a primary focus on identifying the dominant sources of this widespread exposure. While urban noise stems from a vast array of sources, the largest contributor to population exposure and resulting health burden is unequivocally road traffic noise [27–29]. Indeed, the pervasive nature and high prevalence of road traffic noise in densely populated areas lead directly to the chronic exposure it inflicts upon residential and urban spaces [30]. Estimates suggest that road traffic alone accounts for the majority of the population exposed to noise levels exceeding the WHO recommended thresholds, particularly across European regions [31].[11]

11: *"At least 1 million healthy life years are lost annually from traffic-related noise in Western Europe"* - Burden of disease from environmental noise, WHO, 2011 [24].

Beyond vehicular traffic, other primary sources include railway noise and aircraft noise, both often producing high-intensity noise events [27, 28, 32]. Finally, industrial noise and leisure noise also constitute important localised sources that contribute to the overall environmental noise budget, demanding targeted regulatory and planning interventions [24, 31, 33].

Collectively, the output from these diverse, persistent sound sources creates a complex auditory environment, establishing the crucial foundation for the subsequent health consequences.

Indeed, although noise is not an environmental contaminant that accumulates over time, acting instead as an immediate, location-dependent phenomenon, the resulting health risks are critical, spanning from acute

impacts following instantaneous and *short-term* exposure to the substantial, cumulative burden of protracted *long-term* exposure to high noise levels [34].

Historically, the earliest noise regulations mentioned were primarily driven by concerns over its most direct and obvious consequence: damage to the auditory system [21, 22]. Early research and policy, indeed, focused almost exclusively on preventing Noise-Induced Hearing Loss (NIHL) and tinnitus. However, while these remain critical health outcomes [35], non-auditory physiological effects also began to attract attention in the 1970s and are nowadays even more well recognised as significant contributors to the overall health burden caused by noise pollution [30, 32, 34, 36–39].

These non-auditory effects encompass a range of physiological and psychological responses. Protracted exposure to elevated noise levels has been demonstrably linked to a spectrum of adverse health detriments, contributing to an increased vulnerability to conditions such as hypertension, and cardiovascular disease.

The mechanisms underlying these effects are complex and multifaceted, involving both direct physiological stress responses and indirect impacts on behaviour and well-being. For instance, noise exposure can activate the body's stress response systems, leading to elevated levels of stress hormones such as cortisol and adrenaline. Chronic activation of these systems has been linked to hypertension, ischemic heart disease, and stroke [30, 39–43].

Specific segments of the population are demonstrably more susceptible to noise exposure adverse physiological and psychological consequences. This vulnerability is particularly evident in children and adolescents, for whom long-term noise exposure is strongly associated with diminished cognitive function [44–46]. The underlying mechanisms, such as increased stress and sleep disruption [38], negatively impact critical cognitive domains, including attention, memory, and executive functions [44–46]. Furthermore, noisy environments render developing brain regions, such as the left inferior frontal gyrus and the Prefrontal Cortex, more prone to structural and functional alterations, potentially leading to neurodegenerative alterations that affect growth and development [45, 47, 48].

The risk is even more pronounced for individual with pre-existing mental health disorders, where exposure to high noise levels can significantly contribute to the exacerbation of symptoms such as anxiety and depression [49, 50]. Loud and persistent noises from traffic or construction sites are particularly disruptive and perceived as negative and annoying leading to a feeling of frustration and to heightened stress levels, irritability and sleep disturbances [36]. In these individuals, noise exposure may further compromise neural plasticity and worsen existing anomalies, such as structural atrophy and decreased functional activation in key emotional and cognitive processing regions like the Prefrontal Cortex. This disruption impairs the normal connectivity and transmission of information between the prefrontal cortex and other brain areas, potentially deepening the damage [47, 48, 51].

Beyond the chronic effects of sustained exposure, noise events characterised by sudden and high-intensity peaks in noise levels, are also linked to significant adverse outcomes. The immediate physiological and psychological intrusion of these events often results in sleep fragmentation and a reduction in the proportion of restorative sleep stages. Even

when individuals do not fully awaken, these noise peaks can trigger subtle shifts in brain activity, leading to poor sleep quality and resulting daytime fatigue [38]. Furthermore, noise events are a key contributor to annoyance, a multifaceted psychological response often involving feelings of irritation, disturbance and helplessness. This acute annoyance is highly correlated with the unpredictability and suddenness of the noise peaks, serving as a primary pathway through which noise exposure translates into reduced quality of life [37].

The distribution of this environmental health burden is, moreover, highly unequal, often mirroring existing socio-economic disparities. Low-income communities and marginalised populations frequently bear a disproportionately greater burden of noise pollution compared to wealthy areas. This inequity stems from several compounding factors: residences in socio-economically disadvantaged neighbourhoods are often situated near major noise sources, such as heavy traffic corridors, industrial zones, and airports. Furthermore, housing in these areas may be constructed with lower acoustic insulation quality, amplifying indoor noise levels. This consistent environmental injustice creates a dual vulnerability: not only are these populations exposed to higher noise levels, but they may also experience greater susceptibility to noise-related health issues due to co-existing stressors, including financial strain and inadequate access to healthcare [52–56].

In light of the compelling evidence surrounding these multi-faceted health impacts and the documented socio-economic inequities in noise exposure, the need for stringent regulatory action became clear.

This led to the establishment of rigorous, evidence-based guidelines by the World Health Organization (WHO). The WHO Environmental Noise Guidelines for the European Region (2018) serve as a pivotal regulatory document, establishing clear exposure thresholds to mitigate the earlier mentioned health risks. The guidelines strongly recommend that average noise exposure L_{den}, the day-evening-night average from road traffic noise be reduced to below 53 dB. Crucially, to protect sleep quality, the average night noise L_{night} should be maintained below 45 dB for road traffic, with an even lower threshold of 40 dB recommended for highly intrusive sources such as aircraft noise [29, 31, 38].

Despite these clear, evidence-based recommendations, noise pollution remains a pervasive public health challenge. Many urban and peri-urban areas across Europe and even worldwide continue to significantly exceed these thresholds, thereby underscoring the critical and urgent need for more effective planning and management strategies, alongside the development of advanced assessment methodologies.

1.1.3 Environmental Noise: When Sound Becomes Resource

Although the physiological and psychological harms of noise exposure represent a critical domain of environmental psychology and public health, identifying sound solely as a stressor or pollutant fails to capture the full scope of the human acoustic experience. This narrow, pathogen-centric focus risks overlooking sound's equally profound potential for health promotion and wellbeing [57, 58].

Indeed, substantial empirical evidence confirms this positive capacity: places with a high prevalence of natural sounds are consistently rated

as highly relaxing and perceived as more restorative than acoustic environments dominated by sounds from the built environment [59, 60].[12]

12: They also proved that the increase of natural sounds levels does not reduce the positive perception of the environment, differently from anthropic kind of sounds [59].

The efficacy of natural sounds cannot be explained purely by the absence of disturbing urban noise. While urban noise induces adverse psychological states such as anxiety and mental fatigue, natural acoustic environments demonstrate a significant positive impact that extends beyond passive relief [59, 61]. If the benefit were solely due to silence, natural sounds would perform identically to a truly quiet control environment. However, empirical research challenges this notion: exposure to natural sounds results in statistically significant differences compared to quiet control conditions concerning physiological markers such as heart rate, blood pressure and respiratory rate. Thus, natural sounds provide an active, restorative therapeutic effect, validating the focus on the positive enhancement of well-being rather than just noise mitigation [60, 62–65].

Two major theoretical frameworks substantiate the positive effects of natural sound exposure: the *Biophilia Hypothesis* (BET) [66–68] and *Attention Restoration Theory* (ART) [69, 70]. The Biophilia Hypothesis suggests that humans possess an innate, deep-seated tendency to seek affiliations with life and living systems. Thus, natural sounds, particularly those of flowing water or birdsong, are often unconsciously associated with safe, flourishing environments. This inherent affinity primes the listener for a positive affective response and a resultant calming physiological state, thereby providing the foundation for improved well-being [71, 72]. Attention Restoration Theory suggests that exposure to natural environments encourages effortless engagement, allowing the brain's directed attention capacity, usually reduced by the need to focus in complex urban environments, to recover [61, 73, 74].

Crucially, natural sound exposure significantly facilitates recovery from acute stress. Research utilising *Skin Conductance Level (SCL)* as an index of sympathetic activation demonstrates that SCL recovery tends to be faster during exposure to natural soundscapes compared to noisy environments. Listening to natural biotic sounds, such as birdsong, specifically activates the parasympathetic nervous system, having a positive effect on physical relaxation, reducing the overall physiological stress load [60, 75–77]. Listening to bird sounds have been, indeed, largely associated in literature with pleasant stimuli and the possibility to evoke feelings of relaxation and tranquillity, improve attention restoration and stress recovery, enhancing one's mood and overall well-being [78–81]. Also *cortisol*, a primary stress hormone, is reliably modulated by natural sound exposure. Key findings indicate that listening to natural sounds can significantly reduce circulating cortisol levels, providing definitive endocrine evidence of systemic stress relief [82, 83].

Furthermore, exposure to natural acoustic environments supports improved performance on complex cognitive tests, indicating enhanced concentration and superior mental clarity when compared to control or urban acoustic conditions. Individuals exposed to nature-based sounds demonstrate greater attention restoration, proven by significantly improved performance on demanding cognitive tasks, such as mental arithmetic and specific attention tests [58, 74, 84, 85].

This objective efficacy is mirrored in subjective experience. Qualitative studies consistently find that participants perceive nature soundscapes as more relaxing and more restorative than sounds emanating from the built environment [60, 65, 73–75]. However, the observed improvements

in subjective well-being, e.g., the reduction in anxiety and annoyance and the improvement in positive mood, are highly correlated with the objective physiological indicators, such as reduced cortisol and accelerated SCL recovery. This confirms the internal validity of the restorative experience: the subjective feeling of comfort and pleasure is the conscious perception of a measurable, successful physiological shift toward a state of reduced stress. Ultimately, these evidence converge to position natural soundscapes not merely as background ambience, but as a robust and essential resource for human health and cognitive resilience.

1.2 Aims and Objectives

The overarching goal of this thesis is to advance the methodologies for the assessment and prediction of the urban acoustic environment, moving beyond the conventional approach based solely on objective noise levels. The research was primarily structured around two convergent pillars: the detailed modelling of major noise sources in urban environments, specifically road traffic noise, and the analysis of human subjective perception. This dual approach focused on the spatio-temporal evolution of both the physical acoustic reality and the perceived sonic environment, pursuing substantial and parallel advancements in both fields, thereby establishing a significantly more comprehensive and effective analytical basis for sustainable urban planning and acoustic design.

1.2.1 Advancing Urban Noise Source Modelling

The first objective was to conduct an exhaustive **literature review** and critical assessment of existing road traffic noise prediction models, with a specific focus on Noise Emission Models. This involved distinguishing between microscopic, macroscopic, and statistical approaches, in order to identify significant methodological gaps and define the foundational requirements for an innovative predictive framework (**Paper A**).

This critical analysis paved the way for the subsequent development of a **novel stochastic and microscopic noise model** capable of operating beyond the common-used methods by generating individual vehicle kinematics from aggregate data. The objective here was to overcome the inherent limitations of deterministic models and provide more realistic predictions of acoustic emissions in variable traffic flows (**Paper B**).

Building on this foundation, a major focus was set to enhance the predictive accuracy of the novel model by focusing on advanced **spatio-temporal dynamics**.

- In terms of spatial analysis, this included the implementation of a **lane-specific analysis** that utilised topographical data to transition beyond the common literature approach of central road source schematisation (**Paper C**).
- In terms of temporal refinement, the task involved the development of a hybrid model that integrated the microscopic stochastic approach with **Time Series Analysis** for high-resolution noise forecasting (**Paper D**).

1.2.2 Expanding the Scope and Integrating Perception

The second major pillar of this doctoral research is the **soundscape**. While the first pillar focuses on the physical modeling of sound sources, this second phase shifts the analytical lens toward the human element, acknowledging that the acoustic environment is not merely a physical phenomenon but a perceived one. The core objective of this research it to refine and advance methodologies for **mapping subjective perception** by leveraging non-traditional data sources, such as crowdsourced observations and controlled soundwalk, within a robust **spatio-temporal analytic framework**. This mapping methodology is designed and presented fully in **Paper E** and subsequently detailed and validated in **Paper F**, seeking to bridge the gap between objective acoustic metrics and the lived experience of different soundscapes.

To provide a granular understanding of how individuals perceive and experience the surrounding acoustic environment, the research disentangles the complexity of perception into two interdependent dimensions:

- The **spatial** component of this analysis entailed the integration of land use maps to formally assess how the functional "character" of a place modulates the perception of its acoustic environment. By correlating spatial features with subjective feedback, the study identified how urban morphology and visual context can either mitigate or exacerbate the perceived impact of noise (**Paper G**).
- The **temporal** component, conversely, focused on longitudinal analysis to investigate how perception evolves in response to the inherent dynamism of different environments. Recognising that a soundscape is not a static snapshot, this analysis explores how human appraisal changes over time. This includes the assessment of significantly "evolving scenarios", such as the environments in which new infrastructure is introduced, as well as the study of predictable, cyclic fluctuations in source presence (e.g., rush hours vs. nighttime) (**Paper H**).

1.3 Research Questions

In light of the above aims and objectives, this Thesis proposes a transition from the traditional, purely physical approach to noise assessment towards a more holistic human-centered perceptual analysis. While the physical modelling of noise sources remains a critical component, the integration of subjective perception is essential to fully understand and effectively manage the acoustic environment. Two main research questions guide this investigative journey, one for each of the two pillars earlier discussed. Each of these questions is further broken down into specific sub-questions that address the key methodological and analytical challenges identified in the literature review and subsequent research design.

- **RQ1:** How can the predictive accuracy of road traffic noise models be enhanced by incorporating stochastic and microscopic approaches, and what are the implications of integrating spatio-temporal dynamics into these models?
    - How can the inherent limitations of deterministic and macroscopic road traffic noise models be overcome to provide more realistic predictions in complex scenarios?

  - To what extent does a stochastic and microscopic approach, which treats vehicles as individual sound sources with variable speeds, improve the accuracy of noise emission characterization?
  - How does the spatial disaggregation of traffic flows into specific lanes and the use of topographical data impact the precision of near-field noise level assessments?
  - Can time-series forecasting be successfully integrated with microscopic noise models to predict dynamic noise fluctuations in scenarios where direct traffic data is unavailable?

- **RQ2:** How can subjective perception of soundscapes be effectively mapped using non-traditional data sources, and what insights can be gained from analyzing the spatio-temporal evolution of this perception in relation to urban morphology and temporal dynamics?

  - In what ways does the functional "character" of an urban space (represented by land use) modulate human perception and appraisal of its soundscape?
  - How does the human experience and appraisal of a soundscape evolve over time in response to cyclic fluctuations or the introduction of new infrastructure?

1.4 Structure of the thesis

This thesis is structured into two main parts, each dedicated to one of the two pillars outlined in the previous section. The first part focuses on the development and refinement of advanced noise prediction models, while the second part explores the subjective dimension of the acoustic environment through the soundscape approach. The detailed organization of the Chapters is as follows:

- **Chapter 1: Introduction** - This Chapter provides an overview of the research context, outlining the background, aims, and objectives of the thesis. It sets the stage for the subsequent chapters by highlighting the duality of noise as both a pollutant and a resource.

- **Part I: Road Traffic Noise: Review and Modelling**

  - **Chapter 2: A Review of Road Traffic Noise Prediction Models** - This Chapter provides a systematic literature review of Road Traffic Noise Models (RTNMs). It traces the evolution of these models, from early statistical approaches to advanced machine learning techniques. A specific focus is placed on Noise Emission Models, with a critical analysis of their methodologies, assumptions, and limitations, setting the foundation for the development of a novel predictive framework.
  - **Chapter 3: Road Traffic Noise Modelling: A Stochastic and Microscopic Approach** - This Chapter details the development and validation of a microscopic stochastic Road Traffic Noise Model. It describes the methodological innovations that allow for the generation of individual vehicle kinematics from aggregate traffic data, overcoming the limitations of deterministic models and providing more realistic predictions of acoustic emissions in variable traffic flows. Moreover,

the integration of lane-specific analysis and the incorporation of time series forecasting techniques are introduced as key enhancements to the model, demonstrating significant improvements in predictive accuracy.

- **Part II: Soundscape: Mapping Subjective Perception**
  - **Chapter 4: Beyond Physical Indicators: The Soundscape Approach to Map the Intangible** - This Chapter explores the theoretical and practical foundations of the soundscape approach, emphasising its ability to capture subjective acoustic experiences that go beyond traditional physical indicators. An innovative methodology to develop maps of subjective perception of soundscapes is presented, leveraging non-traditional data sources such as crowdsourced observations and controlled soundwalks. The Chapter also details the spatio-temporal analytic framework used to analyse the collected data, providing insights into how perception varies across different areas and over time.

- **Chapter 5: Conclusion** - This Chapter summarises the key findings of the thesis, synthesising the contributions of each Chapter. It reflects on the implications of the research for both noise prediction and soundscape mapping, proposing directions for future investigation. It discusses the practical implications for urban planning and noise mitigation, and suggests directions for future work.
- **Appendices** - This Section includes supplementary materials, organized as follows:
  - **Questionnaires** - The survey instruments used during the soundwalks to collect perceptual data from participants.
  - **Additional Maps** - Supplementary pleasantness maps that support the temporal analysis presented in Chapter 4.
  - **Scientific Papers** - The full text of the scientific papers (Paper A to Paper H) that were published during the course of this doctoral research, providing detailed methodologies, results, and discussions that underpin the findings presented in the main Chapters.

A Review of Road Traffic Noise Prediction Models

2

This Chapter presents a comprehensive review of the most widely adopted literature frameworks for Road Traffic Noise Models (RTNMs). It examines the conventional steps of the modelling chain required to assess noise levels, population exposure, and the resulting impacts of this environmental pollutant. A dedicated and detailed Section is devoted to reviewing Noise Emission Models (NEMs), with a specific focus on approaches that enable the assessment of individual vehicle emissions.

The Chapter also briefly discusses propagation models and methods for assessment at the receiver, thereby contextualising the role of emission modelling within the overall simulation process.

The contents of this Chapter draw primarily upon the material published in appended **Paper A**, complemented by relevant background information derived from **Papers B**, **Paper C**, and **Paper D**.

2.1 The Rationale for Assessing Road Traffic Noise . . 11
2.2 The Road Traffic Noise Modelling Chain 12
2.3 The Evolution of Road Traffic Noise Models (RTNMs) 14
2.4 Noise Emission Models (NEMs): a Comprehensive Overview 24
2.5 Propagation and assessment at the receiver . . . 34
2.6 Assessment at the Receiver 36
2.7 Final Remarks 42

2.1 The Rationale for Assessing Road Traffic Noise

Europe's contemporary landscape is defined by two powerful, intersecting trends: relentless urbanization and the intensification of motorised mobility. Urban areas, including cities, towns, and their suburbs, now host nearly three-quarters of the EU's population and are the primary engines of its economy [86]. Projections indicate this concentration will only increase, with Europe's level of urbanization expected to reach approximately 83.7% by 2050 [87].

This demographic shift, driven by the economic, educational, and social opportunities that cities offer, has been paralleled by a substantial increase in the demand for mobility. Road transport remains the cornerstone of this mobility paradigm, accounting for 73.6% of all energy consumed in the EU transport sector in 2022 [88]. This reliance is reflected in the growing vehicle fleet; between 2013 and 2023 alone, the motorisation rate of passenger cars (i.e., the number per thousand inhabitants) in the EU increased by 13.8% [89]. The confluence of dense human settlement and expanding road traffic has transformed the European acoustic environment, establishing road traffic noise as a pervasive and systemic environmental stressor.[1]

The scale of population exposure to this stressor is a significant public health concern. According to the European Environment Agency (EEA), road traffic is the foremost source of noise pollution in Europe. Latest assessments indicate that at least one in five Europeans is exposed to long-term noise levels considered harmful to health mostly due to road traffic noise. Based on the thresholds established under the EU's Environmental Noise Directive (END) [25], road transport is responsible for the exposure of an estimated 92 million people to harmful day-evening-night average noise levels exceeding 55 decibels [28].[2]

Earlier estimates placed this value even higher, at 113 million people [27]. The problem is particularly acute in many highly populated cities, where more than half of the population is exposed to road noise levels above recommended guidelines. Night-time exposure, which is especially

1: *"We all live close to a road, but not everyone has a railway or an airport nearby."* - Claudio Guarnaccia.

2: *"In comparison, railway noise affects 18 million people during the day-evening-night period while aircraft noise impacts around 2.6 million (day-evening-night)."* - EEA Report 05-2025 [28].

detrimental due to its impact on sleep, is also widespread. It is estimated that 56 million people are exposed to night-time road traffic noise levels above the END threshold of 50 dB [25], a level associated with significant sleep disturbance.[3]

3: A 50-decibel (dB) night-time level is not intuitively high; it is comparable to the ambient noise of a quiet suburban street or a conversation at a low volume. Its disruptive potential, however, lies in its persistence and its nature as an averaged metric. A "quiet" average can disguise frequent high-intensity peaks, such as a single heavy vehicle or a siren, that rise sharply above the background noise. These individual acoustic events, rather than the average volume, often are the responsable of fragmented sleep patterns and, thus, sleep disturbance.

The health implications of this widespread exposure are severe and well-documented. The World Health Organization (WHO) identifies environmental noise as the second-largest environmental cause of ill health in Western Europe, surpassed only by air pollution. Long-term exposure to traffic noise is not merely an annoyance; it is a physiological stressor linked to a cascade of adverse health outcomes [31, 33]. The EEA estimates that chronic noise exposure contributes to 48000 new cases of ischemic heart disease and 12000 premature deaths across Europe each year [24, 31].

Furthermore, 22 million people suffer from chronic high annoyance, and 6.5 million experience chronic high sleep disturbance, conditions that significantly degrade quality of life and are precursors to more severe health problems [27–29]. The scientific consensus, consolidated in the WHO's 2018 Environmental Noise Guidelines for the European Region, recommends even stricter thresholds for health protection, suggesting that road traffic noise should not exceed 53 dB L_{den} and 45 dB L_{night} [90, 91].

This discrepancy suggests that the estimated exposure population, although already alarming, likely underestimates the actual extent of the people at risk.

The persistent and widespread exposure to road traffic noise poses a fundamental challenge to the goals of urban sustainability and public health in Europe. A sustainable urban environment must be a healthy one, yet the sonic environment in many European cities is actively detrimental to well-being. The EU's Zero Pollution Action Plan, indeed, aims to reduce the number of people chronically disturbed by transport noise by 30% by 2030 [92]. This clear objective underscores the necessity to be able to assess the impact of transportation noise accurately.

Therefore, in recent years, considerable effort has been devoted to developing robust methods and models to estimate the impact of road traffic noise, which is a fundamental step in evaluating and managing the acoustic environment of any urban area.[4]

4: A primary example of such a "robust method" is *CNOSSOS-EU (Common Noise Assessment Methods in Europe)* [93], which will be presented in Section 2.4. Mandated by the European Commission (Directive 2015/996) [94], this standardised model aims to resolve historical inconsistencies between different national assessment methodologies and to create comparable, high-resolution strategic noise maps, useful for evaluating population exposure and implementing targeted interventions under the Environmental Noise Directive (END) [25].

2.2 The Road Traffic Noise Modelling Chain

The evaluation of road traffic noise can be accomplished through two primary methodologies: extensive *in situ* measurement campaigns or using computational modelling simulations. However, simulation modelling is frequently preferred over direct empirical measurements for several compelling reasons. Practical and logistical elements to be acknowledged include the substantial financial expenses, the significant temporal constraints related to campaign organization and subsequent analysis, and the requisite for specialised, trained personnel. Furthermore, a fundamental rationale for preferring models lies in their predictive capability. Simulations are indispensable for assessing the potential acoustic impact of road infrastructure still in the design phase, an evaluation that is, by definition, impossible to conduct via *in situ* measurement.[5]

5: The logistical challenge of in situ measurement is non-trivial. A comprehensive, city-wide assessment would require a dense network of calibrated, Type 1 Sound Level Meters (SLMs), often deployed for 24/7 monitoring over extended periods to account for temporal variability. The associated costs (i.e., calibrated hardware, deployment, regular maintenance, security, data management) render such measurements campaigns financially and logistically prohibitive for most municipalities, reinforcing the utility of simulation.

The general framework of any **Road Traffic Noise Model (RTNM)** is to provide a complete assessment of the noise, from its generation at the source to its impact at a receiver. This process is often conceptualised as a "modelling chain" composed of four primary components, as schematised in the figure 2.1.

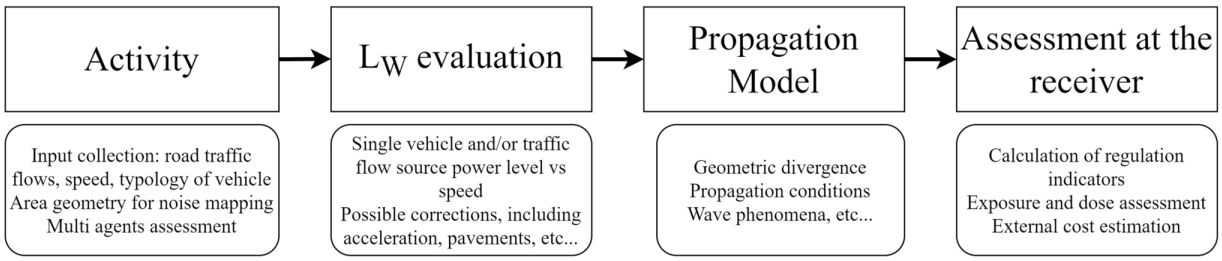


Figure 2.1: Schematic representation of the general modelling chain for Road Traffic Noise Models (RTNMs).

A comprehensive description of each of these components is provided below:[6]

- **Activity:** This foundational step involves the collection of input data. It provides the necessary spatiotemporal distribution of vehicles on the road network, including information on traffic flows or counts, vehicle categories, speeds, and accelerations;
- **Emission:** This component uses the activity data to drive a Noise Emission Model (NEM). The NEM calculates the sound power level L_W of the source, either for aggregated traffic flows or for single vehicles. This step often includes corrections for acceleration, road gradients, and pavement types;[7]
- **Propagation model:** Once the source emission is characterised, this model simulates its propagation through the environment, accounting for geometric divergence, propagation conditions, and wave phenomena;
- **Assessment at the receiver:** The final step calculates the noise impact at the receiver, typically in the form of regulatory indicators, exposure and dose assessment, external cost estimation, or even noise maps and any other useful output.

6: It is worth noting that in some models proposed in the literature, the four steps are not explicitly distinguished; however, this schematic representation still provides a comprehensive understanding of the overall process.

7: The distinction between propulsion (engine) and rolling (tire-road) noise is critical. At speeds above approximately 30 km/h for passenger cars and 50 km/h for heavy vehicles, rolling noise becomes the dominant source. Therefore, an accurate NEM must be able to differentiate the acoustic properties of different asphalts.

Despite the adventange of using models, it is important to acknowledge that they are not without limitations. The accuracy of a model's predictions is inherently tied to the quality and representativeness of its input data, as well as to the assumptions and simplifications embedded within its structure. For instance, models may struggle to capture the full complexity of real-world traffic dynamics, such as stop-and-go conditions, or the influence of microclimatic variations on sound propagation. Additionally, the calibration and validation of models against empirical data are crucial steps that can be resource-intensive and may not always be feasible at the desired spatial and temporal scales. Therefore, while models are indispensable tools for noise assessment and management, their outputs should be interpreted with an understanding of their underlying assumptions and potential sources of uncertainty.

To better contextualise this conceptual framework, several comprehensive studies available in the literature were carefully examined and compared, in order to identify the main approaches, assumptions, and limitations of existing Road Traffic Noise Models (RTNMs). These works provided a valuable overview of the state of the art and helped to delineate the evolution and current trends in noise emission modelling.

A detailed review of the most popular Road Traffic Noise Models (RTNMs) was presented by Steele, in which the early models, together with the methods used at the time of the publication, are presented by reporting the equations and the adopted parameters [95]. Similarly, Mann and Singh provide a specific overview on RTNMs for developing countries [96]. Moreover, by reviewing 11 traffic noise modelling strategies, Ibili et al. found that researchers, probably due to costs and time required to develop new approaches, have developed new RTNMs by starting from earlier models as a baseline, adapting them to their specific conditions [97]. Some other critical and interesting reviews can be find in the work of Garg and Maji and of Rajakumara et al., in which are reported useful resuming tables, with the main features of the RTNMs reviewed. In particular, Garg et al. draw a comparison between the main traffic noise models adopted in different countries on the basis of technical attributes, such as source modelling and sound propagation algorithms [98]. On the other hand, Rajakumara and Gowda compared eight literature models with an "ideal" model to be developed that could overcome several gaps of the literature ones [99].

As for Noise Emission Models (NEMs) of single vehicle, some recent papers have been published, providing critical insights and useful methods. For instance, Rey-Gozalo et al. reported how recent studies results actually could improve the accuracy of road traffic noise assessment and how appropriate action plans could reduce the noise emitted by vehicles [100]. Can and Aumond studied the influence of speed and acceleration in road traffic noise emissions estimation. Using real vehicles trajectories data, taken in a dense urban corridor, they found that commonly used noise emission models could misestimate noise levels under congestion, emphasising the need for additional enhancements in dynamic road traffic noise models [101]. Pascale et al. provided another detailed description of some NEMs, selecting specific models to highlight critical hotspots in the case study [102]. Moreover, they also considered how different typologies of propulsion (namely gazoline, diesel, LPG, and hybrid) contribute to the correct evaluation of sound power level of a vehicle, opening the way to a detailed microscopic modelling that includes also the motorisation of the single vehicle [103].[8]

8: The shift to new propulsion types, particularly electric vehicles, presents a new modelling challenge. At low speeds (<30 km/h), the absence of a combustion engine makes them significantly quieter. However, at higher speeds, where rolling noise dominates, an electric vehicle is acoustically almost identical to its internal combustion counterpart.

Therefore, starting from this existing body of literature, the review presented in this Chapter will focus primarily on the second component of the previously discussed modelling chain, namely the Noise Emission Models (NEMs), after providing an overview of the historical development of RTNMs.

2.3 The Evolution of Road Traffic Noise Models (RTNMs)

The methodologies for road traffic noise assessment have evolved significantly over the decades, moving from early empirical formulae to highly detailed, component-based models and, more recently, to data-driven machine learning techniques. The older approaches consist on collecting large sets of field data in several conditions and then performing statistical regressions with fixed formulae. Such an approach has been then improved including additional parameters and adopting more advanced mathematical algorithms.[9]

9: A crucial limitation of these early statistical models is their *static* nature. Being based on regression analyses of specific datasets, they are "locked in" to the conditions under which they were calibrated (e.g., vehicle fleet composition, pavement types, etc.). They cannot adapt to new technologies and possess very limited "transferability" to different conditions.

2.3.1 Historical Statistical Models

The earliest Road Traffic Noise Models (RTNMs) date back to the 1950s and operate with traffic flow rather than on individual vehicles. Although they rely on a statistical approach that simplifies the actual traffic conditions, these early models generally provide reasonably accurate estimates. They represent the simplest class of RTNMs, requiring only a limited amount of input data and typically yielding the percentile L_{50} or the equivalent continuous sound level L_{eq} as output.[10] Their structure is usually based on regressions analyses performed on specific dataset; consequently, their accuracy is inherently influenced by local factors, such as road geometry, surface characteristics, meteorological conditions, and the composition of the vehicle fleet. The key input parameters typically include traffic flow for the vehicle categories considered (e.g., light and heavy vehicles), characteristics of the road surface, and distance between the carriageway and the receiver.

10: The prevalence of L_{50} (the median sound level, or the level exceeded 50% of the time) in early models was mainly because this metric was feasible to measure and calculate with the technology available at the time. As research progressed, it was found that the total energy of the noise (L_{eq}) and the peaks of the noise (like L_{10}) correlated better with human annoyance and potential health impacts. L_{eq} became the preferred metric because it captures the total energy of the noise, giving more weight to louder, more energetic events, which L_{50} does not.

One of the earliest RTNMs was developed and published in the **Handbook of Acoustic Noise Control**, representing a pioneering attempt to formalise the relationship between traffic parameters and noise levels [104]. This model primarily relied on two inputs: the traffic volume Q (in vehicles per hour) and the distance d (typically in meters) from the observation point to the centre of the traffic lane. The median noise level, the percentile L_{50} in dB, for vehicles travelling at approximately 55-75 km/h and at distances greater that 6 meters, can be estimated using the expression (2.1).

$$L_{50} = 68 + 8.5\log(Q) - 20\log(d) \tag{2.1}$$

It should be underlined that this early model does not provide any specification regarding vehicle types or road characteristics and it assumes a homogeneous vehicle fleet and road characteristics specific to the site where the original measurements were conducted. As a consequence, this model is extremely site-dependent, as other similar early models.

Subsequently, **Nickson** proposed an alternative model that addressed some of these limitations by introducing a constant term, also referred to as C [105]. This constant plays a crucial role in calibrating the model to experimental measurements, allowing its predictions to better match observed noise levels. While still dependent on the conditions of the measurement site, the inclusion of C provides a degree of flexibility by implicitly accounting for local factors not explicitly modelled, such as minor variations in traffic composition and pavement characteristics. The resulting relationship is presented in equation (2.2), representing an early attempt to adjust statistical RTNMs in order to enhance their performance and overcome the limitations associated with site-specific dependencies.

$$L_{50} = C + 10\log\left(\frac{Q}{d}\right) \tag{2.2}$$

Later, **Johnson and Saunders** introduced a more advanced model that extended earlier approaches by incorporating the average vehicle speed v as a key input parameter [106]. This addition started taking into account the effect of average vehicle speed on noise emissions, which was largely neglected in previous flow-based models. In addition, the model included corrective factors to consider ground attenuation and

road gradient, providing a more realistic representation of environmental and infrastructural influences on sound propagation.

These enhancements improved the model predictive capabilities, while still retaining a relatively simple input structure. The resulting relationship is presented in equation (2.3), illustrating how successive refinements, such as the inclusion of speed and environmental corrections, contributed to the gradual evolution of RTNMs toward more accurate and flexible tools for noise assessment.[11]

11: The cubic dependence on speed in Johnson's model reflects an early empirical approximation of the complex, combined physics of noise generation mechanisms.

$$L_{50} = 3.50 + 10 \log \left(\frac{Q v^3}{d} \right) \tag{2.3}$$

Thereafter, **Galloway et al.** proposed a model that introduced the percentage of heavy vehicles P as an additional input [107], as shown in equation (2.4). This addition allowed the model to start taking into account the effect of traffic composition on noise emissions, which had been largely neglected in earlier flow-based models that treated all vehicles equivalently. By explicitly including the proportion of heavy vehicles, the model better captured the contribution of larger, noisier vehicles to overall traffic noise levels.

$$L_{50} = 20 + 10 \log \left(\frac{Q v^2}{d} \right) + 0.4P \tag{2.4}$$

With the introduction of the continuous equivalent level L_{eq} as a standard sound level indicator in several regulations, models capable of predicting this quantity have attracted increasing attention. Among these, one of the most widely adopted is the **Burgess** model [108], presented in equation (2.5). This model employs the same input parameters as earlier statistical RTNMs, i.e., percentage of heavy vehicles, traffic flow, and distances from the source to the receiver, but is specifically designed to estimate the continuous equivalent sound level, providing a more directly applicable metric for regulatory and environmental assessments. Nevertheless, this approach does not consider vehicle speeds, and its predictions remain strongly site-dependent, relying on the conditions under which the original measurement data were collected.

$$L_{eq} = 55.5 + 10.2 \log(Q) + 0.3P - 19.3 \log(d) \tag{2.5}$$

Another model was proposed by **Griffiths and Langdon** in 1968, aiming to compute the continuous equivalent sound level L_{eq} using the percentile levels L_{10}, L_{50} and L_{90} [109], as shown in formula (2.6). Similar to earlier statistical RTNMs and to the model developed by Burgess earlier discussed, this approach considers just the traffic volume Q, the percentage of heavy vehicles P, and the distance d from the source to the receiver as its main input parameters. While it provided a straightforward method to estimate the L_{eq}, it did not account for vehicle speeds and remained strongly site-dependent, being calibrated on measurements with specific features.

$$L_{eq} = L_{50} + 0.018 \left(L_{10} - L_{90} \right)^2 \tag{2.6}$$

Each statistical percentile noise indicator can be computed as in equations (2.7).

$$\begin{aligned} L_{10} &= 61 + 8.4\log(Q) + 0.15P - 11.5\log(d) \\ L_{50} &= 44.8 + 10.8\log(Q) + 0.12P - 9.6\log(d) \\ L_{90} &= 39.1 + 10.5\log(Q) + 0.06P - 9.3\log(d) \end{aligned} \tag{2.7}$$

Later on, **Fagotti and Poggi** investigated the possibility of extending previous RTNMs by including additional vehicle categories, thereby improving model accuracy [110]. Specifically, their model incorporates the flow of motorcycles and buses (i.e., respectively Q_M and Q_{BUS}), in addition to the light-duty and heavy-duty vehicles ones (i.e., Q_L and Q_H). Appropriately calibrated coefficients are used to account for the differing contributions of each vehicle type to the overall noise emissions. The resulting formulation is reported in equation (2.8), representing a significant step toward more detailed and realistic traffic noise modelling.

$$L_{eq} = 10\log(Q_L + Q_M + 8Q_H + 8Q_{BUS}) + 33.5 \tag{2.8}$$

Another model was developed by the French **C.S.T.B** (*Centre Scientifique et Technique du Batiment*), in which the proposed formulation for $L_{A,eq}$ was designed to account for varying road conditions and traffic composition [111]. In particular, the $L_{A,eq}$ is estimated based on the calculation of L_{50}, according to formula (2.9).

This approach allows the model to better reflect differences in vehicle flow and roadway characteristics, while still relying on site-specific measurement data for calibration, making its predictions somehow dependent on the original conditions of the analysed locations.

$$L_{A,eq} = 0.65L_{50} + 28.8 \tag{2.9}$$

The percentile level L_{50} is estimated, using equation (2.10), either in urban or highway scenario with traffic flow lower than 1000 vehicles/hour.

$$L_{50,A} = 11.9\log Q_{eq} + 31.4 \tag{2.10}$$

In urban configuration, where very tall buildings are flanking the street, the width l of the road itself influences the noise levels and it can be taken into account using the equation (2.11).[12]

$$L_{50,A} = 15.5\log Q_{eq} - 10\log l + 36 \tag{2.11}$$

12: The inclusion of the road width l in this equation reflects the influence of *street canyon effects* on noise propagation. Narrower streets can amplify noise levels due to reflections between building façades (i.e., the free-field assumptions of earlier models cannot be used). The term $-10\log l$ attempts to capture this effect, where a narrower street (smaller l) results in higher predicted noise levels.

In both the equations (2.10) and (2.11) the equivalent vehicular flow is calculated as reported in formula (2.12).

$$Q_{eq} = Q\left(1 + \frac{P}{100}(n-1)\right) \tag{2.12}$$

where n is a sort of homogenisation coefficient that accounts for the fact that heavy vehicles generate higher noise emission than light vehicles. This parameter, also referred to as the "acoustical equivalent" of heavy vehicles, represents the number of light vehicles that would produce the same acoustic energy as one heavy vehicle travelling at the same speed. A more detailed formulation of this relationship has been provided in the literature [112], describing the dependence of this relationship on

vehicle speed, giving an explicit expression that links the sound level variation to changes in traffic velocity.

2.3.2 General Equation of the Early Models

Almost all the previously mentioned statistical RTNMs can be traced back to a general formulation of the continuous equivalent noise level:

$$L_{eq} = A \log Q \left[1 + \frac{P}{100}(n-1)\right] + b \log d + C \tag{2.13}$$

where Q represents the traffic volume in vehicles per hour, d is the distance from the observation point to the centre of the traffic lane in meters, P is the percentage of heavy vehicles and n is the acoustic equivalent coefficient previously introduced. The parameters A, b and C are determined through statistical regression analyses, typically performed on large sets of empirical noise measurements covering a variety of traffic, geometric and environmental conditions. This general equation expresses the fundamental empirical relationship between traffic variables and the equivalent noise level observed at a receiver. Despite its apparent simplicity, it encapsulates the essential mechanisms governing road traffic noise generation and propagation, while offering sufficient flexibility to adapt to local contexts through parameter calibration. However, it primarily relies on traffic flow as the key variable for noise estimation, without explicitly accounting for vehicle speed and, consequently, for the dynamic nature of the traffic phenomenon.[13]

As for the homogenisation coefficient n, it can be determined either through regression techniques or through direct acoustic measurements of individual vehicles. This coefficient represents a key parameter for differentiating the acoustic impact of heterogeneous traffic compositions. Indeed, the concept can be extended beyond the light-heavy vehicle dichotomy by defining additional coefficients for other categories, such as motorcycles, buses, or electric vehicles, thus improving the adaptability of the model to more complex or modern fleet compositions.[14]

As discussed earlier, the calibration of these parameters is typically carried out through regression analyses of field data. This process inherently ties the reliability of the resulting model to the quality, quantity, and representativeness of the measurement dataset. Site-specific factors such as local fleet composition, pavement type, and meteorological conditions can strongly influence the estimated coefficients, resulting in models that may perform well locally but exhibit reduced generalisation.[15]

To overcome this limitation, a different approach was proposed in literature [113], who demonstrated that synthetic datasets, generated through computational modelling of various traffic and environmental scenarios, both urban and extra-urban, can effectively replace direct field measurements in the calibration of multi-linear regression models. Such synthetic-based calibration can achieve comparable accuracy to empirical data, provided that the simulated conditions cover an adequate range of variability for the key input parameters. The overall performance of the resulting model, however, remains dependent on the robustness of the reference RTNM employed to generate the synthetic data.

In most cases, the general equation of a regressive RTNM has been further refined by introducing corrective parameters to improve predictive accuracy. These corrections may account for several influencing factors,

13: The reliance on aggregate flow (Q) is one of the weakness of this type of models. It treats traffic as a "fluid" with a uniform density, masking critical acoustic variations. For example, noise emitted by 1,000 vehicles/hour in a free-flowing state (constant speed) is vastly different from 1,000 vehicles/hour in a congested, stop-and-go state (high acceleration/deceleration).

14: Equation 2.8 represents an example of such an extension, where the contributions of motorcycles and buses are explicitly included in the model. The coefficients '8' for heavy-duty vehicles (Q_H) and buses (Q_{BUS}) explicitly quantify this model assumption: one heavy vehicle has the same acoustic energy impact as eight light-duty vehicles (Q_L).

15: The resulting coefficients may capture not only the desired physical relationships but also the random noise and specific co-linearities of the calibration dataset (e.g., a site where heavy trucks only used a specific lane, or where a certain pavement type was always present). This can lead to a model with high "goodness-of-fit" for its source data, but poor "out-of-sample" predictive power when applied to different datasets.

including the average vehicle speed, the type and gradient of the road, meteorological conditions such as temperature or wind, and specific traffic characteristics such as congestion levels or stop-and-go dynamics. In some models, propagation-related corrections are also applied to represent the attenuation caused by barriers, vegetation, or building façades. Although these extensions increase model complexity, they have contributed to bridging the gap between purely empirical formulations and the more physically based approaches that would later emerge. In this sense, the general equation in (2.13) can be regarded as the conceptual foundation upon which subsequent generations of RTNMs were developed, providing a bridge between the first statistical models and the models that characterise the current state of the art.

2.3.3 Overview of National RTNMs

Following the development of early statistical models, several countries began to establish their own national RTNMs, primarily to support regulatory frameworks, environmental assessments, and urban planning policies. These models, while often grounded in the same empirical principles, were adapted to reflect specific national contexts, including local vehicle fleets, driving behaviours, road infrastructures, and meteorological conditions. The following overview presents the most representative national RTNMs, highlighting their methodological foundations, distinctive features, and evolution over time.

The composition of a general formula with several correction factors forms the foundation of the English standard model, commonly known as the **Calculation of Road Traffic Noise** (CoRTN) procedure [114]. The CoRTN model represents one of the first comprehensive national frameworks for traffic noise prediction, designed to support environmental noise assessment and land-use planning in the United Kingdom. Unlike earlier purely statistical approaches, the CoRTN method incorporates not only traffic flow and composition but also the mean vehicle speed, thereby improving the realism of noise level estimations. In its initial formulation, the model assumes idealised reference conditions, such as moderate wind velocity, dry road surface, and open terrain without significant reflective obstacles, as a baseline for the computation. One of the equations proposed in this model allows to assess the hourly noise level at a reference distance of 10 meters from the nearest carriageway, as expressed in equation (2.14):

$$\begin{aligned} L_{10,1h} =& 42.2 + 10\log(Q_{1h}) + \\ &+ \Delta_{flow} + \Delta_G + \Delta_P + \Delta_D + \\ &+ \Delta_S + \Delta_A + \Delta_R \end{aligned} \tag{2.14}$$

Thus, to account for real-world conditions, the CoRTN procedure introduces a set of correction coefficients that adjust the baseline sound level for different influencing factors. Specifically, Δ_{flow} accounts for the variation in traffic flow and composition, Δ_G for the road gradient and Δ_P for the type and condition of the road pavement. The term Δ_D is a distance correction, adjusting the predicted level to distances other than the 10-meters reference. Additional terms include Δ_S, which considers the presence of acoustic shielding, such as barriers or embankments; Δ_A which introduces an angle of view correction related to the receiver's orientation and exposure to the traffic stream; and finally Δ_R, a reflection correction accounting for sound reflections from nearby façades or

surfaces. The introduction of these corrective terms represented a major advancement in the modelling of road traffic noise, as it allowed the CoRTN procedure to be adapted to a wide range of urban and suburban scenarios. Although its underlying structure remains empirical, the modular form of the model makes it flexible and easily applicable to diverse site conditions, providing a practical balance between accuracy and simplicity.[16]

16: The CoRTN model structure represents a pivotal conceptual shift in noise modelling. By establishing a 'baseline' level for idealised conditions and then applying a series of discrete corrections, it creates an extremely modular framework. This "baseline + correction" approach became the dominant paradigm for other national-level models. It allows the models to be easily updated without reformulating it entirely, by refining only correction values.

Another widely adopted approach is represented by the German standard model, known as **RLS 90** (*Richtlinien für den Lärmschutz an Straßen*) [115]. This model, while retaining the core structure of traditional empirical formulations, introduces additional sophistication in the treatment of input parameters. Beyond the standard traffic descriptors, it explicitly includes the average hourly traffic flow, distinguishing among vehicle categories and also considering motorcycles, and the average speed for each class. A distinctive feature of RLS 90 is its capability to evaluate the noise emission from parking areas, an aspect rarely addressed in other national models.[17]

17: The inclusion of parking areas reflects the recognition that stationary vehicles can contribute significantly to urban noise levels. These scenarios are acoustically distinct from free-flowing traffic, as they are dominated by acceleration and deceleration events which produce higher-energy, low-frequency sound (from engines under load) than constant-speed traffic. By considering these events, the model better represents the fluctuating features of urban noise.

Similar to the previously mentioned CoRTN procedure, the RLS 90 model assumes standardised reference conditions to estimate the reference equivalent sound level $L_{m,E}^{(25m)}$, which corresponds to the average sound level at a distance of 25 meters from the centreline of the carriageway, as expressed in equation (2.15).

$$L_{m,E}^{(25m)} = 37.3 + 10\log[Q(1 + 0.082P)] \tag{2.15}$$

Subsequently, a set of correction factors can be applied to such a baseline level in order to account for the actual propagation and environmental conditions. These correction factors can include adjustments for vehicle speed and road surface type, as well as longitudinal gradients, building reflections, ground and atmospheric absorption, topographical variations, and the presence of traffic lights or intersections. Such corrections make RLS 90 a really comprehensive early-generation national models, capable of addressing both emission and propagation influences within a unified empirical framework.

In an effort to adapt the German framework to national conditions, the **Italian National Research Council (C.N.R.)** developed a specific model for the estimation of road traffic noise [116], later refined by Cocchi et al [117]. This model represents an important evolution within the family of empirical approaches, aiming to better reflect the acoustic and infrastructural characteristics of Italian roads. The general expression of the model is reported in equation (2.16).

$$\begin{aligned} L_{A,eq} =& \alpha + 10\log(Q_L + \beta Q_H) - 10\log\left(\frac{d}{d_0}\right) + \\ &+ \Delta_V + \Delta_F + \Delta_B + \Delta_P + \Delta_G + \Delta_{VB} \end{aligned} \tag{2.16}$$

In addition to the parameters already introduced in the German and British models, the C.N.R. formulation incorporates two specific coefficients, α and β, to capture the acoustic characteristics of national vehicle fleets and road infrastructures. In particular, α is related to the single vehicle's noise emission, while β to the heavy vehicle noise emission, adjusting the overall contribution of the heavy vehicle flow Q_H relative to the light vehicle flow Q_L. The reference distance is conventionally set to 25 meters from the road axis.

Several correction terms had been subsequently introduced to account for real-world conditions: Δ_V for the mean traffic speed, Δ_F and Δ_B for the influence of reflective façades located near or opposite the observation point, Δ_P for pavement characteristics, Δ_G for longitudinal gradients, and Δ_{VB} for the presence of intersections, traffic lights, or slow-moving traffic. Overall, the C.N.R. model represents a contextualised evolution of RLS 90, maintaining its empirical robustness while introducing adjustments tailored to Italian traffic dynamics and urban morphology.

In 1999, the **Environmental Research and Training Centre (ERTC) of Thailand** developed a set of empirical equations to estimate the average acoustic power level produced by different vehicle categories, specifically small and large vehicles, through a regression analysis of extensive field measurements [118]. The resulting formulation places a strong emphasis on vehicle speed, reflecting the pivotal role of traffic dynamics in shaping the overall noise levels. Once the power level is obtained as a function of the mean speed, it is used to compute the equivalent continuous sound level L_{eq}, according to equation (2.17).

$$\begin{aligned} L_{eq} =& 67.8 + 20.4 \log v + \\ &+ 10 \log \left[(1 - P) + 53.7P \right] - 10 \log(2dL) \end{aligned} \tag{2.17}$$

where d represents the distance between the traffic lane and the receiver point, while L denotes the average gap distance between successive vehicles, estimated as in formula 2.18.

$$L = \frac{1000v}{Q} \tag{2.18}$$

This formulation explicitly connects the equivalent noise level to the interaction between vehicle flow Q and speed v, thereby offering a more dynamic representation of traffic noise compared to previous flow-based approaches. By directly incorporating the effect of velocity into both the emission and geometrical terms, the ERTC model enhances its predictive capacity under varying traffic conditions, particularly useful in heterogeneous environments such as those commonly observed in Thai urban contexts.

In 2002, **Li et al.** developed a comprehensive road traffic noise model tailored to **Chinese** environmental and traffic conditions [119]. Differently from many earlier empirical approaches, this formulation explicitly incorporated a wider set of local factors, such as vehicle composition, road gradient, ground absorption, and geometric aspects of the propagation path. Vehicles were classified into three categories (light cars, medium trucks, and heavy trucks) to better reflect the heterogeneous composition of the Chinese vehicle fleet.

The model predicts the equivalent continuous sound level $L_{A,eq}$ as a function of the equivalent speed of traffic flow, vehicle density, distance from the source, and several correction factors representing environmental and geometrical influences, as shown in equation (2.19).

$$
\begin{aligned}
L_{A,eq} =& 55.7 + 0.12(v_{eq} - 50) - 8.06 \log v_{eq} + \\
&+ 9.97 \log Q_{eq} + 14.38 \log \left(\frac{d_0}{d} \right) + \\
&+ \Delta_G + \alpha \Delta_{soft} \log \left(\frac{d_0}{d} \right) + \\
&+ 10 \log \left(\frac{\Delta_\phi}{180} \right) + \Delta_s
\end{aligned}
\tag{2.19}
$$

In addition to the coefficients already described in previous models, v_{eq} represents the "equivalent speed" of the traffic flow, reflecting the increasing importance of speed in quantifying traffic noise emission. Δ_G accounts for the influence of road gradient, Δ_{soft}[18] represents the percentage of soft ground cover within the propagation area, while Δ_ϕ denotes the angle subtended by the road segment relative to the receiver position.[19] Finally, Δ_s is a shielding correction that considers the presence of obstacles such as buildings or barriers between the source and receiver.

18: This correction factor is a more physically realistic replacement for the simple $\log(d)$ distance-only term. Sound propagating over "hard" ground combines directly with its reflection, often leading to level amplification at certain frequencies. Conversely, "soft" ground is porous and absorbs sound energy.

19: The angle correction Δ_ϕ captures the effect of the receiver's orientation relative to the traffic flow accounting for the directional nature of traffic noise propagation. This "angles of view" is a foundational principle of all modern propagation models that calculate noise maps in complex geometries.

By integrating multiple corrective factors and explicitly coupling speed, flow, and geometrical configuration, the Li et al. model marked a significant step forward towards context-sensitive noise prediction, providing a more realistic framework for the complex traffic and environmental scenarios typically found in urban China.

In Finland, the **Nordtest** approach was developed under the auspices of the **Nordic Council of Ministers** [120]. The Nordtest model represents one of the earliest coordinated efforts to harmonise road traffic noise assessment procedures across the Nordic countries. It allows for the estimation of the equivalent continuous sound level $L_{A,eq}$ through continuous noise measurements performed over a specified time interval. The methodology provides detailed guidance on measurement procedures, including microphone positioning and data acquisition at specific receiver points, ensuring a high degree of comparability between monitoring campaigns.

The 24-hour equivalent noise level $L_{A,eq,24h}$ is calculated using equation (2.20), which accounts for the independence of the noise levels measured during the day, evening, and night periods—denoted respectively as $L_{A,d}$, $L_{A,e}$, and $L_{A,n}$, each weighted by its corresponding time interval.

$$
L_{A,eq,24h} = 10 \log \frac{1}{T} \left[\Delta t_d 10^{\frac{L_{A,d}}{10}} + \Delta t_e 10^{\frac{L_{A,e}}{10}} + \Delta t_n 10^{\frac{L_{A,n}}{10}} \right] \tag{2.20}
$$

The total duration of the three time intervals equals 24 hours.

In addition to the direct measurement procedure, an alternative estimation method was proposed for cases where actual noise measurements during the night or evening are not available.

This approach relies on average traffic conditions, allowing for a practical yet sufficiently accurate estimation of noise levels. For light vehicles, the corresponding equations are given in (2.21), while for heavy vehicles, reference is made to (2.22). All expressions refer to a standard receiver distance of 10 meters.

$$\begin{aligned} L_{A,e,light} &= 73.5 + 25\log\left(\frac{v}{50}\right); \quad v \geq 40\ km/h \\ L_{A,e,light} &= 71.1 + 25\log\left(\frac{v}{50}\right); \quad 30 \leq v \leq 40\ km/h \end{aligned} \tag{2.21}$$

$$L_{A,e,heavy} = 80.5 + 30\log\left(\frac{v}{50}\right) \tag{2.22}$$

Finally, the equivalent noise level over a one-hour period can be computed using equation (2.23), where n_{light} and n_{heavy} represent the mean hourly traffic flows of the two vehicle categories.[20]

$$L_{eq,A,1h} = 10\log\left[\frac{1}{3600}\left(n_{light}10^{\frac{L_{A,e,light}}{10}} + \right.\right. \\ \left.\left. + n_{heavy}10^{\frac{L_{A,e,heavy}}{10}}\right)\right] \tag{2.23}$$

The Nordtest procedure thus combines empirical modelling with standardised measurement protocols, offering both a robust framework for long-term environmental monitoring and a practical estimation method when direct acoustic data are not available.

20: Equations (2.21) and (2.22) first define the "pass-by" noise level of a single average vehicle ($L_{A,e,light}$ or $L_{A,e,heavy}$) based on its speed. Equation (2.23) then calculates the total L_{eq} by summing the energy of all these discrete pass-by events (e.g., n_{light} events). This "bottom-up" logic, which separates the single-source emission from the traffic count, is the conceptual basis for all modern "component-based" or "microscopic" noise models, showing how the Nordtest approach anticipated later developments in traffic noise modelling, relying on a SEL-based approach.

2.3.4 Machine Learning Models

Following the era of empirical and semi-empirical formulations, which defined explicit relationships between traffic descriptors and emitted sound levels, the field has progressively moved towards data-driven models. One of the latest trends in road traffic noise modelling is the development of **machine learning (ML)** techniques, which can be more reliable and robust in facing non-standard conditions, as stated in [121, 122] and [123]. The Artificial Intelligence (AI) techniques used actually for the prediction of road traffic noise are various, including artificial neural network (ANN), adaptive neuro fuzzy inference system (ANFIS), and genetic algorithm (GA).[21] A bibliographic overview of fifty papers concerning the application of AI-based models in modelling vehicular road traffic noise, selected via a computerised search method, is provided in [124].

21: A significant methodological trade-off in adopting ML models is the loss of "explainability". Unlike the empirical formulations where each term has a discrete physical or statistical meaning, an ML predictive logic is embedded within a complex, non-linear web of weights and biases. This "black box" nature makes it difficult to audit why a model produced a specific result, posing a challenge for regulatory applications where model transparency is often required.

Some examples of the use of ANN in the domain of road traffic noise in the literature are [125] and [126], where the percentage of heavy vehicles, average speed and number of total flowing vehicles are used as input values to implement an ANN model to predict road traffic L_{eq} and L_{10} values in two Indian cities. A similar work implements a model with a higher number of input parameters, accounting for total flowing vehicles, average speed, number of cars, vans, pickup, heavy vehicles and motorcycles, density of building facing the observer and building reflection factor in Tehran [123]. An additional research reported in [127] takes into consideration the same input parameters, adding the type of pavement on the road.

It is particularly relevant that in all these studies, vehicle speeds remain the most influential predictors of the resulting noise level. Thus, even within data-driven frameworks, the dependence of emitted noise on traffic velocity preserves a fundamental and monotonic relationship, similar to that observed in empirical and semi-empirical models. As

speed increases, both rolling and aerodynamic noise components grow, and this trend is captured by ML algorithms, which can refine, rather than replace, the established physical understanding.[22]

22: The success of these data-driven models is entirely contingent on the volume and richness of the training data. While traditional models were calibrated on a finite set of controlled measurements, ML models require vast datasets. To avoid overfitting and ensure generalisability, the training data must capture the full combinatoric spectrum of traffic conditions, meteorological variations, and diverse 3D urban geometries: a significant logistical barrier to their development.

A comparison between ANN and other machine learning techniques has been provided in [128], where authors demonstrated the best prediction results come from ANN compared to other techniques. Similar results have been obtained in [129] and [130], where ANN technique has been compared with regressive approaches and other machine learning techniques respectively. Some noticeable works on ANFIS are the work of Cirianni and Leonardi, [131] who used ANFIS model to predict road traffic noise of two cities in Italy, where in [132] and [133] two models involving fuzzy logic have been developed for prediction and classification of road traffic noise.In the work of Ruiz-Padillo [134] a multicriteria decision methodology was used for the evaluation of traffic noise. In another similar work, equivalent traffic flow, equivalent vehicle speed and honking have been used as input for the implementation of a fuzzy logic for the prediction of road traffic noise [132].

Regarding the usage of GA for road traffic noise prediction, relevant works are [135], [136] and [137], in which this type of AI approach has been successfully implemented for the prediction of road traffic noise.

It is interesting to note how the implementation of machine learning models generally rely on the same road traffic parameters used in historical models, in order to find a predicted noise level at the receiver. Some works introduced new variables, like the presence of buildings in [123] and the type of pavement on the road in [127], but there is still not a comprehensive contribution on this sense, to the author's knowledge. In this regard, the influence of speeds is central not only as a proxy for vehicle dynamics, but also as a key parameter linking emission processes to propagation phenomena, thus bridging classical deterministic approaches and AI-based methodologies. Moreover, another aspect to consider is that, up to the authors knowledge, there is not any AI model working separately on noise emissions or sound propagation, probably because the independent variables to take into consideration to build such a model would not be easily retrieved. These aspects will surely be important in the future development of machine learning techniques for road traffic noise prediction. Anyway, it should be underlined that since the relationships between emission and relevant variables are monotonic, the most interesting contribution of AI tools will be on the improvement of the propagation modelling, where the commonly used approaches can be enhanced.

2.4 Noise Emission Models (NEMs): a Comprehensive Overview

There are several models that, rather than estimating the overall road traffic noise by regression on field data at the receiver, focus on describing the acoustic emission mechanisms at the source level. These approaches, generally referred to as **Noise Emission Models (NEMs)**, are designed to predict the noise levels produced by vehicles by assessing their sound power level L_W.[23] In the context of the modelling chain previously discussed, NEMs specifically address the emission stage, providing the link between traffic activity data and the subsequent propagation step.

23: The sound power level L_W is an intrinsic property of the noise source, representing the total acoustic energy emitted, independent of the environment or distance from the source. This contrasts with sound pressure levels L_p, which vary with distance and environmental conditions. By focusing on L_W, NEMs allows for a clean separation of the "source" (the vehicle) from the "path" (the propagation model), which is the cornerstone of all modern "source-path-receiver" models.

This modelling philosophy enables a detailed representation of the contribution of individual vehicles or vehicle categories, often accounting for their operational conditions (e.g., speed, acceleration, road surface interaction, etc.). It therefore provides a flexible framework for integration with propagation models. The development of such an approach represents a key step toward bridging empirical prediction methods and physically based models, offering the possibility to simulate both standard and non-standard traffic conditions with improved reliability. Indeed, once the emission of an individual vehicle has been simulated and its propagation to the receiver accurately modelled, the cumulative impact of the entire traffic stream can be subsequently assessed by integrating the individual acoustic contributions of all vehicles across both temporal and spatial domains.

Within this framework, the next Subsection delves into microscopic models, which constitute the core of NEM-based approaches. These models investigate the acoustic emission mechanisms of single vehicles, providing essential insights for deriving and validating broader formulations applicable to aggregated traffic flows.

2.4.1 Microscopic Approach: Single Vehicle Noise Emission Models

Microscopic models study the emission process at the level of individual vehicles, allowing a detailed analysis of how specific traffic and operational conditions influence the resulting sound power. These models represent the foundation for understanding the physical mechanisms underlying noise generation and serve as the basis for developing more complex or aggregated formulations.[24]

24: Specific parameters, coefficients, and related technical details for each NEM to be presented in the current Section, are reported in the appended **Paper A**.

Lelong NEM [138]

In 1999, Lelong developed an empirical model to estimate the sound power level L_W of individual vehicles, distinguishing between light and heavy vehicles and considering three main driving conditions: cruising, acceleration, and deceleration. The model formulation reflects the different acoustic behaviours of vehicle categories, providing specific regression coefficients for each case. Equation (2.24) reports the general formulation for light vehicles, while equation (2.25) describes the corresponding relationship for heavy vehicles.

$$L_{w,L} = \alpha_L + \beta_L \log(v) \tag{2.24}$$

$$L_{w,H} = \alpha_H + \beta_H v \tag{2.25}$$

It can be observed that the model expresses a logarithmic dependence on vehicle speed for light vehicles and a linear relationship for heavy vehicles, emphasising the greater influence of speed on the noise emission of heavier traffic categories. This formulation thus provides an early attempt to capture the distinct scaling behaviours of various vehicle categories in relation to operating conditions.

SonRoad NEM [139]

In 2004, a Noise Emission Model calibrated in Switzerland, known as SonRoad, was developed to estimate the sound power level L_W of a single vehicle using key parameters such as vehicle type, speed, road gradient (Δ_G), and surface characteristics (Δ_{BG}).Specifically, two distinct equations are used to assess the sound power level for light and heavy vehicles, as reported respectively in equations (2.26) and (2.27).

$$L_{w,A,L} = 28.5 + \log\Bigg(10^{0.1[7.3+35\log(v)]} + \\ + 10^{0.1[60.5+10\log(1+v/44^{3.5})+\Delta_s]}\Bigg) + \\ + \Delta_{BG} \tag{2.26}$$

$$L_{w,A,H} = 28.5 + \log\Bigg(10^{0.1[16.3+35\log(v)]} + \\ + 10^{0.1[74.7+10\log(1+v/56^{3.5})+\Delta_s]}\Bigg) + \\ + \Delta_{BG} \tag{2.27}$$

The SonRoad model provides a refined representation of vehicle noise emissions by explicitly accounting for physical factors such as slope and ground absorption, thereby improving its adaptability to real-world conditions.[25]

25: The structure of the SonRoad equations (e.g., $10^{0.1[\dots]} + 10^{0.1[\dots]}$) is not just a statistical fit; it is a physically-motivated energetic summation. This formula is the logarithmic equivalent of adding two incoherent sound sources (i.e., rolling and propulsion noise). This model is a key evolutionary step, moving from a single regression (like Lelong's) to a component-based model where the total noise is the sum of its physical parts, which would be later formalised in Harmonoise.

Harmonoise NEM [140]

A major milestone among Noise Emission Models (NEMs), from which subsequent developments led to the standard model currently adopted in Europe, is the Harmonoise model. This model was conceived within the European research project HARMONOISE (*HARMONISEd Accurate and Reliable Methods for the EU Directive on the Assessment and Management of Environmental Noise*), with the main objective of providing a physically based and harmonised framework for road traffic noise prediction.

In this formulation, the sound power level L_W is estimated for five vehicle categories, light, medium-heavy, heavy, special (e.g., tractors and trucks), and motorbikes. It represents one of the first models to explicitly separate the two fundamental components of road traffic noise: propulsion noise $L_{W,propulsion}$, associated with the engine and powertrain, and rolling noise $L_{W,rolling}$, generated by the interaction between tyres and road surface. This distinction allows for a clearer understanding of how different vehicle features and operating conditions influence the overall acoustic emission.

Each component is parameterised through specific frequency-dependent coefficients, $a_p(f)$ for propulsion, and $b_r(f)$ for rolling. These coefficients enable the computation of the corresponding noise contributions across third-octave bands ranging from 25 Hz to 10 kHz, providing a detailed spectral description of the emitted sound.

Moreover, the Harmonoise model introduces a correction term applied to the propulsion component $L_{W,propulsion}$ to account for vehicle acceleration

or deceleration within the range of -2 to +2 m/s^2, represented by the factor Δ_{acc}. This correction reflects the influence of transient driving conditions on noise generation, improving the physical realism of the model.[26]

26: The Harmonoise model shift to frequency-dependent coefficients is a significant advancement. Noise emissions are inherently spectral, with different frequencies being generated by different mechanisms (i.e., low frequencies from engine noise, high frequencies from tyre-road interaction). Moreover, propagation effects (i.e., atmospheric absorption, ground effects) are frequency-dependent. By modelling L_W across third-octave bands, Harmonoise allows for a more accurate representation of both emission and propagation phenomena, which is essential for realistic noise mapping and impact assessment.

The governing equations are reported in (2.28) and (2.29).

$$L_{w,propulsion} = a_p(f) + b_p(f)\left[\frac{v - v_{ref}}{v_{ref}} + \Delta_{acc}\right] \tag{2.28}$$

$$L_{w,rolling} = a_r(f) + b_r(f)\left[\frac{v}{v_{ref}}\right] \tag{2.29}$$

Finally, the total sound power level of a single vehicle is obtained by summing the energetic contributions of propulsion and rolling noise, as shown in equation (2.30).

$$L_{w,TOT} = 10\log\left(10^{\frac{L_{W,propulsion}}{10}} + 10^{\frac{L_{W,rolling}}{10}}\right) \tag{2.30}$$

The Harmonoise model thus represents a fundamental step toward a physically grounded characterisation of vehicle noise sources. By explicitly modelling both the propulsion and rolling components, it provides a robust foundation for the subsequent development of comprehensive European standards such as CNOSSOS-EU, which further refined these concepts for regulatory and large-scale implementation purposes, as will be illustrated in a dedicated part of this Section.

REMEL NEM for US-FHWA Model [141, 142]

In the 1990s, a model was developed in the United States by the U.S. Department of Transportation, Research and Special Programs Administration, in collaboration with the Federal Highway Administration (FHWA). The main objective of this work was to update the technologies used in highway noise assessment and to provide an updated prediction framework for traffic noise along major road infrastructures.

Over the years, the model has undergone several revisions, leading to the most recent version issued in September 2021. This continuous update process reflects the model adaptability to evolving vehicle technologies, pavement types, and acoustic measurement standards.

The formula used to compute the maximum noise emission energy for a single vehicle pass-by is provided in the FHWA technical manual issued by the U.S. Department of Transportation, Research and Special Programs Administration, and is expressed as follows:

$$E_A(v_i) = (0.6214v_i)^{A/10}\,10^{B/10} + 10^{C/10} \tag{2.31}$$

In this equation v_i represents the vehicle speed (in km/h) for the i-th vehicle, and the coefficients A, B, and C depend on the vehicle category, pavement type, and engine throttle condition, and they are defined in the manual itself. The emission energy E_A is then converted into decibels through equation (2.32).

$$L_A(v_i) = 10\log(E_A(v_i)) \tag{2.32}$$

Since the FHWA model performs spectral computations on a one-third octave band basis, the characterisation of noise emission levels can be further refined, as shown in equation (2.33).

$$\begin{aligned} L_{emis,i}(v_i, f) = L_A(v_i) &+ (D_1 + 0.6214 D_2 v_i) \\ &+ (E_1 + 0.6214 E_2 v_i)[\log f] \\ &+ (F_1 + 0.6214 F_2 v_i)[\log f]^2 \\ &+ (G_1 + 0.6214 G_2 v_i)[\log f]^3 \\ &+ (H_1 + 0.6214 H_2 v_i)[\log f]^4 \\ &+ (I_1 + 0.6214 I_2 v_i)[\log f]^5 \\ &+ (J_1 + 0.6214 J_2 v_i)[\log f]^6 \end{aligned} \tag{2.33}$$

In this formulation f is the nominal frequency (Hz) of the considered third-octave band, and coefficients D_1 to J_2 depend on vehicle type, pavement characteristics, and engine throttle.[27]

27: The polynomial structure in $\log f$ allows for a flexible fitting of the spectral shape of the emitted noise, capturing the complex frequency-dependent behaviour of vehicle noise emissions. This fit models the entire spectral shape as one continuous curve, ensuring a smooth spectral shape across all frequencies, in contrast to the EU-countries methods, which often define the spectrum as a series of discrete, stepped values.

Coefficients A, B, and C primarily control the overall emission level, whereas D_1 to J_2 define the spectral shape of the emitted sound. Together, these parameters enable a detailed description of vehicle noise emissions across frequency bands, ensuring consistency between measured pass-by data and model predictions.

NMPB NEM [143–145]

In 1996, the first official release of a road traffic noise predictive model in France was published. The model, known as NMPB ("*Nouvelle Méthode de Prévision du Bruit des Routes*"), was developed under the supervision of the French Ministry of the Environment and has been revised several times, leading to the 2008 edition.

The model is based on the estimation of the source sound power level considering the combined contributions of rolling (L_r) and propulsion (L_p) components. These components are derived from empirical relationships fitted to experimental data obtained through standardised pass-by tests, where the receiver is positioned at a lateral distance of 7.5 m from the road and at a height of 1.2 m above the ground. From the measured maximum A-weighted pass-by levels, the model parameters are determined by fitting the formulation reported in equation (2.34).

$$L_{A,max} = L_r + L_p = 10 \log \left(10^{\frac{L_p}{10}} + 10^{\frac{L_r}{10}} \right) \tag{2.34}$$

Regarding the rolling component, different formulations are proposed for light and heavy vehicles, according to equations (2.35) and (2.36).

$$L_{r,LV} = A_{R,LV} + B_{R,LV} \log \frac{v}{90} \tag{2.35}$$

$$L_{r,HV} = A_{R,HV} + B_{R,HV} \log \frac{v}{80} \tag{2.36}$$

Analogously, the propulsion component follows similar formulations, as shown in equations (2.37) and (2.38).

$$L_{p,LV} = A_{P,LV} + B_{P,LV} \log \frac{v}{90} \tag{2.37}$$

$$L_{p,HV} = A_{P,HV} + B_{P,HV} \log \frac{v}{80} \tag{2.38}$$

The overall power level for an individual vehicle can then be derived from the maximum A-weighted level $L_{A,max}$ using the back-propagation formula reported in equation (2.39).[28]

$$L_W(v) = L_{A,max}(v) + 20 \log \frac{d}{d_0} + 10 \log 2\pi \tag{2.39}$$

d_0 is the reference distance from the road axis, calculated as shown in equation (2.40).

$$\frac{d}{d_0} = \sqrt{7.5^2 + 1.2^2} \tag{2.40}$$

Extensive measurement campaigns were conducted to define the model parameters, involving 450 sites for light vehicles and 150 sites for heavy vehicles, ensuring the model robustness under various traffic and pavement conditions.

28: This "receiver-centric" approach inextricably links the model fundamental L_W definition to the specific geometry of the standardised pass-by test, whereas other models attempt to define L_W as a more absolute, environment-independent source characteristic. This choice simplifies calibration against measured data but complicates the integration with propagation models, which typically require a more general definition of L_W.

CNOSSOS-EU NEM [93, 94, 146]

More recently, the European Union developed the so-called "CNOSSOS model", standing for "*Common NOise aSSessment methOdS*". This framework, inspired by the Harmonoise model introduced earlier, aims to provide a unified methodology for assessing the emissions of major noise sources, both in urban and extra-urban areas, including road traffic. Its main goal is to harmonise such prediction procedures across Member States, enabling consistent and comparable noise mapping as required by Directive 2002/49/EC [25].

The model estimates the source sound power level L_W for each octave band i and for five vehicle categories m: light, medium-heavy, heavy vehicles, powered two-wheelers, and alternative propulsion vehicles. Several correction terms are included to account for influencing factors such as studded tyres, air temperature, road gradient, acceleration or deceleration, and pavement type.

The relationships used to compute the propulsion and rolling sound power levels for an individual vehicle are expressed as shown in equations 2.41 and 2.42 and are calculated for each i-th octave band, from 125 Hz to 4 kHz.

$$L_{w,P,i,m} = A_{P,m}(i) + B_{P,m}(i) \frac{v_m - v_{ref}}{v_{ref}} \tag{2.41}$$

$$L_{w,R,i,m} = A_{R,m}(i) + B_{R,m}(i) \log \frac{v_m}{v_{ref}} \tag{2.42}$$

The coefficients $A_{P,m}$, $B_{P,m}$, $A_{R,m}$, and $B_{R,m}$ vary with the octave band and with the vehicle category considered. v_{ref} denotes the reference speed, which in CNOSSOS is set to 70 km/h, while v_m represents the mean speed of the specific vehicle category.

The original coefficients for categories 1 to 4 were first published in [93] and later refined in [147] and in [94, 146] to include the effects of

surface reflections. Moreover, subsequent studies have proposed further adaptations for vehicle categories not originally included in the CNOSSOS model. For instance, Pallas et al. [148, 149] introduced correction terms for electric vehicles, while Licitra et al. [150] provided updated $A_{P,m}$, $B_{P,m}$, $A_{R,m}$, and $B_{R,m}$ coefficients based on statistical pass-by measurements on reference and crumb rubber pavements.

However, the use of mean speeds for each vehicle category implies that CNOSSOS-EU is not a fully microscopic model, since individual vehicle speeds are not explicitly represented. Nevertheless, the sound power level is still estimated at the single-vehicle level before aggregating emissions along the traffic flow line source, as will be detailed in Section 2.4.2.[29]

29: The CNOSSOS-EU model use of mean speeds per vehicle category is a pragmatic compromise. While it sacrifices some granularity compared to fully microscopic models (which would track individual vehicle speeds), it significantly reduces computational complexity and data requirements. A true microscopic model would be computationally unfeasible for EU-mandated strategic noise mapping. CNOSSOS-EU was designed to use the available data (i.e., time-averaged traffic flow and mean speeds per road segment), making large-scale mapping practical.

The overall propulsion and rolling sound power levels are computed as described in equations (2.43) and (2.44).

$$L_{w,P,m} = 10 \log \sum_{i=125Hz}^{4000Hz} 10^{\frac{L_{w,P,i,m}}{10}} \tag{2.43}$$

$$L_{w,R,m} = 10 \log \sum_{i=125Hz}^{4000Hz} 10^{\frac{L_{w,R,i,m}}{10}} \tag{2.44}$$

Finally, the total source sound power level $L_{W,m}$ for each vehicle category m is obtained as explained in equation (2.45).

$$L_{w,m} = 10 \log \left(10^{\frac{L_{w,P,m}}{10}} + 10^{\frac{L_{w,R,m}}{10}} \right) \tag{2.45}$$

ASJ-RTN NEM [151–153]

In 1975, the Acoustical Society of Japan introduced the first version of a road traffic noise prediction model for free-flowing conditions, known as the ASJ-RTN model. Since its initial release, the model has undergone several revisions, up to the most recent 2018 edition, to incorporate new research findings, comply with updated national regulations, and integrate wave-based computational methods for sound propagation. A comprehensive overview of its evolution can be found in [153]. It represents one of the earliest structured attempts to model vehicle noise emissions in a parametric and adaptable way in Japan, establishing the foundation for subsequent refinements and regional adaptations within Japan's noise prediction framework.

The ASJ-RTN model estimates the A-weighted sound power level $L_{A,W}$ for three vehicle categories, i.e., motorcycles, light vehicles, and heavy vehicles, using the average vehicle speed as the main input variable. In addition, correction terms are available to account for road surface type, road gradient, and the directivity of sound radiation. The general formulation of the model is given in equation (2.46).

$$L_{A,W} = a + b \log v + C \tag{2.46}$$

30: ASJ-RTN model represents a "modal" approach to handling non-free-flow traffic. Instead of applying a continuous correction for acceleration, it changes the entire emission equation (by switching coefficients) for different traffic regimes. This approach simplifies the model structure but may introduce discontinuities in predicted noise levels when transitioning between modes.

In this formulation a and b are regression coefficients, and C is a corrective factor that aggregates adjustments for slope, radiation directivity, and other environmental or operational influences. The parameters a, b, and C are tabulated as a function of flow conditions (steady, non-steady, or decelerating), speed range, vehicle category, and pavement type [154].[30]

Vehicle Noise Specific Power (VNSP) [102]

Recently, a Vehicle Noise Specific Power (VNSP) model has been developed by Pascale et al. with the aim of assessing the sound power level L_W by explicitly considering the vehicle motorisation. The VNSP approach introduces a refinement in the description of vehicle noise emission, as it distinguishes between different powertrain technologies (i.e., diesel, petrol, and hybrid) and models their specific influence on the emitted sound power.

The model establishes a fundamental relationship between L_W and the vehicle speed through a non-linear regression of power levels measured using the statistical pass-by procedure, allowing for a realistic representation of the acoustic behaviour under different operating conditions.

Similarly to the CNOSSOS and Harmonoise formulations, the total sound power level is obtained as the energetic sum of two main components: the propulsion noise, assumed to vary linearly with speed, and the rolling noise, represented by a logarithmic dependence on speed. The general formulation is expressed in equation (2.47).

$$L_W = 10 \log \left(10^{\left(A + B \frac{v - v_{ref}}{v_{ref}}\right)/10} + 10^{\left(C + D \log \frac{v}{v_{ref}}\right)/10} \right) \tag{2.47}$$

The reference speed adopted is consistent with CNOSSOS (i.e., 70 km/h). Nevertheless, a relevant distinction of the VNSP with respect to previous models lies in its direct use of the overall sound power level L_W, instead of performing the regression separately for each octave or third-octave band. This approach simplifies the estimation procedure while maintaining good predictive performance across vehicle categories and operating speeds.

The VNSP model therefore represents an evolution toward a more flexible and technology-sensitive formulation, capable of capturing the growing variability introduced by modern vehicle fleets and alternative powertrains. A practical application of this model and a comparison with results obtained using other NEMs are presented in [103].

Beyond Standardisation: Microscopic Models from Literature

A growing body of research has explored the development of microscopic approaches, in which each vehicle is treated as an individual sound source with its own kinematic state. Unlike macroscopic models, microscopic ones can take into account instantaneous variations in speed, acceleration, and driving dynamics, which play a key role in determining more accurately noise emissions. Several studies have demonstrated the importance of these effects, showing that neglecting vehicle kinematics may lead to significant discrepancies in predicted sound power levels, especially in congested or stop-go traffic [95, 155, 156].[31]

Microsimulation techniques, which reproduce second-by-second vehicle movements, have therefore become increasingly popular for noise modelling applications, as they allow a more realistic representation of the temporal and spatial variability of the phenomenon. For instance, in [157], Can and Botteldooren found out that sound power levels assessed using a microscopic approach differ notably from those estimated using the mean speed approach, particularly in congested traffic conditions and

31: In congested conditions, the mean speed along a road segment may be very low, leading a macroscopic model to predict minimal noise levels. A microscopic approach, however, can capture the true acoustic character of such conditions, which are often "loud" and highly variable due to frequent high-energy, low-gear acceleration events that tend to be masked by temporal averaging.

in urban settings, which are often characterised by ever changing traffic conditions. In their contribution, they noticed that neglecting vehicle kinematics, such as acceleration/deceleration and speed distribution in either congested or stop-and-go scenarios can lead to high disparities, mainly due to actual driving speeds being considerably lower than the speed limit.

In [158], an analysis of the urban and interurban noise frequency spectrum has been performed, comparing a macroscopic approach, which takes into consideration just mean vehicle speeds and flow rates, and a microscopic approach which considers vehicle interactions (respectively called static and dynamic). Even though different noise features were explored, such comparison highlighted how the macroscopic approach systematically underestimates low frequency contributions to continuous equivalent sound pressure levels, being such contributions mainly related to low speeds and accelerating phases.

The inability of macroscopic approaches to consider vehicle kinematics and different traffic patterns also affects $L_{A,eq}$ estimations as also proved in [159] Nygren et al., indeed, highlighted the crucial importance of using a microscopic approach to compute the vehicle-specific noise exposure cost, i.e., the contribution of the single vehicle to the overall noise impact of a road network. Likewise, Baclet et al. proposed the calculation of noise exposure indicators in large urban areas starting through the usage of a microscopic model [160].

In [161], a microscopic approach was employed to assess road traffic noise emission using data collected with "Unmanned Aerial Vehicles" and the CNOSSOS-EU model to simulate each vehicle as an individual source point. Nevertheless, as mentioned earlier, obtaining usable inputs for microscopic models through measurement campaigns is not always possible. To overcome this issue, many scholars utilise meso- or microscopic traffic simulation tools to compute and simulate realistically both road networks and single vehicle behaviors, thereby obtaining speeds and positions of vehicles at the desired time step [162–164].

Several other approaches can be adopted to obtain the necessary traffic data for these models [165]. Direct measurements, video image analysis [166–168], traffic microsimulators [155, 160, 163, 169–172] such as VISSIM or SUMO are among the most common solutions.[32] The combination of these data sources with noise emission and propagation models has led to the development of hybrid methods capable of reproducing complex urban scenarios and evaluating the effects of specific traffic configurations on noise exposure.

32: Tools like SUMO (Simulation of Urban MObility) and VISSIM are "agent-based" or "microscopic" traffic simulators. They do not just model aggregate flow; they simulate the specific behavioural logic (e.g., car-following, lane-changing, gap-acceptance, etc.) of each individual vehicle. For noise modelling, their critical output is a complete, second-by-second kinematic trace (position, speed, and acceleration) for every vehicle in the network.

Among the several approaches developed to enhance the accuracy of road traffic noise predictions, **stochastic methods** have emerged as particularly promising. These methods aim to capture the inherent variability and uncertainty in both traffic flow dynamics and noise generation processes. By incorporating probabilistic elements, such as random variations in vehicle behaviors, traffic composition, and environmental conditions, stochastic approaches allow for a better representation of non-stationary or complex urban scenarios. For instance, in Chapter 3, a stochastic microscopic model developed during this thesis will be presented. In such a model each vehicle speed is randomly drawn from a proper speed distribution curve based on traffic conditions. Several other stochastic road traffic noise models can be found in literature. Li et al. presented noise prediction model based on a Monte Carlo simulation in which, for three different category, single vehicle sound power level from three different types of vehicles is drawn from a probability distribution,

simulating the randomness of real traffic emissions [119], while Wang et al. used mixed probability models for inter-vehicle headways and speeds, applying Monte Carlo sampling to generate detailed noise maps, obtaining very small errors [173].

Lately, the use of **time series analysis** for modelling and forecasting traffic-related phenomena has gained increasing attention too, particularly in the context of intelligent transportation systems and environmental monitoring, intending to forecast real-time traffic to be used as inputs for microscopic noise model. Among the most prominent methods in this domain are the Autoregressive Integrated Moving Average (ARIMA) and its seasonal counterpart (SARIMA), which have proven effective in capturing the temporal dynamics of both traffic flow and its noise emissions. One of the earliest uses of ARIMA in traffic forecasting was introduced by Ahmed and Cook [174], who applied such models to predict freeway traffic volumes and occupancies. Their work laid the foundation for subsequent studies that adopted ARIMA-based approaches as reliable benchmarks for short-term traffic flow forecasting. For example, Guarnaccia et al. and Pascale et al. also employed SARIMA to analyse long-term noise monitoring data in urban areas, respectively in southern Italy [175, 176] and Portugal [177]. Their findings revealed that noise levels, represented by the equivalent continuous sound level, exhibit clear weekly and daily patterns that can be accurately modelled using SARIMA frameworks. These models proved effective not only in fitting historical data but also in providing reliable short-term forecasts, useful for noise mitigation planning and real-time monitoring. However, despite the increasing use of advanced machine learning techniques in the field, as also reported earlier in Section 2.3.4, ARIMA and SARIMA remain popular due to their interpretability, low computational cost, and effectiveness with limited data [178, 179].

The integration of time-dependent forecasting techniques, such as those based on time series analysis, has opened the possibility to simulate temporally evolving noise scenarios. By predicting changes in traffic flow and speed patterns, these methods contribute to a more comprehensive understanding of urban noise dynamics, with potential applications in real-time monitoring and urban planning.[33]

33: A strategic map, as mandated by the EU's Environmental Noise Directive (END) [25], typically represents a yearly average (e.g., L_{den}). A dynamic map, in contrast, can update its predictions on an hourly or even per-minute basis. This has profound implications for public information (e.g., "quiet-route" navigation apps) and short-term policy interventions.

Overall, the literature highlights a progressive shift from standardised, static models toward more detailed and dynamic frameworks. Microscopic and stochastic approaches, by explicitly considering the variability of real traffic conditions, offer a more accurate and physically consistent representation of the mechanisms underlying road traffic noise. This evolution marks an important step beyond standardisation, opening the way to a deeper understanding of the complex interactions between traffic dynamics and acoustic environments.

2.4.2 Micro to macro transition: from single vehicle to traffic flow emission

To achieve a comprehensive assessment of road traffic noise, the emission from individual vehicles must be scaled up to represent the collective contribution of the entire traffic stream along a road segment. In this context, the sound power levels L_W of all vehicles are combined to obtain an overall estimate of the acoustic energy radiated by the flow, which serves as the basis for subsequent propagation and mapping calculations.

Within the CNOSSOS-EU framework [93], a systematic procedure is provided to transition from a single-point source representation to a distributed linear source model, accounting for the cumulative effect of multiple vehicles passing along a roadway. The sound power level of the traffic flow, expressed per meter and per octave band for a given vehicle category m, is computed in the CNOSSOS-EU framework, as shown in equation (2.48).[34]

34: The ratio between $10 \log Q_m$ and $1000 v_m$ yields the density in vehicles per meter. The sound power level of a single average vehicle $L_{W,i,m}$ is scaled by the logarithmic average number of vehicles passing on each one-meter segment of the road at any given instant.

$$L_{W,line,i,m} = L_{W,i,m} + 10 \log \frac{Q_m}{1000\, v_m} \tag{2.48}$$

Here, $L_{W,i,m}$ represents the instantaneous directional sound power level in a semi-free field for a single vehicle, calculated for each i-th octave band from 125 Hz to 4 kHz and for each vehicle category m. The parameters Q_m and v_m denote, respectively, the hourly traffic flow and the average speed of vehicles within category m. In practical implementations, when detailed speed distributions are unavailable, the maximum legal speed for the category is sometimes used as an approximation for this value.

An alternative approach to obtain the total emission from a traffic stream involves an energy-based formulation at the receiver position. In this method, the acoustic energy contributed by each individual pass-by is expressed in terms of its *Sound Exposure Level (SEL)*, and the cumulative traffic noise is obtained by summing the SEL values of all vehicles transiting along the segment within a defined period.[35] This approach inherently accounts for the temporal and energetic characteristics of discrete pass-bys, offering a more microscopic representation of the noise generation process. It has been widely adopted in several research studies and modelling applications, including [166, 167, 180–182], where SEL-based aggregation enables a more accurate assessment of the overall noise emission under varying traffic and environmental conditions.

35: SEL based approach propagates each individual vehicle pass-by to the receiver first, calculating the acoustic "event" of that pass-by. It then sums the energy of all these discrete events at the receiver. It shifts the aggregation from the source to the receiver, allowing for a more detailed temporal representation of noise exposure.

The same principle has been applied in the development of the models to be presented in the Chapter 3, where the aggregation of single pass-by events is used as a foundation to describe and predict the overall traffic noise emission. Their formulation, calibration, and validation procedures are discussed in detail in the next Chapter.

2.5 Propagation and assessment at the receiver

Once the sound power level L_W of the traffic flow has been estimated, either through direct aggregation of individual vehicle emissions or via energy-based methods, the next step involves modelling the propagation of this acoustic energy to the receiver location. This stage is crucial for accurately predicting the noise levels experienced by individuals in the proximity of roadways. Various propagation models can be employed, ranging from simplified empirical approaches to more sophisticated deterministic methods that account for complex environmental factors such as terrain, atmospheric conditions, and ground effects. The choice of propagation model depends on the specific application, required accuracy, and available computational resources.

2.5.1 Propagation models

Once the sound source is characterised by its emission, the vast majority of noise propagation models for noise mapping begin by discretising it into point sources. In the CNOSSOS-EU model, for instance, a vehicle is represented as a point source at a height of 0.05m. Thus, the traffic stream is discretised into an array of point sources, as described earlier, situated along its central axis, at 0.05m height and at regular intervals dependent on the distance between the source and the receiver.[36] The greater this distance, the larger the interval between point sources can be while maintaining the same level of prediction accuracy. If multiple point sources represent the same source, each of these points bears only a fraction of their energy. Once the source is discretised, the next step involves modelling the propagation between the point sources and the receivers within the domain.

36: This standardised height is a 'virtual source' position, not a physical one. It is a modelling convention (adopted by CNOSSOS-EU) designed to simplify the calculation of the "ground effect."

In this regard, several models exist in the literature, which try to balance between precision and computational cost. Pathfinding methods, for instance, involve finding the set of shortest paths between a source and a receiver. In the case of a direct field, it is straightforward: a straight-line segment between these two points, while if a building is present between them, it involves three segments passing over and around the sides of the building. It needs to be acknowledged that in these kind of models there is an inability to represent buildings as arches: the building must be solid, a concept sometimes referred to as 2.5D. When considering reflections, the simulation needs to account for the interaction of sound waves with building surfaces, leading to multiple paths and interactions that contribute to the overall sound field at a receiver.

Once these paths are identified, the next step is to apply a model of sound wave attenuation to each of these paths. The literature contains numerous comparisons between the most commonly used models [183–187], which generally show that, when using detailed input data, most models yield similar results in terms of accuracy.

Most noise propagation models account for the following effects on attenuation:

- **Geometric divergence:** This refers to the attenuation resulting from the loss of energy as the distance increases (-6 dB/doubling of distance for a point source);[37]
- **Atmospheric absorption:** This is influenced by the humidity and temperature of the atmosphere;[38]
- **Absorption and/or reflection of the wave by the ground:** This depends on the type of soil;[39]
- **Terrain shape and topography:** The overall form of the terrain and its topographical features can affect sound propagation;[40]
- **Meteorological effects:** Wind and temperature influence the speed of the sound wave, causing their gradients to have a significant impact on the sound level at the receiver. These are sometimes simplified, as in CNOSSOS-EU or ISO 9613-2, to two distinct conditions, either no effects on propagation or conditions favorable to propagation;[41]
- **Diffraction effects:** These occur at the edges of buildings, acoustic walls, or the ground and can influence the path of sound waves.

37: For a line source, the geometric divergence is -3 dB/doubling of distance.

38: Atmospheric absorption is frequency dependent, with higher frequencies being absorbed more than lower frequencies.

39: "Soft" ground (e.g., grass, soil, etc.) attenuates sound primarily through destructive interference. The sound wave reflecting off the porous ground undergoes a "phase shift". This phase-shifted reflected wave then combines with the direct wave at the receiver. At certain frequencies (typically 250-1000 Hz), this results in significant destructive interference, causing an attenuation "dip" that goes far beyond simple material absorption. Hard ground (pavement) does not cause this phase shift and can lead to constructive interference (amplification).

40: Hills and valleys can create "shadow zones" where sound levels are significantly reduced. Elevated terrain can also act as a barrier, blocking or reflecting sound waves.

41: The simplification to "conditions favourable to propagation" simulates a moderate downwind condition or a slight temperature inversion. In both scenarios, the sound wave's path is refracted (bent) downwards toward the ground, increasing noise levels at a distance. This is a "worst-case" but stable and repeatable condition. Modelling unfavourable conditions (i.e., upwind) is avoided as it can create complex, non-repeatable "sound shadows".

It is crucial to emphasise that, in the context of most large-scale studies, uncertainties in the results are predominantly influenced by factors such as input data and exposure calculations rather than the intricacies of the models themselves [188]. Despite the inherent complexities, numerous

studies with detailed input data have shown acceptable agreement between measurements and simulations in the context of city scale long-term averaged noise levels.

2.6 Assessment at the Receiver

All the models presented in the foregoing Sections and Subsections can be effectively employed to investigate various types of impacts that road traffic noise exerts on the surrounding environment. Depending on the specific objectives of the study, whether the aim is to evaluate compliance with regulations, to understand the spatial distribution of noise exposure, or to estimate its broader societal implications, model outputs can be processed to derive a wide range of impact indicators.

These impacts concern those who can be identified as the *receivers* of road traffic noise, i.e., individuals, communities, or built environments exposed to sound emissions, depending on the spatial and temporal scale of interest. At smaller scales, the focus may be on individual exposure or façade-level sound pressure levels, whereas at larger scales, assessments can encompass entire neighborhoods or urban areas to capture population-wide exposure patterns.

The assessment at the receiver can be performed either directly, by computing energetic indicators as defined by national and international standards, or indirectly, by evaluating secondary consequences such as health outcomes, economic externalities, and variations in property values.

A comprehensive evaluation therefore requires integrating physical, physiological, and socio-economic dimensions of noise exposure. In the following Subsections, three main categories of assessments at the receiver are discussed: (i) regulatory noise indicators, (ii) health-related effects, and (iii) external costs associated with traffic noise.[42]

42: An interesting approach worth to be cited is the *DPSIR (Driver-Pressure-State-Impact-Response)*, which is the standard analytical tool used by the European Environment Agency (EEA) to assess environmental problems. In this framework, the "Driving force" is the traffic demand, the "Pressure" is the noise emission from vehicles, the "State" is the noise level at the receiver, the "Impact" is the negative effect to be analysed, and the "Response" includes policy measures to mitigate noise exposure.

2.6.1 Common Regulation Indicators

A first and most immediate purpose of applying Road Traffic Noise Models (RTNMs) is the computation of standardised noise indicators, which constitute the primary outputs required for environmental assessment and regulatory compliance.

In the European framework, the reference descriptors used for strategic noise mapping and for national regulatory purposes are those defined in the *Environmental Noise Directive* [25]. Among them, the most relevant acoustic descriptor is the *day-evening-night level* (L_{den}), which is an acoustic descriptor computed as shown in equation (2.49).

$$L_{den} = 10 \log \frac{1}{24} \left[12 \cdot 10^{\frac{L_{day}}{10}} + 4 \cdot 10^{\frac{L_{evening}+5}{10}} + 8 \cdot 10^{\frac{L_{night}+10}{10}} \right] \tag{2.49}$$

This formulation integrates the sound energy over the 24-hour period, weighting the different time intervals, i.e., day (12 h), evening (4 h), and night (8 h), with additional penalties of 5 dB and 10 dB for the evening and night, respectively. These corrections account for the increased sensitivity of the population to noise exposure during these periods, reflecting both physiological and behavioural factors.[43]

43: This formulation makes the L_{den} a psycho-acoustic or policy-based indicator, not a purely physical one. A simple 24-hour average ($L_{eq,24h}$) would treat a 60 dB sound at 3 AM as identical to a 60 dB sound at 3 PM. The L_{den}'s +10 dB night penalty effectively states that, from a human annoyance and sleep disturbance perspective, the 60 dB event at 3 AM contributes as much to the 24-hour "dose" as a 70 dB event would during the day.

European Member States are required to employ this indicator for the development of strategic noise maps. Such maps are intended to provide a large-scale assessment of noise exposure, covering all major urban sources, with particular emphasis on road traffic noise. Typically, these assessments are performed using numerical models that simulate both the emission and the propagation of noise from transport and industrial sources, which are often implemented in commercial software environments.

From a modelling standpoint, the ability of an RTNM to produce results consistent with the regulatory indicators is a fundamental requirement for its practical applicability. Two main approaches can be adopted to this end:

- The model can directly output noise levels aggregated over the regulatory time intervals;
- The model can provide instantaneous or time-dependent sound pressure levels $L_p(t)$, which are subsequently processed to derive the equivalent continuous levels and the standardised descriptors.

The latter approach, though computationally more demanding, allows for a more flexible representation of temporal variability and facilitates advanced analyses, such as percentile levels ($L_{A,10}$, $L_{A,50}$, $L_{A,90}$) and event-based indicators (e.g., SEL or L_{Amax}).[44]

In a broader sense, acoustic indicators can be categorised according to their purpose:

- **Energetic indicators**, such as L_{eq} or L_{den}, describe the average acoustic energy over a given period and are typically used for regulatory and mapping purposes;
- **Statistical indicators**, such as $L_{A,10}$, $L_{A,50}$ and $L_{A,90}$, provide information on the temporal distribution of sound levels, enabling the characterisation of background and peak noise conditions;[45]
- **Event-related indicators**, including the Sound Exposure Level (SEL) and the Maximum Sound Level (L_{Amax}), are particularly suited for transient or intermittent sources and can support more detailed analyses of traffic composition and temporal variability.

The computation of these indicators represents the essential interface between the emission modelling phase and the impact assessment phase. They allow the translation of the microscopic variability of vehicular noise emissions into macroscopic, standardised quantities suitable for comparison, regulation, and communication to stakeholders. Furthermore, they serve as the quantitative basis for deriving secondary metrics, such as exposure-response relationships, health impact assessments, and external cost estimations, which will be further addressed in the following Subsections.

44: A macroscopic model that outputs only L_{den} cannot provide the temporal resolution needed to compute percentile levels or event-based indicators. To generate a detailed $L_p(t)$ a microscopic model is needed. Thus $L_p(t)$ can be post-processed to derive any desired indicator, including L_{den}, percentiles, SEL, and L_{Amax}. This flexibility is crucial for comprehensive noise assessments.

45: The statistical indicators L_n (percentile levels) are crucial for describing the character of the noise. $L_{A,90}$ (the level exceeded 90% of the time) is a standard proxy for the "background noise" or "acoustic floor". $L_{A,10}$ (exceeded 10% of the time) is used to represent the "intrusive noise" (e.g., peaks from passing heavy vehicles). A large difference between $L_{A,10}$ and $L_{A,90}$ indicates a highly variable and "spiky" acoustic environment, which is often perceived as more annoying than a steady noise characterised by the same L_{eq}.

2.6.2 Exposure and Effects on Human Health (DALYs)

An alternative approach, particularly relevant when the analysis aims to evaluate population exposure, consists in translating the physical outputs of Road Traffic Noise Models into quantifiable health outcomes. This methodological framework, grounded in the concept of *Environmental Burden of Disease (EBD)* [24, 189], establishes a scientifically consistent linkage between acoustic indicators and health effects [190], and represents a fundamental basis for subsequent applications such as *Health Impact Assessment (HIA)* [191] and *Cost-Benefit Analysis (CBA)* [192].[46]

46: The equations presented in this Subsubsection are based on meta-analyses of epidemiological studies, which have established statistical relationships between noise exposure and specific health outcomes (e.g., annoyance, sleep disturbance, cardiovascular diseases) as reported in [24].

The first methodological step in this conversion is the definition of standardised exposure indicators, which transform acoustic data into a *dose* metric suitable for epidemiological assessment [193]. Within the European Directive 2002/49/EC [25], two harmonised indicators are used to represent population exposure to environmental noise: the day-evening-night level (L_{den}) and the night level (L_{night}). These indicators enable the application of exposure-response (E-R) functions derived from large-scale epidemiological studies. However, a complete HIA framework requires both the acoustic desciptor above mentioned, since different health outcomes (also referred to as "*endpoints*") are associated with different dose metrics.

These E-R functions, mathematical relationships based on meta-analyses of epidemiological data, define the statistical relationship between the level of "dose" (i.e., noise exposure in terms of L_{den} and L_{night}) and the probability of specific health outcomes (i.e., "response") occurring in the exposed population.

Annoyance, for example, is typically associated with daytime noise exposure and is evaluated using the L_{den} indicator. The relationship for percentage annoyed (%A) due to road traffic noise has been modelled as shown in equation (2.50).[47]

47: In the context of Environmental Burden of Disease, "annoyance" (and "high annoyance") is not a trivial discomfort. It is a formal, non-clinical health endpoint defined by the WHO as a "significant degradation in quality of life and well-being." It is treated as a precursor to, and contributor to, more severe stress-related physiological and psychological outcomes, and is therefore quantified as a legitimate component of the total health burden.

$$\%A = 1.795\times10^{-4}(L_{den}-37)^3+2.110\times10^{-2}(L_{den}-37)^2+0.5353(L_{den}-37) \tag{2.50}$$

High annoyance (%HA) is also linked to the L_{den} metric, with the relationship expressed in equation (2.51).

$$\%HA = 9.868\times10^{-4}(L_{den}-42)^3-1.436\times10^{-2}(L_{den}-42)^2+0.5118(L_{den}-42) \tag{2.51}$$

Several factors can influence the annoyance response, including individual sensitivity, cultural context, and the presence of other factors, such as interrupted flows in the traffic phenomenom. Therefore, while these equations provide a general framework for estimating annoyance levels, local adjustments may be necessary to account for specific population characteristics.

Sleep disturbance is more clearly linked to nighttime noise levels, assessed through the L_{night} metric. The percentage of individuals sleep disturbed (%SD) and highly sleep disturbed (%HSD) can be estimated using the relationships shown in equations (2.52) and (2.53) respectively.

$$\%SD = 13.8 - 0.85L_{night} + 0.01670L_{night}^2 \tag{2.52}$$

$$\%HSD = 20.8 - 1.05L_{night} + 0.01486L_{night}^2 \tag{2.53}$$

Cardiovascular effects, such as ischemic heart disease (including myocardial infarction) and hypertension, have also been linked to long-term exposure to road traffic noise. For these health outcomes, odds ratio (OR) (i.e., relative risk) functions are commonly used to quantify the increased risk associated with specific noise exposure levels. For example, the OR for hypertension can be expressed as shown in equation (2.54).

$$\begin{aligned} \mathrm{OR}_{\text{hypertension}} \text{ per } 10 \text{ dB(A)} = 1.13 \quad (95\% \text{ CI} = 1.00 - 1.28), \\ \text{for } L_{den} = 50 - 70 \text{ dB(A)} \end{aligned} \tag{2.54}$$

Similarly, the OR for ischemic heart disease is given in equation (2.55).

$$\begin{aligned} \text{Cubic model:} OR_{IHD} = & 1.629657 - 0.000613 \times (L_{day,16h})^2 \\ & + 0.000007357 \times (L_{day,16h})^3, R^2 = 0.96 \end{aligned} \tag{2.55}$$

These relationships enable the estimation of the increased risk of cardiovascular diseases in populations exposed to varying levels of environmental noise.

To aggregate the various impacts on health (annoyance, sleep disturbance, heart attacks, and even deaths) into a single comparable metric, the standard methodology is the Environmental Burden of Disease (EBD), which uses the *Disability-Adjusted Life Year (DALY)*.

Originally launched in 1990 from Harvard University for the World Bank and backed by the World Health Organization as a measure of the global burden of disease [189], DALYs have been extensively used in the literature to assess the influence of several environmental pollutants on human health worldwide [189, 194, 195]. This indicator quantifies the global human health burden by indicating how many years of healthy life are lost as a consequence of exposure to the analysed pollutant. DALYs are computed as the sum of the *Years of Life Lost (YLL)* due to premature mortality in the population and the *Years Lost due to Disability (YLD)* for people living with a health condition or its consequences. The general formulation is given in equation (2.56).

$$DALY = YLL + YLD \tag{2.56}$$

The YLL component is calculated by multiplying the number of deaths (ND) due to a specific health outcome by the disability weight (DW), which reflects the severity of the condition, and the standard life expectancy (LD) at the age of death, as shown in equation (2.57).

$$YLL = ND \times DW \times LD \tag{2.57}$$

The YLD component is determined by multiplying the number of incident cases (NI) of a particular health condition by the disability weight (DW), and the average duration of the condition (LI), as shown in equation (2.58).[48]

$$YLD = NI \times DW \times LI \tag{2.58}$$

48: Disability weights (DWs) are values between 0 and 1 that represent the severity of a health condition, where 0 indicates perfect health and 1 represents death. These weights are typically derived from population surveys and expert consultations to reflect societal preferences regarding different health states.

European Environment Agency (EEA) estimated that, in 2021, long-term exposure to transport-related noise contributed to approximately 66,000 premature deaths across Europe, alongside 50,000 new cases of cardiovascular diseases and 22,000 new cases of type 2 diabetes. These figures correspond to roughly 0.7% of all newly diagnosed cardiovascular diseases, 1.3% of all new cases of type 2 diabetes, and 1.1% of total premature deaths recorded in that year being attributable to noise from transport sources. [28]

Moreover, emerging evidence suggests that prolonged exposure to transportation noise may also be associated with an increased incidence of

mental health disorders, including depression and dementia as described in Chapter 1.[49] In terms of DALYs, it is estimated that transport noise exposure resulted in the loss of approximately 1.37 million healthy life years each year, with road traffic noise accounting for the majority of this burden [28].[50] These estimates underscore the significant public health impact of transportation noise and highlight the need for effective mitigation strategies to reduce exposure and associated health risks.

In [196] a comprehensive study of effects on health of noise is reported. A correlation between these estimated DALYs and a more punctual noise evaluation on urban context could result in an useful indicators to highlight the profound impact noise has nowadays on our lives. The DALYs approach also reveals how dramatic the impact of noise is on populations in terms of economic costs.

In [197] it is reported an estimation of DALYs due to noise in Netherland, but it is incorporated to the estimation of DALYs due to the more generic air pollution. In detail, it is reported how particulate air pollution accounts for 60% of DALYs, and noise for 24%, with an amount of 17700 DALYs (only for noise) annoyance, 10990 to sleep disturbance, 50 for ischaemic heart disease (IHD) from and 10 DALYs for mortality related to noise.

2.6.3 External Costs of Transportation

External cost, also known as *externalities*, are costs that affect a party who did not choose to incur them. In the context of transportation, external costs refer to the negative impacts of transport activities on society and the environment that are not reflected in the market prices of transport services. These costs include health impacts, traffic congestion, accidents, infrastructure wear and tear but also air pollution, greenhouse gas emissions and noise pollution. Since these costs are largely unaccounted for in the price that transport users have to pay, they tend to not consider the full social cost of their travel decisions, leading to overuse of transportation systems, particularly road transport [198].

A comprehensive methodology to evaluate the external costs of transportation is provided in the *Handbook on estimation of external costs in the transport sector* [104]. This document, published by the European Commission and updated lately [199], offers detailed guidelines and methodologies for estimating the external costs associated with different modes of transportation, including road, rail, air, and maritime transport. Its central aim is to provide a harmonised framework for assessing external costs and to recommend a set of methods and "default values" that can be used by policymakers and analysts.[51]

The central challenge in calculating external costs lies in assigning a monetary value to non-market goods such as human life, clean air, or time. The Handbook framework draws upon several established economic valuation methodologies to address this challenge. The "best practice" and most widely recommended is the *Damage Cost Approach*, which is based on the *Willingness-to-Pay (WTP)* principle. This approach determines the value of an externality by assessing the monetary value of the damages it causes, typically derived from meta-analyses of studies that estimate how much individuals are willing to pay to avoid a negative outcome (e.g., risk of death) or secure a positive one (e.g., environmental quality).[52] Where primary WTP studies are not available or are difficult to apply, other approaches can be used. The *Avoidance Cost Approach* values externalities according to the marginal cost required to achieve a specific, pre-defined

49: The link between noise and mental health (depression, anxiety, cognitive decline) is a critical emerging field. While the physiological pathway (e.g, chronic stress, HPA axis dysregulation, and sleep deprivation) is plausible, the statistical evidence and formal E-R functions are not yet as consolidated as those for cardiovascular disease. The inclusion of these 'emerging endpoints' in future DALYs calculations is expected to significantly increase the total calculated Environmental Burden of Disease from noise.

50: 1.1 million years were lost due to road traffic noise, 230000 healthy years were lost due to railway noise and 21000 healthy years were lost due to aircraft noise [28].

51: The handbook covers a broad range of external cost categories, including accidents, air pollution, climate change, noise, congestion, and infrastructure wear and tear. It provides detailed methodologies for quantifying these costs and offers guidance on data collection and analysis.

52: WTP can be estimated in two ways: (i) *Revealed Preference (RP)* methods, which infer value by observing real-world economic choices. The "hedonic pricing" models (linking property values to noise levels) are a classic example of RP, as they reveal what the market is already willing to pay for quiet; and (ii) *Stated Preference (SP)* methods, which ask people directly (through "contingent valuation" surveys) how much they would hypothetically pay for a non-market good (e.g., *"Would you pay €X more in taxes for a 5 dB reduction in street noise?"*).

policy target (e.g., the cost per tonne of CO_2 to meet the EU's emission reduction objectives), thus providing a pragmatic proxy for collective WTP. The *Replacement or Restitution Cost (RC) Approach* estimates the value of externalities based on the cost of repairing or restoring the damage caused, such as the costs of medical treatments or vehicle repairs following an accident.

The valuation of human costs is generally proxied using the *Value of a Statistical Life (VSL)*, a WTP-based metric derived from a meta-analysis of studies estimating how much individuals are willing to pay for small reductions in mortality risk.[53] The Handbook methodology applies this VSL as a reference standard: fatalities are valued at 100% of the VSL, serious injuries at 13% of the VSL, and slight injuries at 1% of the VSL. Additional direct and indirect economic costs (e.g., lost productivity) are valued at 10% of the VSL and are considered fully external. For material damages, medical costs, and administrative costs, the RC approach is applied to estimate the resources required to restore victims and property to their pre-accident condition.

53: The VSL is a frequently misunderstood metric. It is not the value of a specific, identifiable person's life. Rather, it is a metric related to a *"statistical life"*. It is derived from WTP studies answering: "How much are a large group of people willing to pay for a small reduction in their collective risk of death?" For example, if 100,000 people are each willing to pay €100 for a 1-in-100,000 reduction in mortality risk, the VSL is calculated as (100,000 people × €100) / (1 statistical life saved) = €10 million.

When focusing specifically on noise-related external costs, the Handbook provides detailed methodologies for estimating the economic impact of noise pollution from transportation sources. These costs are typically assessed in terms of health impacts (e.g., annoyance, sleep disturbance, cardiovascular diseases, etc.) and property value depreciation. Valuation methods for noise-related externalities often rely on WTP studies quantifying how much individuals are willing to pay to avoid noise exposure or its associated health effects.

Synthesising the data from the European Commission's Handbook, the full scale of these externalities becomes evident. In 2016, the total external costs of transport in the EU28 amounted to €987 billion. This figure is equivalent to 6.6% of the total Gross Domestic Product (GDP) of the EU28, representing a profound drag on the European economy. The disaggregation of this total reveals the relative importance of each cost category, with some results that challenge common perceptions. In the following list, the main external cost categories and their estimated annual costs in the EU28 are summarised:

- Accidents account for almost €280 billion, highlighting the significant human and economic toll of road traffic accidents;
- Congestion costs are estimated at €270 billion, reflecting the substantial economic impact of traffic delays and inefficiencies;
- Air pollution contributes about €70 billion, underscoring the health impacts of vehicle emissions;
- Climate change costs more than €80 billion, indicating the long-term environmental consequences of road traffic emissions;
- Noise pollution is responsible for nearly €50 billion, reflecting its substantial yet often overlooked impact on public health.

The scientific community has produced a substantial body of literature addressing the evaluation of noise-related external costs, particularly in relation to road traffic noise. These studies employ diverse methodologies to quantify and assess the economic burden of noise in terms of health outcomes, property values, and quality of life. Some research adopts an activity-based perspective, focusing on single-agent exposure assessment [200] or developing indicators for construction-site noise exposure [201]. Regarding airport noise, several relevant applications can be found in [202–204]. Numerous studies have demonstrated a correlation between noise levels and property value variation, indicating that real estate in quieter areas commands higher prices than equivalent properties in noisy

environments [205]. Two main approaches can thus be identified: (i) a bottom-up estimation, computing overall noise levels in a given area as the contribution of each vehicle and then deriving externalities in terms of population health impacts and property depreciation; or (ii) a top-down estimation, correlating noise exposure indicators with economic values to infer external costs more rapidly at large scale. In [206], a linear regression analysis was applied to assess the influence of surface street traffic on both single-family houses and multi-unit rental properties, revealing distinct sensitivities for the two types. Similarly, Del Giudice et al. [207] proposed a theoretical model of environmental externality evaluation based on real estate market analysis, presenting an extensive literature review of works quantifying real estate value reduction due to increasing noise pollution in various American and European cities. Reported depreciation rates range from 0.22% to 1.45% per dBA. Wilhelmsson's work also developed a theoretical model establishing a precise correlation between average noise levels (dBA) and property prices in Stockholm [208]. These approaches rely on established acoustic indicators (e.g., L_{day}, $L_{evening}$, L_{night}, L_{den}) to represent average exposure levels.

It is worth noting that the accurate quantification of noise externalities provides essential information for policymakers. By linking acoustic exposure indicators to their economic consequences, decision-makers can evaluate the cost-effectiveness of mitigation measures, such as traffic flow management, quiet pavement technologies, or urban planning interventions, and prioritise those offering the highest social benefit. In this sense, the integration of noise modelling, exposure assessment, and external cost evaluation represents a crucial step toward a more holistic and evidence-based approach to sustainable mobility planning.

2.7 Final Remarks

The development of effective road traffic noise modelling tools has been a central point in the agenda of the acoustic scientific community in the last decades.

The evolution of the adopted techniques has been presented in this Chapter, starting from the historical formulae, obtained by regression on large datasets collected in different sites. These early models exploited the dependence of traffic noise level from vehicles flows and vehicles category, sometimes including additional parameters and corrections to take into account mean speed of the flow, road grade and pavement, presence of shielding and reflecting vertical surfaces, etc.. On the other hand, recently, the development of more complex models, able to take into account the microscopic features of the traffic flow, has been pursued. These models are based on the simulation of single vehicle pass-by events, that can be merged to reproduce the overall traffic noise emission. The advantages of these models are related to the possibility of including in the simulation several dynamic features of the traffic flow, such as acceleration and deceleration phases, transient speed variations, traffic lights and stop signs effects, that are not easily included in collective models. These microscopic models are particularly suitable for urban context, where the traffic flow is usually not steady and several interactions between vehicles and infrastructures occur.

The latest trend of Artificial Intelligence and Machine Learning techniques for road traffic noise modelling has been also reported, resuming the most popular approaches, such as artificial neural network, random

forest, support vector regression, among the others. The usage of these techniques is obviously strongly dependent on availability of reliable training data, that must be used for the calibration and validation of the models. Despite the popularity of these techniques, in the acoustic scientific community they are considered niche models and they are not included yet in any regulation or standard document, probably because of the strong site-dependence feature of these models, that leads to difficulties in developing a tool that can be easily used anywhere.

A review of single vehicle noise emissions modelling has been extensively reported in the central part of this Chapter. The engine and rolling contributions assessment has been reviewed, considering the most popular Noise Emission Models (NEMs). In particular, the strong relation between emission and vehicle speed has been highlighted, together with the recurrent correction coefficients, usually related to road pavement, grade and acceleration. The ways the single vehicle emission can be merged in a linear source mimicking the road traffic have been briefly reported, to describe the transition from a microscopic simulation to a macroscopic description of the phenomenon.

Finally, the propagation and the assessment at the receivers have been summarised, to complete the road traffic noise modelling and assessment standard scheme, citing the most popular uses of these predictions, such as regulation descriptors calculation, exposure analysis and health risk assessments. The problem of providing quality input data for any road traffic model presented in this Chapter is crucial. Activity models can be developed and used for this purpose, also including dynamic approaches, able to provide the temporal variation of the input data and, consequently of the simulated noise levels.

The main conclusion of this Chapter of the state-of-the-art is that road traffic noise modelling represents a broad and multifaceted research field, encompassing a variety of approaches based on different theoretical and computational techniques. The single-vehicle noise emission assessment is, however, essential for pursuing a microscopic approach that can be effectively employed for noise pollution modelling and control, for instance in eco-routing applications or traffic signal optimization. Conversely, collective models, which often rely on large dataset statistical regressions or machine learning tools, are strongly dependent on the datasets used for their calibration and validation, introducing a potential limitation in their generalisation to different sites or conditions.

The higher level of adherence of microscopic models to the actual dynamics of vehicular traffic, together with their capability to capture context-specific variations in emission behaviour, has motivated the continuation of this research pathway in the present work. The Chapter 3 will therefore present and detail the microscopic modelling framework developed in this thesis, highlighting its formulation, implementation, and validation.

Road Traffic Noise modelling: a Stochastic and Microscopic Approach

3

3.1 The Fundamentals of the Stochastic and Microscopic Approach: Model Architecture and Core Logic 46

3.2 Spatial Analysis: Application of the Stochastic Model Using Variable Level of Aggregation of Traffic Flows 51

3.3 Temporal Analysis: Combination of the Stochastic Approach with Time Series Forecasting . . . 54

3.4 Case Study: The Long-Term Monitoring Station (LTMS) Dataset 58

3.5 Dataset Exploration: Models Implementation and Validation 61

3.6 Final Remarks 104

The comprehensive review of the state of the art presented in Chapter 2 traced the evolution of road traffic noise modelling from early regression-based methods to contemporary computational frameworks. Crucially, this analysis highlighted that current modelling practices are largely dictated by the regulatory landscape governed by the Environmental Noise Directive (2002/49/EC) [25]. Since this directive mandates the production of strategic noise maps to evaluate population exposure, commonly used models predominantly adopt macroscopic or mesoscopic approaches to abstract the traffic stream into aggregated parameters, such as mean flow rates and average speeds. This modelling choice is primarily driven by the nature of strategic mapping, which relies on long-term noise indicators, most notably the L_{den}, that integrate acoustic energy over an entire year. Given this extensive temporal aggregation, the granular detail of microscopic vehicle dynamics is typically regarded as redundant. However, while these conventional models demonstrate efficacy for such standardised, large-scale applications, critical intrinsic limitations were identified in the previous Chapter that compromise their predictive accuracy in complex, real-world scenarios.

The primary shortcoming identified in the literature is the reliance on aggregated input data. Traditional models typically treat the vehicular flow as a homogeneous line source characterised by average variables, such as total hourly flow and mean travel speed. As noted in the review, this "macroscopic" averaging process inherently smooths out the instantaneous fluctuations of dynamic traffic conditions, failing to capture the sound-level variations generated by individual vehicle kinematics. Moreover, in the context of strategic noise mapping already mentioned, it is common practice to assign the maximum legal speed limit as the operating speed for model inputs. Although this choice is motivated by safety and precautionary considerations, it further amplifies the abstraction of real traffic behaviour and may introduce discrepancies with respect to actual driving conditions. Consequently, these models frequently underperform in non-standard conditions, such as stop-and-go traffic, signalised intersections, or scenarios where the speed of single vehicles deviates significantly from the statistical mean.[1]

Furthermore, the literature review revealed that many existing models struggle to represent the stochastic nature of noise generation. By relying on deterministic mean values or regulatory speed limits, these frameworks neglect the random variability of driver behavior, which results in a distribution of speeds rather than single scalar values. This simplification prevents the accurate assessment of dynamic and peak noise events, which are often the primary source of annoyance and environmental impact.[2]

It is upon these specific identified gaps, the inability of macroscopic aggregation to capture traffic dynamics and the absence of a proper representation of the intrinsic randomness of traffic behaviour, that the methodology presented in this Chapter is founded. To overcome these limitations, this research proposes a shift from the "macro" to the "micro" perspective. Moreover, a stochastic and microscopic core approach is presented, capable of simulating the noise immission of the traffic stream by decomposing it into its fundamental components: individual vehicles.

1: This is particularly relevant in urban environments, where traffic dynamics are more complex and variable, and where the noise impact on residents is often most acute.

2: For instance, the noise generated by a single heavy-duty vehicle accelerating from a signalised intersection can significantly exceed the average noise level predicted by a model that assumes constant speed, leading to underestimation of noise exposure for nearby residents.

Thus, rather than modelling the flow as a uniform entity, the proposed methodology assigns a specific, randomly generated speed to each vehicle based on probability distribution curves derived from traffic theory.[3] This approach ensures that the specific acoustic energy of every transit is preserved and calculated individually before aggregation, thereby addressing the loss of resolution inherent in the macromodelling approaches. The detailed implementation of this speed-assignment procedure is further discussed in appended **Paper B**.

3: Adopting a speed distribution rather than a fixed value not only enhances the physical realism of the model but also provides a practical advantage in situations where detailed traffic measurements are unavailable. In design-phase analyses or in contexts characterised by limited or incomplete data, the use of theoretical or empirically derived speed distributions enables the model to account for traffic variability without relying on exhaustive monitoring campaigns.

Building on this foundation, a major focus is set in the subsequent Sections to enhance the predictive accuracy of such a novel model by focusing on advanced spatio-temporal dynamics, thus exploring the full capabilities of such stochastic framework.

In this regard, Section 3.2, dedicated to **spatial analysis**, focuses on utilising the individual vehicle speed and energy calculations to compute noise levels with high precision across different road lanes and receiver distances. This analysis crucially incorporates topographical data to implement this lane-specific analysis, thereby moving beyond the common literature approach of central road source schematisation (as detailed in **Paper C**). This approach addresses the spatial heterogeneity of noise propagation, including the effects of near-field sources and variations in road geometry, providing a lane-by-lane acoustic breakdown.

Subsequently, Section 3.3 introduces the **temporal analysis** through the development of a hybrid noise model. In particular, this model expands the analysis over time, by integrating the microscopic stochastic acoustic energy calculation with Time Series Analysis models for high-resolution noise forecasting (as detailed in **Paper D**). The integration of these two modelling paradigms allows the framework to process dynamic traffic flow data and predict short-term noise level fluctuations with enhanced accuracy.

3.1 The Fundamentals of the Stochastic and Microscopic Approach: Model Architecture and Core Logic

In line with the considerations outlined earlier, and building upon the identified need to preserve the variability intrinsic to road traffic phenomena,[4] the methodology presented in this Section adopts a modular, stochastic, and fully microscopic approach. This framework is specifically structured to retain information at the level of the individual vehicle, thereby enabling an assessment of road traffic noise that does not rely on aggregated representations.

4: E.g., tire-road interaction, engine and aerodynamic noise, exhaust emissions, etc.

In particular, since the acoustical energy emitted by a single vehicle is highly dependent on its speed, it has been decided to assign to each vehicle a single value of speed. Individual speed values can be used if available by means of field measurements, such as in [209] and [182], or using any other calculation tools, such as video image analysis [166–168] or by generating datasets with computational approaches [113], or even by using traffic simulation software as reported in Chapter 2. Another approach could be to randomly derive speed values from a hypothetical speed distribution curve [210]. In this way, the entire vehicular flow is not modelled as a simple source characterised by an average speed value (as usually done by statistic or macroscopic models) but rather it is possible

to associate each vehicle with a peculiar value of speed. Thus, the specific acoustic energy of every transit is preserved and can be used to obtain the total noise level. This method allows us to take into account the different acoustic energy emissions of vehicles also when belonging to the same category, due for instance to different driver behavior or to different maintenance conditions. Thus, the specific acoustic contribution of each vehicle is taken into consideration, and no contribution is mitigated or lost in the averaging processing. The detailed implementation of this speed-assignment procedure is further discussed in **Paper B**.

In Figure 3.1, the flow chart of the proposed model is reported, in which the steps to be followed for a successful implementation of the stochastic model are shown.

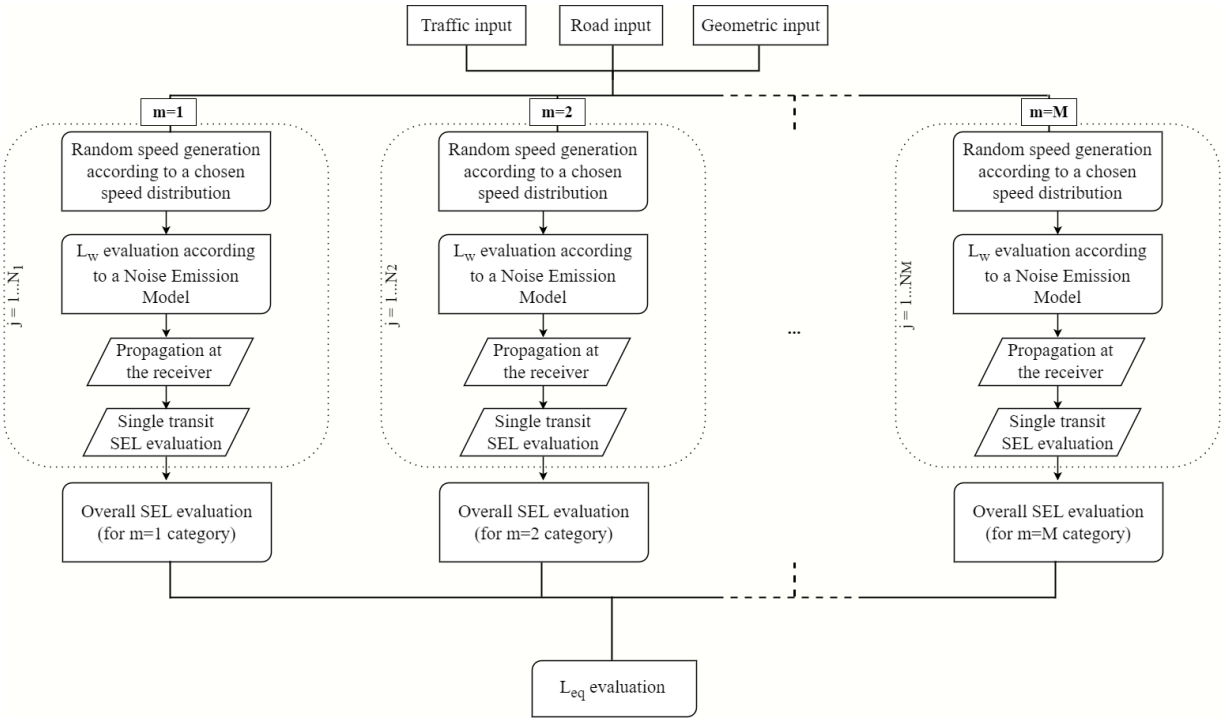


Figure 3.1: Flowchart of the proposed road traffic noise model. The dotted line represents a loop to be repeated for each vehicle considered.

The simulation procedure follows the modelling chain already presented in Chapter 2 and also reported in Figure 2.1.

- **Activity:** This first step involves defining the traffic scenario to be modelled. Indeed, the model first ingests three kinds of necessary data as input.
  - *Traffic data:* This encompasses vehicle flows for each vehicle category considered (e.g., light and heavy-duty vehicles), and their associated mean speeds. It is important to note that the methodology for transforming these aggregate mean speeds into disaggregated, single-vehicle values is detailed immediately below in the description of the stochastic core of the model. Additionally, the specific flow regime (e.g., continuous, pulsed, accelered, etc.) needs to be defined.
  - *Road data:* This includes information about the road type (e.g., highway, urban street, etc.), surface characteristics (e.g., asphalt, concrete, etc.), size, and number of lanes, gradient (slope), and any traffic regulations (e.g., speed limits, lane configurations).

  - *Geometrical data:* This includes information about the road layout, the height of the receiver and the distance between the observation point (the receiver) and the center of the traffic lane (i.e., where the traffic flow source is assumed to be located) in order to adequately propagate the continuous equivalent sound pressure level at the desired distance.

- **Emission:** This component utilises the detailed kinematic data generated in the Activity phase to drive the Noise Emission Model (NEM). In particular, for each individual vehicle j, the Sound Power Level ($L_{W,j}$) is calculated as a function of its specific, randomly assigned speed.
- **Propagation:** Once the source emission is characterised, appropriate sound propagation algorithms has to be taken into account for the attenuation of sound as it travels from the source (the individual vehicles) to the receiver location. This could include considerations for geometric spreading, atmospheric absorption, ground effects, and any relevant barriers or reflections.
- **Assessment at the receiver:** The final step quantifies the noise impact. In the specific case of this approach, the model integrates the instantaneous pressure levels to determine the Sound Exposure Level (SEL) for each transit. These individual contributions are then energetically summed to assess the overall impact in terms of the equivalent continuous sound pressure level $L_{A,eq}$ over the reference time interval.

Following the acquisition of input data, the model advances to its central *stochastic core*: the assignment of individual vehicle speeds derived from an appropriate probability distribution function. Utilising a specific speed distribution curve as a benchmark allows the model to approximate real-world scenarios with high fidelity, even for infrastructure that is yet to be built. However, the traffic flow regime conditions needs to be known or assumed, as they directly influence the selection of the speed distribution function. For example, as demonstrated in the literature [211–213], vehicle speeds under free-flow traffic conditions are well-described by a Gaussian normal distribution, whereas pulsed or congested flows tend to produce skewed distributions, such as Beta or Chi-square [210, 214].[5]

Since the highway segment analysed in the case study exhibits free-flow conditions, a Gaussian distribution was selected (see Section 3.4) with a standard deviation of 10% from the mean value.[6] Thus, the speed $v_{j,m}$ of the j-th vehicle of the m-th category can be extracted from a Gaussian distribution defined by the measured mean speed μ_v and the standard deviation σ_v as reported in equation 3.1.[7]

$$v_{j,m} = \mu_{v,m} + \sigma_{v,m} \cdot \mathcal{N}(0,1) \tag{3.1}$$

Where $\mathcal{N}(0,1)$ is a random number drawn from a standard normal distribution.

Consequently, a physical observable capable of quantifying the acoustic emissions of a single vehicle needs to be chosen. The standard and the most commonly used indicator is the source power level L_W. Numerous NEMs assess such level as a function of vehicle speed, often incorporating correction factors for road gradient, pavement type, and acceleration (See Chapter 2).

A key advantage of the proposed model modular architecture is the flexibility to interchange the selected NEM to calculate L_W based on

5: In particular, Iannone et al. proved that the Beta distribution was a reasonable choice to model speed distributions in pulsed accelerated flow, while the Chi-square distribution was more appropriate for the decelerated flow [210].

6: This value is commonly adopted in the literature to represent speed variability in free-flow traffic conditions [211–213] and it is supported by findings in the literature, such as those in [159].

7: It is imperative to highlight that this stochastic approach assigns a single, however constant speed to each individual vehicle for the entirety of its traversal through the segment. This methodology inherently simplifies the vehicle's kinematics by neglecting any phases of acceleration and deceleration. In real-world congested or pulsed flows, these kinematic transitions significantly alter the acoustic emission profile of the vehicles. However, in a case of free-flow traffic, where the speed variability is relatively low and the majority of vehicles maintain a steady speed, this simplification is justified and does not significantly compromise the model's accuracy. Future iterations of the model could incorporate more complex kinematic profiles to better represent these transient phenomena, particularly in scenarios where acceleration and deceleration are prevalent.

local requirements. For this study, the EU reference model CNOSSOS-EU [93, 94, 146] was adopted to compute the power level $L_{W,j,i,m}$ of the j-th vehicle, for each octave band i and vehicle category m.[8]

The CNOSSOS-EU methodology defines the total noise as the logarithmic sum of *rolling noise* ($L_{W,R,j,i,m}$) and *propulsion noise* ($L_{W,P,j,i,m}$); the former follows a logarithmic dependence, while the latter exhibits a linear dependence on speed. Thus, the sound power level for each vehicle is calculated as shown in Equation 3.2.

$$L_{W,j,i,m}(v_{j,m}) = 10 \log \left(10^{L_{W,R,j,i,m}(v_{j,m})/10} + 10^{L_{W,P,j,i,m}(v_{j,m})/10}\right) \tag{3.2}$$

where $v_{j,m}$ is the speed of the j-th vehicle of category m. The rolling and propulsion noise components are calculated following the formulations in Equations 3.3 and 3.4, respectively, using coefficients (i.e., $A_{R,m}(i)$, $B_{R,m}(i)$, $A_{P,m}(i)$, and $B_{P,m}(i)$) defined in the CNOSSOS-EU guidelines for each vehicle category and octave band. In particular, the updated coefficients reported in [146] have been used in this model. The reference speed v_{ref} is set to 70 km/h. Several correction terms (i.e., $\Delta L_{W,R,j,i,m}$ and $\Delta L_{W,P,j,i,m}$) are also included depending on the actual simulated conditions with respect to the used as standard ones in the CNOSSOS-EU model, as provided in [93, 94, 146].

$$L_{w,R,i,m} = A_{R,m}(i) + B_{R,m}(i) \log \frac{v_m}{v_{ref}} + \Delta L_{W,R,j,i,m}(v_{j,m}) \tag{3.3}$$

$$L_{w,P,i,m} = A_{P,m}(i) + B_{P,m}(i) \frac{v_m - v_{ref}}{v_{ref}} + \Delta L_{W,P,j,i,m}(v_{j,m}) \tag{3.4}$$

Once the source power level $L_{W,j,m}$ has been assessed, the model proceeds to the propagation phase. For the first development and validation of this model, a simplified geometrical propagation scheme is adopted, as illustrated in Figure 3.2. The sound pressure level at the receiver is then calculated based on the position of such a fixed receiver, denoted as R. The dynamic spatial relationship between the moving source and the static observer is governed by the instantaneous vehicle-receiver distance, $r_{j,m}(t)$. This time-dependent variable is analytically derived as shown in equation 3.5.

$$r_{j,m}(t) = \sqrt{d^2 + \left(\frac{S}{2} - v_{j,m} t_{j,m}\right)^2} \tag{3.5}$$

where S is the length of the road segment traveled by the vehicle at speed $v_{j,m}$, and $t_{j,m}$ is the elapsed time. Such length is a fundamental parameter of the model, together with the distance d because they define the angle at which a vehicle traveling on the road significantly contributes to the continuous equivalent sound pressure level at the receiver.

The adopted propagation model deliberately neglects complex attenuation mechanisms, such as atmospheric absorption, ground reflection, and diffraction[9], which typically exert significant influence only over macroscopic distances. Instead, the model assumes omnidirectional point-source propagation, a valid approximation for the short source-to-receiver distances characterising the case study to be presented in Section 3.4.

8: It is worth to note that while the standard CNOSSOS-EU approach operates macroscopically, thus using the average flow speed per category, this model still adopts a fully microscopic approach, leveraging the CNOSSOS-EU spectral coefficients and physical formulation, but applying them to discrete point sources rather than a continuous line source. This shift significantly alters both the emission and propagation phases, though the aggregation of contributions remains straightforward, as road traffic noise sources are treated as incoherent, negating the need to account for interference phenomena.

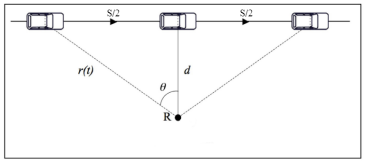


Figure 3.2: Graphical representation of the time-varying distance $r(t)$ between the moving source (vehicle) and the fixed receiver R.

9: See also Section 2.5 for more comprehensive information on the propagation modelling.

However, the modular architecture of the proposed framework allows for the seamless integration of more complex wave phenomena should the analysis be extended to larger spatial scales.

Consequently, the model allows for a precise assessment of the instantaneous acoustic contribution of each vehicle. Based on the calculated distance, the sound pressure level $L_{p,j,m}(t)$ immitted at the receiver R by the j-th vehicle of category m is computed. This calculation, detailed in the equation 3.6, assumes a point source radiating into a specific solid angle over absorbing ground, accounting for source power level and geometric divergence.

$$L_{p,j,m}(t) = L_{W,j,m} - 20\log(r_{j,m}(t)) - 11 \tag{3.6}$$

Here, $L_{W,j,m}$ is the power sound level, $r_{j,m}(t)$ is the distance between source and receiver, as a function of time, and 11 is equal to $10\log_{10}(4\pi)$, which takes into account to the omnidirectional propagation and the absorbing ground factors.

Following the definition of the propagation path, the subsequent analytical phase quantifies the acoustic energy emitted at the receiver point during the vehicle transit. To this end, the SEL was selected as the primary metric. In the context of microscopic traffic modelling, the SEL is methodologically superior to the equivalent continuous sound pressure level ($L_{A,eq}$) for analysing individual pass-bys.[10] The fundamental relationship between the $L_{A,eq}$ over a time interval ΔT and the SEL is expressed in equation 3.7.

10: This is because the duration of a single transit event is variable, fluctuating inversely with vehicle speed; the SEL normalises this energy to a reference duration of 1 second, ensuring comparability between events.

$$SEL = L_{A,eq}(\Delta T) + 10\log(\Delta T) \tag{3.7}$$

where ΔT is the time interval, in seconds, in which the overall $L_{A,eq}$ is evaluated.

Consequently, for the j-th individual vehicle belonging to category m, the $SEL_{j,m}$ is derived by integrating the instantaneous sound pressure level $L_{p,j,m}(t)$ over the transit interval, as detailed in the relationship described in equation 3.8.

$$SEL_{j,m} = 10\log_{10}\left(\frac{1}{t_0}\int_{t_i}^{t_f} 10^{\frac{L_{p,j,m}(t)}{10}}dt\right) \tag{3.8}$$

where t_i and t_f are, respectively, the time instants when the j-th vehicle enters and exits the considered road segment, and t_0 is equal to 1 s.

Once the individual contributions of every vehicle are assessed, the total acoustic energy for each vehicle category is computed. The cumulative SEL_m for category m is indeed obtained by the logarithmic summation of the individual contributions, as shown in equation 3.9.

$$SEL_m = 10\log_{10}\frac{1}{t_0}\left(\sum_{j=1}^{N_m} 10^{\frac{SEL_{j,m}}{10}}\right) \tag{3.9}$$

where N_m is the total number of vehicles in category m.

Finally, the overall equivalent continuous sound pressure level $L_{A,eq}$ at the receiver over the time interval ΔT is derived by aggregating the contributions from all vehicle categories, as expressed in equation 3.10.

$$L_{eq,\Delta T} = 10 \log_{10} \left(\frac{1}{\Delta T} \sum_{m=1}^{M} 10^{\frac{SEL_m}{10}} \right) \tag{3.10}$$

Modelling Procedure Routine Implementation and Operation Phases

The entire modelling procedure has been implemented both within a custom-developed MATLAB ® environment and using a self-written `python` routine.

The algorithm is structured into sequential operational phases, as summarised below:

- **Input Data Acquisition:** All necessary input data have to be imported, including traffic flow rates, mean speeds, road characteristics, and source-receiver geometry. All the parameters required for the selected NEM are defined at this stage too.
- **Speed Stochastic Assignment:** For each vehicle in the traffic stream, a specific speed is assigned based on the selected probability distribution function.
- **Emission modelling:** Using the assigned speeds, the sound power level L_W for each vehicle using the chosen NEM (i.e., CNOSSOS-EU) is computed.
- **Propagation modelling:** The time-varying distance between each vehicle and the receiver is calculated, subsequently determining the instantaneous sound pressure level $L_p(t)$ at the receiver.
- **Single-Event Level Computation:** The instantaneous sound pressure levels over the transit duration to derive the SEL for each vehicle is assessed.
- **Aggregation of Contributions:** Finally, the individual SEL values are aggregated to compute the total equivalent continuous sound pressure level $L_{A,eq}$ at the receiver over the specified time interval.

It is significant to emphasise the architectural flexibility of this model. Although the first application used to validate this approach utilises CNOSSOS-EU emission equations and a simplified propagation model, its modular scheme allows for the seamless substitution of both the NEM and the propagation algorithms should the specificities of a different case study require it.

3.2 Spatial Analysis: Application of the Stochastic Model Using Variable Level of Aggregation of Traffic Flows

While the core innovation of the proposed framework lies in the stochastic assignment of speed to individual vehicles, the noise source position plays an equally critical role in the accuracy of the noise predictions.

Commonly used regulatory models often simplify the complex geometry of multi-lane roads into a single equivalent line source located at the centerline of the carriageway [93, 94, 146]. This abstraction, while computationally and strategically efficient, overlooks the spatial heterogeneity of noise emissions across different lanes and the varying distances

from the receiver. Such a simplification can lead to significant inaccuracies, particularly in scenarios where lane-specific traffic dynamics are pronounced.

This "single-source" assumption, indeed, implies a spatial homogenisation of the traffic flow, where the acoustic energy of all vehicles, regardless of their actual lane of travel, is assumed to radiate from the geometric center of the road. While this approximation may be acceptable for far-field assessments[11], it introduces significant errors in near-field scenarios.[12] In such cases, the difference in propagation distance between the nearest and farthest lanes becomes acoustically relevant: even relatively small distance variations can lead to appreciable differences in the attenuation due to geometrical divergence (*spherical spreading*). As a result, each lane contributes a distinct sound level at the receiver, and the overall field can no longer be represented accurately by a single, homogenised line source.

To address these limitations, the proposed stochastic model has been implemented with a lane-specific analysis, allowing for the discrete representation of each traffic lane as an individual sound source. This approach enables the model to account for the unique acoustic contributions of single vehicles transiting in each distinct lane, considering their specific distances from the receiver. This lane-by-lane breakdown is particularly useful in urban environments or complex road geometries, where the spatial arrangement of sound sources plays a decisive role in shaping the overall acoustic environment. The detailed implementation of this modelling procedure is further discussed in appended **Paper C**.

11: In far-field conditions the receiver is located at a distance much larger than the total width of the road, thus the ratio of the road width to the receiver distance is very small. In such case, the source can be reasonably approximated as a line source: both the geometric extent of the carriageway and the differences in traffic composition or flow across individual lanes have a negligible influence on the resulting sound field.

12: In near-field conditions the receiver is located at a distance comparable to, or only slightly larger than, the total width of the road, resulting in a non-negligible ratio of the road width to the receiver distance. In this case, the line-source approximation becomes inadequate: the geometric extent of the carriageway and the differences in traffic composition or flow across individual lanes can have a significant influence on the resulting sound field.

3.2.1 Spatial Disaggregation of Traffic Flows

The stochastic simulation has been executed using three distinct levels of spatial resolution. As descussed earlier, even if using CNOSSOS-EU NEM to obtain L_W for each transiting vehicle [93, 94, 146], this framework still maintains the discrete nature of the emission using a microscopic approach. Therefore, even when the spatial trajectory is simplified, the acoustic energy is always radiated by individual vehicles treated as moving point sources.

The geometric representation of the different modelling levels used is visually summarised in Figure 3.3.

In the diagrams, the red dashed lines denote the longitudinal trajectories assigned to the simulated vehicular flows, treated acoustically as streams of moving point sources, while the cyan square labelled "R" represents the fixed position of the receiver. The panels illustrate the progressive spatial disaggregation of the traffic stream, moving from a simplified central axis to a detailed lane-specific assignment. In particular, the three adopted spatial configurations, are defined as follows:

1. **Single Source (Centralised Aggregation):** This configuration represents the most abstract level of spatial approximation. Here, the entirety of the traffic flow, regardless of direction or lane occupation, is aggregated into a single sequence of moving point sources travelling along the geometric centerline of the road infrastructure. While computationally efficient, this scheme inherently assumes that the acoustic center of the road coincides with its geometric center. In near-field propagation scenarios, this assumption introduces a systematic error in the calculation of geometrical divergence, as

it artificially increases the distance for vehicles in the near lane and decreases it for vehicles in the far lane, potentially smoothing out peak noise events.

2. **Two Sources (Directional Disaggregation):** This scheme introduces an intermediate level of spatial definition by splitting the flow according to the direction of travel. Two distinct linear trajectories are defined, located at the centerline of each carriageway. Unlike the single-source approach, this configuration allows the model to capture the acoustic asymmetry caused by unequal traffic loads between the two directions. However, within each direction, the traffic is still laterally homogenised; thus, the specific acoustic signature of the slow lane is mathematically averaged with the fast lane, potentially misrepresenting the spectral characteristics of the emission at the receiver.
3. **Four Sources (Lane-Specific Disaggregation):** This configuration constitutes the most rigorous spatial representation proposed in this thesis. The traffic flow is fully disaggregated, generating a dedicated stream of point sources for each lane. The trajectory of every simulated vehicle corresponds strictly to the centerline of the specific lane it occupies. This high-fidelity approach is critical for correctly modelling the *source-to-receiver* geometry. By accounting for the precise lateral position of each vehicle, the model can accurately compute the propagation distance and associated attenuation effects. This level of detail is particularly important in near-field scenarios, where even minor variations in distance can lead to significant differences in the received sound levels.

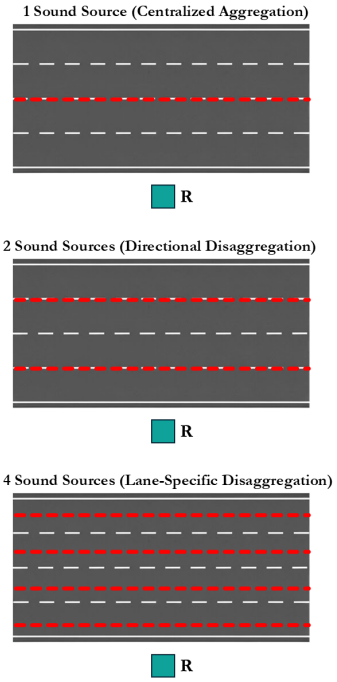


Figure 3.3: Schematic representation of the three spatial modelling levels: Single Source centralised aggregation (top), Two Sources directional disaggregation (middle), and Four Sources lane-specific disaggregation (bottom). The red dashed lines indicate the source trajectories, and R indicates the receiver position.

3.2.2 Mathematical Formulation of the Lane-Specific Stochastic Model

The mathematical implementation of the lane-specific analysis presented in this Section is grounded in the fundamental stochastic architecture presented in Section 3.1. Consequently, the core procedural steps, ranging from input data acquisition to the stochastic assignment of individual vehicle speeds and the calculation of source power levels, remain consistent with the previously detailed methodology and are not reiterated here to avoid redundancy.

Thus, the focus of this Section is exclusively on the extension of the disaggregation logic to account for the spatial decomposition of the source. In this specific implementation, the computational framework processes the traffic flow across K distinct lanes, where the geometric configuration of each source line is uniquely defined by its perpendicular distance d_k from the receiver to the center of the specific lane k.

For every vehicle j of category m traveling within lane k, the individual Sound Exposure Level ($SEL_{j,m,k}$) is computed, following the metholodogy already described earlier. However, this calculation utilises the specific propagation path determined by d_k, strictly adhering to the emission and propagation methodology of the stochastic model developed in Section 3.1.

Consequently, the overall equivalent continuous sound pressure level, $L_{A,eq}$, over the reference time interval ΔT, is derived through a global energetic summation. This aggregation integrates the acoustic energy contributions not only across vehicle categories and individual transits but also across the spatial domain of the lanes, as expressed in equation 3.11:

$$L_{A,eq} = 10\log_{10}\left(\frac{1}{T}\sum_{k=1}^{K}\sum_{m=1}^{M}\sum_{j=1}^{N_{m,k}} 10^{\frac{SEL_{j,m,k}}{10}}\right) \tag{3.11}$$

where $N_{m,k}$ represents the total number of vehicles of category m transiting on lane k. This formulation ensures that the specific spatial geometry of the road lanes and the stochastic nature of the individual vehicle speeds are fully integrated into the final acoustic assessment.

3.3 Temporal Analysis: Combination of the Stochastic Approach with Time Series Forecasting

While the stochastic microscopic model described in Section 3.1 effectively resolves the acoustic contribution of individual vehicles, its application is inherently constrained by the availability of high-resolution input data. In standard practice, detailed kinematic variables are derived from direct field measurements. However, in many scenarios, including the early design phases of transport infrastructure or the assessment of noise in areas lacking sensor coverage, real-time data is unavailable. Nervertheless, traffic noise is not a static phenomenon; it exhibits strong temporal dependencies and trends, characterised by specific cycles, seasonalities, rush-hour peaks, and weekly variances that static regression models fail to capture adequately.

To overcome these limitations and extend the predictive capabilities of the stochastic model beyond the spatial domain addressed in the previous Section (see Section 3.2), this thesis also proposes an expansion into the temporal domain. This *hybrid framework* integrates the stochastic noise simulation core with a time series forecasting module to predict the necessary traffic inputs based on historical patterns, aiming to generate dynamic noise assessments.

Specifically, this approach employs *Seasonal Autoregressive Integrated Moving Average (SARIMA)* models to forecast traffic flows and average speeds for each vehicle category (i.e., the required inputs for the stochastic model). By synergizing stochastic microsimulation with these time-series predictions, the framework reproduces the temporal fluctuations inherent in urban environments more faithfully than static approaches.

While the hybrid model is fully capable of operating with direct measurements when available, its broader strategic objective is to establish a methodology that remains robust even in data-scarce or predictive scenarios, such as during the design phase of new transport infrastructure. In such forward-looking contexts, the model adapts its input generation strategy:

- **Speed Distributions:** These can be defined using design speeds or regulatory limits, following an approach analogous to the CNOSSOS-EU framework, and subsequently adjusted to reflect hypothesised traffic conditions.
- **Traffic Forecasting:** SARIMA models can be calibrated using historical data from comparable existing infrastructures, on the assumption that roads sharing similar geometric and functional characteristics will exhibit analogous traffic patterns. This capability allows the framework to anticipate traffic dynamics in future or

yet-to-be-built scenarios, rather than merely reproducing existing conditions.[13]

13: For instance, if a new highway segment is planned in a region with existing similar highways, historical traffic data from these existing roads can be used to train the SARIMA models. The trained models can then forecast traffic volumes and speeds for the new segment based on expected usage patterns derived from the analogous infrastructure. While forecasting errors are inevitably expected due to site-specific variances, this methodology represents a unique pathway to simulate traffic dynamics, such as daily profiles and flow fluctuations, even during the design phase. Unlike static approaches that rely solely on mean values or theoretical maximum sound levels (worst-case scenarios), this approach captures the time-varying nature of the noise source, offering valuable insights into dynamic exposure patterns even in the absence of direct measurements.

The following analysis outlines the specific procedure employed to forecast traffic inputs through time series modelling. First, the rationale and methodological process for selecting the appropriate forecasting model are outlined, highlighting the key analytical steps used to identify the structure and parameters best suited for capturing temporal dynamics. Subsequently, the integration of these forecasted inputs with the stochastic core is detailed. This modular structure clarifies the individual contributions of each component while highlighting their interdependence in forming a cohesive and comprehensive hybrid modelling approach.

The detailed implementation of this hybridazation modelling procedure is discussed in appended **Paper D**.

3.3.1 First Step: Time-series Forecasting of Traffic Inputs

Road traffic data frequently exhibits strong temporal patterns, such as daily rush hours or weekly fluctuations in volume, which must be accurately captured to simulate realistic acoustic conditions. Traditional regression models or static assumptions often fail to adequately account for such temporal dependencies. Alternatively, time-series forecasting models provide a more appropriate approach, as they are specifically designed to capture both short-term autocorrelations and long-term seasonal patterns. This is made possible by taking into consideration the sequential nature of the data, whereby each observation is stochastically dependent on the previous ones.

To better understand and model such temporal dynamics, time-series data are often decomposed into three key components [215]:

- **Trend:** This component captures the long-term tendency of the data, reflecting underlying growth or decline patterns over time.
- **Seasonality:** This element accounts for regular, periodic fluctuations that occur at consistent intervals, such as daily or weekly cycles.
- **Residual Noise:** This represents the random variations in the data that cannot be explained by either the trend or seasonality, often referred to as *white noise*.

By isolating these components, analysts can better understand the underlying processes driving the observed data and make more accurate forecasts.[14]

14: In traffic analysis, for example, long-term increases or decreases could be observed due to urban growth, even if these are shown alongside daily or weekly peak-hour patterns.

A wide range of models can be employed for time-series forecasting, each designed to uncover underlying structures within temporal data, such as trends, periodic fluctuations, and dependencies, enabling informed predictions about unknown future data [215–217].

A foundational approach is the **Moving Average (MA) model**, which bases predictions on the average of past error terms. This technique is particularly effective in representing short-term variability and in filtering out random noise. It assumes that each observation is a linear function of previous forecast errors and that these errors are uncorrelated. The complexity of the model is determined by its order (q), which specifies the number of lagged error terms included.

In contrast, the **Autoregressive (AR) model** estimates future values using a weighted combination of previous observations. It is well-suited for

capturing long-term dependencies and assumes that future states of the series depend directly on its historical values. The model order (p) indicates how many prior observations are considered in the estimation.

The **Autoregressive Moving Average (ARMA) model** integrates both AR and MA components, allowing it to capture both long-term and short-term patterns in stationary time series. It assumes that observations are influenced by both past values and past errors, and like its simpler components, it requires that error terms be uncorrelated. The orders (p and q) reflect the number of lagged values and errors incorporated.

To address non-stationary data, where statistical properties like mean and variance change over time, the **Autoregressive Integrated Moving Average (ARIMA) model** extends ARMA by including a differencing step. This differencing (of order d) transforms the original series into a stationary one, making the model suitable for series with underlying trends or evolving behavior.

For datasets characterised by seasonal patterns, the **Seasonal ARIMA (SARIMA) model** further extends ARIMA by including seasonal autoregressive, differencing, and moving average terms (denoted by P, D, and Q, respectively). This model effectively captures recurring seasonal fluctuations in addition to long-term and short-term dependencies.

Another widely used family of techniques includes **Exponential Smoothing models**, such as **Simple Exponential Smoothing** and **Holt-Winters methods**. These approaches use exponentially weighted averages of past values, assigning more influence to recent observations. They are particularly useful for smooth data with or without seasonal patterns, and are governed by smoothing parameters that determine how quickly the influence of older data decays.

Clearly, the selection of an appropriate time-series model must be guided by the specific nature of the dataset and the objectives of the forecasting task. By aligning model choice with the data temporal characteristics, it becomes possible to extract meaningful insights and produce accurate, context-aware predictions. Thus, when working with time series data, a rigorous approach needs to be followed in order to select the proper forecasting model [216, 218].

To this end, the initial step involves a comprehensive exploratory data analysis to identify the key temporal features of the dataset. Raw time series are visually inspected to detect trends, seasonal patterns, abrupt changes, or outliers. Strategic use of visualization tools such as time plots and seasonal subseries plots are employed to support this preliminary assessment and to generate hypotheses about the data temporal behavior. Identifying whether the series is stationary or subject to trend and seasonality is particularly important, as it strongly influences the type of model to choose.

A deeper understanding of the series structure is then achieved through decomposition techniques, which separate the data into three fundamental components: trend, seasonality, and residual noise. This decomposition helps to clarify whether an additive or multiplicative structure better describes the series and provides insight into the temporal mechanisms driving the observed values. If a clear seasonal cycle is identified, models that explicitly incorporate seasonal terms, such as SARIMA, may be more appropriate.

After this first phase, in order to support model specification, autocorrelation and partial autocorrelation analyses are conducted. These analyses

help identify the temporal dependencies within the series and guide the selection of autoregressive and moving average terms. The autocorrelation function (ACF) reveals how current values relate to previous values at different lags. In particular, ACF measures the correlation between observations in a time series that are separated by various time lags, quantifying how strongly current values are related to past values across different time intervals. On the other hand, the partial autocorrelation function (PACF) isolates the direct influence of specific lags, excluding the effect of intervening observations. Thus, PACF captures the correlation between a value and its lagged counterpart after removing the effects of the intermediate lags. In other words, it isolates the direct relationship between an observation and its value at a specific lag, without the confounding influence of the values that come in between. This makes PACF particularly useful for identifying the order of an autoregressive (AR) process, as it indicates which past values directly contribute to the present one, beyond the influence of closer lags.

Interpreting the patterns observed in ACF and PACF plots is fundamental in determining the appropriate orders of the AR (p) and MA (q) components in models such as ARMA or ARIMA [217].

Consequently, in this research, after these crucial steps, the model identification and selection were performed using the `auto.arima()` function available in the R forecast package. This automated procedure systematically evaluates a range of candidate ARIMA and SARIMA models, determining the optimal combination of parameters based on the minimisation of information criteria such as the Akaike Information Criterion (AIC), the corrected AIC ($AICc$), or the Bayesian Information Criterion (BIC) [219]. The function also conducts unit root tests to assess stationarity and applies differencing transformations when necessary, thus streamlining the preliminary steps of the modelling process. Moreover, `auto.arima()` includes automatic detection of seasonal components and allows for user-defined constraints on parameter ranges, enhancing both flexibility and interpretability.

Thus, in the application presented in this Chapter, the model selection has been performed using the following specifications: seasonal components were enabled, due to previous investigation on the seasonality of the time series analysed, stepwise search and exact maximum likelihood estimation were enabled, and model selection was made in three different levels, based on the AIC, $AICc$, and BIC information criteria. A maximum order for non-seasonal and seasonal parameters can be set with an iterative approach to achieve a fast convergence of model identification. The trace argument was also set in order to allow for transparent tracking of the selection process. Once a model is selected, residual analysis is performed to ensure that the remaining error terms behave as white noise, uncorrelated, and normally distributed. Forecast accuracy is finally evaluated using common metrics such as the Mean Error (ME), Mean Absolute Error (MAE), Root Mean Squared Error ($RMSE$), and Mean Absolute Percentage Error ($MAPE$), based on a training/test data split or cross-validation approach.[15]

15: However, some inherent limitations of time-series forecasting frameworks in traffic analysis need to be underlined. The robustness of time series models relies heavily on the quality and continuity of historical data; significant gaps or inconsistencies in input observations can hinder the identification of reliable trends and seasonalities. Moreover, being primarily designed to capture periodic temporal structures, these models are often unable to account for external, unpredictable factors such as traffic accidents, sudden road closures, or extreme micrometeorological events. While these anomalies significantly influence real-world traffic patterns and noise emissions, they are not reflected in historical cycles, making the model structurally blind to such non-periodic disruptions. Conversely, these predictive misalignments can be reframed not merely as model failures but as a diagnostic advantage, a sort of informative trigger. When a framework calibrated on longitudinal historical patterns significantly diverges from real-time observations, the resulting discrepancy serves as a recursive indicator for the occurrence of unconventional events. This makes the hybrid framework a valuable decision-support system for public authorities and infrastructure managers, enabling them to distinguish between standard cyclical patterns and unique, non-recurring acoustic events.

3.3.2 Second Step: Integration of the Stochastic Model with Time-Series Forecasting

Following the forecasting of traffic flows and average speeds via SARIMA models, these predicted parameters are directly integrated into the stochastic microscopic noise model detailed in Section 3.1.

This step constitutes the core of the *hybrid modelling approach*, effectively synthesising the predictive capability of time-series analysis with the granular resolution of stochastic simulation. Consequently, the noise model is driven by generated temporal projections rather than empirical measurements, a process schematically illustrated in the workflow of Figure 3.4.

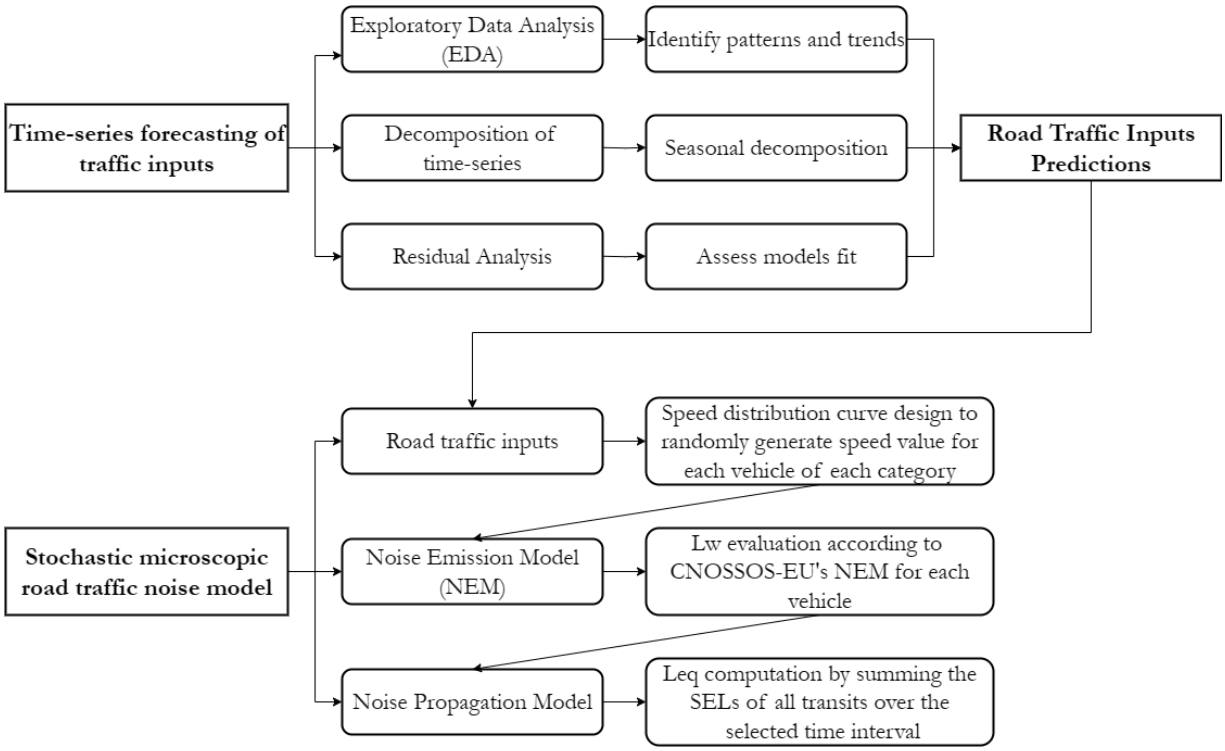


Figure 3.4: Schematic representation of the hybrid approach integrating time-series predictions with the stochastic microscopic noise model.

By incorporating temporally predicted variables, such as traffic volumes and average speeds for each vehicle category, into the noise simulation model, acoustical predictions that evolve dynamically and reflect the inherent temporal variability of urban traffic conditions are provided. This hybridization enables the modelling process to move beyond static scenarios, allowing for a more realistic representation of noise emissions over time.

3.4 Case Study: The Long-Term Monitoring Station (LTMS) Dataset

The primary data source for this research is the *Long-Term Monitoring Station (LTMS)* dataset, collected by a group of researchers belonging to the former IFSTTAR institute ("*Institut Français des Sciences et Technologies des Transports, de l'Aménagement et des Réseaux*"), now merged in the Université Gustave Eiffel, located in Nantes (France).

Such data collection was performed at an experimental station operating 24h a day 365 days a year, for a period of approximately six years (from 2002 to 2007), located in Saint-Berthevin, in proximity of the A81 motorway. The motorway analysed by the French researchers is 93 km long and connects Le Mans to La Gravelle and it is characterised by

two carriageways, two lanes each. During these measurements, acoustic, micrometeorological, and traffic data were measured. The figure 3.5 shows the geographical location of the municipality of Saint-Berthevin, i.e., the site of interest, located in the *Pays de la Loire*, in France. In the upper part of the figure, the location within the french region is highlighted, while in the lower part, a zoomed-in view of the measurement area is provided.

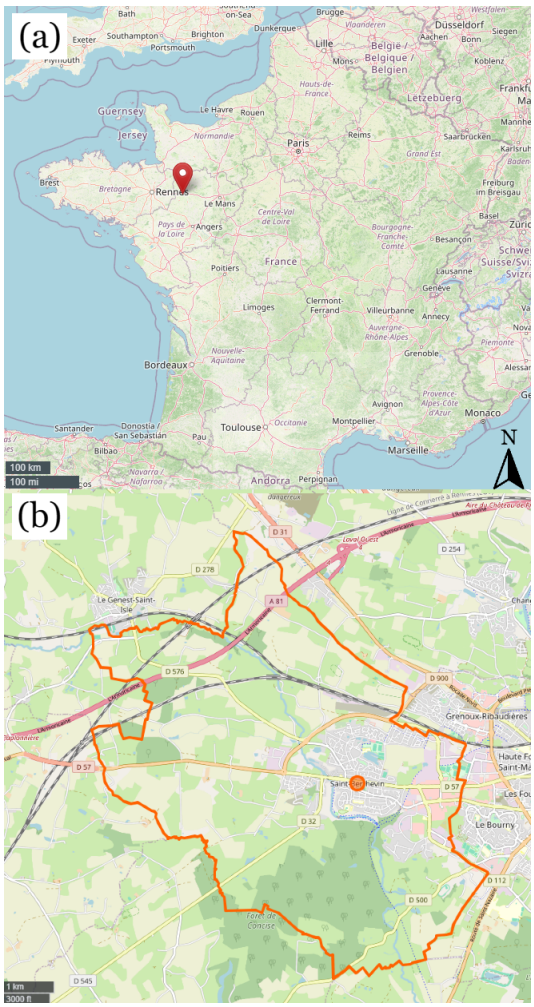


Figure 3.5: Location of Saint-Berthevin: (a) overview within the Pays de la Loire region in France; (b) close-up of the municipality.
(Maps available from: OpenStreetMap®).

The guidelines for this experimental campaign [209] provide a schematic representation of the measurement site and sensors positions; those labelled "A" represent acoustic stations, while "M" refers to meteorological towers. In Figure 3.6, this schematic layout of the measurement site is reported.

Focusing on the noise data, five acoustic stations were installed, which recorded the $L_{A,eq,10s}$ ("A" weighting curve and 1/1 octave from 125 Hz to 4 kHz) at both 2 and 5 meters above the ground. This applies to all stations except for the reference microphone (station A1) located 5 meters above the ground and at a distance of approximately 5 meters from the roadside, which served as the consistent receiver point for all model validations presented in this Chapter.[16] A 01 dB-Stell "outdoor" microphone and 01 dB-Stell SALTO data archives were used by the French researchers responsible of the project to record and store acoustic data.

16: The deliberate choice of the close-field reference microphone (Station A1, located 5 m from the roadside) is strategic. By minimising the propagation distance, this selection allows the research to focus primarily on validating the core methodological innovation, e.g., the stochastic assignment and microscopic emission model, while minimising the influence of complex propagation effects (i.e., ground effects, atmospheric attenuation). The simplicity of the required propagation path (point source, short distance) ensures that the measured errors are predominantly attributable to the source modelling itself. Furthermore, the modular structure of the proposed framework inherently supports future extensions to incorporate sophisticated propagation algorithms (such as CNOSSOS-EU or Nord2000) and utilise far-field measurements; however, such advanced propagation modelling is beyond the scope of this dissertation.

Such measurements were validated with acquisitions taken every 10 seconds.

The measurements were then validated by the same team via a strong cleaning process, which included detecting and removing sound events coming from other sources different from road traffic noise, such as anthropic activity, animals, aircraft, and trains transits, etc. (see [209] for further details). While this thorough cleaning process significantly enhances data reliability, it is important to note that the publicly available dataset does not provide specific information on uncertainties associated with the measurements. Consequently, it was not possible to quantify or exercise direct control over this aspect during the model implementation phase. The cleaned data were then concatenated into 15-minute time intervals and this dataset was made available to the research community.

With regard to vehicle flows, the publicly accessible data is limited to the total number of light and heavy-duty vehicles transiting in the 15-minute time intervals, and the average speed values for the two categories in the same interval.

Crucially, the initial stochastic modelling assumed a single direction and lane due to the aggregated nature of this public data; however, subsequent spatial-enhanced applications, such as the one presented in Section 3.2 utilised specific subsets of raw data to perform single-lane modelling, while the hybrid time-series application in Section 3.3 reverted to the aggregated single-source assumption, proritizing dynamic temporal prediction over fine spatial resolution.[17]

17: Moreover, a comparison with the fully stochastic model using measured speeds was also performed to assess the impact of using forecasted inputs on the accuracy of noise predictions. For consistency, both models maintained the single-source assumption due to the aggregated nature of the available data.

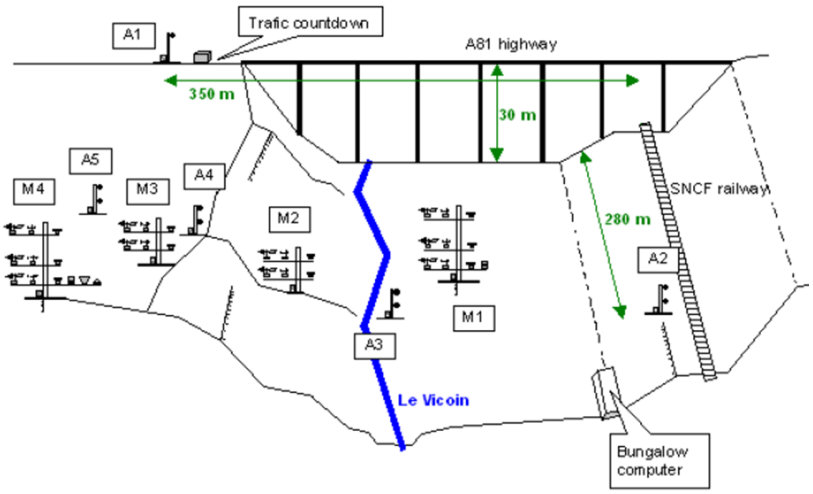


Figure 3.6: Schematic representation of acoustic and meteorological sensor positions [209].

The case under study is characterised by a free-flow traffic condition, as also shown by the exploratory analysis of the dataset (see Section 3.5). This means that vehicle speeds are not significantly influenced by each other due to low flow density, and this assumption is utilised as the core premise for the stochastic methodology across all three models. Such homogeneous traffic condition is described by a Gaussian distribution, as previously discussed, thus needing just its mean speed and a fixed standard deviation to be fully represented [210, 214]. In the case study under analysis, the standard deviation is fixed at a 10% value, based on the free flow assumption [159, 211–213]. Moreover, constant speed values

were used to simulate each vehicle transit, thus no correction factor due to accelaration is considered in this modelling stage.

3.4.1 Raw Data Access and Microscopic Resolution

While the publicly released LTMS dataset provides traffic information aggregated into 15-minute intervals, a comprehensive spatial-enhanced applications surely required a finer level of detail. For these specific analyses (Section 3.2), access was secured to the original raw data thanks to collaboration with the team responsible of the measurements campaign.

This unaggregated dataset offers a significantly higher temporal and spatial resolution, providing:

- **Traffic variables at 10-second intervals:** This represents the maximum temporal granularity of the original measurements campaign. High-frequency data for traffic volume and speed variables a the finest level of detail possible is provided;
- **Lane-specific data:** The detail about which lane has been occupied by the passing vehicles is also present (Lanes 1, 2, 3, and 4), enabling the detailed analysis of flow distributions and the development of the high-resolution 4-Source modelling configuration.

The availability of this 10-second, lane-specific data was fundamental for developing and validating the 4-Source modelling configuration proposed in this thesis, enabling a detailed analysis of flow distributions and mean speeds broken down by each of the four carriageway lanes.

3.5 Dataset Exploration: Models Implementation and Validation

The LTMS dataset, as described in Section 3.4, serves as the foundational dataset for implementing and validating the stochastic microscopic noise model and its subsequent extensions.

This Section is structured to systematically present the validation of each modelling configuration. Specifically, it is organized into distinct Subsections for each model implemented: the baseline stochastic model, the spatial-enhanced lane analysis, and the hybrid time-series forecasting approach. For each application, the following key elements will be presented and discussed:

- **Dataset Description:** An overview on the specific subset of the LTMS dataset chosen for the model implementation will be provided. Any preprocessing steps undertaken to prepare the data for analysis will be described;
- **Exploratory Data Analysis:** The main characteristic of each subset will be examined, including statistical summaries and visualizations to highlight key patterns and trends relevant to the modelling phase;
- **Validation Results and Discussion:** The performance of each model will be evaluated against the measured acoustic data from the LTMS dataset. Key metrics such as Mean Absolute Error (MAE), Root Mean Squared Error (RMSE), and correlation coefficients will be used to quantify the accuracy of the predictions. The results will be

interpreted in the context of the model capabilities and limitations. Comparisons between the different configurations will be made to highlight the benefits of spatial and temporal enhancements in noise prediction accuracy.

3.5.1 Baseline Stochastic Model Implementation and Validation

The baseline stochastic model has been validated using the largest possible subset of the Long-Term Monitoring Station (LTMS) dataset.

This foundational analysis establishes the model effectiveness in predicting road traffic noise levels under free-flow conditions, setting the stage for subsequent enhancements in spatial and temporal resolution.

Dataset Description and Exploratory Analysis

To ensure data integrity and completeness, the initial step involved a thorough cleaning of the LTMS dataset.[18]

18: More details about the LTMS can be found in [209].

This process entailed the removal of entries with missing values. Thus, the used selection criterion was based on using only those 15-minute intervals where all required variables (i.e., traffic flows, average speeds and measured noise levels) were fully available. Therefore, all observations in which one or more input parameters or the $L_{A,eq,15min}$ data were missing were discarded, resulting in a dataset of 30348 usable 15-minute intervals.

Table 3.1: A selection of lines from the dataset used for the baseline stochastic model implementation.

# interval	Date	Time	N_L [veh/15-min]	N_H [veh/15-min]	v_L [km/h]	v_H [km/h]	$L_{A,eq,15min}$ [dBA]
0	01-07-2002	04:30-04:45	229	16	124.1	84.5	72.2
1	01-07-2002	04:45-05:00	227	13	130.1	83.2	72.1
2	01-07-2002	05:00-05:15	264	13	124.3	83.0	72.7
...	...	...	...	...	...	...	...
30345	18-10-2007	07:45-08:00	207	63	126.3	86.5	73.2
30346	18-10-2007	08:00-08:15	160	49	125.5	87.8	72.3
30347	18-10-2007	08:15-08:30	182	53	125.1	88.1	73.1

A closer look at a selection of lines of the obtained dataset composition and its structure can be found in Table 3.1, which shows a selection of lines from the used dataset to illustrate its structure. The 15-minute intervals are indexed by date and time, and for each interval, the traffic flow values for light-duty vehicles (N_L) and heavy-duty vehicles (N_H), their respective average speeds (v_L and v_H), and the measured equivalent continuous sound level ($L_{A,eq,15min}$) are reported.

Table 3.2 summarises the key statistical properties of all the variables, including mean, standard deviation, minimum, maximum, skewness and kurtosis. This statistical overview provides insights into the distribution and variability of the traffic and noise data, which is crucial for understanding the context in which the stochastic model operates.

However, to achieve a clearer overview of the chosen dataset, each variable boxplot has been represented. In these boxplots the horizontal lines represent the median value of the described variable.

Table 3.2: Summary statistics of the main variables within the dataset used for the baseline stochastic model implementation.

Variable	Mean	Std Dev	Min	Max	Skew	Kurt
N_L [veh/15-min]	278.3	171.3	1	1075	0.75	0.47
N_H [veh/15-min]	31.4	21.3	1	222	0.63	0.59
v_L [km/h]	126.1	7.3	40.0	186.2	-0.28	3.34
v_H [km/h]	86.9	4.5	2.0	99.0	-4.95	0.01
$L_{A,eq,15min}$ [dBA]	71.6	2.9	46.3	78.2	-2.04	6.11

The first pair of boxplots in Figure 3.7 describe vehicle flows, distinguishing between light (N_L) and heavy-duty vehicles (N_H). The difference between the amount of light and heavy vehicles is evident observing the medians of the two datasets (i.e., respectively 254 veh/15 min and 28 veh/15 min) and even through their mean values and standard deviations as reported in Table 3.2. As expected regarding the distributions of the outliers, light vehicles distribution shows a higher number of outliers, and they are even more widely distributed than heavy vehicles ones. Variations in road conditions can influence these dynamics, resulting in a greater likelihood of outliers associated with light vehicles.

The second pair of graphs, in Figure 3.8, represents light and heavy vehicles mean speed distributions (v_L and v_H) respectively. The medians of these two distributions are 126.3 km/h and 87.6 km/h respectively, which are in agreement with the speed limits of the motorway of such categories that are 130 km/h for light vehicles and 90 km/h for heavy goods[19] vehicles, although again there are many outliers. This may occur because light vehicles tend to have more diverse acceleration and deceleration patterns due to their maneuverability, making them more susceptible to abrupt changes in speed and noise emissions.

19: With a maximum permissible weight of over 3.5 tonnes and up to 12 tonnes, 100 km/h for public transport vehicles [220, 221].

Finally, the last boxplot in Figure 3.9 represents the distribution of the A-weighted equivalent continuous sound level recorded in the site ($L_{A,eq,15min,meas}$). The median value of this distribution is 72.3 dBA, which is in line with typical noise levels observed on motorways with similar traffic conditions. The outliers of this distribution will be subject of further investigation in this Section.

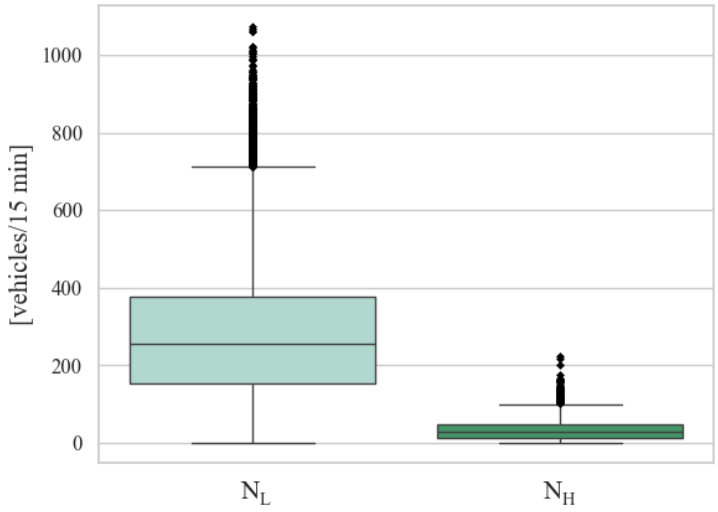


Figure 3.7: Boxplot of light (N_L) and heavy-duty (N_H) vehicle flow.

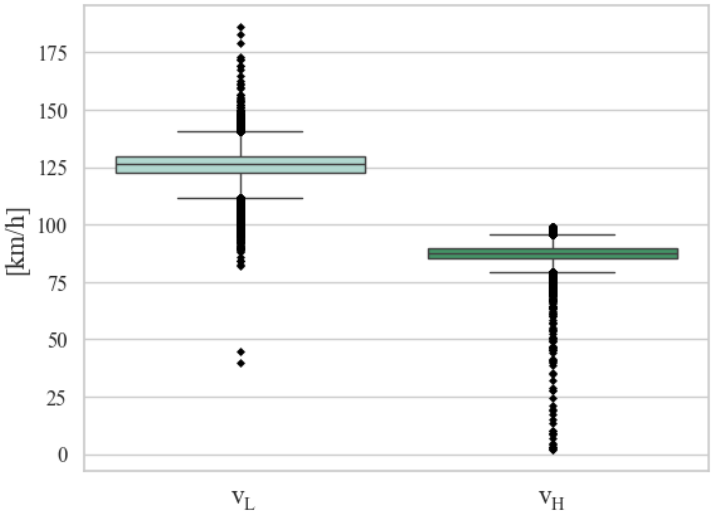


Figure 3.8: Boxplot of light (v_L) and heavy-duty (v_H) vehicle mean speed.

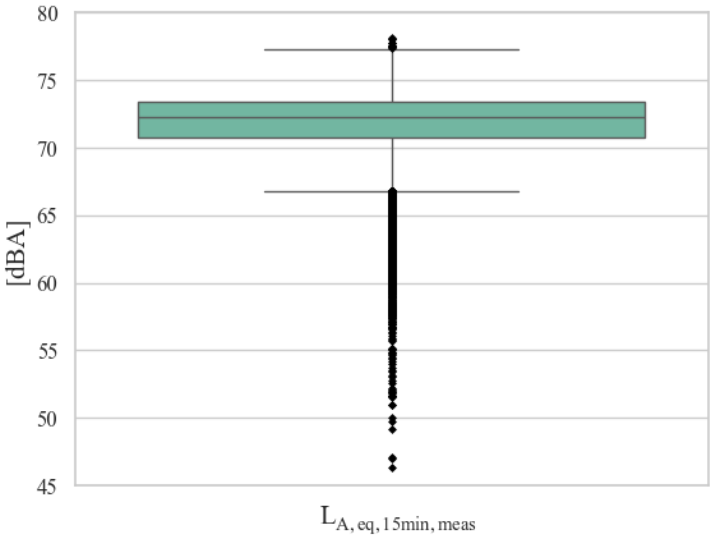


Figure 3.9: Boxplot of the measured equivalent continuous sound level ($L_{A,eq,15min,meas}$).

To further investigate the relationships among the variables, a correlation analysis has been performed. The goal is to investigate whether there is any correlation between the several quantities used as input to the model. From the scatterplot of matrices reported in Figure 3.10, this kind of information can be easily deduced. The graph reports bivariate scatter plots below the diagonal and histograms on the diagonal.

The correlation analysis has been performed using the *Spearman's correlation approach*, utilising `psych`, an R package for statistical analysis. Resulting correlation coefficients are reported above the diagonal.[20] Several insights can be drawn:

- The heavy-duty vehicle mean speeds distribution reveals a bimodal pattern, with two distinct peaks, suggesting the presence of two predominant speed ranges among heavy vehicles (aligning with varying regulatory speed limits for heavy freight);
- The influence heavy vehicle speed (v_H) has on the measured sound level ($L_{A,eq,15min}$) is low, evidenced by a correlation coefficient of

20: The Spearman's correlation coefficients indicate the strength and direction of monotonic relationships between pairs of variables, providing insights into how changes in one variable may be associated with changes in another.

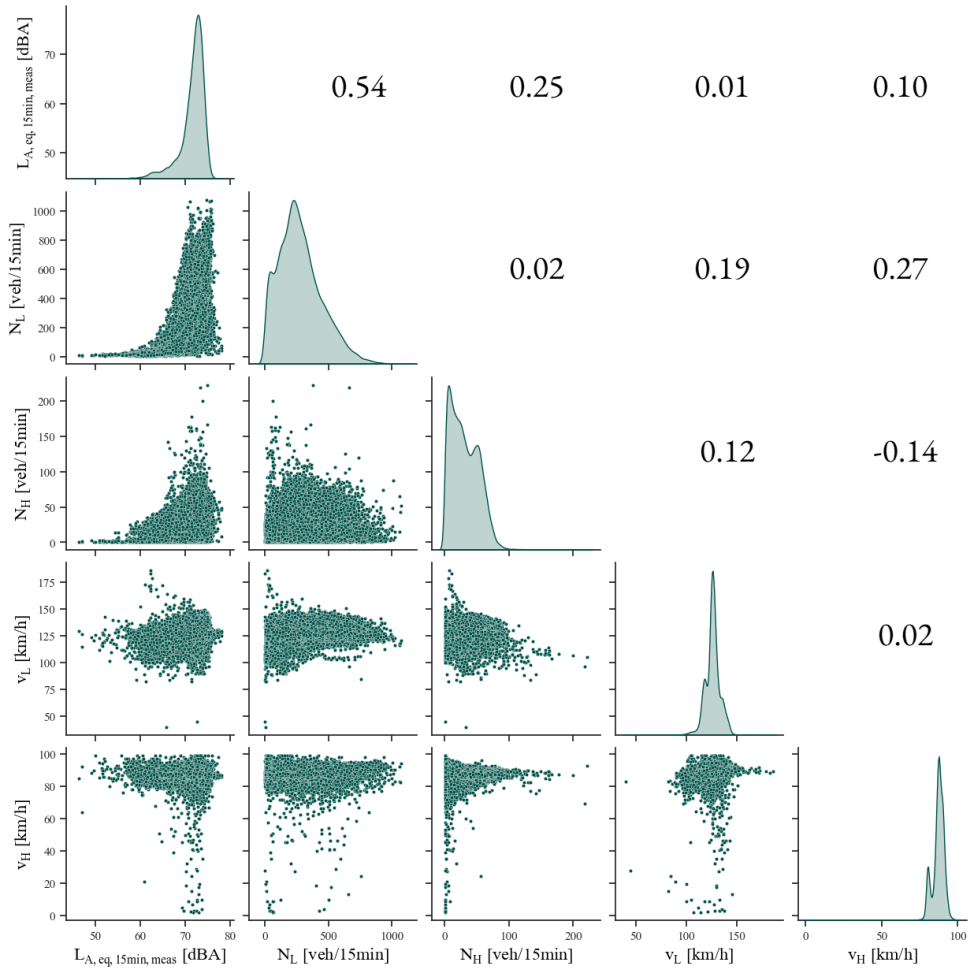


Figure 3.10: Matrix of scatter plots relating all model input variables to each other and their respective Spearman's correlation coefficients.

only 0.10. This suggests that variations in heavy vehicle speeds have a minimal impact on the noise levels recorded at the monitoring station;

- The light vehicle flow (N_L) does not significantly influence speed (v_L), as indicated by a low correlation coefficient (0.19). Since the speeds of single vehicles are not affected by each other, the assumption of a free flow traffic condition, is indeed confirmed to be accurate for describing the dataset;
- The low correlation values observed for both light and heavy vehicle speeds (v_L and v_H) with respect to the respective vehicle flows (N_L and N_H) are largely due to traffic operating below critical density. In such conditions, the road capacity is not reached, allowing individual vehicles to travel at freely chosen speeds without significant influence from surrounding traffic. This decoupling of speed and flow is characteristic of free-flow traffic conditions, where vehicles can maintain their desired speeds regardless of the number of vehicles on the road. Vehicles can travel at freely chosen speeds without significantly influencing flow volume or $L_{A,eq,15min}$ levels. In contrast, a congested traffic scenario, where vehicle interactions are more frequent, would likely exhibit stronger correlations between speed, flow, and noise levels due to the increased influence of traffic density on vehicle behavior.

Validation Results and Discussion

The stochastic simulation has been executed across all 30348 valid 15-minute intervals identified in the dataset. For each interval, simulated equivalent continuous sound levels ($L_{A,eq,15min,sim}$) based on the input traffic parameters (i.e., vehicle flows and average speeds) has been generated. The predicted values are then systematically compared to the corresponding measured sound levels ($L_{A,eq,15min,meas}$) from the LTMS dataset to evaluate the model accuracy.

A crucial preliminary step in validation involved the visual exploration of the sound level distributions, comparing the noise levels as predicted versus those recorded in the measurements. This comparison provides an initial qualitative assessment of the model performance by highlighting any similarities and differences between such values. For this purpose, several graphical representations have been created:

- **Violin Plots:** These plots facilitate a direct visual comparison between the distributions of the measured and simulated sound levels. Figure 3.11 presents violin plots of both the measured and simulated $L_{A,eq,15min}$ values.
- **Histograms:** The comparison of the two distributions is further plotted in Figure 3.12, which shows the histograms of the measured and simulated sound levels overlaid for direct comparison.

From these visualizations, it is evident that the stochastic model effectively captures the overall distribution of measured noise levels:

- The shapes of the two distributions are similar, and they exhibit similar quartiles, as quantified in Table 3.3.
- The distributions also align in terms of main statistics, as reported in Table 3.4, even though the simulated data exhibits a slightly different profile as notable from the skewness and kurtosis values.

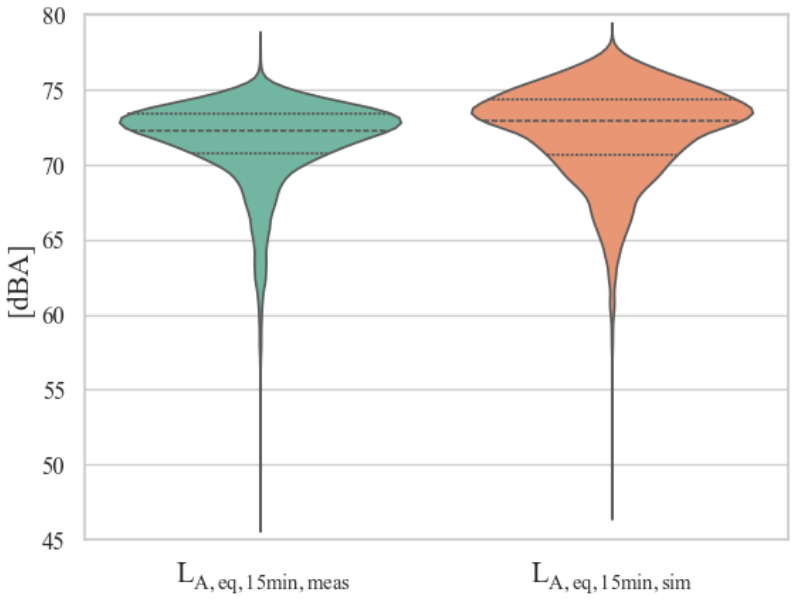


Figure 3.11: Violin plots comparing the distributions of measured (green) and simulated (orange) equivalent continuous sound levels ($L_{A,eq,15min}$).

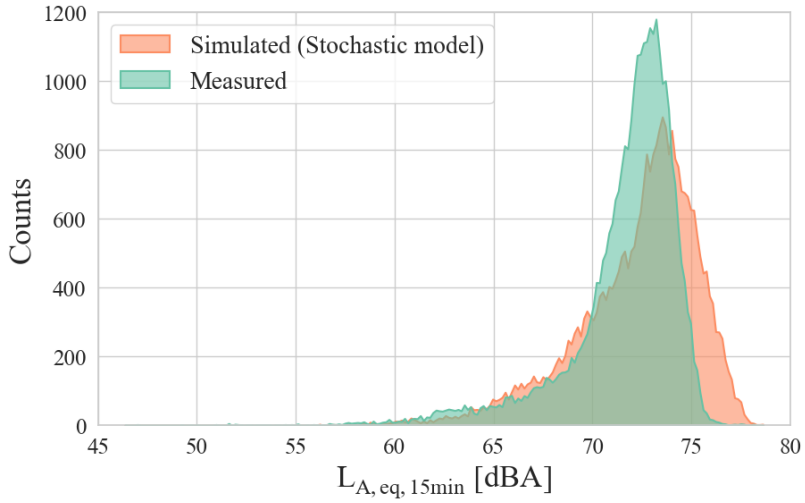


Figure 3.12: Histograms comparing the distributions of measured (green) and simulated (orange) equivalent continuous sound levels ($L_{A,eq,15min}$).

The close alignment between the measured and simulated distributions indicates that the model can replicate both the variability and central tendencies of the measured data. The stochastic microscopic noise model is thus effective in capturing the key dynamics of road traffic noise generation under free-flow conditions.

Table 3.3: Quartiles of measured and simulated equivalent continuous sound levels.

$L_{A,eq,15min}$	**25th quart.** [dBA]	**50th quart.** [dBA]	**75th quart.** [dBA]
$L_{A,eq,15min,meas}$	70.7	72.3	73.4
$L_{A,eq,15min,sim}$	70.6	72.9	74.4

Table 3.4: Summary statistics of measured and simulated equivalent continuous sound levels.

$L_{A,eq,15min}$	**Mean** [dBA]	**Std dev** [dBA]	**Min** [dBA]	**Max** [dBA]	**Skew**	**Kurt**
$L_{A,eq,15min,meas}$	71.6	2.9	46.3	78.2	-2.04	6.11
$L_{A,eq,15min,sim}$	72.2	3.1	47.2	78.7	-1.1	1.8

The simulated A-weighted continuous equivalent sound pressure levels ($L_{A,eq,15min,sim}$) have also been plotted against the corresponding observed data ($L_{A,eq,15min,meas}$) in a bisector plot in Figure 3.13.[21] In this figure, the red solid line indicates the ideal quadrant bisector line where the simulated points would lie if the model predictions perfectly matched the measured values. The analysis reveals that a substantial portion of the data is clustered within the ±2 dBA range, delimited by the black dashed lines. This clustering highlights the model consistency, as 19,501 values, representing approximately 64% of the considered dataset, fall within this acceptable margin of error.

21: This is a standard technique utilised to visually assess the overall model performance in terms of estimation bias (i.e., overestimation or underestimation).

Additional remarks can be drawn by analysing the graph in Figure 3.14, which illustrates the distribution of error through an histogram. The

error is defined as the difference between $L_{A,eq,15min,meas}$, the A-weighted continuous equivalent sound pressure level on the 15-minute interval as measaured during the measaurement campaign, and $L_{A,eq,15min,sim}$, the A-weighted continuous equivalent sound pressure levels during the same 15-minute interval but as simulated using the stochastic model. The obtained error distribution has a mean of (0.6 dBA) and a standard deviation of (2.3 dBA). While the low Mean Error reveals a good overall accuracy of the model, the standard deviation suggests that most of the errors are clustered within an interval of ±2 dBA.

As for the shape of the error distribution, it presents a slight asymmetry towards the right (i.e., positive errors, thus overestimation), as the skewness value is 0.43. Moreover, the distribution is leptokurtic since the kurtosis is equal to 1.91. This implies that the errors are more tightly clustered close to the mean value with respect to what it should be in the case of a normal distribution (kurtosis = 3). However, while the noise levels simulations generally approach the measurements quite well, it is noteworthy that the model exhibits greater residual errors at the extremes of the noise spectrum (i.e., at high levels, (approximately > 70 dBA), and low levels, (approximately < 55 dBA)). The full statistical characterisation of the error distribution is provided in Tables 3.5 and Table 3.6.

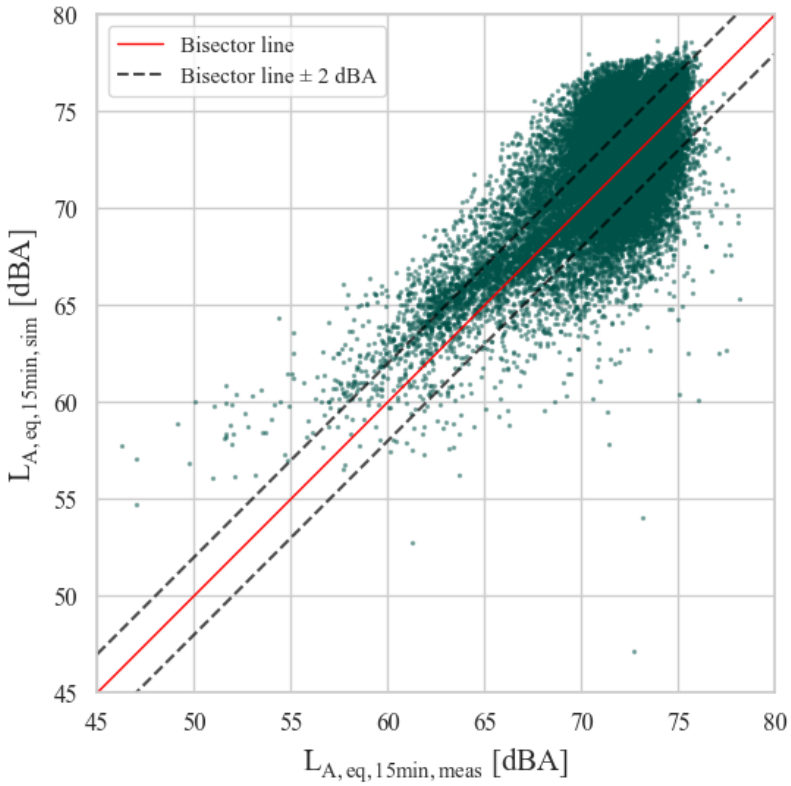


Figure 3.13: Scatter plot of simulated data ($L_{A,eq,15min,sim}$) versus the corresponding measurements ($L_{A,eq,15min,meas}$).

A better insight into the model performances can be achieved by analysing the error distribution tails and, consequently, the model outliers. In Figure 3.15, the A-weighted continuous equivalent sound pressure levels as measured ($L_{A,eq,15min,meas}$) and as simulated ($L_{A,eq,15min,sim}$) are plotted,

respectively, in green and in orange as a function of light vehicle flow (N_L).

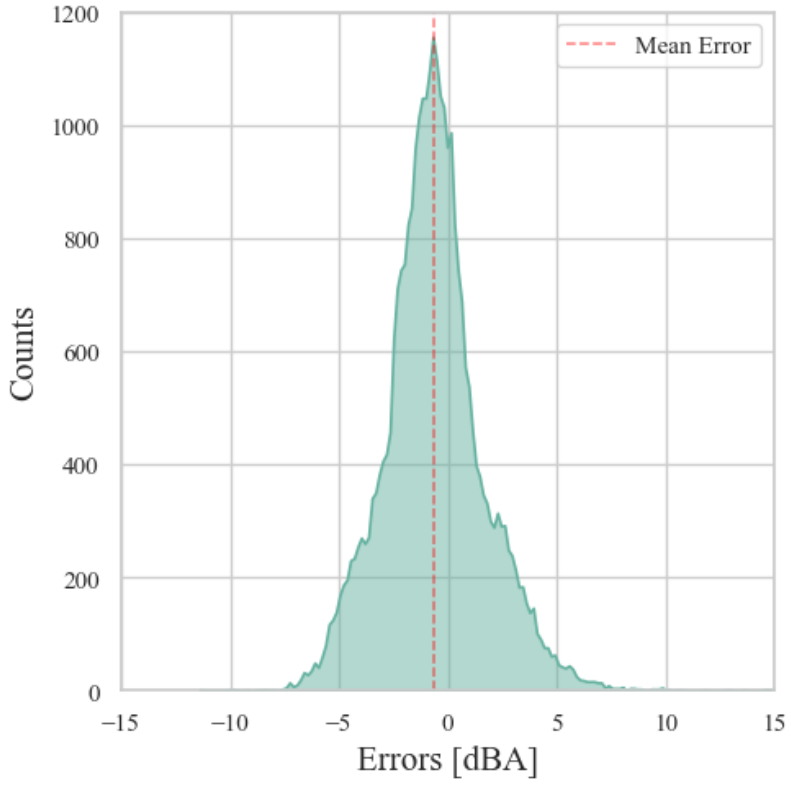


Figure 3.14: Distribution of error values.

Table 3.5: Errors significant quartiles.

	25th quart. [dBA]	**50th quart.** [dBA]	**75th quart.** [dBA]
Errors	-2.0	-0.7	0.5

Table 3.6: Errors summary statistics.

	Mean [dBA]	**Std dev** [dBA]	**Min** [dBA]	**Max** [dBA]	**Skewness**	**Kurtosis**
Errors	-0.6	2.3	-11.5	25.5	0.43	1.91

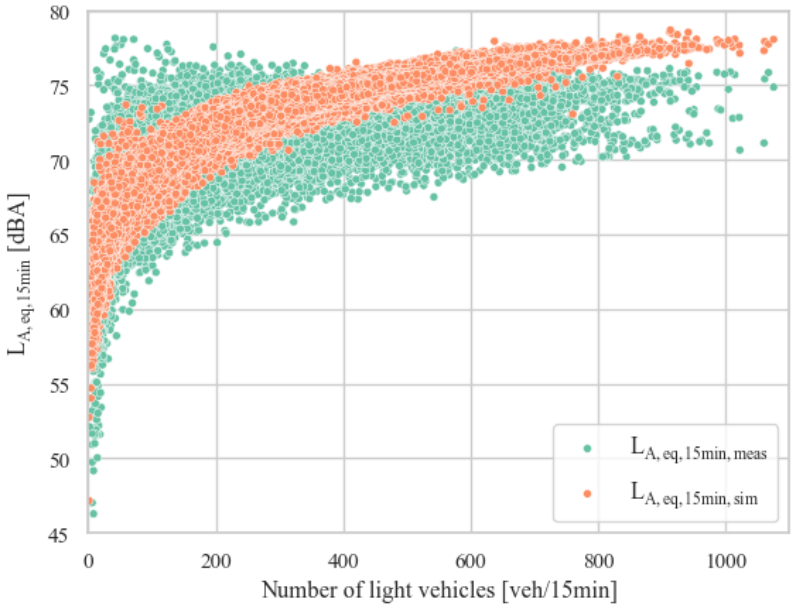


Figure 3.15: Measured and simulated equivalent continuous sound levels as a function of light vehicle flow (N_L).

This visual analysis reveals distinct trends in model errors related to traffic volume:

- **Low Flow Conditions:** For low values of light vehicle flow (i.e., $N_L < 100$ veh/15 min), there is large variability in the measured sound levels, exceeding 20 dBA. This pronounced variability in the measured data likely stems from unordinary conditions, such as the contribution of non-road traffic noise phenomena that were not entirely removed during the original data processing phase;[22]
- **High Flow Conditions:** When analysing low or medium flows, the actual noise level trend is accurately depicted. However, at higher flows, the model consistently exhibits overestimation. This bias is likely attributable to the methodological assumption used to calculate the total noise level at the receiver: the direct summation of SELs. This summation method inherently assumes that individual vehicle transits do not overlap and that each one contributes independently to the overall noise level.[23] As vehicle flow increases, this assumption may not hold true, as overlapping noise events can lead to complex interactions that are not adequately captured by simple additive models. Moreover,with vehicles traversing multiple lanes simultaneously, the spatial distribution of noise sources becomes more complex, further complicating the noise summation process. In this scenario, the higher is the vehicle flow, the more pronounced acoustic and screening overlap effects become, leading to potential overestimations in the predicted noise levels.[24]

Another interesting insight into the model perfomance is gained by examining the error distribution tails, particularly on the model outliers. A focus on 15-minute intervals characterised by significantly prediction errors (i.e., $Errors > +10$ dBA, $Errors < -10$ dBA) is presented in Table 3.7.[25]

- Most error outliers are associated with **night-time intervals**. During these periods, **low traffic flows** may lead to single vehicles traveling

22: The future incorporation of ambient or background noise modelling is necessary to refine the model accuracy in this low-flow regime.

23: This also means that each vehicle contributes 100% of its noise emission to the total noise level, without any attenuation due to overlapping sound events.

24: Future model refinements should consider more sophisticated approaches to account for these interactions, potentially incorporating factors such as temporal overlap and psychoacoustic effects.

25: The continuous equivalent sound levels are noted as $L_{eq,meas}$ and $L_{eq,sim}$ in this table for brevity.

at much higher speeds, resulting in significantly higher measured noise levels than the model simulated, or it may indicate a strong influence of unaccounted background noise;

- High error values are sometimes associated with the **same day** across different 15-minute intervals.[26] This temporal clustering strongly suggests potential issues with the field measurements taken on those days, such as interference from maintenance activity or work in progress, failed to be detected during the original data processing phase.

26: For example, 18/03/07 and 15/10/06 are characterised by similar conditions.

Table 3.7: Details of the selected error outliers.

Date	**Time**	N_L [veh/15-min]	N_H [veh/15-min]	v_L [km/h]	v_H [km/h]	$L_{eq,meas}$ [dBA]	$L_{eq,sim}$ [dBA]	**Error** [dBA]
22-09-04	10:30-10:45	1	1	45.0	28.0	72.7	47.2	25.2
23-09-04	14:30-14:45	4	2	100.0	19.5	73.2	54.0	19.1
18-03-07	05:00-05:15	13	2	127.2	99.0	76.0	60.1	15.9
18-03-07	05:45-06:00	27	2	126.2	98.0	77.4	62.6	14.8
18-03-07	04:15-04:30	16	2	119.7	99.0	75.1	60.4	14.6
08-09-04	11:00-11:15	11	6	82.2	15.2	71.4	57.9	13.6
18-03-07	05:15-05:30	17	4	131.7	94.0	75.5	62.5	13.0
18-03-07	06:00-06:15	42	8	124.9	86.0	78.2	65.4	12.8
26-12-03	08:30-08:45	12	1	127.8	90.0	71.3	59.5	11.8
25-03-07	05:00-05:15	29	1	126.2	95.0	73.5	62.7	10.9
04-03-07	05:15-05:30	35	3	133.0	90.0	75.0	64.3	10.7
09-03-04	08:30-08:45	16	1	127.9	92.0	70.6	60.2	10.5
24-03-07	17:00-17:15	31	13	129.7	85.6	75.2	65.0	10.2
09-03-07	05:45-06:00	51	30	120.4	86.0	77.7	67.6	10.1
01-04-07	06:45-07:00	53	2	129.0	87.5	75.7	65.6	10.1
15-10-06	02:45-03:00	8	1	129.8	85.0	46.3	57.8	-11.5
24-09-06	01:30-01:45	6	2	126.8	92.5	47.0	57.0	-10.0
15-10-06	13:30-13:45	14	1	126.3	99.0	50.0	60.0	-10.0

The analysis of the correlation between both the simulated A-weighted continuous equivalent sound pressure levels ($L_{A,eq,15min,sim}$) and the model errors and all the input variables of the model has been pursued. The results of this analysis are summarised in the scatterplot matrix shown in Figure 3.16, where a Spearman's correlation heatmap is represented.

The errors exhibit a non-negligible negative correlation with the light vehicle flow (N_L), light vehicle speed (v_L), and the simulated sound level ($L_{A,eq,15min,sim}$). This relationship is visually confirmed in Figure 3.17, where the error are plotted versus the input of the model. The errors, indeed, demonstrate a decreasing slope particularly against N_L and $L_{A,eq,15min,sim}$. Moreover, the error variability decreases with an increase in the flow of heavy vehicles (N_H). This suggests that the model predictive accuracy improves as the number of heavy vehicles increases, likely due to the more stable and predictable noise patterns associated with higher heavy vehicle traffic volumes. With higher heavy vehicle flows, indeed, the normal distribution assumption for the speeds is better depicted. On the contrary, when few heavy vehicles pass in the 15-minute time slot, the accuracy of the random speed assignment based on the Gaussian distribution diminishes, leading to greater variability in prediction errors.

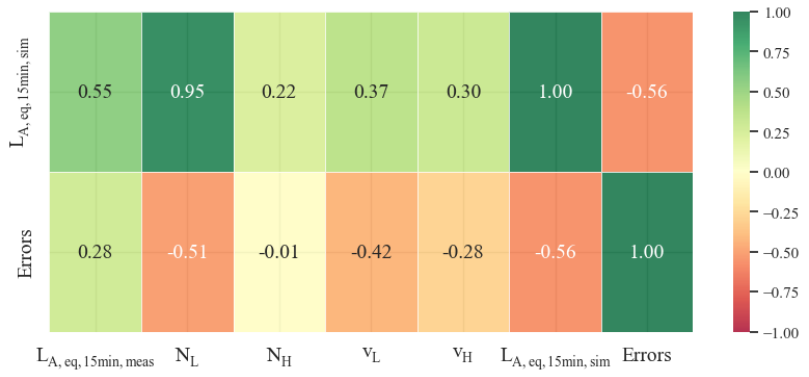


Figure 3.16: Correlation heatmap of the $L_{A,eq,15min,sim}$ and the model errors with $L_{A,eq,15min,meas}$ and model main parameters.

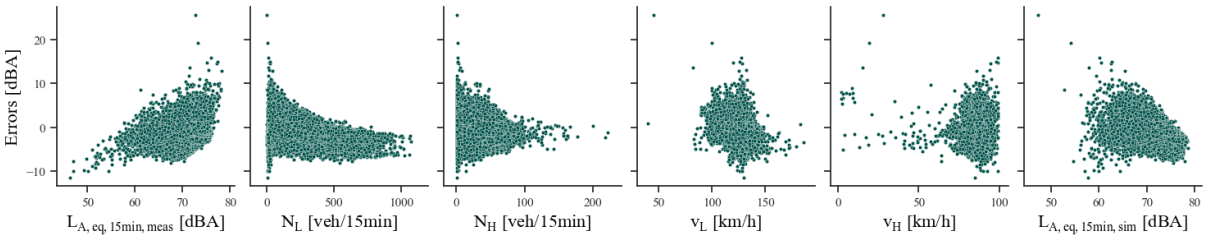


Figure 3.17: Errors plot versus, from left to right, the $L_{A,eq,15min,meas}$, the variables of the model, and the $L_{A,eq,15min,sim}$.

Finally, to quantitatively assess the model predictive performance, several error metrics have been calculated. These metrics provide a comprehensive evaluation of the model accuracy and reliability in simulating road traffic noise levels. The computed error metrics are summarised in Table 3.8. The Mean Absolute Error (MAE) is below 2 dBA, placing the model within the generally accepted range for accurate noise assessment and prediction models [222]. The coefficient of variation of the error (CVE) is notably low at 0.03, indicating that the model errors are relatively small compared to the average measured sound levels. This low CVE suggests that the model consistently produces predictions that are close to the actual measurements, further reinforcing its reliability.

Table 3.8: Summary error metrics of the stochastic model.

ME [dBA]	**Std dev** [dBA]	**MPE** [%]	**MAE** [dBA]	**MSE** $[dBA]^2$	**CVE** [–]
-0.65	2.29	-0.95	1.84	5.67	0.03

Comparison with the CNOSSOS-EU Model

In this Section, the CNOSSOS-EU model is used as a standard reference for evaluating the performance of the proposed modelling techniques. The results obtained from the proposed stochastic microscopic noise model, indeed, have been compared with those derived from the CNOSSOS-EU model, which was applied to the same dataset.

To ensure a rigorous comparison, for each 15-minute time interval, the identical inputs regarding vehicle flows of each considered category were utilised. However, as for the speed values, since the CNOSSOS-EU

model uses mean speeds of the flow per each category (i.e., macroscopic approach) as an input, no random extraction was performed for its implementation, and the empirical average values as provided in the available dataset have been used. In this way, the fundamental methodological difference between the two models lies in their treatment of vehicle speeds and, consequently, the associated noise emission and propagation calculations. Such a comparison, therefore, allows for an isolated assessment of the impact of the stochastic microscopic approach on noise level predictions.

Moreover, the differences in noise levels prediction introduced by the usage of a fully microscopic approach can also be assessed using such a comparison. Unlike microscopic models that treat individual vehicles as distinct point sources with specific speeds, the CNOSSOS-EU model aggregates these contributions into a single line source representing the traffic flow. This approach assumes that all vehicles within the flow travel at a constant speed. Consequently, the sound levels are propagated to the receiver using the cylindrical propagation formula rather than the spherical formula used for point sources.[27] The results revealed notable differences between the two models as can be seen in Figure 3.18, where the distribution curves of measured noise levels are overlapped with simulated ones, both for the stochastic and the CNOSSOS-EU model.

Table 3.9 shows the summary error metrics of the two models, highlighting the performance differences between the stochastic microscopic model and the CNOSSOS-EU. The stochastic model predictions were generally closer to the observed noise levels, as indicated by significantly lower values in key accuracy metrics such as Mean Error (ME), Mean Absolute Error (MAE), and Mean Squared Error (MSE).

27: Since the two models share the same NEM, the different models performances has to be be associated with the different approaches to the source modelling and spatial distribution of acoustic energy. The CNOSSOS-EU model utilises a line source framework with cylindrical geometric divergence ($1/r$), with a fixed distance (the minimum distance between receiver and centre of the carriage, d in Figure 3.3), while the stochastic model treats each vehicle as a point source, leading to omnidirectional radiation characterised by geometric decay that follows an inverse square law ($1/r^2$).

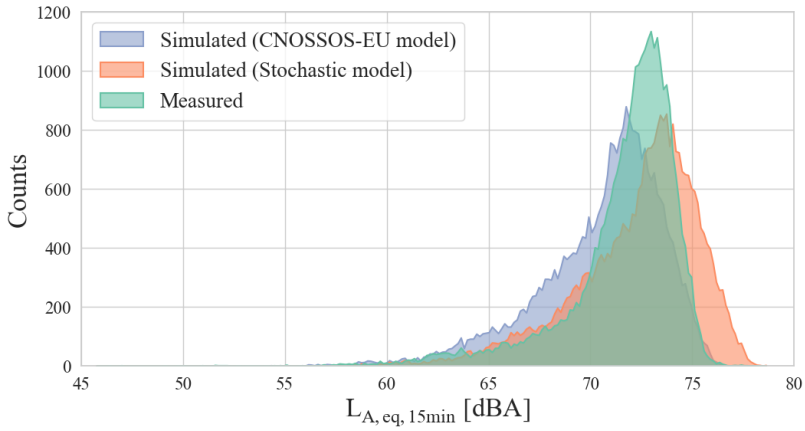


Figure 3.18: Distribution of $L_{A,eq,15min,meas}$ (in green) compared with the distribution of $L_{A,eq,15min,sim}$ computed with CNOSSOS-EU model (in blue) and the proposed stochastic model (in orange).

Table 3.9: Comparison between error metrics of the CNOSSOS-EU model and the proposed stochastic model.

Model used	**ME** [dBA]	**Std dev** [dBA]	**MPE** [%]	**MAE** [dBA]	**MSE** $[dBA]^2$	**CVE** [–]
Stochastic	-0.65	2.29	-0.95	1.84	5.67	0.03
CNOSSOS-EU	1.07	2.28	1.45	1.93	6.37	0.03

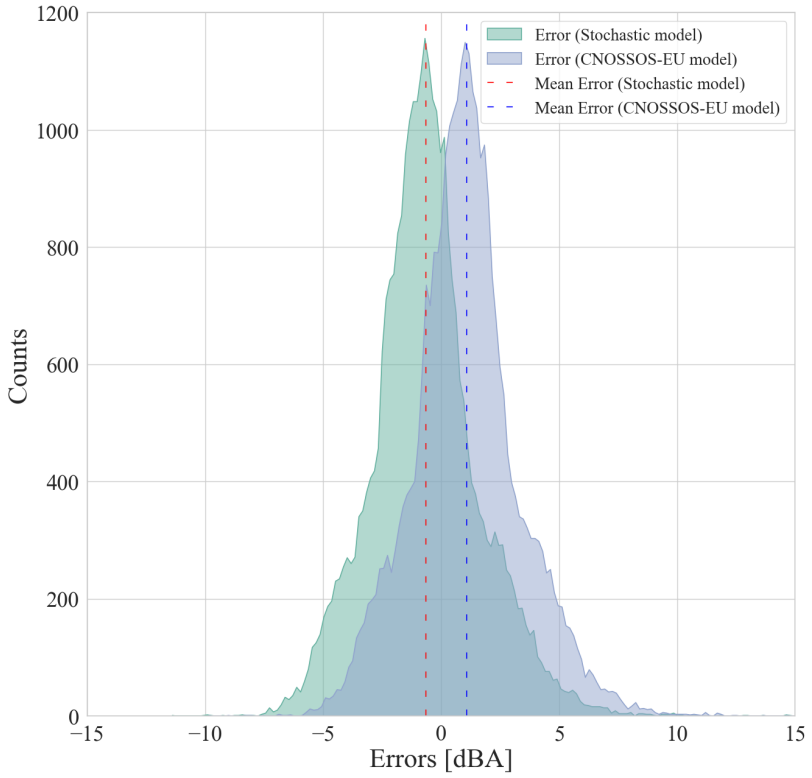


Figure 3.19: Distribution of the stochastic model error values (in green) overlapped with the distribution of CNOSSOS-EU model error values (in blue).

These lower metrics suggest that the stochastic model provides a more accurate and reliable representation of road traffic noise levels compared to the CNOSSOS-EU model, validating the utility of incorporating the microscopic and stochastic elements. These results underscore the potential advantages of incorporating stochastic elements and a fully microscopic approach into traffic noise models.

Even if both the CNOSSOS-EU model and the presented stochastic approach achieve good performances, definitely because they share the same NEM (i.e., the same core of the model when analysing the single vehicle emissions), the stochastic model presents a lower value of MAE and MSE. Moreover, the stochastic model seems to have slightly better performances when the noise levels are lower than 70 dBA, while at higher levels it is more prone to overestimate, unlike the CNOSSOS-EU model which works in the opposite way. This can also be easily noted in Figure 3.19, in which the overlapping of the two errors histograms is presented.

Briefly, the stochastic and microscopic approach overestimates noise levels while CNOSSOS-EU underestimates them. Moreover, the stochastic model predictions are generally closer to the observed noise levels compared to those from CNOSSOS-EU, indicating a comparatively better performance.

However, it is important to note that these metrics are not drastically different, highlighting the ongoing need for refinement in predictive tools to effectively address the complexities of real-world traffic noise.

3.5.2 Spatial Application of the Stochastic Model Using Variable Level of Aggregation of Traffic Flows: Implementation and Validation

To quantify the predictive enhancements yielded by the spatial disaggregation of traffic flows,[28] this Section presents the implementation and validation of the stochastic model in a multi-lane traffic context.

28: Methodologically defined in Section 3.2.

While the core validation in the previous Section established the model reliability using aggregated flows, this specific analysis leverages raw lane-by-lane data to overcome the constraints of the single-source approximation. The primary objective is to investigate the influence of asymmetric lane usage on noise emission and propagation, evaluating the sensitivity of acoustic predictions to the spatial allocation of noise sources in multi-lane configurations.

Dataset Description and Exploratory Analysis

The empirical validation of the spatially disaggregated stochastic model was conducted using a subset of the LTMS dataset presented in Section 3.4. As also mentioned earlier, the infrastructure under study is characterised by two dual-lane carriageways, with each carriageway consisting of two lanes. For the purpose of the multi-source modelling, the lanes are indexed based on their proximity to the noise monitoring station, with Lane 1 being the closest and Lane 4 the farthest. In particular, Lane 1 and 2 serve the West-East direction (towards Le Mans and Paris), while Lane 3 and 4 serve the opposite direction (towards Rennes). Morphologically, Lanes 1 and 4 function as the primary transit lanes, whereas Lane 2 and 3 are the overtaking lanes. This distinction is critical for the acoustic modelling, as traffic dynamics and vehicle distributions can vary significantly between lanes, influencing the overall noise emission profile.

A fundamental aspect of this analysis concerns the availability of lane-specific traffic data. The publicly available LTMS dataset provides traffic counts aggregated over 15-minute intervals, with no lane-specific breakdowns. Therefore, the results to be presented in this Section utilise the raw traffic dataset presented in Section 3.4.1, which are recorded at 10-second intervals. This high-frequency data includes single-lane counts and individual vehicle speeds, allowing for a precise reconstruction of the traffic stream. However, to ensure compatibility with the validation framework established in the previous Section, the 10-second raw data has been systematically processed and aggregated.[29] This procedure compressed the high-frequency raw inputs into 15-minute time slots, calculating the traffic flows and mean speeds for light and heavy vehicles for each of the four lanes over 15-minute intervals.

29: This choice was made to better align with the equivalent continuous sound pressure level measured over 15-minute intervals.

For this investigation, a preliminary screening of the entire LTMS dataset has been performed to define the optimal validation timeframe. Indeed, given the sporadic presence of missing values inherent to the long-term acquisition system the most extensive continuous period characterised by the lowest incidence of data gaps across all required variables needed to be identified. Consequently, a specific subset covering the 28-day interval from March 5th to April 1st, 2007, has been selected. The temporal evolution of light and heavy traffic flows versus the quarter-hour ID, over the 28-day observation period are illustrated in Figures 3.20 and 3.21, respectively, both decomposed by lane index. The graphical representation adopts a specific color-coding scheme to distinguish the

functional role of the infrastructure: the normal transit lane (Lane 1 and Lane 4) are depicted in blue and light-blue, while the overtaking lanes (Lane 2 and Lane 3) are represented in yellow and orange.

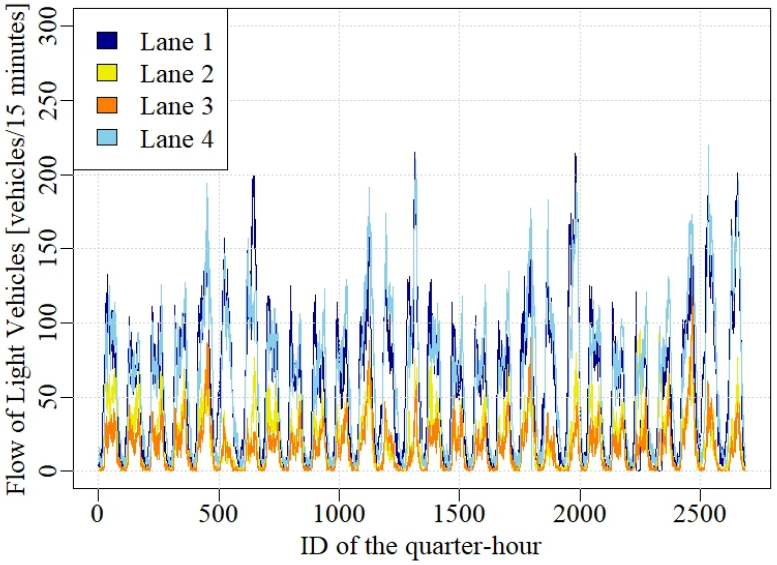


Figure 3.20: Light vehicles flows plotted versus the ID of the quarter-hour, over the 28 days under analysis.

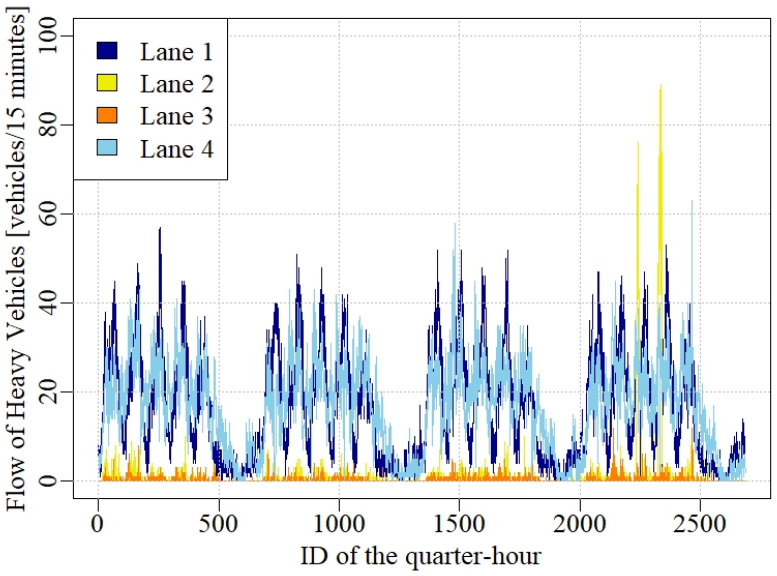


Figure 3.21: Heavy vehicles flows plotted versus the ID of the quarter-hour, over the 28 days under analysis.

The analysis reveals distinct traffic patterns between lanes:

- **Temporal Dynamics:** A distinct pattern characterised by a diurnal cycle is observable across all lane flows, corresponding to the intrinsic day-night oscillations of the traffic behavior. Furthermore,

a macroscopic weekly pattern distinguishes the two vehicle categories: while light vehicle flows remain sustained (or even increase) during weekends due to leisure mobility, heavy vehicle ones exhibit a sharp reduction on Saturdays and Sundays, reflecting typical freight transport patterns and regulations (see also Section 3.5.3 for further details);

- **Spatial Distribution:** Light vehicles mostly utilise the normal transit lanes (Lane 1 and Lane 4). However, it is important to note that the usage of the inner lanes (Lane 2 and Lane 3) is far from negligible. As evidenced by the flow distributions, a consistent portion of the light traffic stream actively utilises these overtaking lanes, indicating a dynamic lane-changing behavior. Conversely, heavy vehicles exhibit a pronounced spatial segregation, being almost entirely confined to the outer lanes (Lane 1 and Lane 4) with negligible presence in the passing lanes (Lane 2 and Lane 3), a behavior consistent with regulatory restrictions;
- **Anomaly Detection:** A significant deviation from these standard patterns is observed during the fourth week of the dataset. The yellow curve (Lane 2) in the heavy vehicles plot exhibits anomalous peaks of high intensity, which strongly contrast with the very low values observed in preceding weeks. A deeper inspection of the raw data reveals that this anomaly corresponds to a specific event: during these intervals, the flow on Lane 1 drops to zero for both categories, indicating a temporary lane closure (likely due to maintenance). This event effectively forced a lateral displacement of the traffic stream, shifting the heavy vehicle load from the proximal lane (Lane 1) to the overtaking lane (Lane 2).[30]

30: This finding is particularly valuable for validation, as it provides a "natural experiment" where the mean source-to-receiver distance is abruptly altered, allowing for an assessment of the model sensitivity to spatial shifts in the noise source.

To further quantify the operational characteristics of the highway segment under analysis, the statistical distribution of traffic flows were analysed using boxplots derived from the high-resolution 10-second raw data. In Figure 3.22 the flow distributions for light vehicles (L) and heavy vehicles (H) are depicted separately for each lane (1 to 4). The analysis of the light vehicle distributions (L) confirms the distinct functional hierarchy of the lanes. The boxplots for the normal transit lanes exhibit significantly higher median values and interquartile ranges compared to the inner lanes. This statistical dominance confirms that Lanes 1 and 4 serve as the primary conduits for the traffic stream, whereas Lanes 2 and 3 function mainly as auxiliary overtaking lanes. In contrast, the heavy vehicle distributions (H) demonstrate a rigid spatial confinement. The flow rates for heavy vehicles in the overtaking lanes (H2 and H3) are negligible, with distributions collapsing near zero. This behavior quantitatively confirms that heavy goods vehicles adhere strictly to regulatory constraints, rarely encroaching upon the overtaking lanes.

These observations are corroborated by the kinematic analysis presented in Figure 3.23, which displays the boxplots of mean speeds obtained by averaging the speeds of the vehicles in each 15-minute slot, starting from the 10-second raw data. A clear velocity gradient is observable between the lanes: the overtaking lanes consistently exhibit higher median speeds compared to the adjacent transit lanes, reflecting the faster dynamics of the passing maneuvers. Furthermore, the heavy vehicle speed distributions are markedly capped, with upper quartiles consistently remaining below 100 km/h, aligning with the specific speed limits enforced for this category on the highway segment under study.

A subtle yet systematic asymmetry emerges from this detailed breakdown. While the outer transit lanes (1 and 4) appear balanced in terms of flow

and speed, a discrepancy is evident between the two overtaking lanes. Specifically, Lane 2 exhibits consistently higher flow and mean speed values compared to its counterpart, Lane 3. This finding is of crucial importance for the acoustic simulations presented in the following Sections; such an asymmetry implies that the acoustic center of the road does not coincide with the geometric center, a nuance that can only be captured by the lane-specific (4-source) model, leading to an expected increase in the simulated levels compared to the centralised approximation.

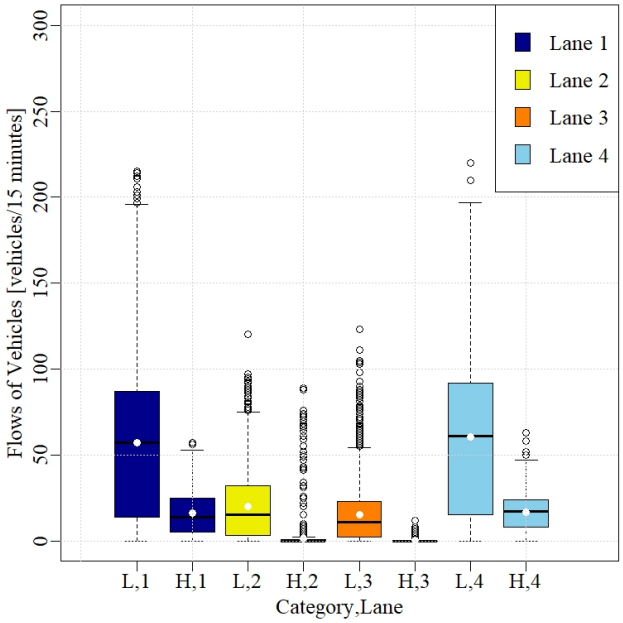


Figure 3.22: Boxplots of light (L) and heavy (H) vehicles flows, divided by lane, over the 28 days under analysis.

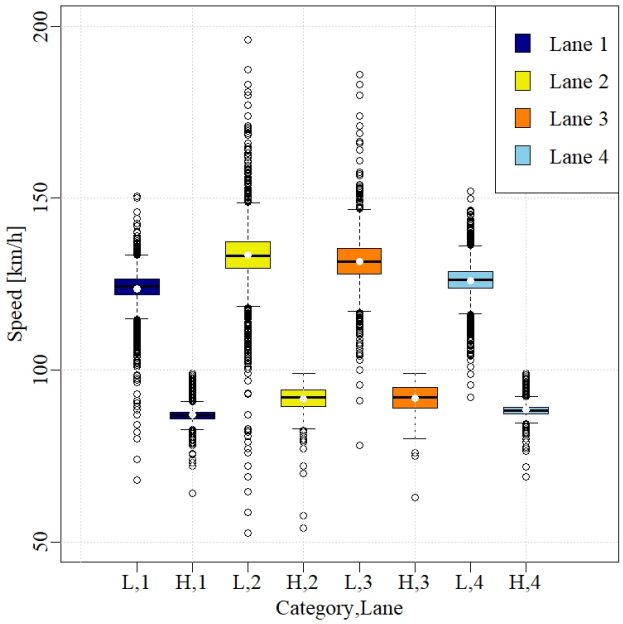


Figure 3.23: Boxplots of light (L) and heavy (H) vehicles mean speeds, divided by lane, over the 28 days under analysis.

Following the exploratory analysis of the dataset, a rigorous data cleaning protocol was implemented to ensure the reliability of the validation phase. As this study aims to quantify the accuracy of the stochastic approach within a spatial multi-source framework, comparing simulated and measured noise levels is essential. Therefore, the availability of the target variable, specifically the measured equivalent continuous sound pressure level ($L_{A,eq,15min}$), is a fundamental prerequisite. Consequently, the dataset was subjected to a strict filtering criterion: all temporal intervals exhibiting missing, invalid, or corrupted acoustic measurements have been systematically excluded from the analysis. This step is critical to ensure that every simulated output corresponds to a verified ground-truth value, thereby enabling a consistent error calculation.

However, this exclusion process inevitably resulted in a reduction of the sample size. From the initial theoretical maximum of 2688 intervals (i.e., 96 distinct 15-minute slots per day over the 28-day observation period), the dataset was refined to a final subset of 443 valid observations. It is important to note that these surviving intervals are not clustered within a single short timeframe but are distributed across the entire four-week duration, thus preserving the temporal heterogeneity of the original dataset (i.e., covering different hours of the day and days of the week).

To verify that this significant reduction did not introduce statistical bias or alter the fundamental characteristics of the sample, a comparative analysis was conducted between the "Raw" (complete) and "Filtered" (reduced) datasets. Table 3.11 presents the descriptive statistics, specifically the mean values and standard deviations, calculated for the key input parameters (flows and speeds) for each lane and vehicle category. Inspection of these metrics reveals that the data cleaning process did not significantly perturb the central tendency or the dispersion of the input distributions. This statistical consistency confirms that the subset of 443 intervals remains fully representative of the general traffic conditions occurring at the site in the period of interest. Consequently, the validation results derived from this filtered dataset can be considered robust and generalisable to the standard operational scenarios of the analysed infrastructure.

Validation Results and Discussion

The comprehensive exploratory data analysis provided critical insights into the complex traffic dynamics characterising the case study area over the selected 28-day testing period. The identification of specific asymmetries in lane usage and kinematic behaviors, particularly the differential load between the overtaking lanes, suggested that the standard "centerline" approximation might oversimplify the acoustic scenario. As reported in Section 3.2, the choice was then to implement the stochastic model in a multi-source configuration, treating each lane as an independent noise source with its specific flow and speed characteristics. This approach allows for a more nuanced representation of the spatial distribution of noise emissions, potentially capturing the effects of lane-specific traffic patterns on the overall sound pressure levels at the receiver location.

In particular, three distinct levels of spatial aggregation have been used and will be compared in this Section:

- **1-Source Model (1S):** A single equivalent source positioned at the geometric center of the carriageway;

- **2-Sources Model (2S):** Two sources representing the centerlines of the opposing directional carriageways;
- **4-Sources Model (4S):** Four distinct sources corresponding to the centerlines of each specific lane.

Thereafter, the propagation geometry for each simulation has been rigorously defined to reflect the physical reality of the site. The source-to-receiver distances have been calculated dynamically, accounting for the fact that Lane 1 is the proximal source (closest to the sound level meter) while Lane 4 is the more distant source. These distances have been computed based on the physical layout of the road segment and the precise location of the measurement point.

This geometric differentiation is visually detailed in Figure 3.24, which depicts the cross-section of the road infrastructure. The cyan axis represents the geometric center used in the 1S model (d_0), while the green axes represent the directional centers for the 2S model (d_{12} and d_{34}). Finally, the red trajectories correspond to the lane-specific distances used in the 4S model (d_1 to d_4).

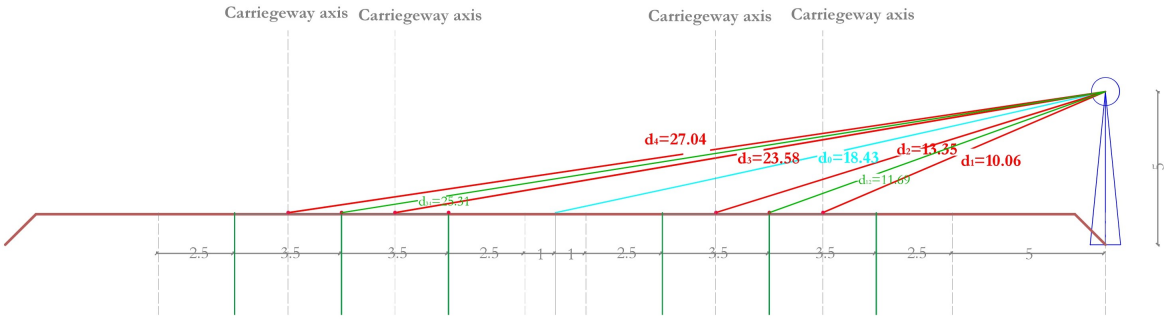


Figure 3.24: Cross-sectional schematic of the case study road segment showing the calculated source-to-receiver distances for the three modelling schemes: single source (d_0, cyan), two sources (d_{12}, d_{34}, green), and four sources (d_1 to d_4, red). The receiver is located 5 m from the roadside at a height of 5 m. Absolute geometric dimensions are indicated in meters.

The specific source-to-receiver distances utilised in each modelling scheme are also summarised in Table 3.10.

Table 3.10: Source-to-receiver distances defined for the three spatial modelling schemes.

Model Scheme	**Source Position**	**Distance** (d) **[m]**
1-Source (1S)	Road Center (d_0)	18.43
2-Sources (2S)	Direction 1 Axis (d_{12})	11.69
	Direction 2 Axis (d_{34})	25.31
4-Sources (4S)	Lane 1 Axis (d_1)	10.06
	Lane 2 Axis (d_2)	13.35
	Lane 3 Axis (d_3)	23.58
	Lane 4 Axis (d_4)	27.04

The visual comparison between the measured and simulated distributions is presented in Figure 3.25, which reports the boxplots for the reference field data alongside the outputs of the three modelling schemes.

The distribution generated by the 4 sources model (yellow boxplot) exhibits the highest degree of alignment with the measured data (green boxplot). While all three simulation schemes exhibit a tendency to underestimate noise levels, indicated by the simulated medians falling

below the measured median, the transition from the centralised (1 source) to the lane-specific (4 sources) approach results in a systematic upward shift of the distribution. This shift effectively reduces the bias, bringing the simulated central tendency significantly closer to the observed reality.

Table 3.11: Mean values and standard deviations of the distributions of parameters for each lane, for both reference databases. Raw databases (before any filtering) include 2688 entries (28 days) while filtered databases (filtering on quarters-hour that include the measured Leq) have 443 entries.

	Parameter calculated over 15 min	**Database**	**Mean value**	**St. dev.**
Lane 1	Flow light [veh/15min]	Raw	57.02	45.24
		Filtered	63.09	46.11
	Flow heavy [veh/15min]	Raw	16.18	12.34
		Filtered	14.97	11.64
	Speed light [km/h]	Raw	123.58	5.73
		Filtered	125.14	4.51
	Speed heavy [km/h]	Raw	86.93	2.50
		Filtered	87.36	2.76
Lane 2	Flow light [veh/15min]	Raw	19.93	19.31
		Filtered	21.00	18.88
	Flow heavy [veh/15min]	Raw	1.20	6.65
		Filtered	1.87	9.44
	Speed light [km/h]	Raw	133.59	10.45
		Filtered	133.84	11.47
	Speed heavy [km/h]	Raw	91.67	4.31
		Filtered	91.54	4.58
Lane 3	Flow light [veh/15min]	Raw	15.02	16.02
		Filtered	14.63	14.10
	Flow heavy [veh/15min]	Raw	0.31	0.82
		Filtered	0.32	0.92
	Speed light [km/h]	Raw	131.64	8.05
		Filtered	133.07	7.33
	Speed heavy [km/h]	Raw	91.73	4.87
		Filtered	90.73	7.38
Lane 4	Flow light [veh/15min]	Raw	60.40	45.73
		Filtered	62.38	41.17
	Flow heavy [veh/15min]	Raw	16.54	9.96
		Filtered	15.37	10.80
	Speed light [km/h]	Raw	126.04	5.33
		Filtered	127.56	4.19
	Speed heavy [km/h]	Raw	88.51	2.31
		Filtered	88.85	2.73

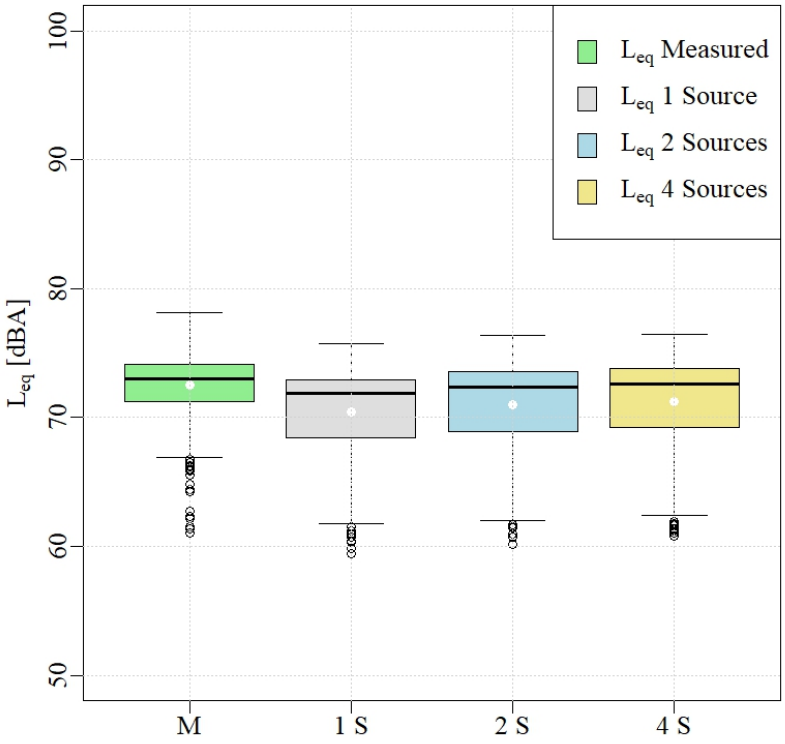


Figure 3.25: Boxplot of measured and simulated sound pressure levels (L_{Aeq}) for the three spatial modelling schemes: single source (1S), two sources (2S), and four sources (4S).

However, all simulated distributions demonstrate a larger spread compared to the measurement dataset, as evidenced by the wider Interquartile Ranges (IQR). This phenomenon is intrinsic to the stochastic nature of the framework: the random generation of individual vehicle speeds introduces a higher degree of instantaneous variability into the system than what is typically captured by the integrated 15-minute field measurements, which naturally smooth out transient kinematic fluctuations.

The qualitative trends observed in the boxplots are also supported by the descriptive statistics reported in Table 3.12.

Table 3.12: Main descriptive statistics of measured and simulated equivalent levels ($L_{A,eq,15min}$) for the three modelling schemes.

$L_{A,eq,15min}$	**Mean** [dBA]	**Median** [dBA]	**Std. Dev.** [dBA]	**Skew**	**Kurt**
Measured	72.50	73.01	2.78	-1.19	2.52
Simulated (1S)	70.46	71.86	3.39	-1.09	0.49
Simulated (2S)	70.99	72.37	3.43	-1.04	0.29
Simulated (4S)	71.25	72.57	3.38	-1.04	0.33

The analysis of the central tendency metrics highlights the progressive improvement achieved through spatial disaggregation. The 1-Source model yields a mean level of 70.46 dBA, which underestimates the measured mean (72.50 dBA) by approximately 2.04 dBA. By moving to the 4-Sources model, the simulated mean rises to 71.25 dBA, thereby narrowing the

discrepancy. A similar convergence is observed in the median values, which increase from 71.86 dBA (1S) to 72.57 dBA (4S). However, as said earlier, the standard deviation of the simulated results remains largely insensitive to the spatial configuration, fluctuating between 3.38 and 3.43 dBA across the three schemes. This indicates that the dispersion of the model outputs is primarily driven by the internal stochastic logic rather than the geometric arrangement of the sources. Consequently, while spatial disaggregation effectively corrects the mean bias (accuracy), it does not significantly alter the precision (spread) of the simulations. To provide a quantitative assessment of the predictive performance, a dedicated error analysis was conducted. The error is here computed as the arithmetic difference between the measured and simulated equivalent levels. The statistical properties of the error distributions are summarised in Table 3.13.

Table 3.13: Main descriptive statistics of the error distributions obtained with the three modelling schemes.

Errors	**Mean** [dBA]	**Median** [dBA]	**Std. Dev.** [dBA]	**Skew**	**Kurt**
Error (1-Source)	2.04	1.00	3.01	1.56	2.82
Error (2-Sources)	1.51	0.46	2.96	1.48	2.37
Error (4-Sources)	1.25	0.14	2.91	1.54	2.52

As noticed from the boxplots analysis, the error statistics confirm a reduction in the magnitude of the error as the spatial resolution increases. The mean error decreases from 2.04 dBA in the 1S configuration to 1.25 dBA in the 4S configuration. Even more significantly, the median error drops to a negligible 0.14 dBA in the 4S model, confirming that the lane-specific simulation provides a highly accurate estimation of the central tendency of the noise emission. As previously observed with the absolute levels, the standard deviation of the error is less sensitive to the spatial modelling, remaining stable around 2.9-3.0 dBA.

Correlation and Outliers Analysis

To investigate the dependencies between the prediction error and the input traffic parameters, a multivariate correlation analysis has been performed and it's represented via pairs panel plot in Figure 3.26. This graphical matrix displays bivariate scatter plots below the diagonal, histograms on the diagonal, and Pearson correlation coefficients above the diagonal. Initial screenings revealed that the prediction errors did not exhibit significant correlation with vehicle speeds (coefficients ranging from -0.07 to -0.09 for light vehicles speeds and from +0.14 to +0.16 for heavy vehicles speeds). Consequently, the analysis focused on the relationship between errors and traffic flows. The scatter plots, indeed, reveal a distinct phenomenon: as the total flow (both light and heavy) increases, the errors tend to asymptotically converge towards zero with reduced dispersion. Conversely, the highest errors are consistently associated with low traffic volumes. This behavior highlights a crucial finding regarding the model sensitivity to external factors.

The scatter plots of Error vs. Measured $L_{A,eq}$ (Figure 3.26, rows 4, 5 and 6, column 3) identify a cluster of data points where measured levels exceed 75 dBA despite being in the low-flow range. In these instances, the error exceeds 5 dBA. Since low traffic flows cannot generate such high

continuous noise levels, these outliers are attributed to external, non-traffic noise sources (e.g., sirens, anthropogenic activity, etc.) present in the field measurements but naturally absent in the simulation. Moreover, the correlation analysis confirms that all three modelling schemes exhibit identical sensitivity patterns regarding traffic flow ranges. This implies that the performance gain observed in the 4 sources model is strictly due to the geometric correction of the source position. The improvement is driven by the specific lane allocation of vehicles, probably more by the shifting of heavy vehicles to the proximal Lane 1, rather than the absolute traffic flows. Significant importance can be also attributed to the asymmetric usage of overtaking lanes by light vehicles, which further skews the acoustic center towards the receiver, with particular relevance due to Lane 2.

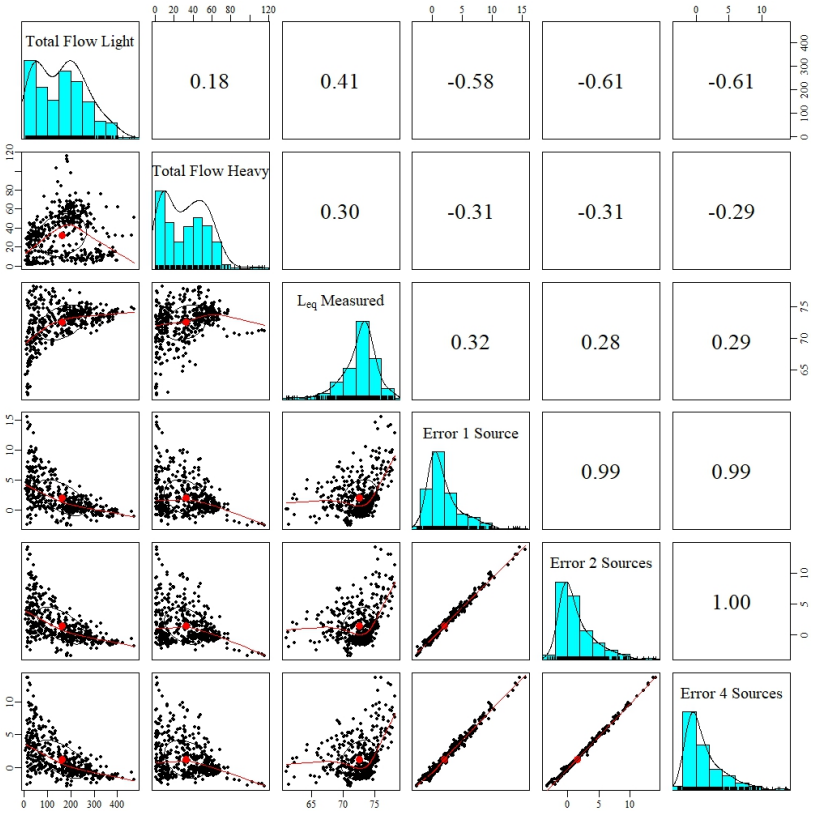


Figure 3.26: Pairs panel of the main input parameters and the error values for the 4-Sources model. Scatter plots are shown below the diagonal, histograms on the diagonal, and Pearson correlation coefficients above the diagonal.

3.5.3 Hybrid Time-Series Forecasting Implementation and Validation

The final validation phase focuses on the hybrid time-series forecasting framework described in Section 3.3. As discussed earlier, this methodology aims to integrate the stochastic microscopic traffic noise model with time series analysis models and techniques to predict noise levels based on traffic historical data. Thus, the validation aims to assess the predictive performance of this integrated framework, comparing its outputs against measured noise levels and evaluating its potential advantages over traditional road traffic noise modelling approaches.

Dataset Description and Exploratory Analysis

The validation of the hybrid time-series forecasting framework was conducted using the same LTMS dataset described in Section 3.4, to ensure consistency and comparability with the previous models presented. With the temporal analysis being the main focus of this modelling approach, no information about lane division was used, and the traffic flows were considered as aggregated over the entire carriageway. Consequently, the simulation framework followed the same logic of the stochastic baseline model,[31] assuming a simplified configuration with a single lane and unidirectional traffic to represent the traffic phenomena. Following the same procedure used for the stochastic baseline model, indeed, each vehicle has been assigned with a constant speed value, and no adjustments are introduced to account for accelaration dynamics in the modelling process. Moreover, with the free flow traffic conditions of the dataset used being confirmed, Gaussian speed distribution curves have been used to generate the individual speeds of the vehicles.

31: For this reason, the public available dataset has been used, which does not include lane-specific information. Thus, the raw dataset used for the lane-specific analysis has not been employed for the time-series forecasting validation.

To enable the integration of traffic and noise modelling within the presented hybrid framework, the model has to be executed at an hourly temporal granularity rather than using the "original" 15-minute intervals. This methodological choice was driven by the need for more stable and temporally consistent data inputs, which are better suited for time-series forecasting and model calibration. Consequently, for each category, hourly traffic volumes were derived by aggregating vehicle counts across four consecutive 15-minute intervals, while mean hourly speeds were determined using the number of vehicles in each subinterval as weighting factors. Regarding acoustic data, the $L_{A,eq,1h}$ values were computed through logarithmic averaging of $L_{A,eq,15min}$ measurements, thereby ensuring the preservation of the energetic characteristics of the sound data. However, it needs to be recalled that, unlike traffic data, which were generally more complete and continuous across the whole dataset, the acoustic measurements presented a greater number of gaps. The reason is to be found primarily in the data cleaning procedures applied by the research team responsible of the measurement campaign to remove non-road noise sources, that could have compromised the reliability of the dataset. Nevertheless, the extent of this preliminary cleaning process is not fully ascertained, as no direct control or possibility of intervention was available at this stage. As a result of these preliminary yet necessary filtering operations, several 15-minute intervals lacked valid noise data $L_{A,eq,15min}$, leading to inconsistencies across the input variables.

However, to ensure the reliability of the forecasting time-series model, it is essential to have a continuous sequence of data without gaps, as missing values can significantly affect the model ability to learn temporal patterns and make accurate predictions. An initial attempt was made to identify the longest available stretch of consecutive 15-minute intervals within the LTMS dataset in which all necessary inputs, both traffic and acoustic data, were present. However, due to the gaps and missing values in the noise measurements it was not possible to isolate a sufficiently long uninterrupted period. Consequently, the analysis was restricted to the most data-dense month available, covering a five-week period from 28 June to 1 August 2004. This timeframe was selected to facilitate the detection of recurring temporal structures in traffic phenomena, spanning both daily and weekly cycles. It must nevertheless be recognised that the selected interval corresponds to a rather specific seasonal context, encompassing the French national holiday on 14 July and coinciding with the peak summer vacation period. Such factors are

likely to influence traffic dynamics, with weekends typically characterised by holiday-related outflows and a reduced presence of heavy vehicles on motorways. These seasonal effects were also reinforced by French regulatory restrictions in force during the summer of 2004, which limited the circulation of heavy vehicles on specific days and times.[32]

The selected period was further divided in accordance with the conventional 80/20 principle often employed in data modelling and analysis: the first four weeks (28 June - 25 July 2004) were allocated for model calibration and training, while the final week (26 July - 1 August 2004) was reserved for model validation.[33] The obtained dataset includes five crucial variables for each 15-minute interval: light vehicles flows N_L, heavy vehicles flows N_H, light vehicles mean speeds v_L, heavy vehicles mean speeds v_H and $L_{A,eq,15min}$, the measured continuous equivalent sound level.

A preliminary exploratory data analysis of the selected timeframe highlighted a minor inconsistency: two records reported a zero flow of heavy vehicles, to which a corresponding zero speed was also assigned. While a zero flow has a clear physical meaning, a zero speed in this context is not physically plausible, since vehicles were not motionless or inactive but rather absent. To avoid inconsistencies in the computation of summary statistics and in the subsequent time series analysis and forecasting models, the flow values in these two records were kept as zero, while the speeds were replaced with the average speed of the heavy vehicles calculated over the entire observation period, apart from these two specific intervals.[34]

A detailed overview of the resulting dataset composition is provided in Table 3.14, whereas Table 3.15 presents a selection of its summary statistics.

32: According to these regulations, vehicles or vehicle combinations used for road freight transport with a maximum authorised gross weight exceeding 7.5 tonnes were prohibited from circulating on Saturdays and the eve of public holidays, from 22:00 on Saturday until 22:00 on Sunday and on public holidays, allowing only permanent exemptions [220, 221].

33: For each hourly record, the number of 15-minute intervals with a corresponding valid noise measurement was also documented, in order to maintain transparency regarding data completeness and quality but this information was not used for any further filtering or weighting of the data.

34: This correction is considered appropriate, as the average speed of heavy vehicles does not exhibit strong fluctuations around its mean, as will be further discussed later.

Table 3.14: A selection of lines from the dataset used for the hybrid model implementation.

# interval	Date	Time	N_L [veh/15-min]	N_H [veh/15-min]	v_L [km/h]	v_H [km/h]	$L_{A,eq,1h}$ [dBA]	15-min count
0	28-06-2004	00:00-00:59	91	20	114.5	83.7	-	0
1	28-06-2004	01:00-01:59	57	30	116.4	80.7	-	0
2	28-06-2004	02:00-02:59	51	32	116.9	80.8	-	0
3	28-06-2004	03:00-03:59	84	46	117.7	80.1	68.2	1
...	...	...	...	...	...	...	...	...
839	01-08-2004	22:00-22:59	284	14	120.9	81.8	69.0	4
840	01-08-2004	23:00-23:59	162	15	122.8	81.5	67.2	2

Table 3.15: Summary statistics of the main variables within the dataset used for the hybrid model implementation.

Variable	Mean	Std Dev	Min	Max	Skew	Kurt
N_L [veh/15-min]	601.6	507.2	7	2504	0.97	0.56
N_H [veh/15-min]	69.0	41.2	0	199	-0.06	-0.96
v_L [km/h]	118.1	3.9	95.4	127.6	-1.73	6.61
v_H [km/h]	81.7	2.4	77.5	92.6	2.04	4.13
$L_{A,eq,1h}$ [dBA]	81.7	2.4	77.5	92.6	2.04	4.13

To provide a clearer representation of the dataset and to highlight potential differences between the calibration and validation sets, the boxplots of the traffic flows, mean speeds, and equivalent sound levels

are respectively reported in Figure 3.27, Figure 3.28, and Figure 3.29, offering a concise summary of their main characteristics. The horizontal lines within each box indicate the median value of the corresponding variable.

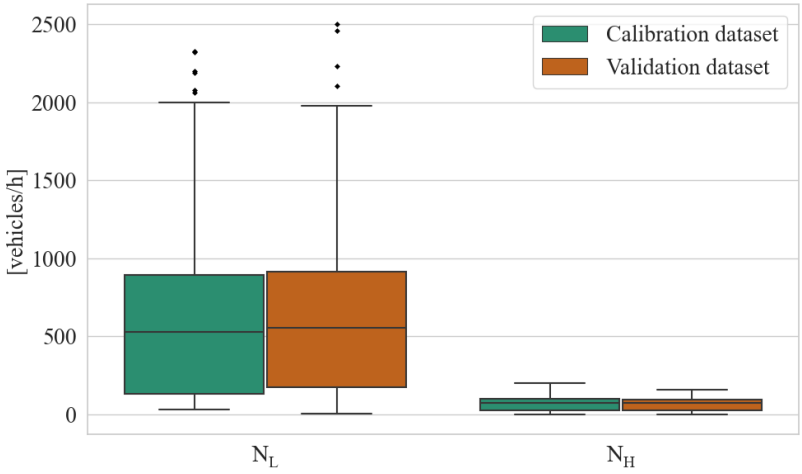


Figure 3.27: Boxplots of light (N_L) and heavy (N_H) vehicle flows, for the calibration and validation sets of the hybrid model.

Specifically, Figure 3.27 illustrates the distributions of traffic flows for light vehicles (N_L) and heavy vehicles (N_H). As expected, light vehicles dominate the traffic composition, with median values of approximately 530 in the calibration dataset and 557 in the validation dataset, whereas heavy vehicles account for a much smaller share, with median values of 74 and 75, respectively. The relatively close alignment of both N_L and N_H between calibration and validation suggests that the traffic structure has been consistently captured in the two datasets. The predominance of light vehicles is consistent with the road typology and usage patterns, and the marginal variation observed between the datasets does not indicate substantial discrepancies in traffic composition.

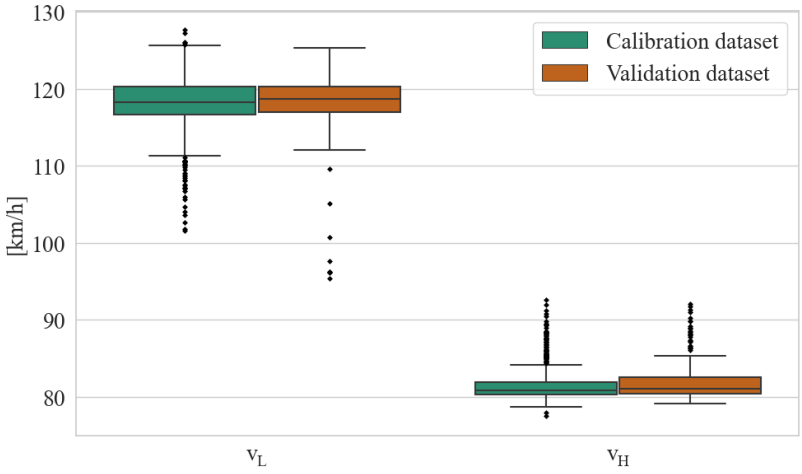


Figure 3.28: Boxplots of light (v_L) and heavy (v_H) vehicles speeds, for the calibration and validation sets of the hybrid model.

Figure 3.28, instead, reports the distributions of average vehicle speeds for both light (v_L) and heavy (v_H) vehicles. The medians confirm that light vehicles travel at considerably higher speeds than heavy vehicles, with values of 118.27 km/h (calibration) and 118.65 km/h (validation) for v_L, compared to 80.87 km/h (calibration) and 81.03 km/h (validation) for v_H. The small differences between the two datasets suggest a strong consistency in speed patterns across the two chosen subsets. Furthermore, the observed gap between v_L and v_H reflects typical traffic dynamics, where heavy vehicles are subject to both technical limitations and regulatory restrictions, leading to systematically lower speeds.

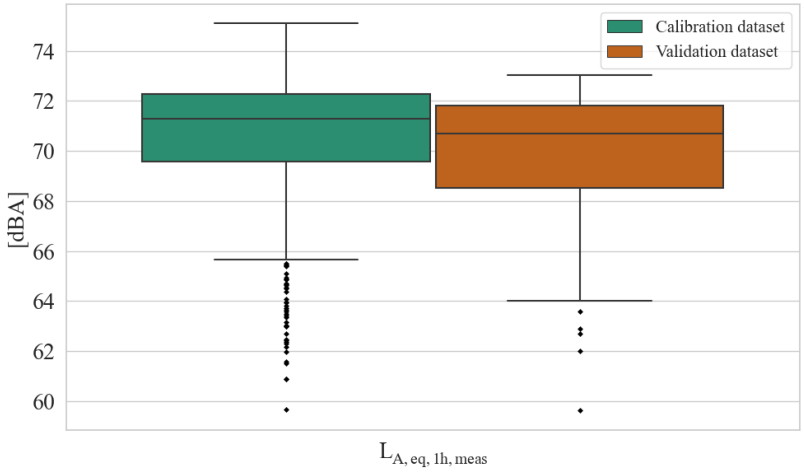


Figure 3.29: Boxplots of equivalent continuous sound level ($L_{A,eq,1h}$), for the calibration and validation sets of the hybrid model.

Finally, Figure 3.29 presents the distributions of the measured equivalent sound levels, $L_{A,eq,1h,meas}$. The median values are 71.29 dBA for the calibration dataset and 70.69 dBA for the validation dataset. Although the difference is modest, it suggests a slightly lower overall acoustic impact during the validation phase. This deviation may be due to minor variations in traffic composition or environmental conditions.

Nevertheless, the general alignment of the two distributions confirms the robustness of the sampling and provides strong evidence that the calibration and validation datasets can be regarded as statistically comparable. The limited differences observed between the two datasets are within the range of expected variability and do not indicate the presence of systematic biases in either the traffic-related or the acoustic variables. This consistency ensures that the validation phase is conducted under representative conditions, thereby reinforcing the reliability of the subsequent model assessments and supporting the robustness of the model calibration process.

Validation Results and Discussion

The following Section outlines the outcomes of the hybrid model. To ensure clarity, the results are organized according to the same framework used in the Section 3.3. Thus, first, the outcomes of the time series forecasting models are reported, highlighting their ability to capture the temporal dynamics of traffic. Next, the acoustic analysis is presented, which encompasses the application of the stochastic microscopic road

traffic noise model and its hybridization with the time series predictions, with the corresponding results critically assessed.

To obtain **time-series forecasting** of the traffic inputs necessary for the running of the microscopic stochastic model, a proper investigation of the temporal structure of the traffic variables had to be conducted. Several seasonal periods have been tested, from 24 hours up to one week, in 24-hour steps. The testing process has been achieved using the `seasonal_decompose` function from *statsmodels* in a self-written `python` routine, chosen for its efficiency in handling large-scale datasets. This function applies a commonly used decomposition method, splitting the original time series into its additive components: long-term trend, repeating seasonal pattern (according to the chosen period), and residual fluctuations. Thus, for each tested period, the proportion of variance explained by the seasonal component has been computed, allowing an objective comparison of the different seasonalities.

Table 3.16 summarises the explained variance across different tested seasonal periods for all variables. The results highlight that N_L and N_H clearly exhibit a strong weekly pattern, while the explained variance is comparatively lower for v_L and v_H. This can be attributed to the higher variability of speed measurements, which are more influenced by stochastic fluctuations and short-term conditions than by systematic weekly cycles. Nevertheless, the weekly period (168 h) still emerges as the dominant seasonal component, confirming its relevance also for the speed variables. Consequently, 168 h has been selected as the reference seasonality for each time series.

Table 3.16: Variance explained by seasonal components for different periods (24-168h).

Variable	24h	48h	72h	96h	120h	144h	168h
N_L	62.30	61.25	61.76	60.74	62.27	63.67	91.25
N_H	13.31	13.85	14.51	15.66	20.18	20.24	85.83
v_L	34.59	36.42	38.55	43.33	45.79	44.51	51.95
v_H	5.87	6.35	7.21	7.58	11.92	15.68	58.90

For each traffic variable, a combined exploratory and decomposition analysis has been performed aiming at obtaining a comprehensive understanding of their temporal dynamics, forming the basis for subsequent correlation analysis and forecasting model specification. Moreover, to further investigate the temporal dependencies and underlying structures within the traffic variables, an autocorrelation (ACF) and partial autocorrelation factor (PACF) analysis has been conducted.

Figure 3.30 and Figure 3.31, Figure 3.32 and Figure 3.33, Figure 3.34 and Figure 3.35, Figure 3.36 and Figure 3.37 show respectively for N_L, N_H, v_L and v_H the results of the decomposition and the ACF and PACF analysis.

The decomposition of N_L in Figure 3.30 highlights a well-defined weekly cycle, with traffic volumes consistently higher on weekends and reduced over weekdays. The trend component shows a medium-term variation that could be reflecting seasonal demand or summer holiday exodus. The seasonal plot instead indicates the cyclical nature of the traffic flows, with peaks at regular intervals which also confirms the corresponding high value of explained variance in Table 3.16. The residuals plot,[35] shows some sharp spikes, which may indicate irregular flows affecting the traffic phenomenon, such as around July 14th and the weekend immediately following.

35: The residuals plot is used to check if any random fluctuations remain after accounting for both the trend and seasonal components.

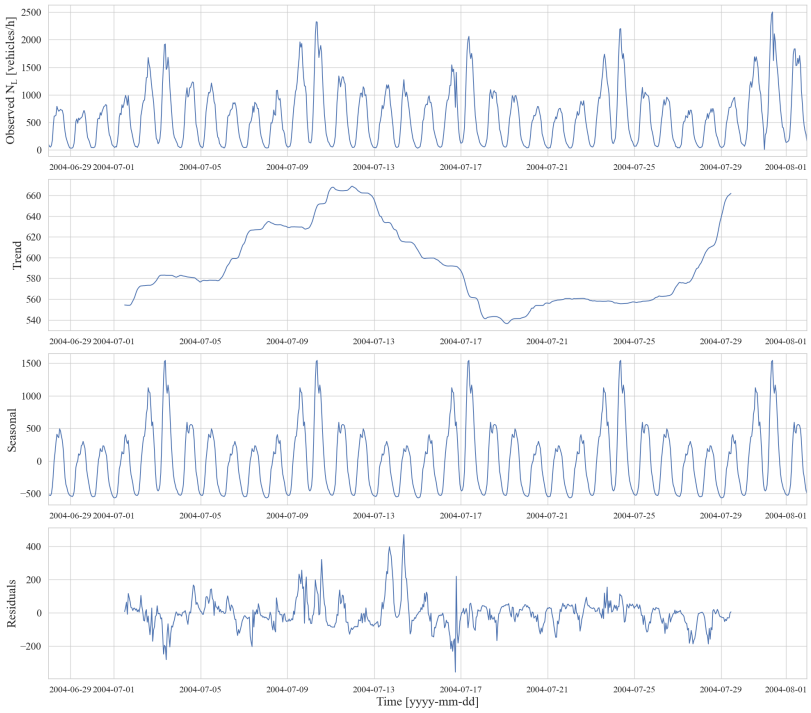


Figure 3.30: Time series and decomposition of the light vehicle flows (N_L). The original time series, the trend component, the seasonal component, and the residuals are represented.

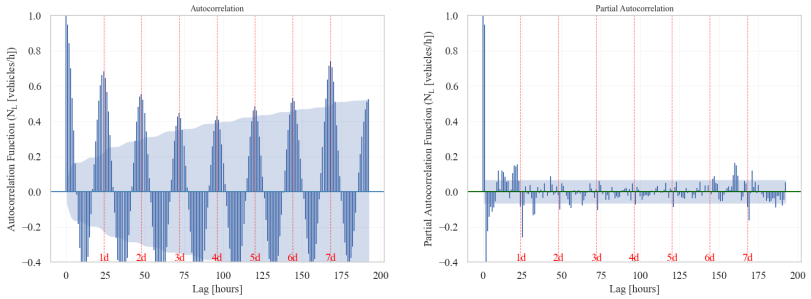


Figure 3.31: Autocorrelation (ACF) and partial autocorrelation (PACF) of the light vehicle flows (N_L).

For N_H, in Figure 3.32, the weekly pattern is even stronger, with a sharp distinction between weekdays, characterised by intense heavy flows, and weekends, when traffic demand is drastically lower. A significant drop is also clear corresponding to July 14th, which is attributable to driving bans during festive days as reported earlier [220, 221]. These insights can be confirmed looking at the trend plot which indicates a noticeable shift in the flow starting around July 10th, where a gradual decrease can be observed, followed by an increase after mid-July. The seasonal component, as in the case of light vehicles flows, clearly dominates the dynamics of the series, while the trend exhibits gradual fluctuations over time. Residuals remain limited, aside from the values measured during July 14th, which being a festive day could be considered as an irregular event in the traffic flow time-series, confirming that most systematic structures are well captured.



Figure 3.32: Time series and decomposition of the heavy vehicle flows (N_H). The original time series, the trend component, the seasonal component, and the residuals are represented.

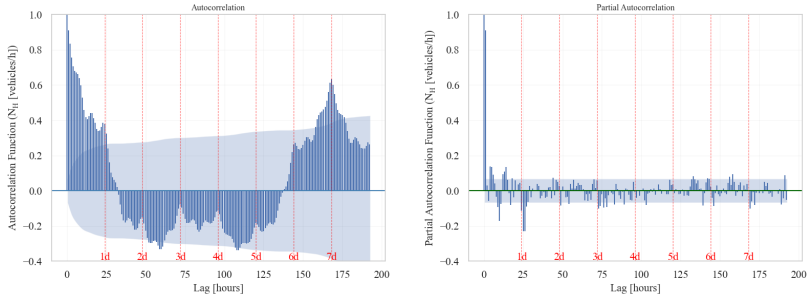


Figure 3.33: Autocorrelation (ACF) and partial autocorrelation (PACF) of the heavy vehicle flows (N_H).

The decomposition of v_L is represented in Figure 3.34. The raw time-series itself shows the data fluctuating with occasional sharp peaks and drops, suggesting high volatility in the measurements of vehicles speed. The trend remains relatively stable, with moderate variations, revealing a gradual increase in average speed, with a noticeable shift around July 14th.

However, when compared to the flow variables, as also confirmed by the explained variance reported in Table 3.16, the light vehicles mean speeds reveal a less pronounced seasonal signal. However, the noise remaining after accounting for both trend and seasonal components seems to be random.

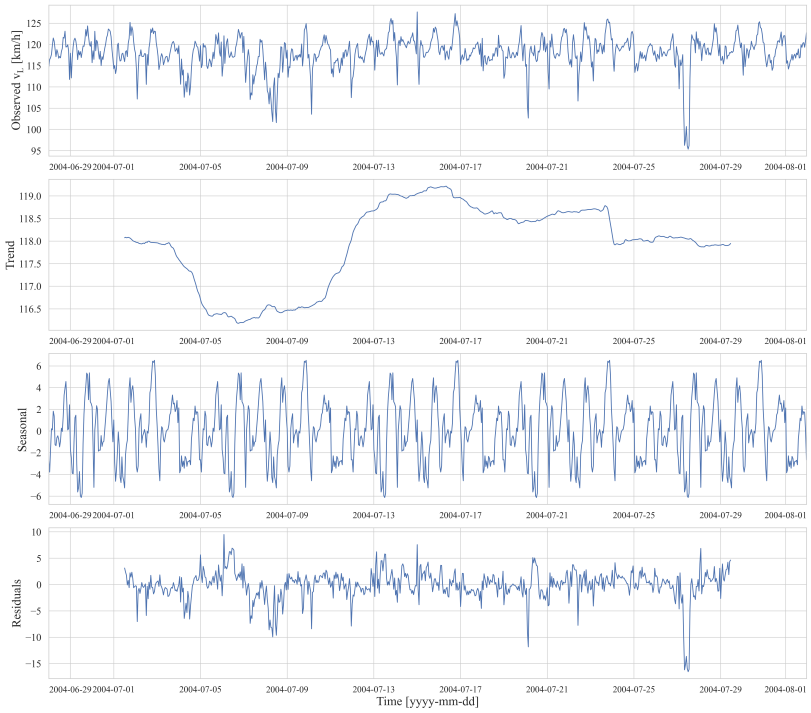


Figure 3.34: Time series and decomposition of the light vehicle speeds (v_L). The original time series, the trend component, the seasonal component, and the residuals are represented.

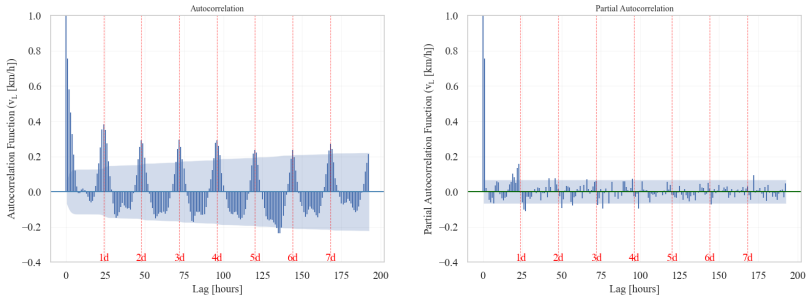


Figure 3.35: Autocorrelation (ACF) and partial autocorrelation (PACF) of the light vehicle speeds (v_L).

Also, in the case of v_H, shown in Figure 3.36, significant fluctuations in the raw data are present, with frequent peaks and valleys. In particular, higher values of mean speeds are measured during the weekends, probably due to the driving ban limits associated with vehicles or vehicle combinations used for road freight transport. Consequently, during these periods, only smaller or even medium vehicles,[36] are permitted to travel, which likely results in higher average speeds. This kind of vehicles may be more maneuverable and capable of faster travel compared to the larger, heavier trucks that are subject to the restriction, thus leading to the observed increase in mean speeds during weekends and holidays. Thus, similarly to the light vehicles mean speeds, the seasonal plot reveals periodic oscillations, suggesting cyclical fluctuations in heavy vehicle speeds. The residuals plot, finally, highlights the remaining noise after extracting the trend and seasonal components, underlying that there may still be unexplained factors affecting the variability in heavy vehicle speeds.

36: Although classified as heavy vehicles, medium vehicles such as vans and light trucks, are not subject to the same restrictions as larger heavy vehicles.



Figure 3.36: Time series and decomposition of the heavy vehicle speeds (v_H). The original time series, the trend component, the seasonal component, and the residuals are represented.

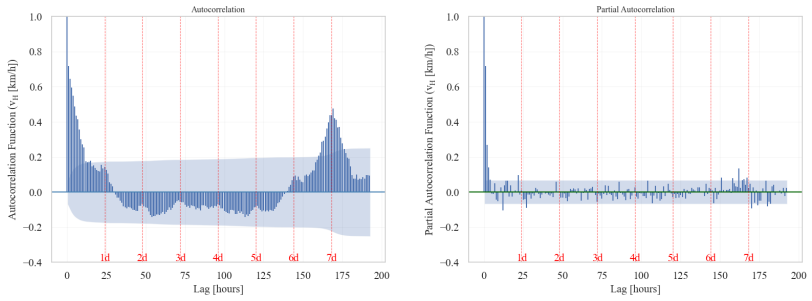


Figure 3.37: Autocorrelation (ACF) and partial autocorrelation (PACF) of the heavy vehicle speeds (v_H).

Regarding the ACF and PACF plots, it is noticeable that the ACF plots reveals always a significant correlation up to approximately 7 days, strongly supporting the idea of a weekly cycle as the dominant seasonality. As for the PACF, the gradual decay that can be observed in all the plots indicates that the dependencies span over several days, and that past observations are relevant for forecasting future values, supporting the choice of 7-day seasonality for the time-series analyses.

Based on this seasonality model identification has been then performed using the *auto.arima()* function in R, which automatically selects the best-fitting SARIMA models. Evaluation of the models has been carried out using the AIC, AICc, and BIC criteria to select the most appropriate fit for each time series. Although the self-written R routine has been implemented to evaluate and select different models based on the minimisation of each individual criteria, the results consistently pointed out to the same model for each variable. This convergence across all four time series indicated that the models selected by *auto.arima()* effectively

minimised the chosen fit criteria without the need for further model tuning or adjustment. Consequently, in Table 3.17 only a single model is indicated for each series, as it aligns with the optimal minimisation of the chosen parameters.

Table 3.17: Selected SARIMA models for each time series.

Variable	Model $(p,d,q)(P,D,Q)_s$	AIC	BIC	AICc
N_L	$(1,1,0)(0,1,0)_{168}$	6053.7	6062.14	6053.7
N_H	$(0,1,1)(0,1,0)_{168}$	4321.9	4330.3	4330.3
v_L	$(1,1,0)(0,0,1)_{168}$	3242.0	3194.2	3260.0
v_H	$(1,0,1)(0,1,0)_{168}$	2104.4	2117.1	2104.4

To assess the forecasting performance of the selected models, a visual comparison between the observed time series and the fitted values over the entire period of interest is presented in Figures 3.38, 3.39, 3.40, 3.41.

Although these visualizations span the full period covered by the dataset itself, thus going from June 28th to August 1st, 2004, it is important to note that for the final validation of the road traffic noise model, only the last week, from July 26th to August 1st, 2004, corresponding to the validation dataset, has been used. These plots provide a qualitative assessment of how well the model captures the underlying patterns in the data, allowing for an initial comparison of the observed and predicted values. However, for a rigorous evaluation, error metrics have been calculated solely on the validation set, in order to provide a more accurate measure of the model predictive ability.

Figure 3.38 shows a good alignment between the observed and predicted N_L values throughout the period. The model appears to fit the data well, capturing the fluctuations in light vehicle traffic with minimal deviation, even if there are some slight mismatches between the observed and predicted values during the last week. In particular, August 1st is characterised by a noticeable underestimation of the predicted values, due to an abnormally higher light traffic flow when compared to the observed one during the previous Sundays of the dataset.

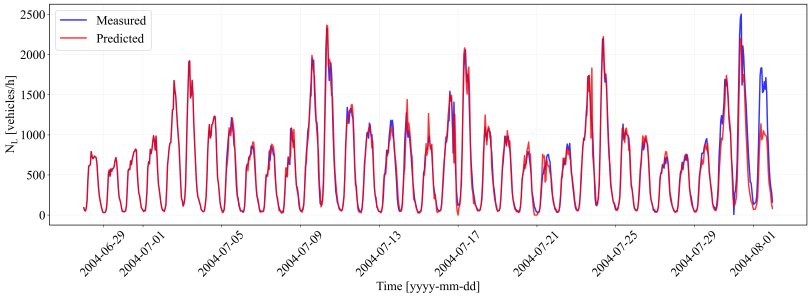


Figure 3.38: Overlapping time series of measured (blue) and predicted (red) values from June 28th to August 1st, 2004 for light vehicle flows (N_L).

Heavy vehicle flows (N_H) predictions can be observed in Figure 3.39. Both the high peaks and the lower traffic periods are reasonably well replicated. However, there are some instances where the model slightly misestimates the flow, such as during July 14th, likely due to the festive day characteristics that might not have been well represented in the training data. Nonetheless, the predictions align well with the general trend, indicating a good overall performance.

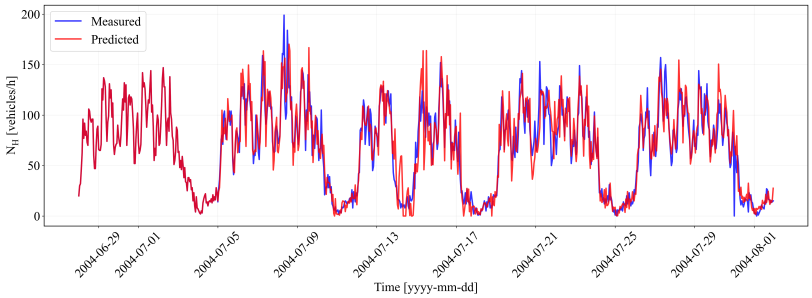


Figure 3.39: Overlapping time series of measured (blue) and predicted (red) values from June 28th to August 1st, 2004 for heavy vehicle flows (N_H).

The model performs well in capturing the overall trend of the light vehicle speed (v_L), but it struggles with accurately predicting the local fluctuations as can be seen in the right part of Figure 3.40. This could be attributed to the choice of a 168-hour periodicity for modelling the seasonality, which fails to account for the finer, more localised oscillations in light vehicle speeds. As indicated by the relatively low explained variance of around 52%, the model does not fully capture the complexity of the underlying dynamics at shorter time scales. Traffic patterns, especially for light vehicles, may exhibit more intricate, possibly daily or sub-daily variations, which are not well represented by a purely weekly seasonality. Moreover, the temporary drop in light vehicle mean speeds observed on the morning of July 27, 2004, remains unexplained, although it coincides with an unusual increase in the speed of heavy vehicles. This pattern could potentially be linked to a temporary disruption in traffic flow, such as the presence of a construction site or a lane closure, which may have created a bottleneck for light vehicles while allowing heavy vehicles to maintain or even increase their speeds. Moreover, this sudden drop in light vehicle speeds could have influenced the model predictive power, as the model might not have been able to account for such a sharp and localised anomaly. Without additional contextual data or real-time traffic information, it remains difficult to definitively pinpoint the cause of this anomaly. However, it is worth underlying that, while the model may not fully explain local fluctuations, it is still able to reflect the broader traffic patterns with reasonable accuracy.

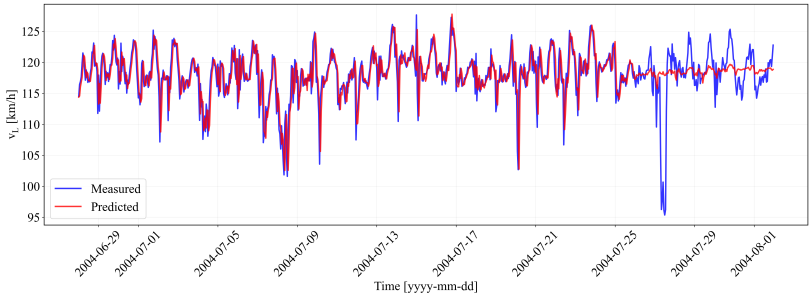


Figure 3.40: Overlapping time series of measured (blue) and predicted (red) values from June 28th to August 1st, 2004 for light vehicle speeds (v_L).

The model seems to capture the broad patterns of heavy vehicle speeds (v_H) fluctuations well as shown in Figure 3.41. However, there are some significant discrepancies which suggest that the model may need further

refinement to handle data better, although it still provides a reasonable estimate of the overall speed trend.

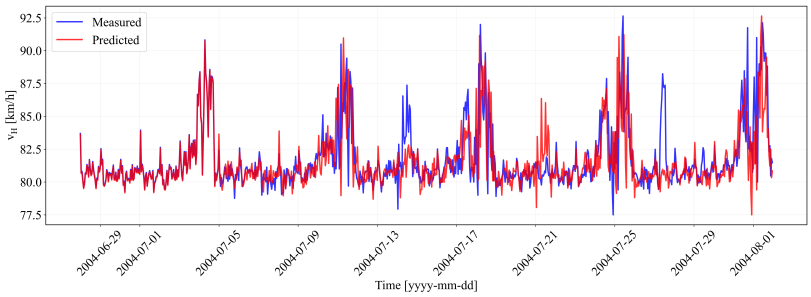


Figure 3.41: Overlapping time series of measured (blue) and predicted (red) values from June 26th to August 1st, 2004 for heavy vehicle speeds (v_H).

While the visual comparison of the observed and predicted time series provides a useful qualitative assessment of the model performance, it is important to also take error metrics into account. In Table 3.18 and Table 3.19, the most relevant residuals and error metrics for each traffic variable (i.e., ME, MAE, RMSE, and MAPE) are presented, respectively for the calibration and validation dataset, providing a quantitative assessment of the model performance.

For light vehicle flow (N_L), the model shows almost no bias during calibration, with an ME close to zero (0.075 vehicles/h). The MAE (46.35 vehicles/h) and the RMSE (84.96 vehicles/h) indicate moderate residual variability, while the MAPE of 11.66% reflects the high dispersion and presence of extreme values in the data. However, in the validation phase, the ME increases substantially, revealing a tendency to underestimate, which aligns with the high variability of the data shown previously in Table 3.15. The MAE and RMSE also rise significantly (122.55 and 208.82 vehicles/h, respectively), suggesting that the model struggles with extreme fluctuations. The MAPE reaches 28.44%, but this can be attributed to the significant variability in the traffic flow, with the presence of outliers likely inflating the error percentage as can be seen in the right part of the relative graph. As for the heavy vehicle flow (N_H), the ME remains very low in both calibration (0.016 vehicles/h) and validation (-3.11 vehicles/h), however indicating a slight overestimation. The MAE and RMSE are stable between the two phases suggesting consistent performance. However, it needs to be underlined that the MAPE is not interpretable due to division by zero values, a known issue when using this metric on traffic datasets with sparse or null flows.

Regarding speed predictions, the model demonstrates strong performance for both vehicle classes. For the light vehicle mean speed (v_L), the ME during calibration is essentially zero, with low MAE (1.91 km/h), RMSE (2.68 km/h), and MAPE (1.63%), confirming accurate estimates. In the validation period, although the ME increases slightly to -0.54 km/h, the MAE and RMSE (2.59 and 4.71 km/h) remain within acceptable ranges. The MAPE increases moderately to 2.33%, indicating a small reduction in performance but still reflecting good predictive accuracy. Similarly, heavy vehicle speed (v_H) is well predicted in both phases. The ME remains small (0.026 km/h in calibration and 0.665 km/h in validation), and both MAE and RMSE remain low (ranging from 0.9 to 1.4 km/h and 1.7 to 2.4 km/h, respectively). The MAPE values, 1.09% in calibration and 1.68% in validation, confirm the model ability to produce

reliable speed estimates even outside the training set. In summary, the model performs well in capturing the dynamics of vehicle speed and heavy vehicle flow across both datasets. However, a noticeable decrease in accuracy is observed for light vehicle flow in the validation phase, suggesting the need for further improvements, particularly in the case of extreme values for light and heavy vehicle flows.

Table 3.18: Residuals metrics for the selected models (Calibrated dataset).

Variable	ME	MAE	RMSE	MAPE
N_L	0.07	46.35	84.96	11.66%
N_H	0.02	9.62	15.19	inf
v_L	0.00	1.90	2.68	1.63%
v_H	0.03	0.90	1.68	1.09%

Table 3.19: Residuals metrics for the selected models (Validation dataset).

Variable	ME	MAE	RMSE	MAPE
N_L	98.51	122.55	208.82	28.44%
N_H	-3.11	10.71	14.33	inf
v_L	-0.54	2.60	4.71	2.33%
v_H	0.66	1.42	2.38	1.68%

Once the time-series forecasts for each traffic variable are obtained, the next step is to run the **stochastic microscopic road traffic noise model** using the predicted values as inputs. Figure 3.42 shows a comparison of the continuous equivalent sound level $L_{A,eq,1h}$ over time during the validation period. In blue the measured values are reported, while the simulated values are depicted in red. The measured data are characterised by gaps mainly present during night-time, due to periods when measurements were not available, while the simulated data are continuously available throughout the week, as the input traffic data derived from time-series forecasting models are consistently present for the simulation. Overall, this comparison highlights the strengths and limitations of the hybrid modelling approach. Measured and simulated data, indeed, exhibit similar temporal patterns, with notable peaks and troughs occurring throughout the days, reflecting the diurnal variations in traffic flow and the corresponding fluctuations in noise levels.

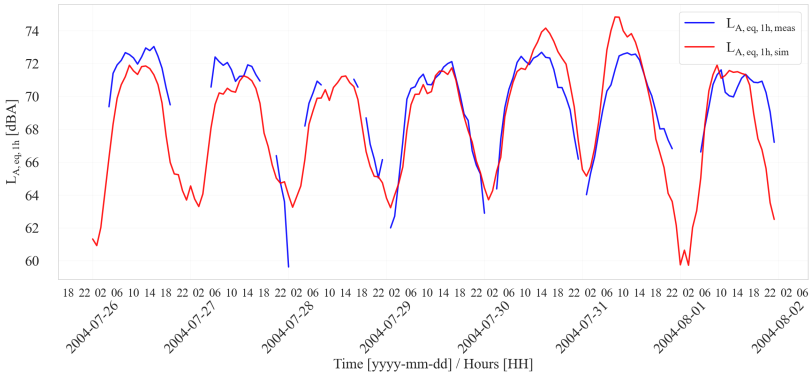


Figure 3.42: Overlapping time series of measured (blue) and predicted (red) $L_{A,eq,1h}$ values from July26th to August 1st, 2004.

However, while the simulation consistently tracks the overall trends and captures the diurnal fluctuations in traffic noise, there are periods where it diverges from the measured values. Such divergence is expected, as the hybrid model relies on two sequential models, meaning that errors from the first model (time-series forecasting) propagate into the second (stochastic traffic noise model).

As such, further calibration of both models may be necessary, particularly to refine the noise predictions during extreme cases as either very low-traffic or peak hours. Nevertheless, this comparison underscores the value of time-series forecasting for generating continuous traffic inputs, which enables noise level predictions even in the absence of direct measurements.

Figure 3.43 shows the $L_{A,eq,1h}$ boxplots for both the measured (blue) and the simulated (red) data, while their quartiles and main statistics are provided in Tables 3.20 and 3.21.

The simulated data exhibit a wider interquartile range compared to the measured data, suggesting that the model predicts more variability in noise levels, capturing a wider spectrum of noise fluctuations even if introducing a level of uncertainty. Additionally, this increased variability could be a result of cascading errors from the time-series forecasting model, as stated earlier, which may propagate through to the noise prediction, amplifying the overall uncertainty in the simulated data.

Moreover, while both datasets display similar median values, as also reported in Table VIII, the simulated data show no outliers, while the measured data include a few, indicating rare extreme noise events. The absence of outliers in the simulated data suggests that the model might not be sensitive to unusual traffic events, which are, however, characteristic of real-world conditions.

Thus, the model may not fully capture the unpredictability of traffic noise, highlighting the need for further model refinement to improve its sensitivity to extreme fluctuations.

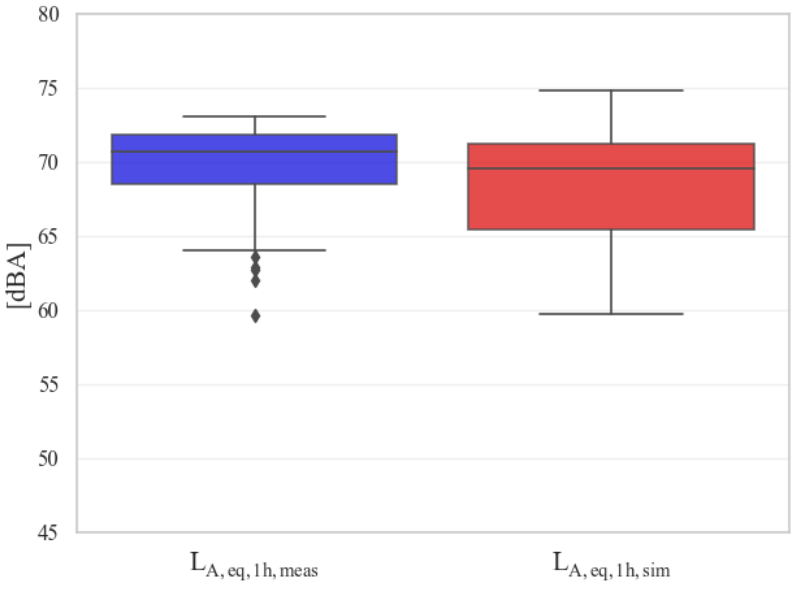


Figure 3.43: Boxplots of measured (blue) and simulated (red) $L_{A,eq,1h}$ values from July 26th to August 1st, 2004.

Table 3.20: $L_{A,eq,1h,meas}$ and $L_{A,eq,1h,sim}$ significant quartiles.

	25th [dBA]	50th [dBA]	75th [dBA]
$L_{A,eq,1h,meas}$	68.50	70.69	71.82
$L_{A,eq,1h,sim}$	65.43	69.58	71.26

Table 3.21: $L_{A,eq,1h,meas}$ and $L_{A,eq,1h,sim}$ main statistics.

	Mean [dBA]	**Std dev** [dBA]	**Min** [dBA]	**Max** [dBA]	**Skew**	**Kurt**
$L_{A,eq,1h,meas}$	69.82	2.67	59.62	73.03	-1.30	1.31
$L_{A,eq,1h,sim}$	68.46	3.51	59.72	74.82	-0.41	-0.81

Similar insights can be retrieved from the scatter plot shown in Figure 3.44, where the simulated continuous equivalent noise levels are plotted against the corresponding measured values. The red solid line represents the ideal bisector line, indicating where the points would lie if the model perfectly matched reality. The majority of points fall within the ±2 dBA range from this line, shown by the black dashed lines, with 81.2% of the points lying within this range. This highlights that the noise model predictions are generally consistent with the observed data, with minor overestimations or underestimations.

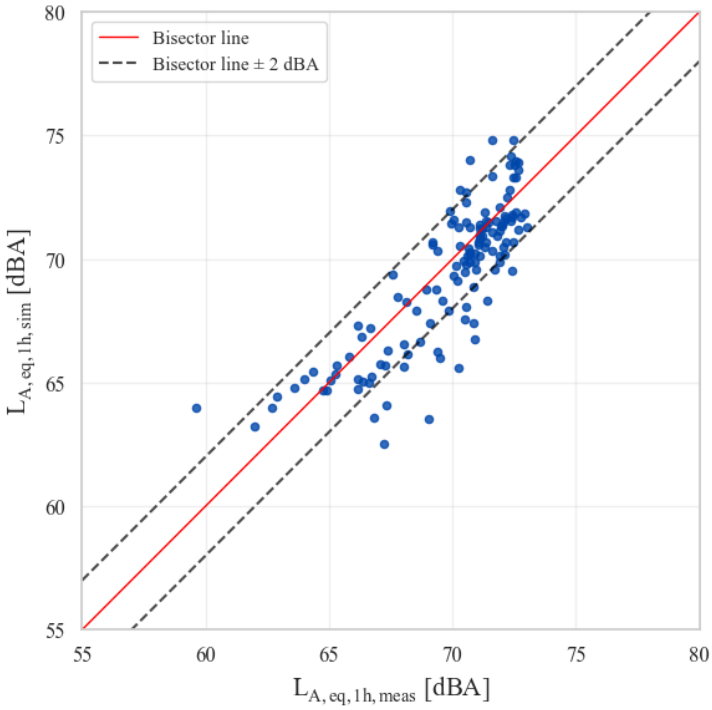


Figure 3.44: Scatter plot of simulated noise level versus the corresponding measurements.

Further observations can be made by observing the graph in Figure 3.45, which represents the error histogram of the hybrid model, and

by analysing the values reported in Table 3.22 and Table 3.24, which summarise all the hybrid model error statistics, providing significant insights into the performance of the model itself and its capability to predict road traffic noise levels.

It can be noticed that the majority of the errors, computed as the difference between measured and simulated levels, are clustered around 0 dBA, indicating that the model predictions are generally close to the observed data. The skewness of 0.23, which is relatively small, suggests that the distribution of errors is fairly symmetric. However, the mean error of 0.43 dBA and the median error of 0.51 dBA imply that there is a slight tendency for the model to overestimate the continuous equivalent noise levels, even if such a small difference confirms that the distribution of errors is not heavily influenced by extreme values, as also confirmed by the low value of skewness. Moreover, the error standard deviation of 1.63 dBA suggests that while the model predictions are generally close to the observed data, there are occasional significant deviations, which is also confirmed by the error range of almost 10 dBA. However, the presence of outliers in both the negative and positive directions, with some predictions deviating significantly from the measured data, suggests that the model does not systematically either overestimate or underestimate even if it still occasionally fails to capture noise levels under specific or dynamic traffic conditions.

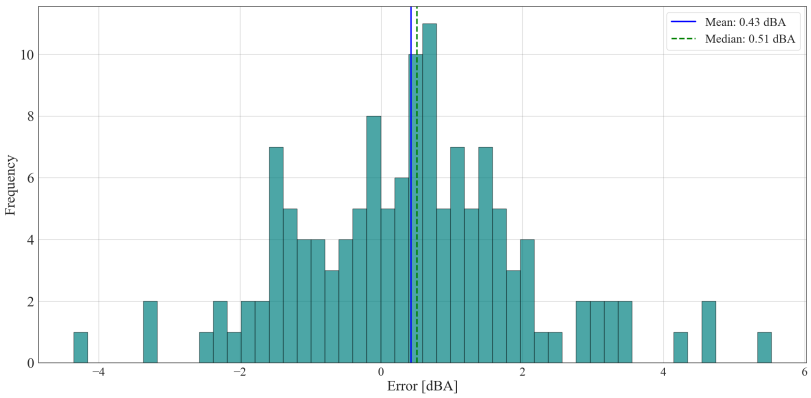


Figure 3.45: Error histogram of the hybrid model.

Table 3.22: Errors significant quartiles.

	25th [dBA]	50th [dBA]	75th [dBA]
Errors	-0.60	0.51	1.37

Table 3.23: Errors main statistics.

	Mean [dBA]	**Std dev** [dBA]	**Min** [dBA]	**Max** [dBA]	**Skew**	**Kurt**
Errors	0.43	1.63	-4.35	5.53	0.23	0.68

Even more interesting is the plot in Figure 3.46 in which the error variation over time is represented. The plot includes several important statistical lines, including the Mean Error (red dashed line), the median error (blue

dashed line), and the Mean Absolute Error (grey dashed lines). The gaps in the plot are attributable to the absence of measured data during certain time intervals.

A noticeable trend is that, aside from the initial part of the graph, corresponding to June 26th, the larger error peaks predominantly occur during the nighttime hours. This suggests that the model predictions tend to deviate more during periods of lower traffic activity, which may be influenced by reduced or more sporadic traffic data input during those times.

On the other hand, high error values can also be observed during the last three days of measurements, from Friday to Sunday. This could reflect increased traffic activity during the weekend, which the model may struggle to predict accurately due to the dynamic nature of traffic flow or other external factors not fully captured by the model, as also commented earlier.

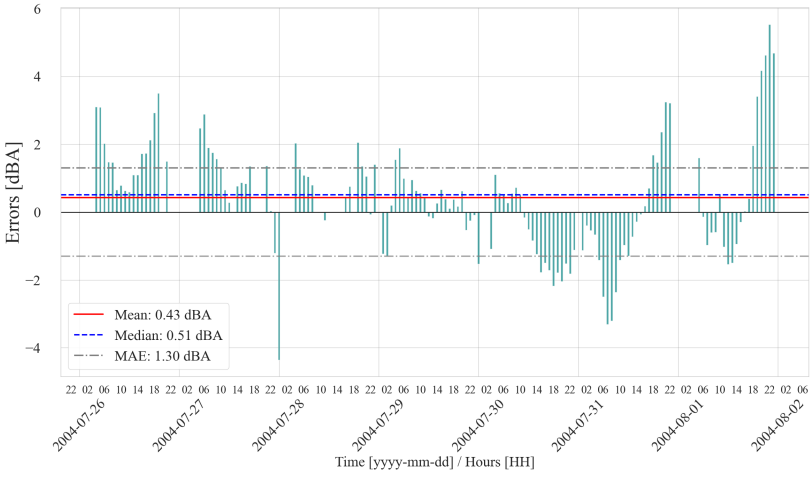


Figure 3.46: Error over time of the hybrid model.

Lastly, the error metrics are presented in Table 3.24, in order to achieve a full comprehension of the hybrid model predictive capabilities.

The MAE of 1.30 dBA is a reasonable error when predicting environmental noise, suggesting that the model is fairly accurate for its purpose. However, the observed discrepancy between the MAE and the RMSE (1.69 dBA) indicates that the model is sensitive to a small number of time intervals with higher predictive errors.[37]

37: Such higher predictive errors may be stemming from the extreme fluctuations in light vehicle traffic recorded during the final validation weekend.

This "penalty" in the squared error metric reflects the challenge of forecasting holiday-related traffic spikes that deviate from the historical seasonal trend. This is also confirmed by the MSE of 2.85 dBA^2, which gives more weight to larger errors and provides a more sensitive measure to larger discrepancies reflecting the overall squared deviation of the model predictions from the observed data.

The MPE of 0.60% and the MAPE of 1.88% are very low percentages, indicating that, on average, the model predictions are very close to the actual values when expressed relative to the measured data. This small percentage error suggests that the model is highly reliable on average, with only minor discrepancies when compared to the observed noise levels.

Table 3.24: Summary error metrics of the hybrid model.

ME [dBA]	**MAE** [dBA]	**MPE** [%]	**MAPE** [%]	**MSE** [dBA^2]	**RMSE** [dBA]
0.43	1.30	0.60	1.88	2.85	1.69

To contextualise the performance of the proposed hybrid model, this Section also provides a **comparative analysis** against two alternative modelling approaches. The first comparison benchmarks the hybrid model against the core stochastic model when supplied only with measured traffic data, thereby isolating the impact of the time-series forecasting component and such two-step modelling chain. Thus, to quantify the impact of this hybridization, the stochastic microscopic model has been re-run for the validation period only (26 July - 1 August 2004) using the actual measured traffic inputs, e.g. flows and mean speeds for each considered vehicle category, instead of the SARIMA-forecasted values. This allows for a direct assessment of the error introduced by the time-series forecasting step.

The second comparison, on the other hand, evaluates the hybrid model against the established CNOSSOS-EU framework, in order to highlight the benefits of a microscopic approach over a more conventional, macroscopic methodology. Figure 3.47 provides a visual comparison between the time histories of the measured noise levels and the predictions from both the hybrid (red line), the stochastic (green line), and the CNOSSOS-EU (grey line) models over the validation week. As depicted in the Figure 3.47, all simulation frameworks successfully capture the characteristic diurnal pattern of traffic noise, with levels rising during the day and falling at night, confirming the fundamental validity of each approach. However, a closer inspection reveals significant differences in their performance and accuracy. The microscopic approaches seem to be more accurate than the macroscopic approach represented by the CNOSSOS-EU formula, being able to follow more correctly the measured noise levels patterns. The CNOSSOS model systematic underestimation, indeed, can be attributed to its macroscopic approach, which relies on averaged inputs and may not fully capture the acoustic energy of the most intense, short-term traffic events that microscopic models are designed to acknowledge.

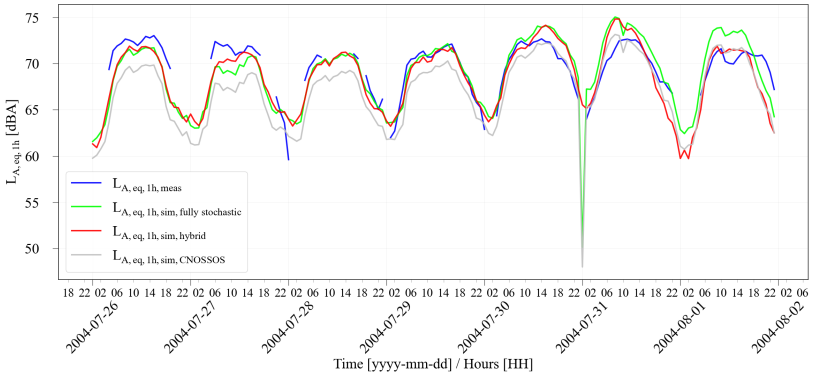


Figure 3.47: Overlapping time series of measured (blue), hybrid model predicted (red), and fully stochastic model predicted (green) $L_{A,eq,1h}$ values from July 26th to August 1st, 2004.

The stochastic model shows good adherence to the measured data where available, confirming the high intrinsic accuracy of the core stochastic noise simulation engine when provided with precise traffic inputs.

An insightful event is observed on July 31st, where an anomalous, sharp dip appears in the predictions of both the stochastic-only and CNOSSOS models. This dip is attributable to the difference between the measured and forecasted input values, which are very far apart for that hour, being significantly lower for both the measured light vehicles and heavy vehicles flows than the predicted ones. This occurrence highlights a critical distinction between real-time monitoring and predictive forecasting. While the forecasting component of the hybrid model proved resilient to this specific input outlier, effectively "smoothing" the acoustic curve to produce a more plausible noise estimation, it is important to categorise this behavior as statistical robustness rather than absolute accuracy. In this instance, the forecasting model is structurally "blind" to non-periodic anomalies, such as the identified sensor maintenance gap or potential temporary road disruptions, that are clearly not reflected in historical weekly patterns. Consequently, while the hybrid framework provides a reliable tool for planning and general environmental assessment where real-time data is unavailable, it does not replace the need for direct measurements when capturing unique, non-recurring acoustic events or sudden micrometeorological shifts is required [223]. Observing the surrounding data, that specific hour could be associated with an erroneous data point within the measured traffic input stream. In particular, high values of traffic flows, both light and heavy vehicles, are observed immediately before and after, and the noise level is actually missing only in such a particular hour, suggesting a maintenance of the measuring stations or a removal of the measured sound level due to the concurrence of external noise sources. Notably, the hybrid model forecasting component proved resilient to this input outlier, producing a more plausible noise estimation and highlighting a key advantage of its approach in handling erroneous data.

A closer analysis of the final day of the validation period reveals a more nuanced aspect of models performances. On August 1st, the hybrid approach exhibits a closer correspondence with the measured data than the fully stochastic approach, even if a strong underestimation in the light vehicle flow predictions has been noticed. This may suggest either that the cascading error expected to be introduced by the double-chain model does not emerge under these conditions or that the hybrid framework is capable of mitigating, at least in part, the propagation of model inaccuracies across successive stages. Nevertheless, it is crucial to recognise that the apparent improvement in predictive accuracy could also result from a compensatory mechanism, whereby errors generated in different components of the model partially offset one another, thus leading to an overall reduction in the discrepancy with the empirical data.[38] Moreover, even if the temporal trend of the predicted noise levels aligns more closely with the measurements, the residual discrepancies remain significant, as clearly illustrated in Figure 3.46.

38: It is plausible that this initial underestimation of light vehicle flows contributes to a compensatory mechanism that offsets the general modelling error, thereby yielding a seemingly improved agreement with the measured sound levels.

Table 3.25 provides a quantitative summary of the error metrics, allowing for a direct comparison of the different approaches performance. The hybrid model emerges as the most accurate predictor overall. This is evidenced by its better performance across the primary accuracy metrics, achieving the lowest MAE, MAPE, and RMSE. Furthermore, it displays the lowest standard deviation of the error, indicating that its predictions are the most consistent. In particular, the reported MAE of 1.30 dBA for the hybrid model represents a significant improvement over the

established CNOSSOS-EU benchmark, which exhibits a notably higher MAE of 2.06 dBA under the same conditions. This underscores the advantage of microscopic modelling over macroscopic approaches in capturing the road traffic acoustic energy. This better performance, even when compared to the model fed with measured data, can be attributed to the forecasting component resilience to anomalies in the input traffic data, which prevents large, isolated errors and results in a more stable and reliable overall prediction. However, it is important to acknowledge a key limitation of this analysis: the comparison is inherently constrained to the time intervals for which measured noise data are available. Given the significant gaps in the acoustic dataset, particularly during nighttime hours, the calculated error metrics may not fully represent the model performance across all operating conditions. It is therefore possible that the true overall error could differ if a complete validation dataset were accessible for comparison.

Table 3.25: Summary error metrics of the compared model.

Model used	**ME** [dBA]	**Std dev** [dBA]	**MAE** [dBA]	**MPE** [%]	**MAPE** [%]	**MSE** [dBA^2]	**RMSE** [dBA]
Fully stochastic model	-0.15	1.84	1.52	-0.24	2.18	3.42	1.85
Hybrid model	0.43	1.63	1.30	0.60	1.88	2.85	1.69
CNOSSOS-EU model	1.71	1.83	2.06	2.43	2.94	6.30	2.51

While the potential for error compensation and the limitations imposed by gaps in the validation data must be carefully considered, the hybrid framework performances confirm it as a highly effective and practical tool. In particular, the hybrid framework seems to be well-suited for forward-looking applications where real-time data are inherently unavailable. This includes critical tasks in urban and infrastructure planning, designing and evaluating the potential effectiveness of noise mitigation strategies before construction, and performing analyses to explore the acoustic consequences of changes in traffic management policies. Therefore, the hybrid model represents a valuable step forward, providing planners and engineers with a reliable method for proactive noise assessment.

3.6 Final Remarks

This Chapter presented the development, implementation, and rigorous validation of a novel microscopic and stochastic framework for road traffic noise modelling. Motivated by the inherent limitations of conventional macroscopic and deterministic approaches, which typically rely on aggregated traffic parameters and centralised line sources, the proposed methodology shifts the analytical focus to the individual vehicle kynematics and dynamics. By assigning specific, randomly generated speeds drawn from probability distribution curves, the stochastic model successfully preserves the distinct acoustic energy of each transit, thereby capturing the intrinsic variability and transient kinematic fluctuations of real-world traffic phenomena.

Applying the standard CNOSSOS-EU emission equations to discrete point sources rather than a homogenised continuous line source enables the model to effectively evaluate the Sound Exposure Level (SEL) for each individual vehicle pass-by. The subsequent energetic aggregation of these discrete transits into an overall equivalent continuous sound level ($L_{A,eq}$) was validated against a robust Long-Term Monitoring Station

(LTMS) dataset. The results demonstrated that this bottom-up, stochastic approach accurately mirrors the actual distribution and central tendencies of measured free-flow noise levels, overcoming the loss of resolution typical of traditional models.

A pivotal enhancement explored in this research was the transition from a simplified, centralised source representation to a fully lane-specific spatial disaggregation. The comparative analysis among the different modelling schematisations of the traffic sound source introduces systematic errors in geometrical divergence, particularly in near-field propagation scenarios. When the spatial homogenisation of traffic flows is overcome by accurately allocating vehicles to their respective lanes, the model's predictive accuracy significantly improves, reducing the Mean Error from 2.04 dBA (in the single and central source configuration) to 1.25 dBA, and dropping the median error to a negligible 0.14 dBA. However, while spatial disaggregation effectively corrects the mean bias to improve overall accuracy, the standard deviation of the error remained largely stable. This indicates that the dispersion of the model output is primarily governed by the internal stochastic logic of the traffic flow, whereas the geometric correction of the source position is paramount for eliminating systematic underestimations.

To extend the framework's applicability to data-scarce scenarios, such as the early design phases of transport infrastructure, a hybrid methodology coupling the stochastic core with Seasonal Autoregressive Integrated Moving Average (SARIMA) time-series forecasting was introduced. By coupling the stochastic core with SARIMA time-series forecasting, the model successfully predicted dynamic traffic flows and average speeds based on historical patterns. The acoustic validation of this hybrid model yielded highly reliable results, achieving a Mean Error of just 0.43 dBA. Notably, prediction errors consistently spiked primarly during low traffic volume periods. Rather than indicating a model flaw, this discrepancy highlights that in low-flow regimes, the acoustic environment ceases to be strictly traffic-dominated and becomes highly susceptible to external, non-recurring anomalous events. The model's deviation from field measurements in these instances thus demonstrates its potential secondary utility as an anomaly-detection tool for environmental monitoring.

Despite these promising outcomes, specific limitations chart the course for future research. The current energetic summation approach assumes independent transits, neglecting the acoustic screening effects that naturally occur between vehicles in high-density scenarios. Moreover, the assignment of constant speeds per transit simplifies the transient kinematics (e.g., accelerations) typical of congested flow. Finally, while the absence of a background noise component highlighted the tool's potential for anomaly detection, future developments must integrate non-traffic ambient noise to refine accuracy during quiet, nighttime regimes, alongside advanced cross-context calibration to minimise the cascading of uncertainties from the forecasting stage.

Ultimately, the microscopic stochastic model developed in this Chapter represents a significant methodological leap beyond standardised macroscopic models. By successfully integrating high-resolution spatial geometries and temporal predictive forecasting, the model provides a highly adaptable, modular, and physically consistent tool. It doesn't enhance the granularity of current environmental noise assessments but it also lays a robust foundation for proactive urban planning, allowing policymakers and engineers to simulate and mitigate dynamic noise exposures long before new infrastructure is built.

Beyond Physical Indicators: the Soundscape Approach to Map the Intangible

4

4.1 Changing the Paradigm: from Physical Metrics to Perceptual Experience Assessment 108
4.2 The Ontology of Soundscape: from its Definition to ISO Standards 110
4.3 The University Campus as a Soundscape Laboratory 118
4.4 Case Study: The Fisciano Campus of the University of Salerno . 121
4.5 Material and Methods: Analyse the Campus Soundscape and Map its Pleasantness 123
4.6 Soundscape Dataset Description and Analysis 130
4.7 Mapping Pleasantness of the Campus Soundscape: Results and Discussion 140
4.8 Final Remarks 155

The assessment of the urban acoustic environment has historically relied on the precision of physical modelling and the rigorous quantification of sound pressure levels. Within the European regulatory framework, the accurate modelling and mapping of transportation noise has represented, indeed, a fundamental milestone in assessing long-term public health risks, and designing technical mitigation measures [25]. Standardised indicators, such as the day-evening-night level (L_{den}), have provided a robust, energy-based metric to quantify noise levels harmful thresholds and their potential impact on human health [24, 25, 27–29, 31, 33]. Yet, as the field of environmental acoustics evolves, it is increasingly evident that a purely physical energetic description of sound, centered on the logarithmic summation of acoustic energy, captures only a partial segment of the phenomenological reality of complex acoustic environments.

This Chapter argues for a necessary transition from the physical management of "noise" to the multi-dimensional, perceptual appraisal of the "soundscape" [224]. This shift acknowledges that the human response to the acoustic environment is not merely a function of intensity, but is deeply rooted in the cognitive interpretation of sounds in context [225, 226]. Building on this novel concept, this Chapter seeks to firstly address the theoretical foundations of this paradigm shift, examining the inherent mismatch between conventional physical metrics and the nuanced reality of human auditory experience. This involves a reorientation from a *pathogenic* perspective, which views sound primarily as a harmful pollutant, to a *salutogenic* one, which views sound as a resource for well-being. Withing this framework, the *Attention Restoration Theory* (ART) [69, 70] and the *ISO 12913 series* [227–229] are presented to provide a standardised scientific vocabulary for soundscape analysis.

The second part of the Chapter transitions to an empirical investigation of a multifaceted soundscape, which is university campus. Using such a setting as a case study, the Chapter delves into capturing the acoustic and perceptive character of different environments, by introducing a novel rigorous methodology to map pleasantness in different areas, comparing objective measurements with subjective evaluations. More specifically, maps obtained through data collected through a crowdsourced approach, are compared with on-site questionnaire and soundwalk ratings. This mixed-methods approach is fully described in appended **Paper E and F**. Drawing directly from this methodological framework, spatial and temporal analyses are then applied to refine such methodologies for mapping subjective perception:

- The **spatial analysis** specifically entailed the integration of land use maps to formally assess how land cover and the characteristics of distinct functional areas with their related sound sources influence the perception of the acoustic environment (**Papers G**).
- The **temporal analysis** focused on longitudinal analysis to understand how perception evolves in response to dynamic changes, such as new infrastructure development (evolving scenarios) or predictable fluctuations in sound sources presence and predominance (**Paper H**).

4.1 Changing the Paradigm: from Physical Metrics to Perceptual Experience Assessment

The historical reliance on energetic metrics reflects a reductionist theoretical perspective, where the acoustic environment is treated primarly as a physical emission to be managed, rather than a sensory experience to be perceived. This "energy-equivalent" paradigm operates on the fundamental assumption that the human auditory system functions analogously to an integrating sound level meter. By accumulating acoustic energy over standardised periods (24 hours for L_{den}, or specific time blocks for L_{day}, $L_{evening}$, and L_{night}) this appoach seeks to produce a single, quantifiable value representing "noise exposure".

While this methodology has been proven robust for estabilishing the thresholds of physiological damage [25, 28], such as noise-induced hearing loss in occupational settings or cardiovascular risk in residential populations exposed to high-intensity transport noise, it exhibits significant limitations when applied to the subtle, multidimensional experience of urban public spaces [30, 32, 34, 38, 39, 189, 224, 230]. The core of this limitation lies in the fact that an acoustics environment is far more than a sum of decibels; it is a complex stream of information that individuals constantly interpret through cognitive and emotional filters [226, 231].

Consequently, a paradigm shift is required to address the inherent gap between physical sound pressure levels and human well-being. As explored in the following Subsections, this transition is not merely a change in measurement techniques, but a theoretical move toward the concept of soundscape. By placing human perception and context at the forefront, the soundscape approach allows for a holistic understanding of the "intangible" qualities of the environment, qualities that traditional energetic metrics inherently fail to capture [232, 233].

4.1.1 The Mismatch Between Physical Metrics and Human Experience

The limitations of the L_{den} and L_{eq} metrics become starkly apparent when examining the "mismatch" between measured levels and reported annoyance or comfort. A solely energy-based approach, indeed, presumes a monotonic dose-response relationship: as sound pressure levels rise, annoyance increases and comfort decreases. However, empirical studies in urban open spaces consistently demonstrate that this linearity breaks down, particularly at moderate sound levels [233]. Yang and Kang, using questionnaires and objective sound level measurements found out that significant differences can be observed between the subjective ratings of sound levels and the acoustic comfort evaluations at the same measured L_{eq} values [234]. Their research indicates that when sound levels fall within below a certain threshold, typically cited around 65-70 dBA, the correlation between sound pressure levels and perceived acoustic comfort weakens significantly. In these scenarios, the *source* of the sound becomes the dominant factor of human response, overshadowing the mere intensity of the sound [234–236]. For example, a heavy goods vehicle and a cascading fountain may generate identical L_{eq} values of 65 dBA over a 15-minute period. Under the energetic paradigm, these two acoustic events are indistinguishable; they contribute an equal "dose" of noise to the environment. Yet, to the human observer, the phenomenological experience is radically different. The vehicle noise is often perceived as

intrusive, rough, and fluctuating in a way that demands involuntary attention, triggering a stress response. Conversely, the fountain is often perceived as soothing, masking other intrusions, and contributing to a sense of "vibrancy" or "calmness" in the environment. This discrepancy clearly highlights the inadequacy of relying solely on energetic metrics to capture the full spectrum of human auditory experience [237, 238].

4.1.2 Theoretical Reorientation: from Pathogenic to Salutogenic

To transcend the limitations of physical metrics, a theoretical reorientation is clearly required: a shift from the pathogenic model of environmental health to the salutogenic model [226]. This shift frames the core argument for the soundscape approach, positioning the acoustic environment not merely as a hazard to be neutralised, but as a resource to be enhanced [224].

As reported earlier, the traditional noise control approach is inherently pathogenic. It is rooted in the assumption that "noise" is the pathogen,[1] while "silence" or "quiet" is compared to a state of health. From this perspective, noise is definetely just an unwanted intrusion, a source of stressors that deplete the individual's coping resources, that must be eliminated or reduced to protect public health. While this perspective is vital for protecting populations from extreme exposure [24, 27, 28, 31, 33], it offers little guidance for the design of environments where people want to be. Such a view neglects the positive aspects of sound and its potential benefits, such as its ability to enhance mood, facilitate social interaction, and contribute to a sense of place and identity [239–241].[2]

1: The term "pathogen" here is used metaphorically to describe noise as an environmental factor that causes harm or adverse health effects.

In a salutogenic framework, on the other hand, the acoustic environment is seen as a dynamic interplay of sounds that can either support or hinder well-being.

The salutogenic orientation, proposed by medical sociologist Aaron Antonovsky, asks a different question: "*What causes health?*" rather than "*What causes disease?*" [242, 243].[3] This approach recognises that stress is ubiquitous and, even more important, unavoidable in human life. Health, therefore, is not the absence of stressors, but the ability to cope with them successfully. This ability depends on the availability of what have been called "*Generalised Resistance Resources*" (GRRs), which can be biological, material, or psychosocial. Applied to acoustics, the salutogenic perspective suggests that the acoustic environment can actually function as a GRR, instead of simply a source of stress. Access to high-quality acoustic spaces, such as quiet courtyards, vibrant social plazas, or naturalistic parks can help individuals recover from the depletion of resources caused by daily urban living. This aligns with the "*Restoration Perspective*" in environmental psychology, which views the environment as a mediator of stress recovery [243, 244].

2: A notable case of sound as a marker of a place identity is seen in the interlude *"No. 29"* by BTS. The track utilizes the resonance of the Sacred Bell of Great King Seongdeok (South Korea's National Treasure No. 29) as a symbolic, heritage-centered transition. This integration demonstrates how even contemporary music and worldwide phenomena like K-pop increasingly recognizes the role of sound as a primary signifier of geographical and cultural identity, leveraging specific sonic artifacts to ground a globalized medium in the ancestral roots of a specific people. The interlude lasts exactly 1 minute and 38 seconds, precisely replicating the decay time required for the bell's harmonic resonance to fade into silence after being struck. By preserving this specific duration, the sound functions as an "acoustic anchor", bridging historical artifact and contemporary medium to reinforce a sense of national and cultural belonging through its unique reverberant profile.

3: *"I hope it will become clear in due course that my concern is no mere semantic quibble and that here, as in all of science, how one poses the question is crucial to the direction one takes in looking for the answers*" - A. Antonovsky, 1979 [242].

The mechanism by which soundscapes support salutogenesis is frequently explained through Kaplan's *Attention Restoration Theory* (ART) [69, 70]. ART suggests that modern urban life places a heavy demand on "directed attention" (voluntary, effortful focus), leading to "mental fatigue". This kind of attentional fascination is also referred to as "*hard fascination*", as it requires significant cognitive effort to maintain focus on specific tasks while filtering out distractions. Prolonged engagement in such environments can deplete cognitive resources, resulting in decreased concentration, irritability, and overall stress [70].

To recover, individuals need access to environments that do not require directed attention but instead engage "involuntary attention" or "*soft fascination*".[4] Natural environments are particularly effective in this regard, as they provide stimuli that capture attention effortlessly, allowing the cognitive system to rest and recover. These natural settings often moderately hold attention, however leaving enough cognitive capacity free for reflection and recovery [70].

For Kaplan, a restorative environment is characterised by four key components:

- **Being Away**: The environment must provide a conceptual or physical sense of escape from routine mental contents;
- **Extent**: The environment must be rich and coherent enough to engage the mind and constitute a "whole other world";
- **Fascination**: The environments must contain elements that effortlessly capture attention.
- **Compatibility**: The environment should align with the individual's purposes and inclinations.

Sound clearly plays a significant role in all four properties. Natural soundscapes, indeed, are archetypal triggers of soft fascination. The complex, non-repeating, yet rhythmic nature of sounds like rustling leaves, bird songs, or flowing water can effortlessly capture attention without draining cognitive resources. Moreover, the acoustic horizon defines the sense of "being away" by creating an auditory boundary that separates the individual from their immediate environment.[5]

Research confirms that soundscapes dominated by natural sounds facilitate recovery from psychological stress more effectively than those dominated by anthropogenic noise [60, 62]. Physiological markers, such as skin conductance levels and heart rate variability, show faster returns to baseline in natural soundscapes. In this regard, several literature studies analyse how the direct exposure to a green environment helps to restore and relax people's mind, contributing to creating a sense of calm and tranquillity and to the overall mental well-being [63].[6] Thus, the soundscape is a tangible public health resource, capable, if well designed, of accelerating the renewal of adaptive resources depleted by urban living.

4: This approach aligns with environmental policies like the EU Environmental Noise Directive (2002/49/EC), which mandates the identification and preservation of "Quiet Areas" in open country and agglomerations. These areas serve as essential urban GRRs, providing the necessary "soft fascination" to recover from cognitive fatigue by shielding individuals from high-intensity anthropogenic noise. Moreover, recent legislations, such as the "Right to Disconnect" proposal, can be seen as an institutional recognition of the need for "soft fascination" in the modern work environment, allowing employees to disengage from work-related communications and recover from cognitive fatigue.

5: If one is visually in a park but aurally surrounded by traffic sirens, the sense of escape is broken. Conversely, a high-fidelity soundscape (where distant sounds are distinct) enhances the sense of "Extent".

6: By designing environments that prioritise pleasant and calming sounds while minimising the "unwanted" noise, indeed, individuals experience reduced stress levels and improved overall well-being as reported in the research of Aletta et al. [57]. Such a target is also in line with the European Environment Agency (EEA) guidelines, which require preserving environmental noise quality where it is good [245].

4.2 The Ontology of Soundscape: from its Definition to ISO Standards

4.2.1 Definitions of Soundscape: What is the Soundscape? - ISO 12913-1: 2014

The transition from "noise" to "soundscape" is not merely semantic; it represents a fundamental change in the ontology of the objective of the study.

The term "*soundscape*" has a dual lineage that has led to significant conceptual divergences [246]. First coined by the urban planner Michael Southworth in 1969 [247], it was used to describe the acoustic properties of city spaces, focusing on how sound influences the perception of urban forms. However, it was popularised and defined more comprehensively by R. Murray Schafer and the World Soundscape Project in the 1970s [248–250]. Schafer, a composer, approached the world as a macrocosmic

musical composition.[7] He introduced terms like "*keynote sounds*" (background sounds that define a place), "*soundmarks*" (unique sounds that are emblematic of a location), and "*acoustic ecology*" (the study of the relationship between humans and their sonic environment) [250].

7: Some extracts from Schafer's work illustrate this perspective: "And the new musicians: anyone and anything that sounds!", "The sounds of the universal orchestra are infinitely varied" - R. Murray Schafer, 1969 [248].

As the concept migrated across disciplines, definitions fractured. For example, in wildlife ecology, "soundscape" refers to the physical collection of sounds in a landscape, categorised into "*biophony*" (living organisms), "*geophony*" (non-biological natural sounds), and "*anthrophony*" (human-made sounds) [251, 252]. Soundscape ecology, indeed, defines soundscape as "*all sounds, those of biophony, geophony and anthrophony, emanating from a landscape to create unique acoustical patterns across a variety of spatial and temporal scales*" [253]. Here, the soundscape exists independently of human perceivers; it is a physical attribute of the ecosystem to be recorded and analysed for biodiversity assessment [253].

In contrast, within urban planning, the focus remains on the human experience. Mitchell et al. analysed the various definitions of soundscape across disciplines and different contexts [246]. According to their review, the definition of the Oxford English Dictionary is "*the sounds which form an auditory environment*" [254]. However, this definition lacks the perceptual and experiential dimensions that are central to the soundscape concept as used in environmental psychology and urban planning.

In contrast, the ISO 12913-1:2014 standard provides a more comprehensive definition that integrates both physical and perceptual dimensions: soundscape is "*an acoustic environment as perceived or experienced and/or understood by a person or people, in context*" [227]. This definition acknowledges that soundscapes are not merely collections of sounds but are fundamentally shaped by human perception, experience, and context. It highlights the subjective nature of soundscapes, recognising that different individuals may perceive the same acoustic environment in diverse ways based on their cultural background, personal experiences, and situational context. Thus, the ontological distinction between soundscape and acoustic environment is even reinforced.[8]

8: This definition parallels the distinction between "*landscape*" (a perceived vista) and "*land*" (the physical terrain). Just as a landscape paiting is an interpretation of the land, a soundscape can be seen as an interpretation of the acoustic environment.

- **Acoustic Environment**: It's the physical reality, the combination of all acoustic sources, natural and artificial, within a given area as modified by the environment, including sound pressure levels, frequency content, and temporal patterns. It is an objective description that can be measured and quantified using acoustic instrumentation.
- **Soundscape**: It's the perceptual construct, the result of the interaction between the acoustic environment and the listener. It encompasses not only the physical properties of sound but also the cognitive and emotional responses they elicit, also influenced by non-acoustic elements, such as the context and the visual setting in which the listener is located.

It is also noteworthy that the "*context*" component in the ISO 12913-1:2014 definition explicetly embeds the soundscape within a triad of interrelated elements: *person*, *activity*, and *place*, in space and time [227]. This triadic model recognises that soundscapes are not experienced in isolation but are deeply intertwined with the individual's identity, the activities they are engaged in, and the specific characteristics of the location.

- **Person**: Perception is moderated by internal factors. Individual differences, including cultural background, personal history, and current psychological state, all influence how a soundscape is perceived.[9]

9: A person who is already stressed may perceive a complex sound environment as "Chaotic", while a relaxed person might perceive the same environment as "Vibrant".

- **Activity**: The nature of the activity being performed (e.g., relaxation, social interaction, work, etc.) shapes the listener's expectations and tolerance for different sounds.[10]
- **Place**: The physical and social characteristics of the location (e.g., urban park, busy street, residential area, etc.) provide a framework within which sounds are interpreted. The context, indeed, encompasses the visual setting, the microclimate, and the cultural expectations, leading to the concept of **soundscape appropriateness**, meaning that certain sounds are deemed suitable or unsuitable depending on the place. Researches shows that visual-audio coherence, where the sound matches the visual expectation, significantly boosts pleasantness ratings [238].[11]

10: A classic example is the difference between "music" and "noise". Violin music can be considered pleasant when one is attending a concert (activity: leisure), but the same music can be perceived as annoying if played loudly while trying to study (activity: concentration).

11: The sound of a diesel bus is expected on a commercial street (high appropriateness, moderate annoyance) but is highly disruptive in a historic cathedral precinct (low appropriateness, high annoyance).

4.2.2 The Measurement of Soundscape Perception: How and What to Measure? - ISO 12913-2:2018 and ISO 12913-3:2019

Having defined soundscape as a perceptual construct, the challenge becomes: how can it be measured? Being a subjective experience, soundscape assessment cannot rely solely on physical instrumentation, nor can it be fully captured through qualitative descriptions. Thus, a psychometric framework that maps the qualitative dimensions of human hearing into quantifiable metrics is required. This is precisely the objective of the ISO 12913-2:2018 and ISO 12913-3:2019 standards [228, 229], which provide guidelines for soundscape data collection and analysis.

Traditional approaches looked at noise annoyance as the primary metric for assessing the impact of sound environments on human well-being [255, 256]. Surveys used in this regard were mainly a single-item question, such as "How annoyed are you by the noise coming from source X?" rated on a numerical scale. While this approach is straightforward, it clearly fails to capture the multidimensional nature of soundscape perception, collapsing the complexity of perception into a single negative axis.[12] Moreover, it implies that exposure to sound in any form is inherently negative, which contradicts the salutogenic perspective discussed earlier, putting the emphasis on the underlaying assumption that sound is primarily a stressor and a waste for the society [257].

12: Using such an approach, different qualities of soundscapes cannot be distinguished. For instance, a "quite, but boring" soundscape cannot be distinguished from a "quiet, but pleasant" one.

The breakthrough came with Axelsson et al. [258], who proposed a two-dimensional model of soundscape perception based on extensive empirical research. By employing Principal Components Analysis (PCA) on a wide range of perceptual attributes (i.e., 116 different attributes) collected through listening experiments, they identified three primary dimensions that encapsulate the majority of variance in soundscape perception: *Pleasantness*, *Eventfulness* and *Familiarity*.[13] Moreover, being the Pleasantness and Eventfulness dimensions orthogonal, which means independent, they could be effectively represented in a two-dimensional space. This means that, urban outdoor soundscapes could be effectively represented by their position in a two-dimensional space defined by Pleasantness and Eventfulness. As reported by Alexsson et al. [258], such a two-dimensional space resembled a circumplex model also reffered to as "*Model of Affect*", a pleasantness-arousal model based on research on environmental psychology, widely used to describe emotional states [259–261].

13: Familiarity is often discarded in simplified models to allow for a 2D representation.

The circumplex model for soundscape perception, now enshrined in the ISO 12913-3:2019 [229], is a powerful tool for visualizing and interpreting

soundscape data. It allows for the categorisation of soundscapes into distinct quadrants obtained through the intersection of the Pleasantness (X-axis) and Eventfulness (Y-axis) dimensions. Each quadrant represents a unique combination of these dimensions, identifying eight key attributes arranged at 45-degree intervals.[14] In Figure 4.1, the circumplex model is illustrated as represented in the ISO 12913-3:2019 standard [229]. The bipolar structure of the circumplex itself dictates that these states are mutually exclusive; for instance, a soundscape cannot be perceived as both Calm and Chaotic simultaneously, as they necessitate diametrically opposed levels of both Pleasantness and Eventfulness.

14: Some differences in the angles can be found when languages aside from English are used. The *Soundscape Attributes Translation Project* (SATP) provides validated translations of soundscape attributes in several languages, obtained using listening experiments and surveys [262–264].

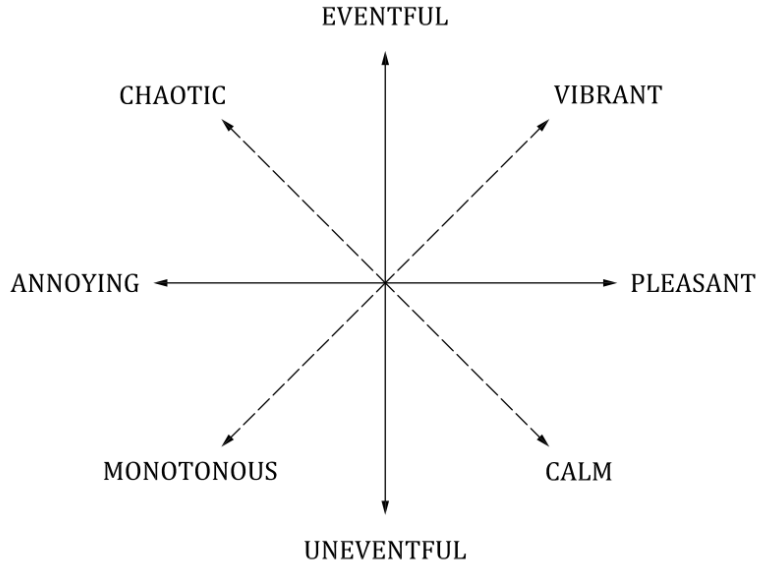


Figure 4.1: Circumplex model of soundscape perception based on Pleasantness and Eventfulness dimensions as represented in ISO 12913-3:2019 [229].

Thus, in line with the ISO 12913-2:2018 [228], eight key parameters are identified to capture the perceptual dimensions of soundscapes:

- **Eventful:** The extent to which the environment is perceived as lively and dynamic;
- **Vibrant:** Describes an environment that is lively and energetic, often characterised by changing but positive sound events;
- **Pleasant:** Represents the degree of enjoyment derived from the sound environment;
- **Calm:** Indicates a tranquil and soothing soundscape, often associated with low levels of activity and minimal sound events;
- **Uneventful:** Characterises a soundscape that lacks significant sound events, a static acoustic environment;
- **Monotonous:** Describes an environment that is repetitive and unchanging;
- **Annoying:** Reflects the degree of discomfort associated with the sound environment;
- **Chaotic:** Indicates a disordered and overwhelming soundscape, often characterised by high levels of unpredictable and conflicting sound events.

Table 4.1 provides a concise overview of the relationship between these attributes and the underlying perceptual dimensions of Pleasantness and Eventfulness, facilitating a deeper understanding of how different acoustic environments are experienced by individuals.

Table 4.1: Characteristics of the four diagonal soundscape attributes in the Pleasantness-Eventfulness circumplex.

Attribute	Coordinates	Soundscape characteristics	Examples
Vibrant	High Pleasantness (+) High Eventfulness (+)	Active, engaging, lively and energetic	Urban plaza, market
Calm	High Pleasantness (+) Low Eventfulness (-)	Inactive, tranquil, restorative soothing and peaceful	Park, garden, library
Monotonous	Low Pleasantness (-) Low Eventfulness (-)	Inactive, dull, unchanging, repetitive, boring and oppressive silence	Empty alley, room with constant HVAC noise
Chaotic	Low Pleasantness (-) High Eventfulness (+)	Active, disordered, overwhelming, confusing unpredictable and stressful noise	Construction site, heavy traffic site

However, to integrate perceptual data into such an analysis, a methodology to convert subjective and multi-dimensional evaluations into spatial representations is required. The ISO 12913-3:2019 also provides a framework to transform subjective data (often collected through Likert scales from 1 to 5 for each attribute) into continuous Cartesian coordinates, mostly referred to as $ISO_{Pleasantness}$ and $ISO_{Eventfulness}$ [229]. This trigonometric projection allows for the plotting of users' soundscape perceptions within the circumplex model, enabling a visual representation of how different environments are perceived. Equation 4.1 and equation 4.2 illustrate this transformation.

$$ISO_{\text{Pleasant}} = \frac{1}{4+\sqrt{32}} \cdot \Big[(\text{Pleasant - Annoying}) + \cos(45^\circ)(\text{Calm - Chaotic}) + \cos(45^\circ)(\text{Vibrant - Monotonous}) \Big] \tag{4.1}$$

$$ISO_{\text{Eventful}} = \frac{1}{4+\sqrt{32}} \cdot \Big[(\text{Eventful - Uneventful}) + \cos(45^\circ)(\text{Chaotic - Calm}) + \cos(45^\circ)(\text{Vibrant - Monotonous}) \Big] \tag{4.2}$$

The denominator $(4 + \sqrt{32})$ serves as a normalisation factor, ensuring that the resulting $ISO_{Pleasantness}$ and $ISO_{Eventfulness}$ values are scaled appropriately within the circumplex model, typically ranging between -1 and 1.

To standardise the data collection procedures, ISO 12913-2:2018 provides a robust and detailed framework. It includes guidelines for survey design and sampling strategies and it explains how to be sure that the input data possess ecological validity and covers the necessary dimensions of human perception [228].

Methodologies recommended by the standard include both *in-situ* surveys, where participants evaluate the soundscape in its natural context, and *laboratory-based listening experiments*, which allow for controlled manipulation of acoustic stimuli. The standard emphasises the importance of capturing a diverse range of contexts, activities, and individual differences to ensure that the collected data accurately reflects the multifaceted nature of soundscape perception.

As for *in-situ* measurements campaigns several approaches are listed and suggested in the ISO 12913-2:2018 [228], one of which are **soundwalks**. A soundwalk involves guided tours through different acoustic environments, where participants provide real-time evaluations of their perceptions.

A specific route to be followed must be carefully planned to cover either a variety of soundscapes, including areas of high and low variation, different dominant sound sources and varying visual contexts, or the entirety of the area to investigate. During the soundwalk activity, data collection occurs by filling out structured questionnaires at designated stops along the route. The standard implies that participants should be indeed exposed to the environment to be evaluated for a sufficient duration at each stop, typically at least three minutes, to form a stable impression of the soundscape before rating it. In this regard, a crucial step in the soundwalk design is the selection and training of participants. The standard recommends recruiting a diverse sample of individuals to capture a wide range of perceptual responses. Moreover, participants needs to be briefed on the purpose of the study, the meaning of the soundscape attributes, and the rating scales to ensure consistency in data collection. They must be instructed to focus on the soundscape rather than simply detecting noise sources.[15]

Another method outlined in the ISO 12913-2:2018 for collecting soundscape data are **binaural recordings**.[16] This approach involves utilising specific instrumentation (i.e., binaural microphones or dummy head) to capture the acoustic environment as it would be perceived by a human listener. Binaural recordings, indeed, preserve spatial cues, such as directionality and distance, which are crucial for accurately representing the soundscape experience of a person. The standard emphasises the importance of a strict calibration procedure of the recording equipment to ensure that the captured sound accurately reflects the true acoustic environment. This type of setup is able to capture sound with the same time delays (*Interaural Time Difference ITD*) and level differences (*Interaural Level Difference ILD*) as the human head. It also captures the spectral filtering effects of the pinnae (outer ears), head, and torso (*Head-Related Transfer Functions HRTF*).

Once recorded, these recordings can be played back in controlled laboratory settings, allowing participants to evaluate the soundscape under standardised conditions. This method is particularly useful for isolating specific acoustic features and examining their impact on perception.

However, to standardise the collection of subjective data in a more systematic way, ISO 12913-2:2018 [228] provides at least three data collection protocols, designated as Method A, Method B, and Method C. These methods are distinct in their structure, granularity, and intended application, though Method A has emerged as the dominant protocol in the scientific literature [265].

Method A is a structured quantitative approach designed to be administered *in situ*, typically during a soundwalk. Its core is the assessment of

15: This framing effect can significantly alter the resulting data; if participants believe they are "noise monitors," they may rate mechanical sounds more harshly than if they are "soundscape evaluators".

16: Simple mono/stereo recordings for soundscape analyses are indeed not recommended by the standard, which suggests to rely on binaural techniques for the acquisition of such data. A mono recording collapses the sound field into a single point, destroying the spatial cues that allow humans to segregate sources, also referred to as the *"cocktail party effect"*.

the eight main soundscape attributes mentioned earlier, also referred to as *Perceived Affective Quality* (PAQ), through a standardised questionnaire. Participants rate these attributes on a 5-point Likert scale, ranging from "Strongly Disagree" (1) to "Strongly Agree" (5).[17]

In addition to the affective qualities, Method A requires participants to assess the dominance of various sound sources. This is not a binary "present/absent" checklist but a dominance rating, usually on a similar 5-point scale.[18] The standard also categorises sounds into a taxonomy to ensure consistency.

Method A also includes a high-level assessment of the overall soundscape quality since it suggests to ask participants to rate the environment appropriateness for its intended use, bridging the gap between the acoustic character and the functional context of the space.[19]

Method B is less commonly used in the literature but often offers a complementary perspective on soundscape assessment [265]. While sharing the objective of quantifying soundscape perception mainly during a soundwalk activity, it utilises a different set of attribute descriptors as well as a different question structure. This approach is a more exploratory approach and it focuses on collecting qualitative data through open-ended questions, allowing participants to describe their soundscape experiences in their own words.[20] Since its nature is more qualitative, it does not provide a direct mapping onto the Pleasantness-Eventfulness circumplex but can yield rich insights into the subjective experience of soundscapes. This method, indeed, is particularly useful for uncovering nuanced perceptions and emotional responses that may not be captured through structured questionnaires.

Finally, **Method C** represents a departure from the quantitative focus of Methods A and B, embracing the qualitative tradition of social sciences. It prescribes a protocol for narrative interviews, which are typically conducted off-site or after the exposure to the acoustic environment. This method, instead of "forcing" the participants to choose between predefined attributes, encourages them to articulate their experiences and perceptions in a more open-ended manner. The interviews are usually semi-structured, allowing for flexibility in exploring topics that arise during the conversation. This approach is particularly valuable for capturing the depth and complexity of soundscape experiences, as it allows participants to express their thoughts and feelings without the constraints of fixed response options. For this reason, this approach can be even more valuable in exploratory studies or when investigating complex environments where the context heavily modifies perception (e.g., cultural heritage sites or religious spaces). It can be also used to validate the attributes used in Methods A and B, ensuring that the standardised terms remain relevant to the public's actual vocabulary. The data collected through Method C can be analysed using qualitative techniques, such as thematic analysis or narrative analysis, to identify common themes and patterns in soundscape perception.

4.2.3 Current Developments in Soundscape Standardisation - ISO 12913-4

The ongoing advancement of the ISO 12913 series is most recently evidenced by the development of ISO/TS 12913-4, provisionally titled "*Acoustics — Soundscape — Part 4: Design and intervention*". While the initial tripartite foundation of the series, comprising conceptual definitions

17: The suggested question to collect data about PAQ is: "For each of the 8 scales below, to what extent do you agree or disagree that the present surrounding sound environment is..." with the attribute to be rated.

18: The suggested question in this regard is the following: "To what extent do you presently hear the following four types of sounds?". The sound source to be rated are grouped into four categories: traffic noise (e.g., cars, buses, trains, air planes), other noise (e.g., sirens, construction noise, industry, loading of goods), sounds from human beings (e.g., conversation, laughter, children at play, footsteps), natural sounds (e.g., singing bird, flowing water, wind in vegation).

19: The suggested questions for this aspect are: "Overall, how would you describe the present surrounding sound environment?" with a 5-point scale ranging from "Very good" (1) to "Very bad" (5), and "Overall, to what extent is the present surrounding sound environment appropriate to the present place?" with a 5-point scale ranging from "Not at all" (1) to "Perfectly" (5).

20: The suggested questions are: "How loud is it here?", "How comfortable is it here?" and "How appropriate is the sound to the surrounding?" with a 5-point scale ranging from "Not at all" (1) to "Extremely" (5). It suggests also to ask about the willing to visit the place under analysis again, specifically with the question "How often would you like to visit this place again?" with a 5-point scale ranging from "Never" (1) to "Very often" (5). Finally, it proposes to include an overall impression question to be answered with open text, such as: "What is going through your mind?".

(Part 1), data collection requirements (Part 2), and analysis protocols (Part 3), established a robust methodological baseline for soundscape characterisation, Part 4 aims to a pivotal transition from purely descriptive research toward prescriptive application.

This forthcoming technical specification is designed to provide urban planners, architects, and environmental acousticians with a standardised, structured framework for the implementation and validation of soundscape "interventions". Thus, the significance of Part 4 lies in its capacity to operationalise soundscape theory within the built environment. By providing a unified language and actionable guidelines, ISO/TS 12913-4 may bridge the long-standing disconnect between academic soundscape research and professional urban development. It will empower stakeholders to integrate acoustic comfort into the earliest stages of the planning process, treating the soundscape as an intentional design element rather than an accidental byproduct of construction.

Consequently, this standard is poised to become a cornerstone in the creation of sustainable urban environments, effectively transforming sound from a pollutant to be mitigated into a functional tool for enhancing public health and social well-being.

4.2.4 Soundscape Design Interventions in Urban Environments

The transition of soundscape design from theoretical discourse to tangible urban interventions manifest the previously discussed paradigm shift, aiming to move beyond the reductive pursuit of silence to prioritise the intentional introduction of restorative auditory stimuli [266, 267]. By treating acoustic quality as a fundamental pillar of public health, these interventions demonstrate these theoretical principles are translated into functional, sensory experiences. To illustrate this practical viability, the following Subsection presents key real-world cases where intentional acoustic planning has successfully transformed the urban fabric.[21]

21: A comprehensive catalogue of soundscape interventions all around the world can be found in [268].

The remodelling of **Nauener Platz** in Berlin, for instance, realised between 2008 and 2010, serves as a pioneering example of soundscape-centric urban design that transcends the mere reduction of sound pressure levels [269–271]. During this project, the qualitative resident expertise, termed "new experts", was synthesised with quantitative psychoacoustic metrics to rehabilitate a square compromised by intrusive traffic noise. Rather than relying on traditional, isolating noise barriers, the intervention implemented a sophisticated dual strategy that combined structural protection with cognitive masking. Specifically, the square was shielded by gabion walls engineered not just to block sound, but to scatter and absorb incident waves, effectively preventing harsh acoustic reflections. This physical shielding was complemented by the installation of "audio islands", sound benches that allowed users to intentionally introduce natural sounds, such as birdsong or flowing water, into the environment. While these additions did not lower the physical decibel levels of the adjacent traffic, they successfully altered the "acoustic meaning" of the space by providing a soothing auditory backdrop that masked the mechanical stressor. By shifting the focus from a pathogenic hazard to a salutogenic resource, the project demonstrated that urban well-being is fostered through "acoustic harmony" rather than absolute silence. The success of this approach is evidenced by post-implementation surveys, which indicated significant improvements in residents' perceptions of

acoustic comfort and overall well-being, even though the objective noise intensity remained relatively constant.

Transitioning from a static square to an incredibly dynamic street corridor, the research surrounding the **Sheffield Gold Route**, a series of connected public spaces linking the railway station to the city's heart, further refined this methodology by establishing a rigorous taxonomy of "active" and "passive" sounds [239, 240]. This body of work emphasised that the impact of sound is heavily dependent on source identification and perceived authenticity.[22] Furthermore, the Sheffield studies provided a precise technical toolkit for deploying water as a "primary soundscape quality" to manipulate the urban atmosphere. This intervention included a sophisticated distinction between the broadband, low-frequency masking capabilities of heavy cascades, designed to neutralise the "hum" of adjacent traffic, and the high-frequency "sparkle" of thin trickles, which provides a delicate auditory focal point that masks higher-pitched mechanical distractions while improving the perceived freshness of the air to the pedestrian experience. Crucially, these water features were integrated into structures made of "Sheffield Steel", specifically using Corten steel and stainless steel to pay homage to the city's industrial legacy. The choice of material was not merely aesthetic; the metallic surfaces provide a distinct acoustic reflection that complements the "crispness" of the water sounds, grounding the salutogenic experience in the tangible, local identity of the "Steel City".

22: For instance, while live musical performances serve as powerful social attractors that enhance "place-making," "canned" or disembodied music is often rejected as "acoustic litter" due to its lack of spatial relevance.

At the macro-scale of city-wide planning, the **Sounding Brighton** initiative exemplifies the integration of soundscape principles into municipal policy to address the friction between a vibrant tourism hub and its residential core [241, 272]. A key component was the **West Street Tunnel experiment**, which targeted a subterranean pedestrian artery historically characterised by harsh acoustic reflections, poor lighting, and a high incidence of antisocial behavior [273, 274]. The intervention utilised behavioral modulation through a curated atmospheric soundscape. By installing a multi-channel sound system that broadcasted a blend of natural soundscapes and low-tempo acoustic textures, the project neutralised the tunnel's hostile "echo-chamber" effect. This "acoustic curation" fundamentally altered the environmental affordance of the space: the transformation of a neglected transit-way into a perceived "cultural space" psychologically discouraged social aggression and loitering. The experiment proved that by replacing mechanical reverberation with an organized auditory narrative, acoustic comfort can serve as a non-invasive tool for public safety, fostering a sense of "civic stewardship" among pedestrians.

Collectively, these interventions illustrate that strategically shaping the auditory environment can transform the experience of urban living, shifting from a defensive posture of noise reduction toward the creation of a functional, restorative, and social resource.

4.3 The University Campus as a Soundscape Laboratory

The imperative to study the university soundscape extends far beyond the traditional boundaries of classroom acoustics. Today, the campus represents a primary habitat for a significant and rapidly expanding segment of the global population. For millions of students and academics,

the university is a "*total environment*", a space where the functions of domestic life, professional labor, and social recreation overlap within a single geographic footprint. Unlike a typical office or residential district, the campus requires an acoustic environment that can simultaneously support high-level cognitive focus, restorative sleep for those who live on-site within dormitories or nearby housing, and vibrant social interaction. When the soundscape fails to balance these needs, it doesn't just hinder learning; it impacts the long-term mental health and physiological well-being of a population that "inhabits" the campus on a continuous basis.

The urgency of researching university soundscapes is underscored by the radical transformation of campuses from quiet retreats into dense urban nodes. Historically, the university was defined by monastic seclusion. The medieval "cloister" model was, indeed, purposefully designed as an island of silence, physically walled off to protect scholars from the "noises and distractions" of the secular city [275–277].[23]

23: In the medieval "Cloister" model, the pursuit of silence was rooted in both functional necessity and moral philosophy. The university aimed to establish the *tranquillitas scholarum* (the tranquillity of scholars), a concept codified as early as the 1215 in the Statutes of Paris. Within the walls of such environments, noise was often equated with "earthly pleasures" that acted as "lascivious sirens," leading scholars away from the path of wisdom. A striking example is found in the 1497 statutes of the Collegium Sapientiae in Freiburg, where playing musical instruments was strictly forbidden. The only exceptions were the clavichord, accepted mainly because of its extremely soft tone. This enforced quietude stood in stark contrast to the "*bawling and brawling*" of undisciplined students in the city's taverns and streets. In this era, the acoustic boundary of the campus served a dual purpose: it was a physical shield against urban chaos and a moral barrier against the "*raucous behavior*" that defined the secular world [276].

However, as the university evolved from an elite institution into a driver of global development, this isolation became unsustainable. The 20th and 21st centuries ushered in a "massification" of higher education, shifting a campus from a secluded sanctuary to a high-density habitat [278, 279]. The scale of this shift is staggering. Student enrollment has more than doubled between 2000 and 2020, reaching approximately 235 million; projections even suggest that this number could reach 600 million by 2040 [280, 281].

As university campuses become increasingly dense and complex, they function as "micro-cities" that integrate diverse environments, from quiet focus areas and academic buildings to vibrant leisure spaces, internal road networks, and parking lots. This environmental heterogeneity makes the university campus an ideal laboratory for testing innovative soundscape analysis tools and exploring the interplay between physical acoustic parameters and human perception.

Moreover, given that students often spend extended hours on campus for both academic and social activities, it is imperative to evaluate and design university campuses soundscape. This is not merely for acoustic comfort, but to ensure a sustainable high quality of life for a population that increasingly relies on the campus as their primary living and working environment. Consequently, a robust body of literature is dedicated to analysing how specific acoustic campus features affect student health and even social outcomes.

Foulkes et al., for example, showed that campus noise has a crucial impact on physical and mental health of undergraduate students living in dormitories. Specifically, noise-induced sleep remains a precursor to feeling of sadness and frustration, which ultimately undermines academic achievement [282]. Beyond these well-being outcomes, the detrimental effects of chronic noise exposure on cognitive process, extensively studied in the literature with reference to children, have also been observed among university-level students, showing that higher-order cognitive functions such as problem solving and memory development are particularly affected by noise exposure [283].

A review of studies regarding the negative effect of noise on students is also reported in [284], in which it is underlined how noise pollution within university campuses affects students' academic performance and their overall well-being. Ibrahim also studied noise effects on students' lives using questionnaires [285]. He indicated that the acoustic environments of university campuses are, indeed, a crucial element as they directly

impact students' learning experiences, communication effectiveness, and overall well-being [282, 286, 287].

Given these impacts, numerous studies have focused on evaluating acoustic conditions within these educational settings through extensive noise measurement campaigns [288–291]. This body of research emphasises the importance of identifying specific sound sources that disrupt the educational acoustic environment. Notable examples include the intrusive honking of passing trains [289], the presence of street vendors on peripheral roads [290], and the proximity of campuses to highways and railway stations [291].

On this basis, several other studies can be found in the literature which have pursued the introduction of soundscape principles into campuses environments. A study of the Polytechnic Center of the Federal University of Paraná combined both objective acoustic measurements and the soundscape approach aiming to understand not only if noise levels in the campus fall within acceptable and regulatory limits, but also determining if its population was actually sensitive to noise pollution [292, 293]. For instance, Puspagarini et al. illustrated how the soundscape of the Yogyakarta campus in Indonesia is shaped by a complex interplay of anthrophony and natural sounds, much like an urban park, where insects, water, and human voices compete with road traffic [294]. Lu and Fu, instead, investigated the perceived restorative factors of a campus outdoor environment and found it to be positively correlated with natural features of the area [295]. Methodological diversity is also evident in the work of Aletta et al. at the University of Sheffield, who utilised music stimuli to measure users' willingness to stay in open public spaces [296].

However, a university acoustic character cannot be described as spatially uniform; rather, it requires a nuanced approach that accounts for the spatial heterogeneity of the campus. Research by Zhuang and Shang in Linyi University Campus, China, highlights this variability, showing that while teaching areas and green spaces often comply with national noise standards, zones such as dormitories, cafeterias, sports fields, and main gates frequently exceed them due to human activity and traffic [297]. Similarly, Anuar et al. reported that in campus areas, natural sounds are often insufficient to mitigate or mask negatively perceived noise sources [298].

Moreover, it needs to be taken into account that university campuses are often located in urban areas, and thus, they are often surrounded by streets with high traffic flow volume, which affect the overall quality of the external spaces. This is the case of several Italian Universities, for example, the Roma TRE University analysed by D'Alessandro et al. [299]. In their research, the investigation on how natural features, visual aspects and thermal conditions can affect the users' judgment of the environment was carried out. Research efforts have also been directed towards understanding the influence of acoustic environments on various indoor settings within university campuses. Indrani et al., for instance, found out that even work behaviour depends on the acoustic characteristics of the workplace and on its perception [300].

Researchers at McGill University in Montreal, Canada, have also contributed significantly to this field by exploring the relationship between campus soundscapes and student well-being. Collaborating with the artist collective Audiotopie [301], the team installed four sound art pieces in a park setting (a proxy for campus green space) in the dense Plateau Mont-Royal neighborhood. The sounds played back include human voices and abstractions of natural sounds, such as water and birdsong

[302]. Their studies have demonstrated that the addition of sound, even if it is a counter-intuitive approach, reduced the perceived loudness of the existing urban noise, serving as a distractor from unwanted sounds.

Moreover, the perception of a campus soundscape is not a monolith; it is fractured by the role of the user (i.e., student vs. staff) and their cultural background [303]. While conducted in a secondary school setting, the study at St. Oscar Romero Catholic School in the UK offers significant insights applicable to the university context. In particular, a stark difference has been found: teachers predominantly perceived the school soundscape as "engaged" (high comfort and content), whereas students often perceived it as "detached". The research suggests that this gap, and thus the difference perception of a soundscape, could be driven by the control that the user has on it. Teachers have authority over the acoustic environment (silencing a class, closing a door), while students are passive recipients of the soundscape.

Given the complex overlap of these multifaceted variables, ranging from the interaction between several different sound sources to the internal psychological and behavioral responses of the users, it is evident that the campus environment cannot be analysed in isolated fragments. Instead, these factors coexist in a delicate balance where physical, sensory, and functional dimensions merge. To reflect this complexity, a comprehensive understanding of the campus soundscape must integrate the dynamic interactions between the built environment, landscape features, and temporally fluctuating acoustic sources.

Against this backdrop, this Chapter turns to the **Fisciano campus of the University of Salerno** as a real-world soundscape laboratory. The campus is first presented in its physical and functional structure, followed by a description of the measurement campaigns designed to collect subjective perceptual data. These data are then analysed in accordance with the ISO soundscape framework [227–229], providing a robust basis for subsequent interpretation.[24]

Finally, the Chapter introduces the central contribution achieved: a novel methodological approach for mapping soundscape attributes, particularly the pleasantness, resulting in an intuitive and user-friendly tool that mirrors the accessibility and readability of conventional noise maps. By providing an output that is readily usable and interpretable, this approach aims to empower designers and policy makers to reach informed decisions supported by data within standard planning procedures. Spatial and temporal analysis of the soundscape maps are then presented, in order to uncover the acoustic dynamics of the campus environment and to obtain a comprehensive characterisation of its soundscape.

24: Please note that the case study is presented before the methodology Section, in order to provide the reader with a clear understanding of the context in which the research has been conducted, being the methodology site-specific. However, the underlying framework remains extrapolable and scalable to other scenarios; with the appropriate contextual analysis and site-specific adjustments, the proposed methodology can be effectively applied to diverse environments, allowing for a comprehensive understanding of soundscape perception across different contexts.

4.4 Case Study: The Fisciano Campus of the University of Salerno

The Fisciano campus of the University of Salerno (UNISA) is located in the Campania region of Southern Italy. Established in 1988, the campus has evolved into a sprawling educational complex that serves over 30,000 students and staff members. Its strategic location, approximately 60 kilometers east of Naples, positions it within a semi-urban context that blends natural landscapes with urban infrastructure. The campus is nestled between rural surroundings and major regional transportation infrastructures, creating a high-density habitat that serves as a transition

zone between the built environment and the natural landscape. In particular, the campus is adjacent to the A30 motorway, a critical artery that connects Salerno to Caserta and Naples, facilitating substantial vehicular traffic flow [304]. Figure 4.2 illustrates the geographical positioning of the campus.

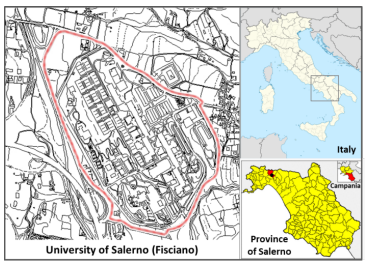


Figure 4.2: Location of the Fisciano campus of the University of Salerno (Italy). Red line in the left plot is the campus border, while the right plot shows a zoomed-out view of the campus area in the Campania region.

Due to its intricate environmental configuration and diverse functional zones, the Fisciano campus of the University of Salerno serves as an exemplary case study for soundscape analysis and for this reason it has been chosen as a case study for this research.[25] Spanning a vast area of approximately 1,200,000 m^2, the campus is organized as a "micro-city", integrating a diverse mosaic of functional zones, each characterised by distinct acoustic and social signatures [304]. While these areas tend to follow consistent auditory patterns, they are not static; rather, they exhibit significant variability driven by the time of the day, seasonal transitions, and fluctuating weather conditions.

Several primary environments that reflect the multifacated nature of university life can be observed within the campus:

- **Quiet study and academic zones:** the central core of the campus is occupied by the main academic infrastructure, which includes lecture halls, laboratories, faculty offices, libraries, and the canteen. In these sectors, the soundscape is primarily dominated by human sounds such as conversations and footsteps. These environments are highly dynamic, characterised by temporal peaks in noise levels during class transitions and breaks, contrasting with markedly quieter periods during active lecture hours or outside standard working times. Furthermore, seasonal factors introduce specific technical sounds, such as the operation of heating systems during the winter months;
- **Internal road networks and parking facilities:** multiple internal roadways and extensive parking facilities introduce persistent vehicular noise into the campus environment. These traffic-related sounds fluctuate according to the academic calendar; vehicular movement intensifies during peak hours, particularly immediately before and after class starts, and shows distinct variations between standard course periods and intensive exam sessions. A terminal bus is also present, serving as a hub for public transportation and contributing to the overall soundscape with bus engine noise and passenger activity;
- **Vibrant leisure spaces:** these zones are characterised by a lively acoustic environment, where the auditory experience is defined by social interactions, recreational activities, and occasional organized events. The acoustic signature of these spaces reflects the social vitality of the university, with human speech and activity forming a dense and ever-changing soundscape;
- **Green areas and parks:** many sectors of the campus are defined by significant greenery, where the acoustic experience is characterised by natural sounds such as birdsong and the rustle of wind through foliage. These parks and tree-lined walkways provide a tranquil atmosphere and function as vital buffer zones, mitigating the propagation of road traffic noise from the near highway and road networks in general. However, these zones are subject to seasonal shifts that influence the presence of wildlife and the density of vegetation, while weather conditions like rain or wind further alter sound propagation and user perception.

25: The Fisciano campus of the University of Salerno has also been selected as a case study in previous research works [305–307].

4.5 Material and Methods: Analyse the Campus Soundscape and Map its Pleasantness

This Section outlines the dual-methodological framework designed to bridge the gap between objective acoustic measurements and subjective human perception. Two main approaches have been employed to investigate the campus soundscape: first, a standardised qualitative assessment via soundwalks to interpret the soundscape at specific hotspots; and second, a large-scale crowdsourcing data collection using the NoiseCapture application to assess the spatial distribution of soundscape attributes across the entire campus.

Finally an Inverse Distance Weighting (IDW) interpolation to draw pleasantness maps of the campus environment has been applied. In the following Subsections each of these methods is described in more detail, highlighting their respective roles in the comprehensive analysis of the campus soundscape.

4.5.1 Campus Soundscape Analysis via Standardised Soundwalks

To provide a rigorous interpretation of the campus soundscape, a series of soundwalks were conducted following the protocols established by the ISO/TS 12913-2:2018 standard [228].

The adopted soundwalks were strategically planned to cover a diverse range of campus environments, ensuring a comprehensive assessment of its different areas. A total of 3 soundwalks were carried out within the campus:

- **Soundwalk 1:** conducted on March 8, 2019, approximately from 10:00 AM to 12:00 PM, covering six strategic measurement points. Both Method A and Method B from ISO 12913-2:2018 [228] were employed during this soundwalk;
- **Soundwalk 2:** conducted on November 5, 2024, approximately from 3:00 PM to 5:30 PM, covering nine strategic measurement points (i.e., the six points from soundwalk 1 plus three additional points). Method A from ISO 12913-2:2018 [228] was employed during this soundwalk. [26]

The soundwalks were conducted at various times of day and under different weather conditions to try to capture the dynamic nature of the campus soundscape. Figure 4.3 illustrates the measurement points where data were collected during the soundwalks. The points in red are from the first soundwalk, while the ones in blue are the additional points added in the second and third soundwalks. Table 4.2 summarises the key details and characteristics of the investigated points, including their locations, surrounding features, and anticipated acoustic influences.

26: Notice that a third soundwalk activity was conducted on November 7, 2025, approximately from 9:30 AM to 11:30 AM, covering nine strategic measurement points (i.e., same points from soundwalk 2) using questionnaires from Method A from ISO 12913-2:2018 [228]. However, this soundwalk specifically aimed at testing the individuation and application of **Soundscape Perception Index** (SPIs). SPIs are designed to compress multidimensional perceptual data into context-dependent single-value scores, facilitating a direct comparison of environmental quality with the aim of proposing a more intuitive and user-friendly tool for designers and policy makers to reach informed decisions supported by data within standard planning procedures [308]. As this activity took place during the final stages of the doctoral research, it falls outside the primary scope of this work. Moreover the questionnaires results from this soundwalk activity have not been used in the methodological validation presented herein. For this reason, outputs and results from this soundwalk are not included in the analysis and discussion of the Chapter. It is nonetheless cited for the sake of completeness in reporting the full range of activities associated with the study of the soundscape of this area.

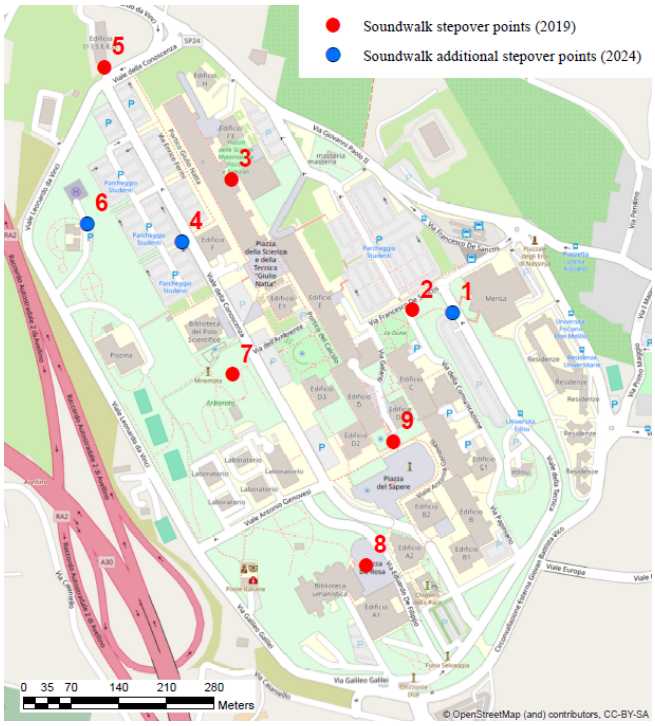


Figure 4.3: Map of the Fisciano campus of the University of Salerno from Open Street Map [309] with soundwalks stepover points: red points are from the first soundwalk, while blue points are the additional points from the second and third soundwalks.

Table 4.2: Soundwalk stepover points characteristics with corresponding IDs from 2019 and 2024 soundwalk. Points order is the same as in Figure 4.3.

Point	Point ID 2019	Point ID 2024	Description	Main Sound Sources
1	-	1	Street, near the canteen building and the terminal bus	Chatting, road traffic noise
2	6	2	Green area, near parking lots and academic buildings	Chatting, road traffic noise, nature
3	5	3	Academic building area	Chatting, HVAC implants in winter
4	-	4	Academic building area, near parking lots	Chatting, road traffic noise
5	1	5	Street, near parking lots and academic buildings	Chatting, road traffic noise, nature
6	-	6	Green area	Nature
7	2	7	Green area	Nature, road traffic noise
8	3	8	Square area	Chatting
9	4	9	Square area	Chatting

In each point along the soundwalk routes, participants engaged in a 3-minute period of passive listening to fully immerse themselves in the local acoustic context. Following each session, they filled out questionnaires to rate the soundscape across several perceptual attributes, including:[27]

- The dominance of various sound sources (traffic noise, human sounds, natural sounds, and other noise sources) on a 5-point Likert scale;
- The eight main soundscape attributes on a 5-point Likert scale;
- The overall soundscape quality through questions regarding the appropriateness and the overall evaluation of the environment for its intended use;

27: Please refer to Appendix A for the full questionnaire used during the soundwalks.

- Additional information, such as demographic data and subjective comments.

During the first edition of the soundwalk, also questions retrieved from Method B were included in the questionnaire, such as the perceived loudness of the environment and its related unpleasantness.

It is also significant that soundwalks participants were mostly students attending courses related either to environmental acoustics or Physics of the Bachelor in Civil Engineering and Environmental Engineering programs of the University of Salerno. Gender equality was ensured among participants, with an equal representation of male and female students. They were asked in anonymous way if they had any hearing impairments, and they were trained about foundamentals in acoustics. Moreover, before each soundwalk, participants were briefed on the study's objectives and trained on basic soundscape concepts. Instructions were also provided on soundwalk protocols and how to complete the questionnaires to ensure consistency in data collection. This choice was made to ensure that participants had a basic understanding of acoustic concepts, which could enhance the reliability of their perceptual assessments and to have "local experts" assessing the soundscape within the campus, as suggested by the standards [227–229].[28]

28: Please find additional details about the soundwalks activities carried out in Table 4.3 (noted as "SW").

4.5.2 Campus Soundscape Assessment via Crowdsourcing Science

In an effort to overcome the spatial limitations of soundwalk fixed-point measurements and to try to capture the multifaceted nature of the Fisciano campus entirely, a large-scale crowdsourcing approach has been implemented. This methodology transforms the campus community into a mobile sensor network, providing a high-resolution dataset that reflects the complex spatio-temporal dynamics of the university environment.

To ensure a high density of soundscape crowdsourced data, a series of dedicated events were organized within the campus, encouraging mainly students and research fellows to actively participate in the data collection process. These volunteer-based participatory events (i.e., "**NoiseCapture parties**" [310]) aimed specifically at raising awareness about environmental noise pollution while simultaneously promoting the use of tools for environmental noise assessment, particularly those developed within the framework of the Noise-Planet initiative [311].[29]

29: A group of French researchers from the "Joint Research Unit in Environmental Acoustics" (UMRAE) and the "Centre for Studies on Risks, Mobility, Land Planning and the Environment" (CEREMA), and the "DECIDE" team from the "Research laboratory in information and communication science and technology" (Lab-Sticc) developed such initiative.

Seven NoiseCapture parties have been organized within the campus, involving almost 360 participants:

- NoiseCapture Party@Unisa 2018: 17th May 2018;
- NoiseCapture Party@Unisa 2019: 24th May 2019;
- NoiseCapture Party@Unisa 2022: 16th May 2022;
- NoiseCapture Party@Unisa 2022 fall edition: 9th November 2022;
- NoiseCapture Party@Unisa 2023: 26th October 2023;
- NoiseCapture Party@Unisa 2024: 5th November 2024.[30]

30: A seventh NoiseCapture party was organized on November 7, 2025, but it is not included in the analysis of this Chapter as it took place during the final stages of the doctoral research. Moreover, since the main focus of this Chapter is on the methodological approach for mapping soundscape attributes, any other details about this event are not provided here since it has not been used in the methodological validation presented herein. It is nonetheless cited for the sake of completeness in reporting the full range of activities associated with the study of the soundscape of this area.



Figure 4.4: Routes followed during the NoiseCapture parties organized within the Fisciano campus of the University of Salerno.

During these events, participants were divided into several groups and encouraged to explore different areas of the campus following a precise route as represented in Figure 4.4, while using the **NoiseCapture smartphone application** [312] to record sound levels and provide perceptual ratings of the soundscape.[31]

Through the use of the NoiseCapture mobile application, indeed, participants can measure sound levels using their mobile phones' microphones and provide the ratings of the pleasantness of the soundscape experienced on a unipolar continuous-category scale of the location in which the measurement took place.[32] The identification of the predominant sound sources operating during the measaurement is also allowed.

The measurement is embedded with the device identifier and the GPS position and, once stopped, it can be uploaded to the cloud that feeds an online and real time map available on the Noise-Planet project website [311]. In Figure 4.5, a screenshot of the NoiseCapture app is shown, illustrating the user interface during a measurement session.

As for the participants, similarly to those engaging in the soundwalk activities, they were mostly students attending courses related to environmental acoustics of the Bachelor in Civil Engineering and Environmental Engineering programs of the University of Salerno. Gender equality was ensured among participants, with an equal representation of male and female students. A proper training session was organized before the events, during which the participants were instructed about foundamentals in acoustics, with specific focus on the soundscape approach and its potential applications. Specifically, since the pleasantness rating given by the user at the end of the measurement is then automatically attributed to each point along the trajectory followed during the measurement, participants were trained about the crucial importance of stopping the measurement whenever significant changes in the soundscape occurred, providing homogeneous and consistent information on the investigated acoustic environments.

These measurements constitute the crowdsourced dataset that has been used to generate soundscape attribute maps of the campus environment. In particular, since the pleasantness is the attribute assessed during the NoiseCapture measurements, **pleasantness maps** of the campus have been produced.

31: Please note that the routes followed during the NoiseCapture parties are similar but not identical to those followed during the soundwalks, as the main aim of the NoiseCapture parties was to cover the campus area as much as possible.

32: Mobile phones must be calibrated before any reliable sound level measurement can be taken. The calibration procedure can be achieved in four ways, namely, using road traffic noise, by manually calibrating the mobile microphone from a reference device or from a calibrator device (in this case, a plug-in external microphone is required), and by automatically estimating the correction factor through a comparison with a pre-calibrated device. In order to ensure a basic level of reliability of the sound level measurements, the majority of the participants smartphones have been calibrated either through a direct comparison with a first-class sound level meter (i.e., the reference device) or by sharing the correction factors obtained by a pre-calibrated device. However, since in the research to be presented in this Chapter, the main focus is clearly the soundscape assessment, any other details on this procedure are not provided here.

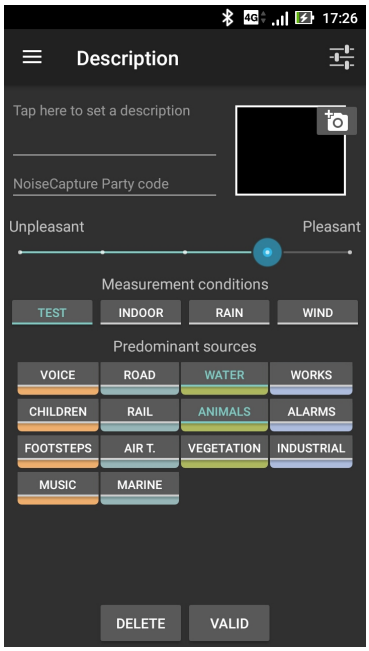


Figure 4.5: Screenshot of the NoiseCapture app during a measurement session.

The recorded measurements, along with the corresponding pleasantness ratings, can be retrieved from a public repository, allowing users to freely access and analyse the collected data. Different type of datasets can be downloaded, including point, track and area datasets. Pleasantness values are available in both the point and area datasets. In the point dataset, pleasantness values are assigned to each point along the trajectory, with all the point collectively representing the track followed during the measurement. As for the area dataset, pleasantness values are calculated as the average of all the individual point-based ratings that fall within each predefined hexagonal grid cell. By averaging the rating from all the points within the hexagon, this approach provides a temporally aggregated representation of how users perceive the acoustic environment in any specific area, averaged over time. Table 4.3 summarises the key details and characteristics of the soundwalk activities ("SW") and of the NoiseCapture parties ("NC") within the campus.

Table 4.3: NoiseCapture parties and soundwalks activities characteristics within the Fisciano campus of the University of Salerno.

Event	Date	Season	Time of Day	Number of participants	Number of points
NC	17/05/2018	Spring	Morning	25	5104
SW	08/03/2019	Winter	Morning	22	6
NC	24/05/2019	Spring	Morning	39	11766
NC	16/05/2022	Spring	Afternoon	40	4902
NC	09/11/2022	Autumn	Morning	113	24056
NC	26/10/2023	Autumn	Afternoon	78	12560
NC	05/11/2024	Autumn	Afternoon	64	23984
SW	05/11/2024	Autumn	Afternoon	52	9

4.5.3 Pleasantness Mapping via Inverse Distance Weighting (IDW) Interpolation

As mentioned earlier, the crowdsourced pleasantness dataset collected through the NoiseCapture app during the NoiseCapture parties has been utilised to generate soundscape attribute maps of the Fisciano campus. The goal is to provide a tool that can be easily interpreted and used by designers and policy makers within standard planning procedures, similar to conventional noise maps.[33]

33: Note that similar approaches can be found in the literature. Margaritis and van Kann presented a smartphone-based method for noise and soundscape analysis in a university campus that underwent a renovation plan. The authors used statistical and geographic information system (GIS) tools to examine the spatio-temporal variability of noise and soundscape and the influence of landscape features. Some maps of perceived annoyance but also stress escapes and quietness were produced. However, no soundscape attributes were mapped [313].

The raw data packages (i.e., points, trajectories and areas datasets) collected during the NoiseCapture parties are updated on a daily basis and can be downloaded from the Noise-Planet data repository [311], selecting the country, in a compressed folder of the measurements uploaded by users. Once downloaded, the data can be imported and handled in any GIS software for further analysis and, in this specific case, mapping.

To build a reliable dataset, the "*Accuracy*" of each measurement point has also been considered, where "Accuracy" refers to the GPS localisation accuracy in meters, i.e., the radius within which there is a 68% probability that the actual location of the measurement point lies. Only points with an accuracy of less than 10 meters have been considered for the mapping procedure, in order to ensure a sufficient level of spatial precision. Moreover, points with missing pleasantness values have been discarded. In Table 4.3, the total number of points after the cleaning process used for the mapping procedure is reported for each NoiseCapture party.

In order to obtain a map of pleasantness of the campus environment, it is necessary to spatially interpolate the point-based pleasantness ratings

collected during the NoiseCapture parties. For this reason, an approach based on an **Inverse Distance Weighting (IDW)** interpolation, a widely used geostatistical technique for spatial interpolation, has been used. IDW interpolation operates on the principle that points closer to the location of interest have a greater influence on the estimated value than those further away. This method is particularly suitable for environmental data, where spatial autocorrelation is often present. The Inverse Distance Weighting (IDW) interpolation is mathematically expressed as follows:

$$P(x_0) = \frac{\sum_{i=1}^{N} \frac{P(x_i)}{d(x_0,x_i)^k}}{\sum_{i=1}^{N} \frac{1}{d(x_0,x_i)^k}} \tag{4.3}$$

where $P(x_0)$ is the estimated pleasantness at the location of interest x_0, $P(x_i)$ is the known pleasantness at location x_i, $d(x_0, x_i)$ is the distance between the locations x_0 and x_i, k is the power parameter that controls the rate of decay of influence with distance, and N is the total number of known points used in the interpolation. In the case under study, a power parameter of $k = 2$ has been selected, which is a common choice in environmental applications, as it provides a balanced weighting scheme that emphasises nearby points while still considering the influence of more distant observations [314].

This mapping procedure heavily relies on soundscape homogeneity. A crucial parameter to implement the IDW interpolation is, indeed, the **search radius**, also called "influence radius". This value describes the circular area within which points have to be considered for the interpolation at each location of interest. Therefore, in this case, it indicates the maximum distance from which pleasantness ratings are taken into account to estimate the pleasantness at a specific location on the campus map. In this study, the search radius has been firstly set at 50 meters, in order to capture local variations in pleasantness while maintaining a balance between detail and generalisation. However, sensitivity analyses have been then conducted to assess the impact of varying its value on the maps. The results of sensitivity analyses performed can be found in Section 4.7 for further details about the sensitivity analyses performed.

In this research work, QGIS software [315] has been used to perform the IDW interpolation and to generate the pleasantness maps of the campus environment [316]. The obtained maps have been finally validated through a comparison with the soundwalks questionnaires results, ensuring that the spatial patterns observed in the maps align with the perceptual assessments collected. Further details about the validation procedure are provided in Section 4.7.

To achieve this comparison, it is worthy to notice that the pleasantness values provided by the NoiseCapture data are given in percentage, rating from 0% (i.e., very unpleasant) to 100% (i.e., very pleasant), with steps of 25%. On the other hand, the data collected during the soundwalks according to the ISO 12913-2:2018 standard [228] are rated on a 5-point Likert scale, ranging from 5 (i.e., "strongly agree" with the experienced soundscape being pleasant) to 1 (i.e., "strongly disagree" with the experienced soundscape being pleasant). The two scales are not directly comparable, thus a normalisation procedure has to be applied to convert the 5-1 scale of Method A to 100%-0% scale used in NoiseCapture data. This procedure has been performed having access to the raw data collected during the soundwalks, thus converting each single rating from each participant in each point. When using questionnaires' results from

Method B, since they refer to the soundscape unpleasantness rating,[34] they have been converted into the mean pleasantness by assuming that "non pleasant" is the complementary of "pleasant". This procedure, of course, can lead to misestimations of the pleasantness values, since the subjective rating of how much a location is unpleasant may be affected by the question structure. Moreover, asking about the unpleasantness, indeed, may influence the participant and let them focus on the negative factors more than on the positive ones, and vice versa.[35]

34: In this regard, the suggested question in Method B is: "How unpleasant is it here?" with a 5-point Likert scale ranging from 1 (i.e., "not at all") to 5 (i.e., "extremely").

35: This peculiarity of Method B will be confirmed by a general understimation in the pleasantness results presented in the following Section 4.7 and it has lead us to use Method A results for validation of the mapping, adopting the scale in percentage, as proposed in the NoiseCapture application. The app, indeed, asks to rate the unpleasantness/pleasantness perception in a more neutral way, using a five-point unipolar scale as shown in Figure 4.5. This choice is also coherent with other studies in literature, such as the study by Aletta et al. [57], in which the results of Method A and Method B questionnaires during a soundwalk through the Department of Engineering of the University of Roma Tre were compared. It was observed that choosing a protocol over another could have an effect on the soundscape data that are being gathered, confirming the necessity of performing a comparison between the two methods. Moreover, as reported earlier, Method A has clearly emerged as the dominant protocol in the scientific literature [265].

Spatial and Temporal Analysis of Pleasantness Maps

To gain deeper insights into the spatial and temporal dynamics of the campus soundscape, comprehensive analyses of the generated pleasantness maps have been conducted, aiming at uncovering patterns and trends in the perceived pleasantness across different areas of the campus and at various times of the day.

The **spatial analysis** focuses on identifying patterns in the distribution of high and low pleasantness areas, examining how they correlate with specific campus features. For instance, the obtained pleasantness maps could be directly compared with sound levels, interweaving soundscapes' information with noise maps of the interested area to identify potential relationships between physical parameters and perceptual factors. In the case of the Fisciano campus, particular attention has been paid to the relationship between pleasantness levels and different land uses within the campus, looking into how the composition of the acoustic environment contributes to defining the overall pleasantness of a location, mainly investigating the role of sound sources. By overlaying the pleasantness maps with the campus land use and facility map, it is possible to discern how different functional zones within the campus, and their associated predominant sound sources, influence soundscape perception. Furtermore, an additional comparison between these insights and the information collected during the soundwalk activity about subjective perceived predominance sound sources has been carried out. This aims to evaluate the presence of any masking effects or variations in the perception of the acoustic environment, due to the complexity overlapping of numerous and various typologies of possible sound sources present in any area of the campus. A resume of the steps followed for the spatial analysis is provided in Figure 4.6.

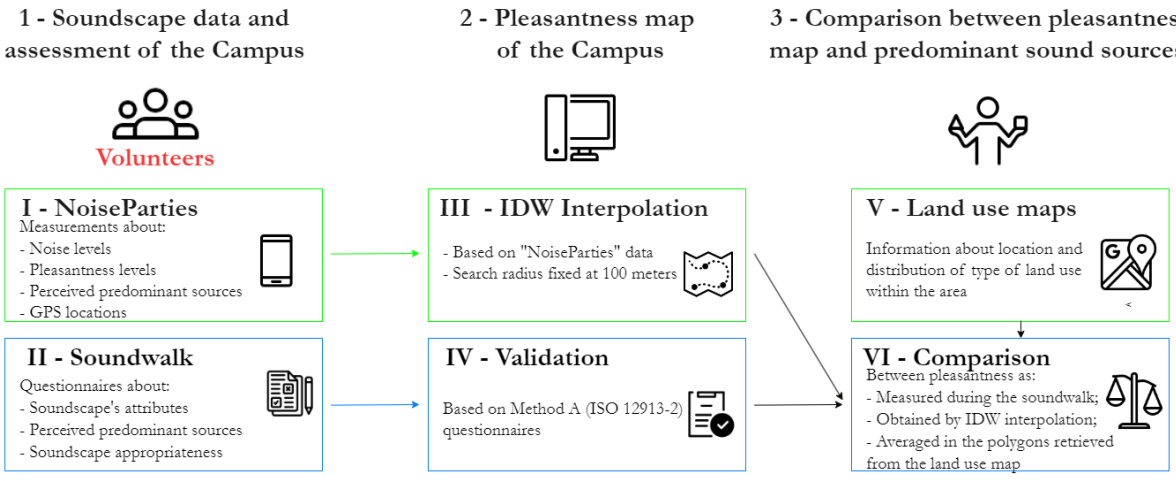


Figure 4.6: Flowchart resuming the steps followed for the spatial analysis of the pleasantness maps.

However, soundscape variation occurs both spatially, as different sound sources shape the acoustic environment in distinct areas, and temporally, as the soundscape transforms over time due to daily activity patterns, seasonal changes, and particular events. Having this in mind, a **temporal analysis** has been coupled to the spatial one, in order to obtain deeper insights into the interplay between physical parameters, perceptual evaluations, and the acoustic environment dynamics.

To reach this goal, different maps for each edition of NoiseCapture party have been generated, allowing for an investigation the campus soundscape evolution over time, year-by-year. To do so, data from the point-based layer have been used, considering the timestamp associated with each measurement point, in order to properly differentiate the measurements collected during each NoiseCapture party. This analysis is particularly relevant in a dynamic environment, where the acoustic landscape and its sound sources can change significantly based on daily activities and seasonal variations.

4.6 Soundscape Dataset Description and Analysis

This Section provides a comprehensive analysis of the perceptual data collected during the soundwalks conducted at the Fisciano campus of the University of Salerno. Specifically, a longitudinal approach has been adopted, comparing the results from the March 2019 soundwalk with those from the November 2024 soundwalk. The objective is to characterise the soundscape of the campus environment, analysing it coherently with the ISO 12913-2:2018 standard [228].

To ensure data integrity and completeness, the initial step involved a rigorous cleaning of the dataset. Specifically, entries with missing values were removed.[36] Moreover, "straight-lining" responses, i.e., cases where participants provided identical ratings for all eight perceptual attributes regardless of the acoustic environment, were also removed. Such entries were deemed non-representative of actual perception and were excluded to prevent a reduction in the model sensitivity. After this filtering phase, the final dataset comprised a total of $N = 542$ valid responses ($N_{2019} = 127$ and $N_{2024} = 415$). Thus, following the approach proposed by the ISO 12913-2:2018 standard [228], the analysis is structured in two main steps: first, an examination of the perceived dominance of different sound sources across the investigated points; second, an analysis of the eight perceptual attributes associated with the campus soundscape.

36: Missing values were exclusively associated with the paper-based questionnaires used in the 2019 campaign. Conversely, the 2024 survey was implemented using Computer-Assisted Web Interviewing (CAWI) tools (i.e., Google Forms) which allowed for the setting of mandatory fields, thereby eliminating the possibility of incomplete responses at the source.

4.6.1 Sound Sources Predominance Analysis

In this Subsection, the perceived dominance of different sound sources across the investigated points is analysed. The sound sources are categorised into four main types: traffic noise, other noise source, human sounds and natural sounds, as also defined earlier.

In Figure 4.7 and Figure 4.8, the results of the sound source predominance analysis are presented.[37] The results are presented in terms of the percentage of responses indicating the dominance of each sound source type at each point, allowing for a comparative analysis between the two soundwalk campaigns and providing insights into the acoustic

37: Note that in this analysis, the point IDs refer to the 2024 soundwalk.

environment of the campus. Further consideration about the results of the sound source predominance analysis are provided in Section 4.7.2, where the relationship between the objectively present sound sources, the subjective predominant sound sources, and the pleasantness levels across the campus are investigated.

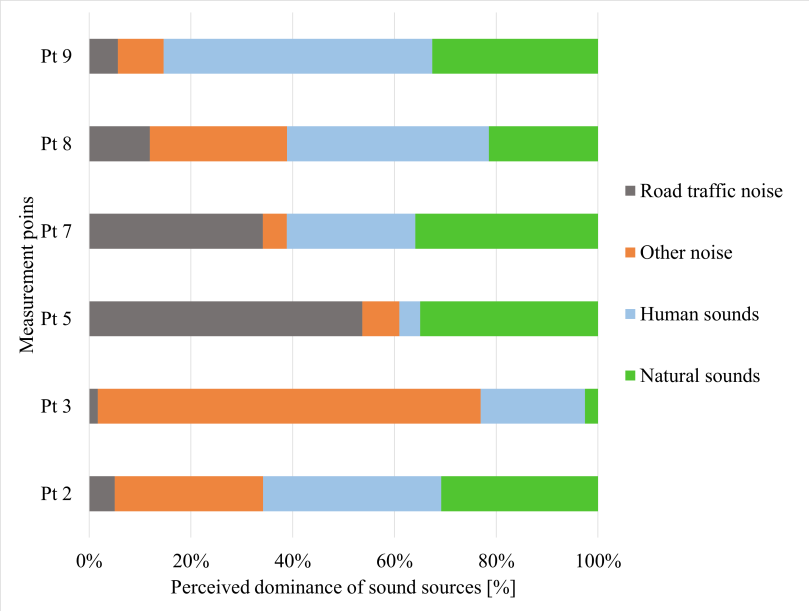


Figure 4.7: Predominant perceived sound sources detected during the soundwalk activity in the six selected points (2019 soundwalk).

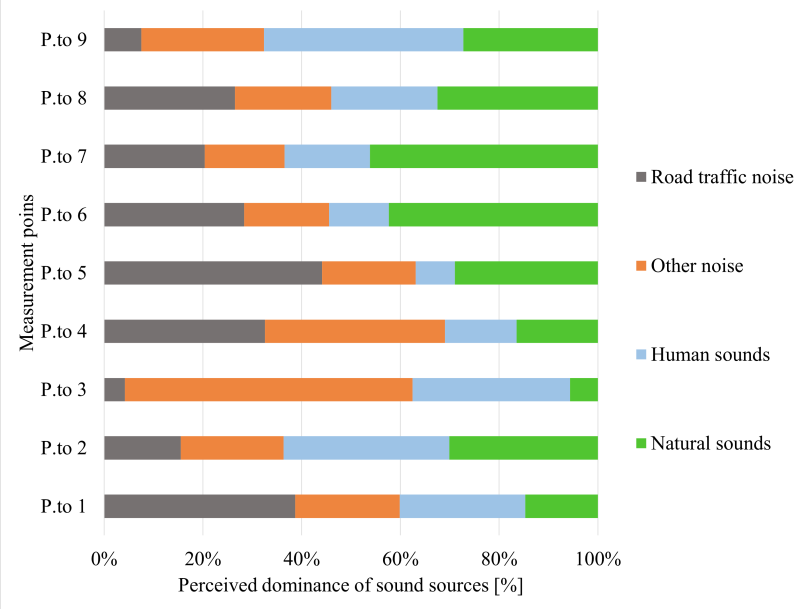


Figure 4.8: Predominant perceived sound sources detected during the soundwalk activity in the six selected points (2024 soundwalk).

Global Circumplex Analysis

To comply with the ISO 12913-2:2018 standard [228], a global circumplex analysis of the soundscape perceptual attributes has been performed and is used to present the soundscape dataset obtained through the soundwalk activities. In Figure 4.9 and Figure 4.10, the circumplex diagrams for the 2019 and 2024 soundwalks are shown, respectively. These diagrams visually represent the distribution of the eight perceptual attributes in a two-dimensional space, allowing for an intuitive understanding of the overall soundscape perception at each point.

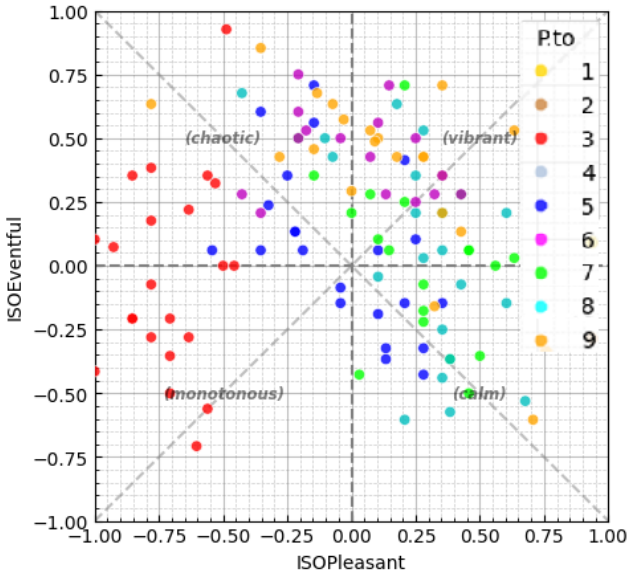


Figure 4.9: Global circumplex analysis of the soundscape perceptual attributes for the six selected points (2019 soundwalk).

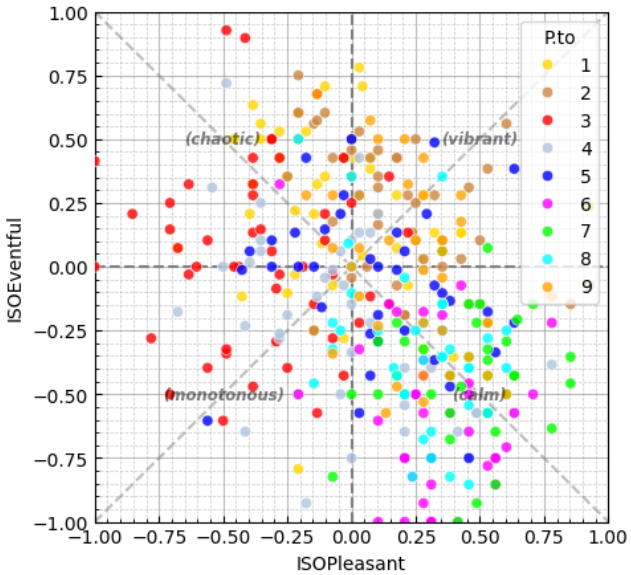


Figure 4.10: Global circumplex analysis of the soundscape perceptual attributes for the six selected points (2024 soundwalk).

4.6.2 Point-specific Circumplex Analysis

Since the soundscape perception can vary significantly across different locations within the campus, using a single global circumplex diagram to represent the overall soundscape perception may not capture the unique characteristics of each point. Therefore, in addition to the global circumplex analysis, a point-specific circumplex analysis has also been performed to capture the unique perceptual characteristics of each investigated point in a more detailed and readable way. Thus, in the following Figures, for each point investigated during the soundwalks, a circumplex diagram is presented for both the 2019[38] and 2024 soundwalks, allowing for a comparative analysis of the soundscape perception at each location across the two campaigns.

Figure 4.11 offers a compelling snapshot of the psychoacoustic landscape at point 1, which is in a pedestrian street near the canteen building and the terminal bus. A high degree of eventfulness, characterised by a notable dispersion between the vibrant and chaotic can be observed, likely influenced by the presence of road traffic noise and human sounds.

38: While the 2024 dataset is more complete, and for this reason a circumplex for each point is present, the 2019 dataset is less comprehensive and only available points are shown.

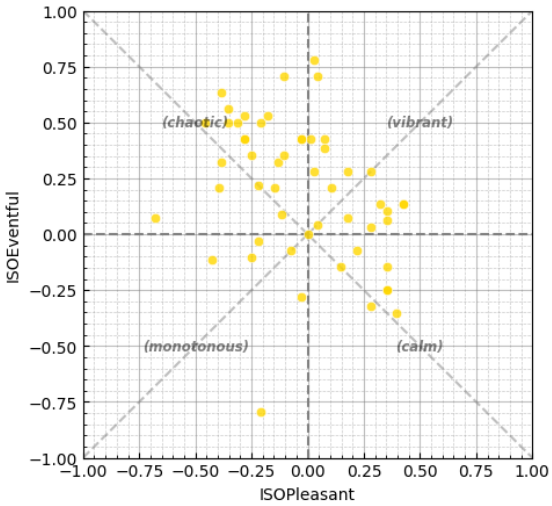


Figure 4.11: Point 1 circumplex (2024 soundwalk).

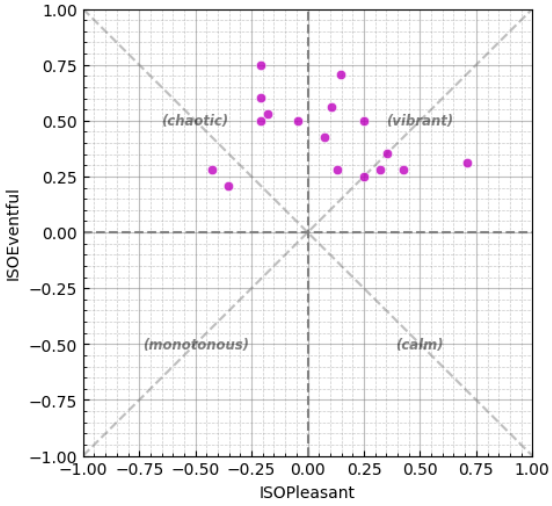


Figure 4.12: Point 2 circumplex (2019 soundwalk).

Point 2 depected in Figure 4.12 and Figure 4.13, shows a significant shift in the soundscape perception between the two campaigns. In 2019, the acoustic environment was more concentrated in the vibrant and chaotic quadrants, probably dominated by the campus activities and the road traffic noise from the nearby parking lot. However, in 2024, there is a noticeable migration toward the calm and pleasant sector; while the space remains eventful, the increased density of points in the lower-right quadrant indicates that the greenery and natural elements have become dominant.

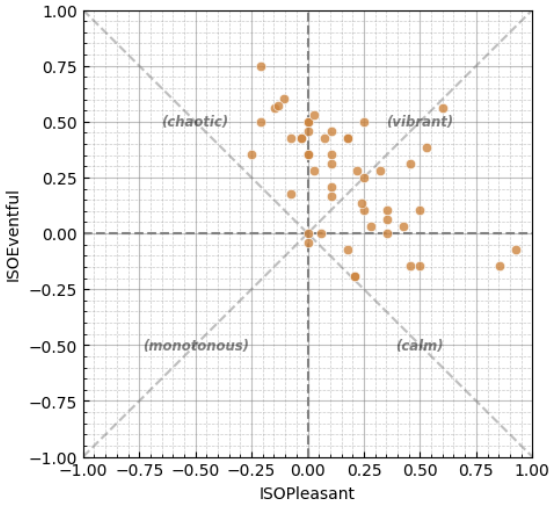


Figure 4.13: Point 2 circumplex (2024 soundwalk).

An interesting case is represented by point 3, located near academic buildings and a HVAC system. 2019 data reflexts a soundscape heavily constrained by constant mechanical noise, with responses clustered in the left side of the graph. The pervasive HVAC hum appears to have 'masked' the potential for any pleasant perception, effectively anchoring the site in a negative affective state. In the 2024, the data points migrate slightly toward the center, probably due to the systems being deactivated.[39]

39: The balance between mechanical noise and human noise is crucial in this point. The change in predominant perceived sound sources is evident in the graphs presented in Figure 4.7 and Figure 4.8.

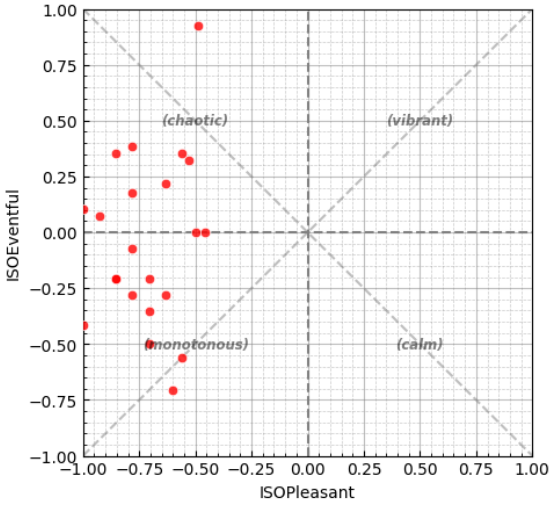


Figure 4.14: Point 3 circumplex (2019 soundwalk).

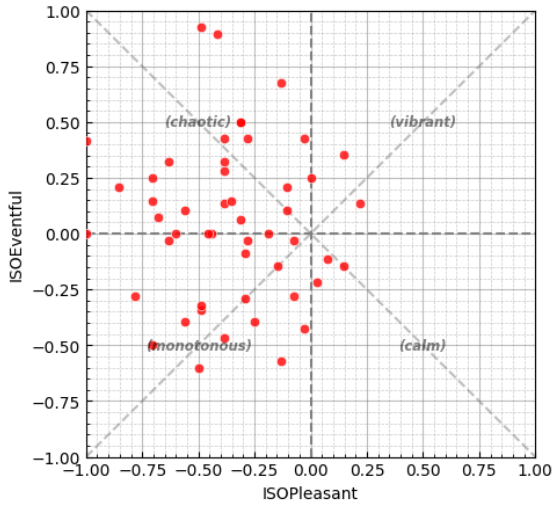


Figure 4.15: Point 3 circumplex (2024 soundwalk).

Point 4 is located near the central road axis of the campus, close to a building site.

This area has been object of significant changes in its landscape due to the construction of a new building, which has led to a significant increase in the presence of construction noise and road traffic noise, as also confirmed by the sound source predominance analysis shown in Figure 4.8.

The soundscape perception at this point appears to be extremely heterogeneous, with a wide dispersion of responses across all quadrants. This is likely due to the complex interplay of various sound sources, including road traffic noise, construction noise, and human activity, which contribute to a highly dynamic acoustic environment.

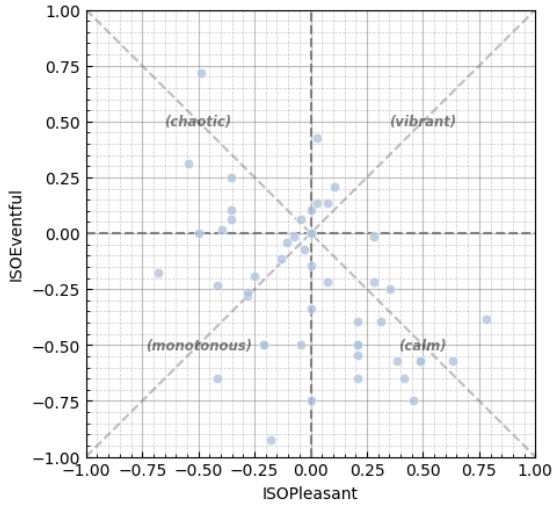


Figure 4.16: Point 4 circumplex (2024 soundwalk).

Point 5 appears to be somehow stable, with a wide dispersion of responses across all quadrants in both campaigns, likely due to the presence of a variety of sound sources, including road traffic noise, human sounds, and natural sounds, which contribute to a complex and dynamic acoustic

environment. However, a slight shift toward the calm and pleasant sector can be observed in 2024, probably due to the increased presence of natural sounds and the reduction of road traffic noise.

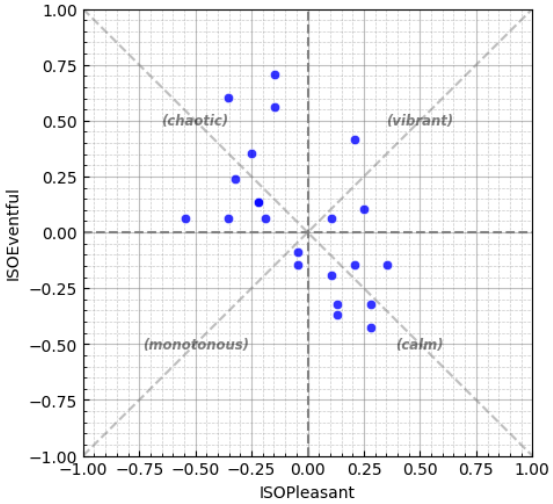


Figure 4.17: Point 5 circumplex (2019 soundwalk).

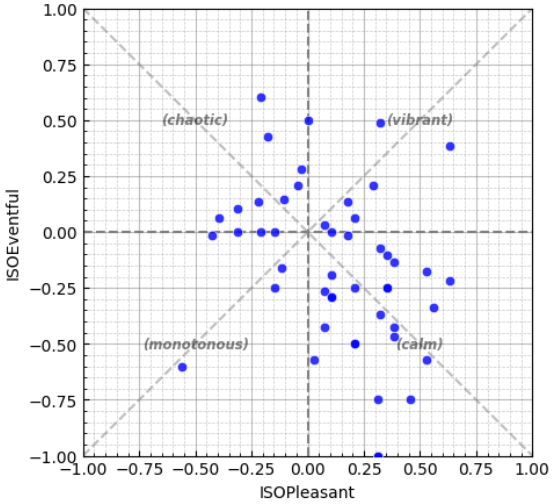


Figure 4.18: Point 5 circumplex (2024 soundwalk).

Point 6 is located in a green area close to the external road axis of the campus and the nearby highway which is directly visible due to the lack of natural barriers. Despite the presence of these noise sources, the soundscape perception at this point is predominantly calm and pleasant in both campaigns, as also shown by Figure 4.19.

This point clearly describes a calm and pleasant soundscape, with a high degree of uneventfulness. This area, even if it is located near the external road axis of the campus and the nearby highway, is characterised by a significant presence of natural sounds, which appear to have a strong influence on the soundscape perception, confirming the importance of natural elements in shaping the acoustic environment and in enhancing the pleasantness of the soundscape.

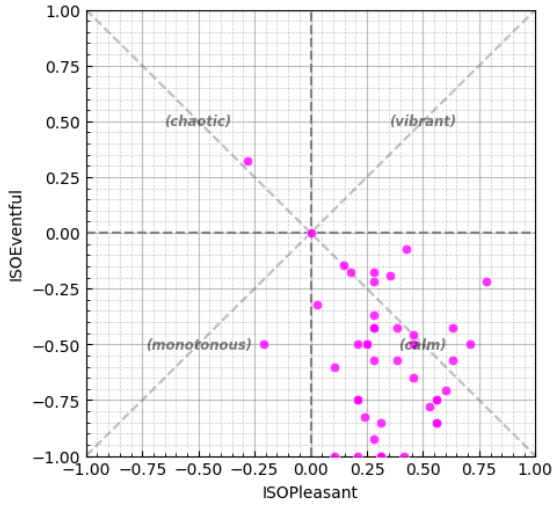


Figure 4.19: Point 6 circumplex (2024 soundwalk).

The perception of the main park of the campus is depicted in Figure 4.20 and Figure 4.21.

Differently from the point 6, this area is located in the central part of a green area, thus the nearby road axis and the highway are not directly visible, being separated by natural barriers and greenery. Thus, a calm and even more pleasant soundscape is expected to be perceived in this location.

However, the soundscape perception of this point in the 2019 soundwalk appears to be more eventful, with a significant dispersion of responses across the vibrant and calm quadrants, likely due to the presence of a variety of sound sources, including human voices.

In 2024, a shift toward the calm and pleasant sector can be observed, likely due to the increased presence of natural sounds with respect to the other sound sources, as also confirmed by the sound source predominance analysis shown in Figure 4.7 and Figure 4.8. The decrease in pedestrian activity, shaped the soundscape perception in this area, allowing the natural sounds to become more perceptually dominant, thus enhancing the overall pleasantness of the soundscape.

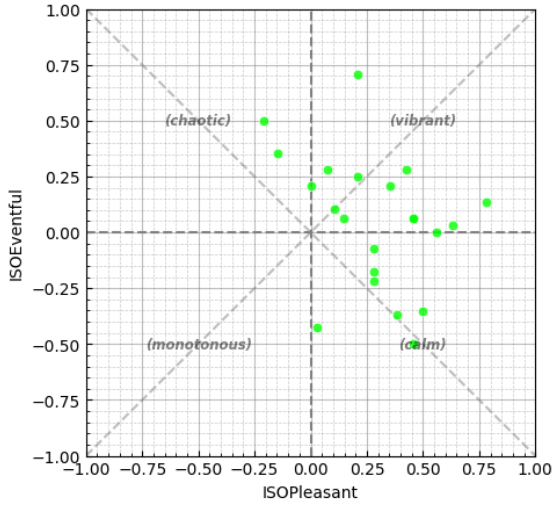


Figure 4.20: Point 7 circumplex (2019 soundwalk).

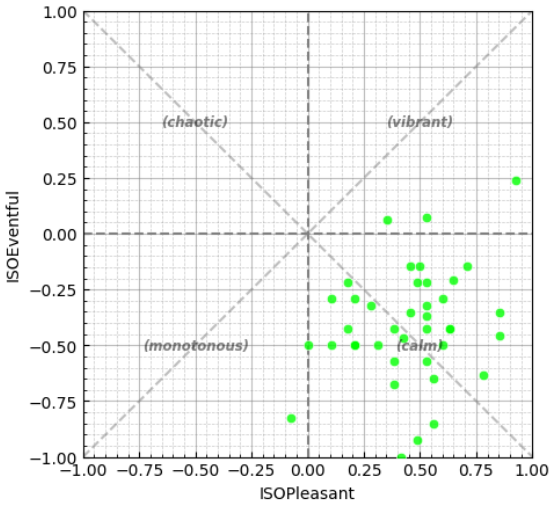


Figure 4.21: Point 7 circumplex (2024 soundwalk).

Similar insights can be drawn for point 8 and 9 which are located in two different squares of the campus, which are normally characterised by a high level of pedestrian activity, especially during the breaks between lessons, and by the presence of several facilities such as bars and stationery bookshops. However, the soundscape perception in these areas seems to have undergone a significant change between the two campaigns, as shown by Figure 4.22, Figure 4.23, Figure 4.24 and Figure 4.25.

Both points, 8 and 9, exhibit a similar trend in the evolution of their soundscape perception. In 2019, the soundscape perceptions in these areas were more concentrated in the vibrant and chaotic quadrants. The 2019 soundwalk, indeed, being conducted during the morning, captured the soundscape during a period of high pedestrian activity, which likely contributed to the perception of a more eventful and less pleasant soundscape. However, in 2024, there is a noticeable migration toward the calm and pleasant sector, likely due to the reduction of pedestrian activity and the increased presence of pleasant sounds.[40] The 2024 soundwalk, being conducted during the afternoon, captured the soundscape during a period of lower activity, which likely contributed to the perception of a more calm and pleasant soundscape.[41]

40: The reduction of pedestrian activity is also confirmed by the sound source predominance analysis shown in Figure 4.7 and Figure 4.8.

41: More details about the evolution of the soundscape over the time are provided in Section 4.7.3, where the pleasantness levels across the campus in different years and in different period of the day are investigated in a more detailed way.

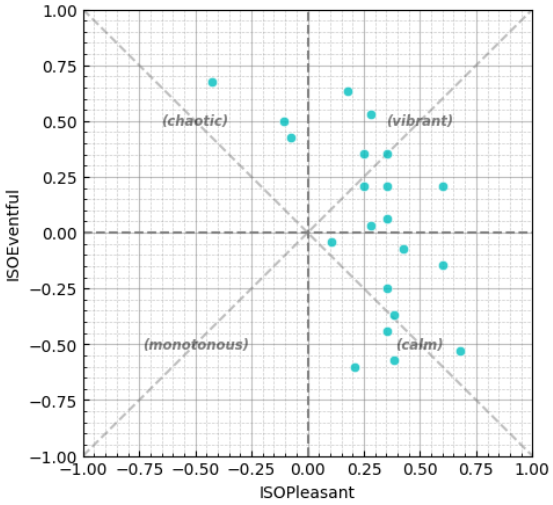


Figure 4.22: Point 8 circumplex (2019 soundwalk).

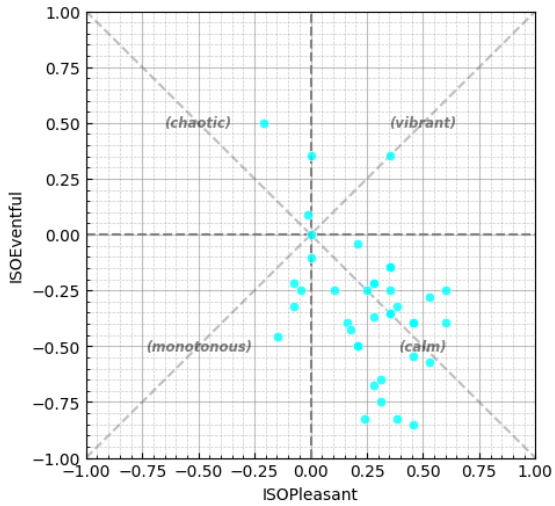


Figure 4.23: Point 8 circumplex (2024 soundwalk).

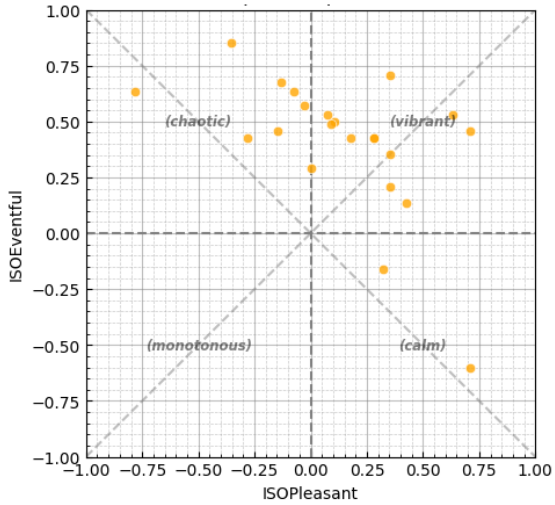


Figure 4.24: Point 9 circumplex (2019 soundwalk).

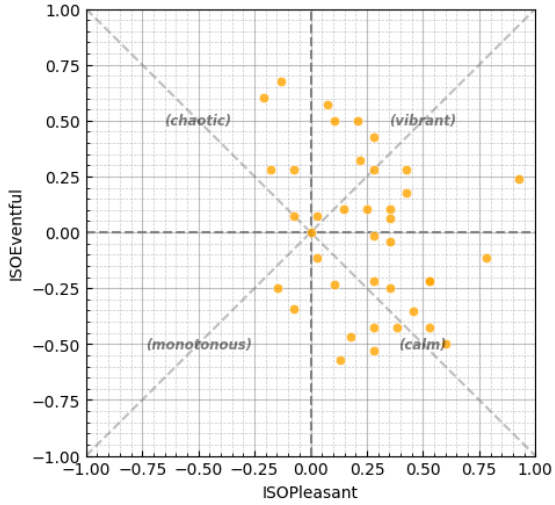


Figure 4.25: Point 9 circumplex (2024 soundwalk).

4.7 Mapping Pleasantness of the Campus Soundscape: Results and Discussion

In this Section the results obtained from the pleasantness mapping of the Fisciano campus soundscape are presented and discussed. The generated maps provide a visual representation of the spatial distribution of perceived pleasantness across the campus and they have been validated through a comparison with the soundwalks questionnaires' results, ensuring that the spatial patterns observed in the maps align with the perceptual assessments collected.

Further, a detailed spatial and temporal analysis of the pleasantness maps is provided, uncovering patterns and trends in the perceived pleasantness across different areas of the campus during different period.

4.7.1 Pleasantness Mapping Interpolation Results

The first pleasantness map of the Fisciano campus of the University of Salerno has been generated using the crowdsourced dataset collected from several NoiseCapture Party, specifically the first four editions have been used, i.e., NoiseCapture Party@Unisa 2018, NoiseCapture Party@Unisa 2019, NoiseCapture Party@Unisa 2022 and NoiseCapture Party@Unisa 2022 fall edition. During these events, a total of 217 participants actively engaged in the data collection process.[42]

Figure 4.26 illustrates the resulting pleasantness map of the campus environment, generated through the Inverse Distance Weighting (IDW) interpolation method. It visually represents the spatial distribution of pleasantness ratings across the campus, with colour gradients indicating varying levels of perceived pleasantness.

The fixed search radius for this interpolation has been set to 50 meters. The classification into different pleasantness levels ranges has been performed using the *Natural Breaks* method available in QGIS software [315], which identifies natural groupings inherent in the data.

Regarding the validation of the map, as mentioned earlier, a comparison with the soundwalks questionnaires' results has been carried out. It needs to be underlined that this validation procedure, together with the sensitivity analysis of the results with respect with the changing search radius to be presented in the current section, is limited to six points rather than the full set of nine. This reflects the project timeline: at this specific phase, only the results from the first soundwalk campaign (2019) were available as ground-truth for the mapping procedure, as subsequent campaigns were conducted after this initial methodology was established.[43]

42: Please note that at this stage, no cleaning procedure has been applied to the raw datasets, thus all the points collected during the NoiseCapture parties have been used for the mapping procedure. The followed rationale is to evaluate the methodology's robustness when applied to the raw participatory output. By using the unfiltered dataset, we establish a performance baseline that reflects the immediate nature of crowdsourced noise data; this allows for a more transparent assessment of the mapping procedure before the subsequent implementation of refined quality-control and data-cleaning protocols.

43: For this reason, please refer to Table 4.2 for the correspondence between the point IDs from the 2019 soundwalk and those from the 2024 soundwalk. In this Section, IDs' points refer to the 2019 soundwalk.

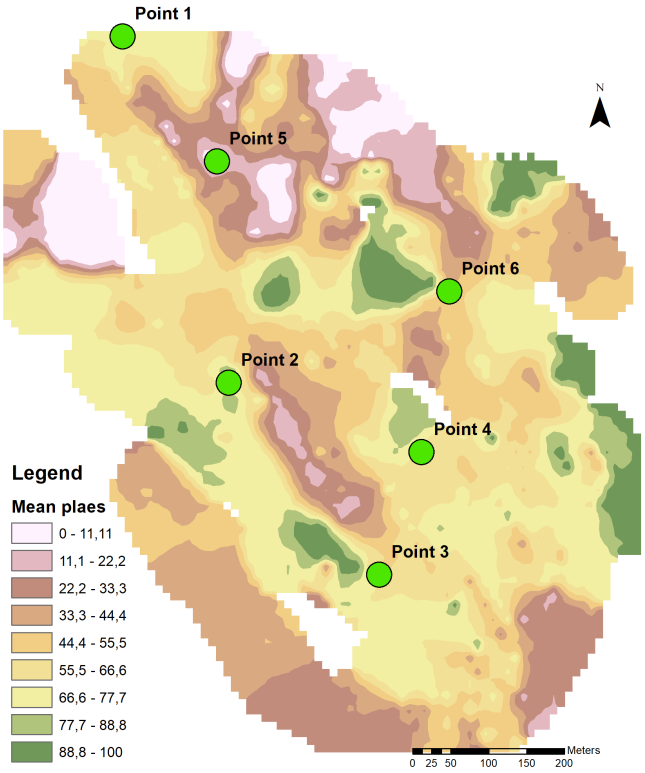


Figure 4.26: Pleasantness map of the Fisciano campus generated using IDW interpolation with a 50-meter search radius.

Moreover, since the soundscape assessments gathered during the 2019 soundwalk were used, both Method A and Method B were employed to validate the generated map. This approach facilitated a comparative analysis of the two protocols, aiming to determine which approach to use as the ground-truth reference for the final assessment and validation of the results obtained by the IDW interpolation in the six points of the soundwalk. These data are resumed in Table 4.4.

Figure 4.27 provides a visual comparison of the mean pleasantness values obtained from Method A, Method B, and the IDW interpolation at each of the six soundwalk points.

The comparison highlights that the IDW interpolation is in good agreement with the Method A responses, in almost all the points, except for point 1. It is important to note that this point is affected by a lack of surrounding measured data which can lead to a misestimation of the pleasantness value at that specific location. To overcome this issue, a mean of the pleasantness recorded in the nearest points in a range of 100 meters has been calculated, resulting in a value of 60.4%, which is more in line with the soundwalk results from both methods. This could be considered a good option to overcome the problem of missing data in the interpolation dataset. However, the choice of a bigger radius for the proximity analysis has to be carefully evaluated and supported by the homogeneity of the soundscape within the area. In the case under analysis, indeed, the soundscape is homogeneous in a range of 100 meters from point 1, being primarly influenced by road traffic noise and parking lots. The influnce of the selected search radius to consider a measurement "close enough" to influence the pleasantness in a given point is of course a key point of this approach. When applying the same procedure and

calculating the mean pleasantness of nearby measurements for the other points, results are not always converging to the soundwalk responses.

Table 4.4: Mean pleasantness measured with the soundwalk methods and simulated with IDW mapping.

Point	Method A [%]	Method B [%]	IDW Mapping [%]
Point 1	52.3	50.9	75.0
Point 2	72.7	58.6	77.5
Point 3	67.1	57.2	60.3
Point 4	61.4	52.8	61.0
Point 5	2.3	9.0	4.9
Point 6	54.4	46.0	46.6

Considering the Method A as the benchmark of this validation, indeed, in point 5 the inclusion of measurements that are 100 meters away from the point itself led to a value of 35.3%, that is very much higher than 2.3% obtained from the questionnaire evaluation pleasantness mean value. Point 5 is very close to noisy, cooling/heating implants (see Table 4.2), that strongly affects the soundscape perception in that area, leading to very low pleasantness ratings during the soundwalk. However, since this point is located in an open area, measurements taken at a distance of 100 meters are likely to be less influenced by this specific sound source, thus leading to a higher pleasantness value when averaging them. This confirms the importance of carefully selecting the search radius for the proximity analysis, taking into account the soundscape homogeneity in the area.

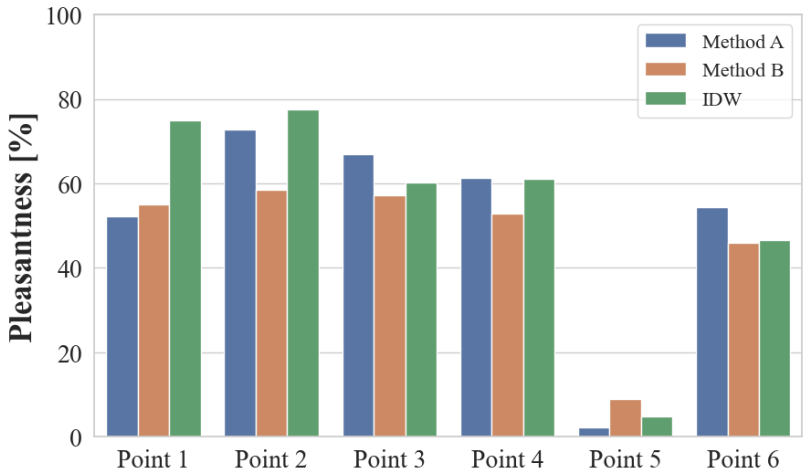


Figure 4.27: Comparison of mean pleasantness measured with the two methods during the soundwalk and simulated with the IDW interpolation of the NoiseCapture parties data at each of the six soundwalk points.

However, it's hard and even misleading to give a fixed value for the "influence radius", that can be considered acceptable in diverse applications and areas, since it strongly depends on the specific soundscape characteristics of the area under study and for this reason it should be estimated in terms of soundscape homogeneity.

Moreover, as reported earlier, Method B may be affected by the formulation of the question during the survey which asks to rate how much

the soundscape is unpleasant, rather than pleasant as in Method A. This can lead to a bias in the responses, as participants may focus more on negative aspects of the soundscape when asked about unpleasantness, explaining the general underestimation of pleasantness values obtained from Method B. Point 2 is a good example for this aspect. It is located in the main green park of the campus, full of nature and greenery.

Anyway, the soundscape of this point is affected by the highway that runs very close to the campus border, a few hundred meters away from the park. The participants gave a high rating in Method A questionnaires about how much pleasant this site is, probably also affected by the presence of natural masking sounds and by the visual aspects. However, when they are asked about the unpleasantness, they probably started to notice the presence of the annoying noise coming from the highway and the overall results are worse than the one measured with Method A. This effect is not included in the NoiseCapture parties data, in which this evaluation is asked in a more neutral way.

Overall, the agreement between the IDW interpolation results and the soundwalk Method A responses suggests that the mapping procedure is effective in capturing the spatial distribution of pleasantness across the campus. The Mean Errors are equal to -2.5% and -8.5% respectively for Method A and Method B, confirming the better performance of Method A for this specific application.[44] It should be also noticed that the general overestimation of the IDW map is influenced by the results in point 1. Excluding this point from the calculation of the error, based on the bad interpolation due to missing measured data, the Mean Error for Method A decreases to +1.5%, and -5.3% for Method B, confirming the good reliability of the mapping procedure.

44: Errors are calculated as the different between the measured pleasantness (i.e., defined as the mean questionnaire score obtained from Method A for each point) and the simulated value (i.e., derived from the IDW interpolation).

Sensitivity Analysis on the Search Radius: the Significance of Soundscape Homogeneity

As stated earlier, when performing an IDW interpolation, one of the most important paramters is the search radius. This radius influences the amount of data included in the interpolation and, in this specific analysis, from the physical point of view, it expresses the distance among data that can be considered somehow related to an homogeneous soundscape. As addressed by the insights gained by the obtained map, this distance must change according to the areas and the sources occurring within the site of interest.

For instance, moving inside a big parking area or along a main road of the campus, such as the path that goes from point 1 to point 2 of the soundwalk perfomed in 2019, allow for the usage of a large search radius, since this path is approximately 450 meters and its soundscape is quite homogeneous. When approaching point 2, the soundscape changes quickly over space. The main park of the campus is lying below the main campus road level and is clearly characterised by natural sounds.

However, the highway in front of the campus is a relevant noise source, that affects the appropriateness of the park soundscape. Thus, at the conjunction between these two areas, the search radius must be reduced, to consider the sharp variations in the soundscape and the different perception of it by people staying in those areas. To address this issue of nonhomogeneous soundscape, a sensitivity analysis has been performed, by varying the search radius of the IDW interpolation, to find if an optimal choice for the case under study can be identified.

Specifically, search radius from 50 to 300 meters have been tested. In each simulation, the values of the mean pleasantness in the six points under study have been retrieved from the maps and the variations have been analysed. The obtained results are reported in Table 4.5 and Figure 4.28.

It can be noticed that as the search radius increases, there is a general trend of decreasing pleasantness values across most points. This trend can be attributed to the inclusion of more diverse soundscape data from a broader area, which may introduce data from soundscape characterised by different sound sources into the interpolation.

Looking at Figure 4.28, it is noticeable that the choice of the search radius significantly affects the obtained pleasantness values. However, all the curves present some variations in a closer range (i.e., less that 100 meters), exhibiting a flat scope increasing the search radius. The pleasantness error, calulated as the difference between the IDW simulation results and the mean pleasantness obtained during the soundwalk with Method A, is reported in Figure 4.29 and Table 4.6.

Table 4.5: IDW pleasantness ([%]) in the six considered points with different search radius values.

Radius [m]	Point 1	Point 2	Point 3	Point 4	Point 5	Point 6
50	75.00	77.52	60.28	62.68	4.86	46.59
60	66.95	77.02	60.03	62.91	6.19	52.74
70	68.17	76.26	59.61	62.37	7.17	50.54
80	62.87	75.70	59.85	63.08	8.89	52.91
90	63.03	75.31	59.91	63.26	9.54	51.72
100	60.79	74.99	60.35	63.72	9.94	53.91
150	59.68	74.15	60.24	59.78	11.69	53.62
200	55.65	73.58	59.66	59.34	12.46	53.42
300	53.06	73.06	59.18	59.92	13.43	52.20

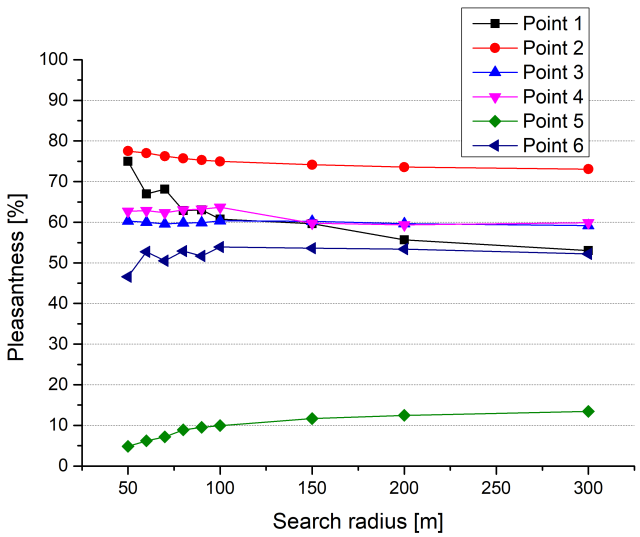


Figure 4.28: Sensitivity analysis of the mean pleasantness values at the six soundwalk points by varying the search radius from 50 to 300 meters.

Table 4.6: Difference [%] between IDW simulated values and soundwalk measurement, i.e., pleasantness error.

Radius [m]	Point 1	Point 2	Point 3	Point 4	Point 5	Point 6
50	22.73	4.79	-6.77	1.32	2.59	-7.82
60	14.68	4.30	-7.02	1.54	3.92	-1.68
70	15.90	3.54	-7.43	1.01	4.90	-3.87
80	10.60	2.98	-7.20	1.72	6.62	-1.50
90	10.76	2.58	-7.13	1.89	7.27	-2.69
100	8.52	2.26	-6.70	2.35	7.66	-0.50
150	7.41	1.43	-6.81	-1.58	9.41	-0.80
200	3.38	0.86	-7.38	-2.03	10.19	-1.00
300	0.79	0.34	-7.87	-1.44	11.15	-2.21

Point 1 shows the highest variability of the error as the search radius varies, and it diminishes as the distance increases. Point 6 also shows a decrease of the error. Point 5, on the contrary, presents an increasingly higher value of error when increasing the search radius. The other points have smaller oscillations as it can be noticed for point 3 error line, for instance, that is basically flat. These results indicate how the soundscape homogeneity is variable within the area under study.

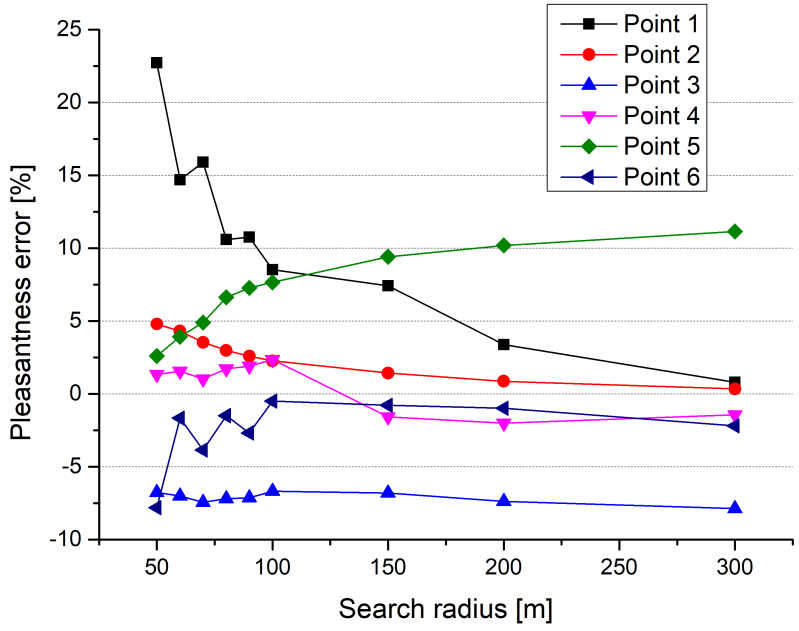


Figure 4.29: Variation of pleasantness error at each soundwalk point as the search radius changes.

In more detail, the specific features of each point are relevant to understand the slope of the error curves. Point 2, for example, is a large green area. Considering the common features of the entire soundscape, the perception of a quiet and pleasant environment is basically maintained throughout the whole area. As a consequence, the mean IDW pleasantness value is quite stable even if considering increasingly larger spaces, leading to a stable error when the search radius increases.

Similar conclusions can be drawn for point 1. Here, a remarkable variation of the pleasantness error is evident, with lower errors as the search

radius increases. As it happens for point 2, this is consequential to the homogeneity of the soundscape under investigation. By taking this homogeneity into account and enlarging the radius used to compute the IDW interpolation, as also stated earlier, more data can be included in the analysis, enabling a better fit with the results obtained during the soundwalk. However, if point 5 is taken into consideration, the opposite effect can be noticed, as commented earlier.

Another interesting remark is that pleasantness errors variation is more evident for search radius between 50 and 150 meters, but at a greater distance, the values remain more or less constant. A crucial output of this analysis is that it's very difficult if not impossible to define a unique value for the search radius that can be considered acceptable in the entire area of study or in different contexts, since the influence distance should be estimated is terms of soundscape homogeneity.

Nevertheless, the size of the area under study is a relevant parameter. The Fisciano Campus of the University of Salerno is a large area, thus a large variability of the soundscape needs to be acknowledged. Smaller areas, such as urban parks, industrial or residential areas, and areas along main transporation infrastructures, may allow the usage of a single smaller search radius.[45]

45: Thus, in some cases, an average value of the search radius could be identified, still being able to provide reliable and robust soundscape maps, consistent with the perceived sound environment.

4.7.2 Spatial Analysis of Pleasantness Maps: The Influence of Predominant Sound Sources

To gain deeper insights into the spatial dynamics of the campus soundscape, a comprehensive spatial analysis of the generated pleasantness maps has been conducted. This analysis aims to uncover patterns and trends in the perceived pleasantness across different areas of the campus, examining how they correlate with specific campus features and predominant sound sources. In order to achieve this goal, land use and facility maps of the campus have been considered, aiming to identify key sound sources that could affect the overall perception of the acoustic environment. Although the search radius to be used to perform the IDW interpolation cannot be uniformly fixed across the entire campus area, the sensitivity analysis previously presented has shown that, when set at 100 meters, the discrepancy observed during the validation process between the interpolation approach results and the soundwalk questionnaires answers stabilised itself. For this reason, a search radius of 100 meters has been selected for the spatial analysis of the pleasantness maps. Moreover, it needs to be underlined that, since the temporal analysis is not the focus of this Section, the pleasantness map has been generated using data from all four NoiseCapture parties; only the results from 2019's soundwalk have been used, as previously done for the validation procedure.[46]

46: For this reason, as in the validation procedure, point IDs from the 2019 soundwalk have been used. Please refer to Table 4.2.

Figure 4.30 illustrates the resulting pleasantness map of the campus, generated through the Inverse Distance Weighting (IDW) interpolation method with a search radius of 100 meters. Also in this case, as mentioned earlier, the classification into different pleasantness level ranges have been performed using the *Natural Breaks* method available in QGIS software [315]. However, only five classes have been used to classify the pleasantness levels, to have a clearer overview of the soundscape perception across the campus area. Thereafter, Figure 4.31 shows the land use and facility map of the Fisciano campus, used to perform the comparison between pleasantness map and objective predominant sound sources.[47]

47: In this context, "*objective*" distinguishes the land-use and facility data, which are derived from physical site characteristics and functional zoning, from the "*subjective*" perceptual data gathered through participant assessments.

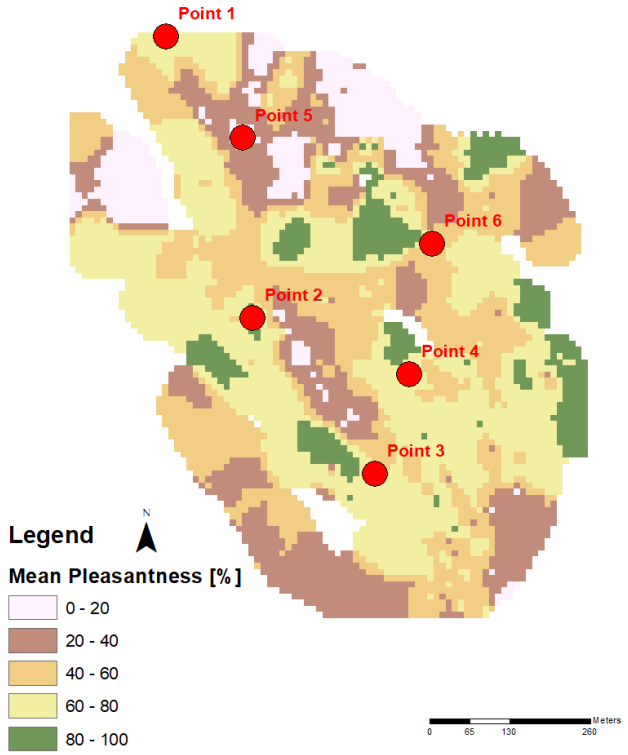


Figure 4.30: IDW interpolated map of pleasantness across the Fisciano Campus with a search radius of 100 meters. The measurement points refer to the 2019 soundwalk activity.

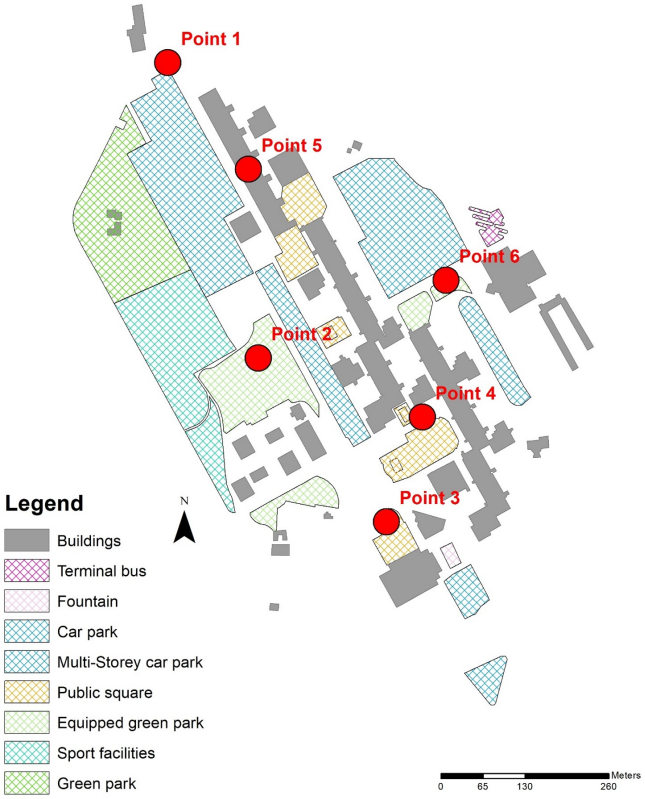


Figure 4.31: Land use and facility map of the Fisciano Campus.

Through the overlapping of these two maps, represented in Figure 4.32,

useful insights on the influence of sound sources on human perception of a soundscape could be gained.[48]

48: To obtain a readable map, the pleasantness map has been changed, preferring a grey colour scale from white to black.

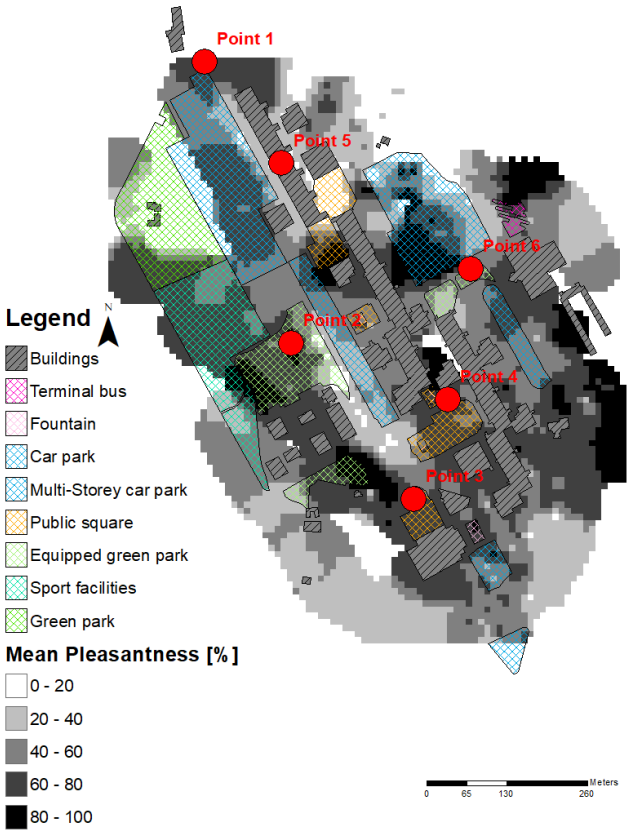


Figure 4.32: Overlapping of the pleasantness IDW map with the land use and facility map of the Fisciano Campus.

Higher pleasantness values are focused mostly in green areas of the campus, where natural sounds are most probably to be heard. Very high values of pleasantness can also be found in vibrant areas, such as in the southern part where squares are located and it is expected to have a lot of human sounds due to people chatting passing by. However, similar values are also observed within specific sectors of the campus two primary parking facilities; this phenomenon may be attributed to their spatial proximity to adjacent zones characterised by positive sound sources and diverse environmental features. It can be noticed, indeed, that the parking lot in the North-East part of the campus exhibits a portion with low pleasantness, close to the main external road and to the terminal bus, and another part with high pleasantness, near the canteen and a small green area. The parking lot in the North-West area exhibits a similar pattern, with a low pleasantness portion close to a not equipped green area and a high pleasantness region near the main green park. Thus, it can be deduced that road traffic noise is not the predominant sound source in these areas, as expected by only looking at the land use map, but the influence of nearby areas, which are characterised by more pleasant sound sources, such as natural sounds and human sounds, plays a significant role in shaping the overall soundscape perception within these parking facilities, contributing to such a better perception.

On the other hand, it seems that lower values of pleasantness are focused on the main road axis of the campus, the central parking lots and on the

green area in the North-West part of the campus. As for the latter, the low values of the pleasantness are probably due to its proximity to the highway located just in front of this area, to the ring road internal to the campus and to the parking lots. Moreover, the green area under analysis is not equipped (i.e., it is not provided with benches or resting areas), thus people do not tend to stay there for a long time, probably perceiving the soundscape as less pleasant. The visual impact of the highway, indeed, could also play a role in the overall soundscape perception.[49]

Mean pleasantness values in each polygon of the facilities and land use map has also been computed. Results are graphically represented in Figure 4.33.[50] It can be noticed that most of the areas of the campus have a pleasantness in a medium-high class. Only the mentioned earlier green area in the North-West part of the campus and the area close to point 5 show a low value of the mean pleasantness.

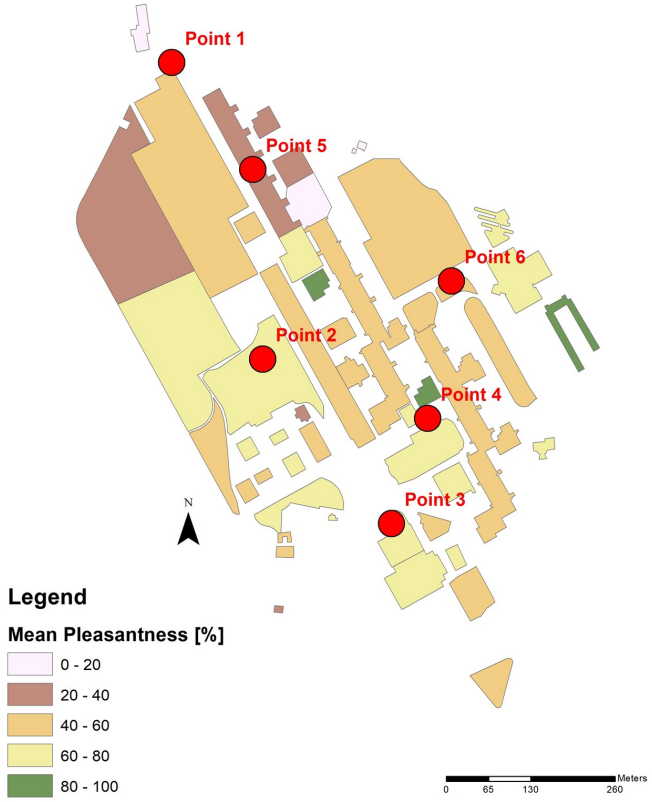


Figure 4.33: Mean pleasantness values in each polygon of the facilities and land use map of the Fisciano Campus.

While the intersection between the land use and pleasantness maps helps to provide interesting insights into the relation between the pleasantness and the presence of different sound sources, it is even more significant to identify the link between such soundscape attributes and actually perceived sound sources. This has been achieved by analysing the results of the soundwalk questionnaires. Participants in the soundwalk activity gave selected sound sources a score from 0% to 100% in each of the six points, indicating the predominance of each one over the others. The selected sound sources to be investigated, as requested by the standards [228], were: road traffic noises, other noises (i.e., industrial, construction works, and similar ones), human sounds and natural sounds. Figure 4.34 illustrates the mean predominance percentages of each sound in the selected points.[51]

49: Although several academic buildings with classrooms and offices are depicted on the map, it must be emphasised that these insights can only be applied to outdoor spaces, as "NoiseCapture parties" only collected data in outdoor areas. The indoor soundscape has not been analysed in this work, although a similar methodology applied to smaller areas could be used to study the soundscape of academic buildings.

50: In Figure 4.33, the colour of the buildings does not refer to the pleasantness indoor, but to the surrounding soundscape.

51: Scores assigned to each noise source during the soundwalk were first averaged and then normalised to 100% so that a comparison between the four sources could be achieved.

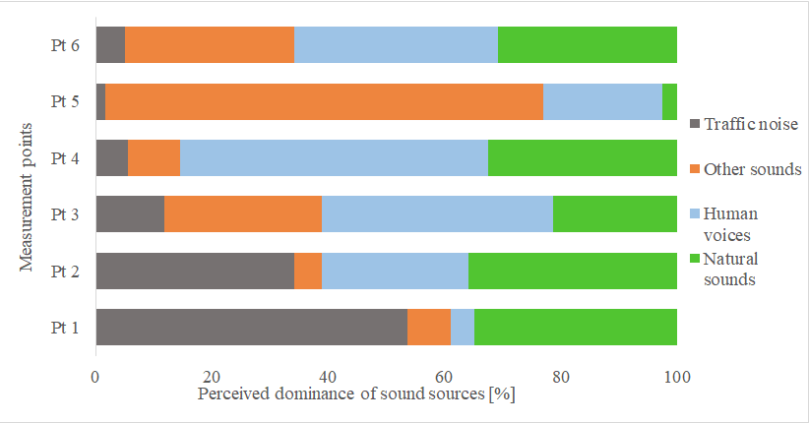


Figure 4.34: Mean percentages of each sound source predominance in the selected points of the Fisciano Campus.

As reported earlier and looking at Figure 4.32, it can be seen that even if point 1 is located near a parking lot, it has an intermediate pleasantness value, which agrees with previous comments about the influence of nearby areas characterised by more pleasant features. This is also confirmed by the analysis of the subjective responses regarding predominant sound sources obtained by Method-A questionnaires in Figure 4.34: natural sounds have been perceived just slightly less predominant than road traffic, determining a positive masking effect. The same observation applies to point 6 in which the proximity to parking lots and roads is not felt as negative, thanks to the predominance of natural sounds and chatting. On the other hand, in the main park of the campus (i.e., point 2), natural sounds are not perceived as the most predominant, since traffic noise and human voices also influence human perception. However, the pleasantness of this point is not as low as this aspect might suggest. This indicates that the visual aspect has a great influence on how the user perceives the soundscape.[52]

Point 3 and point 4 are similar in several aspects: human voices and natural sounds are the perceived predominant sound sources and they are located near public squares. The high levels of pleasantness here reported suggest the positive influence of these kinds of sounds on human perception of an acoustic environment. Finally, point 5 is near HVAC machines, which explains the high value assigned to the "other sounds" category, and the very low pleasantness value recorded in this area.

A quantitative comparison of the pleasantness in each point, as measured during the soundwalk activity, as obtained by IDW interpolation map (Figure 4.30) and as averaged in the polygon retrieved from the land use map (Figure 4.33) has also been performed. Results are reported in Table 4.7. When compared with the pleasantness values measured during the soundwalk activity, the results retrieved by the IDW interpolated map, built with a search radius of 100 meters, shows a good agreement in all the six points. Moreover, looking at the data in Table 4.7, it is evident that mean pleasantness values computed in the polygon of the land use map do not describe the soundscape in a whole area properly, since in the selected points they do not achieve good agreement with soundwalk values. This is mostly due to the edge effects already discussed, and thus the proximity between different acoustic environments that can affect the overall soundscape perception in a given area, that at this stage of the research has not been fully considered.[53]

52: This inevitably suggests that further analysis could be carried out from this point of view, also considering visual features alongside perceptual and acoustical ones. However, in this thesis, the focus is on soundscape mapping and analysis, thus visual features have not been considered.

53: This approach was initially intended to define a synthetic indicator to characterise the soundscape of a specific area. However, the results suggest that soundscape pleasantness lacks the necessary spatial homogeneity to be averaged within land-use boundaries, as the acoustic environment is shaped by fluid transitions rather than discrete land-use zones.

Table 4.7: Summary of pleasantness values in %, measured during the soundwalk activity, obtained by IDW interpolation map and averaged in the polygon retrieved from the land use map.

Point	Soundwalk pleas. values	IDW map pleas. values	Mean pleas. values in land use map areas
1	52.3	60.8	56.7
2	72.7	75.0	64.1
3	67.1	60.3	65.7
4	61.4	63.7	60.2
5	2.3	9.9	32.2
6	54.4	53.9	50.3

4.7.3 Temporal Analysis of Pleasantness Maps: The Evolution of Soundscape over Time

To further explore the dynamics of the soundscape within the Fisciano Campus, a temporal analysis of the pleasantness maps has been conducted. This investigation aims to understand how perceived pleasantness fluctuates across different time periods, accounting for variations in daily routines, weekly schedules and seasonal changes. The analysis has been performed by generating distinct pleasantness maps for each edition of "NoiseCapture party" events held on campus, employing the previously established IDW interpolation method.

As noted earlier, these maps have been generated using the point-based layer to isolate measurements recorded during each specific event.[54] To establish a robust framework for this temporal analysis, the initial step involved merging data from all NoiseCapture parties into a single dataset to create an overall pleasantness map, consistent with the results previously presented. This map has been used as a baseline for comparison against individual yearly maps, allowing the identification of potential temporal shifts. For the interpolation process, fixed search radii of 50 and 100 meters were adopted to assess variations at different spatial scales. Table 4.8 presents a comparative analysis of pleasantness values as measured through the soundwalk activity and estimated via IDW interpolation using both the 2024 dataset and the total cleaned dataset with different search radii.[55] Alongside this data, the equivalent continuous sound level $L_{A,eq}$ at each point measured during the 2024 soundwalk edition is also reported, offering a direct correlation between the perceptual data and the acoustic measurements at the specified locations.

The pleasantness values obtained through the IDW maps demonstrate relative stability across the different influence radii with both dataset. Moreover, comparing values from the total dataset with those of 2024 shows that some points remained relatively stable over time while others changed significantly.

For instance, point 2 and point 3 exhibit only minor variations between the IDW-interpolated values from the total dataset and those from the 2024 dataset, suggesting that the acoustic and environmental conditions at these locations have not changed a lot. Specifically, for point 2, the IDW values for both datasets and both search radii remain within a narrow range (approximately 53-58%), and the soundwalk measaurement (56.80%) aligns well with these estimates. Similarly, at point 3, the IDW values for the total dataset (30.71% for *r=50m* and 30.98% for *r=100m*) are

54: Previous results in this Chapter relied on the area-based layer, using mean values of pleasantness aggregated over several years. While that approach provided a comprehensive spatial overview, it precluded a more granular temporal assessment. In contrast, in this Section, the point-based data have been used to facilitate a year-by-year comparison, capturing the evolution of the perceived acoustic environment.

55: For consistency across the temporal comparison, points IDs from the 2024 soundwalk have been used (please refer to Table 4.2). Data from the 2018 NoiseCapture party, though present in earlier stages of this study, have been excluded from this specific analysis to ensure that the interpolation is based on a dataset with uniform sampling density and the same rigorous validation criteria used for the most recent campaigns.

very close to those from the 2024 dataset (24.71% for *r=50m* and 26.86% for *r=100m*), while the soundwalk results (21.00%) is just slightly lower, reinforcing the consistency and stability of the soundscape perception at this location over time.

Conversely, some points show considerable changes over time, likely due to modifications in their acoustic environment. In point 1, for example, while the IDW interpolation for the total dataset shows relatively high pleasantness values (86.30% for *r=50m* and 84.95% for *r=100m*), the 2024 dataset indicates a significant drop (33.43% for *r=50m* and 41.14% for *r=100m*). The soundwalk measurement (44.81%) corroborates this decline, suggesting either that the soundscape at this location has deteriorated over time, or that recent conditions have negatively influenced human perception of the area. This decline may be related to the fact that 2024 measurements were taken during peak hours, when vehicular noise from the near parking lot was at its highest, as shown also by the high $L_{A,eq}$ value recorded at this point (61.1 dBA). Moreover, ongoing construction work in the canteen building likely masked more pleasant sounds, reducing the perceived pleasantness. Since such works in progress were not present in previous years, this change highlights the dynamic nature of the acoustic environment and the impact of temporary but significant alterations in the soundscape.

Point 4 has undergone a noticeable change. Previously, this location was primarily a parking lot, but a new building has been constructed in recent years in this area, altering both the soundscape and the overall environmental perception. The IDW-interpolated pleasantness values have consequently changed, with a slight decrease compared to the total dataset (from approximately 60% to 35% in the 2024 with *r=50m*). The soundwalk measurement (52.55%) indicates a more moderate perception of pleasantness, suggesting that while the new building may have introduced some negative elements, the overall soundscape is still perceived relatively positively by users, probably due to the presence of residual green area.

Point 5 is characterised by IDW interpolation values that have remained relatively stable between the total dataset and the 2024 dataset (around 47-48% for both search radii). However, the soundwalk measurement (60.20%) is significantly higher than that, suggesting that direct human perception of pleasantness at this location is more favorable than predicted by the interpolation method. Given the noise level ($L_{A,eq}$ = 50.8dBA), this discrepancy might be explained by additional environmental factors, such as the presence of green spaces and, thus, natural sounds, which enhance the overall experience. The stability of the IDW values suggests that this location has not undergone major transformations, but the difference between the interpolated and the measured values underscores the limitations of relying solely on interpolation methods without considering direct human feedback.

Point 6, instead, exhibits a unique pattern due to data limitations. While an IDW-interpolated value was available for the total dataset for *r=100m* (48.39%), the absence of a value for *r=50m* in both datasets suggests a lack of sufficient nearby data points, likely due to fewer participants passing through that area or due to the cleaning process. Consequently, the interpolation may not accurately capture the complexity of local sound conditions, which is instead completely acknowledged during the soundwalk. With influence radius of 100 meters, the inclusion of data from more distant points allowed for the generation of estimates. However, these data are predominantly from points near the external

road, where perceived pleasantness is likely much lower than in the surroundings of the green area in point 6 itself. This aspect underscore the crucial role of the search radius in IDW interpolation, as it defines the spatial extent within which surrounding data points affect the estimation at a given location.

Another interesting case is point 7, where pleasantness values have remained high but still show variations between datasets. However, the 2024 dataset shows a slight decrease in interpolated values (70.30% for *r=50m* compared to 79.60% for the total dataset). The soundwalk measurement (86.58%) confirms that the area remains one of the most pleasant location of the campus, but the interpolation discrepancy suggests that the location possesses specific attributes, likely visual or environmental factors, such as greenery, that enhance the positive perception when stationary but may not be fully captured by a moving listener during data collection, such as happens during the NoiseCapture party approach.[56]

Point 8 and 9 have a similar trend. While IDW determines relatively stable pleasantness values between the total dataset, the soundwalk measurement tends to be considerably higher, indicating that participants perceived the area as more pleasant than estimated. This discrepancy, however, may be influenced by the different times at which participants engaged in the two activities. While both activities started simultaneously, participants in the 2024 NoiseCapture party edition completed their routes more quickly, passing through certain points earlier in the day, when background noise levels were still elevated due to ongoing academic and social activities. In contrast, the soundwalk included scheduled stops and required participants to answer questionnaires, resulting in a longer duration and a later passage through some locations. By that time, the acoustic environment may have been quieter, enhancing the perception of pleasantness. More specifically, participants in the soundwalk activity passed by point 8 and 9 around 6:00 P.M. when academic activities were almost over and a quiet environment was experienced, while the NoiseCapture party participants, passing by during peak hour around 4:00 P.M., had the full experience of a crowded and chaotic acoustic environment, which may not be perceived as fully pleasant.

56: As reported earlier in Section 4.2.1, the nature of the activity being performed while experiencing the soundscape actually shapes the listerner's perception. In this case, the soundwalk activity, which includes scheduled stops and questionnaires, allows participants to engage more deeply with the environment, potentially leading to a heightened awareness of pleasant features that may be overlooked during a more dynamic activity like the NoiseCapture party.

Table 4.8: Comparison of pleasantness as measured through soundwalk activity and computed through IDW interpolation with 2024 data and with the total cleaned dataset with different search radius *r*.

Point	$L_{A,eq}$ [dBA]	**IDW map** (total, *r=50m*)	**IDW map** (total, *r=100m*)	**IDW map** (2024, *r=50m*)	**IDW map** (2024, *r=100m*)	**Soundwalk** (2024)
1	61.1	86.30	84.95	33.43	41.14	44.81
2	51.1	53.80	54.00	58.09	56.80	61.00
3	57.8	30.71	30.98	24.71	26.86	21.00
4	51.0	60.69	59.59	35.29	28.80	52.55
5	50.8	47.49	47.67	47.00	-	60.20
6	47.1	-	48.39	-	38.08	77.27
7	44.6	79.60	73.49	70.30	63.34	86.58
8	49.3	62.31	62.92	-	61.37	71.25
9	47.2	53.09	53.88	52.63	53.25	71.15

Table B.1 provides a comparison of pleasantness values computed through IDW interplation for each year's dataset with search radius of 100 meters. This comparison allows to observe the evolution of the soundscape **over the years**, highlighting any significant changes in perceived pleasantness at each point. A clear distinction emerges between areas where the acoustic environment has remained relatively stable and those where it

has undergone significant transformations. For instance, location such as point 2 and 7 exhibit only minor fluctuations, indicating that the environmental and acoustic conditions at these sites have remained mostly unchanged over the years. This stability may be attributed to the consistency of the surrounding areas and the lack of significant alterations in land use or infrastructure. In contrast, other points of the campus have seen considerable shifts. Several ongoing construction activities have been present lately on the campus, in particular near point 1, 4 and 5. These modifications in the campus infrastructure have likely led to an increased auditory presence of disruptive elements, overshadowing the more pleasant sounds that once contributed to the area positive acoustic perception. For instance, the introduction of a new building near point 4 appears to have altered the local soundscape, with the IDW interpolation suggesting a drop in pleasantness value in 2024.

While the temporal evolution of the campus over the years reveals broader trends, a closer examination of the daily changes in the soundscape at specific points offers additional insights into its fluctuating nature. Analysing the data from Table B.1 gives a more nuanced understanding of how the soundscape at particular locations evolves. For instance, point 1 demonstrates a marked decrease in perceived pleasantness in the first edition of the 2022 and 2024 datasets compared to previous years, likely due to increased vehicular noise from nearby parking facilities during peak hours when such activities took place. Thereafter, point 7 which is characterised mainly by green spaces and relatively low noise levels, maintains a high perception of pleasantness. However, a slight decrease is observed between the 2024 and the total dataset, suggesting that **time-of-the-day factors** shape the acoustic experience. The timing of the NoiseCapture party activities, which occurred during peak traffic hours, may have contributed to a more intrusive soundscape at this location, probably due to a nearby external road. Similarly, the discrepancies notable in point 8 and 9 can be attributed to the fact that, while both activities started simultaneously, participants in the 2024 NoiseCapture party edition completed their routes more quickly, passing through certain points earlier in the day, when background noise levels were higher due to ongoing activities, whereas the soundwalk included scheduled stops and required participants to answer questionnaires, resulting in a longer duration and a later passage through some locations. By that time, the acoustic environment may have been quieter, enhancing the perception of pleasantness, as also discussed earlier.

Table 4.9: Comparison of pleasantness computed through IDW interpolation with different datasets and search radius *r=100m*, and measured during soundwalks.

Point	**IDW '19** Morning	**IDW '22(i)** Afternoon	**IDW '22 (ii)** Morning	**IDW '23** Afternoon	**IDW '24** Afternoon	**IDW Total**	**SW** ('19)	**SW** ('24)
1	74.26	38.34	77.56	65.51	41.14	84.95	-	44.81
2	57.02	30.57	59.74	46.51	56.80	54.00	54.40	61.00
3	48.36	25.31	25.43	26.61	26.68	30.98	2.30	21.00
4	75.31	100.00	69.53	41.77	39.31	59.59	-	52.55
5	-	-	-	-	46.77	47.67	52.30	60.20
6	61.00	-	60.85	75.00	38.08	48.39	-	77.27
7	77.42	-	75.94	75.43	63.34	73.49	72.70	86.58
8	66.82	100.00	56.03	76.35	61.37	62.92	67.10	71.25
9	55.65	100.00	49.75	63.68	53.25	53.88	61.40	71.15

4.8 Final Remarks

The investigation presented in this Chapter marks a fundamental theoretical and methodological pivot from the traditional, pathogenic management of environmental noise toward a holistic, salutogenic appraisal of the urban soundscape. By utilising the Fisciano campus of the University of Salerno as a representative "*micro-city*" laboratory, the research successfully operationalises the premise that human response to the acoustic environment is not merely a function of cumulative sound energy, but a complex cognitive interpretation moderated by spatial, temporal, and functional contexts.

A primary achievement of this work is the development and validation of a novel methodology for mapping perceptual attributes, specifically "pleasantness", by leveraging the synergy between standardised soundwalk protocols [228, 229] and large-scale participatory crowdsourcing data. Translating subjective, intangible responses into spatially continuous maps via Inverse Distance Weighting (IDW) interpolation provides a highly intuitive and robust tool for urban designers. This approach mirrors the accessibility of conventional noise maps while successfully capturing the nuanced reality of human auditory perception. Furthermore, the combined spatial and temporal analyses yielded valuable insights into the dynamics of acoustic comfort, demonstrating practically how positive auditory stimuli, such as natural environments and social vibrancy, can effectively mask mechanical stressors and elevate the perceived quality of spaces even in close proximity to major transportation infrastructures.

However, examining these findings through a critical scientific lens reveals several inherent limitations in current soundscape mapping techniques that warrant further attention. Foremost among these is the profound challenge of defining and quantifying soundscape homogeneity. The spatial sensitivity analysis demonstrated that the optimal search radius for IDW interpolation is highly variable and context-dependent. Assuming uniform spatial continuity across abrupt morphological or functional boundaries inevitably leads to edge effects, where the mathematical aggregation of perceptual data risks smoothing over the sharp transitions that define complex urban acoustic ecosystems.

Furthermore, a critical methodological vulnerability emerges from the observed discrepancies between the two data collection paradigms. The stationary, deliberate evaluations conducted during the soundwalks frequently yielded different perceptual outcomes compared to the dynamic, transient assessments recorded via the crowdsourced application. This divergence underscores a crucial nuance: a listener's specific activity, level of environmental engagement, and duration of exposure fundamentally modulate their acoustic appraisal. The evaluation of a soundscape given by users during a soundwalk could not mirror the fluid and dynamic experience of the same soundscape in quotidian life, where individuals are often in motion and less consciously attuned to their surroundings. This raises important questions about the ecological validity of soundscape assessments and suggests that future research should explore more integrative methodologies that can capture both the depth of stationary perception and the breadth of dynamic experience.

Translating the inherent subjectivity of human acoustic perception into continuous, tangible spatial representations offers a profound advantage for urban environmental analysis. These pleasantness maps successfully capture the nuanced perceptual reality of a specific temporal window,

functioning as highly informative acoustic *photographs*. However, from a practical standpoint, acknowledging this snapshot-like quality highlights a widespread limitation in current planning methodologies, where the inherent dynamicity of the soundscape is frequently overlooked. Existing approaches often present a supposedly comprehensive soundscape review of a given area, yet such evaluations remain inevitably bounded by the specific timeframe of data collection. Given that transitory acoustic events and daily traffic fluctuations can drastically alter a localised environment, these static representations, while invaluable for visualizing spatial patterns, demonstrate that future strategies must move beyond time-fixed evaluations to actively incorporate the continuous, lived temporal depth of the urban acoustic ecosystem.

Ultimately, while the methodology developed in this Chapter successfully delivers a powerful tool for translating human perception into spatial maps as accessible as conventional noise maps, it also reveals the profound complexity and fluidity of acoustic perception. The observed edge effects and temporal discrepancies underscore that the soundscape is not a static, homogenous entity that can be neatly mapped, but rather a dynamic, context-sensitive experience that defies simple spatial aggregation. As such, while these maps provide critical insights and tools for urban planners, they also highlight the need for future research to develop more sophisticated, adaptive methodologies that can capture the full temporal and experiential richness of the soundscape. Moving forward, the goal of acoustic planning must evolve from mapping the invisible to actively orchestrating it. This requires a bold shift toward highly context-sensitive and temporally adaptive strategies, ensuring that the acoustic environments of our future cities are not just incidentally tolerable, but intentionally resonant, restorative, and vividly alive.

Conclusions 5

5.1 Synthesis of the Research: Key Findings and Contributions 157
5.2 Implications for Theory and Practice 158
5.3 Limitations of the Study 159
5.4 Future Research Directions 161

The world is never truly silent; rather, it is woven from a constant and complex acoustic tapestry that envelops our everyday existence. This thesis embarked upon a critical inquiry to bridge the historical chasm between the objective, physical measurement of sound and the profound, subjective reality of human perception. By weaving together the disparate threads of engineering, physics, and environmental psychology, this thesis has sought to redefine how we assess, predict, and ultimately perceive the acoustic scenario of our environments. Crucially, advancing toward a soundscape paradigm does not necessitate abandoning the rigorous foundations of traditional noise assessment. Rather, a dual-lens framework emerges as essential: retaining the fundamental physics of noise assessment and mitigation while simultaneously integrating the subjective, human-centered art of soundscape orchestration. By acknowledging that noise is a physical pollutant to be systematically controlled, and sound is a vital resource to be intentionally curated, this thesis establishes methodologies to investigate and analyse urban scenarios from different points of view. This integrated perspective recognises that a truly sustainable environment must not only protect its inhabitants from auditory harm, by assessing and mitigating noise pollution in a scientifically rigorous manner, but also actively nurture their psychological well-being through positive acoustic stimuli.

5.1 Synthesis of the Research: Key Findings and Contributions

To operationalise this dual-lens philosophy and fully decipher the urban acoustic tapestry, the research was strategically structured around two distinct, yet complementary, methodological pillars. Together, these pillars establish a comprehensive framework that examines the acoustic environment through both its physical and perceptual dimensions. The overarching aim was to develop a versatile toolkit: on one side, advancing the objective prediction of physical noise through a highly granular Road Traffic Noise Model, and on the other, establishing a spatial framework for mapping human-centered, subjective appraisals. Acknowledging that physical noise mitigation and perceptual soundscape curation serve different, yet equally, vital purposes, this research proves that both operational avenues could be effectively utilised to comprehensively manage and elevate the acoustic environment.

The first pillar advanced noise source modelling through the development and validation of a novel stochastic and microscopic Road Traffic Noise Model. By generating individual vehicle kinematics from aggregate data and assigning probability-driven speeds to each transit, this model successfully breaks down traffic into its fundamental components. This stochastic core was further refined through granular spatial disaggregation, treating individual lanes as distinct noise sources, and temporal enhancement via Seasonal Autoregressive Integrated Moving Average (SARIMA) forecasting of the traffic inputs. The findings have definitively established that lane-specific disaggregation can significantly reduce the systematic underestimations inherent in centralised line-source assumptions, preserving the unique acoustic energy of individual vehicular

transits. This advancement not only enhances the fidelity of noise predictions but also provides a more nuanced understanding of the acoustic contributions from different traffic lanes, which is crucial for targeted noise mitigation strategies. Furthermore, the temporal enhancement through SARIMA forecasting offers greater modelling flexibility and potential for noise predictions, allowing a more sophisticated characterisation of the dynamic temporal fluctuations of traffic noise. This dual spatial-temporal advancement provides a highly realistic and dynamic representation of acoustic contributions, which remains absolutely critical for developing responsive, targeted physical noise management strategies capable of adapting to fluid and complex urban traffic conditions.

The second pillar shifted the analytical focus from the physical noise source to the subjective listener. Utilising the Fisciano campus of the University of Salerno as a "micro-city" living laboratory, the intangible aspects of subjective perception were mapped using crowdsourced observations alongside standardised ISO soundwalks. Through Inverse Distance Weighting (IDW) interpolation, the subjective attribute of pleasantness was successfully translated into spatially continuous maps. The most valuable contribution of this perceptual framework is the empirical validation that human acoustic comfort extends far beyond the mere absence of high-energy noise. It demonstrates that restorative auditory stimuli, such as natural elements and the vibrancy of social presence, function as powerful modulators that actively enhance the perceived quality of a space. By translating these intangible experiences into continuous spatial data, the research effectively captures the "acoustic DNA" of the acoustic scenario in which people are immersed. This insight disrupts the traditional, strictly pathogenic paradigm of noise control, proving the necessity of integrating qualitative, perceptual metrics into common urban design approaches. Therefore, by highlighting the role of positive auditory stimuli and social vibrancy, this research aims at opening new avenues for urban soundscape management that not only mitigate noise but also actively enhance the acoustic environment to promote well-being and social cohesion. This shift towards a more holistic approach to soundscape management has the potential to transform urban environments into more livable, enjoyable spaces that foster a sense of community and improve overall quality of life.

5.2 Implications for Theory and Practice

The methodologies employed in this thesis offer robust, pragmatic solutions to tangible challenges in urban planning and environmental engineering. Theoretically, this research catalyzes a profound methodological evolution by formalising a dual-lens framework. Rather than advocating for a wholesale replacement of traditional noise assessment with soundscape approaches, this thesis demonstrates that both paradigms can coexist and can complement each other to provide a more comprehensive understanding of the acoustic environment.

The traditional, pathogenic approach to noise management remains indispensable for identifying and mitigating sources of harmful noise pollution. Moreover, it provides the scientific rigor necessary for regulatory compliance and the protection of public health. Practically, addressing the physical lens of this framework, the integration of time-series forecasting with the stochastic road traffic noise model tackles a complex real-world challenge: the acoustic assessment of infrastructure that does not yet

exist. By learning temporal traffic patterns from analogous existing infrastructures or from traffic microsimulators, this hybrid tool can generate dynamic, highly realistic noise predictions during the critical early design phases. Policymakers, urban planners, and environmental engineers must leverage these predictive models to proactively simulate dynamic noise exposures and include targeted mitigation strategies in the designing phase.

However, standard acoustic metrics alone are insufficient to capture the full spectrum of human experience in urban environments. This thesis proved that physical metrics should be seamlessly integrated with a holistic, salutogenic appraisal of the urban soundscape that actively considers the psychological and social dimensions of acoustic experience in order to fully understand and manage the acoustic environment. By demonstrating that subjective perception can be rigorously quantified and spatially mapped alongside physical measurements and noise maps, this dual approach aims to bridge the historical gap between the physics of acoustic engineering and the qualitative insights of environmental psychology. In doing so, it effectively operationalises the modern concept of an "acoustically high-quality area". Rather than merely discussing this as a theoretical ideal, this research provides robust empirical evidence to the growing consensus in the body of soundscape research that acoustic quality is achieved not only through the reduction of harmful noise, as traditionally defined, and the consequent improvement of physical acoustic metrics, but through the balanced coexistence of mitigated noise levels and the presence of meaningful, restorative sound.

This insight has profound practical implications for urban design and soundscape management. The pleasantness mapping techniques developed herein can be actively used to pinpoint vulnerable acoustic zones and map perceptual landscape. It suggests that decision-makers must adopt a holistic approach to acoustic management that goes beyond simply reducing energy levels. Through intentional "acoustic curation", urban planners should actively seek to enhance these environments by integrating positive sound elements into their design strategies. This could involve the intentional incorporation of green spaces, water features, and areas for social interaction that provide restorative auditory stimuli and enhance the overall soundscape quality. Ultimately, this proactive, dual-lens approach to management, simultaneously mitigating harmful noise and cultivating positive sound, has the potential to transform urban environments into more livable, enjoyable spaces that promote public health, well-being, and social cohesion.

5.3 Limitations of the Study

While this thesis establishes a robust, dual-lens framework for the comprehensive analysis of the urban soundscape, the theoretical and methodological ambition of this work inevitably reveals specific boundaries that must be critically acknowledged. A rigorous evaluation of these constraints is indeed essential not only for contextualising the current findings but also for defining the operational limits of the proposed methodologies.

Within the physical acoustic framework, the fundamental architecture of the stochastic microscopic Road Traffic Noise Model, while innovative, is not without its limitations. At this stage, the model introduces certain simplifications. The current energetic summation approach relies on the

assumption that individual vehicle transits are independent, acoustically transparent point sources. From a critical physical perspective, this simplification neglects the complex acoustic screening and multiple-reflection phenomena that naturally occur between vehicle bodies in high-density, congested traffic scenarios. By treating dense queues as a sum of independent energies, the model risks overestimating the propagated noise in heavily saturated conditions. Consequently, the current version of the model may not fully capture and accurately predict noise propagation within such complex urban traffic scenarios.

Furthermore, assigning constant, probability-driven speeds per individual transit introduces a degree of simplification within the inherent transient kinematics of traffic flow. Urban mobility is characterised by a dynamic interplay of accelerations and decelerations, with interrupted flows, bottlenecks, and stop-and-go patterns that can be present in real-world traffic scenarios. Sudden accelerations can significantly alter not just the overall sound pressure level, but the spectral signature of the noise, shifting the acoustic energy toward low-frequency engine rumble. By not fully capturing these transient kinematic phases, the model predictive fidelity is relatively constrained when applied to highly complex environments, where the acoustic impact of such transient events can be particularly pronounced. This means that while the model provides a significant improvement over traditional approaches, there is still room for refinement to capture the full complexity of real-world traffic noise, especially in scenarios characterised by high congestion and dynamic traffic patterns.

In the perceptual domain, moving from discrete subjective evaluations to continuous spatial maps exposed inherent methodological challenges. The application of IDW interpolation assumes uniform spatial continuity (i.e., isotropy). However, the acoustic environment within campuses and urban areas is inherently anisotropic, fractured by functional zones, physical barriers, and morphological discontinuities. Because IDW is a purely mathematical, distance-decay algorithm, it is "blind" to physical barriers and functional boundaries. Consequently, it is highly vulnerable to edge effects and risks creating a misleading spatial continuity that does not reflect the true heterogeneity of the acoustic environment. Moreover, it risks creating a "spatial blurring" effect, for instance, interpolating a smooth transition between a noisy and unpleasant area and a quiet and pleasant one, when in reality such transition may be abrupt and highly localised, due to the presence of a physical barrier, such as a building.

Moreover, the application of two distinct perceptual data collection paradigms shed light on how the assessment method itself can influence the nature of the data collected and the subsequent interpretations. Some discrepancies between the stationary, deliberate evaluations conducted during ISO soundwalks and the dynamic, transient assessments gathered via the crowdsourced NoiseCapture application were observed. Crucially, the standardised ISO soundwalks, which require participants to stop and evaluate their surroundings, may induce a state of acoustic hyper-awareness that could not be fully representative of how individuals typically experience their acoustic environment during everyday activities. By explicitly instructing individuals to halt and evaluate their surroundings, participants are compelled to dedicate focused cognitive resources to the acoustic environment, actively isolating and analysing nuances, distant sources, and background murmurs that they would instinctively filter out during their everyday routines. Consequently, an artificially heightened, highly analytical vision of the soundscape that diverges significantly from the passive, subconscious manner in which

citizens naturally experience and navigate urban sounds on a day-to-day basis could actually be assessed. In contrast, the crowdsourced method used in this research predominantly captures a fleeting perspective, reflecting the specific scenario of passersby who are in motion and may not be consciously evaluating their acoustic environment. This discrepancy suggests that different data collection methods can be used to capture different facets of the acoustic experience, and that the choice of method can significantly influence the insights gained about how people perceive and interact with their acoustic environment.

5.4 Future Research Directions

To systematically address the methodological constraints encountered and fully realise the potential of the dual-lens framework, future research must pursue advanced integrations in both the physical and perceptual domains.

Within the physical acoustic framework, future efforts must prioritise the refinement of the stochastic Road Traffic Noise Model to capture higher degrees of kinematic dynamism, by embedding acceleration and deceleration profiles. Furthermore, developing advanced computational algorithms capable of simulating vehicle-to-vehicle acoustic screening in congested, high-density traffic configurations will be imperative to prevent energy overestimation. Finally, the predictive architecture must be expanded to incorporate non-traffic ambient background noise, in order to provide high predictive performance also during quieter nighttime or off-peak hours.

Transitioning to the perceptual domain, advancing soundscape mapping methodologies requires moving beyond purely geometric, isotropic interpolation. Future investigations could explore the integration of machine learning algorithms to dynamically weight spatial variables during interpolation, and create a dynamic search radius that can adapt to the local heterogeneity of the environment. By training models to recognise functional urban boundaries and physical topographies, the edge effects that currently compromise spatial continuity assumptions could be effectively mitigated.

Simultaneously, future inquiries must rigorously address the psychological divergence between stationary, deliberate evaluation and mobile, transient engagement. A critical next step is the development of hybrid protocols for capturing the duality of the "perceived" (actively evaluated) versus the "experienced" (passively navigated) soundscape. Additionally, there is a need for longitudinal studies that track individual listeners' acoustic appraisals over time, considering their activities and exposure durations to better understand how these factors may influence soundscape perception. This nuanced understanding will be crucial for designing interventions that effectively respond to both the immediate, momentary perceptions of passersby and the more reflective appraisals of stationary listeners. Ultimately, maintaining this continuous effort will be essential to engineering environments that are not only quieter, but sonically richer, healthier, and profoundly attuned to the subtleties of the human experience.

Appendix

A

Questionnaire used during the soundwalk activities

Please mind that the questionnaire is in Italian, as the soundwalk activity was held in Italy and the participants were Italian speakers. Moreover, the questionnaire was designed to be filled in by hand, so it is not possible to provide a digital version of it. The PDF file included in this chapter is a scan of the original paper questionnaire.

As for the questionnaire used during the 2024 soundwalk activity, same questions were asked, but the questionnaire was designed to be filled in digitally.

Sesso ____ , Età _____ , Note _____

Data _____ Orario ____ : ____ Punto di misura _____

In che misura percepisci i seguenti 4 tipi di suoni?

Scegli *una sola* risposta per ogni tipo di suono

	Per niente	Poco	Moderatamente	Molto	Domina completamente
Rumore da traffico veicolare (auto, bus, treni, aerei, ...)	☐	☐	☐	☐	☐
Altri rumori (sirene,industre, costruzioni, carico e scarico merci, ...)	☐	☐	☐	☐	☐
Souni provenienti da altre persone (risate, conversazioni, bambini che giocano, passi, ...)	☐	☐	☐	☐	☐
Suoni naturali (uccelli che cinguettano, acqua che scorre, vento, ...)	☐	☐	☐	☐	☐

Per ognuno degli attributi indicati, in che misura sei d'accordo (o non) che l'ambiente acustico che ti circonda è:...

Scegli *una sola* risposta per ogni valore

	Molto d'accordo	D'accordo	Né d'accordo né in disaccordo	In disaccordo	Molto in disaccordo
Piacevole	☐	☐	☐	☐	☐
Caotico	☐	☐	☐	☐	☐
Vivace (vibrante)	☐	☐	☐	☐	☐
Non movimentato	☐	☐	☐	☐	☐
Tranquillo	☐	☐	☐	☐	☐
Fastidioso	☐	☐	☐	☐	☐
Movimentato	☐	☐	☐	☐	☐
Monotono	☐	☐	☐	☐	☐

Complessivamente, come descriveresti l'ambiente acustico che ti circonda?

Ottimo	Buono	Nè buono né cattivo	Cattivo	Pessimo
☐	☐	☐	☐	☐

Complessivamente, in che misura l'ambiente acustico che ti circonda è appropriato per il luogo dove ti trovi?

Per niente	Poco	Moderatamente	Molto	Perfettamente
☐	☐	☐	☐	☐

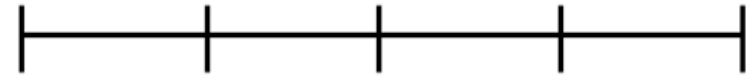
Quanto è rumoroso (*loud*) questo posto?

Segna la tua impressione/sensazione in un punto *qualsiasi* della scala seguente



Quanto è sgradevole (*unpleasant*) questo posto?

Segna la tua impressione/sensazione in un punto *qualsiasi* della scala seguente



Quanto è appropriato (*appropriate*) questo posto?

Segna la tua impressione/sensazione in un punto *qualsiasi* della scala seguente



Quanto spesso vorresti visitare questo posto?

Segna la tua impressione/sensazione in un punto *qualsiasi* della scala seguente



Elenca le sorgenti sonore che hai individuato inziando dalla più evidente.

Limitati a *8* sorgenti sonore

Ulteriori informazioni

Scrivi i tuoi *pensieri* e i tuoi *sentimenti* dopo aver ascoltato l'ambiente circostante

B

Maps of Pleasantness During the Years

In this Appendix, the maps of pleasantness obtained during each edition of the NoiseCapture party are reported. The maps are obtained through an Inverse Distance Weighted (IDW) interpolation using a search radius of 100m and a power parameter of 2.

To improve the readability of the maps, Table B.1 has been reported in this Appendix. The Table shows the values of pleasantness obtained through IDW interpolation at the points of the soundwalk routes, for each edition of the NoiseCapture party, and the values of pleasantness measured during the soundwalks. The comparison between these values allows to better understand the differences between the maps obtained through IDW interpolation and the perceived pleasantness during the soundwalks.

Table B.1: Comparison of pleasantness computed through IDW interpolation with different datasets and measured during soundwalks.

Point	**IDW '19** Morning	**IDW '22(i)** Afternoon	**IDW '22 (ii)** Morning	**IDW '23** Afternoon	**IDW '24** Afternoon	**IDW Total**	**SW** ('19)	**SW** ('24)
1	74.26	38.34	77.56	65.51	41.14	84.95	-	44.81
2	57.02	30.57	59.74	46.51	56.80	54.00	54.40	61.00
3	48.36	25.31	25.43	26.61	26.68	30.98	2.30	21.00
4	75.31	100.00	69.53	41.77	39.31	59.59	-	52.55
5	-	-	-	-	46.77	47.67	52.30	60.20
6	61.00	-	60.85	75.00	38.08	48.39	-	77.27
7	77.42	-	75.94	75.43	63.34	73.49	72.70	86.58
8	66.82	100.00	56.03	76.35	61.37	62.92	67.10	71.25
9	55.65	100.00	49.75	63.68	53.25	53.88	61.40	71.15

In the following pages, the maps of pleasantness obtained through IDW interpolation for each edition of the NoiseCapture party are reported. The maps are ordered chronologically, starting from the 2019 edition and ending with the 2024 edition. Each map is accompanied by a caption that indicates the edition of the NoiseCapture party when the measurements were taken.

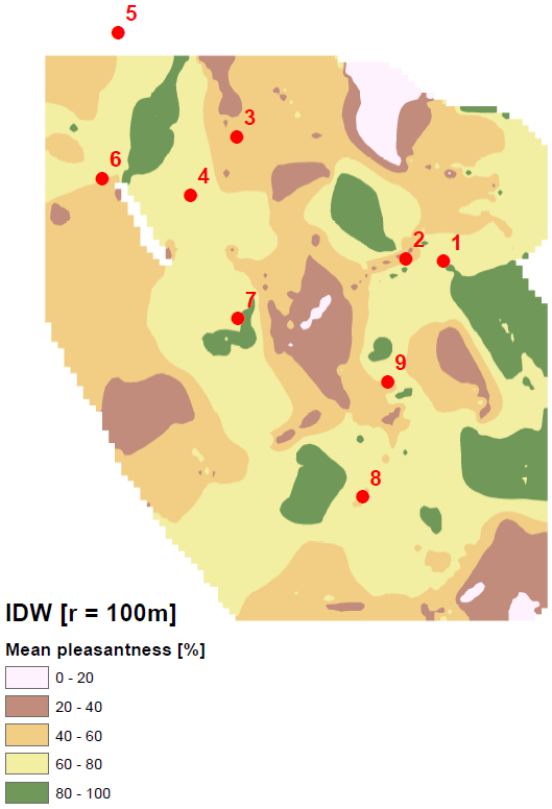


Figure B.1: Pleasantness map of the 2019 edition of the NoiseCapture party.

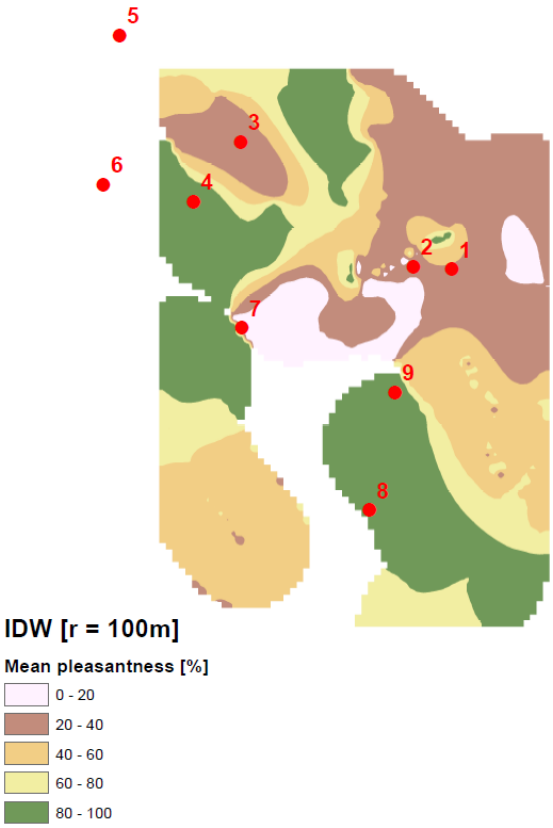


Figure B.2: Pleasantness map of the 2022i edition of the NoiseCapture party.

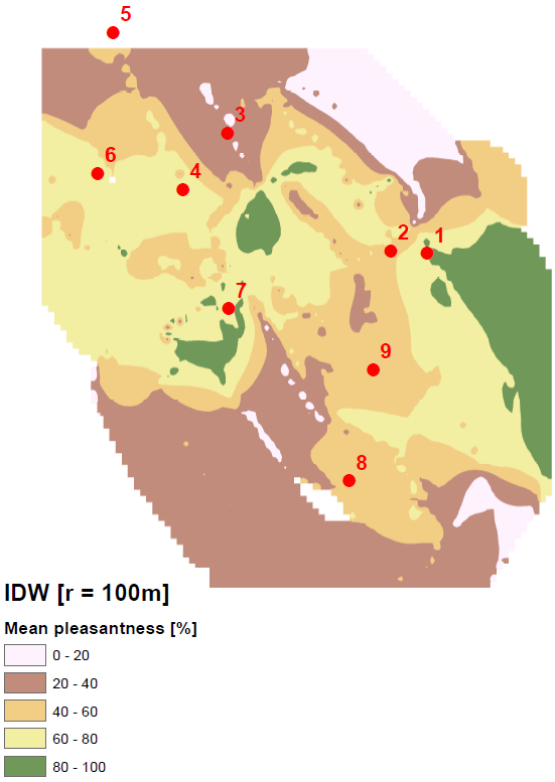


Figure B.3: Pleasantness map of the 2022ii edition of the NoiseCapture party.

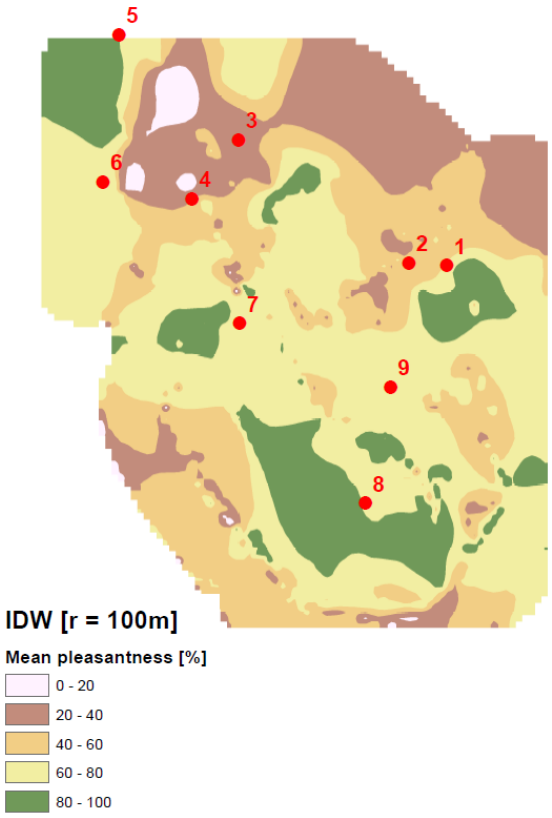


Figure B.4: Pleasantness map of the 2023 edition of the NoiseCapture party.

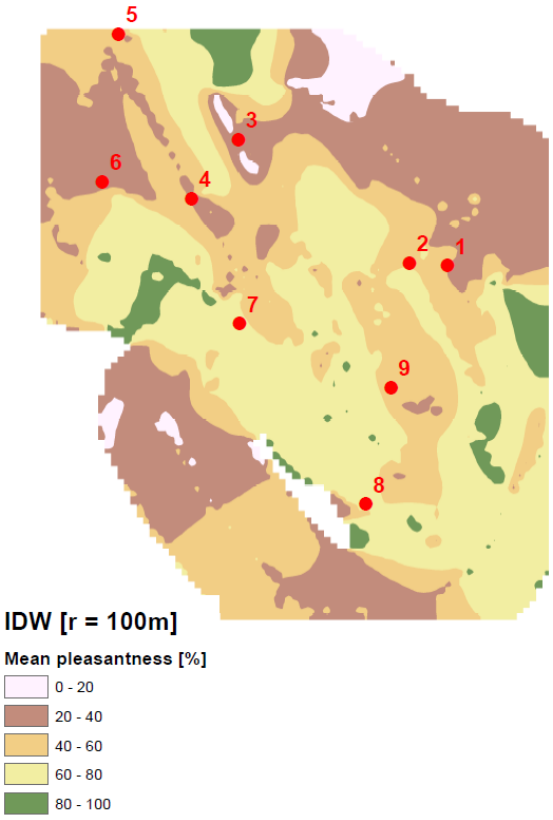


Figure B.5: Pleasantness map of the 2024 edition of the NoiseCapture party.

C

Appended Papers

Paper A

Claudio Guarnaccia, **Aurora Mascolo**, Pierre Aumond, Arnaud Can, Domenico Rossi. (2024). 'From early to recent models: A review of the evolution of road traffic and single vehicles noise emission modelling'. *Current Pollution Reports* 10(4), pp. 662-683 (2024).

Paper B

Aurora Mascolo, Domenico Rossi, Alessandro Ruggiero, Claudio Guarnaccia. 'A stochastic and microscopic model to predict road traffic noise by random generation of single vehicles' speeds'. *The Journal of the Acoustical Society of America* 157(2), pp. 721-737 (2025).

Paper C

Aurora Mascolo, Domenico Rossi, Mariangela Nigro, Benoit Gauvreau, Claudio Guarnaccia. 'Comparison of stochastic and microscopic road traffic noise models using variable level of aggregation of traffic flows'. *Conference proceedings of* 11th *Forum Acusticum Euronoise 2025, European Acoustics Association* (2025).

Paper D

Aurora Mascolo, Domenico Rossi, Claudio Guarnaccia. 'Combination of time series forecasting models with a microscopic and stochastic approach to predict road traffic noise'. *The Journal of the Acoustical Society of America* 159 (3), pp. 2754-2778 (2026).

Paper E

Aurora Mascolo, Domenico Rossi, Michele Grimaldi, Claudio Guarnaccia.'Soundscape indicators assessment and mapping in a university campus'. *Conference proceedings of* 10th *Forum Acusticum, European Acoustics Association* (2023).

Paper F

Aurora Mascolo, Domenico Rossi, Michele Grimaldi, Claudio Guarnaccia. 'Soundscape maps of pleasantness in a university campus by crowd-sourced measurements interpolation' *Noise Mapping*, 11(1), 20220178 (2024).

Paper G

Aurora Mascolo, Domenico Rossi, Michele Grimaldi, Claudio Guarnaccia. 'Study of pleasantness maps and perceived predominant sound sources in a university campus soundscape analysis' *INTER-NOISE and NOISE-CON Congress and Conference Proceedings* 270(7), pp. 4838-4852 (2024).

Paper H

Aurora Mascolo, Domenico Rossi, Michele Grimaldi, Claudio Guarnaccia. 'The role of pleasantness mapping in a university campus for studying soundscape subjective perception in evolving environments' *Conference proceedings of* 11th *Forum Acusticum Euronoise 2025, European Acoustics Association* (2025).

Current Pollution Reports (2024) 10:662–683
https://doi.org/10.1007/s40726-024-00319-5

A

REVIEW

From Early to Recent Models: A Review of the Evolution of Road Traffic and Single Vehicles Noise Emission Modelling

Claudio Guarnaccia[1] · Aurora Mascolo[1] · Pierre Aumond[2] · Arnaud Can[2,3] · Domenico Rossi[1]

Accepted: 19 June 2024 / Published online: 30 July 2024
© The Author(s) 2024

Abstract

Purpose of the Review This paper is devoted to the review of the most popular literature Road Traffic Noise Models (RTNMs) frameworks, from the oldest ones to the recent machine learning techniques. A dedicated section is reserved to the review of Noise Emission Models (NEMs), with specific focus on approaches that allow the assessment of single vehicles' emissions. Finally, some propagation models are also briefly presented, along with the assessment of the impact on the population of road traffic noise, in terms of time-averaged indicators and exposure descriptors.

Recent Findings In recent years, many efforts have been devoted to developing methods and models to assess the impact of environmental noise. Considering the primary role of road traffic as a noise source, estimating its impact is fundamental when evaluating the acoustic environment of a specific urban area. The scope of RTNMs is to provide an assessment of the noise emitted by the source in terms of traffic flows, propagate it at any desired point, including possible corrective factors, assess the impact at the receiver, and use this information to provide maps and other useful outputs.

Summary This review summarizes the so-far developed approaches for road traffic noise evaluation and furthermore underscores the ongoing necessity for research to develop more precise tools useful for managing road traffic noise's adverse effects on urban environments and public well-being. Challenges and limitations of such models are discussed in the conclusions, highlighting the need for providing high quality input data and avoiding site-dependent approaches.

Keywords Road traffic noise · Modelling · Single vehicle noise emission · Micro to macro modelling · Propagation and assessment

Introduction

The ongoing urbanization and population growth that characterize modern cities have resulted in an increased demand for mobility, consequently contributing to the degradation of acoustic environments in urban scenarios. As a result, a significant amount of people, about 20% of the European population, live in areas where noise levels are considered harmful to human health due to long-term exposure to high levels of noise, with road traffic consistently identified as the most annoyance noise source [1]. The potential consequences of prolonged exposure to noise, both psychological and physical well-being, include sleep disturbances, hearing loss, cardiovascular issues, anxiety, and stress, among others [1–3]. Considering that one of the main EU objectives is to reduce the number of people chronically disturbed by transport noise by at least 30% within the year 2030 [4], it appears clear the necessity to be able to assess the impact of transportation noise. Therefore, in recent years, considerable

✉ Claudio Guarnaccia
cguarnaccia@unisa.it

✉ Aurora Mascolo
amascolo@unisa.it

Pierre Aumond
pierre.aumond@univ-eiffel.fr

Arnaud Can
arnaud.can@univ-eiffel.fr

Domenico Rossi
drossi@unisa.it

[1] Department of Civil Engineering, University of Salerno, Via Giovanni Paolo II, 132, Fisciano I-84084, Italy

[2] Université Gustave Eiffel, CEREMA, UMRAE, F-44344 Bouguenais, France

[3] WAVES Research Group, Department of Information Technology, Ghent University, 4 Technologiepark 126, Zwijnaarde, 9052 Ghent, Belgium

effort has been devoted to developing methods and models to assess the impact of environmental noise. In particular, considering the primary role of road traffic as a noise source [1], the estimation of its impact is fundamental when evaluating the acoustic environment of a specific urban area. This evaluation can be carried out either through extensive in situ measurement campaigns or using appropriate modelling simulations. However, the use of simulations over in situ measurements can be preferred due, for example, to the high costs involved, the time burden related to the organization and any follow-up studies of such measurement campaigns, as well as the need for appropriately trained staff and so on. Finally, a fundamental and non-trivial reason that might lead to a preference for the use of models over actual measurements is that the impact on the urban noise environment of a road still in the design phase might want to be assessed and, as such, it cannot yet be the subject of measurements.

A detailed review of the most popular Road Traffic Noise Models (RTNMs) was presented by Steele in [5], in which the author presented the early models, together with the methods used at the time of the publication, by reporting the equations and the adopted parameters. Mann et al. provide a specific overview on RTNMs for developing countries [6]. Moreover, by reviewing 11 traffic noise modelling strategies, Ibili et al. found that researchers, probably due to costs and time required to develop new models, have developed new RTNMs by starting from earlier models as a baseline, adapting them to their specific conditions [7]. Some other critical and interesting reviews can be find in the work of Garg et al. and of Rajakumara et al. [8, 9], in which useful resuming tables, reporting the main features of the RTNMs under review, can be found. In particular, Garg et al. [8] draw a comparison between the main traffic noise models adopted in different countries on the basis of technical attributes, such as source modelling and sound propagation algorithms. On the other hand, Rajakumara et al. [9] compared eight literature models with an "ideal" model to be developed that could overcome several gaps of the literature ones.

Focusing on Noise Emission Models (NEMs) of single vehicle and road traffic, some recent papers have been published, providing critical insights and useful methods. For instance, in [10••], Rey-Gozalo et al. reported how recent studies' results actually could improve the accuracy of road traffic noise assessment and how appropriate action plans could reduce the noise emitted by vehicles.

In [11], Can and Aumond studied the influence of speed and acceleration in road traffic noise emissions estimation. Using real vehicles trajectories data, taken in a dense urban corridor, they found that commonly used noise emission models could misestimate noise levels under congestion, emphasizing the need for additional enhancements in dynamic road traffic noise models.

Another detailed description of some NEMs can be found in [12] in which the selected models were tested to highlight critical hotspots in the case study. In [13•], Pascale et al. also considered how different typologies of propulsion (namely gazoline, diesel, LPG, and hybrid) contribute to the correct evaluation of sound power level of a vehicle, opening the way to a detailed microscopic modelling that includes also the motorization of the single vehicle.

Once the single vehicle noise emission has been estimated with any microscopic NEM, it is possible to define impact indicators. In [14], two indicators based on the second-by-second sound power level of a single vehicle are defined, namely the overall and the average sound power level emitted during a route. They can be used for eco-routing applications, such as in [14, 15], or for signal setting design, as for example in [16], expanding the potential applications of road traffic noise assessment. Moreover, the problem of variability in single vehicle sound power levels of mixed fleet can occur. This is mainly due to variation in emissions of a fleet of vehicles, affecting both static and dynamic modelling. In [17•], the authors suggested that noise emission levels calculated through usual static noise prediction models should be corrected using a correcting factor that depends on the variance of the residuals distribution.

The general idea of any Road Traffic Noise Model is to provide an assessment of the noise emitted by the source in terms of traffic flows, to propagate it at any desired point, including possible corrective factors, to assess the impact at the receiver, and to use this information to provide maps and other useful outputs. Figure 1 illustrates the four main

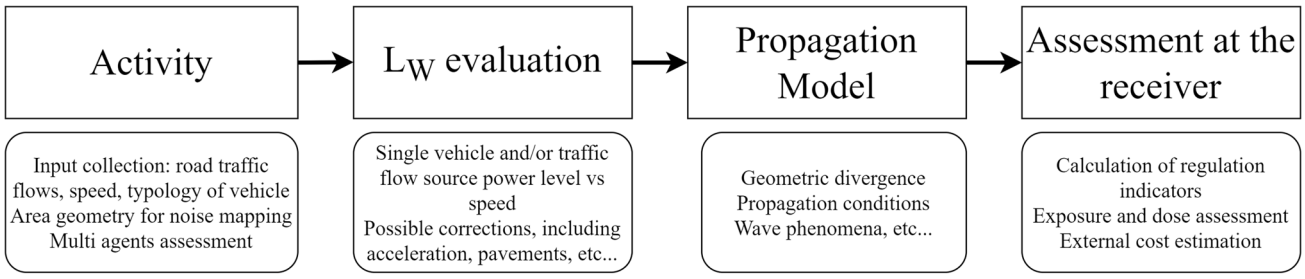


Fig. 1 Flowchart of the common road traffic noise modelling chain

components of road traffic noise modelling framework. It is noteworthy that certain models proposed by the community do not entirely separate the different models, but this schematic view nonetheless allows for their comprehensive understanding.

In this paper, the authors aim to present the most popular modelling frameworks that have been proposed in recent years. For the sake of brevity, the focus of the paper will be on emission models, with special care on models that allow the assessment of single vehicles' emissions. These models, in fact, can be used in a microscopic modelling of a complex network, combined with a micro-to-macro process and a propagation model, to assess the road traffic noise impact at any receiver, as it is done in most macroscopic models. A detailed report about how the input of the models is obtained, i.e. the study of the activity of the source, will be postponed to a forthcoming paper, as well as a review of the propagation models and the assessment at the receiver. For these reasons, after resuming in "Evolution of Road Traffic Noise Modelling: from Early Statistical Models to Machine Learning Approaches" section the evolution of road traffic noise modelling approach, from early models to recent AI and machine learning techniques, an overview of the most up-to-date approaches to assess the sound power level L_W of road traffic, namely the NEMs is provided in "NEMs Review" section. The propagation models of road traffic noise are briefly presented in "Propagation and Assessment at the Receiver" section, together with the assessment at the receiver, in which the possible uses of RTNMs predictions are presented. To assess the impact on the population of road traffic noise, in fact, collective and time-averaged indicators must be estimated to compare prediction results with regulation limits, as well as exposure descriptors to provide insight on health effects. Finally, in "Conclusions" section, the conclusions are given. It is noteworthy to underline that the variables and symbols of the models reported in this paper may sometimes be slightly different from the original versions. This choice was made for coherence purposes and to improve the readability of the paper.

Evolution of Road Traffic Noise Modelling: from Early Statistical Models to Machine Learning Approaches

Many models have been developed and used to assess road traffic noise. The older approach consists on collecting large sets of field data in several conditions and then performing statistical regressions with fixed formulas. Such an approach has been then improved including additional parameters and adopting more advanced mathematical algorithms.

Historical Models

The earliest RTNMs date back to the 1950s and work with traffic flow, instead of individual vehicles. Although based on a statistical approach that simplifies the actual traffic conditions, they are usually able to provide fairly accurate results. These are generally the simplest type of models, characterized by a small amount of input data required and providing as an output the percentile L_{50} or the L_{eq}. They are usually based on regressions that are typically performed on specific dataset. Thus, they are influenced by local conditions, both in terms of road and weather characteristics and vehicle types, which leads them to a limited accuracy. Indeed, the key inputs are usually traffic flows for the vehicle categories considered (i.e. light and heavy vehicles), characteristics of the road surface, and distance between carriage and receivers.

An early RTNM was developed in the *Handbook of Acoustic Noise Control* [18]. This model primarily relied on two inputs: Q is the traffic volume in vehicles per hour, and d is the distance from the observation point to the center of the traffic lane. The percentile L_{50} for vehicles with a speed of about 55–75 km/h and a distance greater that 6 m can be computed following the formula (1):

$$L_{50} = 68 + 8.5Log(Q) - 20Log(d) \tag{1}$$

It has to be underlined that this model does not provide any kind of specification with respect to vehicle types or road characteristics.

Subsequently, Nickson et al. introduced an alternative model that included a constant term, also referred to as C essential for aligning the model with experimental data [19]. The formula used is presented in Eq. (2)

$$L_{50} = C + 10Log\left(\frac{Q}{d}\right) \tag{2}$$

Later, Johnson et al. presented a model that also considered the average vehicle speed v as input data, along with some corrective factors related to ground attenuation and gradient, as shown in formula (3) [20]:

$$L_{50} = 3.50 + 10Log\left(\frac{Qv^3}{d}\right) \tag{3}$$

Galloway et al. in [21] made some improvements to the previous model, introducing the percentage of heavy vehicles P as in Eq. (4).

$$L_{50} = 20 + 10Log\left(\frac{Qv^2}{d}\right) + 0.4P \tag{4}$$

With the introduction in several regulations of the equivalent level L_{eq} as a sound level indicator, one of the most used

models that uses the same inputs to compute the equivalent level is the Burgess model [22] presented in Eq. (5).

$$L_{eq} = 55.5 + 10.2Log(Q) + 0.3P - 19.3Log(d) \quad (5)$$

Another model was proposed by Griffiths and Langdon in 1968, with the aim of computing the L_{eq} using the percentile levels L_{10}, L_{50}, and L_{90} as in formula (6) [23].

$$L_{eq} = L_{50} + 0.018\left(L_{10} - L_{90}\right)^2 \quad (6)$$

Each statistical percentile noise indicator can be computed as in Eq. (7).

$$\begin{aligned} L_{10} &= 61 + 8.4Log(Q) + 0.15P - 11.5Log(d) \\ L_{50} &= 44.8 + 10.8Log(Q) + 0.12P - 9.6Log(d) \\ L_{90} &= 39.1 + 10.5Log(Q) + 0.06P - 9.3Log(d) \end{aligned} \quad (7)$$

Later on, Fagotti et al. explored the possibility of introducing other vehicle categories into the previous models, making them more accurate. Specifically, their RTNM considers the motorcycles and buses flow (i.e. respectively Q_M and Q_{BUS}), aside from the light-duty and heavy-duty vehicles ones (i.e. Q_L and Q_H) using appropriately calibrated coefficients to take into account their different contributions. The formulation is reported in (8) [24].

$$L_{eq} = 10Log(Q_L + Q_M + 8Q_H + 8Q_{BUS}) + 33.5 \quad (8)$$

Another model was developed by the French C.S.T.B (Centre Scientifique et Technique du Batiment), in which the proposed formulation for $L_{eq,A}$ helps to consider different conditions of road and vehicle flow [25]. In particular, the $L_{eq,A}$ is calculated using the estimation of L_{50} according to formula (9):

$$L_{eq,A} = 0.65L_{50} + 28.8 \quad (9)$$

The percentile level L_{50} is estimated, using, either in urban or highway scenario with traffic flow lower than 1000 vehicles/hour, Eq. (10):

$$L_{50,A} = 11.9LogQ_{eq} + 31.4 \quad (10)$$

or in urban configuration, where very tall buildings are flanking the street, taking into account the width l of the road itself, as in formula (11):

$$L_{50,A} = 15.5LogQ_{eq} - 10Logl + 36 \quad (11)$$

In both the Eqs. (10) an (11), the equivalent vehicular flow is calculated as reported in formula (12):

$$Q_{eq} = Q\left(1 + \frac{P}{100}(n-1)\right) \quad (12)$$

where n is a sort of homogenization coefficient, helping to consider that heavy vehicles cause a greater noise emission than light ones, also called "acoustical equivalent" of heavy vehicles. This coefficient provides the number of equivalent light vehicles that produce the same acoustic energy as a heavy vehicle, travelling at the same speed. A formulation of its dependence from speed is given in [26].

General Equation of the Early Models

Almost all the previously mentioned statistical RTNMs can be traced back to a general equation of the equivalent noise level:

$$L_{eq} = ALogQ\left[1 + \frac{P}{100}(n-1)\right] + bLogd + C \quad (13)$$

where Q is the traffic volume in vehicles/hour, d is the distance from the observation point to the center of the traffic lane, P is the percentage of heavy vehicles, and n is the acoustic equivalent coefficient above presented. The A, b, and C parameters can be computed using a regression approach on many L_{eq} data with different values of the input variables (Q, P, d). As for n, similar regressive approaches can be used or it can be even established by single vehicle emission measurements. Obviously, several homogenization coefficients could be defined to consider different categories in addition to the heavy one (i.e. motorcycles, buses).

As already mentioned earlier, the calibration of these parameters is usually performed by means of regression on field data. A different approach is presented in [27], in which the authors showed that a computed dataset, depicting several different scenarios of traffic, both urban and extra-urban, can replace field measurements in calibrating a multi-linear regressive model with good results. The performance of such a model depends mostly on the selected ranges of variables and on the RTNM adopted to simulate the equivalent levels.

The general equation of a regressive model is often modified by means of several corrective parameters that, depending on the model considered, include the role of average speed, kind of road (gradient, asphalt, etc.), weather and traffic conditions, the presence of disturbing elements to the propagation of sound waves such as barriers, building, etc.

CoRTN English Model

The composition of a general formula with several correction factors is at the basis of the English standard model, referred to as CoRTN procedure [28]. CoRTN model takes into consideration, aside from the traffic flow and composition, the mean speed too. In the first step, the other

conditions are idealized, for example assuming the hypothesis of moderate wind velocity and a dried road surface. One of the equations proposed in this model allows to assess the hourly noise level at a distance of 10 m from the nearest roadway as in Eq. (14). Then, the computed level can be corrected through the use of different coefficients to consider the actual conditions of the road infrastructure under study as shown by the several coefficients.

$$L_{10,1h} = 42.2 + 10Log(Q_{1h}) + \Delta_{flow} + \Delta_G + \Delta_P + \Delta_D + \Delta_S + \Delta_A + \Delta_R \quad (14)$$

Thus, several corrective coefficients are considered, Δ_{flow} due to traffic flow adjustment, Δ_G due to the road's gradient, Δ_P due to the type of road pavement, Δ_D is a distance adjustment, Δ_S due to the presence of shielding, Δ_A take into consideration the angle of view adjustment, and Δ_R the reflection adjustment.

RLS 90 German Model

Another model is the one used as the German standard, *RLS 90* model [29]. The needed inputs for this model, aside from the "classic" ones, collect information about the average hourly traffic flow, considering also the motorcycles category and the average speed of each category. A peculiar characteristic of this model is its potential to assess the noise emission of a parking lot. As the aforementioned CoRTN model, RLS 90 model uses ideal conditions to assess $L_{m,E}^{(25\,m)}$, an average noise level at a distance of 25 m from the centre of the carriageway as reported in Eq. (15).

$$L_{m,E}^{(25m)} = 37.3 + 10Log[Q(1 + 0.082P)] \quad (15)$$

Several corrective factors are then added to such value, to take into account speed limits, different road surfaces and vehicle speeds, rises and falls along the route, the presence of buildings, air absorption, ground and atmospheric conditions, topography characteristics, and presence of traffic lights.

C.N.R. Italian Model

To obtain an adaptation of the German model to the Italian framework, it has been developed the Italian *National Research Center (C.N.R.)* model [30], then improved by Cocchi et al. [31]. The model formulation is reported in Eq. (16).

$$L_{eq.A} = \alpha + 10Log(Q_L + \beta Q_H) - 10Log\left(\frac{d}{d_0}\right) + \Delta_V + \Delta_F + \Delta_B + \Delta_P + \Delta_G + \Delta_{VB} \quad (16)$$

In addition to what has already been explained for the German and the UK models, in the C.N.R. model, two new parameters have been considered, α and β, in order to evaluate the characteristics of countries roads and vehicles. In particular, α is related to the single vehicle's noise emission and β to the heavy vehicle's noise emissions. Moreover, Q_L and Q_H are respectively light and heavy vehicle traffic flow, while d_0 is a fixed reference distance of 25 m. Several corrective coefficients are then considered, Δ_V due to mean tflow velocity, Δ_F and Δ_B due to the presence of a reflective facade near or in the opposite direction of the observation point, and Δ_{VB} due to the presence of traffic lights or slow traffic conditions.

ERTC Thailand Model

In 1999, the *Environmental Research and Training Centre (ERTC)* of Thailand established several equations to assess the average power level due to small and large vehicle groups through a regression approach of measured data [32]. Once the power level is obtained as a function of the speed, it has been used for estimating the L_{eq}, as in Eq. (17).

$$L_{eq} = 67.8 + 20.4Logv + 10Log((1 - P) + 5.37P) - 10Log2dL + \Delta_{diff} + \Delta_P \quad (17)$$

where d is the distance from a traffic line to receiving point, Δ_{diff} is the correction value for diffraction attenuation and L is the average gap distance estimated as follows (18):

$$L = 1000v/Q \quad (18)$$

Li et al. Chinese Model

In 2002, a road traffic noise model has been developed by *Li et al.* in the Chinese area, considering local environmental conditions, vehicle types, and traffic conditions. They classified vehicles into three types, namely, light cars, medium trucks, and heavy trucks. The model gave as output the equivalent noise level with respect to speed, traffic flow, distance, gradient, ground absorption, finite length of road segment, and the presence of any shielding adjustment as shown in formula (19) [33].

$$L_{eq,A} = 55.7 + 0.12(v_{eq} - 50) - 8.06Logv_{eq} + 9.97LogQ_{eq} + 14.38Log\left(\frac{d_0}{d}\right) + \Delta_G + \alpha\Delta_{soft}Log\left(\frac{d_0}{d}\right) + 10Log\left(\frac{\Delta_\phi}{180}\right) + \Delta_S \quad (19)$$

In addition to the coefficients characterized by the same notation as those presented in previous models, v_{eq} is the equivalent speed of traffic flow, Δ_G, as above, is an adjustment

for the road gradient, Δ_{soft} is the percentage of soft ground cover within the road segment considered, and Δ_{ϕ} is the angle subtended by road segment relative to the receiver.

Nordtest Finnish Model

In Finland, the *Nordtest* approach was developed under the auspices of the Nordic Council of Ministers [34]. The Nordtest model permits to assess the L_{eq} by performing noise measurements in a continue way for certain time interval period. It describes how to measure the noise level in a precise point and using several microphone positions. The 24 h equivalent noise level $L_{eq,24\,h}$ formula is reported in (20), in which it is clear also the independence of noise levels measured during the day, evening, and night periods, respectively $L_{d,A}$, $L_{e,A}$, $L_{n,A}$ to which correspond time intervals indicated by the same indices.

$$L_{eq,A,24h} = 10Log\frac{1}{T}\left[\Delta t_d 10^{\frac{L_d}{10}} + \Delta t_e 10^{\frac{L_e}{10}} + \Delta t_n 10^{\frac{L_n}{10}}\right] \quad (20)$$

where the sum of the three considered time interval is 24 h. They also proposed an alternative method to assess the traffic conditions during night or evening period, by considering average traffic conditions instead of taking actual measurements. For the light vehicles, the used equations are reported in (21).

$$\begin{aligned} L_{e,A,light} &= 73.5 + 25Log\left(\frac{v}{50}\right); \quad for\, v \geq 40km/h \\ L_{e,A,light} &= 71.1; \quad for\, 30 \leq v \leq 40km/h \end{aligned} \quad (21)$$

while for heavy vehicles, reference is made to (22). All three equations refer to a distance of 10 m.

$$\begin{aligned} L_{e,A,heavy} &= 80.5 + 30Log\left(\frac{v}{50}\right); \quad for\, 50 \leq v \leq 90km/h \\ L_{e,A,heavy} &= 80.5; \quad for\, 30 \leq v \leq 50km/h \end{aligned} \quad (22)$$

Finally, one can compute the equivalent noise level in 1 h span as in (23).

$$L_{eq,A,1h} = 10Log\left[\frac{1}{3600}\left(n_{light}10^{\frac{L_{e,A,light}}{10}} + n_{heavy}10^{\frac{L_{e,A,heavy}}{10}}\right)\right] \quad (23)$$

where n_{light} and n_{heavy} are the mean traffic flow per hours of the two considered categories.

Machine Learning Models

One of the latest trends in road traffic noise modelling is the development of machine learning models. A new way of approaching the traffic noise modelling problem is the Artificial Intelligence (AI) approach, which can be more reliable and robust in facing non-standard conditions, as stated in [35, 36] and [37]. The AI techniques used nowadays for the prediction of road traffic noise are various, including the artificial neural network (ANN), adaptive neuro fuzzy inference system (ANFIS), and genetic algorithm (GA). A bibliographic overview of fifty papers concerning the application of artificial intelligence (AI)-based models in modelling vehicular road traffic noise, selected via a computerized search method, is provided in [38•]. Some examples of the use of ANN in the domain of road traffic noise in the literature are [39] and [40], where the percentage of heavy vehicles, average speed, and number of total flowing vehicles are used as input values to implement an ANN model to predict road traffic L_{eq} and L_{10} values in two Indian cities. A similar work [37] implements a similar model but with a higher number of input parameters (total flowing vehicles, average speed, number of cars, vans, pickup, heavy vehicles and motorcycles, density of building facing the observer, and building reflection factor) in Teheran. An additional research reported in [41] takes into consideration the same input parameters, adding the type of pavement on the road.

A comparison between ANN and other machine learning techniques has been provided in [42], where authors demonstrated the best prediction results come from ANN compared to other techniques. Similar results have been obtained in[43] and [44], where ANN technique has been compared with regressive approaches and other machine learning techniques, respectively.

Some noticeable works on ANFIS are the work of Cirianni and Leonardi [45], who used ANFIS model to predict road traffic noise of two cities in Italy, where in [46] and [47], two models involving fuzzy logic have been developed for prediction and classification of road traffic noise.

In the work of Ruiz-Padillo [48], a multicriteria decision methodology was used for the evaluation of traffic noise. In another similar work, equivalent traffic flow, equivalent vehicle speed, and honking have been used as input for the implementation of a fuzzy logic for the prediction of road traffic noise [46]. Regarding the usage of GA for road traffic noise prediction, relevant works are [49, 50], and [51], in which this type of AI approach has been successfully implemented for the prediction of road traffic noise.

It is interesting to note how the implementation of machine learning models generally relies on the same road traffic parameters used in historical models, in order to find a predicted noise level at the receiver. Some works introduced new variables, like the presence of buildings in [37] and the type of pavement on the road in [41], but there is still not a comprehensive contribution on this sense. Moreover, another aspect to consider is that, up to the authors knowledge, there is not any AI model working separately on noise emissions or sound propagation, probably because the independent variables to take into consideration to build such a model would not be easily retrieved. These aspects will

surely be important in the future development of machine learning techniques for road traffic noise prediction. Anyway, it should be underlined that since the relationships between emission and relevant variables are monotonic, the most interesting contribution of AI tools will be on the improvement of the propagation modelling, where the commonly used approaches can be improved.

NEMs Review

There are several models that, rather than estimating the overall road traffic noise by regression on field data at the receiver, focus on estimating the noise levels produced by vehicles through the use of Noise Emission Models (i.e. NEMs) aimed at assessing the sound power level L_W of the source. In the following, the single vehicle approach will be presented together with the potential applications of such an assessment. In addition, the possible methods to move from single vehicle to traffic flow noise emissions will be resumed at the end of the section. The main parameters of the presented models are reported in Appendix.

Microscopic Approach: Single Vehicle Noise Emission

Lelong et al. NEM

In 1999, Lelong et al. developed an empirical model to estimate the sound power level L_W of the individual vehicle, distinguishing it in two different equations for light and heavy vehicles, and taking into account three driving conditions: cruise driving, acceleration, and deceleration conditions [52]. Equation (24) reports the general equation used in Lelong's model for the light vehicle and equation (25) the one used for the heavy vehicle.

$$L_{w,L} = \alpha_L + \beta_L Log(v) \tag{24}$$

$$L_{w,H} = \alpha_H + \beta_H v \tag{25}$$

One could notice the different dependence of these sound power levels on speed, logarithmic for light vehicles and linear for heavy vehicles.

SonRoad NEM

In 2004, a NEM calibrated in Switzerland, also known as SonRoad, was developed to estimate the sound power level L_W of a single vehicle using the vehicle type, speed, grade of the road (i.e. Δ_G), and surface type (i.e. Δ_{BG}) as main inputs [53]. In particular, two different equations are used to assess the sound power level for light and heavy vehicles as reported respectively in Eqs. (26) and (27).

$$L_{w,A,L} = 28.5 + 10Log\left(10^{0.1[7.3+35Log(v)]} + 10^{0.1[60.5+10Log(1+(v/44)^{3.5})+\Delta_G]}\right) + \Delta_{BG} \tag{26}$$

$$L_{w,A,H} = 28.5 + 10Log\left(10^{0.1[16.3+35Log(v)]} + 10^{0.1[74.7+10Log(1+(v/56)^{3.5})+\Delta_G]}\right) + \Delta_{BG} \tag{27}$$

Harmonoise NEM

A very important NEM, from which subsequent developments led to the model canonically used in Europe, is the Harmonoise one, in which the sound power level L_W is estimated for five different vehicle categories (i.e. light, medium-heavy, heavy, special (tractors, trucks), and motorbikes). It is one of the first model to separate the contribution of engine noise, also called propulsion noise $L_{W,propulsion}$, from that of tyre rolling on the road surface $L_{W,rolling}$, using coefficients as a_P and b_P and a_R and b_R that also lead to compute such contributions for each third octave band f from 25Hz to 10kHz. Moreover, Harmonoise's model introduces a correction term to propulsion sound power level $L_{W,propulsion}$ to take into account acceleration or deceleration values between -2 and +2 m/s^2 factor for (i.e. Δ_{acc}) [54]. Model equations are reported in formulas (28) and (29):

$$L_{w,propulsion} = a_P(f) + b_P(f)\left[\frac{v - v_{ref}}{v_{ref}} + \Delta_{acc}\right] \tag{28}$$

$$L_{w,rolling} = a_R(f) + b_R(f)Log\left(\frac{v}{v_{ref}}\right) \tag{29}$$

Finally, the overall sound power level of single vehicle is computed per each category as in formula (30):

$$L_{w,TOT} = 10Log\left(10^{\frac{L_{W,propulsion}}{10}} + 10^{\frac{L_{W,rolling}}{10}}\right) \tag{30}$$

REMEL NEM for US-FHWA Model

In the 90 s, a model was developed for the United States of America by the U.S. Department of Transportation, Research and Special Programs Administration, in support of the Federal Highway Administration, also referred to as the FHWA model [55]. The main objective of their work was to update the previous technologies used and to develop a new highway traffic noise prediction model. Over the years, several updates to this model have been produced until the most recent, which was issued in September 2021 [56]. The formula to compute the maximum noise emission energy for a single vehicle pass-by is given in the technical manual

issued by the U.S. Department of Transportation, Research and Special Programs Administration, as follows:

$$E_A(v_i) = \left(0.6214 v_i\right)^{A/10} 10^{B/10} + 10^{C/10} \tag{31}$$

where v_i is the vehicle speed in kilometers per hour for the i-th vehicle and A, B, and C are variables that depend on vehicle type, pavement type and engine throttle, and they are defined in the manual itself. E_A is then converted in dB scale as follows:

$$L_A(v_i) = 10 Log_{10}(E_A(v_i)) \tag{32}$$

Since the FHWA RTNM computes various adjustment factors on a one-third octave band basis, the characterization of noise emission levels is then refined.

$$\begin{aligned} L_{emis,i}(v_i, f) = {} & L_A(s_i) + (D_1 + 0.6214 D_2 v_i) + (E_1 + 0.6214 E_2 v_i)[Log_{10} f] \\ & + (F_1 + 0.6214 F_2 v_i)[Log_{10} f]^2 + (G_1 + 0.6214 G_2 v_i)[Log_{10} f]^3 \\ & + (H_1 + 0.6214 H_2 v_i)[Log_{10} f]^4 + (I_1 + 0.6214 I_2 v_i)[Log_{10} f]^5 \\ & + (J_1 + 0.6214 J_2 v_i)[Log_{10} f]^6 \end{aligned} \tag{33}$$

where f is the nominal frequency (in Hz) of the considered third octave band and D_1 to J_2 are parameters that depend on vehicle type, pavement type, and engine throttle. They are not reported in this work for the sake of brevity, but they are defined in the above mentioned manual [56]. A, B, and C coefficients control the overall level, while D_1 to J_2 control the spectral shape of the emissions.

NMPB NEM

In 1996, the first release of a Road Traffic Noise predictive model in France was published. The model known as NMPB, that stands for "Nouvelle Méthode de Prévision du Bruit des Routes" has been updated several times, up to the 2008 edition, as reported in the work of Dutilleux et al. in [57]. The model is based on the estimation of the source sound power level considering the contributions of rolling (L_r) and propulsion (L_p) [58, 59]. These components are determined through fit of experimental data obtained with pass-by tests, in which the receiver is at a lateral distance from the road of 7.5 m and at a height of 1.2 m above the ground. From the measurements of the maximum A-weighted pass-by levels, the model parameters are obtained fitting the following relationship:

$$L_{A,max} = L_r + L_p = 10 Log\left(10^{\frac{L_p}{10}} + 10^{\frac{L_r}{10}}\right) \tag{34}$$

where L_p and L_r represent the power level for propulsion and the sound emission level for rolling, respectively. Regarding the rolling contribution, different formulations are proposed for light and heavy vehicles, according to Eqs. (35) and (36).

$$L_{r,LV} = A_{R,LV} + B_{R,LV} log \frac{v}{90} \tag{35}$$

$$L_{r,HV} = A_{R,HV} + B_{R,HV} log \frac{v}{80} \tag{36}$$

The same differences can be noticed for the propulsion contribution.

$$L_{p,LV} = A_{P,LV} + B_{P,LV} log \frac{v}{90} \tag{37}$$

$$L_{r,HV} = A_{P,HV} + B_{P,HV} log \frac{v}{80} \tag{38}$$

The power level for an individual vehicle is thus obtained from the level $L_{A,max}$, using the following back-propagation formula:

$$L_w(v) = L_{A,max}(v) + 20 Log \frac{d}{d_0} + 10 Log 2\pi \tag{39}$$

where

$$\frac{d}{d_0} = \sqrt{7.5^2 + 1.2^2} \tag{40}$$

Measurements were carried out on a large number of samples. Specifically, the measurement campaign involved 450 sites for light vehicles and 150 sites for heavy ones [57].

CNOSSOS-EU NEM

More recently, the European Union delivered the so called "CNOSSOS model", which stands for "Common NOise aSSessment methOdS". This model is inspired by the Harmonoise model presented in "Harmonoise NEM" section and aims at assessing the emission of the major noise sources, both in urban and extraurban areas, including road traffic [60]. It has as a main goal to harmonize the procedures and enable all member countries to create noise maps as imposed by the regulation 2002/49/CE. The model assesses the source power level L_W for each band of octave i, for five categories of vehicles m: light, medium-heavy, and heavy vehicles, powered two-wheelers, and alternative propulsion cars. Different correction terms are considered to take into account the effects on the noise emissions of studded tyres, air temperature, road gradient, acceleration and deceleration phase, type of road surface, and so on. The relationships used to compute the sound power level due to propulsion and rolling noise of the individual vehicle are given in Eqs. (41) and (42). They are calculated for each i-th octave band from 125 Hz to 4 kHz.

$$L_{w,P,i,m} = A_{P,m}(i) + B_{P,m}(i) \frac{v_m - v_{ref}}{v_{ref}} \tag{41}$$

$$L_{w,R,i,m} = A_{R,m}(i) + B_{R,m}(i) Log \frac{v_m}{v_{ref}} \quad (42)$$

The coefficients $A_{P,m}$, $B_{P,m}$, $A_{R,m}$, and $B_{R,m}$ change with respect to each octave band and to vehicles' category considered. v_{ref} is a reference speed that in the CNOSSOS model is set at 70 km/h, while v_m is the average speed of the vehicle's category considered. The coefficients for categories from 1 to 4 have been firstly published in [60] and then amended in [61], in order to take into account surface reflection effects. Latest official version of the coefficients is available in [62]. In addition, several works in literature also aim to provide such coefficients for vehicle categories not yet included in the CNOSSOS model. For example, regarding electric vehicles in [63] and in [64], Pallas et al. provided some correction terms to be applied to obtain the emission of electrically powered vehicles. In [65], Licitra et al. proposed the coefficients $A_{P,m}$, $B_{P,m}$, $A_{R,m}$, and $B_{R,m}$ to be applied when referring to electric vehicles, computed after fitting statistical pass-byes for a reference pavement and compared with results obtained with a crumb rubber pavement. A list of the main coefficients to be used for CNOSSOS application is given in Appendix. The use of mean speed for each vehicle's category makes the CNOSSOS' NEM a not fully microscopic model, as it does not consider the individual car's speed, even though the single vehicle sound power level is estimated separately before merging all the vehicles emissions in the traffic flow line source, as will be described in the next subsection.

The propulsion and rolling overall sound power levels are computed as follows:

$$L_{w,P,m} = 10 Log \sum_{i=125Hz}^{4000Hz} 10^{\frac{L_{w,P,i,m}}{10}} \quad (43)$$

$$L_{w,R,m} = 10 Log \sum_{i=125Hz}^{4000Hz} 10^{\frac{L_{w,R,i,m}}{10}} \quad (44)$$

Finally, one can compute the overall source sound power level $L_{W,m}$ for each single vehicle's category m as

$$L_{w,m} = 10 Log\left(10^{\frac{L_{w,P,m}}{10}} + 10^{\frac{L_{w,R,m}}{10}}\right) \quad (45)$$

ASJ-RTN NEM

In 1975, the Acoustic Society of Japan delivered the first release of a road traffic noise predictive model for free-flowing conditions, also referred to as ASJ-RTN [66, 67]. The ASJ-RTN has been updated several times up to 2018, following research's results, the promulgation of different regulations and to consider wave-based computational methods for sound propagation. In [68], the history of the development of this model is reported, up to the 2018 version. This model estimates $L_{W,A}$ for three categories of vehicles, i.e. motorcycles, light vehicles, and heavy vehicles, using their average speed as input variable. Moreover, some correction terms to consider the type of road surface, the slope, and the directivity factor can be applied [69]. The general equation of ASJ-RTN is reported in (46):

$$L_{W,A} = a + bLogv + C \quad (46)$$

where a and b are regression coefficient and C is a corrective factor that includes terms for road gradient, sound radiation directivity, and other factors. Parameters a, b, and C are given as a function of flow condition (steady, non-steady, deceleration), speed range, category of vehicle, and pavement typology.

Vehicle Noise Specific Power

Recently, a Vehicle Noise Specific Power (VNSP) model has been developed by Pascale et al. with the aim of assessing the sound power level L_W considering vehicle motorization. VNSP establishes a fundamental relationship between L_W and speed, with respect to three types of motorization of cars (diesel, petrol, and hybrid), by a non-linear regression on power levels measured through the statistical pass-by standard procedure. As in CNOSSOS and Harmonoise models, the engine contribution is assumed to have a linear dependence by the speed, while the rolling noise is modelled with a logarithmic function of the speed. More details are reported in [12]. The equation used is reported below (47):

$$L_w = 10 Log\left(10^{\left(A+B\frac{v-v_{ref}}{v_{ref}}\right)/10} + 10^{\left(C+DLog\frac{v}{v_{ref}}\right)/10}\right) \quad (47)$$

The speed used as a reference is the same as CNOSSOS' one (i.e 70 km/h). The main difference between VNSP and the previous models is that VNSP adopts the overall sound power level L_W, instead of fitting the function per each octave band or third octave band. A practical application of this model and the comparison with results obtained with other NEMs are presented in [13•].

Micro to Macro Transition: from Single Vehicle to Traffic Flow Emission

To achieve an overall assessment of the road traffic noise levels, the single vehicle emission needs to be extended at the road segment level. The sound power level L_W of all the vehicles must be merged together, to provide assessment of the traffic flow emission.

The CNOSSOS model provides an approach to move from the single point source to a linear source by considering

multiple passing-by vehicles on the road [60]. The sound power level of traffic in the m-th category per meter per frequency band of the linear source is given in (48):

$$L_{w,line,i,m} = L_{w,i,m} + 10Log\frac{Q_m}{1000v_m} \quad (48)$$

where $L_{w,i,m}$ is the instantaneous directional sound power level in a semi-free field of a single vehicle, calculated for each i octave band from 125 Hz to 4 kHz and for each vehicle's category m. Hourly traffic flow data Q_m and average speed v_m are considered for each vehicle category, even if in some cases the maximum legal speed for the vehicle category is used.

Another way to move from single vehicle to traffic flow is to consider the acoustic energy immitted at the receiver by the single pass-by by means of SEL calculation and then to sum up the SELs of all the vehicles. In several models and applications (for example in [68, 70, 71, 72•, 73]), such a procedure is used to calculate the SELs of the vehicles travelling on a given road segment, to assess the overall traffic flow emission.

Propagation and Assessment at the Receiver

Propagation Models

Once the sound source is characterized by its emission, the vast majority of noise propagation models for noise mapping begin by discretizing it into point sources. In the CNOSSOS-EU model, for instance, a car may be represented as a point source at a height of 0.05 m. Subsequently, a road is discretized into an array of point sources, situated along its central axis, at 0.05 m height and at regular intervals dependent on the distance between the source and the receiver. The greater this distance, the larger the interval between point sources can be while maintaining the same level of prediction accuracy. Then, if multiple point sources represent the same source, each of these points bears only a fraction of their energy. Once the source is discretized, the next step involves modelling the propagation between the point sources and the receivers within the domain.

Similar to the discretization process, there is a homogenization of models for noise mapping due to a well-balanced trade-off between precision and computational cost in path-finding methods. Pathfinding methods involve finding the set of shortest paths between a source and a receiver. In the case of a direct field, it is straightforward—a straight-line segment between these two points. If a building is present between them, it involves three segments passing over and around the sides of the building. In these models, there is an inability to represent buildings as arches; the building must be solid, a concept sometimes referred to as 2.5D. When considering reflections, the simulation needs to account for the interaction of sound waves with building surfaces, leading to multiple paths and interactions that contribute to the overall sound field at a receiver. Once these paths are identified, the next step is to apply a model of sound wave attenuation to each of these paths. The literature contains numerous comparisons between the most commonly used models [74–78].

Most noise propagation models account for the following effects on attenuation:

- Geometric divergence: This refers to the attenuation resulting from the loss of energy as the distance increases (-6 dB/doubling of distance for a point source).
- Atmospheric absorption: This is influenced by the humidity and temperature of the atmosphere.
- Absorption and/or reflection of the wave by the ground: This depends on the type of soil.
- Terrain shape and topography: The overall form of the terrain and its topographical features can affect sound propagation.
- Meteorological effects: Wind and temperature influence the speed of the sound wave, and so their gradients have a significant impact on the sound level at the receiver. These are sometimes simplified, as in CNOSSOS-EU or ISO 9613-2, to two distinct conditions, either no effects on propagation or conditions favourable to propagation.
- Diffraction effects: These occur at the edges of buildings, acoustic walls, or the ground and can influence the path of sound waves.

It is crucial to emphasize that, in the context of most large-scale studies, uncertainties in the results are predominantly influenced by factors such as input data and exposure calculations rather than the intricacies of the models themselves [79]. Despite the inherent complexities, numerous studies with detailed input data have shown acceptable agreement between measurements and simulations in the context of city scale long-term averaged noise levels.

Assessment at the Receiver

All the models presented in the foregoing sections and subsections can be effectively used in order to investigate several types of road traffic noise's impacts on the surroundings. Depending on which specific feature has to be analyzed or highlighted through the analysis itself, or in general what is the aim of the study, model outputs could be used to produce different kinds of impacts' indicators. These impacts affect those who can be identified as "receivers" of road traffic noise, and they can be assessed either in a direct way, estimating the energetic indicators defined by national and international regulation, or indirect, evaluating secondary effects, such as health consequences, external costs, and

influence on property prices. In this subsection, three different macro-categories of assessments at the receiver will be introduced and explored, namely the usual regulation indicators, the health effects, and the external costs.

Common Regulation Indicators

A first and most obvious desired derivable from the application of RTNMs could be the computation of noise indicators usually used by regulations. Concerning European countries, for instance, the standard indicators to be used for strategic noise mapping and for national regulation issues have been defined in the "Environmental Noise Directive" [80]. The most relevant noise level indicator is called "acoustic descriptor day-evening-night", computed as in the following formula:

$$L_{den} = 10Log\frac{1}{24}\left[12 \cdot 10^{\frac{L_{day}}{10}} + 4 \cdot 10^{\frac{L_{evening}+5}{10}} + 8 \cdot 10^{\frac{L_{night}+10}{10}}\right] \tag{49}$$

This formulation computes the different times regarding the amount of hours for each period (12 h for the day, 4 h for the evening, and 8 h for the night) and adds some penalties for the noise emitted at evening and night times. European countries must use this indicators for strategic map duties, for which all the main sources in urban areas must be assessed, with special care to road traffic noise. This mapping is usually performed by using algorithms for emission and propagation of noise coming from roads, railways, airports, and industrial sources, commonly included in commercial software. As for road traffic noise modelling, it is evident that a usable and reliable model—that could be largely used and accepted—has to produce results comparable with the acoustic descriptor used by the regulations. There are two ways to get such type of results: the model can supply an aggregated output of noise level comparable with the time periods of regulations (like in [81]) or give as output a time dependent sound pressure level L_p, which has to be subsequently aggregated according to the time period required. As reported in the previous sections, some RTNMs do not offer as output the noise indicators as identified in the regulations, but rather some of them allow the calculation of pressure levels as a function of time, later to be aggregated into summary indicators, or percentile sound pressure levels (i.e. L_{night}, $L_{A,10}$, $L_{A,50}$, $L_{A,90}$).

Exposure and Effects on Human Health (DALYs)

Originally launched by the World Bank and backed by the World Health Organization as a measure of the global burden of disease, DALYs (disability adjusted life years) have been extensively used in literature to assess the influence of several pollutants on the life of citizens all through the World [82, 83]. Noise has been one of these pollutants, especially in the recent past, due to its pervasiveness and to the constant increasing number of people exposed to high levels of noise. DALYs quantify the amount of impact by suggesting how many years of life people lose due to the exposure to the analyzed pollutant. In [84], it is reported an estimation of DALYs due to noise in Netherland, but it is incorporated to the estimation of DALYS due to the more generic air pollution. In detail, it is reported how particulate air pollution accounts for 60% of DALYs, and noise for 24%, with an amount of 17,700 DALYs (only for noise) annoyance, 10,990 to sleep disturbance, 50 for ischaemic heart disease (IHD), and 10 DALYs for mortality related to noise. In 2011, WHO Europe published a work where the impact of noise in terms of DALYs was evident [85]: more than 1,700,000 DALYs were lost in EU member states and other Western European countries for heart and blood diseases, sleep disturbances, tinnitus, and annoyance. In [86], a comprehensive study of effects on health of noise is reported. A correlation between these estimated DALYs and a more punctual noise evaluation on urban context could result in useful indicators to highlight the profound impact noise has nowadays on our lives. The DALYs approach also reveals how dramatic is the impact of noise on populations in terms of economic impact on the population.

External Costs of Transportation

A proper characterization of environmental noise—especially on urban areas—also takes into account the externalities of the noise itself. Whether the negative externalities of road transportation are easier to identify (environmental and road damage, accidents, congestion, and oil dependence) and their relative costs are subject of policy attention [87], the economic costs of noise are not directly addressed and not commonly investigated. Some papers consider a single-agent exposure by proposing an activity-based assessment [88••] and possible indicators for construction sites noise exposure impact [89]. As for airport noise, examples of noise cost assessment can be found in [90–92].

Regarding the road traffic noise, the costs are mainly investigated in terms of health cost. Many works show the direct correlation between noise and health problems like annoyance, depression and anxiety [93–96], sleep disturbance [93, 97–100], and cardiovascular diseases [101–103]. Out of these correlations is immediate to retrieve externalities in terms of costs on national health systems. A different group of studies relates the noise level to the variation of the prices of the estates, identifying how properties on quieter places are more expensive than properties on noisy ones. In [104], a linear regression technique is used to evaluate and characterize the influence of surface street traffic on both single-family houses and multi-unit rental residential

property, obtaining different results for the two types of properties. In [105], a theoretical model of evaluation of environmental externalities based on the analysis of real estate prices is provided. This work, in particular, presents a comprehensive literature review of works evaluating the reduction of real estate values for increasing of noise pollution in many American and EU cities. The percentage value spans from a minimum of 0.22% to a maximum of 1.45%. The work of Wilhemssons [106] also shows a theoretical model to extract a precise correlation between the average noise level (dBA) and the prices of estates in Stockholm. Such approaches evaluate the noise level as final entities influencing the externalities' severity and request a noise measurements or a theoretical inference of the noise level itself. The described actions all take in consideration, to assess noise levels, the indicators commonly used in scientific literature (L_{day}, $L_{evening}$, L_{night}, L_{den}), which report the average noise level exposure during day specific sections.

A different approach is the possibility to infer the drop or raising of selling or renting estate pricing per dB. In [107], it is reported an interim EU-wide economic value of 23.5 euros/dBA/household/year. Two different approaches are then possible: the computation of the overall noise level on a certain area as the contribution of the noise coming from each single vehicle transiting, and then the corresponding externalities on population living in the area, in terms of health issues and economic evaluation of estates (bottom-top approach). On the other hand, it would be possible to get an indicator correlating the noise level to an economic value to easily infer how it could impact on the externalities on populations. It is interesting to note how the precise evaluation of externalities of the noise in a certain area can help policy makers in making choice between the possible measures to mitigate noise.

Conclusions

The development of effective road traffic noise modelling tools has been a central point in the agenda of the acoustic scientific community in the last decades. The evolution of the adopted techniques has been presented in this paper, starting from the historical formulas, obtained by regression on large datasets collected in different sites. These early models exploited the dependence of traffic noise level from vehicle flows and vehicle category, sometimes including additional parameters and corrections to take into account mean speed of the flow, road grade and pavement, presence of shielding and reflecting vertical surfaces, etc. The latest trend of Artificial Intelligence and machine learning techniques for road traffic noise modelling has been also reported, resuming the most popular approaches that are mainly artificial neural network, random forest, support vector regression, among others. The usage of these techniques is obviously strongly dependent on availability of reliable training data that must be used for the calibration and validation of the models. Despite the popularity of these techniques, in the acoustic scientific community, they are considered niche models and they are not included yet in any regulation or standard document, probably because of the strong site-dependence feature of these models that leads to difficulties in developing a tool that can be easily used anywhere. A review of single vehicle noise emissions modelling has been extensively reported in the central part of the paper. The engine and rolling contributions assessment has been reviewed, considering the most popular NEMs. In particular, the strong relation between emission and vehicle speed has been highlighted, together with the recurrent correction coefficients, usually related to road pavement, grade, and acceleration. The ways the single vehicle emission can be merged in a linear source mimicking the road traffic have been briefly reported to describe the transition from a microscopic simulation to a macroscopic description of the phenomenon. Finally, the propagation and the assessment at the receivers have been summarized to complete the road traffic noise modelling and assessment standard scheme, citing the most popular uses of these predictions, such as regulation descriptors calculation, noise mapping, exposure analysis, and health risk assessments. The problem of providing quality input data for any road traffic model presented in this review is crucial. Activity models can be developed and used for this purpose, also including dynamic approaches, able to provide the temporal variation of the input data and, consequently, of the simulated noise levels.

The main conclusion of this review is that road traffic noise modelling is a wide field of study that may include several approaches based on different techniques. The single vehicle noise emission assessment is mandatory for pursuing a microscopic approach that can be easily used for noise pollution modelling and control, for instance in eco-routing applications and traffic signal setting design. On the contrary, collective models that can be based on large dataset statistical regressions or machine learning tools are dependent on the databases used for the calibration and validation, introducing a potential limitation on the extension of these models to any site under study.

Appendix: Main Coefficients of the Reviewed Models

Table A Lelong's coefficient for light vehicles

Vehicle's conditions	**Parameters**	
	α_L [dBA]	β_L [dBA]
Cruising or decelerating ($v \geq 11.5km/h$)	53.6±0.3	26.8±0.2
Accelerating ($v \geq 25km/h$)	53.6±0.3	26.8±0.2
Vehicle's conditions	$\boldsymbol{L_w}$ **[dBA]**	
Cruising or decelerating ($v \leq 11.5km/h$)	$L_w = 82$	
Accelerating ($v \leq 25km/h$)	$L_w = 90.5$	

Table B Lelong's coefficient for heavy vehicles

Vehicle's conditions	**Parameters**	
	α_H [dBA]	β_H [dBA]
Cruising ($v \geq 21km/h$)	100.6	0.089
Decelerating ($v \geq 18km/h$)	91.0	0.20
Vehicle's conditions	$\boldsymbol{L_w}$ **[dBA]**	
Cruising ($v \leq 21km/h$)	$L_w = 102.5$	
Decelerating ($v \leq 18km/h$)	$L_w = 94.5$	
Accelerating ($v \geq 20.5km/h$)	$L_w = 104.5$	

Table C SonRoad's parameters

Surface type	$\boldsymbol{\Delta_{BG}}$**[dBA]**
Dense asphalt concrete, type AB 10,11,16	0
Cement concrete	+2
Drainasphalt, type DRA 10,11 for $v > 70km/h$	-4
Gussaphalt (mastic asphalt), type GA	0
Rauhasphalt (Macro-Rugeux) MR6,11	-1
Stone mastic asphalt, type SMA 6	-1
Stone mastic asphalt, type SMA 8,11	0
Splittasphalt, type SPA 6,8,11	0
Teerasphaltbeton, type TA 10	0
Teerasphaltbeton, type TA 16	+1
Road gradient	$\boldsymbol{\Delta_G}$
Only for uphill road	$0.8g$

Table D Harmonoise's rolling noise coefficients

Octave frequency bands	**Category 1**		**Category 2**		**Category 3 (4 axles)**	
[Hz]	α_R [dBA]	β_R [dBA]	α_R [dBA]	β_R [dBA]	α_R [dBA]	β_R [dBA]
25	69.9	33	76.5	33	79.5	33
31.5	69.9	33	76.5	33	79.5	33
40	69.9	33	76.5	33	79.5	33
50	74.9	30	78.5	30	81.5	30

Octave frequency bands	Category 1		Category 2		Category 3 (4 axles)	
[Hz]	α_R [dBA]	β_R [dBA]	α_R [dBA]	β_R [dBA]	α_R [dBA]	β_R [dBA]
63	74.9	30	79.5	30	82.5	30
80	74.9	30	79.5	30	82.5	30
100	79.3	41	82.5	41	85.5	41
125	82.5	41.2	84.3	41.2	87.3	41.2
160	81.3	42.3	84.7	42.3	87.7	42.3
200	80.9	41.8	84.3	41.8	87.3	41.8
250	78.9	38.6	87.4	38.6	90.4	38.6
315	78.8	35.5	88.2	35.5	91.2	35.5
400	80.5	31.7	92	31.7	95.0	31.7
500	85.7	21.5	94.1	21.5	97.1	21.5
630	87.7	21.2	93.8	21.2	96.8	21.2
800	89.2	23.5	94.4	23.5	97.4	23.5
1000	90.6	29.1	92.2	29.1	95.2	29.1
1250	89.9	33.5	89.6	33.5	92.6	33.5
1600	89.4	34.1	88.9	34.1	91.9	34.1
2000	87.6	35.1	86.5	35.1	89.5	35.1
2500	85.6	36.4	83.1	36.4	86.1	36.4
3150	82.5	37.4	81.1	37.4	84.1	37.4
4000	79.6	38.9	79.2	38.9	82.2	38.9
5000	76.8	39.7	77.3	39.7	80.3	39.7
6300	74.5	39.7	77.3	39.7	80.3	39.7
8000	71.9	39.7	77.3	39.7	80.3	39.7
10000	69.0	39.7	77.3	39.7	80.3	39.7

Table E Harmonoise's propulsion noise coefficients

Octave frequency bands	Category 1		Category 2		Category 3 (4 axles)	
[Hz]	α_P [dBA]	β_P [dBA]	α_P [dBA]	β_P [dBA]	α_P [dBA]	β_P [dBA]
25	85.8	0	97	0	97.7	0
31.5	87.6	0	97.7	0	97.3	0
40	87.5	0	98.5	0	98.2	0
50	87.5	0	98.5	0	103.3	0
63	96.6	0	101.5	0	109.5	0
80	97.2	0	101.4	0	105.3	0
100	91.5	0	97	0	100.8	0
125	86.7	0	96.5	0	101.2	0
160	86.8	0	95.2	0	99.9	0
200	84.9	0	99.6	0	102.3	0
250	86	8.2	100.7	8.5	103.5	8.5
315	86	8.2	101	8.5	104.0	8.5
400	85.9	8.2	98.3	8.5	101.6	8.5
500	80.6	8.2	94.2	8.5	99.2	8.5
630	80.2	8.2	92.4	8.5	99.4	8.5
800	77.8	8.2	92.1	8.5	95.1	8.5
1000	78	8.2	93.8	8.5	95.8	8.5
1250	81.4	8.2	94.3	8.5	95.3	8.5
1600	82.3	8.2	95.2	8.5	93.8	8.5
2000	82.6	8.2	94.9	8.5	93.9	8.5

Octave frequency bands	Category 1		Category 2		Category 3 (4 axles)	
[Hz]	α_P [dBA]	β_P [dBA]	α_P [dBA]	β_P [dBA]	α_P [dBA]	β_P [dBA]
2500	81.5	8.2	93.3	8.5	92.7	8.5
3150	80.7	8.2	91.2	8.5	91.6	8.5
4000	78.8	8.2	89.3	8.5	90.9	8.5
5000	77	8.2	87.3	8.5	87.9	8.5
6300	76	8.2	85.3	8.5	87.9	8.5
8000	74	8.2	84.3	8.5	81.8	8.5
10000	72	8.2	83.3	8.5	80.2	8.5

Table F Harmonoise's corrective term due to acceleration

Vehicle's category	C [dBA]
Category 1	4.4
Category 2	5.6
Category 3	5.6

Table G NMPB's rolling noise coefficient—light vehicles

Rolling noise component	$A_{R,LV}$	$B_{R,LV}$
R_1	73.3	31.0
R_2	77.3	30.1
R_3	79.8	31.4

Table H NMPB's rolling noise coefficient—heavy vehicles

Rolling noise component	$A_{R,HV}$	$B_{R,HV}$
R_1	82.5	30.0
R_2	85.6	30.0
R_3	86.6	30.0

Table I NMPB's propulsion noise coefficient—light vehicles

Vehicle's conditions	Coefficient	
	$A_{P,LV}$ [dBA]	$B_{P,LV}$ [dBA]
Steady and $v = 20 - 30$ km/h	60.6	0
Steady and $v = 30 - 110$ km/h	66.3	12.0
Steady and $v = 110 - 130$ km/h	64.6	31.3
Accelerating and $v = 5 - 20$ km/h	85.7	24.1
Accelerating and $v = 20 - 100$ km/h	70	0
Accelerating and $v = 100 - 130$ km/h	68.2	38.6
Decelerating and $v = 5 - 10$ km/h	55.5	0
Decelerating and $v = 10 - 25$ km/h	73.3	18.7
Decelerating and $v = 25 - 80$ km/h	66.0	5.5
Decelerating and $v = 80 - 110$ km/h	66.3	12.0
Decelerating and $v = 110 - 130$ km/h	64.6	31.3

Table J NMPB's propulsion noise coefficient—heavy vehicles

Vehicle's conditions	Coefficient	
	$A_{P,LV}$ [dBA]	$B_{P,LV}$ [dBA]
Steady and $v = 5 - 70km/h$)	73	0
Steady and $v = 70 - 100km/h$)	0	13.0

Table K CNOSSOS' coefficients for category m=1 (passenger cars), 2012

Octave band centre frequency	A_R	B_R	A_P	B_P	a	b
[Hz]	[dBA]	[dBA]	[dBA]	[dBA]	[dBA]	[dBA]
63	79.7	30.0	94.5	-1.3	0	0
125	85.7	41.5	89.2	7.2	0	0
250	84.5	38.9	88.0	7.7	0	0
500	90.2	25.7	85.9	8.0	2.6	-3.1
1000	97.3	32.5	84.2	8	2.9	-6.4
2000	93.9	37.2	86.9	8	1.5	-14
4000	84.1	39.0	83.3	8	2.3	-22.4
8000	74.3	40.0	76.1	8	9.2	-11.4

Table L CNOSSOS' coefficients for category m=2 (medium-heavy vehicles), 2012

Octave band centre frequency	A_R	B_R	A_P	B_P
[Hz]	[dBA]	[dBA]	[dBA]	[dBA]
63	84.0	30.0	101.0	-1.9
125	88.7	35.8	96.5	4.7
250	91.5	32.6	98.8	6.4
500	96.7	23.8	96.8	6.5
1000	97.4	30.1	98.6	6.5
2000	90.9	36.2	95.2	6.5
4000	83.8	38.3	88.8	6.5
8000	80.5	40.1	82.7	6.5

Table M CNOSSOS' coefficients for category m=3 (heavy-duty vehicles), 2012

Octave band centre frequency	A_R	B_R	A_P	B_P
[Hz]	[dBA]	[dBA]	[dBA]	[dBA]
63	87.0	30.0	104.4	0.0
125	91.7	33.5	100.6	3.0
250	94.1	31.3	101.7	4.6
500	100.7	25.4	101.0	5.0
1000	100.8	31.8	100.1	5.0
2000	94.3	37.1	95.9	5.0
4000	87.1	38.6	91.3	5.0
8000	82.5	40.6	85.3	5.0

Table N CNOSSOS' coefficients for category m=4a (powered two-wheelers ≤ 50*cc*), 2012

Octave band centre frequency	A_R	B_R	A_P	B_P
[Hz]	[dBA]	[dBA]	[dBA]	[dBA]
63	0	0	88.0	4.2
125	0	0	87.5	7.4
250	0	0	89.5	9.8
500	0	0	93.7	11.6
1000	0	0	96.6	15.7
2000	0	0	98.8	18.9
4000	0	0	93.9	20.3
8000	0	0	88.7	20.6

Table O CNOSSOS' coefficients for category m=4b (powered two-wheelers > 50*cc*), 2012

Octave band centre frequency	A_R	B_R	A_P	B_P
[Hz]	[dBA]	[dBA]	[dBA]	[dBA]
63	0	0	95.0	3.2
125	0	0	97.2	5.9
250	0	0	92.7	11.9
500	0	0	92.9	11.6
1000	0	0	94.7	11.5
2000	0	0	93.2	12.6
4000	0	0	90.1	11.1
8000	0	0	86.5	12.0

Table P CNOSSOS' latest coefficients for category m=1 (passenger cars), 2020

Octave band centre frequency	A_R	B_R	A_P	B_P
[Hz]	[dBA]	[dBA]	[dBA]	[dBA]
63	83.1	30.0	97.9	-1.3
125	89.2	41.5	92.5	7.2
250	87.7	38.9	90.7	7.7
500	93.1	25.7	87.2	8.0
1000	100.1	32.5	84.7	8.0
2000	96.7	37.2	88.0	8.0
4000	86.8	39.0	84.4	8.0
8000	76.2	40.0	77.1	8.0

Table Q CNOSSOS' latest coefficients for category m=2 (medium-heavy vehicles), 2020

Octave band centre frequency	A_R	B_R	A_P	B_P
[Hz]	[dBA]	[dBA]	[dBA]	[dBA]
63	88.7	30.0	105.5	-1.9
125	93.2	35.8	100.2	4.7
250	95.7	32.6	100.5	6.4
500	100.9	23.8	98.7	6.5
1000	101.7	30.1	101.0	6.5

Octave band centre frequency	A_R	B_R	A_P	B_P
[Hz]	[dBA]	[dBA]	[dBA]	[dBA]
2000	95.1	36.2	97.8	6.5
4000	87.7	38.3	91.2	6.5
8000	83.6	40.1	85.0	6.5

Table R CNOSSOS' latest coefficients for category m=3 (heavy-duty vehicles), 2020

Octave band centre frequency	A_R	B_R	A_P	B_P
[Hz]	[dBA]	[dBA]	[dBA]	[dBA]
63	91.7	30.0	108.8	0.0
125	96.2	33.5	104.2	3.0
250	98.2	31.3	103.5	4.6
500	104.9	25.4	102.9	5.0
1000	105.1	31.8	102.6	5.0
2000	98.5	37.1	98.5	5.0
4000	91.1	38.6	93.8	5.0
8000	85.6	40.6	87.5	5.0

Table S CNOSSOS' latest coefficients for category m=4a (powered two-wheelers $\leq 50cc$), 2020

Octave band centre frequency	A_R	B_R	A_P	B_P
[Hz]	[dBA]	[dBA]	[dBA]	[dBA]
63	0	0	93.0	4.2
125	0	0	93.0	7.4
250	0	0	93.5	9.8
500	0	0	95.3	11.6
1000	0	0	97.2	15.7
2000	0	0	100.4	18.9
4000	0	0	95.8	20.3
8000	0	0	90.9	20.6

Table T CNOSSOS' latest coefficients for category m=4b (powered two-wheelers $> 50cc$), 2020

Octave band centre frequency	A_R	B_R	A_P	B_P
[Hz]	[dBA]	[dBA]	[dBA]	[dBA]
63	0	0	99.9	3.2
125	0	0	101.9	5.9
250	0	0	96.7	11.9
500	0	0	94.4	11.6
1000	0	0	95.2	11.5
2000	0	0	94.7	12.6
4000	0	0	92.1	11.1
8000	0	0	88.6	12.0

Table U ASJ-RTN coefficients a and b for dense asphalt pavement (steady and non-steady traffic flow sections), for Three-category and Two-category vehicles classifications

Classification	Steady traffic flow section		Non-steady traffic flow section	
	a	*b*	*a*	*b*
Three-category				
Light vehicles	45.8	30	82.3	10
Medium-sized vehicles	51.4	30	87.1	10
Large-sized vehicles	54.4	30	90.0	10
Two-category				
Light vehicles	45.8	30	82.3	10
Heavy vehicles	53.2	30	88.8	10
Motorcycles	49.6	30	85.2	10

For $L_{W,A}$ in deceleration running condition on expressways (10 km/h $\leq V$), the coefficients a and b are given by those of the steady traffic flow section

Table V VNSP's coefficients for three different motorization

Car's motorization	A	B	C	D
Diesel	98.77	15.28	102.76	35.74
Gasoline	98.02	17.61	105.06	31.08
Hybrid	22.06	-65.81	104.44	34.25

Acknowledgements C. Guarnaccia and D. Rossi acknowledge the support of the MOST - Sustainable Mobility National Research Center, funded by the European Union Next-GenerationEU (PIANO NAZIONALE DI RIPRESA E RESILIENZA (PNRR) - MISSIONE 4 COMPONENTE 2, INVESTIMENTO 1.4 - D.D. 1033 17/06/2022, CN00000023). This manuscript reflects only the authors' views and opinions, neither the European Union nor the European Commission can be considered responsible for them.

Funding Open access funding provided by Università degli Studi di Salerno within the CRUI-CARE Agreement.

Open Access This article is licensed under a Creative Commons Attribution 4.0 International License, which permits use, sharing, adaptation, distribution and reproduction in any medium or format, as long as you give appropriate credit to the original author(s) and the source, provide a link to the Creative Commons licence, and indicate if changes were made. The images or other third party material in this article are included in the article's Creative Commons licence, unless indicated otherwise in a credit line to the material. If material is not included in the article's Creative Commons licence and your intended use is not permitted by statutory regulation or exceeds the permitted use, you will need to obtain permission directly from the copyright holder. To view a copy of this licence, visit http://creativecommons.org/licenses/by/4.0/.

References

Papers of particular interest, published recently, have been highlighted as:
• Of importance
•• Of major importance

1. Agency European Environment. Environmental noise in Europe -, 22/2019. Luxembourg: Publications Office of the European Union; 2020. p. 2020.
2. Héroux ME, Babisch W, Belojevic G, Brink M, Janssen S, Lercher P, et al. WHO environmental noise guidelines for the European region. Euronoise. 2015;2015:2589–93.
3. World Health Organization. Environmental noise guidelines for the European region. Regional Office for Europe: World Health Organization; 2018.
4. European Commission. Pathway to a healthy planet for all. EU action plan: 'towards zero pollution for air, water and soil'. COM(2021) 400 final. 2021; p.22.
5. Steele C. A critical review of some traffic noise prediction models. Appl Acoust. 2001;62(3):271–87.
6. Mann S, Singh G. Traffic noise monitoring and modelling–an overview. Environ Sci Pollut Res. 2022;29(37):55568–79.
7. Ibili F, Adanu EK, Adams CA, Andam-Akorful SA, Turay SS, Ajayi SA. Traffic noise models and noise guidelines: a review. Noise Vib Worldw. 2022;53(1–2):65–79.
8. Garg N, Maji S. A critical review of principal traffic noise models: strategies and implications. Environ Impact Assess Rev. 2014;46:68–81.
9. Rajakumara H, Gowda RM. Road traffic noise prediction models: a review. Int J Sustain Dev Plan. 2008;3(3):257–71.
10.•• Rey-Gozalo G, BarrigónMorillas JM, MontesGonzález D. Analysis and Management of Current Road Traffic Noise. Curr Pollut Rep. 2022;8(4):315–27. **This review paper presents the state of the art about road traffic noise control measures, within the framework of countries regulation, considering the possible interventions at the source and at the propagation path and receiver.**
11. Can A, Aumond P. Estimation of road traffic noise emissions: the influence of speed and acceleration. Transp Res Part D: Transp Environ. 2018;58:155–71.
12. Pascale A, Fernandes P, Bahmankhah B, Macedo E, Guarnaccia C, Coelho MCA, vehicle noise specific power concept. In:

Forum on Integrated and Sustainable Transportation Systems (FISTS). IEEE. 2020;2020:170–5.
13.• Pascale A, Fernandes P, Guarnaccia C, Coelho MC. A study on vehicle Noise Emission Modelling: correlation with air pollutant emissions, impact of kinematic variables and critical hotspots. Sci Total Environ. 2021;787:147647. **In this paper, 7 vehicle noise emission models and the VSP methodology are used to estimate noise and pollutants emissions of a vehicle along different routes, to highlight critical hotspots.**
14. Graziuso G, Mancini S, Guarnaccia C. Comparison of single vehicle noise emission models in simulations and in a real case study by means of quantitative indicators. Int J Mech. 2020;14:198–207.
15. Bandeira JM, Guarnaccia C, Fernandes P, Coelho MC. Advanced impact integration platform for cooperative road use. Int J Intell Transp Syst Res. 2018;16:1–15.
16. Di Pace R, Storani F, Guarnaccia C, de Luca S. Signal setting design to reduce noise emissions in a connected environment. Physica A: Statistical Mechanics and its Applications; 2023. p. 129328.
17.• Rey-Gozalo G, Aumond P, Can A. Variability in sound power levels: implications for static and dynamic traffic models. Transp Res D Transp Environ. 2020;84:102339. **In this paper, road traffic noise emission levels calculated through usual static noise prediction models are corrected using a factor that depends on the variance of the residuals distribution.**
18. Bolt B, Newman i, Bolt RH, Rosenblith WA. Handbook of Acoustic Noise Control. No. v. 1 in Handbook of Acoustic Noise Control. Wright Air Development Center, Air Research and Development Command, United States Air Force; 1953. Available from: https://books.google.it/books?id=BOZSaHASDOoC.
19. Nickson A. Can community reaction to increased traffic noise be forecast? Proceeding of 5th International Congress on Acoustics; 1965.
20. Johnson D, Saunders E. The evaluation of noise from freely flowing road traffic. J Sound Vib. 1968;7(2):287–309.
21. Galloway WJ, Clark WE, Kerrick JS. Highway noise measurement, simulation, and mixed reactions. NCHRP Rep. 1969;78.
22. Burgess M. Urban traffic noise prediction from measurements in the metropolitan area of Sydney. Appl Acoust. 1977;10.
23. Griffiths I, Langdon FJ. Subjective response to road traffic noise. J Sound Vib. 1968;8(1):16–32.
24. Fagotti C, Poggi A. Traffic noise abatement strategies: the analysis of real case not really effective. In: Proceeding of 18th International Congress for Noise Abatement; 1995. p. 223–233.
25. Centre Scientifique et Technique du Batiment. Etude théorique et expérimentale de la propagation acoustique. Revue d'Acoustique. 1991;70.
26. Guarnaccia C. Advanced tools for traffic noise modelling and prediction. WSEAS Trans Syst. 2013;12(2):121–30.
27. Rossi D, Mascolo A, Guarnaccia C. Calibration and validation of a measurements-independent model for road traffic noise assessment. Appl Sci. 2023;13(10):6168.
28. Department of Transport, UK Welsh Office. Calculation of road traffic noise. 1988.
29. BUNDESMINISTER FV, WOHNUNGSWESEN B. Richtlinien für den Lärmschutz an Straßen (RLS 90). Verkehrsblatt: Amtsblatt des Bundesministers für Verkehr der Bundesrepublik Deutschland (VkBl) Nr. 1990;7.
30. Cannelli G, Glück K, Santoboni S. A mathematical model for evaluation and prediction of the mean energy level of traffic noise in Italian towns. Acta Acust Acust. 1983;53(1):31–6.
31. Cocchi A, Farina A, Lopes G. Modelli matematici per la previsione del rumore stradale: verifica ed affinamento del modello CNR in base a rilievi sperimentali nella città di Bologna. In: Atti XIX Convegno Nazionale AIA, Napoli; 1991.
32. Suksaard T, Sukasem P, Tabucanon SM, Aoi I, Shirai K, Tanaka H. Road traffic noise prediction model in Thailand. Appl Acoust. 1999;58(2):123–30. https://doi.org/10.1016/S0003-682X(98)00069-3.
33. Li B, Tao S, Dawson R, Cao J, Lam K. A GIS based road traffic noise prediction model. Appl Acoust. 2002;63(6):679–91.
34. Nielsen HL. Road traffic noise: Nordic prediction method. Stationery Office: Temanord Series; 1997.
35. Codur MY, Atalay A, Unal A. Performance evaluation of the ANN and ANFIS models in urban traffic noise prediction. Fresenius Environ Bull. 2017;26:4254–60.
36. Hamad K, Khalil MA, Shanableh A. Modeling roadway traffic noise in a hot climate using artificial neural networks. Transp Res Part D: Transp Environ. 2017;53:161–77.
37. Mansourkhaki A, Berangi M, Haghiri M, Haghani M. A neural network noise prediction model for Tehran urban roads. J Environ Eng Landsc Manag. 2018;26(2):88–97.
38.• Umar IK, Adamu M, Mostafa N, Riaz MS, Haruna SI, Hamza MF, et al. The state-of-the-art in the application of artificial intelligence-based models for traffic noise prediction: a bibliographic overview. Cogent Eng. 2024;11(1):2297508. **This paper presents a review of artificial intelligence (AI)-based models for road traffic noise assessment, analyzing fifty published articles from 2007 to 2023, regarding several aspects, including input data and modeling techniques.**
39. Kumar P, Nigam S, Kumar N. Vehicular traffic noise modeling using artificial neural network approach. Transp Res Part C Emerg Technol. 2014;40:111–22.
40. Garg N, Mangal S, Saini P, Dhiman P, Maji S. Comparison of ANN and analytical models in traffic noise modeling and predictions. Acoust Aust. 2015;43:179–89.
41. Cirianni F, Leonardi G. Artificial neural network for traffic noise modelling. ARPN J Eng Appl Sci. 2015;10(22):10413–9.
42. Bravo-Moncayo L, Lucio-Naranjo J, Chávez M, Pavón-García I, Garzón C. A machine learning approach for traffic-noise annoyance assessment. Appl Acoust. 2019;156:262–70.
43. Nedic V, Despotovic D, Cvetanovic S, Despotovic M, Babic S. Comparison of classical statistical methods and artificial neural network in traffic noise prediction. Environ Impact Assess Rev. 2014;49:24–30.
44. Genaro N, Torija A, Ramos-Ridao A, Requena I, Ruiz DP, Zamorano M. A neural network based model for urban noise prediction. J Acoust Soc Am. 2010;128(4):1738–46.
45. Cirianni F, Leonardi G. Road traffic noise prediction models in the metropolitan area of the Strait of Messina. In: Proceedings of the Institution of Civil Engineers-Transport. vol. 164. Thomas Telford Ltd; 2011. p. 231–239.
46. Sharma A, Vijay R, Bodhe G, Malik L. Adoptive neuro-fuzzy inference system for traffic noise prediction. Int J Comput Appl. 2014;98(13).
47. Sharma A, Vijay R, Bodhe G, Malik L. An adaptive neuro-fuzzy interface system model for traffic classification and noise prediction. Soft Comput. 2018;22:1891–902.
48. Ruiz-Padillo A, Ruiz DP, Torija AJ, Ramos-Ridao Á. Selection of suitable alternatives to reduce the environmental impact of road traffic noise using a fuzzy multi-criteria decision model. Environ Impact Assess Rev. 2016;61:8–18.
49. Rahmani S, Mousavi SM, Kamali MJ. Modeling of road-traffic noise with the use of genetic algorithm. Appl Soft Comput. 2011;11(1):1008–13.
50. Khouban L, Ghaiyoomi AA, Teshnehlab M, Ashlaghi AT, Abbaspour M, Nassiri P. Combination of artificial neural networks and genetic algorithm - gamma test method in prediction of road traffic noise. Environ Eng Manag J (EEMJ). 2015;14(4).

51. Chen P, Xu L, Tang Q, Shang L, Liu W. Research on prediction model of tractor sound quality based on genetic algorithm. Appl Acoust. 2022;185:108411.
52. Lelong J. Vehicle noise emission: evaluation of tyre/road and motor-noise contributions. In: Proceedings of Internoise 99, Fort Lauderdale, Florida, USA, 6-8 December 1999, Vol. 1; 1999.
53. Heutschi K. SonRoad: new Swiss road traffic noise model. Acta Acust Acust. 2004;90(3):548–54.
54. Watts G. Harmonoise prediction model for road traffic noise. Transp Res Lab; 2005.
55. Fleming GG, Rapoza AS, Lee CS. Development of national reference energy mean emission levels for the FHWA traffic noise model (FHWA TNM), version 1.0. United States. Federal Highway Administration; 1995.
56. Federal HighwayAdmnistritaion OoNE. Technical Manual, Traffic Noise Model 3.1. U.S. Department of Transportation; 2021.
57. Dutilleux G, Defrance J, Ecotière D, Gauvreau B, Bérengier M, Besnard F, et al. NMPB-routes-2008: the revision of the French method for road traffic noise prediction. Acta Acust Acust. 2010;96(3):452–62.
58. Besnard F, Hamet JF, Lelong J, LeDuc E, Guizard V, Fürst N, et al. Road noise prediction 1-calculating sound emissions from road traffic. Bagneux: SETRA; 2009.
59. Hamet JF, Besnard F, Doisy S, Lelong J, Le Duc E. New vehicle noise emission for French traffic noise prediction. Appl Acoust. 2010;71(9):861–9.
60. Kephalopoulos S, Paviotti M, Anfosso-Lédée F. Common noise assessment methods in Europe (CNOSSOS-EU). Publications Office of the European Union; 2012.
61. Kok A, van Beek A. Amendments for CNOSSOS-EU: description of issues and proposed solutions. RIVM Lett Rep. 2019.
62. Commission Delegated Directive (EU) of 21.12.2020 amending, for the purposes of adapting to scientific and technical progress, Annex II to Directive 2002/49/EC of the European Parliament and of the Council as regards common noise assessment methods, 2020.
63. Pallas MA, Berengier M, Chatagnon R, Czuka M, Conter M, Muirhead M. Towards a model for electric vehicle noise emission in the European prediction method CNOSSOS-EU. Appl Acoust. 2016;113:89–101.
64. Czuka M, Pallas MA, Morgan P, Conter M. Impact of potential and dedicated tyres of electric vehicles on the tyre-road noise and connection to the EU noise label. Transp Res Proc. 2016;14:2678–87.
65. Licitra G, Bernardini M, Moreno R, Bianco F, Fredianelli L. CNOSSOS-EU coefficients for electric vehicle noise emission. Appl Acoust. 2023;211:109511.
66. Ishii K. Prediction of road traffic noise (part 1), method of practical calculation. J Acoust Soc Jpn. 1975;31:507–17. (In Japanese).
67. Ikegaya K. Mathematical models and estimation for predicting the road traffic noise. J Acoust Soc Jpn. 1975;31:559–65. (In Japanese).
68. Sakamoto S. Road traffic noise prediction model ASJ RTN-Model 2018: report of the research committee on road traffic noise. Acoust Sci Technol. 2020;41(3):529–89. https://doi.org/10.1250/ast.41.529.
69. Yamamoto K. Road traffic noise prediction model ASJ RTN-Model 2008: report of the research committee on road traffic noise. Acoust Sci Technol. 2010;31(1):2–55.
70. Quartieri J, Iannone G, Guarnaccia C. On the improvement of statistical traffic noise prediction tools. In: Proceedings of the 11th WSEAS International Conference on Acoustics & Music: Theory & Applications (AMTA'10), Iasi, Romania; 2010. p. 201–207.
71. Guarnaccia C. EAgLE: equivalent acoustic level estimator proposal. Sensors. 2020;20(3):701.
72.• Pascale A, Macedo E, Guarnaccia C, Coelho MC. Smart mobility procedure for road traffic noise dynamic estimation by video analysis. Appl Acoust. 2023a;208:109381. **This paper presents a microscopic road traffic noise model that considers single vehicle speed and category, obtained via video analysis automatic tool.**
73. Pascale A, Guarnaccia C, Macedo E, Fernandes P, Miranda AI, Sargento S, et al. Road traffic noise monitoring in a Smart City: sensor and model-based approach. Transp Res Part D: Transp Environ. 2023b;125:103979.
74. Khan J, Ketzel M, Jensen SS, Gulliver J, Thysell E, Hertel O. Comparison of Road Traffic Noise prediction models: CNOSSOS-EU, Nord 2000 and TRANEX. Environ Pollut. 2021;270:116240.
75. Attenborough K, VanRenterghem T. Predicting outdoor sound. CRC Press; 2021.
76. Van Renterghem T, Botteldooren D. Landscaping for road traffic noise abatement: model validation. Environ Model Software. 2018;109:17–31.
77. Ecotiere D, Foy C, Dutilleux G. Comparison of engineering models of outdoor sound propagation: NMPB2008 and Harmonoise-Imagine. In: Acoustics 2012; 2012. .
78. Hart CR, Reznicek NJ, Wilson DK, Pettit CL, Nykaza ET. Comparisons between physics-based, engineering, and statistical learning models for outdoor sound propagation. J Acoust Soc Am. 2016;139(5):2640–55.
79. Aumond P, Can A, Mallet V, Gauvreau B, Guillaume G. Global sensitivity analysis for road traffic noise modelling. Appl Acoust. 2021;176:107899.
80. European Union. Directive 2002/49/EC relating to the Assessment and Management of Environmental Noise. Official Journal of the European Communities; 2002.
81. European Commission Directive. 2015/996 of 19 May 2015 establishing common noise assessment methods according to Directive 2002/49/EC of the European Parliament and of the Council. Official Journal of the European Communities; 2015.
82. World Bank. World Development Report 1993: investing in health, Volume1. The World Bank; 1993.
83. Murray CJ, Lopez AD, Organization WH. The global burden of disease: a comprehensive assessment of mortality and disability from diseases, injuries, and risk factors in 1990 and projected to 2020: summary. World Health Organization; 1996.
84. deHollander AE, Melse JM, Lebret E, Kramers PG. An aggregate public health indicator to represent the impact of multiple environmental exposures. Epidemiology. 1999; p. 606–617.
85. World Health Organization. Burden of disease from environmental noise: quantification of healthy life years lost in Europe. Regional Office for Europe: World Health Organization; 2011.
86. Stansfeld SA. Noise effects on health in the context of air pollution exposure. Int J Environ Res Public Health. 2015;12(10):12735–60.
87. Santos G, Behrendt H, Maconi L, Shirvani T, Teytelboym A. Part I: Externalities and economic policies in road transport. Res Transp Econ. 2010;28(1):2–45. https://doi.org/10.1016/j.retrec.2009.11.002.
88.•• Nygren J, LeBescond V, Can A, Aumond P, Gastineau P, Boij S, etal. Agent-specific, activity-based noise impact assessment using noise exposure cost. Sustain Cities Soc. 2024; p. 105278. **This paper presents an agent-specific and activity-based method for traffic noise exposure, by merging agent-based simulation in MATSim, existing traffic noise prediction tools and noise exposure cost methodologies.**
89. Hankach P, Le Bescond V, Gastineau P, Vandanjon PO, Can A, Aumond P. Individual-level activity-based modeling and indicators for assessing construction sites noise exposure in urban areas. Sustain Cities Soc. 2024;101:105188.
90. Nero G, Black JA. A critical examination of an airport noise mitigation scheme and an aircraft noise charge: the case of capacity expansion and externalities at Sydney (Kingsford Smith) airport. Transp Res Part D: Transp Environ. 2000;5(6):433–61.

91. Tomkins J, Topham N, Twomey J, Ward R. Noise versus access: the impact of an airport in an urban property market. Urban studies. 1998;35(2):243–58.
92. Ekici F, Orhan G, Gümüş Ö, Bahce AB. A policy on the externality problem and solution suggestions in air transportation: the environment and sustainability. Energy. 2022;258:124827.
93. Kim M, Chang SI, Seong JC, Holt JB, Park TH, Ko JH, et al. Road traffic noise: annoyance, sleep disturbance, and public health implications. Am J Prev Med. 2012;43(4):353–60.
94. Dzhambov AM, Lercher P. Road traffic noise exposure and depression/anxiety: an updated systematic review and meta-analysis. Int J Environ Res Public Health. 2019;16(21):4134.
95. De Kluizenaar Y, Janssen SA, Vos H, Salomons EM, Zhou H, Van den Berg F. Road traffic noise and annoyance: a quantification of the effect of quiet side exposure at dwellings. Int J Environ Res Public Health. 2013;10(6):2258–70.
96. Urban J, Máca V. Linking traffic noise, noise annoyance and life satisfaction: a case study. Int J Environ Res Public Health. 2013;10(5):1895–915.
97. Elmenhorst EM, Griefahn B, Rolny V, Basner M. Comparing the effects of road, railway, and aircraft noise on sleep: exposure-response relationships from pooled data of three laboratory studies. Int J Environ Res Public Health. 2019;16(6):1073.
98. Kawada T. Noise and health–sleep disturbance in adults. J Occup Health. 2011;53(6):413–6.
99. Muzet A. Environmental noise, sleep and health. Sleep Med Rev. 2007;11(2):135–42.
100. Foulkes L, McMillan D, Gregory AM. A bad night's sleep on campus: an interview study of first-year university students with poor sleep quality. Sleep Health. 2019;5(3):280–7.
101. Fyhri A, Aasvang GM. Noise, sleep and poor health: modeling the relationship between road traffic noise and cardiovascular problems. Sci Total Environ. 2010;408(21):4935–42.
102. Sørensen M, Hvidberg M, Andersen Z, Nordsborg R, Lillelund K, Jakobsen J, et al. Road traffic noise and stroke: a prospective cohort study. Epidemiology. 2011;22(1):S51.
103. Münzel T, Gori T, Babisch W, Basner M. Cardiovascular effects of environmental noise exposure. Eur Heart J. 2014;35(13):829–36.
104. ELarsen J, PBlair J. Price effects of surface street traffic on residential property. Int J Hous Mark Anal. 2014;7(2):189–203.
105. Del Giudice V, De Paola P, Manganelli B, Forte F. The monetary valuation of environmental externalities through the analysis of real estate prices. Sustainability. 2017;9(2):229.
106. Wilhelmsson M. The impact of traffic noise on the values of single-family houses. J Environ Plan Manag. 2000;43(6):799–815.
107. Navrud S. The economic value of noise within the European union - a review and analysis of studies. Acta Acustica (Stuttgart). 2003;89(SUPP.).

JASA ARTICLE

A stochastic and microscopic model to predict road traffic noise by random generation of single vehicles' speeds

Aurora Mascolo,[1,a)] Domenico Rossi,[1] Alessandro Ruggiero,[2] and Claudio Guarnaccia[1,b)]
[1]*Department of Civil Engineering, University of Salerno, Via Giovanni Paolo II 132, I-84084 Fisciano, Italy*
[2]*Department of Industrial Engineering, University of Salerno, Via Giovanni Paolo II 132, I-84084 Fisciano, Italy*

ABSTRACT:
Road traffic noise is the major component of acoustic environmental pollution both in urban and rural areas. For this reason, much effort has been put into developing models to assess its impact. However, literature models are often suitable for standard conditions but can fail in non-standard ones, i.e., when the single vehicle speed cannot be neglected. Moreover, input data to literature models are not always available, e.g., if the road infrastructure is still in the design phase. The presented approach aims to try to overcome these shortcomings using a microscopic and stochastic-core model, in which the speed of each vehicle can be randomly generated using a specific speed distribution. The validation of the model, investigated through a statistical analysis of simulated continuous equivalent sound pressure levels, the error distribution, and the calculation of commonly used error metrics suggests that the proposed methodology provides good estimations of traffic noise. The errors of the model computed as the differences between measured and simulated sound levels, can be described as a distribution curve with a −0.6 dBA mean and a standard deviation of 2.3 dBA. The error metrics confirm the model's goodness, with a mean absolute error of 1.84 dBA and a coefficient of variation error of 0.03.
© *2025 Author(s). All article content, except where otherwise noted, is licensed under a Creative Commons Attribution (CC BY) license (https://creativecommons.org/licenses/by/4.0/).* https://doi.org/10.1121/10.0035570
(Received 13 August 2024; revised 7 January 2025; accepted 7 January 2025; published online 3 February 2025)
[Editor: Francesco Aletta] Pages: 721–737

18 February 2026 18:56:06

I. INTRODUCTION

The environmental impact of noise pollution is a critical issue in both urban and interurban areas within the framework of modern cities and settlements. Noise is, indeed, the second most relevant environmental problem, only behind air pollution.[1–4] However, in some European countries, the societal cost of noise pollution has been estimated to surpass that of air pollution. Although not as evident as air pollution, the effects of noise pollution can still be very harmful.[5] Although not as evident as the air one, the effects of noise pollution can be still very harmful. According to the World Health Organization (WHO), prolonged exposure to high levels of noise may be associated with the occurrence of negative consequences for people's physiological and psychological health.[6–8] Negative impacts are also proved to be associated with social vulnerability in several European Countries.[5,9] For example, noise particularly affects children's cognitive performances.[10–14] Also, shift workers,[15–18] noise-sensitive people, and people with pre-existing health conditions[19,20] are particularly affected by noise exposure. In particular, continuous noise exposure could lead to potential short-term effects, such as morning tiredness, hearing problems, and sleep disorder, and thus in general a bad influence on the quality of life, or even long-term effects, such as contributing to the development of cardiovascular problems or chronic hypertension.[21–31] In such a scenario, road traffic is a significant noise source within the urban and interurban environment, with cars or passenger vehicles being the dominant form of transportation for internal urban mobility.[32] To this regard, the European Environmental Agency (EEA) has estimated that in Europe the population exposed to a day-evening-night noise level L_{den} of at least 55 decibels dBA, i.e., the value above which the occurrence of negative effects is associated, due only to road traffic is around 113×10^6 people.[1,2] In addition, 22×10^6 people are exposed to similar noise levels due to rail traffic, 4×10^6 people to noise from air traffic, and less than 1×10^6 people are exposed to high noise levels due to industrial areas.[1,2] Moreover, it has also been predicted that noise pollution will still be increasing due to the population growth in urban settings and the resulting increase in people's mobility needs.[32] Given that, it is clear why one of the primary European Union (EU) targets is to decrease the percentage of individuals who are chronically disturbed by transportation noise by at least 30% by the year 2030.[33]

For these reasons, in the last few decades, many efforts have been made for the development of methods and models that could help to assess environmental noise impact. More specifically, taking into consideration the main role played by road traffic noise, the assessment of noise impact in the proximity of existing or under-design road infrastructure plays a significant role in evaluating the acoustic environment of an urban and interurban settlement. Such evaluation

[a)]Email: amascolo@unisa.it
[b)]Email: cguarnaccia@unisa.it

 ©Author(s) 2025.

can be pursued both by planning and carrying out a wide enough measurement campaign activity *in situ* or through simulations using specific algorithms. However, several conditions may contribute to making measurement activities not feasible: for example, it must be considered the high economic burden of these campaigns or even the fact that the designing phase of the infrastructure under analysis may still be ongoing. Hence, the use of appropriate models to estimate the continuous equivalent sound pressure level produced by any road infrastructure could be of essential support during the designing phase of a new road infrastructure and also to avoid unnecessary mitigation actions; this way any measurement campaigns can be minimized and used just for the calibration of the model. These aspects, along with the relevant references, will be further developed and discussed in the following.

Modelling road traffic noise could be very challenging, especially due to the presence of several random elements associated with the characteristics of the phenomenon under study. To achieve an adequate simulation of the actual acoustic environment studied, very precise mathematical modelling of the surrounding area, the sound sources, and the sound propagation laws should be taken into consideration.[34]

However, a lot of the commonly used road traffic noise models (RTNMs) are mainly statistic-based models and their intrinsic nature inherently has several shortcomings, among which prevails the inability to consider the random core of the traffic dynamics. In this regard, in the last few decades, numerous countries have developed their specific models to estimate road traffic noise. Most of them are statistic-based models and specifically framed on national regulations and fleets. Examples of such models are the CoRTN model,[35] developed in the United Kingdom, which is based on a regression approach, as well as RLS90, which is the German national model.[36] A similar methodology is used in the C.N.R. Model, promoted in Italy,[37] and in Thailand, the ERTC model.[38] However, a lot of them can be considered macroscopic or mesoscopic, since they use average or limit speed for each vehicle's category, which implies many approximations. Examples of these approaches are the French NMPB-Routes model,[39] the Swiss SonRoad model,[40] the Scandinavian Nord2000,[41] the American FHWA model,[42] and the European reference model, i.e., CNOSSOS-EU model.[43,44]

These models are particularly suitable for standard conditions (fluid flow, intermediate traffic volume, etc.), but they can fail in non-standard ones, or whenever the single vehicle speed influence cannot be neglected. This is especially true in cases of non-free flow traffic, traffic jams, in the proximity of road intersections or traffic lights, as well as during extremely high or low traffic volume or speed. Indeed, as specifically investigated by Garg and Maji,[45] even though commonly used models such CNOSSOS-EU model[46–49] recommend using mean speed measurements or limit speeds as inputs for noise emission models (NEMs), to obtain accurate noise levels predictions when in interrupted traffic flow or near a junction and other types of traffic delaying structures such as speed bumps, it is necessary to micro-simulate road traffic. This includes accounting for dynamic effects that alter the speed homogeneity of the traffic flow.

Thus, a robust baseline for the development of a predicting road traffic noise model that can be applied to contexts with different characteristics from the standard ones is achievable using a microscopic approach, i.e., based on the noise emission of the single vehicle. Several studies in the literature aim to develop microscopic models of road traffic noise to assess the local influence of traffic dynamics on noise emissions. In Ref. 50, a microscopic approach has been used to correct the noise level predictions obtained using a macroscopic model in proximity of road junctions. The relevance of analyzing the single vehicle behavior in either roundabouts or road junctions has been proved also in Ref. 51 where the authors propose a method to describe the performance of roundabouts starting from traffic volumes, noise level, pollutant emission, and representative speed profile.

In Ref. 52, Can and Botteldooren found out that sound power levels assessed using a microscopic approach differ notably from those estimated using the mean speed approach, particularly in congested traffic conditions and in urban settings, which are often characterized by ever changing traffic conditions. In their contribution, they noticed that neglecting vehicle kinematics, such as acceleration/deceleration and speed distribution in either congested or stop-and-go scenarios can lead to high disparities, mainly due to actual driving speeds being considerably lower than the speed limit. In Ref. 53, the authors focused on the analysis of the urban and interurban noise frequency spectrum, comparing a macroscopic approach, which takes into consideration just mean vehicle speeds and flow rates, and a microscopic approach which considers vehicle interactions (respectively called static and dynamic[53]). Even though different noise features were explored, such comparison led to similar conclusions, highlighting how the macroscopic approach systematically underestimates low frequency contributions to continuous equivalent sound pressure levels, being such contributions mainly related to low speeds and accelerating phases. The inability of macroscopic approaches to consider vehicle kinematics and different traffic patterns also affects $L_{A,eq}$ estimations as also proved in Ref. 54. Nygren *et al.*[55] highlighted the crucial importance of using a microscopic approach to compute the vehicle-specific noise exposure cost, i.e., the contribution of the single vehicle to the overall noise impact of a road network. Likewise, Baclet *et al.*[56] proposed the calculation of noise exposure indicators in large urban areas starting through the usage of a microscopic model.

In Ref. 57, a microscopic approach was employed to assess road traffic noise emission using data collected with Unmanned Aerial Vehicles and the CNOSSOS-EU model to simulate each vehicle as an individual source point.

Nevertheless, as mentioned earlier, obtaining usable inputs for microscopic models through measurement

18 February 2026 18:56:06

https://doi.org/10.1121/10.0035570

campaigns is not always possible. To overcome this issue, many scholars utilize meso- or microscopic traffic models to compute and simulate realistically both road networks and single vehicle behaviors, thereby obtaining speeds and positions of vehicles at the desired time step.[58–60] In this regard, another approach that can be found in the literature is the specific combination of traffic simulating software and noise models. An example is the model developed by École Polytechnique Fédérale de Lausanne (EPFL), dynamic road traffic noise (drone), which uses AVENUE and ASJ-RTN-1998, respectively, as a traffic simulation and noise model.[61] In Ref. 62, the authors use PARAMICS for the traffic inputs and a noise model based on the Nord2000 database. Also, in Ref. 63, a similar approach to the problem can be found, with the combination of the open-source tool NoiseModelling, which uses the CNOSSOS-EU model to estimate noise levels, with MATSim.

Nevertheless, the main objective and novelty of this contribution is to address the inherent shortcomings of macroscopic approaches by adopting a microscopic model based only on aggregated data. Having as a starting point the aggregate characteristics of any road infrastructure, for example, the flow distributions of vehicle silhouettes and their speeds, the idea of this work is to develop a "micro to macro" energy-based model.

By doing so, the presented methodology allows us to achieve accurate results, even when only data suitable for macroscopic analysis are available. This is possible thanks to the stochastic core of the presented model: the speed of the single vehicle can be randomly generated knowing the speed mean and traffic conditions, which lead to a specific speed distribution. Once this random speed assignment has been made, the distribution of acoustical energies emitted by transiting vehicles and, consequently, the continuous equivalent sound pressure level (L_{eq}) can be estimated. Finally, such sound pressure level L_{eq} could be used to compute noise indicators as often established by government institutions, for instance, concerning the European regulation, L_{day}, $L_{evening}$, L_{night}, or L_{den}.

Such information can be used in the design of new roads, i.e., when just a hypothesis on the road infrastructure conditions can be made, or in the management of existing infrastructures, as well as in the maintenance and design of any noise abatement operations. Furthermore, not needing the imputation of microscopic data through traffic simulating software, the model presented in this paper is a simple and user-friendly tool, useful to better assist urban planning technicians in accurately foretelling the potential noise repercussions of road infrastructure during both the phase of design and conception. Thus, in this paper, following the introduction section, in which the significance of modeling traffic noise and the various challenges in this field have been presented, a comprehensive description of the stochastic model utilized in the study is provided in the methodology section. The process of generating individual vehicle speeds and calculating the A-weighted continuous equivalent sound pressure level ($L_{A,eq}$) is therefore explained.

Subsequently, the case study section focuses on a database collected in France, which contains six years of traffic data. This section illustrates how the data has been used to implement the proposed model effectively. Next, the results and discussion section detail the findings derived from applying the model to the earlier mentioned data, showcasing the outcomes of the traffic noise predictions. To better investigate the potential of the presented approach, a comparison between the results of the stochastic approach and the CNOSSOS-EU model has also been performed.

Finally, the paper concludes with a conclusion that summarizes the key results and offers insights into future research directions in traffic noise modeling.

II. MATERIALS AND METHODS

In order to be able to investigate the intrinsic random nature of road traffic phenomena, such as tire-road interaction, engine noise, aerodynamic noise, and exhaust systems, without omitting data about the single vehicle, the authors decided to develop a modular, stochastic, and microscopic approach. In particular, since the acoustical energy emitted by a single vehicle is highly dependent on its speed, it has been decided to assign to each vehicle a single value of speed. Individual speed values can be used if available by means of field measurements, such as in Refs. 64 and 65, or using any other calculation tools, such as video image analysis,[66,67] generating datasets with computational approaches,[68] or even using traffic simulation software as reported in Sec. I. Otherwise, speeds can be randomly derived from a hypothetical speed distribution curve.[69] In this way, the entire vehicular flow is not modelled as a simple source characterized by an average speed value (as usually done by statistic or macroscopic models in the literature[43,44]) but rather it is possible to associate each vehicle with a peculiar value of speed.

This method allows us to take into account the different acoustic energy emissions of vehicles also when belonging to the same category, due for instance to different driver behavior. Thus, the specific acoustic contribution of each vehicle is taken into consideration, and no contribution is mitigated or lost in the averaging processing.

In Fig. 1, the flow chart of the proposed model is reported, in which the steps to be followed for a successful implementation of the stochastic model are shown.

The model uses three different kinds of data as input. First, traffic flow data are taken into account. In this step, information is gathered on the traffic flow of each vehicle category considered (for example light and heavy-duty vehicles), mean speeds, and flow typologies (continuous, pulsed, accelerated, etc.). Then geometry and road parameters are evaluated, such as the height of the receiver and the distance between the observation point (the receiver) and the center of the traffic lane (i.e., where the traffic flow source is assumed to be located) in order to adequately

18 February 2026 18:56:06

propagate the continuous equivalent sound pressure level at the desired distance. Finally, data about the road characteristics are considered, such as the type of road, the pavement, size, and number of lanes, gradient (slope), etc.

Thereafter the crucial step of collecting data inputs, the model moves to its central stochastic core: the random selection of single vehicle speed from an appropriate speed distribution. Using a specific speed distribution curve as a benchmark to describe current or to be expected traffic conditions (i.e., if the road infrastructure does not yet exist), can result in a model that closely approximates real scenarios. For instance, in Refs. 70–72, it has been shown that vehicle speeds in free-flow traffic conditions can be described by a Gaussian normal distribution, while pulsed flows produce skewed speed distributions, such as Beta and Chi-square.[73] In this paper, the highway segment analyzed as a case study presented free-flow conditions, which led to the selection of a Gaussian speed distribution (see Sec. III).

The next step is to evaluate a physical observable that could be used to describe the acoustic emissions of the single vehicle. The commonly used indicator is the source power level, L_W, and many models in the literature assess the vehicle's power level as a function of the vehicle speed v. These models are usually named NEMs[74] and provide the vehicle's noise emission curve as a function of the vehicle speed, sometimes including correcting factors about road slope, pavement, acceleration, etc. The modular structure of the proposed model allows for the changing of the selected NEM to be used to compute L_W according to the case study location or any other significant variables. In this paper, the choice was to follow the EU reference model CNOSSOS-EU[43,44] approach for computing the $L_{W,j,i,m}$ of the jth vehicle, as a function of its speed, for each octave band i and for each vehicle category m. CNOSSOS-EU model suggests to log-sum of the contributions of propulsion noise, $L_{W,P,j,i,m}$, and rolling noise, $L_{W,R,j,i,m}$, being the former linearly dependent on the speed and assuming a logarithmic dependence for the latter. Nevertheless, differently from the CNOSSOS-EU approach, which uses the average speed of the flow per each category (i.e., macroscopic approach), since in this model the single vehicle speed v_j is used (i.e., microscopic approach), for each vehicle the jth vehicle source power level is computed as in Eq. (1). Thus, the inspiration for the CNOSSOS-EU model is restricted to the modelling of overall source power level as the log-sum of propulsion and rolling contributions, using the CNOSSOS-EU coefficients. The CNOSSOS-EU model considers the traffic flow as a line source and then propagates the continuous equivalent sound pressure levels at the receiver, treating individual vehicles as point sources and then merging them to represent a line source. In contrast, the presented model is fully microscopic, considering each vehicle considered as a point source. This shift changes the modelling approach significantly, both in the emission and propagation phases. However, no interference phenomena need to be accounted for, as in road traffic noise modelling, vehicles are considered incoherent sources, simplifying the aggregation of contributions,

$$L_{W,j,i,m}(v_{j,m}) = 10\log_{10}\left(10^{L_{WR,j,i,m}(v_{j,m})/10} + 10^{L_{WP,j,i,m}(v_{j,m})/10}\right). \quad (1)$$

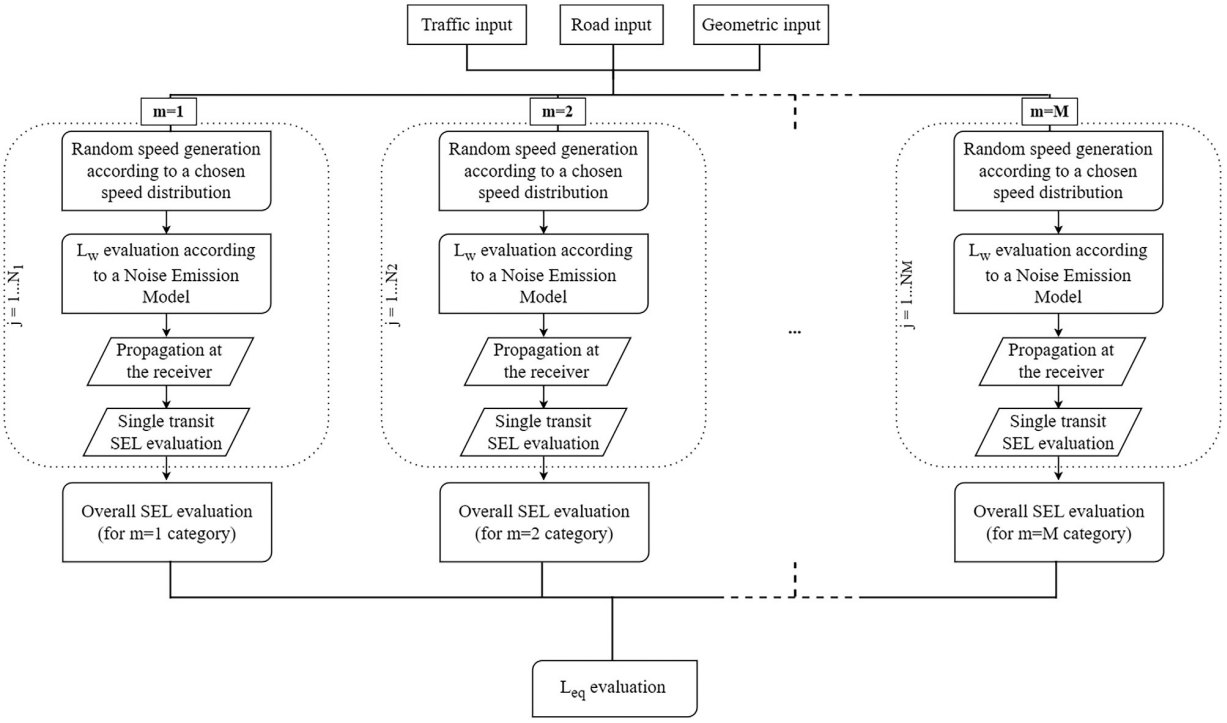


FIG. 1. Flowchart of the proposed road traffic noise model. The dotted line represents a loop to be repeated for each vehicle considered.

18 February 2026 18:56:06

https://doi.org/10.1121/10.0035570

Rolling noise $L_{W,R,j,i,m}$ $(v_{j,m})$ and propulsion noise, $L_{W,P,j,i,m}$ $(v_{j,m})$ are computed according to Eq. (2) and Eq. (3), using coefficients (i.e., $A_{R,i,m}$, $B_{R,i,m}$ and $A_{P,i,m}$, $B_{P,i,m}$) depending on the vehicles category considered and different corrective factors (i.e., $\Delta L_{W,R,j,i,m}$, and $\Delta L_{W,P,j,i,m}$) depending on the actual simulated conditions with respect to the used as standard ones in the CNOSSOS-EU model, as provided in Refs. 43 and 44,

$$L_{W,R,j,i,m}(v_{j,m}) = A_{R,i,m} + B_{R,i,m}\log_{10}\left(\frac{v_{j,m}}{v_{rif}}\right) + \Delta L_{W,R,j,i,m}(v_{j,m}), \quad (2)$$

$$L_{W,P,j,i,m}(v_{j,m}) = A_{P,i,m} + B_{P,i,m}\left(\frac{v_{j,m} - v_{ref}}{v_{ref}}\right) + \Delta L_{W,P,j,i,m}(v_{j,m}). \quad (3)$$

However, after several studies in the literature,[75,76] the coefficients provided by the CNOSSOS-EU document have been lately updated[44] in order to consider surface reflection effects. These latter coefficients have been used in this paper. Nevertheless, many studies in the literature aim at computing these coefficients for vehicle categories that are still not considered in the CNOSSOS-EU model.[77,78] For example, in Ref. 79, the coefficients for electric vehicles are provided after fitting statistical pass-byes for a reference pavement and compared with results obtained with a crumb rubber pavement.

Having calculated the sound power level L_W, it is possible to move on to the following step in which the authors decide to assume a simple type of propagation as the one reported in Fig. 2. Point R is the fixed receiver at which the continuous equivalent sound pressure level has to be calculated, while $r_{j,m}(t)$ is the variable (time dependent) single vehicle-receiver distance that could be easily computed as reported in Eq. (4),

$$r_{j,m}(t) = \sqrt{d^2 + \left(\frac{S}{2} - v_{j,m}t_{j,m}\right)^2}, \quad (4)$$

where S is the length of the road segment traveled by the vehicle at speed $v_{j,m}$, and $t_{j,m}$ is the elapsed time. Such length is a fundamental parameter of the model, together with the distance d because they define the angle at which a vehicle traveling on the road significantly contributes to the continuous equivalent sound pressure level at the receiver. The simplified propagation model adopted in this study deliberately omits more complex effects, such as atmospheric attenuation, ground reflection, and diffraction, which become significant over greater distances. Instead, the model assumes omnidirectional propagation from a point source, which is more appropriate for shorter distances, as in the vehicle-receiver setup considered in the scenario presented later in the case study section. Nonetheless, due to the modular nature of the approach, the propagation formula can easily be adapted to incorporate wave phenomena and other propagation effects if larger distances need to be analyzed.

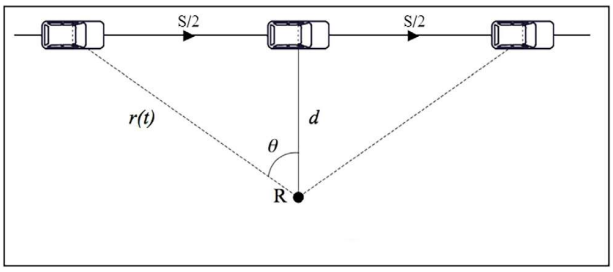


FIG. 2. Graphical representation of the distance between the source (vehicle) whose position varies over time with $r(t)$ and the point R which is assumed to be the fixed receiver.

It therefore makes it possible to assess what the actual contributions to the continuous equivalent sound pressure level at the receiver are.

Starting from this distance, the sound pressure level $L_{p,j,m}$ immitted at the receiver R by a single jth vehicle belonging to the m category, can be calculated as a function of time t, under the assumption of a point source combining the source power level with the geometrical spreading and the solid angle part, considering absorbing ground, as shown in Eq. (5),

$$L_{p,j,m}(t) = L_{W,j,m} - 20\log_{10}(r(t)) - 11. \quad (5)$$

Here, $L_{W,j,m}$ is the power sound level, $r(t)$ is the distance between source and receiver, as a function of time, and 11 is 10 $\log_{10}$ (4π), due to the omnidirectional propagation and the absorbing ground.

At this point, the next crucial step involves calculating a physical parameter to assess the overall pressure level assessed at the receiver during the vehicle transit. Since the focus of this phase is to evaluate the acoustical energy emitted to the receiver by the single vehicle, the authors decided to use the single event sound exposure level (SEL). In the application presented, SEL appears to be more suitable than the $L_{A,eq}$ of the single transit since the single vehicle pass-by must be analyzed, and the corresponding time interval changes from vehicle to vehicle according to the speed. The relation between $L_{A,eq}$ and SEL is given by the Eq. (6),

$$SEL = L_{eq}(\Delta T) + 10\log_{10}(\Delta T), \quad (6)$$

where ΔT is the time interval, in seconds, in which the overall $L_{A,eq}$ is evaluated.

Starting from the jth individual pass-by, the $SEL_{j,m}$ is calculated following Eq. (7),

$$SEL_{j,m} = 10\log_{10}\frac{1}{t_0}\int_{t_i}^{t_f} 10^{L_{p,j,m}(t)/10}dt, \quad (7)$$

where t_i and t_f are, respectively, the time instants when the jth vehicle enters and exits the considered road segment, and t_0 is equal to 1 s.

18 February 2026 18:56:06

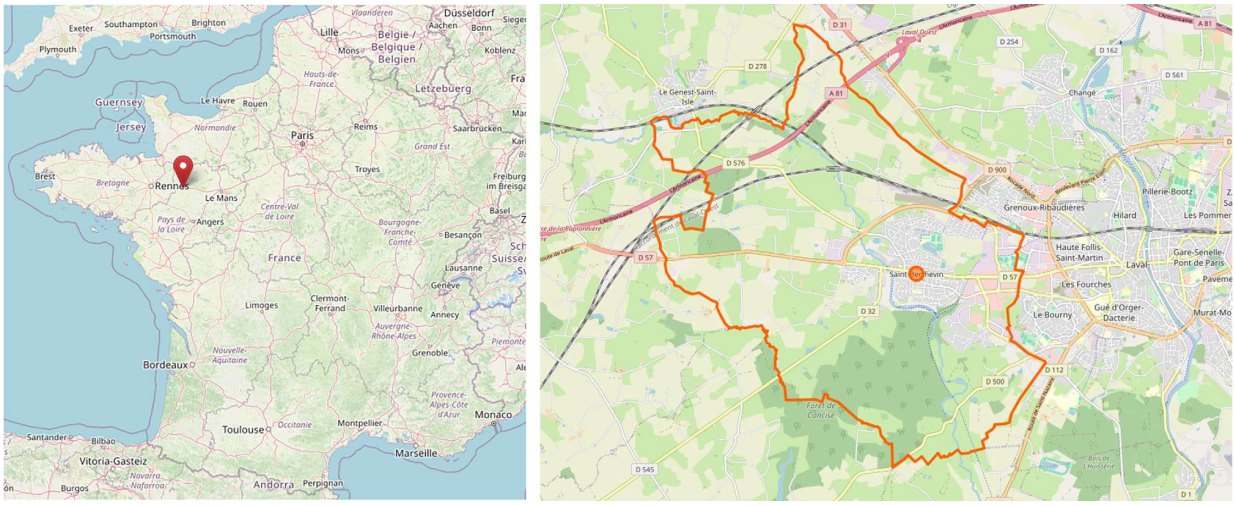


FIG. 3. Geographical location of the municipality of Saint-Berthevin located in the region of *Pays de la Loire*, France (maps available from: OpenStreetMap®).

After that, all the SELs of vehicles belonging to the same category m are appropriately combined to obtain the total SELs of the corresponding category following Eq. (8),

$$SEL_m = 10\,\log_{10}\frac{1}{t_0}\left(\sum_{j=1}^{N_m} 10^{SEL_{j,m}/10}\right). \tag{8}$$

Finally, the last step requires the calculation of the overall $L_{A,eq}$, through the log-sum of the SELs of all vehicle categories considered in the analyzed ΔT time interval, as shown in Eq. (9),

$$L_{eq_{\Delta T}} = 10\log_{10}\frac{1}{\Delta T} + 10\log_{10}\sum_{m=1}^{M} 10^{SEL_m/10}. \tag{9}$$

Nevertheless, as mentioned earlier, even if in this application the equations from the CNOSSOS-EU model were used to compute the single vehicle sound power level and what can be considered as a quite simple propagation model, the modular scheme of the presented model makes it easy to change both the NEM and the propagation model to be used if the case study or analysis pursued suggests so.

The whole procedure has been developed using a self-written MATLAB® code. In such a routine, several phases can be distinguished, following the explained methodology. The first one in which all the input parameters of the model are defined and the dataset is being uploaded for further use. Then the random speed extraction from a proper distribution for each vehicle in each time interval has been performed. Subsequently, the source power level is computed using the CNOSSOS-EU formulation for each vehicle and the propagation has been taken into account. Finally, the continuous equivalent sound pressure level has been calculated on the desired time basis.

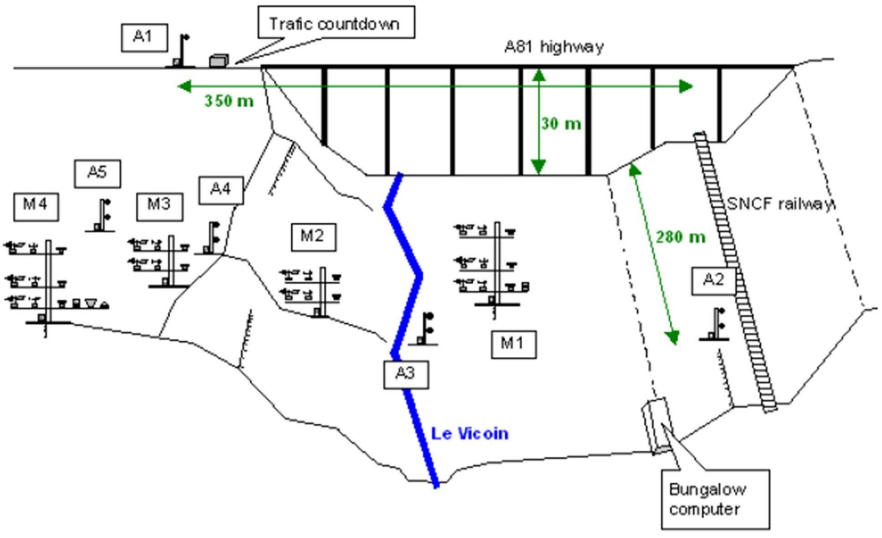


FIG. 4. Schematic representation of acoustic and meteorological sensors' positions. Ref. 64.

18 February 2026 18:56:06

https://doi.org/10.1121/10.0035570

TABLE I. A selection of lines from the used dataset.

# Interval	Date	Time interval	N_L [veh/15 min]	N_H [veh/15 min]	v_L [km/h]	v_H [km/h]	$L_{A,\mathrm{eq,15min,meas}}$ [dBA]
0	01-07-2002	04:30– 04:45	229	16	124.1	84.5	72.2
1	01-07-2002	04:45– 05:00	227	13	130.1	83.2	72.1
2	01-07-2002	05:00– 05:15	264	13	124.3	83.0	72.7
—	—	—	—	—	—	—	—
30 345	18-10-2007	07:45–08:00	207	63	126.3	86.5	73.2
30 346	18-10-2007	08:15–08:30	160	49	125.5	87.8	72.3
30 347	18-10-2007	08:30– 08:45	182	53	125.1	88.1	73.1

Moreover, a comparison between the results of the application of this approach and the CNOSSOS-EU model will be pursued with the aim of getting insights into the capabilities of the stochastic approach with respect to the commonly used methods.

A. Error metrics

Since the presented model is descriptive of a phenomenon characterized by its random nature and by the interaction of many factors (e.g., the input data presented in the previous subsection), it is expected to obtain a certain number of errors from its application. In order to deepen the evaluation of the model performances the authors computed several error metrics. In particular, "mean error" (ME), "mean percentage error" (MPE), and "mean absolute error" (MAE) are implemented and calculated, as well as the "mean squared error" (MSE) and the "coefficient of variation of the error" (CVE). The ME is obtained as indicated in Eq. (10), by adding the differences between the measured and simulated value and dividing the result by the total number of values, n. It can be defined as a measure of the uncertainty of the simulation performed, which allows us to understand whether the model overestimates or underestimates the data on average,

$$\mathrm{ME} = \frac{\sum_{t=1}^{n} \left(Y_t - \widehat{Y}_t\right)}{n}, \tag{10}$$

where Y_t is the measured value and $\widehat{Y}_t$ is the simulated one.

The MPE has been calculated through Eq. (11), to obtain a value expressed as a percentage of such error metrics,

$$\mathrm{MPE} = \frac{\sum_{t=1}^{n} \left(\frac{Y_t - \widehat{Y}_t}{Y_t}\right)}{n}. \tag{11}$$

The MAE was also evaluated using Eq. (12). Specifically, the MAE is obtained by calculating the absolute error, so that negative and positive values do not cancel each other out, and then calculating its mean value,

$$\mathrm{MAE} = \frac{\sum_{t=1}^{n} \left|Y_t - \widehat{Y}_t\right|}{n}. \tag{12}$$

To better understand whether the best fit was found, MSE has been evaluated with Eq. (13),

$$\mathrm{MSE} = \frac{\sum_{t=1}^{n} \left(Y_t - \widehat{Y}_t\right)^2}{n}. \tag{13}$$

Finally, CVE computation has been performed following Eq. (14), to obtain a statistical measure of the dispersion of the dataset's values around its mean.

$$\mathrm{CVE} = \frac{\sqrt{\frac{\sum_{t=1}^{n} \left(Y_t - \widehat{Y}_t\right)^2}{n}}}{\overline{Y}}, \tag{14}$$

where $\overline{Y}$ is the mean value of the measured data in the considered time range t.[80]

III. CASE STUDY APPLICATION

The study carried out in this work involves the application of the methodology explained in Sec. II to experimental

TABLE II. Summary statistics of the used dataset.

	Mean	Standard deviation (Std. dev.)	Min. value	Max. value	Skewness	Kurtosis
N_L [veh/15 min]	278.3	171.3	1	1075	0.75	0.47
N_H [veh/15 min]	31.4	21.3	1	222	0.63	0.59
v_L [km/h]	126.1	7.3	40	186.2	−0.28	3.34
v_H [km/h]	86.9	4.5	2	99	−4.95	0.01
$L_{A,\mathrm{eq,15min,meas}}$ [dBA]	71.6	2.9	46.3	78.2	−2.04	6.11

18 February 2026 18:56:06

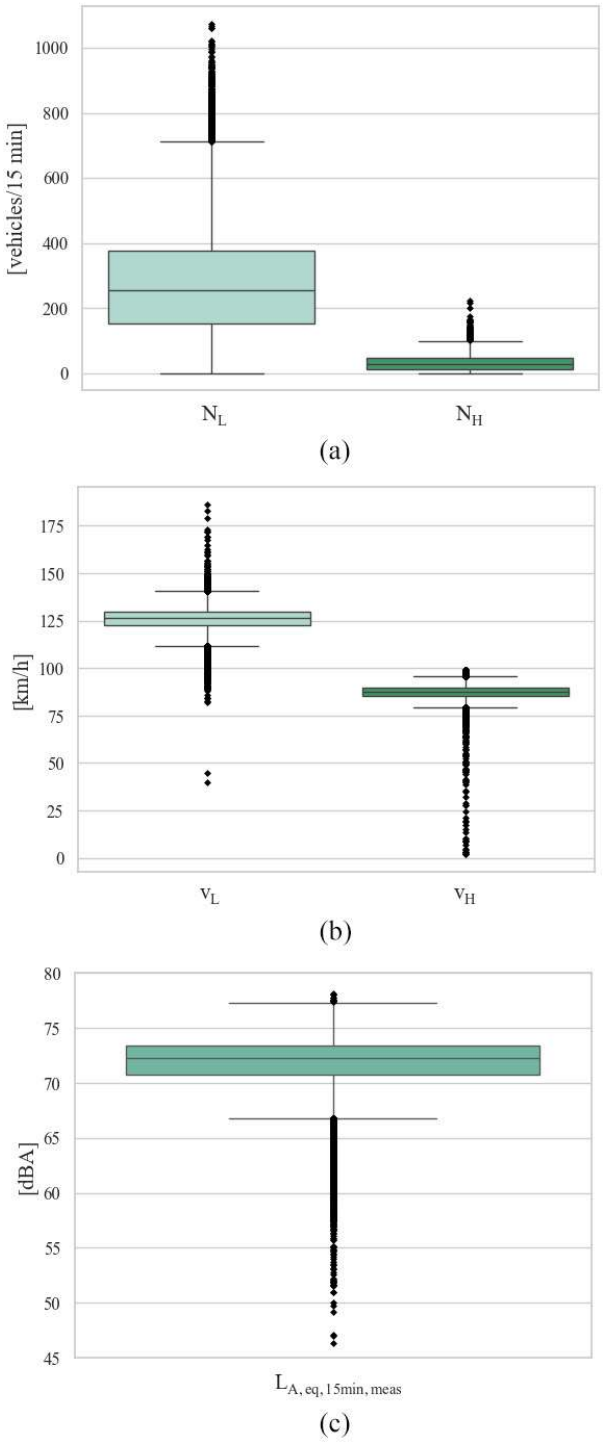


FIG. 5. Boxplot of (a) Light (N_L) and heavy (N_H) vehicles flow, (b) Light (v_L) and heavy (v_H) vehicles' speed, (c) A-weighted continuous equivalent sound pressure levels ($L_{A,eq,15min,meas}$) recorded.

data referred to as Long Term Monitoring Station (LTMS) database,[64] collected by a group of researchers belonging to the former IFSTTAR institute (*"Institut français des sciences et technologies des transports, de l'aménagement et des réseaux"*), now merged in the Université Gustave Eiffel, located in Nantes (France).

Such data collection was performed at an experimental station operating 24 h a day 365 days a year, for a period of approximately six years (from 2002 to 2007), located in Saint-Berthevin, in proximity of the A81 motorway. The motorway analyzed by the French researchers is 93 km long and connects Le Mans to La Gravelle and it is characterized by two carriageways, two lanes each. During these measurements, acoustic, micrometeorological, and traffic data were measured.

Figure 3 shows the geographical location of the municipality of Saint-Berthevin, i.e., the site of interest, located in the *Pays de la Loire*, in France.

Figure 4 shows a schematic representation of the sensors' positions, where those indicated with the letter "A" are the acoustic stations while "M" refers to the meteorological towers.

Focusing on the noise data, five acoustic stations were installed, which recorded the $L_{A,eq,10s}$ ("A" weighting curve and 1/1 octave from 125 Hz to 4 kHz) at both 2 and 5 m above the ground. This applies to all stations except for the reference microphone (station A1) located 5 m above the ground and at a distance of approximately 5 m from the roadside, which is the one considered for this application. A 01 dB-Stell "outdoor" microphone and 01 dB-Stell SALTO data archives were used by French researchers to record and store acoustic data. Such measurements were validated with acquisitions taken every 10 s.

These measurements were then validated by the French researchers involved in the project via a strong cleaning process, for example detecting and removing sound events coming from other sources, different from road traffic noise, such as anthropic activity, animals, aircraft, and trains transits, etc. (see Ref. 64 for further details). While this thorough cleaning process significantly enhances data reliability, it is important to note that the publicly available dataset does not provide specific information on uncertainties associated with the measurements. Any inherent uncertainties related to the detection, identification, and discrimination of sound sources should be acknowledged. The cleaned data were then concatenated into 15-min time intervals and such a dataset was made available to the research community.

With regard to vehicle flows, the only accessible data in the cleaned dataset is the total number of light and heavy-duty vehicles transiting in the 15-min time intervals. There is no distinction between the lane or the direction in which each vehicle transits, which is why the simulation assumes a single direction and a single lane to describe the road traffic.

As for the vehicle speeds, the only public data is the average speed values of the two categories considered for each 15-min time interval.

However, the case under study is characterized by a free-flow traffic condition, as also shown by the exploratory analysis of the dataset (see Sec. IV) meaning that due to a sufficiently low flow density with respect to the road's capacity, the vehicles' speeds are not influenced by each other. Free flow condition could be considered as a homogeneous traffic condition, and so vehicle speeds could be

18 February 2026 18:56:06

https://doi.org/10.1121/10.0035570

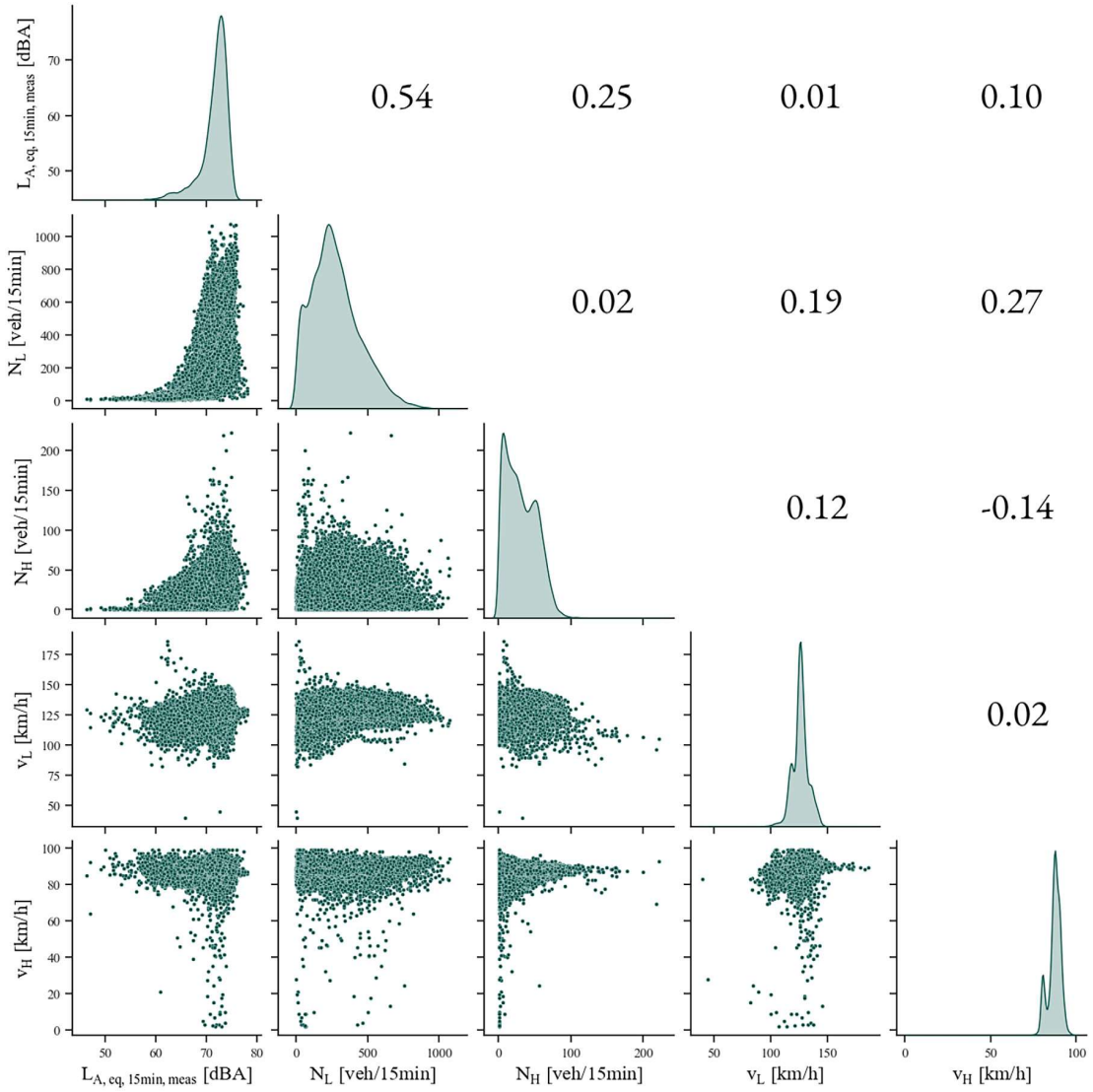


FIG. 6. Matrix of scatter plots relating all model input variables to each other and their respective Spearman's correlation coefficients.

easily summarized using a Gaussian distribution.[70–72] Being a normal distribution, it can be built if the mean and standard deviation are known. In the case under analysis, as mentioned earlier the mean speed for each category for each 15-min time interval is known, while the standard deviation is being fixed by the authors at a 10% value, based on the characteristics of the traffic data and the assumption of a free flow condition. This approach is supported by findings in the literature, such as those in Ref. 55. Being in a free flow condition, constant values of speed were used to simulate each vehicle transit, thus no correction factor due to acceleration is considered at this stage of the proposed model.

Since not every 15-min time intervals present all the aforementioned data, the authors decided to use only the intervals in which all the necessary information for each of the considered categories was measured (i.e., traffic flows and mean speeds). Therefore, at this stage, all the observations in which one or more input parameters of the model or even the $L_{A,eq,15min}$ data were missing were discarded, resulting in a total of 30 437 usable 15-min intervals.

A closer look at the obtained dataset composition can be found in Table I, while in Table II some of the summary statistics of it can be found.

To achieve a clearer overview of the dataset used, the variables' boxplots have been represented in Fig. 5 to summarize their main characteristics. Mind that the horizontal lines represent the median value of the described variable.

The first pair of boxplots in Fig. 5(a) describes vehicle flows, distinguishing between light and heavy-duty vehicles, namely, N_L and N_H. The difference between the amount of light and heavy vehicles is evident observing the medians of the two datasets (i.e., respectively 254 veh/15 min and 28 veh/15 min) and even through their mean values and

18 February 2026 18:56:06

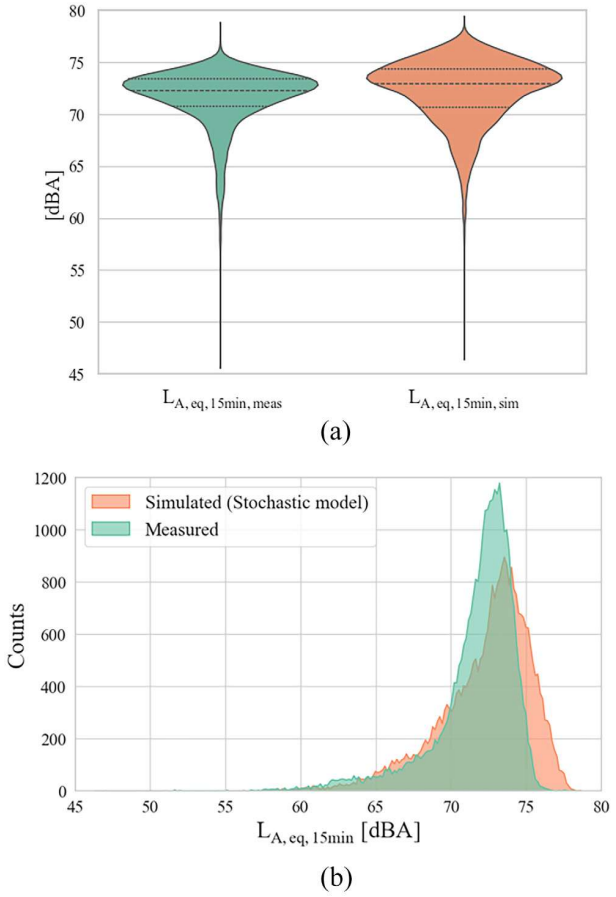


FIG. 7. Distribution of $L_{A,\mathrm{eq,15min,meas}}$ compared with the distribution of $L_{A,\mathrm{eq,15min,sim}}$ computed with the proposed model through the use of (a) violin plots, (b) overlapped distributions.

standard deviations as reported in Table II. As expected regarding the distributions of the outliers, light vehicles distribution shows a higher number of outliers, and they are even more widely distributed than heavy vehicles. Several factors contribute to this phenomenon, including driver behavior, road conditions, and traffic dynamics. Light vehicles tend to have more diverse acceleration and deceleration patterns due to their maneuverability, making them more susceptible to abrupt changes in speed and noise emissions. Additionally, variations in road conditions can further influence these dynamics, resulting in a greater likelihood of outliers associated with light vehicles.

The second pair of graphs [Fig. 5(b)] represent respectively light and heavy vehicles' mean speed distributions, respectively indicated as v_L and v_H. The medians of these two distributions are, respectively, 126.3 and 87.6 km/h,

TABLE III. $L_{A,\mathrm{eq,15min,meas}}$ and $L_{A,\mathrm{eq,15min,sim}}$ signifiant quartiles.

	25th quart. [dBA]	50th quart. [dBA]	75th quart. [dBA]
$L_{A,\mathrm{eq,15min,meas}}$	70.7	72.3	73.4
$L_{A,\mathrm{eq,15min,sim}}$	70.6	72.9	74.4

TABLE IV. $L_{A,\mathrm{eq,15min,meas}}$ and $L_{A,\mathrm{eq,15min,sim}}$ summary statistics.

	Mean [dBA]	Std dev. [dBA]	Min. value [dBA]	Max. value [dBA]	Skewness	Kurtosis
$L_{A,\mathrm{eq,15min,meas}}$	71.6	2.9	46.3	78.2	−2.04	6.11
$L_{A,\mathrm{eq,15min,sim}}$	72.2	3.1	47.2	78.7	−1.1	1.8

which are in agreement with the speed limits of the motorway of such categories that are 130 km/h for light vehicles 90 km/h for heavy goods vehicles with a maximum permissible weight of over 3.5 tonnes and up to 12 tonnes, 100 km/h for public transport vehicles, although again there are many outliers.

Finally, the last box plot in Fig. 5(c) describes the A-weighted continuous equivalent sound pressure level recorded in the site, referred to as $L_{A,\mathrm{eq,15min,meas}}$, and it is characterized by a median value of 72.3 dBA. The outliers will be the subject of further investigation in Sec. IV.

However, a different kind of graph could be useful to investigate whether there is a correlation between the different quantities used as input to the model. From the scatterplot of matrices reported in Fig. 6, this kind of information can be easily deduced. It reports bivariate scatter plots below the diagonal and histograms on the diagonal. An analysis of the correlation has been performed using *psych*, an R® package for statistical analysis. The regression has been pursued using Spearman's correlation approach. The resulting correlation coefficients between the several variables have been reported above the diagonal. An analysis of the speed distribution of heavy vehicles reveals a bimodal pattern in the histogram shown in Fig. 6 (the last distribution on the bottom right). This histogram exhibits two distinct peaks, reflecting the presence of different speed groups among heavy vehicles. While this bimodal distribution exists, it has only a low influence on the measured sound level, as evidenced by the correlation coefficient of 0.10. This observation aligns with the varying speed limits for vehicles transporting heavy freight on the motorway under analysis, as previously mentioned. Additionally, the low correlation values observed for both light and heavy vehicle mean speeds with flow volumes are largely due to the traffic operating below critical density. In such conditions, the road capacity is not reached, allowing individual vehicles to travel at freely chosen speeds without significantly influencing flow volume or $L_{A,eq}$. In contrast, a congested situation, where critical density is reached or even exceeded, would likely result in stronger correlations among speed, flow, and sound levels.

It is also worth focusing on the relationship between the light vehicles flow N_L (i.e., the largest part of vehicle flow) and their speeds v_L. N_L does not significantly influence v_L and this can also be noticed from the correlation coefficient, which is equal to 0.19. Since the speeds of single vehicles are not affected by each other, the assumption of a free flow traffic condition, and thus a Gaussian distribution curve for speeds, is indeed confirmed to be accurate for describing the

18 February 2026 18:56:06

https://doi.org/10.1121/10.0035570

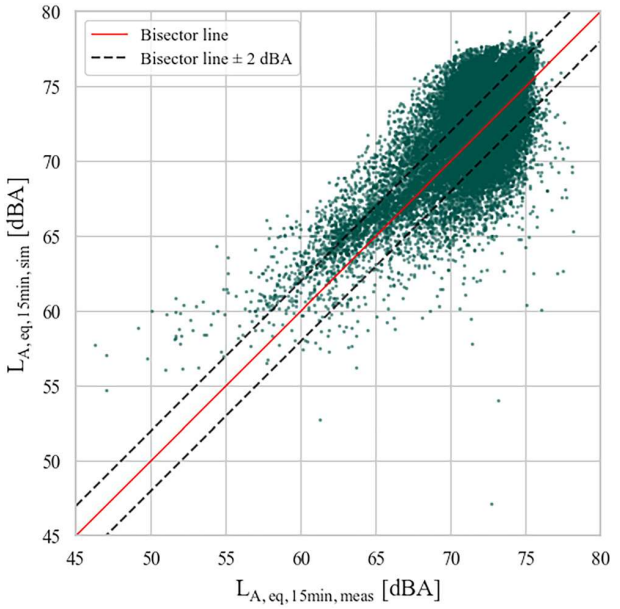


FIG. 8. Scatter plot of simulated data ($L_{A,eq,15min,sim}$) versus the corresponding measurements ($L_{A,eq,15min,meas}$).

dataset. The same can be said by observing the corresponding values for heavy vehicles, confirming the hypothesis made earlier.

More details about the LTMS database can be found in Ref. 64.

IV. RESULTS AND DISCUSSION

The results obtained from the simulation pursued as presented earlier, are reported in this section. Figure 7(a) shows the violin plots of both the measured ($L_{A,eq,15min,meas}$)

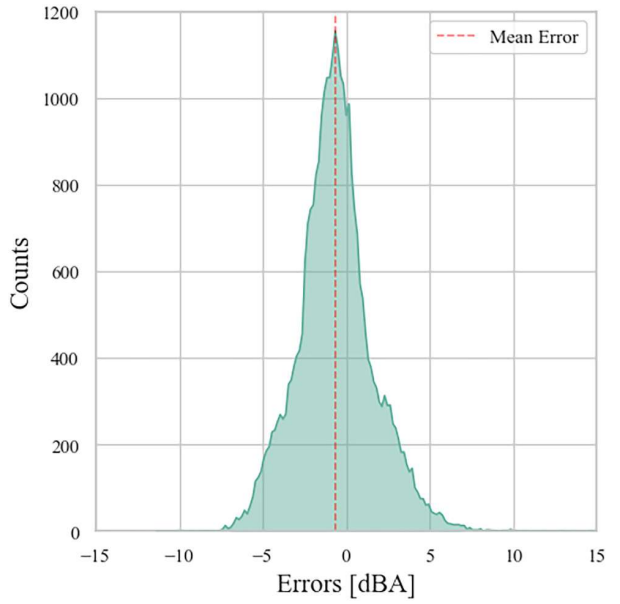


FIG. 9. Distribution of error values.

TABLE V. Errors significant quartiles.

	25th quart. [dBA]	50th quart. [dBA]	75th quart. [dBA]
Errors	−2.0	−0.7	0.5

and simulated ($L_{A,eq,15min,sim}$) A-weighted continuous equivalent sound pressure levels over the 15-min time intervals. The dotted lines represent the quartiles of the distributions, whose values are also reported in Tables III and IV. The comparison of the two distribution curves, as plotted in Fig. 7(b), shows that they present similar quartiles, as quantified in Table III, and main statistics, as reported in Table IV, even if skewness and kurtosis are different.

Moreover, the $L_{A,eq,15min,sim}$ distribution curve roughly has the same skewness that can be observed in the $L_{A,eq,15min,meas}$ distribution.

The simulated A-weighted continuous equivalent sound pressure levels have also been plotted in a bisector plot versus the corresponding observed data in Fig. 8, in order to specifically highlight the overall performances in terms of either overestimation or underestimation of the model itself. In particular, the red solid line indicates the graph's quadrant bisector line, where the points would ideally lie if the model's predictions were closer to the measured values. However, it is possible to notice that a large portion of the points is included in the ± 2dBA range, identified on the graph by the black dashed lines, which highlight how the model can be considered to provide values rather consistent with the measured ones. Specifically, 19 501 values are within such range, i.e., approximately 64% of the considered dataset.

Additional remarks can be drawn by analyzing the graph in Fig. 9, which is the error histogram. Errors have been calculated as the difference between $L_{A,eq,15min,meas}$, the A-weighted continuous equivalent sound pressure level on the 15-min interval as measured during the measurement

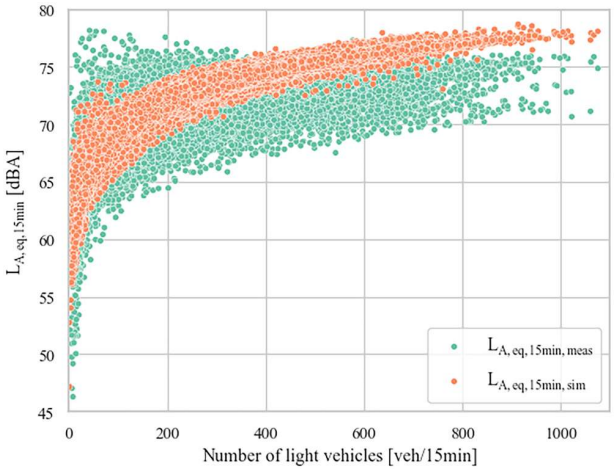


FIG. 10. Overlapping of measured ($L_{A,eq,15min,sim}$) and simulated ($L_{A,eq,15min,sim}$) A-weighted continuous equivalent sound pressure levels plotted against the number of light vehicles transiting (N_L).

18 February 2026 18:56:06

TABLE VI. Errors summary statistics.

	Mean [dBA]	Std dev. [dBA]	Min. value [dBA]	Max. value [dBA]	Skewness	Kurtosis
Errors	−0.6	2.3	−11.5	25.5	0.43	1.91

TABLE VII. Details of the selected error outliers.

Date	Time interval	N_L [veh/15 min]	N_H [veh/15 min]	v_L [km/h]	v_H [km/h]	$L_{A,\mathrm{eq,15min,meas}}$ [dBA]	$L_{A,\mathrm{eq,15min,sim}}$ [dBA]	Errors [dBA]
22-09-2004	10:30–10:45	1	1	45.0	28.0	72.7	47.2	25.2
23-09-2004	14:30–14:45	4	2	100.0	19.5	73.2	54.0	19.1
18-03-2007	05:00–05:15	13	2	127.2	99.0	76.0	60.1	15.9
18-03-2007	05:45–06:00	27	2	126.2	98.0	77.4	62.6	14.8
18-03-2007	04:15–04:30	16	2	119.7	99.0	75.1	60.4	14.6
08-09-2004	11:15–11:30	11	6	82.2	15.2	71.4	57.9	13.6
18-03-2007	05:15–05:30	17	4	131.7	94.0	75.5	62.5	13.0
18-03-2007	06:00–06:15	42	8	124.9	86.0	78.2	65.4	12.8
26-12-2003	08:30–08:45	12	1	127.8	90.0	71.3	59.5	11.8
25-03-2007	05:00–05:15	29	1	126.2	95.0	73.5	62.7	10.9
04-03-2007	05:15–05:30	35	3	133.0	90.0	75.0	64.3	10.7
09-03-2004	08:30–08:45	16	1	127.9	92.0	70.6	60.2	10.5
24-03-2007	17:00–17:15	31	13	129.7	85.6	75.2	65.0	10.2
09-03-2007	05:45–06:00	51	30	120.4	86.0	77.7	67.6	10.1
01-04-2007	06:45–07:00	53	2	129.0	87.5	75.7	65.6	10.3
15-10-2006	02:45–03:00	8	1	129.8	85.0	46.3	57.8	−11.5
24-09-2006	01:30–01:45	6	2	126.8	92.5	47.0	57.0	−10.0
15-10-2006	13:30–13:45	14	1	126.3	99.0	50.0	60.0	−10.0

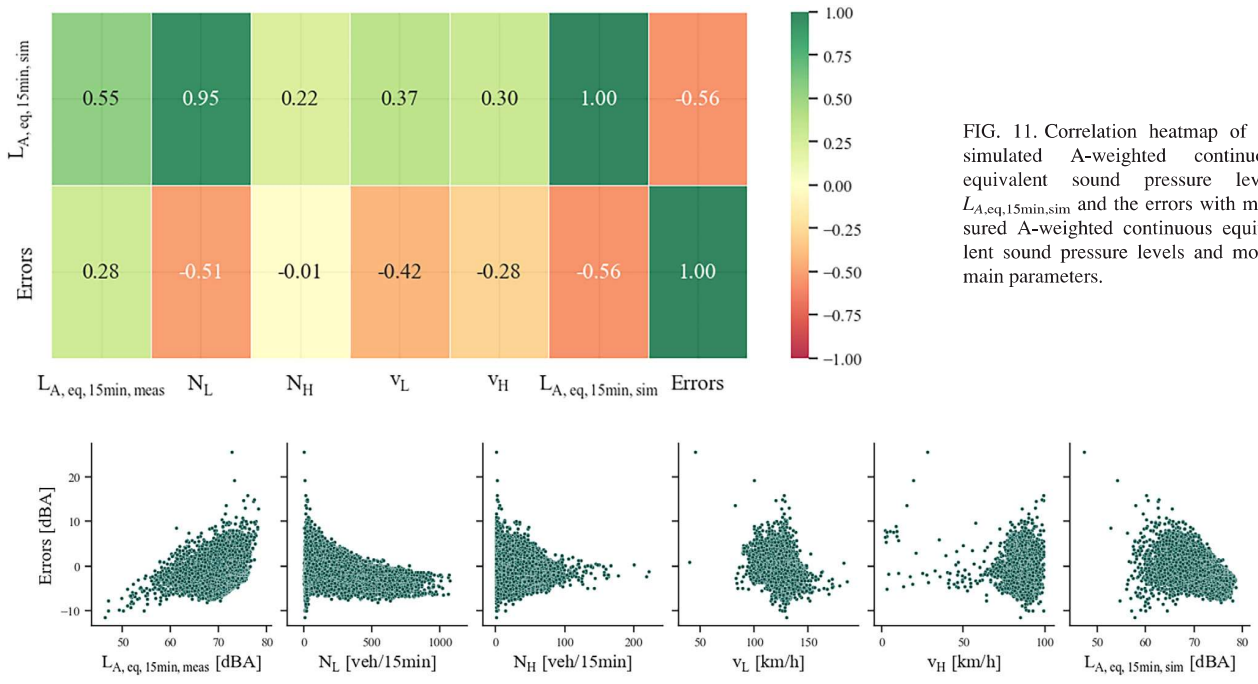


FIG. 11. Correlation heatmap of the simulated A-weighted continuous equivalent sound pressure levels $L_{A,\mathrm{eq,15min,sim}}$ and the errors with measured A-weighted continuous equivalent sound pressure levels and model main parameters.

FIG. 12. Errors plot versus, from left to right, the measured A-weighted continuous equivalent sound pressure levels $L_{A,\mathrm{eq,15min,meas}}$, the variables of the model, and the simulated A-weighted continuous equivalent sound pressure levels $L_{A,\mathrm{eq,15min,sim}}$.

TABLE VIII. Summary error metrics of the stochastic model.

ME [dBA]	Std deviation [dBA]	MPE [%]	MAE [dBA]	MSE [dBA^2]	CVE
−0.65	2.29	−0.95	1.84	5.67	0.03

18 February 2026 18:56:06

https://doi.org/10.1121/10.0035570

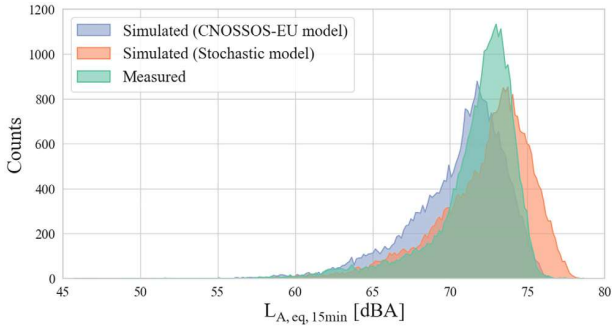


FIG. 13. Distribution of $L_{A,eq,15min,meas}$ (in green) compared with the distribution of $L_{A,eq,15min,sim}$ computed with CNOSSOS-EU model (in blue) and the proposed stochastic model (in orange).

campaign, and $L_{A,eq,15min,sim}$, the A-weighted continuous equivalent sound pressure levels during the same 15-min interval but as simulated using the model.

The obtained error distribution has a mean value of –0.6 dBA and a standard deviation of 2.3 dBA. While the low ME reveals a good accuracy of the model, the standard deviation suggests that most of the errors are within an interval of ± 2dBA. As for the shape of the error distribution, it presents a slight asymmetry towards the right, as the skewness value is 0.43. Overall, the distribution is leptokurtic since the kurtosis is equal to 1.91. This leads to the state in which the errors are more clustered close to the mean value with respect to what it should be in the case of a normal distribution (kurtosis = 3).

Overall, the model simulations approach the measurements quite well, with greater errors at high and low noise levels (approximately $>$ 70 dBA and $<$ 55 dBA).

The statistics of the error distribution are reported in Tables V and VI.

A better insight into the model performances can be achieved by analyzing the error distribution tails, and thus the model outliers. In Fig. 10, the A-weighted continuous equivalent sound pressure levels as measured, i.e., $L_{A,eq,15min,meas}$, and as simulated, i.e., $L_{A,eq,15min,sim}$, are plotted, respectively, in green and in orange as a function of light vehicle flow N_L. For low values of N_L, there is a large variation of $L_{A,eq,15min,meas}$, of more than 20 dBA. This variability could be due to values recorded in unordinary conditions, such as, for instance, a phenomenon aside from the road traffic noise itself that may not be cleaned during the processing phase. In addition, background noise should be also taken into account and this even finer improvement of the model could help to reduce error values in that area. However, Fig. 10 shows that the actual trend in noise levels is quite well depicted by the model when low or medium flows are analyzed. At higher flows, the model exhibits an overestimation, probably due to the use of the sum of SELs performed to calculate the noise level at the receiver. This approach, indeed, assumes that the single vehicle transits do not overlap in any way, but are considered and calculated individually and then added together. As vehicle flow increases, the larger error could be due to the overlap that is likely to occur in reality between vehicles traveling in different lanes at the same time. These details will certainly be further investigated in future research.

A detailed list of some error outliers is given in Table VII. The authors decided to report the 15-min intervals characterized by errors greater than +10 dBA and less than −10 dBA, along with the corresponding model inputs. Most of the error outliers can be associated with nighttime intervals, where low traffic flows would either favour higher single vehicle speeds and thus much higher noise levels than the one simulated. Moreover, it is possible to see that high error values can be associated with the same day, even if in different 15-min time intervals (for instance 18/03/2007 and 15/10/2006), which suggests that there may have been problems with the measurements taken at those times, such as work in progress.

Following the approach used in Sec. III, a detailed analysis of the correlation between both the simulated A-weighted continuous equivalent sound pressure levels $L_{A,eq,15min,sim}$ and the model's errors and all the input variables of the model has been pursued, plotting a Spearman's correlation heatmap (Fig. 11). It can be seen that the errors show a non-negligible negative correlation with N_L, v_L, and $L_{A,eq,15min,sim}$. This is confirmed also by Fig. 12, in which the errors are plotted versus the input of the model, and, especially for N_L and $L_{A,eq,15min,sim}$, the plots show a decreasing slope. It is also interesting to notice that the error variability decreases when the flow of heavy vehicles increases.

It is also interesting to notice that the error variability decreases when the flow of heavy vehicles increases. It can be seen that the spread of the error on the vertical axis reduces when NH grows, probably because with higher heavy vehicle flows the normal distribution assumption for the speeds is better depicted. On the contrary, when few heavy vehicles pass in the 15 min time slot, the random assignment of speed according to Gaussian distribution may more easily fail to properly describe the flow.

Finally, Table VIII summarizes the error metrics evaluated after applying the model. As already discussed earlier, when commenting on the error distribution, the model exhibits good performances in terms of error metrics. In particular, the MAE being below 3 dBA is within the range in

TABLE IX. Comparison between error metrics of the CNOSSOS-EU model and the proposed stochastic model.

Model used	ME [dBA]	Std dev. [dBA]	MPE [%]	MAE [dBA]	MSE [dBA^2]	CVE
Stochastic model	−0.65	2.29	−0.95	1.84	5.67	0.03
CNOSSOS-EU model	1.07	2.28	1.45	1.93	6.37	0.03

18 February 2026 18:56:06

which a model can be assumed to be correct, as reported in Ref. 81.

B. Comparison with the CNOSSOS-EU model

A comparative analysis between the results obtained from the presented stochastic model and the outcomes from applying the CNOSSOS-EU model has been then pursued.

To ensure a rigorous comparison, both models were applied to the same dataset. For each 15-min time interval, the same data of traffic flows for light and heavy-duty vehicles have been used. However, as for the speed values, since the CNOSSOS-EU model uses mean speeds of the flow per each category (i.e., macroscopic approach) as an input, no random extraction has been performed, and the average values as provided in the available dataset have been used. This comparison could help to get insights into the capabilities of the stochastic core of the presented model. Indeed, as mentioned earlier, the stochastic model takes into account for each vehicle of each category a single and peculiar value of speed (i.e., microscopic approach). In such a comparison, the differences in noise levels' prediction introduced by the fully microscopic approach can also be assessed. The CNOSSOS-EU model, indeed, aggregates the contributions of single vehicle point sources, assuming that they run at the same speed, in a line source representing the traffic flow, and then propagates the sound levels at the receiver with the cylindric propagation formula. The presented model is fully microscopic, considering the single vehicle, with its specific speed, as a point source, and propagating with the related formula (see Sec. II). The results revealed notable differences between the two models as can be seen in Fig. 13, where the distribution curves of measured noise levels are overlapped with simulated ones, both for the stochastic and the CNOSSOS-EU model.

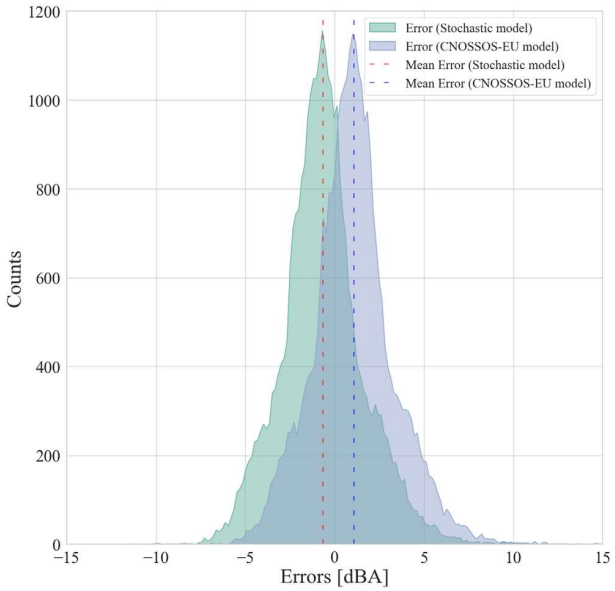


FIG. 14. Distribution of the stochastic model's error values (in green) overlapped with the distribution of CNOSSOS-EU model's error values (in blue).

Since the two models share the same NEM, the different models' performances could be associated with the different approaches to the source modelling and spatial distribution of acoustic energy. The CNOSSOS-EU model utilizes a line source framework with cylindrical geometric divergence ($1/r$), with a fixed distance (the minimum distance between receiver and centre of the carriage, d in Fig. 2), while the presented stochastic model treats each vehicle as a point source, leading to omnidirectional radiation characterized by geometric decay that follows an inverse square law ($1/r^2$).

Table IX shows the summary error metrics of the two models. The obtained comparison showed that the stochastic model's predictions were generally closer to the observed noise levels. Specifically, the stochastic model exhibits lower values in key metrics such as ME, MAE, and MSE. These metrics indicate that the predictions from the stochastic model are more closely aligned with the observed noise levels compared to those generated by the CNOSSOS-EU model.

These results underscore the potential advantages of incorporating stochastic elements and a fully microscopic approach into traffic noise models. Even if both the CNOSSOS-EU model and the presented stochastic approach achieve good performances, with low error metrics, definitely because they share the same NEM (i.e., the same core of the model when analyzing the single vehicle emissions), the stochastic model presents a lower value of MAE and MSE.

Moreover, the stochastic model seems to have slightly better performances when the noise levels are lower than 70 dBA, while at higher levels it is more prone to overestimate, unlike the CNOSSOS-EU model which seems to work in the opposite way. This can also be easily noted in Fig. 14, in which the overlapping of the two histograms of the errors of both models is presented. Averagely, indeed, the stochastic approach overestimates noise levels while CNOSSOS-EU underestimates them.

Nevertheless, as mentioned earlier, the predictions of the stochastic model's sound levels are generally closer to the observed noise levels compared to those from the CNOSSOS-EU model. This results in smaller errors, indicating a comparatively better performance. However, it is important to note that the metrics are not drastically different, highlighting the ongoing need for refinement in predictive tools to effectively address the complexities of real-world traffic noise. An advanced and extended comparison with more detailed propagation models will be the subject of future developments in this research.

V. CONCLUSIONS

In this paper, a new microscopic approach for predicting road traffic noise was presented, based on random generation of single vehicles' speeds.

18 February 2026 18:56:06

Considering that the acoustical energy emitted by a vehicle is known to be highly dependent on its speed, the idea was to use the single vehicle speed influence on road traffic noise levels, to better analyze and assess the continuous equivalent sound pressure levels at the receiver. In this way, the presented approach deviates from commonly used and statistical ones, which tend to use mean speed as an aggregate value, thereby failing to capture the complexities associated with individual vehicle behaviour in road traffic flow.

A second key feature of the presented model is its stochastic nature. Single vehicles' speeds are not always known or available by means of field measurements. Thus, the traffic flow can be modelled using either specific or hypothetical speed distribution curves, according to the traffic conditions and the categories of the vehicles considered.

Moreover, the proposed approach is very versatile, as the two main components of the model itself, one concerning the calculation of noise emission by a NEM (in the presented case study, CNOSSOS-EU with updated coefficients) and the second involving the propagation and the assessment at the receiver (in the presented case study, the sum of SELs of single vehicle transits), can be modified by the user according to whatever the specific conditions of the case study are. Additionally, the modularity of the presented model allows it to be compatible with any national model and facilitates the integration of diverse propulsion systems, including also electric and hybrid engines.

The validation of the model on a large dataset available in the literature, regarding road traffic noise levels measured in a free-flow highway condition, has provided interesting results. The error distribution, in fact, was shown to be quite symmetric and slightly leptokurtic, with a mean value of –0.6 dBA, and a standard deviation of 2.3 dBA. Error metrics also confirmed the model's goodness, in particular with MAE of 1.84 dBA and a CVE of 0.03.

The features of the model and the encouraging results obtained in the validation suggest that it can be used in a wide range of situations, such as calculating regulation indicators (L_{den}, L_{night}, etc.), both for existing infrastructures, by using measured or specific speed distributions, or for under development projects, by making hypothesis on the possible speeds behaviour.

However, the model has some limitations up until now, mainly related to the sum of SELs produced by each vehicle transit at the receiver, which is a necessary step to sum up the contributions of single vehicles, in the proposed fully microscopic model. This choice could lead to noise level overestimations with high flow occurrences (see Figs. 7 and 10) since it neglects any overlapping of transiting vehicles and assumes that each vehicle's contribution is independent of the others. By treating each transit as an independent event and neglecting the effects of overlapping vehicles at high flow rates, indeed, the model may inaccurately overestimate the overall noise level. An analysis of errors as a function of traffic flow, as reported in Figs. 11 and 12, has highlighted a correlation between the model's performance and light vehicle flows. Investigating this relationship further will lead to refining the model's applicability across diverse traffic conditions, from light to congested flows, as well as traffic flow distribution over the four lanes, enhancing the accuracy of predictions in real-world scenarios where vehicle interactions are significant.

Thus, future developments will be devoted to solving these issues by distributing the transiting vehicles on all the carriageways, considering the possibility of screening effects due to their overlapping in the proximity of the receiver.

Another limitation is the absence of background noise, which will be added in a further revision of the model, to improve the comparison with real world measured values.

Moreover, the presented model will be tested in variable traffic conditions, using different speed distribution curves. The latter development will aim to test alternative traffic flow distributions to improve the model's accuracy in scenarios with varying or congested traffic, capturing potential interactions between overlapping vehicles and their contributions to the overall noise level.

ACKNOWLEDGMENTS

This study was carried out within the MOST—Sustainable Mobility National Research Center and received funding from the European Union Next-GenerationEU (PIANO NAZIONALE DI RIPRESA E RESILIENZA (PNRR)—MISSIONE 4 COMPONENTE 2, INVESTIMENTO 1.4—D.D. 1033 17/06/2022, CN00000023). This manuscript reflects only the authors' views and opinions, neither the European Union nor the European Commission can be considered responsible for them. The authors are also grateful to Rosa Maria Taddeo for participating in this research during her master's thesis.

AUTHOR DECLARATIONS

Conflict of Interest

The authors have no conflicts to disclose.

DATA AVAILABILITY

The data that support the findings of this study are available in [LTMS 2002–2007 A reference experimental database for environmental acoustics] at http://doi.org/10.1016/j.apacoust.2013.01.008, Ref. 64

[1]European Environment Agency, "Exposure of Europe's population to environmental noise" (EEA, Copenhagen, Denmark, 2017).
[2]European Environment Agency, "Environmental noise in Europe—2020" (EEA, Copenhagen, Denmark, 2017).
[3]European Parliament, Council of the European Union, "Living well, within the limits of our planet: The 7th EAP (2014-20)" (COEU, Brussels, Belgium, 2013).
[4]European Environment Agency, "Noise in Europe 2014," EEA Report No. 10/2014 (EEA, Copenhagen, Denmark, 2014).
[5]European Environment Agency, "Unequal exposure and unequal impacts: Social vulnerability to air pollution, noise and extreme temperatures in Europe," EEA Report No 22/2018 (EEA, Copenhagen, Denmark, 2018).

18 February 2026 18:56:06

[6]B. Berglund, T. Lindvall, and D. H. Schwela, "Guidelines for community noise" (WHO, Copenhagen, Denmark, 1999).
[7]WHO Europe, *Night Noise Guidelines for Europe* (WHO, Copenhagen, Denmark, 2009).
[8]World Health Organization, "Environmental noise guidelines for the European region" (WHO, Copenhagen, Denmark, 2018).
[9]WHO Europe, *Environmental Health Inequalities in Europe. Assessment Report* (WHO, Copenhagen, Denmark, 2012).
[10]European Commission, "Links between noise and air pollution and socio-economic status," In-Depth Report 13, Science for Environment Policy (European Commission, Brussels, Belgium, 2016).
[11]C. Clark and K. Paunovic, "WHO environmental noise guidelines for the European region: A systematic review on environmental noise and cognition," Int. J. Environ. Res. Public Health **15**(2), 285 (2018).
[12]K. V. Weyde, N. H. Krog, B. Oftedal, P. Magnus, S. Øverland, S. Stansfeld, M. J. Nieuwenhuijsen, M. Vrijheid, M. d C. Pascual, and G. M. Aasvang, "Road traffic noise and children's inattention," Environ. Health **16**(1), 127 (2017).
[13]L. Pérez-Crespo, M. López-Vicente, A. Valentín, M. Burgaleta, M. Foraster, H. Tiemeier, and M. Guxens, "Association between residential exposure to road traffic noise and cognitive and motor function outcomes in children and preadolescents," Environ. Int. **183**, 108414 (2024).
[14]A. M. Dzhambov, P. Lercher, and D. Botteldooren, "Childhood sound disturbance and sleep problems in Alpine valleys with high levels of traffic exposures and greenspace," Environ. Res. **242**, 117642 (2024).
[15]A. Muzet, "Environmental noise, sleep and health," Sleep Med. Rev. **11**(2), 135–142 (2007).
[16]A. Lie, M. Skogstad, H. A. Johannessen, T. Tynes, I. S. Mehlum, K. C. Nordby, B. Engdahl, and K. Tambs, "Occupational noise exposure and hearing: A systematic review," Int. Arch. Occup. Environ. Health **89**, 351–372 (2016).
[17]L. R. Teixeira, F. Pega, A. M. Dzhambov, A. Bortkiewicz, D. T. C. da Silva, C. A. F. de Andrade, E. Gadzicka, K. Hadkhale, S. Iavicoli, M. S. Martínez-Silveira, M. Pawlaczyk-Łuszczyńska, B. M. Rondinone, J. Siedlecka, A. Valenti, and D. Gagliardi, "The effect of occupational exposure to noise on ischaemic heart disease, stroke and hypertension: A systematic review and meta-analysis from the WHO/ILO Joint Estimates of the Work-Related Burden of Disease and Injury," Environ. Int. **154**, 106387 (2021).
[18]A. K. Guha and S. Gokhale, "Urban workers' cardiovascular health due to exposure to traffic-originated PM2.5 and noise pollution in different microenvironments," Sci. Total Environ. **859**, 160268 (2023).
[19]M. Crous-Bou, M. Gascon, J. D. Gispert, M. Cirach, G. Sánchez-Benavides, C. Falcon, E. M. Arenaza-Urquijo, X. Gotsens, K. Fauria, J. Sunyer, M. J. Nieuwenhuijsen, and J. L. Molinuevo, "Impact of urban environmental exposures on cognitive performance and brain structure of healthy individuals at risk for Alzheimer's dementia," Environ. Int. **138**, 105546 (2020).
[20]J. Weuve, J. D'Souza, T. Beck, D. A. Evans, J. D. Kaufman, K. B. Rajan, C. F. M. de Leon, and S. D. Adar, "Long-term community noise exposure in relation to dementia, cognition, and cognitive decline in older adults," Alzheimers Dement **17**(3), 525–533 (2021).
[21]M. Gascon, G. Sánchez-Benavides, P. Dadvand, D. Martínez, N. Gramunt, X. Gotsens, M. Cirach, C. Vert, J. L. Molinuevo, M. Crous-Bou, and M. Nieuwenhuijsen, "Long-term exposure to residential green and blue spaces and anxiety and depression in adults: A cross-sectional study," Environ. Res. **162**, 231–239 (2018).
[22]W. Babisch, "The noise/stress concept, risk assessment and research needs," Noise Health **4**(16), 1–11 (2002).
[23]World Health Organization, "Burden of disease from environmental noise: Quantification of healthy life years lost in Europe" (WHO, Copenhagen, Denmark, 2011).
[24]M. Basner and S. McGuire, "WHO environmental noise guidelines for the European region: A systematic review on environmental noise and effects on sleep," Int. J. Environ. Res. Public Health **15**(3), 519 (2018).
[25]K. Sygna, G. M. Aasvang, G. Aamodt, B. Oftedal, and N. H. Krog, "Road traffic noise, sleep and mental health," Environ. Res. **131**, 17–24 (2014).
[26]J. Hegewald, M. Schubert, A. Freiberg, K. Romero Starke, F. Augustin, S. G. Riedel-Heller, H. Zeeb, and A. Seidler, "Traffic noise and mental health: A systematic review and meta-analysis," Int. J. Environ. Res. Public Health **17**(17), 6175 (2020).
[27]D. Petri, G. Licitra, M. A. Vigotti, and L. Fredianelli, "Effects of exposure to road, railway, airport and recreational noise on blood pressure and hypertension," Int. J. Environ. Res. Public Health **18**(17), 9145 (2021).
[28]C. Krittanawong, Y. K. Qadeer, R. B. Hayes, Z. Wang, S. Virani, M. Zeller, P. Dadvand, and C. J. Lavie, "Noise exposure and cardiovascular health," Curr. Probl. Cardiol **48**(12), 101938 (2023).
[29]E. Van Kempen and W. Babisch, "The quantitative relationship between road traffic noise and hypertension: A meta-analysis," J. Hypertens **30**(6), 1075–1086 (2012).
[30]T. Münzel, T. Gori, W. Babisch, and M. Basner, "Cardiovascular effects of environmental noise exposure," Eur. Heart J **35**(13), 829–836 (2014).
[31]O. Hahad, J. H. Prochaska, A. Daiber, and T. Muenzel, "Environmental noise-induced effects on stress hormones, oxidative stress, and vascular dysfunction: Key factors in the relationship between cerebrocardiovascular and psychological disorders," Oxid. Med. Cell. Longev **2019**, 4623109.
[32]Y. Gao and J. Zhu, "Characteristics, impacts and trends of urban transportation," Encyclopedia **2**(2), 1168–1182 (2022).
[33]European Commission, Communication from the commission to the European Parliament, the Council, the European Economic and Social Committee and the Committee of the Regios: Pathway to a Healthy Planet for All EU Action Plan: "Towards Zero Pollution for Air, Water and Soil," COM(2021) 400 final.
[34]C. Guarnaccia, A. Mascolo, P. Aumond, A. Can, and D. Rossi, "From early to recent models: A review of the evolution of road traffic and single vehicles noise emission modelling," Curr. Pollut. Rep. **10**(4), 662–683 (2024).
[35]Department of Transport (UK), "Calculation of road traffic noise" (Department of Transport UK, London, UK, 1988).
[36]Der Bundesminister Für Verkehr (Germany) "Richtlinien für den Lärmschutz an Straßen RLS-90" (Abteilung Straßenbau, Ausgabe 1990) [The Federal Minister for Transport, "Guidelines for noise protection on roads RLS-90" (Road Construction Directorate-General, Edition 1990)].
[37]G. B. Cannelli, K. Glück, and S. Santoboni, "A mathematical model for evaluation and prediction of the mean energy level of traffic noise in Italian towns," Acta Acust. united Ac. **53**(1), 31–36.
[38]T. Suksaard, P. Sukasem, S. M. Tabucanon, I. Aoi, K. Shirai, and H. Tanaka, "Road traffic noise prediction model in Thailand," Appl. Acoust. **58**(2), 123–130 (1999).
[39]G. Dutilleux, J. Defrance, D. Ecotière, B. Gauvreau, M. Bérengier, F. Besnard, and E. L. Duc, "NMPB-routes-2008: The revision of the French method for road traffic noise prediction," Acta Acust. united Ac. **96**(3), 452–462 (2010).
[40]K. Heutschi, "SonRoad: New Swiss road traffic noise model," Acta Acust. united Ac. **90**(3), 548–554 (2004).
[41]Danish Environmental Protection Agency, "Nord2000: Nordic noise prediction method" (DEPA, Odense, Denmark, 2020).
[42]G. G. Fleming, A. S. Rapoza, and C. S. Lee, "Development of national reference energy mean emission levels for the FHWA traffic noise model," FHWA TNM, version 1.0 (U.S. Federal Highway Administration, Washington, DC, 1995).
[43]S. Kephalopoulos, M. Paviotti, and F. Anfosso-Lédée, "Common noise assessment methods in Europe (CNOSSOS-EU)," in *EUR 25379 EN* (Publications Office of the European Union, Luxembourg, 2012).
[44]Commission Delegated Directive (EU) "21.12.2020 amending, for the purposes of adapting to scientific and technical progress, Annex II to Directive 2002/49/EC of the European Parliament and of the Council as regards common noise assessment methods" (European Union, Brussels, Beglium, 2020).
[45]N. Garg and S. Maji, "A critical review of principal traffic noise models: Strategies and implications," Environ. Impact Assess. Rev. **46**, 68–81 (2014).
[46]DEFRA, *Working Group on the Assessment of Environmental Noise (WG-AEN), Good Practice Guide for Strategic Noise Mapping and the Production of Associated Data on Noise Exposure—Version 2* (DEFRA, London, UK, 2006).
[47]S. Kephalopoulos, M. Paviotti, F. Anfosso-Lédée, D. Van Maercke, S. Shilton, and N. Jones, "Advances in the development of common noise assessment methods in Europe: The CNOSSOS-EU framework for strategic environmental noise mapping," Sci. Total Environ. **482–483**, 400–410 (2014).

18 February 2026 18:56:06

https://doi.org/10.1121/10.0035570

[48]J. Khan, M. Ketzel, S. S. Jensen, J. Gulliver, E. Thysell, and O. Hertel, "Comparison of Road Traffic Noise prediction models: CNOSSOS-EU, Nord2000 and TRANEX," Environ. Pollut. **270**, 116240 (2021).
[49]A. Kok, "Refining the CNOSSOS-EU calculation method for environmental noise," in *Proceedings of Internoise 2019*, Madrid, Spain (June 16–19, 2019), pp. 1842–1849.
[50]B. De Coensel, D. Botteldooren, F. Vanhove, and S. Logghe, "Microsimulation based corrections on the road traffic noise emission near intersections," Acta Acust. united Ac. **93**(2), 241–252 (2007).
[51]P. Fernandes, R. Tomás, F. Acuto, A. Pascale, B. Bahmankhah, C. Guarnaccia, A. Granà, and M. C. Coelho, "Impacts of roundabouts in suburban areas on congestion-specific vehicle speed profiles, pollutant and noise emissions: An empirical analysis," Sustainable Cities Soc. **62**, 102386 (2020).
[52]A. Can and D. Botteldooren, "Towards traffic situation noise emission models," Acta Acust. united Ac. **97**(5), 900–903 (2011).
[53]A. Can, L. Leclercq, J. Lelong, and D. Botteldooren, "Traffic noise spectrum analysis: Dynamic modeling vs. experimental observations," Appl. Acoust. **71**(8), 764–770 (2010).
[54]A. Can and P. Aumond, "Estimation of road traffic noise emissions: The influence of speed and acceleration," Transp. Res. Part D: Transp. Environ. **58**, 155–171 (2018).
[55]J. Nygren, S. Boij, R. Rumpler, and C. J. O'Reilly, "Vehicle-specific noise exposure cost: Noise impact allocation methodology for microscopic traffic simulations," Transp. Res. Part D: Transp. Environ. **118**, 103712 (2023).
[56]S. Baclet, K. Khoshkhah, M. Pourmoradnasseri, R. Rumpler, and A. Hadachi, "Near-real-time dynamic noise mapping and exposure assessment using calibrated microscopic traffic simulations," Transp. Res. Part D: Transp. Environ. **124**, 103922 (2023).
[57]J. Espadaler-Clapés, E. Barmpounakis, and N. Geroliminis, "Traffic congestion and noise emissions with detailed vehicle trajectories from UAVs," Transp. Res. Part D: Transp. Environ. **121**, 103822 (2023).
[58]A. Can, L. Leclercq, J. Lelong, and J. Defrance, "Accounting for traffic dynamics improves noise assessment: Experimental evidence," Appl. Acoust. **70**(6), 821–829 (2009).
[59]E. Chevallier, A. Can, M. Nadji, and L. Leclercq, "Improving noise assessment at intersections by modeling traffic dynamics," Transp. Res. Part D: Transp. Environ **14**(2), 100–110 (2009).
[60]L. Estévez-Mauriz and J. Forssén, "Dynamic traffic noise assessment tool: A comparative study between a roundabout and a signalised intersection," Appl. Acoust. **130**, 71–86 (2018).
[61]A. Bhaskar, E. Chung, and M. Kuwahara, "Development and implementation of the areawide Dynamic ROad traffic NoisE (DRONE) simulator," Transp. Res. Part D: Transp. Environ **12**(5), 371–378 (2007).
[62]B. De Coensel, T. De Muer, I. Yperman, and D. Botteldooren, "The influence of traffic flow dynamics on urban soundscapes," Appl. Acoust. **66**(2), 175–194 (2005).
[63]V. Le Bescond, A. Can, P. Aumond, and P. Gastineau, "Open-source modeling chain for the dynamic assessment of road traffic noise exposure," Transp. Res. Part D: Transp. Environ. **94**, 102793 (2021).
[64]B. Gauvreau, "Long-term experimental database for environmental acoustics," Appl. Acoust. **74**(7), 958–967 (2013).
[65]A. Pascale, C. Guarnaccia, E. Macedo, P. Fernandes, A. I. Miranda, S. Sargento, and M. C. Coelho, "Road traffic noise monitoring in a Smart city: Sensor and model-based approach," Transp. Res. Part D: Transp. Environ. **125**, 103979 (2023).
[66]C. Guarnaccia, "EAgLE: Equivalent acoustic level estimator proposal," Sensors **20**(3), 701 (2020).
[67]A. Pascale, E. Macedo, C. Guarnaccia, and M. C. Coelho, "Smart mobility procedure for road traffic noise dynamic estimation by video analysis," Appl. Acoust. **208**, 109381 (2023).
[68]D. Rossi, A. Mascolo, and C. Guarnaccia, "Calibration and validation of a measurements-independent model for road traffic noise assessment," Appl. Sci **13**(10), 6168 (2023).
[69]G. Iannone, "Improvements in the acoustical modelling of traffic noise prediction: Theoretical and experimental results," Ph.D. thesis, UNISA, Fisciano, Italy (2011).
[70]D. Helbing, "Derivation and empirical validation of a refined traffic flow model," Phys. A **233**(1-2), 253–282 (1996).
[71]D. Helbing, "Empirical traffic data and their implications for traffic modeling," Phys. Rev. E **55**(1), R25–R28 (1997).
[72]D. Helbing, "Fundamentals of traffic flow," Phys. Rev. E **55**(3), 3735–3738 (1997).
[73]G. Iannone, C. Guarnaccia, and J. Quartieri, "Speed distribution influence in road traffic noise prediction," Environ. Eng. Manag. J. **12**(3), 493–501 (2013).
[74]A. Pascale, P. Fernandes, C. Guarnaccia, and M. C. Coelho, "A study on vehicle noise emission modelling: Correlation with air pollutant emissions, impact of kinematic variables and critical hotspots," Sci. Total Environ. **787**, 147647 (2021).
[75]B. Peeters and G. van Blokland, "Interface between the CNOSSOS-EU road traffic noise emission model and the propagation model," M+P report. RIVM **17**(1), 13 (2017).
[76]A. Kok and A. van Beek, Amendments for CNOSSOS-EU: Description of issues and proposed solutions (NIPHE, Bilthoven, the Netherlands, 2019).
[77]M. A. Pallas, M. Berengier, R. Chatagnon, M. Czuka, M. Conter, and M. Muirhead, "Towards a model for electric vehicle noise emission in the European prediction method CNOSSOS-EU," Appl. Acoust. **113**, 89–101 (2016).
[78]M. A. Pallas, J. Kennedy, I. Walker, R. Chatagnon, M. Berengier, and J. Lelong, "Noise emission of electric and hybrid electric vehicles: Deliverable FOREVER (No. Forever WP2_D2-1-V4)," Ph.D. thesis, IFSTTAR, Champs-sur-Marne, France (2015).
[79]G. Licitra, M. Bernardini, M. Ricardo, F. Bianco, and L. Fredianelli, "CNOSSOS-EU coefficients for electric vehicle noise emission," Appl. Acoust. **211**, 109511 (2023).
[80]C. Guarnaccia, J. G. Cerón Bretón, J. Quartieri, C. Tepedino, and R. M. Cerón Bretón, "An application of time series analysis for forecasting and control of carbon monoxide concentrations," Int. J. Math. Models Methods Appl. Sci. **8**, 505–515 (2014).
[81]D. M. Gómez, A. M. Jaramillo, and J. Ochoa, "Analysis of the measurement uncertainty and its effects on noise mapping validations," J. Environ. Manag. **266**, 110606 (2020).

18 February 2026 18:56:06

DOI: 10.61782/fa.2025.0233

FORUM ACUSTICUM EURONOISE 2025

C

COMPARISON OF STOCHASTIC AND MICROSCOPIC ROAD TRAFFIC NOISE MODELS USING VARIABLE LEVEL OF AGGREGATION OF TRAFFIC FLOWS

Aurora Mascolo[1*] Domenico Rossi[1] Mariangela Nigro[1]
Benoit Gauvreau[2] Claudio Guarnaccia[1]
[1] Department of Civil Engineering, University of Salerno, Italy
[2] UMRAE, Université Gustave Eiffel, CEREMA, France

ABSTRACT

The problem of assessing road traffic noise levels by means of predictive models is strictly related to the issue of using reliable and easy-to-obtain input data. This work focuses on evaluating the performance of a stochastic and microscopic traffic noise prediction model, using traffic flow inputs aggregated in two ways: by grouping multiple lanes together or analysing them separately.
The model incorporates stochastic distributions to account for the variability in single vehicle speeds, and consequently in noise emissions. It uses microscopic simulations to consider the motion of individual vehicles and to calculate the Sound Exposure Level (SEL) of each transit. To assess model effectiveness, predictions obtained using both aggregated and disaggregated traffic data are compared to field measurements collected in a long-term monitoring station site in France.
Results suggest that disaggregating traffic flow by lanes modifies the equivalent continuous sound levels distributions, by acting on the distances between each lane and the receiver point, particularly when the flows are asymmetric.
The study underlines the adaptability of the developed stochastic and microscopic model and provides valuable insights into optimizing the balance between accuracy and efficiency when dealing with traffic flow data collection at different levels of aggregation.

[*] ***Corresponding author***: *amascolo@unisa.it*
Copyright: *©2025 First author et al. This is an open-access article distributed under the terms of the Creative Commons Attribution 3.0 Unported License, which permits unrestricted use, distribution, and reproduction in any medium, provided the original author and source are credited.*

Keywords: *road traffic noise, microscopic modelling, stochastic modelling, single lane linear source, experimental data validation.*

1. INTRODUCTION

The study of road traffic noise has become increasingly relevant due to its significant impact on urban health and environmental quality. As cities grow and traffic density rises, accurately modelling noise emissions is essential for both research and policy-making. This paper examines the effectiveness of stochastic and microscopic models in predicting road traffic noise, with a particular focus on how different levels of traffic flow aggregation influence noise estimates. The motivation for this study arises from a well-documented connection between prolonged noise exposure and adverse health effects, including cardiovascular diseases and metabolic disorders [1-3]. Moreover, traditional noise prediction models often struggle to capture the complex and dynamic nature of urban and non-urban traffic, highlighting the need for more refined methodologies [4-5]. In recent years, advancements in road traffic noise modelling have introduced a range of approaches, from empirical models to data-driven techniques such as machine learning. While empirical models, like many of those resumed in [6], remain widely used, they often fail to account for transient variations in traffic conditions [5, 7], or in correspondence of signal setting intersections [8]. On the other hand, machine learning methods, particularly artificial neural networks (ANNs), have demonstrated considerable promise in enhancing prediction accuracy by incorporating real-time traffic data [10-11]. Research indicates that ANNs, when

trained on detailed traffic characteristics, can outperform traditional statistical models in noise prediction [10]. Additionally, recent studies have explored the incorporation of stochastic elements into microscopic models, enabling a more detailed simulation of vehicle interactions and their cumulative impact on noise emissions [11-12].

The current direction in traffic noise modelling emphasizes context-sensitive and dynamic approaches. Various factors, such as vehicle type, speed, and road surface conditions, play a crucial role in noise propagation and should be incorporated into predictive models [5-6, 13]. For instance, Zuo et al. in [1] stress the importance of assessing individual noise exposure, which can vary significantly based on local urban design and traffic patterns. Moreover, recent efforts to integrate graph theory into noise modelling have opened new possibilities for analysing the relationships between traffic flow and noise emissions [14]. Such approaches allow for a more comprehensive understanding of how different traffic scenarios influence overall noise levels, offering valuable insights for urban planners and policymakers.

In conclusion, a comparative analysis of stochastic and microscopic road traffic noise models can provide a deeper understanding of noise dynamics in urban settings. By considering different levels of traffic flow aggregation, this study aims to contribute to the ongoing discourse on effective noise mitigation strategies and their implications for public health and sustainable urban planning.

2. MATERIALS AND METHODS

The starting point of this research can be retrieved in the development of microscopic Road Traffic Noise Models (RTNMs) developed and used by the authors in several case studies, for instance in [15-18]. In all these applications, the contribution at the receiver of the single vehicle is estimated in terms of the Sound Exposure Level (SEL) of the transit. This descriptor depends on the speed of the single vehicle, which, together with the category of the vehicle, mostly influences the noise emission and thus the pressure level at the receiver. In [19] a stochastic approach for assigning a speed to each transiting vehicle has been successfully calibrated and validated on a large dataset collected by a long-term monitoring station operating in France in the period 2002-2007 [20]. Anyway, in [19] the overall traffic flow over 15 minutes has been used as input of the stochastic model, considering an ideal linear source placed in the centre of the carriage, without separating traffic flows per lane. Despite the good results obtained, the detailed investigation of the errors and the outliers of the model reported in [19] suggested that further development can be pursued by considering the traffic flows in each lane and by modelling the highway with four different linear sources, placed at different distances from the receiver, i.e. the position of the sound level meter used for validation.

2.1 Resume of the stochastic and microscopic model

The model used in this paper, presented in [19], assumes that the vehicles' speeds are distributed according to a probability distribution whose shape depends on the traffic condition. For instance, steady-state flows are described by a normal distribution, while accelerating and decelerating conditions can be described by skewed distributions [21]. The idea of the model is to randomly assign a speed to each transiting vehicle and estimate the corresponding noise emission using the CNOSSOS-EU emission model [22-23], using its recent updates [24-25]. Then, the point-like source propagation formula is used to propagate the emitted noise at the receiver. This calculation is performed as a function of time and the resulting L_p is used to calculate the SEL, according to the standard formula, using the transit time as a temporal range. Then the SELs of all the vehicles are summed up and then the result is converted to the L_{eq} over 15 minutes.

This procedure exhibits some limitations that are listed below:

- Underestimation of noise at low traffic flows, due to the assumption that the equivalent level is made only of noise coming from vehicles. When a few vehicles pass, the background noise is not negligible anymore.
- Possible overestimation at high traffic flows, due to the overlapping of vehicles transits. The model assumes that each vehicle contributes at 100%, neglecting possible overlapping and screening effects.
- Single linear source placed in the centre of the road.

As for the first two limitations, they are related to the computational core of the model and need to be addressed by operating on the step that merges the single vehicle contributions.

The third limitation is addressed in this paper by performing a more detailed modelling of the source, i.e. by considering a linear source per each lane. Of course, each source has a different distance and will contribute differently to the overall equivalent level.

2.2 Case study description

The dataset adopted in this work comes from an extensive data collection performed by researchers affiliated with the former IFSTTAR institute ("*Institut français des sciences et technologies des transports, de l'aménagement et des*

réseaux"), now merged into Université Gustave Eiffel in Nantes, France. This database is known as the Long-Term Monitoring Station (LTMS) database and it has been fully described in [20].

This data collection took place at an experimental station operating continuously, 24 hours a day, 365 days a year, over approximately six years (2002-2007). The monitoring site was situated in Saint-Berthevin, near the A81 motorway, in the link from Le Mans to La Gravelle. This highway consists of two carriageways, each with two lanes. Lane 1 and lane 2 are respectively the normal transit and overtaking lanes in the direction West-East (to Le Mans and Paris), while lanes 3 and 4 are respectively the transit and overtaking lanes in the other direction (to Rennes). This numbering will be used throughout the paper to identify each lane.

During the data collection period, acoustic, meteorological, and traffic data were systematically recorded in several points of the area. In this work, we will focus only on traffic counting in each lane and on equivalent continuous sound levels measured at the closer sound level meter (reference microphone), positioned 5 meters above ground and approximately 5 meters from the roadside, close to lane 1.

Data measured were validated at 10-second intervals, with cleaning of noise events unrelated to road traffic and then aggregated in 15-minute time slots.

Regarding vehicle flow data, the available dataset includes only the total number of light and heavy-duty vehicles recorded within each 15-minute interval. However, thanks to the availability of raw data provided by one of the coauthors, it was possible to work on single lane counts and speeds per 10-second intervals, making it possible to perform the analysis presented in the following sections.

As already shown in [19], the case study under analysis exhibits free-flow traffic conditions and allows to use of Gaussian distributions for the speed. The mean speeds per category per 15-minute intervals are available in the public database. As for the dispersion of the distribution, starting from the 10-second raw data, it is possible to calculate the standard deviation of speeds in each 15-minute interval. Anyway, to compare with previous studies (e.g., in [19]), the choice was to set the standard deviation at 10% of the mean speed. Under free-flow conditions, constant speed values were assigned for vehicle transits, meaning acceleration effects were not factored into the model at this stage.

2.3 Dataset presentation and analysis

The case study presented above has been used in [19] for the validation of the model. Due to occasional missing data, only complete 15-minute intervals containing all necessary variables (traffic flow, mean speeds, and $L_{A,eq,15min}$) were included in the analysis. As a result, the dataset was refined to 30437 usable 15-minute intervals. Anyway, in this application, since the aim is to highlight the variations of model performance when using more detailed input data, i.e. when using information for a single lane or the two directions of the highway, a subset of the entire dataset has been selected. After running the model on different periods, for the sake of brevity, only results obtained in the period from March 5 to April 1, 2007, will be presented.

In Figure 1, the light (top plot) and heavy (bottom plot) vehicles' flows are represented versus the ID of the quarter-hour, over the 28 days under analysis, i.e. 2688 15-minute intervals.

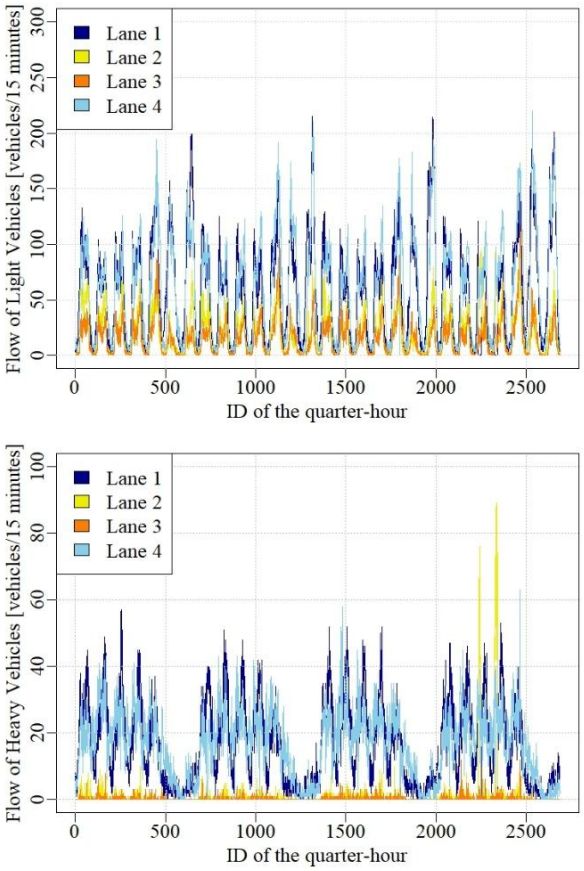


Figure 1. Light (top) and heavy (bottom) vehicles flows plotted versus the ID of the quarter-hour, over the 28 days under analysis.

Lane 1 (blue curve) and lane 4 (light-blue curve) are normal transit lanes, with lane 1 closer to the sound level meter position, while lane 2 (yellow curve) and lane 3 (orange curve) are the overtaking lanes. In each lane flow, there is a seasonal pattern with regular peaks, related to the day-night oscillation. A seasonality related to the working days and weekends of the 28-day period is also observed, showing that during Saturday and Sunday, there is an increase in light vehicles' flows and a decrease in heavy vehicles. The normal march lanes (1 and 4) show higher traffic volumes than the passing lanes (2 and 3), as expected.

As for the heavy vehicles' flows in 15 minutes (Figure 1b), the curves follow the same colour scheme. The flow of heavy vehicles is generally lower than that of light vehicles, and it is almost entirely running on the normal march lanes (1 and 4). Overtaking lane 2 flows curve (yellow line in the plot) shows peaks of heavy traffic during the fourth week of the observation period. Going more in depth with the analysis, it was found that during those two periods, lane 1 was closed, in fact, the flows in that lane were zero for both light and heavy vehicles categories.

Figure 2 shows the boxplots of vehicle flows on the four lanes, distinguishing between light (L) and heavy (H) vehicles, using the 10-second raw data. The comparison of the flows' distributions makes it possible to analyse the different uses of the lanes and to make some considerations about the overall behaviour of light and heavy traffic.

The flows of light vehicles in normal transit lanes (L1 and L4) are the highest. This confirms that lanes 1 and 4, which are configured as normal march traffic lanes, are largely used in comparison to lanes 2 and 3 which are occasionally used for overtaking.

The flow of heavy vehicles in lanes 2 and 3 (H2 and H3) is basically negligible, confirming that heavy vehicles rarely use the overtaking lane, probably for regulation reasons.

All the above comments are confirmed by looking at the boxplots of the mean speeds in Figure 3, calculated by averaging the speeds of the vehicles in each 15-minute slot, starting from the 10-second raw data. It is evident that the overtaking lanes (L2 and L3) exhibit higher speeds with respect to the normal transit lanes (L1 and L4), and that the heavy vehicles' mean speeds are always lower than 100 km/h, i.e. the speed limit in the highway segment under study for such category.

It must be noticed that, while lanes 1 and 4 are basically balanced in all the parameters, lane 2 shows slightly higher light vehicles' flows and mean speed than lane 3. This small asymmetry will be commented in the equivalent continuous sound levels results since it will produce an increase of the simulated levels when moving from 1 source to 4 sources.

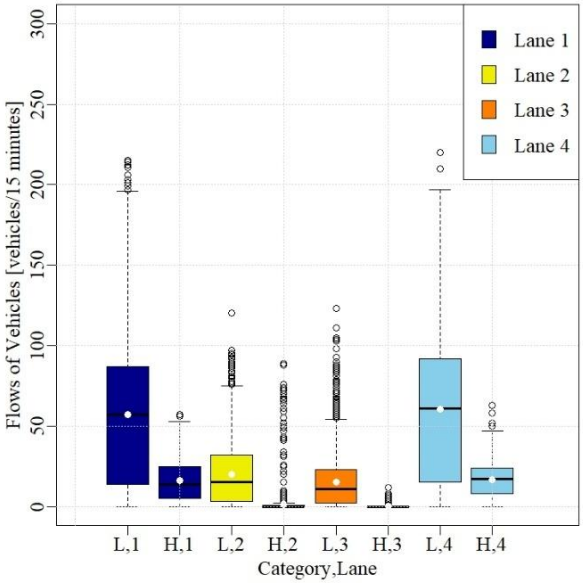


Figure 2. Boxplots of light and heavy vehicles flows, divided by lane, over the 28 days under analysis.

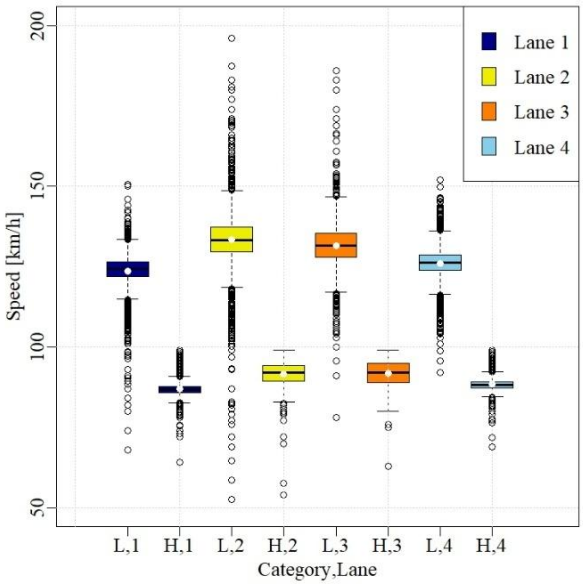


Figure 3. Boxplots of light and heavy vehicles mean speeds, divided by lane, over the 28 days under analysis.

2.4 Cleaning procedure of the dataset

After the careful analysis of the input data performed and reported in subsection 2.3, cleaning of the dataset has been performed. To validate the model results compared with measured equivalent levels on 15 minutes, all the entries of the database in which the measured levels were missing have been discarded. This process reduced the number of 15-minute slots from 2688 (96 slots for 28 days) to 443, spread over the entire 4-week original period.

A comparison between mean values and standard deviations for each parameter, per single lane, calculated on the raw database and the filtered dataset is reported in Table 1. It can be noticed that the filtering of the dataset didn't change drastically the central tendency and the dispersion of the parameters' distributions, since mean values and standard deviations are very similar before and after the data cleaning.

3. RESULTS

The detailed exploratory data analysis performed on the input data of the noise model, resumed in section 2, allowed to gain useful insights into the traffic phenomenon in the case study area, in the 28 days selected for testing. The asymmetries found suggest that a modelling of the source that considers the different flows in the directions and the lanes, could improve the performance of the microscopic and stochastic model presented in [19].

The model has then been run in three different configurations:

- Single source, placed in the middle of the carriageway (1-source model)
- Two sources, placed in the middle of each direction (2-sources model)
- Four sources, placed in the middle of each lane of the carriageway (4-sources model)

Of course, the source-receiver distances were fixed according to the source simulation scheme, considering that lane 1 is the closest to the receiver (i.e., the sound level meter position) and lane 4 is the farthest.

The results of the simulations with the above-listed source modelling schemes are reported in Figure 4, in which the measured levels boxplot is compared with the simulated ones. It can be noticed that the boxplot that best approaches the simulated distribution is the one produced with the 4-sources model. Anyway, all the simulated distributions present a larger spread of the data, being the interquartile ranges greater than that of the measured distribution.

The main descriptive statistics are reported in Table 2. It can be noticed that the central tendency metrics, mean and median, of the simulated distributions are always lower than the measured ones, but, moving from 1 source to 4 sources, the discrepancy is lower. The standard deviations of the simulated distributions do not change significantly, meaning that the different modelling schemes do not affect the dispersion of the simulations.

Table 1. Mean values and standard deviations of the distributions of parameters for each lane, for both reference databases. Raw databases (before any filtering) include 2688 entries (28 days) while filtered databases (filtering on quarters-hour that include the measured L_{eq}) have 443 entries.

	Parameter calculated over 15 min	Database	Mean value	St. dev.
Lane 1	Flow light [veh/15min]	Raw	57,02	45,24
		Filtered	63,09	46,11
	Flow heavy [veh/15min]	Raw	16,18	12,34
		Filtered	14,97	11,64
	Speed light [km/h]	Raw	123,58	5,73
		Filtered	125,14	4,51
	Speed heavy [km/h]	Raw	86,93	2,50
		Filtered	87,36	2,76
Lane 2	Flow light [veh/15min]	Raw	19,93	19,31
		Filtered	21,00	18,88
	Flow heavy [veh/15min]	Raw	1,20	6,65
		Filtered	1,87	9,44
	Speed light [km/h]	Raw	133,59	10,45
		Filtered	133,84	11,47
	Speed heavy [km/h]	Raw	91,67	4,31
		Filtered	91,54	4,58
Lane 3	Flow light [veh/15min]	Raw	15,02	16,02
		Filtered	14,63	14,10
	Flow heavy [veh/15min]	Raw	0,31	0,82
		Filtered	0,32	0,92
	Speed light [km/h]	Raw	131,64	8,05
		Filtered	133,07	7,33
	Speed heavy [km/h]	Raw	91,73	4,87
		Filtered	90,73	7,38
Lane 4	Flow light [veh/15min]	Raw	60,40	45,73
		Filtered	62,38	41,17
	Flow heavy [veh/15min]	Raw	16,54	9,96
		Filtered	15,37	10,80
	Speed light [km/h]	Raw	126,04	5,33
		Filtered	127,56	4,19
	Speed heavy [km/h]	Raw	88,51	2,31
		Filtered	88,85	2,73

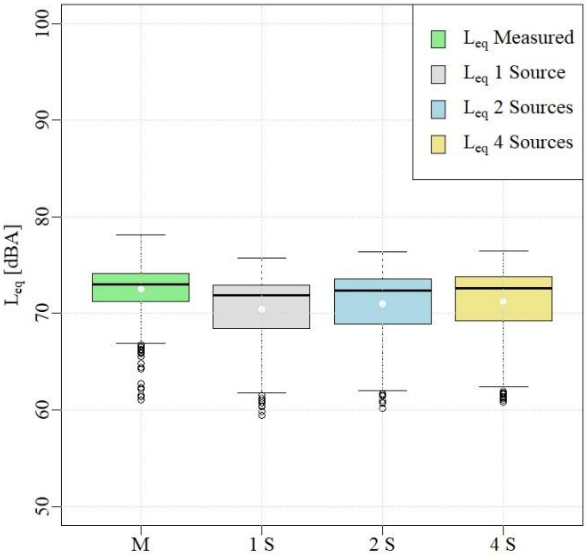


Figure 4. Boxplots of measured and simulated equivalent levels calculated in the 15-minutes time slots. The results obtained with the three modelling schemes are plotted.

Table 2. Main descriptive statistics of measured and simulated equivalent levels with the three modelling schemes.

	Mean [dBA]	Median [dBA]	Std. dev. [dBA]	Skew	Kurt
Measured $L_{eq.15min}$	72.50	73.01	2.78	-1.19	2.52
Simulated $L_{eq.15min}$ 1-source	70.46	71.86	3.39	-1.09	0.49
Simulated $L_{eq.15min}$ 2-sources	70.99	72.37	3.43	-1.04	0.29
Simulated $L_{eq.15min}$ 4-sources	71.25	72.57	3.38	-1.04	0.33

3.1 Error analysis

To provide a quantitative assessment of the modelling scheme performances, an error analysis has been pursued, calculating the error as the difference between measured and simulated equivalent levels. Such a definition leads to assessing an overestimation when the error is negative and, vice versa, an underestimation is associated with a positive error. The error distributions statistics are reported in Table 3. The mean and median of the errors are reduced when using a more detailed modelling of the source. Standard deviation is less sensitive, due to the same reasons explained above.

Table 3. Main descriptive statistics of error distributions, obtained with the three modelling schemes.

	Mean [dBA]	Median [dBA]	Std. dev. [dBA]	Skew	Kurt
Error (1-source)	2.04	1.00	3.01	1.56	2.82
Error (2-sources)	1.51	0.46	2.96	1.48	2.37
Error (4-sources)	1.25	0.14	2.91	1.54	2.52

A further analysis is provided in Figure 5, in which a pairs panel plot is given. In this plot, the variables are plotted one versus the other below the diagonal in bivariate scatter plots, while numbers above the diagonal are the Pearson correlation coefficients. The histograms of the variables are reported in the diagonal.

The pairs-panel plot was first performed using all the variables, to check the correlations between errors and input data. Since the errors did not correlate significantly with the speeds (correlation coefficients ranging from -0.07 to -0.09 for light vehicles' speed and from 0.14 to 0.16 for heavy vehicles' speed), Figure 5 reports only the pairs between errors and total light and heavy vehicles' flows.

Looking at the scatter plots between the errors (for all the modelling schemes) and total flow light and heavy, it is evident that, when the flows increase, the errors tend to converge to low values with low dispersion. This is an interesting finding since it confirms that greater errors are obtained when the flow is small. The plots of errors versus L_{eq} measured (rows 4, 5 and 6, column 3) show that for equivalent levels higher than 75 dBA the errors are always greater than 5 dBA. Those measurements can be found also in row 3, column 1, in the low flow range. This means that those high errors are probably due to external reasons, such as other sources. In addition, since all the source modelling schemes present the same behaviours versus the plotted variables, the presented approach is sensitive to the parameters' ranges in the same way, regardless of the

source modelling. This result shows that the improvement obtained when moving from 1-source to 4-sources scheme is dependent on the lanes where the vehicles transit rather than on the absolute traffic flow values.

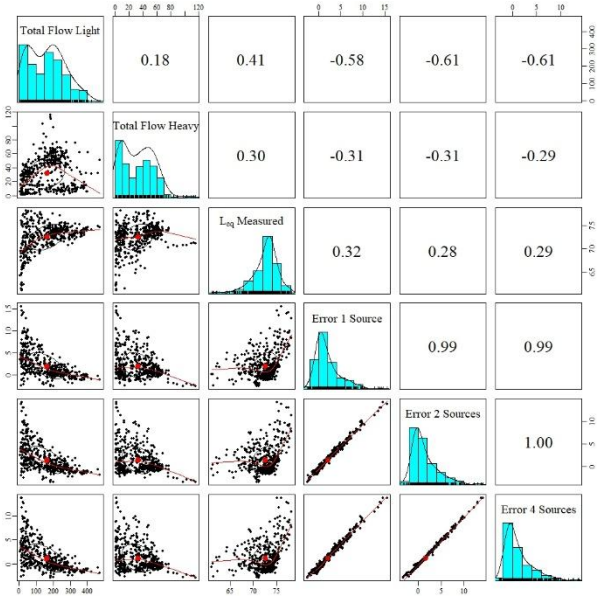


Figure 5. Pairs panel of the errors, obtained with the three modelling schemes, versus the total flow of light and heavy vehicles.

4. CONCLUSIONS

In this paper, a microscopic and stochastic model for road traffic noise prediction has been tested with variable levels of aggregation of input parameters. In particular, traffic flows and mean speeds for light and heavy vehicles, estimated on 15 minutes, have been considered per single lane, per direction (grouped by two lanes) and aggregated, to simulate three different schemes for the noise source.

After presenting a detailed exploratory data analysis, useful to understand the scenarios occurring in the case study area and to infer information for noise model performances understandings, the authors implemented the modelling schemes, using a single source in the middle of the carriageway (1-source model), two sources in the centre of each direction (2-sources model) and four sources in the middle of each lane (4-sources model).

The results show an improvement of the prediction, in terms of mean and median errors. The standard deviation of the error does not improve significantly, suggesting that the dispersion of simulations need to be furtherly investigated, for instance with a parameter sensitivity analysis. An outlier analysis can be also performed, to better understand the non-standard conditions that occur in the case study location.

In conclusions, standing the parsimony principle, that, with similar performances, suggests using the model with lower parameters, the 4-sources model is a good candidate for replacing the 1-source approach. The presented results confirm that in cases in which the traffic flows are asymmetric, the single line source placed in the middle of the carriageway is not anymore a suitable choice and that a more detailed modelling of the source is able to better predict the equivalent continuous sound levels.

5. ACKNOWLEDGMENTS

This study was carried out within the MOST – Sustainable Mobility National Research Center and received funding from the European Union Next-GenerationEU (PIANO NAZIONALE DI RIPRESA E RESILIENZA (PNRR) – MISSIONE 4 COMPONENTE 2, INVESTIMENTO 1.4 – D.D. 1033 17/06/2022, CN00000023). This manuscript reflects only the authors' views and opinions, neither the European Union nor the European Commission can be considered responsible for them.

6. REFERENCES

[1] L. Zuo, X. Chen, M. Liu, L. Chen, W. Xu, H. Chen, S. Dong, Y. Wei, L. Li, S. Peng & G. Hao: "Road traffic noise, obesity, and the risk of incident type 2 diabetes: a cohort study in UK biobank", *International Journal of Public Health*, vol. 67, 2022.

[2] Z. Kupcikova, D. Fecht, R. Ramakrishnan, C. Clark, & Y. Cai: "Road traffic noise and cardiovascular disease risk factors in UK biobank", *European Heart Journal*, vol. 42, no. 21, 2072-2084, 2021.

[3] J. Thacher, A. Poulsen, U. Hvidtfeldt, O. Raaschou-Nielsen, J. Brandt, C. Geels, J. Khan, T. Münzel & M. Sørensen: "Long-term exposure to transportation noise and risk for type 2 diabetes in a nationwide cohort study from Denmark", *Environmental Health Perspectives*, vol. 129, no. 12, 2021.

[4] S. Ahac, M. Ahac, J. Domitrović, & V. Dragčević: "Modeling the influence of roundabout deflection on its efficiency as a noise abatement measure", *Sustainability*, vol. 13, no. 10, 5407, 2021.

[5] M. Zefreh and Á. Török: "Theoretical comparison of the effects of different traffic conditions on urban road traffic noise", *Journal of Advanced Transportation*, art. ID 7949574, pp. 1-11, 2018.
[6] C. Guarnaccia, A. Mascolo, P. Aumond, A. Can and D. Rossi: "From Early to Recent Models: A Review of the Evolution of Road Traffic and Single Vehicles Noise Emission Modelling", *Current Pollution Reports*, vol. 10, pp. 662–683, 2024.
[7] X. Lü, J. Kang, P. Zhu, J. Cai, F. Guo & Y. Zhang: "Influence of urban road characteristics on traffic noise", *Transportation Research Part D Transport and Environment*, vol. 75, 136-155, 2019.
[8] R. Di Pace, F. Storani, C. Guarnaccia, S. de Luca: "Signal setting design to reduce noise emissions in a connected environment", *Physica A*, vol. 632, 129328, pp. 1-15, 2023.
[9] X. Zhang, H. Kuehnelt & W. Roeck: "Traffic noise prediction applying multivariate bi-directional recurrent neural network", *Applied Sciences*, 11, no. 6, 2714, 2021.
[10] P. Kim, H. Ryu, J. Jeon & S. Chang: "Statistical road-traffic noise mapping based on elementary urban forms in two cities of South Korea", *Sustainability*, vol. 13, no. 4, 2365, 2021.
[11] D. Singh, A. Francavilla, S. Mancini & C. Guarnaccia: "Application of machine learning to include honking effect in vehicular traffic noise prediction", *Applied Sciences*, vol. 11, no. 13, 6030, 2021.
[12] P. Cao, "Stochastic microscopic modelling of traffic flow for automated driving validation", in *Proc. SPIE 13224 of the 4th International Conference on Internet of Things and Smart City,* (Hangzhou, China), 13224, vol. 10, 2024.
[13] H. Qi and Y. Ying, Y.: "A stochastic two-dimensional intelligent driver car-following model with vehicular dynamics", *Chinese Physics B*, vol. 32, no. 4, 044501, 2023.
[14] A. Țițu, A. Boroiu, S. Mihăilescu, A. Pop & A. Boroiu: "Assessment of road noise pollution in urban residential areas—a case study in Pitești, Romania", *Applied Sciences*, vol. 12, no. 8, 4053, 2022.
[15] C. Guarnaccia: "EAgLE: Equivalent Acoustic Level Estimator Proposal", *Sensors*, vol. 20, no. 3, 701, 2020.
[16] A. Pascale, E. Macedo, C. Guarnaccia, M.C. Coelho: "Smart mobility procedure for road traffic noise dynamic estimation by video analysis", *Applied Acoustics*, Vol. 208, 109381, 2023.
[17] C. Guarnaccia, U. Catherin, A. Mascolo, D. Rossi: "Improvement and Validation of a Smart Road Traffic Noise Model Based on Vehicles Tracking Using Image Recognition: EAgLE 3.0", *Sensors*, vol. 25, no. 6, 1750, 2025.
[18] D. Rossi, A. Mascolo, A. Pascale, M. C. Coelho, C. Guarnaccia: "The problem of obtaining vehicles speed input for road traffic noise microscopic models: a comparison between field measurements and a stochastic approach", *Proc. of the* I*NTER-NOISE and NOISE-CON Congress and Conference Proceedings*, (Nantes, France), 270 (7), pp. 4979-4988, 2024.
[19] A. Mascolo, D. Rossi, A. Ruggiero, C. Guarnaccia: "A stochastic and microscopic model to predict road traffic noise by random generation of single vehicles' speeds", *The Journal of the Acoustical Society of America*, vol. 157, pp. 721-737, 2025.
[20] B. Gauvreau: "Long-term experimental database for environmental acoustics", *Applied Acoustics*, vol. 74, no. 7, pp. 958–967, 2013.
[21] G. Iannone, C. Guarnaccia, J. Quartieri: "Speed distribution influence in road traffic noise prediction", *Environmental Engineering and Management Journal*, vol. 12, no. 3, pp. 493-501, 2013.
[22] S. Kephalopoulos, M. Paviotti, F. Anfosso-Lédée, "Common noise assessment methods in Europe (CNOSSOS-EU)", Publications Office of the European Union, 2012.
[23] S. Kephalopoulos, M. Paviotti, F. Anfosso-Lédée, D. Van Maercke, S. Shilton & N. Jones: "Advances in the development of common noise assessment methods in Europe: The CNOSSOS-EU framework for strategic environmental noise mapping", *Science of the Total Environment*, 482, 400-410, 2014.
[24] A. Kok, A. van Beek, "Amendments for CNOSSOS-EU: description of issues and proposed solutions", RIVM Lett Rep, 2019.
[25] Commission Delegated Directive (EU): "21.12.2020 amending, for the purposes of adapting to scientific and technical progress, Annex II to Directive 2002/49/EC of the European Parliament and of the Council as regards common noise assessment methods" Brussels, Belgium, 2020.

JASA ARTICLE

CrossMark

Combination of time series forecasting models with a microscopic and stochastic approach to predict road traffic noise

Aurora Mascolo,[a] Domenico Rossi, and Claudio Guarnaccia
Department of Civil Engineering, University of Salerno, Via Giovanni Paolo II 132, I-84084 Fisciano, Italy

ABSTRACT:
Road traffic noise represents a major source of environmental pollution, and its prediction remains a critical task. This challenge particularly emerges when traffic data are not available, such as during the design phases of new infrastructures, where it becomes necessary to predict the noise exposure affecting nearby residents, even in the absence of measurement data. To address this issue, this work augments a previously developed microscopic and stochastic-core traffic noise model, integrating it with forecasting time series models for traffic flows and average vehicle speeds. This integration produces a hybrid model that enables the estimation of hourly traffic noise levels based solely on historical traffic patterns, even in the absence of direct traffic observations for the period under investigation. The methodology has been evaluated through a statistical analysis of simulated noise levels, with a focus on error distribution and conventional error metrics. The mean error of 0.43 dBA and the mean absolute error of 1.30 dBA confirm the accuracy of the proposed approach for estimating road traffic noise in data-scarce scenarios. A comparison with the CNOSSOS-EU model's performance highlights the possibility of using such methodology in early-stage infrastructure design and planning.
© *2026 Author(s). All article content, except where otherwise noted, is licensed under a Creative Commons Attribution (CC BY) license (https://creativecommons.org/licenses/by/4.0/).* https://doi.org/10.1121/10.0043155
(Received 10 October 2025; revised 26 February 2026; accepted 2 March 2026; published online 24 March 2026)
[Editor: Francesco Aletta] Pages: 2754–2778

04 April 2026 14:08:15

I. INTRODUCTION

Road traffic noise is increasingly recognized as one of the most pervasive environmental pollutants across European cities. In Europe, over 110×10^6 people, representing more than 20% of the population, live in areas where noise levels exceed harmful thresholds, with road traffic being the predominant sound source in both urban and non-urban settings.[1–4] The adverse effects of prolonged exposure to such high noise levels on human health and quality of life are well documented: chronic exposure above 55 dB(A) has been linked to stress, sleep disturbance, cardiovascular and cognitive impairments, and may also contribute to premature mortality.[5–12]

In response to growing awareness of the significant health and environmental impacts of noise pollution, both the European Union and the World Health Organization have analysed European and global exposure to various sources of noise, proposing and adopting ambitious strategies aimed at mitigating its effects.[13–19] This broader commitment is reflected in key European objectives, including the goal of reducing the population exposed to harmful noise levels by at least 30% by 2030 to improve public health and promote sustainable urban development.[19]

Effective planning and mitigation strategies rely heavily on accurate noise predictions. In this context, the scientific literature offers a wide range of models specifically developed to estimate noise levels generated by road traffic.[20] Conventional road traffic noise models are generally structured as a combination of a noise emission model (NEM), which quantifies the sound power level generated by the source (i.e., traffic flow or single vehicle assessment), and an acoustic propagation model, which simulates the transmission of sound through the environment to the receiver.

However, a significant gap remains between the requirements of regulatory compliance and the physical reality of urban traffic. Conventional frameworks and commonly used models are fundamentally macroscopic; they rely on "aggregated" inputs like total vehicle flows and mean speeds to estimate noise levels. While effective when realizing strategical mapping, these models inherently smooth out the instantaneous fluctuations of real-world dynamic traffic, fundamentally preventing them from capturing the true second-by-second variability of noise emission. Moreover, even if they can be effective under standard conditions (e.g., conditions in which they were calibrated and developed), they may present some intrinsic limitations: they have a site-depending nature, often reflecting local regulatory frameworks and vehicle fleet compositions. For instance, the CoRTN model, developed in the UK, adopts a regression-based approach using empirical data to link

[a]Email: amascolo@unisa.it

 ©Author(s) 2026.

https://doi.org/10.1121/10.0043155

traffic parameters with expected noise levels.[21] Similarly, the German model RLS-90 relies on standardized traffic and infrastructure conditions, applying correction factors based on vehicle type and road surface.[22] Italy's C.N.R. Model follows a comparable structure, offering a simplified statistical treatment of emission sources.[23] Other models, such as the ERTC model developed in Thailand, also belong to this category, relying on average traffic data and empirical correlations.[24]

Some further studies, and thus models developed more recently, attempt to improve noise level predictions by distinguishing between the main physical components of vehicle noise emissions, namely, propulsion and rolling noise, and by differentiating among vehicle categories (e.g., light, heavy, motorcycles, etc.). Nevertheless, these approaches generally remain macroscopic or mesoscopic. They commonly rely on averaged or regulatory speed values rather than real-time traffic dynamics, which introduces significant approximations to the traffic schematization and modelling, making them liable to error in peculiar traffic conditions, such as stop-and-go or congested traffic. Examples of this class include France's NMPB-Routes (now replaced by NMPB-2008),[25] Switzerland's SonRoad,[26] the Scandinavian Nord2000 model,[27] the American FHWA model,[28] and the European CNOSSOS-EU framework.[29,30]

As said earlier, although these models have proven effective in standardized conditions, such as steady, free-flowing traffic, they often underperform in complex scenarios. For instance, Ascari *et al.* introduced the possibility of tuning user-defined pavements in CNOSSOS-EU, to consider the variation of asphalts with respect to the standard ones listed in the EU model, with the aim of producing reliable estimates of road noise exposure.[31] The low noise pavements, in fact, are a new trend solution for mitigating road traffic noise exposure levels.[32] Another approach to predict noise levels in complex areas could be to build prediction models based on the urban features of streets themselves, rather than traffic variables.[33] Moreover, complex scenarios, such as congested environments, signalized intersections, traffic-calming installations (e.g., speed bumps or roundabouts), or highly variable flow regimes need to be addressed relying on dynamic flow data.[34,35] In such cases, relying on mean or limit speeds, as many models recommend, is not sufficient to represent the dynamic fluctuations in vehicle behavior that strongly influence noise emissions. Khan *et al.*, indeed, highlight that static models can oversimplify the conditions under which they operate, limiting their application in urban environments marked by fluctuating traffic situations.[36] Moreover, "static" prediction models lack the capability to represent the dynamic variations of noise, also over short time intervals. The absence of detailed vehicle-level dynamics within these frameworks means they cannot precisely account for the transient noise generated by individual vehicle kinematics, such as the distinct acoustic signatures of acceleration, deceleration, or idling. The significance of fluctuations has been also investigated by Benocci *et al.*, which demonstrated that through extensive measurement campaign in cities like Milan, it is possible to identify statistically repetitive temporal trends for different road categories, allowing for the prediction of dynamic noise levels across vast areas using minimal number of real-time measurement points.[37,38]

Thus, to capture the fluctuating nature of traffic noise, researchers have been developing dynamic and microscopic approaches. Clearly, the primary challenge when using microscopic models is the data acquisition phase. Traditional deterministic microscopic simulators require exhaustive, second-by-second trajectory data for every vehicle in the stream. For example, Chevallier *et al.* showed that microsimulation-based noise modeling significantly outperforms models in which speed values do not change at signalized intersections, capturing queue formation and stop–go waves that static models miss.[39] Also, Can and Aumond proved that road traffic noise emissions are highly sensitive to vehicle kinematics variables, fully understandable when using microscopic models.[40] Such detailed telemetry is typically unavailable to urban planners and is inherently nonexistent during the design phases of new infrastructure. This creates a "data-scarcity paradox": planners need microscopic accuracy to assess the impact of new road geometries, but they lack the microscopic data required to drive such models. To address this, an advanced approach is coupling microscopic traffic simulators with detailed noise emission and propagation models. In this kind of strategy, a traffic microsimulator (e.g., VISSIM, SUMO) generates individual vehicle trajectories (positions, speeds, accelerations) on a second-by-second basis, which are then fed into noise emission formulas and used to compute noise levels at the receivers.[39,41–44]

In addition to traffic microsimulation, several other methods can be employed to obtain traffic data. These include, for instance, video image analysis using computer vision techniques,[45,46] as well as the generation of artificial datasets through computational approaches based on probabilistic models or neural networks.[47] Such methods are particularly valuable in scenarios where observational data are scarce, incomplete, or difficult to access.

Among the several approaches developed to enhance the accuracy of road traffic noise predictions, stochastic methods have emerged as particularly promising. These methods aim to capture the inherent variability and uncertainty in both traffic flow dynamics and noise generation processes. By incorporating probabilistic elements, such as random variations in vehicle behaviors, traffic composition, and environmental conditions, stochastic approaches allow for a better representation of non-stationary or complex urban scenarios.

For instance, Mascolo *et al.* proposed a stochastic microscopic model in which each vehicle's speed is randomly drawn from a Gaussian distribution based on measured mean values.[48]

Moreover, Li *et al.* presented noise prediction model based on a Monte Carlo simulation in which each vehicle's sound power level from three different types of vehicles is

04 April 2026 14:08:15

drawn from a probability distribution, simulating the randomness of real traffic emissions,[49] while Wang *et al.* used mixed probability models for inter-vehicle headways and speeds, applying Monte Carlo sampling to generate detailed noise maps, obtaining very small errors.[50]

Lately, the use of time series analysis for modeling and forecasting traffic-related phenomena has gained increasing attention too, particularly in the context of intelligent transportation systems and environmental monitoring, intending to forecast real-time traffic into such microsimulation-based noise predictions. Among the most prominent methods in this domain are the autoregressive integrated moving average (ARIMA) and its seasonal counterpart (SARIMA), which have proven effective in capturing the temporal dynamics of both traffic flow and the resulting noise emissions. One of the earliest uses of ARIMA in traffic forecasting was introduced by Ahmed and Cook,[51] who applied such models to predict freeway traffic volumes and occupancies. Their work laid the foundation for subsequent studies that adopted ARIMA-based approaches as reliable benchmarks for short-term traffic flow forecasting. For example, Guarnaccia *et al.* and Pascale *et al.* also employed SARIMA to analyze long-term noise monitoring data in urban areas, respectively in southern Italy[52] and Portugal.[53] Their findings revealed that noise levels, represented by the equivalent continuous sound level (L_{eq}), exhibit clear weekly and daily patterns that can be accurately modeled using SARIMA frameworks. These models proved effective not only in fitting historical data but also in providing reliable short-term forecasts, useful for noise mitigation planning and real-time monitoring.

Despite the increasing use of advanced machine learning techniques in the field,[54–57] ARIMA and SARIMA remain popular due to their interpretability, low computational cost, and effectiveness with limited data.[58,59]

In this context, the present paper introduces a hybrid microscopic–stochastic model for road traffic noise prediction. The foundation of this work is the model previously proposed by the authors in Ref. 49, which combines a microscopic framework with a stochastic core. In that model, starting from known traffic flows for each category under analysis, the speed of each individual vehicle is randomly drawn from a Gaussian distribution centered around empirically measured mean values, thus capturing the inherent variability of real-world traffic behavior. Unlike deterministic microscopic models that rely on detailed vehicle telemetry, the usage of probability distribution curves to assign kinematics using a stochastic core approach, significantly reducing input data requirements while preserving the physical resolution of the simulation. Once the speed of each vehicle is determined, a NEM is applied to calculate the sound power level L_w for each vehicle, which is then used to estimate the overall equivalent continuous sound level L_{eq} by applying an appropriate propagation model.

Building upon this framework, this research aims to address the limitations of static noise modelling by developing a hybrid modelling framework that integrates time series forecasting of road traffic parameters with a stochastic microscopic noise model, enabling reliable predictions in data-scarce scenarios. The hybridization of stochastic microsimulation with time-series analysis allows for the generation of temporally dynamic noise predictions that can reflect actual urban variability. Moreover, while both components of the hybrid model can operate with measured data when available, the broader objective is to develop a methodology that remains applicable even in data-scarce or predictive scenarios, such as during the design phase of transport infrastructure. In such cases, speed distributions can be defined using design speeds or regulatory limits, following an approach similar to the one adopted in the CNOSSOS-EU framework,[29,30] and then adjusted to reflect hypothesized traffic conditions. Likewise, time series models used to forecast traffic parameters can be calibrated using data from comparable existing infrastructures, under the assumption that roads with similar geometric and functional characteristics will exhibit analogous traffic patterns. This makes it possible to use time-series forecasting not only for reproducing existing conditions, but also for anticipating traffic dynamics in future or yet-to-be-built scenarios.

The performance of the proposed approach will be compared against the core stochastic model when only supplied with measured traffic data. This comparison serves as a crucial benchmark, since it helps to isolate and evaluate the impact of the hybrid model's time-series forecasting component, and thus the presented two-step modelling chain. Additionally, the established CNOSSOS-EU framework and performances will also be considered to highlight the advantages of a microscopic model over a more conventional, macroscopic methodology. This dual comparison aims to demonstrate the presented model's improved ability to capture short-term noise fluctuations and produce realistic estimates of time-varying environmental noise exposure.

The manuscript is organized into several key sections to address these objectives. Section II introduces the proposed hybrid methodology, detailing the time-series forecasting framework, the stochastic microscopic noise simulation, and their subsequent integration. Section III presents the case study application and the dataset used. Section IV provides a comprehensive discussion of the results, including the assessment of traffic predictions, while the comparative performance analysis is presented in Sec. V. Finally, Sec. VI summarizes the main findings and suggests directions for future research.

II. MATERIALS AND METHODS

As outlined earlier, the proposed hybrid model is composed of two principal components: (1) a time-series forecasting module used to predict traffic-related inputs and (2) a stochastic microscopic model for the simulation of road traffic noise. Accordingly, this section is structured into three main subsections. Section II A is dedicated to the presentation of the forecasting framework, further used to predict traffic volumes and average speeds. It also outlines the

04 April 2026 14:08:15

https://doi.org/10.1121/10.0043155

rationale and methodological process followed to select an appropriate model, including the key analytical steps used to identify the most suitable structure and parameters for capturing the temporal dynamics of the traffic data.

Section II B delves into the stochastic noise model, detailing how individual vehicles are assigned unique speed values and modeled as discrete acoustic sources.

Section II C provides a brief synthesis, illustrating how these two components are integrated. This modular structure not only clarifies the individual contributions of each component but also highlights their interdependence in forming a cohesive and comprehensive hybrid modeling approach. Finally, Section II D presents the model evaluation criteria used in this paper.

A. Time-series forecasting of traffic inputs

Traffic data often exhibits strong temporal patterns, such as daily rush hours or weekly fluctuations in volume, which must be accurately captured to simulate realistic acoustic conditions. Traditional regression models or static assumptions often fail to account for such temporal dependencies. Alternatively, time-series forecasting models provide a more appropriate approach, as they are specifically designed to capture both short-term autocorrelations and long-term seasonal patterns. This is made possible by taking into consideration the sequential nature of the data, whereby each observation is influenced by the previous ones.

To better understand and model such temporal dynamics, time-series data are often decomposed into three key components: trend (e.g., long-term tendency of the data), seasonality (e.g., regular periodic fluctuations), and residual noise (e.g., random variations in the data that cannot be explained either by the trend or the seasonality).[60] In traffic analysis, for example, long-term increases or decreases could be observed due to urban growth, even if these are shown alongside daily or weekly peak-hour patterns.

A wide range of models can be employed for time-series forecasting, each designed to uncover underlying structures within temporal data, such as trends, periodic fluctuations, and dependencies, enabling informed predictions about unknown future data.[60–62]

One foundational approach is the moving average (MA) model, which bases predictions on the average of past error terms. This technique is particularly effective in representing short-term variability and in filtering out random noise. It assumes that each observation is a linear function of previous forecast errors and that these errors are uncorrelated. The complexity of the model is determined by its order (q), which specifies the number of lagged error terms included.

In contrast, the autoregressive (AR) model estimates future values using a weighted combination of previous observations. It is well-suited for capturing long-term dependencies and assumes that future states of the series depend directly on its historical values. The model order (p) indicates how many prior observations are considered in the estimation.

The autoregressive moving average (ARMA) model integrates both AR and MA components, allowing it to capture both long-term and short-term patterns in stationary time series. It assumes that observations are influenced by both past values and past errors, and like its simpler components, it requires that error terms be uncorrelated. The orders (p and q) reflect the number of lagged values and errors incorporated.

To address non-stationary data, where statistical properties like mean and variance changeover time, the ARIMA model extends ARMA by including a differencing step. This differencing (of order d) transforms the original series into a stationary one, making the model suitable for series with underlying trends or evolving behavior.

For datasets characterized by seasonal patterns, the seasonal ARIMA (SARIMA) model further extends ARIMA by including seasonal AR, differencing, and MA terms (denoted by P, D, and Q, respectively). This model effectively captures recurring seasonal fluctuations in addition to long-term and short-term dependencies.

Another widely used family of techniques includes exponential smoothing models, such as simple exponential smoothing and Holt-Winters methods. These approaches use exponentially weighted averages of past values, assigning more influence on recent observations. They are particularly useful for smooth data with or without seasonal patterns and are governed by smoothing parameters that determine how quickly the influence of older data decays.

Ultimately, the selection of an appropriate time-series model must be guided by the specific nature of the dataset and the objectives of the forecasting task. By aligning model choice with the data's temporal characteristics, it becomes possible to extract meaningful insights and produce accurate, context-aware predictions. Thus, when working with time series data, a rigorous approach needs to be followed in order to select the proper forecasting model.[61,63]

In the presented application, the process begins with an initial exploratory analysis of the data, where the raw time series is visually examined to reveal potential trends, recurring seasonal patterns, abrupt shifts, or outliers. Visualization tools such as time plots and seasonal subseries plots are also employed to support this preliminary assessment and to generate hypotheses about the data's temporal behavior. At this stage, identifying whether the series is stationary or subject to trend and seasonality is particularly important, as it strongly influences the type of model to choose.

A deeper understanding of the series structure is then achieved through decomposition techniques, which separate the data into three fundamental components: trend, seasonality, and residual noise. This decomposition helps to clarify whether an additive or multiplicative structure better describes the series and provides insight into the temporal mechanisms driving the observed values. If a clear seasonal cycle is identified, models that explicitly incorporate seasonal terms, such as SARIMA, may be more appropriate.

After this first phase, in order to support model specification, autocorrelation and partial autocorrelation analyses

04 April 2026 14:08:15

are conducted. These analyses help identify the temporal dependencies within the series and guide the selection of AR and MA terms. The autocorrelation function (ACF) reveals how current values relate to previous values at different lags. In particular, ACF measures the correlation between observations in a time series that are separated by various time lags, quantifying how strongly current values are related to past values across different time intervals.

On the other hand, the partial autocorrelation function (PACF) isolates the direct influence of specific lags, excluding the effect of intervening observations. Thus, PACF captures the correlation between a value and its lagged counterpart after removing the effects of the intermediate lags. In other words, it isolates the direct relationship between an observation and its value at a specific lag, without the confounding influence of the values that come in between. This makes PACF particularly useful for identifying the order of an AR process, as it indicates which past values directly contribute to the present one, beyond the influence of closer lags.

Interpreting the patterns observed in ACF and PACF plots is fundamental in determining the appropriate orders of the AR (p) and MA (q) components in models such as ARMA or ARIMA.[62]

In this work, after these crucial steps, the model identification and selection were performed using the *auto.arima()* function available in the R *forecast* package. This automated procedure systematically evaluates a range of candidate ARIMA and SARIMA models, determining the optimal combination of parameters based on the minimization of information criteria such as the Akaike information criterion (AIC), the corrected AIC (AICc), or the Bayesian information criterion (BIC).[64] The function also conducts unit root tests to assess stationarity and applies differencing transformations when necessary, thus streamlining the preliminary steps of the modeling process. Moreover, *auto.arima()* includes automatic detection of seasonal components and allows for user-defined constraints on parameter ranges, enhancing both flexibility and interpretability. In the present study, the model selection was performed using the following specifications: seasonal components were enabled, due to previous investigation on the seasonality of the time series analyzed, stepwise search and exact maximum likelihood estimation were enabled, and model selection was made in three different levels, based on the AIC, AICc, and lately BIC information criteria. A maximum order for non-seasonal and seasonal parameters can be set with an iterative approach to achieve a fast convergence of model identification. The trace argument was also set in order to allow for transparent tracking of the selection process. Once a model is selected, residual analysis is performed to ensure that the remaining error terms behave as white noise, uncorrelated, and normally distributed. Forecast accuracy is evaluated using common metrics (see Sec. II D), based on a training/test data split or cross-validation approach.

However, some inherent limitations of time-series forecasting frameworks in traffic analysis need to be underlined. The robustness of time series models relies heavily on the quality and continuity of historical data; significant gaps or inconsistencies in input observations can hinder the identification of reliable trends and seasonalities. Moreover, being primarily designed to capture periodic temporal structures, these models are often unable to account for external, unpredictable factors such as traffic accidents, sudden road closures, or extreme micrometeorological events. While these anomalies significantly influence real-world traffic patterns and noise emissions, they are not reflected in historical cycles, making the model structurally blind to such non-periodic disruptions. Conversely, these predictive misalignments can be reframed not merely as model failures but as a diagnostic advantage, a sort of informative triggers. When a framework calibrated on longitudinal historical patterns significantly diverges from real-time observations, the resulting discrepancy serves as a recursive indicator for the occurrence of unconventional events. This makes the hybrid framework a valuable decision-support system for public authorities and infrastructure managers, enabling them to distinguish between standard cyclical patterns and unique, non-recurring acoustic events.

B. Stochastic microscopic road traffic noise model

The main objective underlying the usage of a microscopic and stochastic model to assess road traffic noise level is its ability to comprehend the inherently random dynamics of road traffic without losing any resolution at the level of individual vehicles. Moreover, since the acoustic energy produced by a vehicle is strongly influenced by its speed, rather than relying on an average or limit speed, as is commonly done in statistical or macroscopic approaches,[20] a specific speed value, drawn from a theoretical distribution function, is assigned to each individual vehicle,[65] thereby preserving variability within the traffic stream.

This modeling choice enables a more realistic representation of the vehicular flow, where each vehicle is treated as a distinct entity with its own dynamics. It also allows for the differentiation of acoustic emissions even among vehicles belonging to the same category, accounting for variations such as those arising from driver behavior. As a result, the model captures the unique acoustic contribution of each vehicle, avoiding the loss of detail and potential underestimation that can occur when relying on aggregated or averaged parameters.

For a comprehensive and detailed description of the stochastic model, the reader is referred to Ref. 48. Moreover, to further support understanding of the model's formulation, the complete set of equations and illustrative figures can also be found in the same reference. A summarized outline of the framework is nonetheless provided below for clarity.

The required basic inputs are traffic information (e.g., flow typologies, vehicle classification, and speed distribution curves if drawable or hypothesized), geometric data (e.g., the distance between the traffic lane and the receiver, as well as the height of the observation point, to enable accurate

04 April 2026 14:08:15

https://doi.org/10.1121/10.0043155

modelling of sound propagation), road-specific features (e.g., pavement type, road gradient, and number of lanes).

Thus, the stochastic core of the model is performed with the assignment of speeds to each individual vehicle based on the specific speed distribution. For instance, free-flow conditions are modelled using a Gaussian speed distribution, while skewed distributions such as Beta or Chi-square are employed to represent more irregular or congested traffic patterns.[34,66–68]

Thereafter, the sound power level L_W for each vehicle is estimated, by referencing the CNOSSOS-EU NEM, which decomposes the total vehicle noise emission into two main components: propulsion noise $L_{W,P}$ and rolling noise $L_{W,R}$. Both of such components are modelled as functions of speed, with linear and logarithmic dependencies respectively, and are combined using a logarithmic sum to yield the total source power level. The usage of the CNOSSOS-EU NEM ensures that the core of the acoustic simulation remains independent of site-specific calibration, as it utilizes standardized regulatory formulas to calculate sound power levels. Moreover, this characteristic is essential for the model's applicability in predictive or data-scarce scenarios, such as the design phases of new transport infrastructures, where measurement data for tuning are absent.

Then, the time-varying distance between each moving vehicle and the fixed receiver is computed, using geometric relations based on the vehicle's position along the road segment. This allows for the calculation of instantaneous sound pressure levels L_p at the receiver, under the assumption that each vehicle acts as an isotropic point source.

To quantify the acoustic impact of each individual transit event, the model employs the sound exposure level (*SEL*), a metric that captures the cumulative energy of a single pass-by. The total *SEL* for each vehicle category is computed by aggregating individual *SEL*s via a logarithmic sum. Ultimately, the L_{eq} over a specified time interval is determined through another logarithmic aggregation of *SEL*s from all vehicle categories, enabling a complete temporal and categorical integration of the acoustic data.

Despite relying on CNOSSOS-based equations and a simplified propagation model for demonstration purposes, the authors highlight the adaptability of their modular framework. Both the NEM and the propagation scheme can be easily substituted to suit the needs of alternative use cases or specific geographic contexts.

The full procedure was implemented using a custom PYTHON routine, consisting of distinct phases: input parameter configuration and data loading; random vehicle speed generation based on a specified probability distribution; computation of sound power levels using the CNOSSOS formula; noise propagation estimation; and final aggregation into the equivalent continuous sound level.

C. "Hybrid" noise model

The finale phase, which is the one that can be regarded as a hybrid modelling approach, aims at combining the strengths of two distinct yet complementary methodologies. Specifically, the traffic input data used to drive the stochastic microscopic noise model are not derived from direct measurements alone but are instead generated through the implementation of a time-series forecasting model, as previously described. From a computational standpoint, this process is structured as a two-step procedure: the forecasting analysis is performed in the R environment (v4.3) using *forecast* library and *statsmodels* library in PYTHON; the resulting predicted traffic variables are then imported into and processed by a custom-written PYTHON (v3.14) routine that handles the stochastic microscopic simulation using *numpy*, *pandas*, and *scipy* for mathematical and statistical processing. This dual-modular workflow ensures that each analytical step is handled by the most efficient tool: preliminary tests, indeed, were adopted, which demonstrated that, while both environments produced identical numerical results, the R implementation was significantly faster and more computationally efficient for the forecasting phase. The entire computational workflow was executed on a standard professional-grade workstation running Windows 10 (64-bit), equipped with an Intel Xeon E3-1245 v5 processor (3.50 GHz), 16 GB of RAM, and an AMD Radeon Pro WX 2100 GPU with 2 GB of dedicated memory. Such a configuration resulted in a computational time of about 4–5 h in producing each traffic input time series model and few minutes in calculating the road traffic noise levels in the second step. This outcome highlights the framework's practical feasibility in real-world operational environments, such as infrastructure design and urban planning, by demonstrating that high-fidelity noise assessments can be achieved without requiring high-performance computing (HPC) resources.

It is important to remark on the evolution of this framework compared to the previously published stochastic-core model.[48] While the underlying acoustic simulation logic (the assignment of speeds via probability distributions) remains consistent, the current hybridization with time-series forecasting fundamentally alters the model's operational scope. Unlike the stochastic framework, which requires empirically measured traffic inputs and thus it is a diagnostic assessment tool, the hybrid framework presented here is capable of predicting noise levels in the absence of direct traffic observations by leveraging historical temporal structures, which makes it a prognostic predictive tool.

This process is schematically illustrated in the flow chart of Fig. 1, which provides a concise overview of the two combined methodologies.

By incorporating temporally predicted variables, such as traffic volumes and average speeds for each vehicle category, into the noise simulation model, the system becomes capable of producing acoustical predictions that evolve dynamically and reflect the inherent temporal variability of urban traffic conditions. This hybridization enables the modelling process to move beyond static scenarios, allowing for a more realistic representation of noise emissions over time.

To assess the effectiveness and predictive capacity of this hybrid procedure, a series of error metrics will be

04 April 2026 14:08:15

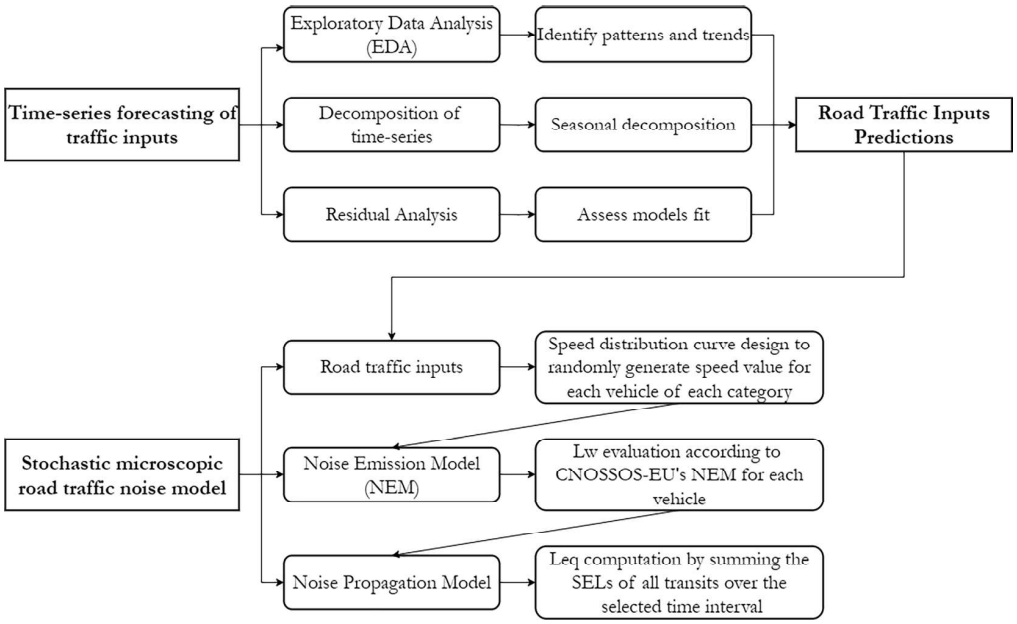


FIG. 1. Schematic representation of the hybrid approach integrating time-series predictions with the stochastic microscopic noise model.

computed and analysed to quantify the performance of the model and highlight potential strengths or limitations in capturing real-world acoustical phenomena. Furthermore, the outcomes generated by the hybrid model will be systematically compared with those obtained from the stochastic model alone, when fed with actual measured traffic data and with the CNOSSOS-EU macroscopic framework. This comparative analysis aims to evaluate the added value of the time-series forecasting component, thereby offering insights into the potential of the integrated approach for future applications in traffic noise prediction and urban sound environment assessment.

D. Model evaluation metrics

To rigorously assess the performance of the proposed hybrid framework, a multi-stage evaluation methodology is implemented. This analysis is divided into the evaluation of the traffic forecasting module and the validation of the resulting acoustic output. Specifically, the accuracy of the SARIMA models for each traffic input parameter is assessed during both the calibration phase (analysis of residuals) and the validation phase (prediction error). This is achieved by employing several widely adopted error metrics such as mean error (ME), mean absolute error (MAE), mean percentage error (MPE), mean absolute percentage error (MAPE), mean square error (MSE), and root mean square error (RMSE); the mathematical formulations for these error metrics can be found in Ref. 48. The same set of metrics have been consistently applied to quantify the predictive accuracy of each component within the hybrid model.

To provide a comprehensive insight into the error structure of the hybrid model, other diagnostic tools have been employed. An error distribution analysis has been utilized to visualize the frequency and symmetry of deviations. This statistical analysis also includes also the mean, standard deviation, range, skewness, kurtosis, and the distribution quartiles, to further understand the model's reliability. Furthermore, a continuous time-series plot of errors is provided to detect temporal patterns or specific intervals where the simulation precision might fluctuate.

Finally, the significance of the proposed hybrid model is established through a comparative analysis with established approaches in the literature. In particular, the hybrid model's results are benchmarked against those obtained from the fully stochastic model and the CNOSSOS-EU model.

III. CASE STUDY APPLICATION

A real-world dataset known as the "Long Term Monitoring Station LTMS database"[69] has been used as a case study. This dataset was originally collected by a team of researchers affiliated with the former IFSTTAR institute ("*Institut français des sciences et technologies des transports, de l'aménagement et des réseaux*"), which has since become part of Université Gustave Eiffel, headquartered in Nantes, France.

The monitoring campaign took place over a continuous six-year period (2002–2007) at a dedicated experimental site located in Saint-Berthevin. Figure 2 illustrates the location of Saint-Berthevin within the Pays de la Loire region, in France. The chosen site was near a motorway, which extends for approximately 93 km, linking Le Mans and La Gravelle, and features two carriageways with two lanes in each direction. The monitoring system was equipped to operate continuously, collecting data throughout the years in the proximity of such a motorway. In particular, multiple

04 April 2026 14:08:15

JASA
https://doi.org/10.1121/10.0043155

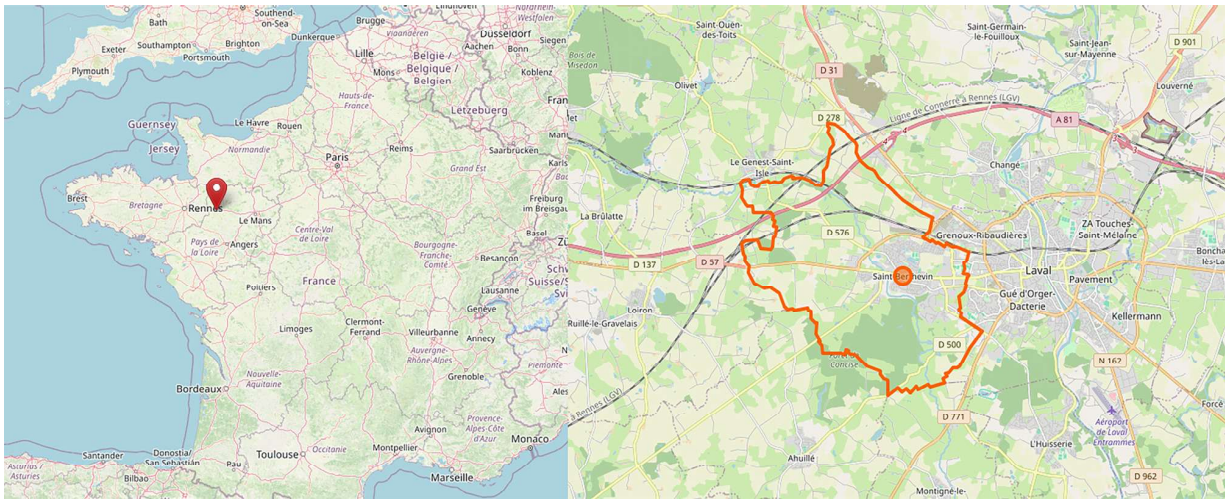


FIG. 2. Saint-Berthevin's position within the *Pays de la Loire* region in France (maps available from OpenStreetMap®) (Ref. 48).

data types were recorded, including acoustic levels, micrometeorological variables, and detailed traffic parameters.

With regard to the acoustic data, five monitoring stations were deployed to record A-weighted equivalent continuous sound levels ($L_{eqA,10s}$) across 1/1 octave bands ranging from 125 Hz to 4 kHz, at two different heights: 2 and 5 m above the ground for each measurement point. An exception is the designated reference point for this study, positioned 5 m high and approximately 5 m from the roadside. The acoustic data acquisition was performed using professional-grade instrumentation designed for high-precision, long-term outdoor monitoring. The system utilized 01 dB-Stell "outdoor" microphones, which are class 1 certified to ensure high metrological accuracy and stability under varying environmental conditions. The road traffic counts are collected with a SIREDO, type ELSI, sensor. These were coupled with the SALTO acquisition system, a multi-channel platform capable of synchronous logging of the acoustic and traffic parameters. Acoustic levels were logged every 10 s and subsequently validated by the French research team through a cleaning process aimed at eliminating non-traffic-related events (see Ref. 69 for further information). The validated data were then aggregated into 15-min intervals and made available to the scientific community.

Concerning traffic data, the publicly available dataset provides only aggregate counts of light and heavy-duty vehicles recorded over 15-min intervals, with no information about lane division. Consequently, the simulation framework assumes a simplified configuration with a single lane and unidirectional traffic to represent the road scenario. Similarly, the publicly available data include only the average speeds for each vehicle category within the same 15-min interval.

It has to be underlined that the examined site exhibits free-flow traffic conditions, as also confirmed by the preliminary data analysis performed by the authors,[48] indicating that vehicle speeds are not significantly affected by surrounding traffic due to low traffic density in relation to the road capacity. Under such conditions, traffic can be considered homogeneous, and vehicle speeds can be effectively modeled using a Gaussian distribution.[66–68] Given the nature of the normal distribution, it can be defined by specifying the mean and standard deviation. In this study, the mean speed is directly extracted from the dataset, while the standard deviation is set to 10% of the mean value, consistent with the approach used in the literature.[48,70]

This choice of a unified dispersion coefficient reflects the physical constraints typical of high-speed motorway environments. In a free-flow regime, the absence of intersections or significant gradient changes minimizes the kinematic variability between different vehicle categories, as both light and heavy vehicles tend to maintain a steady speed centered around their respective regulatory limits or prevailing flow conditions. From an acoustical perspective, the 10% standard deviation provides a stable stochastic foundation; since $L_{A,eq}$ is an energetic average, its value is highly robust to minor fluctuations in the width of the speed distribution.

Based on these considerations, in this contribution, each vehicle has been simulated with a constant value of speed, and no adjustments are introduced to account for acceleration dynamics in the modeling process.

To enable the integration of traffic and noise modeling within the presented hybrid framework, the analysis was conducted at the hourly level rather than using the "original" 15-min intervals. This methodological choice was driven by the need for more stable and temporally consistent data inputs, which are better suited for time-series forecasting and model calibration. Thus, hourly traffic data were obtained by summing the vehicle flows across four consecutive 15-min intervals, while average speeds were computed for each vehicle category, using the number of vehicles in each subinterval as weighting factors. Similarly, acoustic measurements were aggregated by applying logarithmic averaging to the $L_{A,eq,15min}$ values over the course of each

04 April 2026 14:08:15

hour, thereby preserving the energetic characteristics of the sound data.

However, unlike traffic data, which were generally more complete and continuous across the whole dataset, the acoustic measurements presented a greater number of gaps. The reason is to be found primarily in the rigorous data cleaning procedures applied by the research team to remove non-road noise sources, such as human activity, animals, aircraft, and railways, that could compromise the reliability of the dataset. Nevertheless, the extent of this preliminary cleaning process is not fully ascertained, as no direct control or possibility of intervention was available at this stage. As a result of these preliminary yet necessary filtering operations, several 15-min intervals lacked valid noise data ($L_{A,eq,15min}$), leading to inconsistencies across the input variables. To construct a continuous time series suitable for forecasting purposes, an initial attempt was made to identify the longest available stretch of consecutive 15-min intervals in which all necessary inputs, both traffic and acoustic data, were present. This would also enable the construction of complete hourly aggregates based on reliable 15-min data. However, due to the earlier described data gaps, particularly in the noise measurements, it was not possible to isolate a sufficiently long uninterrupted period. Consequently, the analysis was restricted to the most data-dense month available, covering a five-week period from 28 June to 1 August 2004. This timeframe was selected to facilitate the detection of recurring temporal structures in traffic phenomena, spanning both daily and weekly cycles. It must nevertheless be recognized that the selected interval corresponds to a rather specific seasonal context, encompassing the French national holiday on 14 July and coinciding with the peak summer vacation period. Such factors are likely to influence traffic dynamics, with weekends typically characterized by holiday-related outflows and a reduced presence of heavy vehicles on motorways. These seasonal effects were also reinforced by French regulatory restrictions in force during the summer of 2004, which limited the circulation of heavy vehicles on specific days and times. According to these regulations, vehicles or vehicle combinations used for road freight transport with a maximum authorized gross weight exceeding 7.5 tonnes were prohibited from circulating on Saturdays and the eve of public holidays, from 22:00 on Saturday until 22:00 on Sunday and on public holidays, allowing only permanent exemptions.[71,72]

The selected period was further divided in accordance with the conventional 80/20 principle often employed in data modelling and analysis: the first four weeks (28 June to 25 July 2004) were allocated for model calibration and training, while the final week (26 July to 1 August 2004) was reserved for model validation. For each hourly record, the number of 15-min intervals with a corresponding valid noise measurement was also documented, in order to maintain transparency regarding data completeness and quality.

The obtained dataset includes five crucial variables for each 15-min interval: N_L, light vehicles flows, N_H, heavy vehicles flows, v_L, light vehicles mean speeds, v_H heavy vehicles mean speeds and $L_{A,eq,1h,meas}$, the measured continuous equivalent sound level.

A preliminary exploratory data analysis of the selected timeframe highlighted a minor inconsistency: two records reported a zero flow of heavy vehicles, to which a corresponding zero speed was also assigned. While a zero flow has a clear physical meaning, a zero speed in this context is not physically plausible, since vehicles were not motionless or inactive but rather absent. To avoid inconsistencies in the computation of summary statistics and in the subsequent time series analysis and forecasting models, the flow values in these two records were kept as zero, while the speeds were replaced with the average speed of heavy vehicles calculated over the entire observation period, apart from these two specific intervals. This correction is considered appropriate, as the average speed of heavy vehicles does not exhibit strong fluctuations around its mean, as will be further discussed later. A detailed overview of the resulting dataset's composition is provided in Table I, whereas Table II presents a selection of its summary statistics.

To provide a clearer representation of the dataset and to highlight potential differences between the calibration and validation sets, the boxplots of the variables are reported in Fig. 3, offering a concise summary of their main characteristics. The horizontal lines within each box indicate the median value of the corresponding variable.

Figure 3(a) illustrates the distributions of traffic flows for light vehicles (N_L) and heavy vehicles (N_H). As expected, light vehicles dominate the traffic composition, with median values of approximately 530 in the calibration dataset and 557 in the validation dataset, whereas heavy vehicles account for a much smaller share, with median values of 74 and 75, respectively. The relatively close

TABLE I. A subset of entries from the dataset used in the analysis.

# Interval	Date	Time interval	N_L [veh/h]	N_H [veh/h]	v_L [km/h]	v_H [km/h]	$L_{A,eq,1h,meas}$ [dBA]	15-min count
0	28-06-2004	00:00–00:59	91	20	114.5	83.7	—	0
1	28-06-2004	01:00–01:59	57	30	116.4	80.7	—	0
2	28-06-2004	02:00–02:59	51	32	116.9	80.8	—	0
3	28-06-2004	03:00–03:59	84	46	117.7	80.1	68.2	1
…	…	…	…	…	…	…	…	…
839	01-08-2004	22:00–22:59	284	14	120.9	81.8	69.0	4
840	01-08-2004	23:00–23:59	162	15	122.8	81.5	67.2	2

04 April 2026 14:08:15

https://doi.org/10.1121/10.0043155

alignment of both N_L and N_H between calibration and validation suggests that the traffic structure has been consistently captured in the two datasets. The predominance of light vehicles is consistent with the road typology and usage patterns, and the marginal variation observed between the datasets does not indicate substantial discrepancies in traffic composition.

Figure 3(b) reports the distributions of average vehicle speeds for both light (v_L) and heavy (v_H) vehicles. The medians confirm that light vehicles travel at considerably higher speeds than heavy vehicles, with values of 118.27 km/h (calibration) and 118.65 km/h (validation) for v_L, compared to 80.87 km/h (calibration) and 81.03 km/h (validation) for v_H. The small differences between the two datasets suggest a strong consistency in speed patterns across the two time intervals. Furthermore, the observed gap between v_L and v_H reflects typical traffic dynamics, where heavy vehicles are subject to both technical limitations and regulatory restrictions, leading to systematically lower speeds.

Figure 3(c) presents the distributions of the measured equivalent sound levels, $L_{A,eq,1h,meas}$. The median values are 71.29 dBA for the calibration dataset and 70.69 dBA for the validation dataset. Although the difference is modest, it suggests a slightly lower overall acoustic impact during the validation phase. This deviation may be due to minor variations in traffic composition or environmental conditions.

Nevertheless, the general alignment of the two distributions confirms the robustness of the sampling and provides strong evidence that the calibration and validation datasets can be regarded as statistically comparable. The limited differences observed between the two datasets are within the range of expected variability and do not indicate the presence of systematic biases in either the traffic-related or the acoustic variables. This consistency ensures that the validation phase is conducted under representative conditions, thereby reinforcing the reliability of the subsequent model assessments and supporting the robustness of the model calibration process.

It needs to be underlined that the selection of the LTMS dataset as a case study for the hybrid framework validation serves a specific methodological objective. Since this dataset was previously utilized to validate the stochastic microscopic noise model in Ref. 48, its reuse here aims at establishing a controlled benchmarking environment. This setup is essential for isolating the error propagation inherent in the proposed two-step modelling chain. It allows for an individuation of the discrepancy introduced solely by the SARIMA-based traffic forecasting component, as the baseline performance of the acoustic engine is already documented for this site. By maintaining consistency in the validation site, this approach aims at providing a transparent assessment of the "forecasting cost," demonstrating the hybrid model's reliability for prognostic purposes.

TABLE II. Statistical summary of the variables included in the dataset.

Variable	Mean	Std. dev.	Min. value	Max. value	Skewness	Kurtosis
N_L [veh/h]	601.6	507.2	7	2504	0.97	0.56
N_H [veh/h]	69.0	41.2	0	199	−0.06	−0.96
v_L [km/h]	118.1	3.9	95.4	127.6	−1.73	6.61
v_H [km/h]	81.7	2.4	77.5	92.6	2.04	4.13
$L_{A,eq,1h,meas}$ [dBA]	70.3	2.8	59.6	75.1	−1.27	1.34

IV. RESULTS AND DISCUSSION

The following outlines the outcomes of the presented study and discusses their relevance in the context of the proposed methodology. To ensure clarity, the results are organized according to the same framework used in the

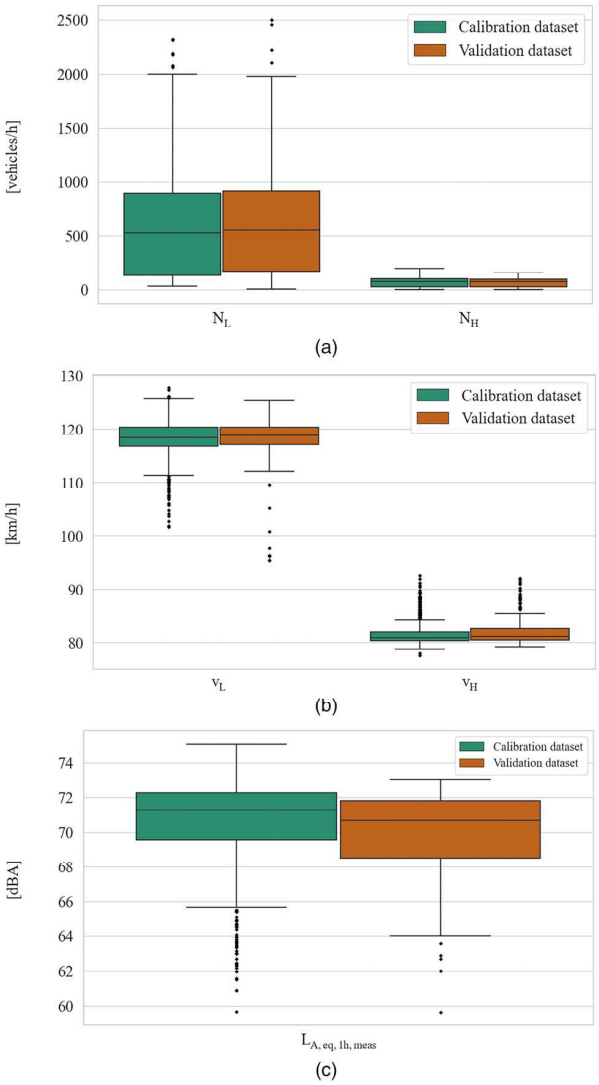


FIG. 3. Boxplot of (a) light (N_L) and heavy (N_H) vehicles flows, (b) light (v_L) and heavy (v_H) vehicles' speeds, (c) equivalent noise levels ($L_{A,eq,1h,meas}$) recorded. Calibration data are shown in green; validation data in orange.

04 April 2026 14:08:15

TABLE III. Variance explained by seasonal components for different periods (24–168 h).

Variable	24h	48h	72h	96h	120h	144h	168h	Best period
N_L	62.30	61.25	61.76	60.74	62.27	63.67	91.25	168h
N_H	13.31	13.85	14.51	15.66	20.18	20.24	85.83	168h
v_L	34.59	36.42	38.55	43.33	45.79	44.51	51.95	168h
v_H	5.87	6.35	7.21	7.58	11.92	15.68	58.90	168h

methodology. First, the outcomes of the time series forecasting models are reported, highlighting their ability to capture the temporal dynamics of traffic. Next, the acoustic analysis is presented, which encompasses the application of the stochastic microscopic road traffic noise model and its hybridization with the time series predictions, with the corresponding results critically assessed.

A. Time-series forecasting of traffic inputs: Results and assessment

To investigate the temporal structure of the traffic variables under analysis, several seasonal periods has been tested, from 24 h up to one week, in 24-h steps. The testing process has been achieved using the *seasonal_decompose* function from *statsmodels* in a self-written Python routine, chosen for its efficiency in handling large-scale datasets. This function applies a commonly used decomposition method, splitting the original time series into its additive components: long-term trend, repeating seasonal pattern (according to the chosen period), and residual fluctuations. Thus, for each tested period, the proportion of variance explained by the seasonal component has been computed, allowing an objective comparison of the different seasonalities. Table III summarizes the explained variance across different tested seasonal

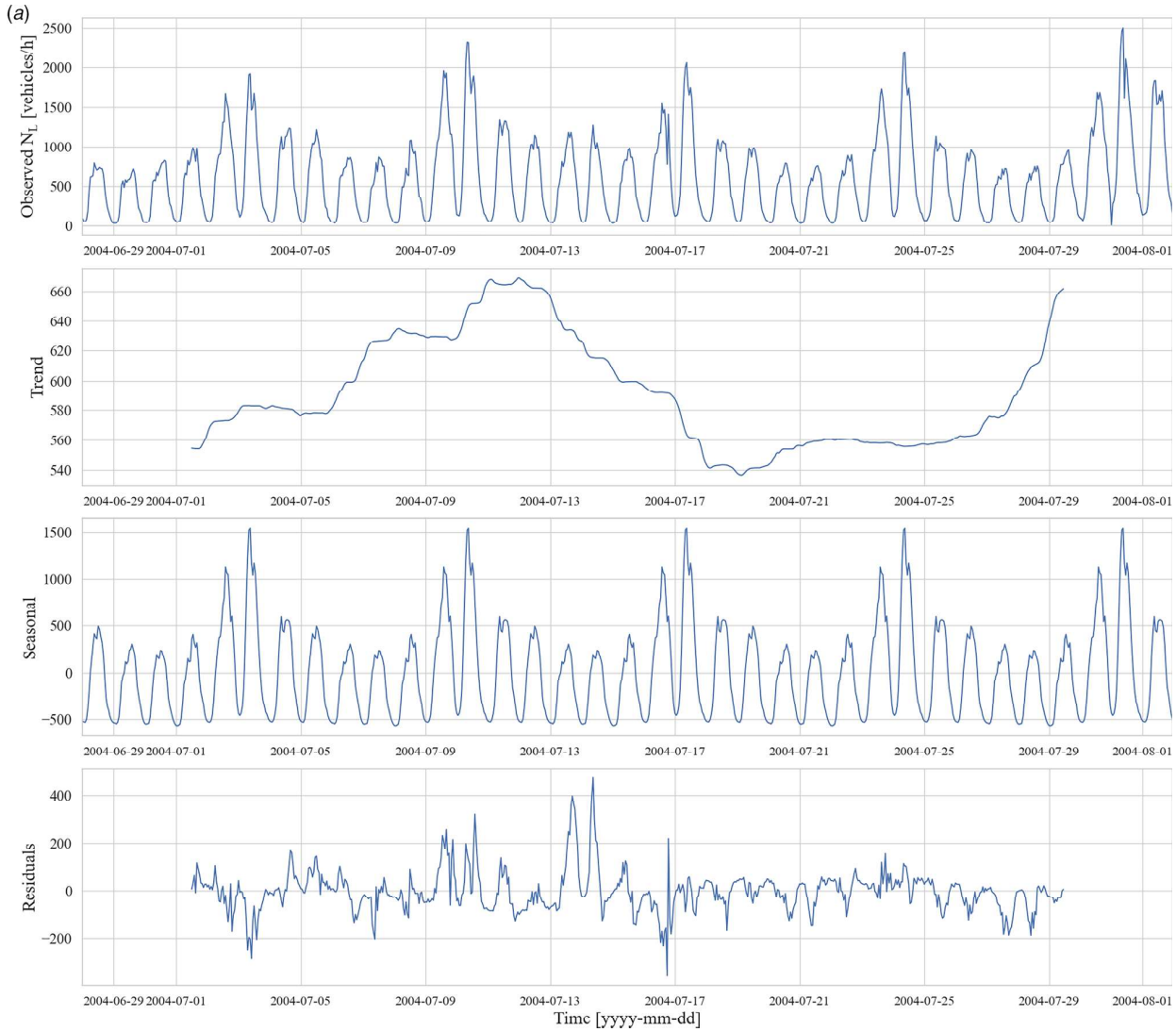


FIG. 4. Time series and decomposition of the traffic variables: (a) light vehicle flows (N_L), (b) heavy vehicle flows (N_H), (c) light vehicle mean speeds (v_L) and (d) heavy vehicle mean speeds (v_H). For each time series the original series, the trend component, the seasonal component, and the residuals are represented.

04 April 2026 14:08:15

https://doi.org/10.1121/10.0043155



FIG. 4. (*Continued.*)

periods for all variables. The results highlight that N_L and N_H clearly exhibit a strong weekly pattern, while the explained variance is comparatively lower for v_L and v_H. This can be attributed to the higher variability of speed measurements, which are more influenced by stochastic fluctuations and short-term conditions than by systematic weekly cycles. Nevertheless, the weekly period (168 h) still emerges as the dominant seasonal component, confirming its relevance also for the speed variables. Consequently, 168 h has been selected as the reference seasonality for each time series, and it has been used to decompose them into their trend, seasonal, and residual components.

Figure 4 show, for each variable, both the full time series and its decomposition.

The decomposition of N_L, shown in Fig. 4(a), highlights a well-defined weekly cycle, with traffic volumes consistently higher on weekends and reduced over weekdays. The trend component, however, shows a medium-term variation that could be reflecting seasonal demand or summer holiday exodus. The seasonal plot clearly indicates the cyclical nature of the traffic flows, with peaks at regular intervals, especially during weekends as explained earlier, which also confirms the corresponding high value of explained variance reported in Table III. The residuals plot, used to check if any random fluctuations remain after accounting for both the trend and seasonal components, shows some sharp spikes, which may indicate irregular flows or special events that affect the traffic phenomenon, such as around July 14th and the weekend immediately following.

For N_H, in Fig. 4(b), the weekly pattern is even stronger, with a sharp distinction between weekdays, characterized by intense heavy flows, and weekends, when traffic demand is drastically lower. A significant drop is also clear in corresponding of July 14th, which is attributable to driving bans during festive days as reported earlier.[72,73] These insights can be confirmed looking at the trend plot which indicates a

04 April 2026 14:08:15

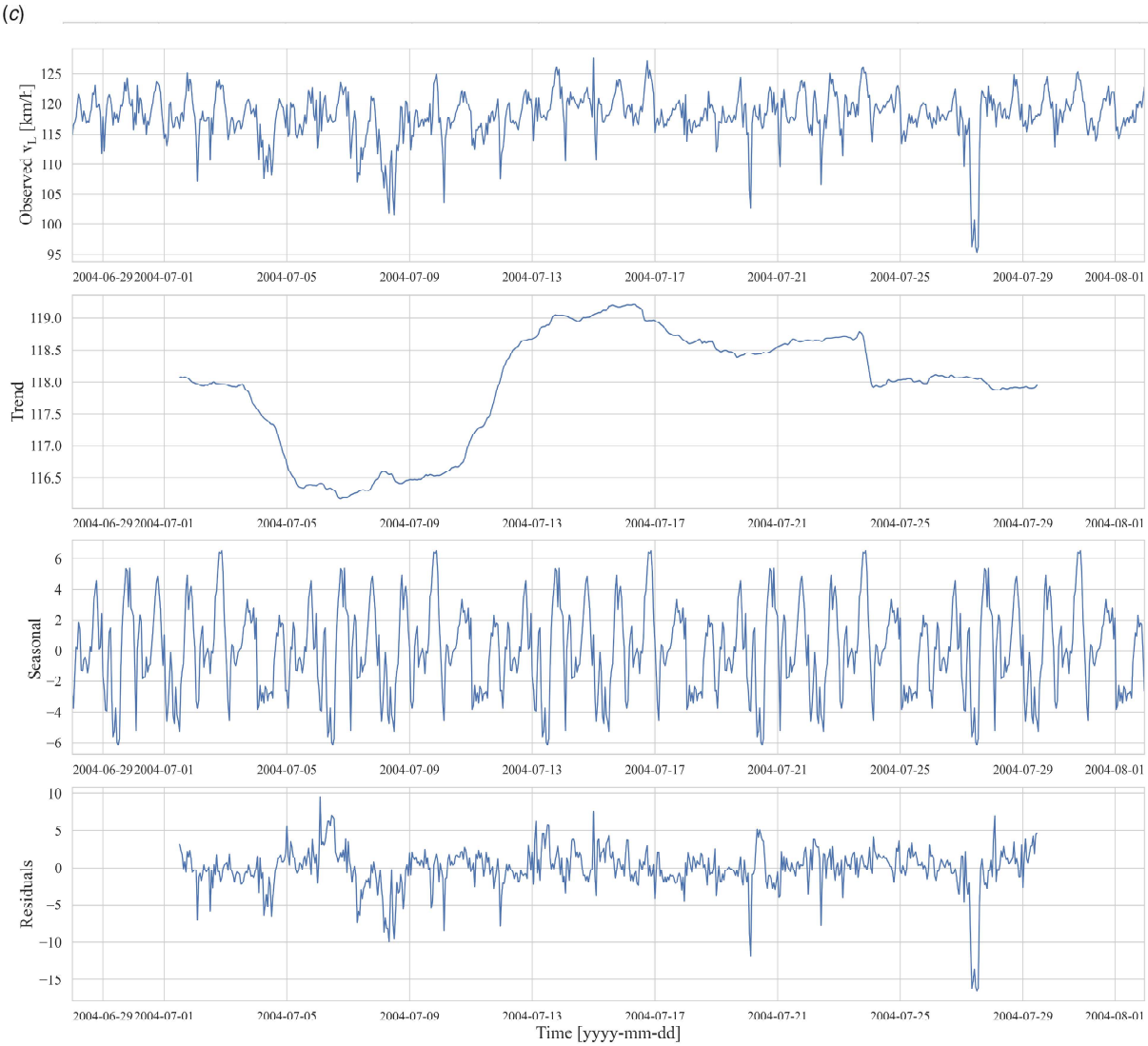


FIG. 4. (*Continued.*)

noticeable shift in the flow starting around July 10th, where a gradual decrease can be observed, followed by an increase after mid-July. The seasonal component, as in the case of light vehicles flows, clearly dominates the dynamics of the series, while the trend exhibits gradual fluctuations over time. Residuals remain limited, aside from the values measured during July 14th, which being a festive day could be considered as an irregular event in the traffic flow time-series, confirming that most systematic structures are well captured.

The decomposition of v_L is represented in Fig. 4(c). The raw time-series itself shows the data fluctuating with occasional sharp peaks and drops, suggesting high volatility in the measurements of vehicles speed. The trend remains relatively stable, with moderate variations, revealing a gradual increase in average speed, with a noticeable shift around July 14th. However, when compared to the flow variables, as also confirmed by the explained variance reported in Table III, the light vehicles mean speeds reveal a less pronounced seasonal signal. However, the noise remaining after accounting for both trend and seasonal components seems to be random.

Also, in the case of v_H, shown in Fig. 4(d), significant fluctuations in the raw data are present, with frequent peaks and valleys. In particular, higher values of mean speeds are measured during the weekends, probably due to the driving ban limits associated with vehicles or vehicle combinations used for road freight transport. Consequently, during these periods, only smaller or even medium vehicles, although classified as heavy vehicles, are permitted to travel, which likely results in higher average speeds. This kind of vehicle may be more maneuverable and capable of faster travel compared to the larger, heavier trucks that are subject to the restriction, thus leading to the observed increase in mean speeds during weekends and holidays. Thus, similarly to the light vehicles' mean speeds, the seasonal plot reveals

04 April 2026 14:08:15

https://doi.org/10.1121/10.0043155

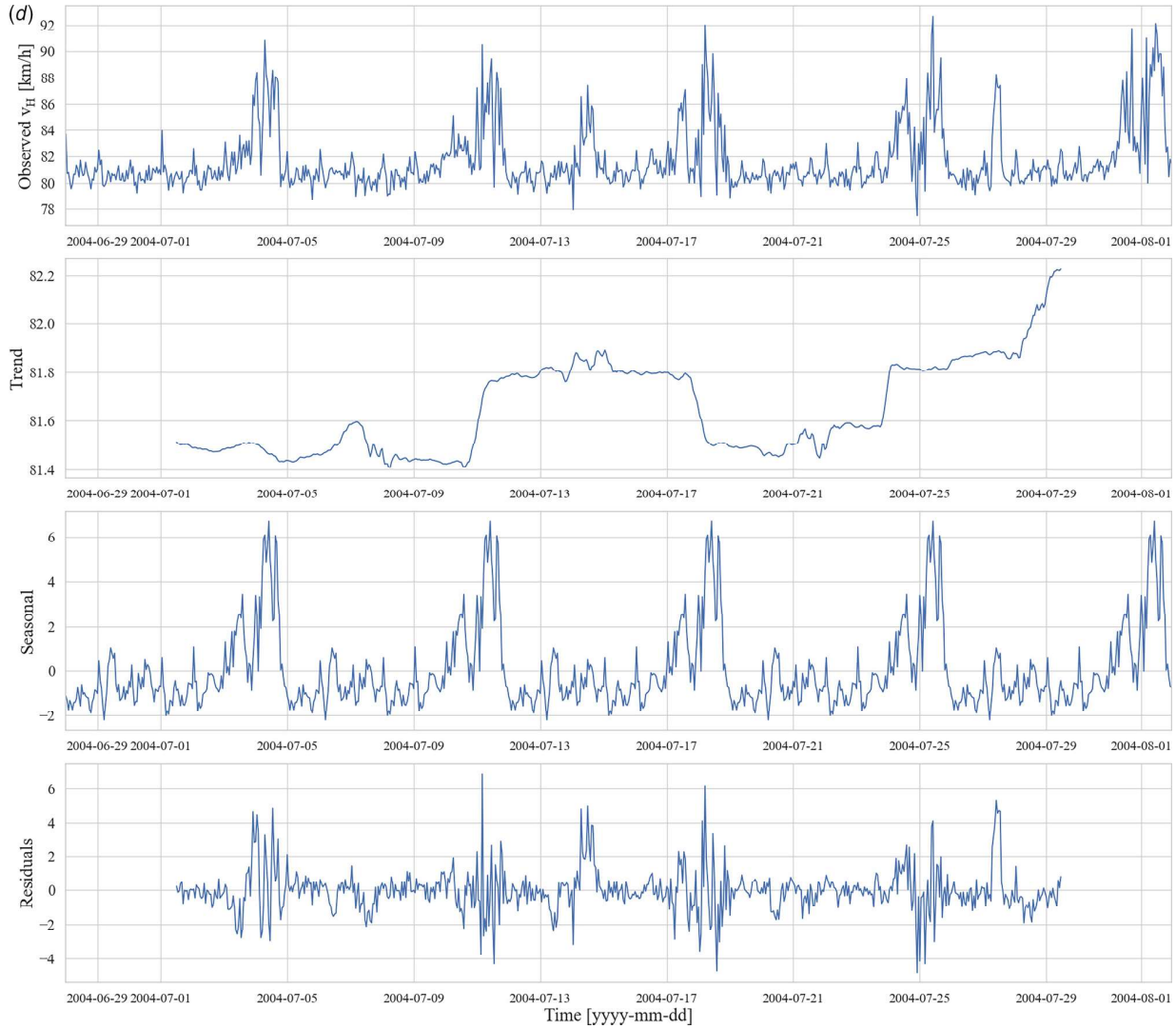


FIG. 4. (*Continued.*)

periodic oscillations, suggesting cyclical fluctuations in heavy vehicle speeds. The residuals plot, finally, highlights the remaining noise after extracting the trend and seasonal components, underlying that there may still be unexplained factors affecting the variability in heavy vehicle speeds, which should be object of further investigation.

This combined exploratory and decomposition analysis, provides a comprehensive understanding of the temporal dynamics of the traffic variables, forming the basis for subsequent correlation analysis and forecasting model specification. Nevertheless, to further investigate the temporal dependencies and underlying structures within the traffic variables, an autocorrelation (ACF) and partial autocorrelation factor (PACF) analysis has been conducted. Figure 5 reports the graphs for ACF and PACF for all the investigated variables. It is noticeable that the ACF plots reveals always a significant correlation up to approximately 7 days, strongly supporting the idea of a weekly cycle as the dominant seasonality. As for the PACF, the gradual decay that can be observed in all the plots indicates that the dependencies span over several days, and that past observations are relevant for forecasting future values, supporting the choice of 7-day seasonality for the time-series analyses.

Based on the 7-day seasonality observed in the previous analysis, model identification has been then performed using the *auto.arima()* function in R, which automatically selects the best-fitting SARIMA models. Evaluation of the models has been carried out using the AIC, AICc, and BIC criteria to select the most appropriate fit for each time series. Although the self-written R routine has been implemented to evaluate and select different models based on the minimization of each individual criteria, the results consistently pointed out to the same model for each variable. This convergence across all four time series indicated that the models selected by *auto.arima()* effectively minimized the chosen fit criteria without the need for further model tuning or adjustment. Consequently, in Table IV only a single

04 April 2026 14:08:15

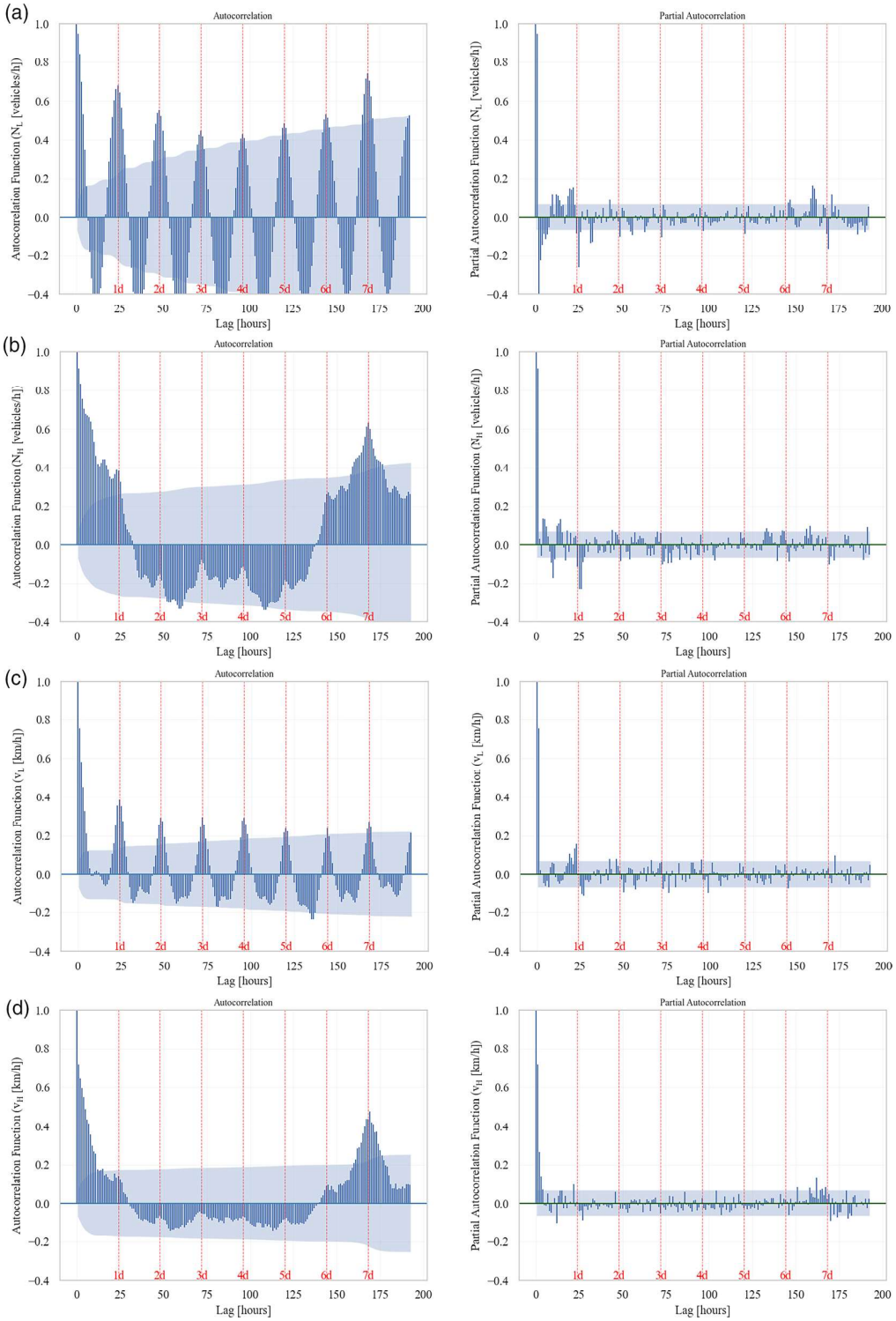


FIG. 5. Autocorrelation function (ACF) and partial autocorrelation function (PACF) plots for (a) light vehicle flows (N_L), (b) heavy vehicle flows (N_H), (c) light vehicle mean speeds (v_L), and (d) heavy vehicle mean speeds (v_H).

model is indicated for each series, as it aligns with the optimal minimization of the chosen parameters.

To assess the forecasting performance of the selected models, a visual comparison between the observed time series and the fitted values over the entire period of interest is presented in Fig. 6.

Although these visualizations span the full period covered by the dataset itself, thus going from June 28th to

04 April 2026 14:08:15

https://doi.org/10.1121/10.0043155

TABLE IV. Selected SARIMA models for each time-series.

Variable	Model $(p,d,q)(P,D,Q)_S$	AIC	BIC	AICc
N_L	$(1,1,0)(0,1,0)_{168}$	6053.7	6062.14	6053.7
N_H	$(0,1,1)(0,1,0)_{168}$	4321.9	4330.3	4330.3
v_L	$(1,1,0)(0,0,1)_{168}$	3242.0	3194.2	3260.0
v_H	$(1,0,1)(0,1,0)_{168}$	2104.4	2117.1	2104.4

August 1st, 2004, it is important to note that for the final validation of the road traffic noise model, only the last week, from July 26th to August 1st, 2004, corresponding to the validation dataset has been used. These plots provide a qualitative assessment of how well the model captures the underlying patterns in the data, allowing for an initial comparison of the observed and predicted values. However, for a rigorous evaluation, error metrics have been calculated solely on the validation set, in order to provide a more accurate measure of the model's predictive ability.

Figure 6(a) shows a good alignment between the observed and predicted N_L values throughout the period. The model appears to fit the data well, capturing the fluctuations in light vehicle traffic with minimal deviation, even if there are some slight mismatches between the observed and predicted values visible during the last week. In particular, August 1st is characterized by a noticeable underestimation of the predicted values, due to an abnormally higher light traffic flow when compared to the observed one during the previous Sundays of the dataset.

Heavy vehicle flows N_H predictions can be observed in Fig. 6(b). Both the high peaks and the lower traffic periods are reasonably well replicated. However, there are some instances where the model slightly underestimates the flow, such as during July 14th, likely due to the festive day characteristics that might not have been well represented in the training data. Nonetheless, the predictions align well with the general trend, indicating a good overall performance.

The model performs well in capturing the overall trend of the light vehicle speed v_L, but it struggles with accurately predicting the local fluctuations as can be seen in the right part of Fig. 6(c). This could be attributed to the choice of a 168-h periodicity for modelling the seasonality, which fails to account for the finer, more localized oscillations in light vehicle speeds. As indicated by the relatively low explained variance of around 52%, the model does not fully capture the complexity of the underlying dynamics at shorter time scales. Traffic patterns, especially for light vehicles, may exhibit more intricate, possibly daily or sub-daily variations, which are not well represented by a purely weekly seasonality. Moreover, the temporary drop in light vehicle mean speeds observed on the morning of July 27, 2004, remains unexplained, although it coincides with an unusual increase in the speed of heavy vehicles. This pattern could potentially be linked to a temporary disruption in traffic flow, such as the presence of a construction site or a lane closure, which may have created a bottleneck for light vehicles while allowing heavy vehicles to maintain or even increase their speeds. Moreover, this sudden drop in light vehicle speeds could have influenced the predictive model, as the model might not have been able to account for such a sharp and localized anomaly, thus affecting its overall performance. Without additional contextual data or real-time traffic information, it remains difficult to definitively pinpoint the cause of this anomaly. However, it is worth underlying that, while the model may not fully explain local fluctuations, it is still able to reflect the broader traffic patterns with reasonable accuracy.

The model seems to capture the broad patterns of heavy vehicles speed fluctuations well as shown in Fig. 6(d). However, there are some significant discrepancies which suggest that the model may need further refinement to handle data better, although it still provides a reasonable estimate of the overall speed trend.

While the visual comparison of the observed and predicted time series provides a useful qualitative assessment of the model's performance, it is important to take into account also error metrics. In Tables V and VI, the most relevant residuals and error metrics for each traffic variable, e.g., ME, MAE, RMSE, and MAPE, are presented, respectively for the calibration and validation dataset, providing a quantitative assessment of the model's performance.

For light vehicle flow (N_L), the model shows almost no bias during calibration, with a ME close to zero (0.075 vehicles/h). The MAE (46.35 vehicles/h) and the RMSE (84.96 vehicles/h) indicate moderate residual variability, while the MAPE of 11.66% reflects the high dispersion and presence of extreme values in the data. However, in the validation phase, the ME increases substantially, revealing a tendency to underestimate, which aligns with the high variability of the data shown previously in Table II. The MAE and RMSE also rise significantly (122.55 and 208.82 vehicles/h, respectively), suggesting that the model struggles with extreme fluctuations. The MAPE reaches 28.44%, but this can be attributed to the significant variability in the traffic flow, with the presence of outliers likely inflating the error percentage as can be seen in the right part of the relative graph.

As for the heavy vehicle flow N_H, the ME remains very low in both calibration (0.016 vehicles/h) and validation (−3.11 vehicles/h), however indicating a slight overestimation. The MAE and RMSE are stable between the two phases suggesting consistent performance. However, it needs to be underlined that the MAPE is not interpretable due to division by zero values, a known issue when using this metric on traffic datasets with sparse or null flows.

Regarding speed predictions, the model demonstrates strong performance for both vehicle classes. For the light vehicle mean speed v_L, the ME during calibration is essentially zero, with low MAE (1.91 km/h), RMSE (2.68 km/h), and MAPE (1.63%), confirming accurate estimates. In the validation period, although the ME increases slightly to −0.54 km/h, the MAE and RMSE (2.59 and 4.71 km/h) remain within acceptable ranges. The MAPE increases moderately to 2.33%, indicating a small reduction in performance but still reflecting good predictive accuracy.

04 April 2026 14:08:15

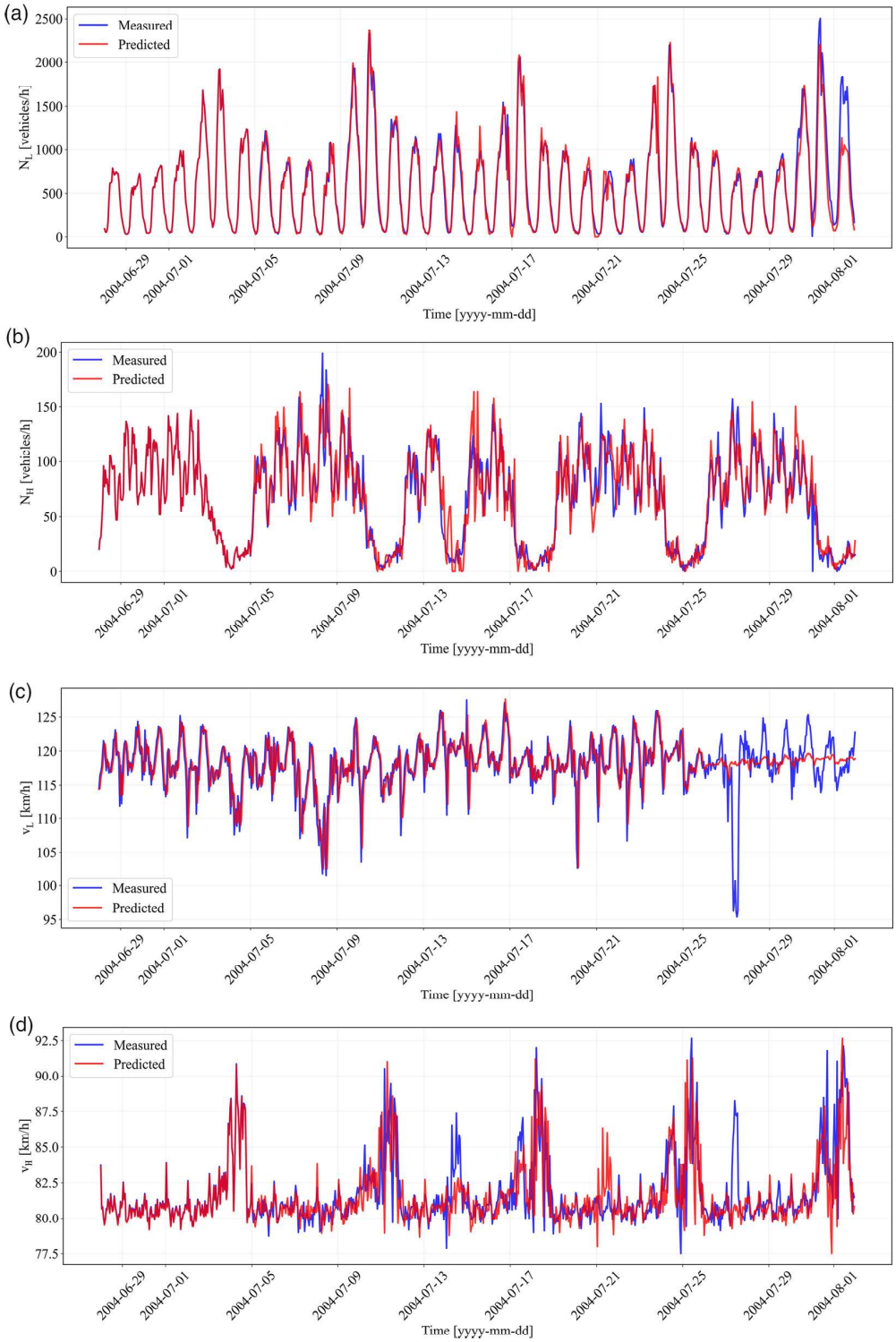


FIG. 6. Overlapping time series of measured (blue) and predicted (red) values from June 28th to August 1st, 2004 for (a) light vehicle flows (N_L), (b) heavy vehicle flows (N_H), (c) light vehicle mean speeds (v_L), and (d) heavy vehicle mean speeds (v_H).

Similarly, heavy vehicle speed v_H is well predicted in both phases. The ME remains small (0.026 km/h in calibration and 0.665 km/h in validation), and both MAE and RMSE remain low (ranging from 0.9 to 1.4 km/h and 1.7 to 2.4 km/h, respectively). The MAPE values, 1.09% in calibration and 1.68% in validation, confirm the model's ability to produce reliable speed estimates even outside the training set.

04 April 2026 14:08:15

https://doi.org/10.1121/10.0043155

TABLE V. Residuals metrics for the selected models (calibration dataset).

Variable	ME	MAE	RMSE	MAPE
N_L	0.07	46.35	84.96	11.66%
N_H	0.02	9.62	15.19	inf
v_L	0.00	1.90	2.68	1.63%
v_H	0.03	0.90	1.68	1.09%

TABLE VI. Error metrics for the selected models (validation dataset).

Variable	ME	MAE	RMSE	MAPE
N_L	98.51	122.55	208.82	28.44%
N_H	−3.11	10.71	14.33	Inf
v_L	−0.54	2.60	4.71	2.33%
v_H	0.66	1.42	2.38	1.68%

In summary, the model performs well in capturing the dynamics of vehicle speed and heavy vehicle flow across both datasets. However, a noticeable decrease in accuracy is observed for light vehicle flow in the validation phase, suggesting the need for further improvements, particularly in the case of extreme values for light and heavy vehicle flows.

B. Stochastic microscopic road traffic noise model: Results and assessment

In this section, the results of the road traffic noise model, as predicted using the stochastic approach using traffic inputs retrieved from the time-series forecasting models discussed earlier, are presented.

Figure 7 shows a comparison of the continuous equivalent sound level $L_{A,eq,1h}$ over time, plotted during the validation week, between the measured (blue) and simulated (red) noise levels. The measured data are characterized by gaps mainly present during nighttime, due to periods when measurements were not available, while the simulated data are continuously available throughout the week, as the input traffic data derived from time-series forecasting models are consistently present for the simulation. Overall, this comparison highlights the strengths and limitations of the hybrid modelling approach. Measured and simulated data, indeed, exhibit similar temporal patterns, with notable peaks and troughs occurring throughout the days, reflecting the diurnal variations in traffic flow and the corresponding fluctuations in noise levels.

However, while the simulation consistently tracks the overall trends and captures the diurnal fluctuations in traffic noise, there are periods where it diverges from the measured values. Such divergence is expected, as the hybrid model relies on two sequential models, meaning that errors from the first model (time-series forecasting) propagate into the second (stochastic traffic noise model). As such, further calibration of both models may be necessary, particularly to refine the noise predictions during extreme cases as either very low-traffic or peak hours. Nevertheless, this comparison underscores the value of time-series forecasting for generating continuous traffic inputs, which enables noise level predictions even in the absence of direct measurements.

Figure 8 shows the $L_{A,eq,1h}$ boxplots for both the measured (blue) and the simulated (red) data, while their quartiles and main statistics are provided in Tables VII and VIII.

The simulated data exhibit a wider interquartile range compared to the measured data, suggesting that the model predicts more variability in noise levels, capturing a wider spectrum of noise fluctuations even if introducing a level of uncertainty. Additionally, this increased variability could be a result of cascading errors from the time-series forecasting model, as stated earlier, which may propagate through to the noise prediction, amplifying the overall uncertainty in the simulated data.

Moreover, while both datasets display similar median values, as also reported in Table VIII, the simulated data show no outliers, while the measured data include a few, indicating rare extreme noise events. The absence of outliers

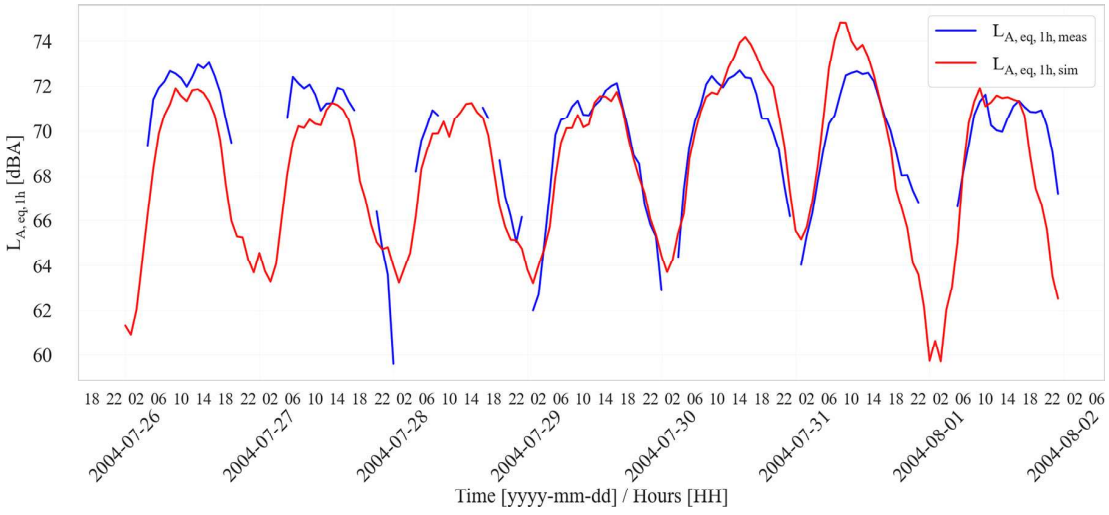


FIG. 7. Overlapping time series of measured (blue) and predicted (red) $L_{A,eq,1h}$ values from July 26th to August 1st, 2004.

04 April 2026 14:08:15

TABLE VII. $L_{Aeq,1h,meas}$ and $L_{Aeq,1h,sim}$ significant quartiles.

	25th quart. [dBA]	50th quart. [dBA]	75th quart. [dBA]
$L_{Aeq,1h,meas}$	68.5	70.69	71.82
$L_{Aeq,1h,sim}$	65.43	69.58	71.26

in the simulated data suggests that the model might not be sensitive to unusual traffic events, which are, however, characteristic of real-world conditions. Thus, the model may not fully capture the unpredictability of traffic noise, highlighting the need for further model refinement to improve its sensitivity to extreme fluctuations.

Similar insights can be retrieved from the scatterplot shown in Fig. 9, where the simulated continuous equivalent noise levels are plotted against the corresponding measured values. The red solid line represents the ideal bisector line, indicating where the points would lie if the model perfectly matched reality. The majority of points fall within the ±2 dBA range from this line, shown by the black dashed lines, with 81.2% of the points lying within this range. This highlights that the noise model's predictions are generally consistent with the observed data, with minor overestimations or underestimations.

Further observations can be made by observing the graph in Fig. 10, which represents the error histogram of the hybrid model, and by analysing the values reported in Tables IX and X, which summarise all the hybrid model error statistics, providing significant insights into the performance of the model itself and its capability to predict road traffic noise levels.

It can be noticed that the majority of the errors, computed as the difference between measured and simulated levels, are clustered around 0 dBA, indicating that the model's predictions are generally close to the observed data. The skewness of 0.23, which is relatively small, suggests that the distribution of errors is fairly symmetric. However, the ME of 0.43 dBA and the median error of 0.51 dBA imply that there is a slight tendency for the model to overestimate the continuous equivalent noise levels, even if such a small difference confirms that the distribution of errors is not heavily influenced by extreme values, as also confirmed by the low value of skewness. Moreover, the error's standard deviation of 1.63 dBA suggests that while the model's predictions are generally close to the observed data, there are occasional significant deviations, which is also confirmed by the error range of almost 10 dBA. However, the presence of outliers in both the negative and positive directions, with some predictions deviating significantly from the measured data, suggests that the model does not systematically either overestimate or underestimate. While the model is

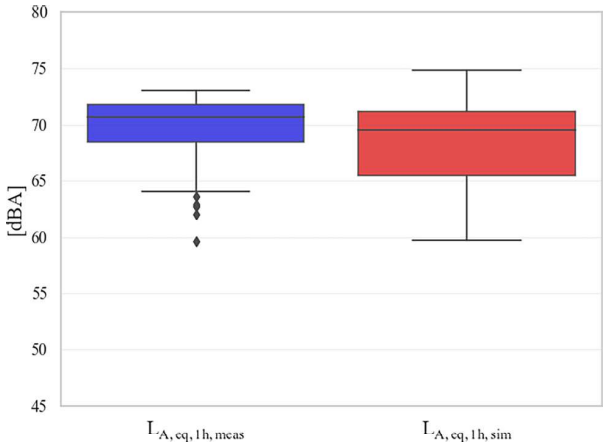


FIG. 8. Boxplots of the $L_{A,eq,1h}$ as measured (blue) and as simulated (red).

reasonably accurate, it still occasionally fails to capture noise levels accurately, particularly under specific or dynamic traffic conditions.

Even more interesting is the plot in Fig. 11 in which it is possible to visualize how the errors vary over time. The plot includes several important statistical lines, including the ME (red dashed line), the median error (blue dashed line), and the MAE (gray dashed lines). It needs to be underlined that, also in this case, the gaps in the plot are attributable to the absence of measured data during certain time intervals.

A noticeable trend is that, aside from the initial part of the graph, corresponding to June 26th, the larger error peaks predominantly occur during the nighttime hours. This suggests that the model's predictions tend to deviate more during periods of lower traffic activity, which may be influenced by reduced or more sporadic traffic data input during those times. On the other hand, high error values can also be observed during the last three days of measurements, from Friday to Sunday. This could reflect increased traffic activity during the weekend, which the model may struggle to predict accurately due to the dynamic nature of traffic flow or other external factors not fully captured by the model, as also commented earlier.

Last, the error metrics are presented in Table XI, in order to achieve a full comprehension of the hybrid model's predictive capabilities.

The MAE of 1.30 dBA is a reasonable error when predicting environmental noise, suggesting that the model is fairly accurate for its purpose. However, the observed discrepancy between the MAE and the RMSE (1.69 dBA) indicates that the model is sensitive to a small number of time intervals with higher predictive errors, likely stemming from the extreme fluctuations in light vehicle traffic recorded

TABLE VIII. $L_{Aeq,1h,meas}$ and $L_{Aeq,1h,sim}$ summary statistics.

	Mean [dBA]	Std dev. [dBA]	Min. value [dBA]	Max. value [dBA]	Skewness	Kurtosis
$L_{Aeq,1h,meas}$	69.82	2.67	59.62	73.03	−1.30	1.31
$L_{Aeq,1h,sim}$	68.46	3.51	59.72	74.82	−0.41	−0.81

04 April 2026 14:08:15

https://doi.org/10.1121/10.0043155

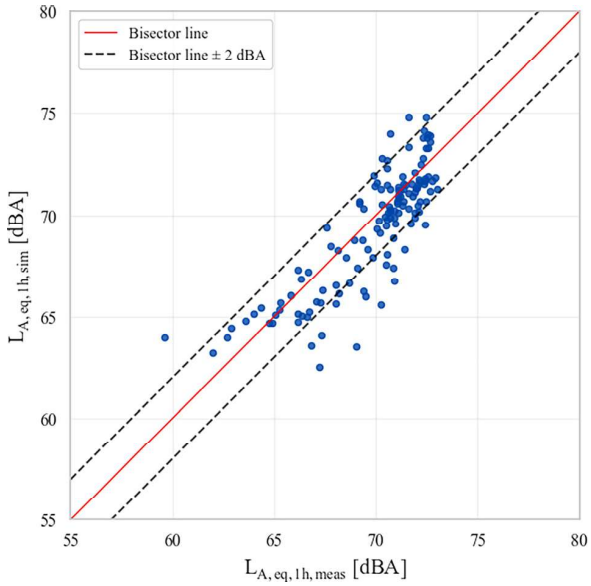


FIG. 9. Scatter plot of simulated noise level versus the corresponding measurements.

during the final validation weekend. This "penalty" in the squared error metric reflects the challenge of forecasting holiday-related traffic spikes that deviate from the historical seasonal trend. This is also confirmed by the MSE of 2.85 dBA,[2] which gives more weight to larger errors and provides a more sensitive measure to larger discrepancies reflecting the overall squared deviation of the model's predictions from the observed data. The MPE of 0.60% and the MAPE of 1.88% are very low percentages, indicating that, on average, the model's predictions are very close to the actual values when expressed relative to the measured data. This small percentage error suggests that the model is highly reliable on average, with only minor discrepancies when compared to the observed noise levels.

V. COMPARATIVE PERFORMANCE ANALYSIS

To contextualize the performance of the proposed hybrid model, this section provides a comparative analysis against two alternative modelling approaches. The first comparison benchmarks the hybrid model against the core stochastic model when supplied only with measured traffic data, thereby isolating the impact of the time-series forecasting component and such two-step modelling chain. The primary innovation of the presented work, indeed, is the integration of a time-series forecasting module to enable noise prediction in the absence of real-time traffic data. Thus, to quantify the impact of this hybridization, the stochastic microscopic model has been re-run for the validation period only (26 July to 1 August 2004) using the actual measured traffic inputs, e.g., flows and mean speeds for each considered vehicle's category, instead of the SARIMA-forecasted values. This allows for a direct assessment of the error introduced by the time-series forecasting step.

TABLE IX. Errors significant quartiles.

	25th quart. [dBA]	50th quart. [dBA]	75th quart. [dBA]
Errors	−0.60	0.51	1.37

The second comparison, on the other hand, evaluates the hybrid model against the established CNOSSOS-EU framework, in order to highlight the benefits of a microscopic approach over a more conventional, macroscopic methodology.

Figure 12 provides a visual comparison between the time histories of the measured noise levels and the predictions from both the hybrid (red line), the stochastic (green line), and the CNOSSOS-EU (gray line) models over the validation week.

As depicted in the figure, all simulation frameworks successfully capture the characteristic diurnal pattern of traffic noise, with levels rising during the day and falling at night, confirming the fundamental validity of each approach. However, a closer inspection reveals significant differences in their performance and accuracy. The microscopic approaches seem to be more accurate than the macroscopic approach represented by the CNOSSOS-EU formula, being able to follow more correctly the measured noise levels patterns. The CNOSSOS model's systematic underestimation, indeed, can be attributed to its macroscopic approach, which

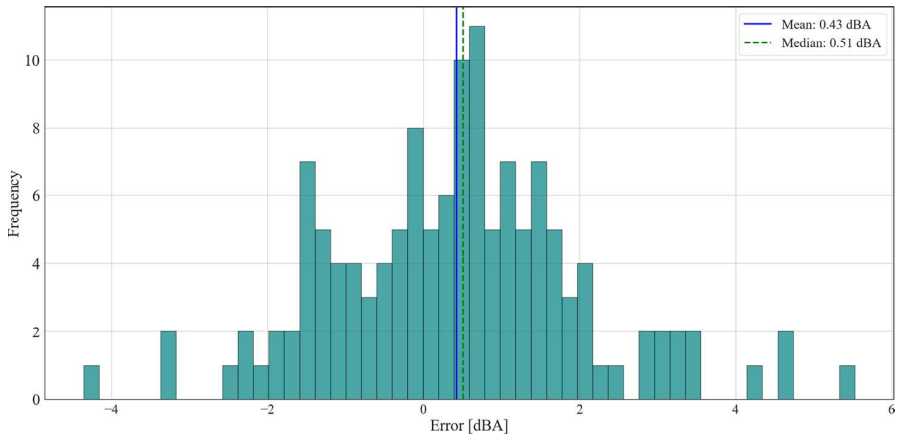


FIG. 10. Errors' histogram.

04 April 2026 14:08:15

TABLE X. Errors summary statistics.

	Mean [dBA]	Std dev. [dBA]	Min. value [dBA]	Max. value [dBA]	Skewness	Kurtosis
Errors	0.43	1.63	−4.35	5.53	0.23	0.68

relies on averaged inputs and may not fully capture the acoustic energy of the most intense, short-term traffic events that the microscopic model is designed to simulate.

The stochastic model shows good adherence to the measured data, where available, confirming the high intrinsic accuracy of the core stochastic noise simulation engine when provided with precise traffic inputs. An insightful event is observed on July 31st, where an anomalous, sharp dip appears in the predictions of both the stochastic-only and CNOSSOS models. This dip is attributable to the difference between the measured and forecasted input values, which are very far apart for that hour, being significantly lower for the measured both light vehicles and heavy vehicles flows than the predicted ones. This occurrence highlights a critical distinction between real-time monitoring and predictive forecasting. While the forecasting component of the hybrid model proved resilient to this specific input outlier, effectively "smoothing" the acoustic curve to produce a more plausible noise estimation, it is important to categorize this behavior as statistical robustness rather than absolute accuracy. In this instance, the forecasting model is structurally "blind" to non-periodic anomalies, such as the identified sensor maintenance gap or potential temporary road disruptions, that are clearly not reflected in historical weekly patterns. Consequently, while the hybrid framework provides a reliable tool for planning and general environmental assessment where real-time data is unavailable, it does not replace the need for direct measurements when capturing unique, non-recurring acoustic events or sudden micrometeorological shifts is required.[73]

Observing the surrounding data, that specific hour could be associated with an erroneous data point within the measured traffic input stream. In particular, high values of traffic flows, both light and heavy vehicles, are observed immediately before and after, and the noise level is actually missing only in such a particular hour, suggesting a maintenance of the measuring stations or a removal of the measured sound level due to the concurrence of external noise sources. Notably, the hybrid model's forecasting component proved resilient to this input outlier, producing a more plausible noise estimation and highlighting a key advantage of its approach in handling erroneous data.

A closer analysis of the final day of the validation period reveals a more nuanced aspect of models' performances. On August 1st, the hybrid approach exhibits a closer correspondence with the measured data than the fully stochastic approach, even if a strong underestimation has been noticed in the light vehicle flow predictions. This may suggest either that the cascading error expected to be introduced by the double-chain model does not emerge under these conditions or that the hybrid framework is capable of mitigating, at least in part, the propagation of model inaccuracies across successive stages. Nevertheless, it is crucial to recognize that the apparent improvement in predictive accuracy could also result from a compensatory mechanism, whereby errors generated in different components of the model partially offset one another, thus leading to an overall reduction in the discrepancy with the empirical data. It is plausible that this initial underestimation of light vehicle flows

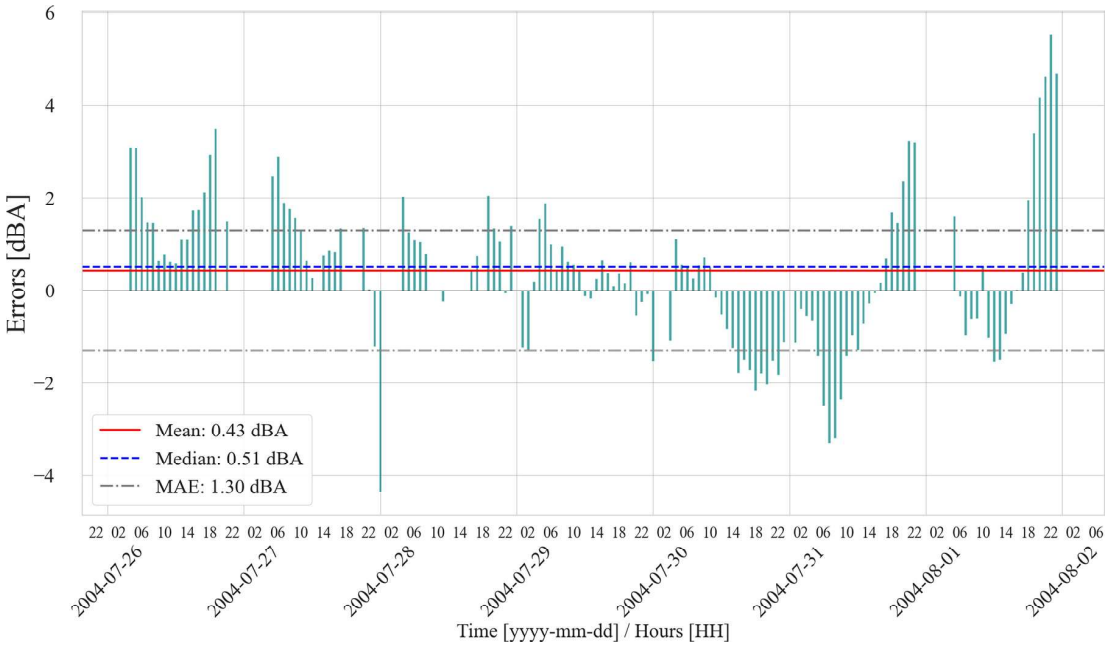


FIG. 11. Errors' time history.

04 April 2026 14:08:15

https://doi.org/10.1121/10.0043155

TABLE XI. Summary error metrics of the hybrid model.

ME [dBA]	MAE [dBA]	MPE. [%]	MAPE [%]	MSE [dBA^2]	RMSE [dBA]
0.43	1.30	0.60	1.88	2.85	1.69

contributes to a compensatory mechanism that offsets the general modeling error, thereby yielding a seemingly improved agreement with the measured sound levels. Moreover, even if the temporal trend of the predicted noise levels aligns more closely with the measurements, the residual discrepancies remain significant, as clearly illustrated in Fig. 11.

Finally, Table XII provides a quantitative summary of the error metrics, allowing for a direct comparison of the different approaches' performance. The hybrid model emerges as the most accurate predictor overall. This is evidenced by its superior performance across the primary accuracy metrics, achieving the lowest MAE, MAPE, and RMSE. Furthermore, it displays the lowest standard deviation of the error, indicating that its predictions are the most consistent. In particular, the reported MAE of 1.30 dBA for the hybrid model represents a significant improvement over the established CNOSSOS-EU benchmark, which exhibits a notably higher MAE of 2.06 dBA under the same conditions. This underscores the advantage of microscopic modelling over conventional macroscopic approaches in accurately capturing the acoustic energy generated by discrete traffic events.

This better performance, even when compared to the model fed with measured data, can be attributed to the forecasting component's resilience to anomalies in the input traffic data, which prevents large, isolated errors and results in a more stable and reliable overall prediction. However, it is important to acknowledge a key limitation of this analysis: the comparison is inherently constrained to the time intervals for which measured noise data are available. Given the significant gaps in the acoustic dataset, particularly during nighttime hours, the calculated error metrics may not fully represent the model's performance across all operating conditions. It is therefore possible that the true overall error could differ if a complete validation dataset were accessible for comparison.

While the potential for error compensation and the limitations imposed by gaps in the validation data must be carefully considered, the hybrid framework's performance confirms it as a highly effective and practical tool. In particular, the hybrid framework seems to be well-suited for forward-looking applications where real-time data is inherently unavailable. This includes critical tasks in urban and infrastructure planning, designing and evaluating the potential effectiveness of noise mitigation strategies before construction, and performing analyses to explore the acoustic consequences of changes in traffic management policies. The model, therefore, represents a valuable step forward, providing planners and engineers with a reliable method for proactive noise assessment.

VI. PRACTICAL IMPLICATIONS AND FUTURE DEVELOPMENTS

The hybrid framework presented in this study offers immediate practical implications for environmental noise management. By integrating SARIMA forecasting with a microscopic stochastic engine, high-fidelity noise assessment could be achieved for existing infrastructures even when real-time telemetry is interrupted or unavailable. This reduces the reliance on continuous, expensive measurement campaigns, allowing for high-quality acoustic monitoring based on a standard workstation's computational power. Beyond simple estimation, the model could be used as a diagnostic decision-support system: since the framework is calibrated on longitudinal seasonal cycles, any significant

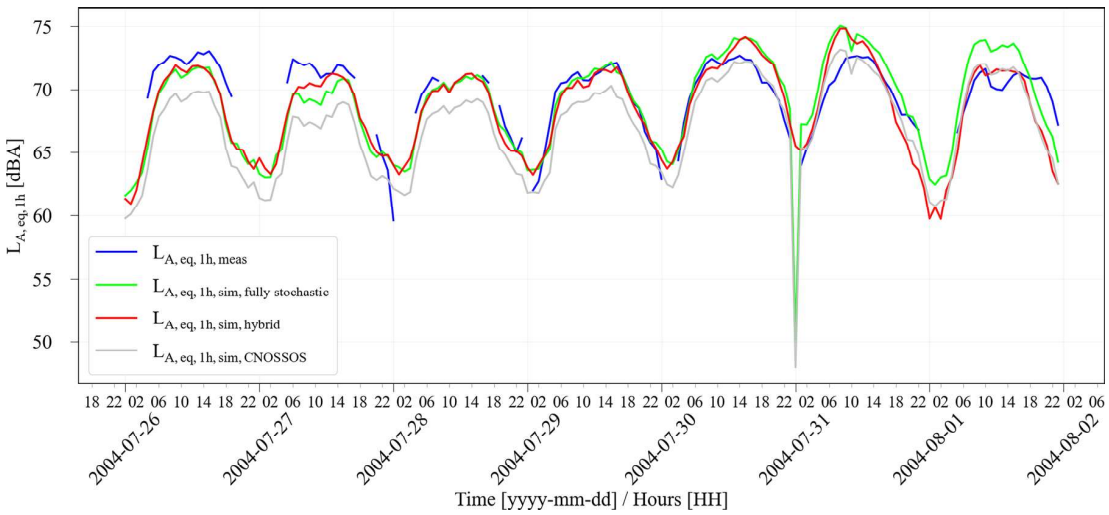


FIG. 12. Overlapping time series of measured (blue), hybrid model predicted (red), and fully stochastic model predicted (green) $L_{A,eq,1h}$ values from July 26th to August 1st, 2004.

04 April 2026 14:08:15

TABLE XII. Summary error metrics of the compared model.

Model used	ME [dBA]	Std dev [dBA]	MAE [dBA]	MPE. [%]	MAPE [%]	MSE [dBA^2]	RMSE [dBA]
Fully stochastic model	−0.15	1.84	1.52	−0.24	2.18	3.42	1.85
Hybrid model	0.43	1.63	1.30	0.60	1.88	2.85	1.69
CNOSSOS-EU model	1.71	1.83	2.06	2.43	2.94	6.30	2.51

divergence from real-time observations acts as an informative trigger. This discrepancy enables authorities and infrastructure managers to identify non-periodic disruptions or unconventional events, effectively distinguishing them from standard cyclical patterns.

The most significant future development of this research concerns the data-scarcity issue in the design phase of new infrastructures. Since historical data are inherently absent for non-existent roads, the next research milestone will be to investigate the transferability of seasonal traffic patterns. The goal is to evaluate whether historical traffic structures from an existing "proxy" site (sharing the same road category and functional classification) can be successfully used as an input for the hybrid model to predict the noise impact of a planned infrastructure. Validating this "pattern-transfer" methodology is essential to transforming the framework into a proactive design tool.

Furthermore, future iterations will explore the inclusion of additional external factors (e.g., local weather conditions or holiday calendars) to improve the forecasting of non-seasonal traffic anomalies that deviate from regular seasonal trends. In this context, while the SARIMA architecture was selected for the present study due to its optimal balance between statistical interpretability and seasonal robustness, future research could evaluate the integration of alternative forecasting algorithm. Testing machine learning or deep learning methodologies, such as long short-term memory networks, would provide a valuable comparative benchmark to evaluate the trade-offs between predictive precision and computational complexity within the hybrid modelling chain.

Ultimately, by converting historical patterns into prognostic intelligence and predictive misalignments into diagnostic triggers, this methodology have the potentialities to transform the challenge of data scarcity into a strategic asset for more resilient, responsive, and sustainable urban planning.

VII. CONCLUSIONS

In this paper, a hybrid modelling framework that combines time-series forecasting with a stochastic microscopic road traffic noise model has been presented.

The goal of the research activities was to establish a hybrid modelling framework that integrates time-series forecasting with stochastic microscopic traffic noise simulation. While the presented methodology is adaptable to scenarios in which measurement campaigns can be done and thus data is available, the broader objective was to develop a methodology still useful when data are scarce or even in predictive scenarios, such as during the design phase of transport infrastructure.

By integrating the temporal structure captured through SARIMA forecasting modelling with the detailed emission modelling of the stochastic approach,[48] both the traffic random phenomenon and its acoustic dynamics have been effectively reproduced.

Moreover, the presented approach is very adaptable and versatile, as the two main parts of the hybrid model itself, one regarding the time-series forecasting of traffic inputs and the other considering the stochastic microscopic road traffic noise model, can be adapted by the user according to whatever the specific conditions of the case study are.

The validation of the hybrid model has been performed on a large dataset available upon request to the authors of Ref. 69, the same used to validate the stochastic model, even if for computational reasons, just a part of it has been successfully used. The dataset regards road traffic noise levels measured in a free-flow highway condition, during a period of five weeks in the summer of 2004. The findings confirm that this approach not only enhances the representation of temporal traffic dynamics through SARIMA-based forecasting but also incorporates stochastic variability at the vehicle level, thereby providing more realistic noise predictions.

A strong influence of weekly periodicity has been found for both light and heavy vehicle flows, while a slightly lower influence of such periodicity has been found for their mean speeds. SARIMA model performance has been investigated for each time series, providing both graphs and error metrics for each model, revealing that the model performs well in predicting both traffic flow and vehicle speed, even if some areas where improvements could be made have been noticed, particularly in the case of extreme values for light and heavy vehicle flows.

The time-series predictions have been then used as traffic input to the stochastic road traffic noise model, leading to an enhanced predictive capacity, with simulated equivalent noise levels aligning more closely with measured data. In particular, the hybrid approach achieved MAEs below 1.5 dBA and root mean squared errors (RMSE) around 2 dBA, thereby showing good outcomes in terms of accuracy and robustness, highlighting the benefits of reproducing the temporal dynamics of traffic flows and adopting a microscopic perspective to simulate noise levels.

Nevertheless, the hybridization strategy inherits some of the inherent limitations of its components. The stochastic component is constrained by the assumption of constant speed values, which does not fully reflect the complexity of

04 April 2026 14:08:15

real driving conditions, particularly when taking into account accelerations and decelerations. Moreover, some limitations of the stochastic approach, mainly regarding the propagation assessment, i.e., the sum of *SEL*s produced by each vehicle transit at the receiver, which could lead to noise level overestimations with high flow occurrences and the background noise that is not taken into consideration at this stage, may affect the outcomes of this analysis. At the same time, the two-step modelling chain implies that uncertainties from the time-series forecasting of traffic inputs inevitably propagate into the acoustic simulations, introducing compounded errors that can reduce reliability under particularly variable conditions.

Despite these limitations, the proposed methodology demonstrates clear advantages in adaptability and predictive accuracy. It represents a step forward toward more integrated frameworks capable of reflecting both the temporal and stochastic nature of traffic noise phenomena. Future developments will focus on a more detailed examination of dataset characteristics, such as the influence of the number of 15-min intervals with valid acoustic measurements within each hourly record, and how this factor affects model errors. Comparative analyses will also be undertaken to evaluate the performance of the hybrid framework against the stochastic model applied directly to the available traffic data, without the integration of time-series forecasts.

A crucial line of development will be to assess whether a model calibrated on a data-rich case study can reliably predict noise dynamics in comparable contexts, characterized by similar infrastructure and traffic loads, thereby enhancing its applicability to scenarios where only limited or no measurements are available, such as the design phase of new transport infrastructures, providing a solid foundation for more reliable environmental noise assessment in real-world contexts.

ACKNOWLEDGMENTS

This study was carried out within the MOST–Sustainable Mobility National Research Center and received funding from the European Union Next-GenerationEU (PIANO NAZIONALE DI RIPRESA E RESILIENZA (PNRR)–MISSIONE 4 COMPONENTE 2, INVESTIMENTO 1.4–D. D. 1033 17/06/2022, CN00000023). This manuscript reflects only the authors' views and opinions; neither the European Union nor the European Commission can be considered responsible for them.

AUTHOR DECLARATIONS

Conflict of Interest

The authors have no conflicts to disclose.

DATA AVAILABILITY

The data that support the findings of this study are available in Ref. 69.

[1]European Environment Agency, "Exposure of Europe's population to environmental noise" (2017).
[2]European Environment Agency, "Environmental noise in Europe—2020," Publications Office of the European Union, Luxembourg (2020).
[3]European Parliament, Council of the European Union, "Living well, within the limits of our planet: The 7th EAP (2014-20)" (2013).
[4]European Environment Agency, "Noise in Europe 2014," EEA Report No. 10/2014 (2014).
[5]T. Münzel, F. P. Schmidt, S. Steven, J. Herzog, A. Daiber, and M. Sørensen, "Environmental noise and the cardiovascular system," JACC **71**(6), 688–697 (2018).
[6]T. Münzel, A. Daiber, N. Engelmann, M. Röösli, M. Kuntic, and J. L. Banks, "Noise causes cardiovascular disease: It's time to act," J. Exposure Sci. Environ. Epidemiol. **35**(1), 24–33 (2025).
[7]European Commission, "Links between noise and air pollution and socio-economic status," In-depth Report No. 13, Science for Environment Policy (2016).
[8]K. V. Weyde, N. H. Krog, B. Oftedal, P. Magnus, S. Øverland, S. Stansfeld, M. J. Nieuwenhuijsen, M. Vrijheid, M. de Castro Pascual, and G. M. Aasvang, "Road traffic noise and children's inattention," Environ. Health **16**(1), 127 (2017).
[9]L. Pérez-Crespo, M. López-Vicente, A. Valentín, M. Burgaleta, M. Foraster, H. Tiemeier, and M. Guxens, "Association between residential exposure to road traffic noise and cognitive and motor function outcomes in children and preadolescents," Environ. Int. **183**, 108414 (2024).
[10]A. M. Dzhambov, P. Lercher, and D. Botteldooren, "Childhood sound disturbance and sleep problems in Alpine valleys with high levels of traffic exposures and greenspace," Environ. Res. **242**, 117642 (2024).
[11]A. Muzet, "Environmental noise, sleep and health," Sleep Med. Rev **11**(2), 135–142 (2007).
[12]O. Hahad, J. H. Prochaska, A. Daiber, and T. Muenzel, "Environmental noise-induced effects on stress hormones, oxidative stress, and vascular dysfunction: Key factors in the relationship between cerebrocardiovascular and psychological disorders," Oxid. Med. Cell. Longevity **2019**, 623109 (2019).
[13]B. Berglund, T. Lindvall, and D. H. Schwela, "Guidelines for community noise" (1999).
[14]WHO Europe, *Night Noise Guidelines for Europe* (World Health Organization, Copenhagen, Denmark, 2009).
[15]World Health Organization, *Environmental Noise Guidelines for the European Region* (World Health Organization, Geneva, Switzerland, 2018).
[16]C. Clark and K. Paunovic, "WHO Environmental Noise Guidelines for the European Region: A systematic review on environmental noise and cognition," Int. J. Env. Res. Public Health **15**(2), 285 (2018).
[17]World Health Organization, *Burden of Disease From Environmental Noise: Quantification of Healthy Life Years Lost in Europe* (World Health Organization, Geneva, Switzerland, 2011).
[18]M. Basner and S. McGuire, "WHO environmental noise guidelines for the European region: A systematic review on environmental noise and effects on sleep," Int. J. Env. Res. Public Health **15**(3), 519 (2018).
[19]European Commission, Directorate-General for Environment, "EU Action Plan: Towards Zero Pollution for Air, Water and Soil," COM **400**, 22 (2021).
[20]C. Guarnaccia, A. Mascolo, P. Aumond, A. Can, and D. Rossi, "From early to recent models: A review of the evolution of road traffic and single vehicles noise emission modelling," Curr. Pollut. Rep. **10**(4), 662–683 (2024).
[21]Department of Transport (UK), "Calculation of road traffic noise" (1988).
[22]D. B. Für Verkehr, "Richtlinien für den Lärmschutz an Straßen RLs 90" ("Guidelines for noise protection on roads RLs 90") (1990).
[23]G. B. Cannelli, K. Glück, and S. Santoboni, "A mathematical model for evaluation and prediction of the mean energy level of traffic noise in Italian towns," Acta Acust. united Ac. **53**(1), 31–36 (1983).
[24]T. Suksaard, P. Sukasem, S. M. Tabucanon, I. Aoi, K. Shirai, and H. Tanaka, "Road traffic noise prediction model in Thailand," Appl. Acoust. **58**(2), 123–130 (1999).
[25]G. Dutilleux, J. Defrance, D. Ecotière, B. Gauvreau, M. Bérengier, F. Besnard, and E. L. Duc, "NMPB-routes-2008: The revision of the French method for road traffic noise prediction," Acta Acust. united Ac. **96**(3), 452–462 (2010).
[26]K. Heutschi, "SonRoad: New Swiss road traffic noise model," Acta Acust. united Ac. **90**(3), 548–554 (2004).

04 April 2026 14:08:15

[27]Danish Environmental Protection Agency (EPA), "Nord2000: Nordic noise prediction method" (2020).
[28]G. G. Fleming, A. S. Rapoza, and C. S. Lee, "Development of national reference energy mean emission levels for the FHWA traffic noise model," FHWA TNM, version 1.0 (U.S. Federal Highway Administration, Washington, DC, 1995).
[29]S. Kephalopoulos, M. Paviotti, and F. Anfosso-Lédée, "Common noise assessment methods in Europe (CNOSSOS-EU)" (2012).
[30]Commission Delegated Directive (EU) of 21.12.2020 amending, for the purposes of adapting to scientific and technical progress, Annex II to Directive 2002/49/EC of the European Parliament and of the Council as regards common noise assessment methods.
[31]E. Ascari, M. Cerchiai, L. Fredianelli, D. Melluso, and G. Licitra, "Tuning user-defined pavements in CNOSSOS-EU towards reliable estimates of road noise exposure," Transp. Res. D: Transp. Environ. **130**, 104195 (2024).
[32]E. Ascari, M. Cerchiai, L. Fredianelli, D. Melluso, F. Rampino, and G. Licitra, "Decision trees and labeling of low noise pavements as support for noise action plans," Environ. Pollut. **337**, 122487 (2023).
[33]A. L. Montenegro, G. Rey-Gozalo, J. P. Arenas, and E. Suárez, "Streets classification models by urban features for road traffic noise estimation," Sci. Total Environ. **932**, 173005 (2024).
[34]G. Iannone, C. Guarnaccia, and J. Quartieri, "Speed distribution influence in road traffic noise prediction," Environ. Eng. Manag. J. **12**(3), 493–501 (2013).
[35]F. Li, H. Wang, C. Du, Z. Lan, F. Yu, and Y. Rong, "Probabilistic prediction model for expressway traffic noise based on short-term monitoring data," Sustainability. **16**(16), 6841 (2024).
[36]J. Khan, M. Ketzel, S. S. Jensen, J. Gulliver, E. Thysell, and O. Hertel, "Comparison of road traffic noise prediction models: CNOSSOS-EU, Nord2000 and TRANEX," Environ. Pollut. **270**, 116240 (2021).
[37]R. Benocci, A. Molteni, M. Cambiaghi, F. Angelini, H. E. Roman, and G. Zambon, "Reliability of Dynamap traffic noise prediction," Appl. Acoust. **156**, 142–150 (2019).
[38]R. Benocci, H. E. Roman, C. Confalonieri, and G. Zambon, "Investigation on clusters stability in DYNAMAP's monitoring network during COVID-19 outbreak," Noise Map **7**(1), 276–286 (2020).
[39]E. Chevallier, A. Can, M. Nadji, and L. Leclercq, "Improving noise assessment at intersections by modeling traffic dynamics," Transp. Res. D: Transp. Environ. **14**(2), 100–110 (2009).
[40]A. Can and P. Aumond, "Estimation of road traffic noise emissions: The influence of speed and acceleration," Transp. Res. D: Transp. Environ. **58**, 155–171 (2018).
[41]J. Heltimo, J. Niittymäki, and E. Björk, "A microlevel method for road traffic noise prediction," WIT Trans. Built. Environ. **60**, 10 (2002).
[42]S. Baclet, K. Khoshkhah, M. Pourmoradnasseri, R. Rumpler, and A. Hadachi, "Near-real-time dynamic noise mapping and exposure assessment using calibrated microscopic traffic simulations," Transp. Res. D: Transp. Environ. **124**, 103922 (2023).
[43]V. Le Bescond, A. Can, P. Aumond, and P. Gastineau, "Open-source modeling chain for the dynamic assessment of road traffic noise exposure," Transp. Res. D: Transp. Environ. **94**, 102793 (2021).
[44]B. De Coensel, D. Botteldooren, F. Vanhove, and S. Logghe, "Microsimulation based corrections on the road traffic noise emission near intersections," Acta Acust. united Ac. **93**(2), 241–252 (2007).
[45]C. Guarnaccia, U. Catherin, A. Mascolo, and D. Rossi, "Improvement and validation of a smart road traffic noise model based on vehicles tracking using image recognition: EAgLE 3.0," Sensors **25**(6), 1750 (2025).
[46]L. Fredianelli, S. Carpita, M. Bernardini, L. G. Del Pizzo, F. Brocchi, F. Bianco, and G. Licitra, "Traffic flow detection using camera images and machine learning methods in ITS for noise map and action plan optimization," Sensors **22**(5), 1929 (2022).
[47]D. Rossi, A. Mascolo, and C. Guarnaccia, "Calibration and validation of a measurements-independent model for road traffic noise assessment," Appl. Sci. **13**(10), 6168 (2023).
[48]A. Mascolo, D. Rossi, A. Ruggiero, and C. Guarnaccia, "A stochastic and microscopic model to predict road traffic noise by random generation of single vehicles' speeds," J. Acoust. Soc. Am. **157**(2), 721–737 (2025).
[49]F. Li, S. S. Liao, and M. Cai, "A new probability statistical model for traffic noise prediction on free flow roads and control flow roads," Transp. Res. D: Transp. Environ. **49**, 313–322 (2016).
[50]H. Wang, Z. Wu, and J. Chen, "A prediction method for city traffic noise based on traffic simulation under a mixed distribution probability," Sustainability **16**(16), 7065 (2024).
[51]M. S. Ahmed and A. R. Cook, "Analysis of freeway traffic time-series data by using Box-Jenkins techniques" (1979), p. 722.
[52]C. Guarnaccia, J. Quartieri, N. E. Mastorakis, and C. Tepedino, "Development and application of a time series predictive model to Acoustical noise levels," WSEAS Trans. Syst. **13**, 745–756 (2014).
[53]A. Pascale, S. Mancini, P. M. d'Orey, C. Guarnaccia, and M. C. Coelho, "Correlating the effect of Covid-19 lockdown with mobility impacts: A time series study using noise sensors data," Transp. Res. Proc. **62**, 115–122 (2022).
[54]I. K. Umar, M. Adamu, N. Mostafa, M. S. Riaz, S. I. Haruna, M. F. Hamza, O. S. Ahmed, and M. Azab, "The state-of-the-art in the application of artificial intelligence-based models for traffic noise prediction: A bibliographic overview," Cogent Eng. **11**(1), 2297508 (2024).
[55]L. Bravo-Moncayo, J. Lucio-Naranjo, M. Chávez, I. Pavón-García, and C. Garzón, "A machine learning approach for traffic-noise annoyance assessment," Appl. Acoust. **156**, 262–270 (2019).
[56]M. Y. Codur, A. Atalay, and A. Unal, "Performance evaluation of the ANN and ANFIS models in urban traffic noise prediction," Fresenius Environ. Bull. **26**, 4254–4260 (2017).
[57]D. Rossi, A. Pascale, A. Mascolo, and C. Guarnaccia, "Coupling different road traffic noise models with a multilinear regressive model: A measurements-independent technique for urban road traffic noise prediction," Sensors **24**(7), 2275 (2024).
[58]N. Garg, K. Soni, T. K. Saxena, and S. Maji, "Applications of Auto Regressive Integrated Moving Average (ARIMA) approach in time-series prediction of traffic noise pollution," Noise Cont. Eng. J. **63**(2), 182–194 (2015).
[59]N. Garg, M. K. Sharma, K. S. Parmar, K. Soni, R. K. Singh, and S. Maji, "Comparison of ARIMA and ANN approaches in time-series predictions of traffic noise," Noise Cont. Eng. J. **64**(4), 522–531 (2016).
[60]P. J. Brockwell and R. A. Davis, *Introduction to Time Series and Forecasting*, 3rd ed. (Springer, New York, 2016).
[61]G. E. Box, G. M. Jenkins, G. C. Reinsel, and G. M. Ljung, *Time Series Analysis: Forecasting and Control* (Wiley, New York, 2015).
[62]P. J. Brockwell and R. A. M. Davis, *Time Series: Theory and Methods* (Springer Science & Business Media, New York, 2009).
[63]G. Box and G. M. Jenkins, *Analysis: Forecasting and Control* (Holden-Day, San Francisco, CA, 1976).
[64]R. H. Shumway and D. S. Stoffer, *Time Series Analysis and Its Applications: With R Examples* (Springer, New York, 2006).
[65]G. Iannone, "Improvements in the acoustical modelling of traffic noise prediction: Theoretical and expérimental results," Ph.D. thesis, University of Salerno, Salerno, Italy (2011).
[66]D. Helbing, "Derivation and empirical validation of a refined traffic flow model," Phys. A **233**(1-2), 253–282 (1996).
[67]D. Helbing, "Empirical traffic data and their implications for traffic modeling," Phys. Rev. E **55**(1), R25–R28 (1997).
[68]D. Helbing, "Fundamentals of traffic flow," Phys. Rev. E **55**(3), 3735–3738 (1997).
[69]B. Gauvreau, "Long-term experimental database for environmental acoustics," Appl. Acoust. **74**(7), 958–967 (2013).
[70]J. Nygren, S. Boij, R. Rumpler, and C. J. O'Reilly, "Vehicle-specific noise exposure cost: Noise impact allocation methodology for microscopic traffic simulations," Transp. Res. D: Transp. Environ. **118**, 103712 (2023).
[71]French Government, "Lois et décrets (version papier numérisée) n° 21 du 25/01/1995 relatif à l'interdiction de circulation des véhicules de transport de marchandises" ("Laws and decrees No. 21 of 25/01/1995 relating to the prohibition of circulation of goods transport vehicles"), J. Officiel République Française.
[72]French Government, "Lois et décrets (version papier numérisée) n° 0302 du 31/12/2003 relatif aux interdictions complémentaires de circulation pour 2004 des véhicules de transport de marchandises et de transport de matières dangereuses" ("Laws and decrees No. 0302 of 31/12/2003 relating to additional prohibitions on the circulation for 2004 of vehicles transporting goods and dangerous goods"), J. Officiel République Française.
[73]R. J. Hyndman and G. Athanasopoulos, *Forecasting: Principles and Practice* (OTexts, Melbourne, Australia, 2018).

04 April 2026 14:08:15

DOI: 10.61782/fa.2023.0511

E

forum acusticum 2023

SOUNDSCAPE INDICATORS ASSESSMENT AND MAPPING IN A UNIVERSITY CAMPUS

A. Mascolo[1*] **D. Rossi**[1] **M. Grimaldi**[1]
C. Guarnaccia[1*]
[1] Department of Civil Engineering, University of Salerno, Italy

ABSTRACT

The acoustic environment of a University campus is very complex since it usually includes i) zones in which the quietness is very important, to foster concentration needed for working and studying, ii) parking lots and internal road networks, iii) vibrant areas, populated by students and personnel during free time. For this reason, the campuses can be a very interesting case study for testing soundscape analyses tools, as well as to perform research of innovative methodologies for soundscape assessment and mapping. In this paper, the Fisciano campus of the University of Salerno (Italy) is presented as a case study, in which several measurements have been performed. In particular, the results of a soundwalk performed according to the ISO TS 12913 will be presented, together with the data obtained in crowdsourcing mode, collected within the celebration of NoiseCapture parties, organized in the campus during the last years. The NoiseCapture app, in fact, allows to collect both the physical sound levels and the pleasantness rated by participants during the events. The available data of mean pleasantness recorded along the campus will give the chance to test new methodologies for mapping of the detected soundscape. In particular, an Inverse Distance Weighting (IDW) interpolation technique will be proposed and validated on the mean pleasantness measured during the soundwalk. The results will give interesting hints about the proposed methodology.

Keywords: *Soundwalk, GIS mapping, NoiseCapture app, sound perception, pleasantness.*

[*] ***Corresponding authors***: *{amascolo, cguarnaccia}@unisa.it*
Copyright: *©2023 A. Mascolo et al. This is an open-access article distributed under the terms of the Creative Commons Attribution 3.0 Unported License, which permits unrestricted use, distribution, and reproduction in any medium, provided the original author and source are credited.*

1. INTRODUCTION

The soundscape research is becoming more and more relevant in the scientific literature, thanks to a large awareness of the damages and risks deriving from living in noisy and annoying environments. Beside the development of new techniques for noise assessment and modeling, in fact, there is a large part of the acoustic community that is now turning on soundscape analyses to involve the subjective perception in their studies.

In this framework, the study of particular locations such as schools, universities, workplaces, vibrant areas, sport facilities, etc., is very important to highlight possible peculiarities in the soundscape, according to the land use and to the activities pursued in the site under study. There are several studies, for example, devoted to the investigation of the natural soundscape in parks or green areas. Uebel et al. provided more evidence to the idea that natural sounds can improve the quality of the perceived acoustic environment and even mask urban noises. In particular, their studies proved that the increase of natural sounds levels does not reduce the positive perception of the environment, differently from anthropic kinds of sounds. [1]. Liu et al. proposed questionnaire surveys to assess the relationship between soundscape perception and public visiting experience in the city parks, focusing on the changing of sound source characteristics in the urbanization process. [2].

Furthermore, a study by Masullo et al. assessed the possibility that even being surrounded by historical-artistic art forms could be just as relevant as a natural component for people's restorative capacity. [3]

The perceptive side was combined with the physical one in the research of Can et al. that proposed a procedure to physically describe and to categorize urban sound environments making it possible to determine particular

areas and periods remarkably suitable for stress recovery [4].
Also, the ecoacoustic soundscape studies are more and more developed, using sound recordings to calculate ecoacoustic indexes and to infer details about health quality of the natural area under study [5-6].
As for University campuses, some studies can be found in literature.
Puspagarini et al. reported how the soundscape in the campus of Yogyakarta, in Indonesia, was influenced both by anthrophony and natural sound sources, as any urban park. With respect to different locations, different sources were analyzed and found to be dominant, including animals and in particular insects, water sounds, road traffic noise and even human voices [7].
In [8], Aletta et al. estimated the willingness of users to stay in an open public space at the University of Sheffield (UK), measuring people staying time under different music stimuli and in a controlled condition.
In [9], the soundscape of the campus of Fisciano of the University of Salerno, Italy, was assessed by means of a soundwalk organized by some of the authors, using the recommendation reported in the ISO 12913–2 [10]. The results confirmed the expectations that the vibrant areas, as well as the small park in the campus, were the locations with the best soundscape in terms of appropriateness and willingness to return.
In [11], the same data has been used for a deeper investigation, including also a circumplex model 2D plane plot, that relates all the soundscape attributes and shows the relations among them.
In this paper, the authors propose a soundscape mapping of the campus of Fisciano, University of Salerno, based on pleasantness data recorded with a trained crowdsourcing technique. The data, in fact, are provided by students of the Engineering Departments, trained by some of the authors to provide reliable sound level measurements and assessment of the soundscape quality. Results will be compared with the data collected during the soundwalk activity and presented in [9] and [11], to validate the mapping procedure and to highlight strength points and/or possible shortcoming of the proposed methodology.

2. MATERIALS AND METHODS

In this paper a methodology to draw a soundscape map of the campus under study is presented, starting from the sound perception rating provided by the participants to 4 events at the University of Salerno (Figure 1), named after "NoiseCapture parties".

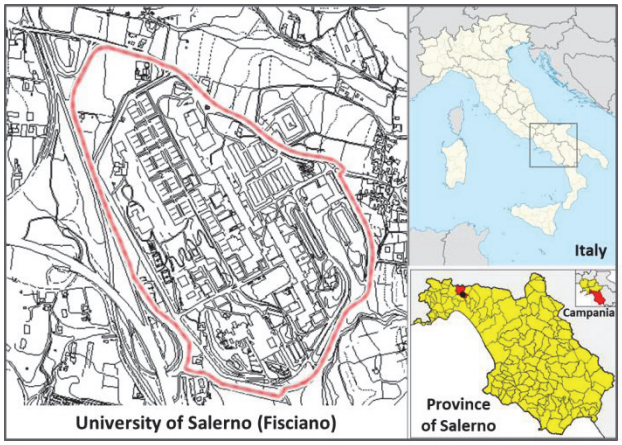


Figure 1. Location of the campus of Fisciano, University of Salerno [11]. Red line in the left plot is the Campus border.

These parties have been organized by some of the coauthors, under the patronage of the Noise-Planet project team [12], with the aim of spreading the noise awareness among future engineers (all the participants were students of engineering disciplines) and promoting the tools for environmental noise assessment developed within the project. Among these tools, in fact, the colleagues from Université Gustave Eiffel, CEREMA, UMRAE, France, developed the NoiseCapture app for Android, for measuring the sound levels with the mobile phone's microphone [13]. At the end of each measurement, the user can provide a rating of the pleasantness, on a five-points unipolar continuous-category scale, together with the identification of the predominant sources operating during the measurement (see Figure 2). The measurement is embedded with the device identifier and the GPS position and, once stopped, can be uploaded on a cloud that feeds the online and real time map available at the Noise-Planet project website [12]. The pleasantness rated by the user is assigned to the measurement and averaged with all the pleasantness recorded in the same hexagonal area.
The raw data packages are updated on a daily basis and can be downloaded from a repository, selecting the country, in a compressed folder including points, areas and trajectories files of the measurements uploaded by the users. Once downloaded, the data can be imported and handled in any GIS software.

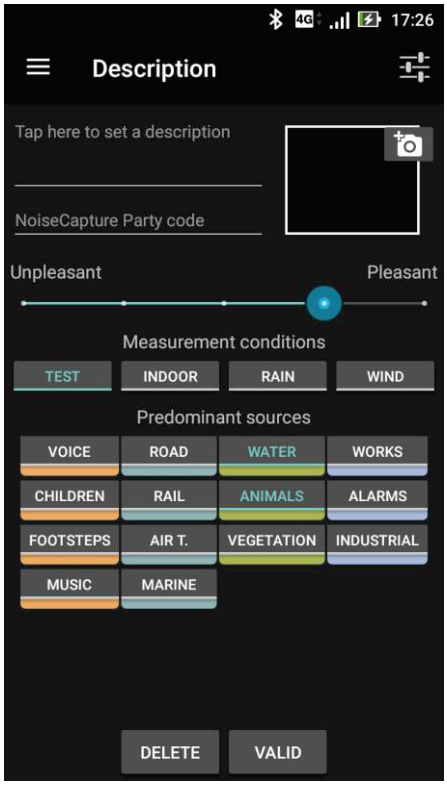


Figure 2. Screen of the app NoiseCapture at the end of measurement, with the five-points unipolar scale to provide pleasantness rating and predominant sources [12].

The idea presented in this paper is to use the mean pleasantness recorded by trained users during selected sessions of NoiseCapture measurements, that are the NoiseCapture parties, to draw soundscape maps of the area under study.

During a NoiseCapture party the participants are firstly asked to calibrate their mobile phone's microphone with one of the several possible techniques listed in the app itself. In the University of Salerno's events, calibration of the used devices has been achieved either by the comparison with a first-class sound level meter or by the spreading of the proper sound level correction factors from a calibrated mobile phone to another via wireless connection.

The students have been divided in 5 teams, each of them including at least 3 calibrated mobile phones, and they have been asked to walk along the route assigned to each group, as in Figure 3a, measuring the environmental sound level. The students have been asked to stop the measurement each time a relevant variation of the soundscape occurred, in order to provide homogeneous information about pleasantness and predominant sources. This rule leads to many short measurements that can be handled in a GIS environment and can be used for mapping purposes. In this case, the authors used QGIS©.

In addition to the NoiseCapture parties, the authors organized a soundwalk, performed following the ISO 12913-2 [10], using questionnaires proposed in method A and method B reported in Annex C3. The soundwalk was carried out on March 8, 2019, with the participation of 22 students, following the route and the points reported in Figure 3b. The selected students regularly frequent the campus and, thus, have been considered local experts of the area under study. This kind of contribution is crucial to collect and analyze ecologically valid acoustical and perceptual data [10]. More details about the soundwalk are reported in [11], in which a comprehensive description of the activity is reported, together with a detailed data analysis. Table 1 reports a summary of the main features of the selected points, as well as the sound continuous equivalent levels measured in each point, with a calibrated class 1 sound level meter (Fusion, 01dB).

Table 1. Description of the measurement points and L_{eq} results.

Location	Description	L_{eq} [dBA]
Point 1	Vehicles entrance and parking lots	55.2
Point 2	Main park, close to the scientific library	53.3
Point 3	Rectorate square, close to the main library	48.3
Point 4	Central square, close to a fountain and a bar	57.0
Point 5	External area, close to HVAC plants	68.2
Point 6	Pedestrian road to the bus station and canteen	55.4

This soundwalk provided robust subjective data about the soundscape of the campus that will be used for comparison with the pleasantness map produced in this paper, to validate the methodology proposed.

It is worthy to notice that the pleasantness provided by the NoiseCapture data is given in percentage, rating from 0% to 100%, respectively from unpleasant to pleasant, with steps of 25%. On the other hand, the data collected according to

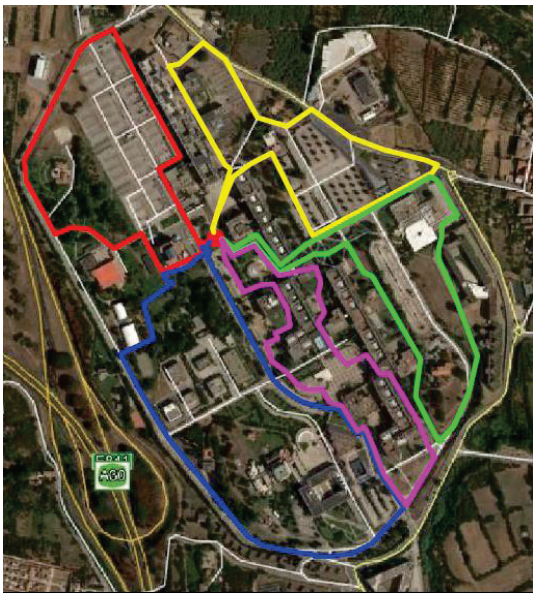
method A of the ISO standard are given in a scale from 5 to 1, from "strongly agree" to "strongly disagree" about how pleasant the soundscape of each point is. The two scales are not directly comparable, thus the authors converted the 5-1 scale of method A to 100%-0%. This was possible because of the availability of the single questionnaire results.
As for method B results, since they refer to the soundscape unpleasantness rating, they have been converted into the mean pleasantness by assuming that "non unpleasant" is "pleasant". This procedure, of course, can lead to a misestimation of the pleasantness, since the subjective rating of how much a location is unpleasant may be affected by the question structure. Asking about the unpleasantness, in fact, may influence the participant and let her/him focus on the negative factors more than on the positive ones, and vice versa. This peculiarity of method B will be confirmed by a general underestimation in the pleasantness results presented in the next section and will lead the authors to use method A results for validation of the mapping, adopting the scale in percentage, as proposed in the NoiseCapture application. The app, in fact, asks to rate the unpleasantness/pleasantness perception in a more neutral way, using a five-point unipolar scale (see Figure 2).

3. CASE STUDY AND RESULTS

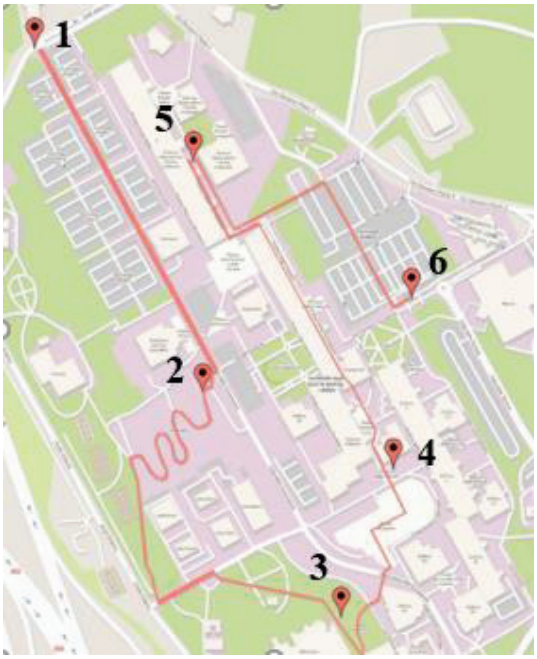
The case study presented in this paper is the campus of Fisciano of the University of Salerno. The authors downloaded the data related to Italy and to Salerno province, in which the campus is located. A filter on the date and on the hour has been implemented, to select only the measurements performed during the NoiseCapture party events, celebrated in:

- NoiseCapture@Unisa 2018: 17th of May
- NoiseCapture@Unisa 2019: 24th of May
- NoiseCapture@Unisa 2022: 16th of May
- NoiseCapture@Unisa 2022 fall edit.: 9th of November

This allowed to work with controlled data, recorded by trained users, that are the students involved in the events, thus reducing the probability of corrupted data uploading. Firstly, the mean pleasantness attribute present in each hexagonal area of the campus has been plotted with a color gradient scale (Figure 4). At this stage, the map does not include any spatial interpolation of the data, but only serves as a "guide for the eye" and represents the database used for the following analysis.



(a)



(b)

Figure 3. (a) Paths of the NoiseCapture parties (modified from Google Maps©) and (b) route of the soundwalk [11].

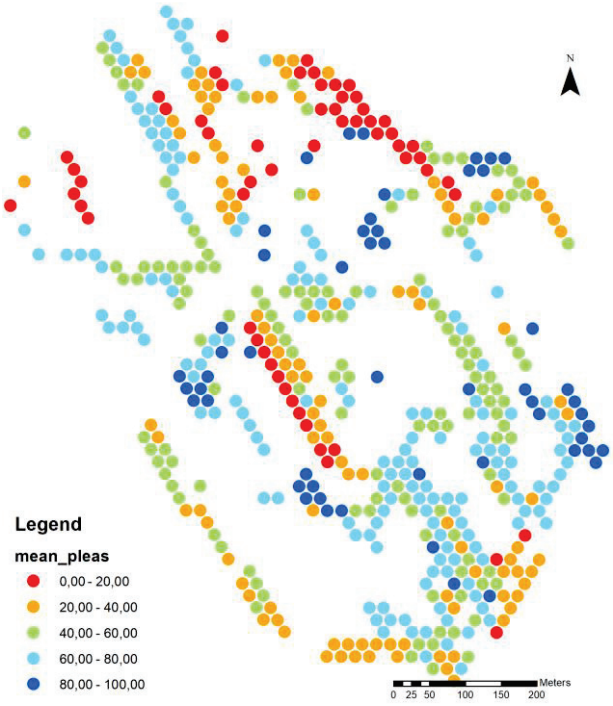


Figure 4. Mean pleasantness measured during the NoiseCapture parties, aggregated on the centroids of the hexagonal grid elements of the OnoMap used for Noise-Planet project.

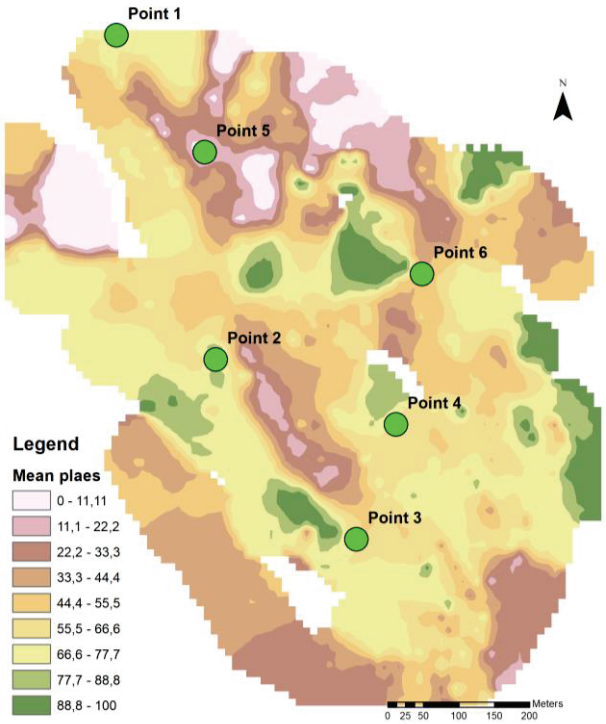


Figure 5. IDW interpolation map of the mean pleasantness in the Campus of Fisciano. The green points are the soundwalk stations.

Preliminary comments have been drawn, noting that the areas in which the mean pleasantness is low correspond to those locations in which there is a relevant noise coming from heating/cooling systems or from the nearby roads. On the contrary, the areas with higher pleasantness in the map correspond to locations generally with a better soundscape, for instance the parks and the vibrant areas.

Table 2. Mean pleasantness measured with the soundwalk methods and simulated with IDW mapping.

Point	Method A [%]	Method B [%]	IDW map [%]
Point 1	52.3	50.9	75.0
Point 2	72.7	58.6	77.5
Point 3	67.1	57.2	60.3
Point 4	61.4	52.8	61.0
Point 5	2.3	9.0	4.9
Point 6	54.4	46.0	46.6

Starting from the mean pleasantness recorded during the NoiseCapture parties in each hexagonal area, the authors decided to perform an Inverse Distance Weighting (IDW) interpolation to produce a map of the campus pleasantness. The fixed search radius for the IDW interpolation has been set to 50 m. The classification has been obtained with natural break method. The resulting map is reported in Figure 5.

The map built with the above-described procedure has been then compared with the pleasantness recorded during the soundwalk performed by a group of students, as described in section 2. In particular, the pleasantness measured during the soundwalk, according to method A and method B, has been compared with the results obtained by the IDW interpolation in the 6 points of the soundwalk (see Figure 3b and Figure 5). These data are resumed in Table 2 and plotted in Figure 5.

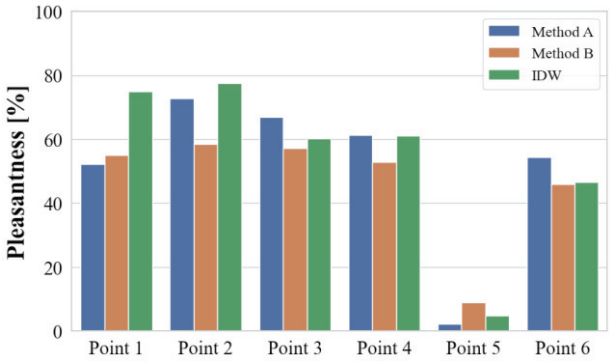


Figure 6. Comparison of mean pleasantness measured with the two methods during the soundwalk and simulated with the IDW interpolation of the NoiseCapture parties data.

The comparison highlights that the IDW interpolation is in a quite good agreement with method A in almost all the points, except for Point 1. It is important to note that this point is affected by lack of surrounding measured data (see Figure 4). To overcome this problem, a mean of the pleasantness recorded in the nearest points in a range of 100 m has been calculated, resulting in a value of 60.4%, that is much closer to the value measured during the soundwalk. This could be considered a good option to overcome the problem of missing data in the interpolation dataset. The choice of 100 m for the proximity analysis was supported by the homogeneity of the soundscape of the area, in which roads and parking lots are present as main sources. The influence of the radius selected to consider a measurement "close enough" to influence the pleasantness in a given point is of course a key point of this calculation. When applying the same procedure and calculating the mean pleasantness of nearby measurements for the other points, in fact, results are not always converging to the method A measured pleasantness, that can be considered as a benchmark. In point 5, in fact, the inclusion of measurements that are 100 meters away from the point led to a value of 35.3%, that is much higher than 2.3% of method A result and is not in line with the personal experience of the authors. Point 5, in fact, is very close to noisy cooling/heating plants [11]. In the authors' point of view, it's hard to give a fixed value for the "influence radius", that can be considered acceptable in all the applications, since the proximity should be estimated in terms of soundscape homogeneity. A more detailed analysis of sensitivity to distance radius could be performed in further studies, to obtain optimal thresholds ranges.

As already discussed in section 2, method B is affected by the formulation of the question during the survey, since it asks to rate from 1 to 5 how much unpleasant the location under study is, influencing the participant to focus on the negative factors of the site. Point 2 result is a good example of this comment. It is located in a green park of the campus, full of natural sounds and greenery. Anyway, the soundscape of this point is affected by the highway that runs very close to the campus border, a few hundreds of meters away from the park. For this reason, the same participants gave a high rating in method A questionnaires about how much pleasant this site is, including also the visual factors and the presence of the natural sounds. However, when they concentrated about the unpleasantness, they focused on the presence of the annoying noise coming from the highway and the overall results were worse than the one measured with method A. This effect is not included in the NoiseCapture parties data, in which the question about pleasant-unpleasant soundscape is given in a more neutral way.

Despite the comments reported above, the agreement between the IDW interpolated map and the results of the soundwalk is reasonable. The mean errors are about -2.5% and -8.5%, respectively for method A and method B. The general overestimation of the IDW map is influenced by the results in point 1. Excluding this point from the calculation of the error, because of the bad interpolation due to missing measured data, the mean errors are respectively +1.5% and -5.3%.

4. CONCLUSIONS

The need to map soundscape attributes and indices is becoming more and more important. In this paper, the authors proposed a methodology to map the pleasantness of a University campus, by using crowdsourced data, provided by the NoiseCapture app during the celebration of "NoiseCapture parties at Unisa", with a selected group of trained students. These data, averaged in a hexagonal grid, have been used for building a IDW interpolation map. The results of the mapping have been validated on 6 points included in a soundwalk carried out by some of the authors in the same campus, according to the ISO standards.

The validation showed that the mean pleasantness obtained by the IDW mapping in the 6 points was comparable with the values measured with method A of the ISO, assumed as benchmark, with a slight overestimation and a mean error of -2.5%. Considering the first point as an outlier, because there were no nearby points for the IDW interpolation, the mean error was +1.5%.

More in general, it can be concluded that the map of the pleasantness obtained with the IDW interpolation of the NoiseCapture parties data is a reliable tool to provide information about the spatial distribution of the phenomenon, even though the results can be affected by the homogeneity of the soundscape of the site. Anyway, a proper choice of the simulation parameters and the possibility to merge results from nearby points may be useful to finely tune the mapping procedure and to produce even more robust results.

5. ACKNOWLEDGMENTS

The authors are grateful to all the students that took part in the NoiseCapture parties along the years. The authors also acknowledge the contribution of the bachelor and master students that worked on this project during their thesis activity. A special thank goes to the students Antonio Marino, Valentina Pepe, David Vuto, Simone Toscano and Francesca Castella, that voluntarily realized the short videos of the events, published at [14].

6. REFERENCES

[1] K. Uebel, M. Marselle and A.J. Dean, “Urban green space soundscapes and their perceived restorativeness”. *People and Nature* vol 3, pp 756–769, 2021.

[2] L. Jiang, X. Yichao, W. Yajun and L. Tuo, "Soundscape effects on visiting experience in city park: A case study in Fuzhou, China." *Urban forestry & urban greening* vol 31, pp 38-47, 2018.

[3] M. Masullo, A.O. Bilen, R.A. Toma, G.A. Guler and L.Maffei,"The restorativeness of outdoor historical sites in urban areas: Physical and perceptual correlations." *Sustainability* vol 13.10, no5603 pp 1-23, 2021.

[4] A. Can and B. Gauvreau, "Describing and classifying urban sound environments with a relevant set of physical indicators." *The Journal of the Acoustical Society of America* vol 137.1 pp: 208-218, 2015.

[5] R. Benocci, H.E: Roman, A. Bisceglie, F. Angerlini, G. Brambilla and G. Zambon, "Auto-correlations and long time memory of environment sound: The case of an Urban Park in the city of Milan (Italy)." *Ecological Indicators* vol 134 no 108492, 2022.

[6] A. Farina, R. Righini, S. Fuller, P.Li and G.Pavan, "Acoustic complexity indices reveal the acoustic communities of the old-growth Mediterranean forest of Sasso Fratino Integral Natural Reserve (Central Italy)." *Ecological Indicators* vol 120 no 106927, 2021.

[7] D.A. Puspagarini, S.S. Utami, A.S. Sudarsono and R.F. Fela “Soundscape study of an urban campus park”. in AIP Conference Proceedings (2019, March vol. 2088, No. 1, p. 050011). AIP Publishing LLC.

[8] F. Aletta, F. Lepore, E. Kostara-Konstantinou, J. Kang and A. Astolfi, “An experimental study on the influence of soundscapes on people’s behaviour in an open public space”. *Applied sciences*, vol 6(10), no 276, 2016.

[9] A. Mascolo, S. Mancini, G. Graziuso, J. Quartieri and C. Guarnaccia, *Comparison between Sound Pressure Levels and Perception: a Soundscape Application in a University Campus.* in Journal of Physics: Conference Series (2020, September, Vol. 1603, No. 1, p. 012026). IOP Publishing.

[10] International Organization for Standardization 2018 ISO/TS 12913–2:2018 acoustics —soundscape — part 2: data collection and reporting requirements, ISO, Geneva.

[11] S. Mancini, A. Mascolo, G. Graziuso and C. Guarnaccia, Soundwalk, questionnaires and noise measurements in a university campus: A soundscape study. *Sustainability*, vol 13(2), no 841, 2021.

[12] https://noise-planet.org/index.html , last accessed on April 26, 2023.

[13] G. Guillaume, P. Aumond, E. Bocher, A. Can, D. Écotière, N. Fortin, C. Foy, B. Gauvreau, G. Petit, and J. Picaut, “Noisecapture smartphone application as pedagogical support for education and public awareness,” *The Journal of the Acoustical Society of America,* vol. 151, no. 5, pp. 3255–3265, 2022.

[14] Playlist of NoiseCapture parties@UNISA videos, https://www.youtube.com/playlist?list=PL1rZllzl1ke_wfUqVfkxcuvh5V7uXjS-4, last accessed on April 27, 2023

F

Research Article

Aurora Mascolo, Domenico Rossi, Michele Grimaldi, and Claudio Guarnaccia*

Soundscape maps of pleasantness in a university campus by crowd-sourced measurements interpolation

https://doi.org/10.1515/noise-2022-0178
received December 06, 2023; accepted December 23, 2023

Abstract: A university campus is a complex environment, as it comprises many areas, each with distinctive acoustic characteristics. There are zones where a quiet environment is crucial for work and study, parking lots and internal road networks, as well as vibrant spaces where students and personnel stay during leisure time. Thus, university campuses clearly offer a remarkable opportunity for the evaluation of soundscape analysis tools and the exploration of new methodologies for assessing and mapping soundscapes. In this work, the Fisciano campus of the University of Salerno (Italy) has been depicted as a case study. Specifically, the outcomes of a soundwalk conducted following ISO/TS 12913 standards will be presented, together with data gathered through crowd-sourcing during NoiseCapture parties. The data from NoiseCapture parties have been used to test and validate an innovative methodology based on an inverse distance weighting interpolation to produce soundscapes' attributes maps, using the mean pleasantness as an example and exploring the relative influence of the maximum distance used to characterize an homogeneous sound environment to build the maps themselves. The results will offer valuable insights into the proposed methodology.

Keywords: soundscape mapping, soundwalk, crowdsourced data, IDW interpolation

*** Corresponding author: Claudio Guarnaccia**, Department of Civil Engineering, University of Salerno, Salerno, Italy, e-mail: cguarnaccia@unisa.it
Aurora Mascolo: Department of Civil Engineering, University of Salerno, Salerno, Italy, e-mail: amascolo@unisa.it
Domenico Rossi: Department of Civil Engineering, University of Salerno, Salerno, Italy, e-mail: drossi@unisa.it
Michele Grimaldi: Department of Civil Engineering, University of Salerno, Salerno, Italy, e-mail: migrimaldi@unisa.it

1 Introduction

The soundscape research is becoming more and more relevant in the scientific literature, thanks to a large awareness of the damages and risks deriving from living in noisy and annoying environments. Beside the development of new techniques for noise assessment and modelling, in fact, there is a large part of the acoustic community that is now turning on soundscape analyses to involve the subjective perception in their studies.

However, such studies and analyses should not remain at a theoretical level, and indeed, in recent years, one of the main lines of research has been to bring these notions to a practical and valid level for planning and designing more livable and pleasant cities and urban environments. This is due also to the impulse coming from national and international institutions that ask to combine the standard noise mapping strategies with the soundscape approach, as affirmed by the European environmental agency (EEA) in the Good Practice Guide on Quiet Areas [1]. Thus, the assessment and understanding of soundscapes has become increasingly important as it provides a distinctive point of view into the social and cultural dimensions of urban settings. By paying attention to the combination of sounds that collectively define a particular place, researchers can learn more about how people actually experience and understand their surroundings. This exploration provides details not only about how deep people engage with the environment but also about how the places they are in affect their well-being and quality of life, furnishing useful information that could be used into the design of urban areas. In this perspective, it must be taken into account that nowadays people occupy different types of environments while working or simply spending time on a daily basis. All of them are characterized by the presence of several sound sources and by their characteristic combination. In this framework, the study of particular locations such as schools, universities, workplaces, vibrant areas, and sport facilities is very important to highlight possible

Open Access. © 2024 the author(s), published by De Gruyter. This work is licensed under the Creative Commons Attribution 4.0 International License.

peculiarities in the soundscape, according to the land use and the activities pursued in the site under study.

Yang and Kang [2] investigated the acoustic comfort in urban open public space finding out that the subjective evaluation of sound level generally relates well with the mean L_{eq}, but it varies in different cities and sites, being it influenced by the sound source type, the background sound level, and the demographic factors. This article also shows that visual and auditory aspects interact with each other and affect the overall comfort evaluation. Aletta *et al.* [3] suggested that country-specific factors should be considered too when designing urban soundscapes, as different communities may have different preferences for acoustic environments.

Moreover, there are several studies devoted to the investigation of the natural soundscape in parks or green areas. Uebel *et al.* provided more evidence to the idea that natural sounds can improve the quality of the perceived acoustic environment and even mask urban noises. In particular, their studies proved that the increase of natural sounds levels does not reduce the positive perception of the environment, differently from anthropic kinds of sounds [4]. Liu *et al.* proposed questionnaire surveys to assess the relationship between soundscape perception and public visiting experience in the city parks, focusing on the changing of sound source characteristics in the urbanization process [5]. Jeon *et al.* [6] confirmed that natural environments had higher restorative effects than urban environments, and that visually attractive and spatial-natural landscapes and acoustically supportive and tranquil soundscapes should be created to improve restoration response. Similar conclusions were drawn from the work of Chen and Kang [7].

Furthermore, a study by Masullo *et al.* assessed the possibility that even being surrounded by historical-artistic art forms could be just as relevant as a natural component for people's restorative capacity [8]. The perceptive side was combined with the physical one in the research of Can and Gauvreau that proposed a procedure to physically describe and to categorize urban sound environments making it possible to determine particular areas and periods remarkably suitable for stress recovery [9]. Also, the ecoacoustic soundscape studies are more and more developed, using sound recordings to calculate ecoacoustic indexes and to infer details about health quality of the natural area under study [10,11].

As for university campuses, some studies can be found in the literature. Puspagarini *et al.* reported how the soundscape in the campus of Yogyakarta, in Indonesia, was influenced by both anthrophony and natural sound sources, as any urban park. With respect to different locations, different sources were analyzed and found to be dominant, including animals and in particular insects, water sounds, road traffic noise, and even human voices [12]. Moreover, it needs to be taken into account that university campuses are often located in urban areas, and thus, they are often surrounded by streets with high traffic flow volume, which affect the overall quality of the external spaces. This is the case of several Italian Universities, for example, the Roma TRE University analyzed by D'Alessandro *et al.* [13]. In their research, the investigation on how natural features, visual aspects and thermal conditions can affect the users' judgment of the environment was carried out. Other studies in university campuses have been carried out, with particular attention to indoor soundscape such as in the study by Indrani *et al.* [14] finding out that even work behaviour depend on the acoustic characteristics of the workplace and on its perception, which is influenced by physiological, psychological, and social-cultural characteristics in the local environment. Aletta *et al.* [15] estimated the willingness of users to stay in an open public space at the University of Sheffield (UK), measuring people staying time under different music stimuli and in a controlled condition. Margaritis *et al.* [16] presented a smartphone-based method for noise and soundscape analysis in a university campus that underwent a renovation plan. The authors used statistical and geographic information system (GIS) tools to examine the spatiotemporal variability of noise and soundscape and the influence of landscape features, and also presented some maps of several perceptual factors of these areas. Anyway, Margaritis and van Herry [16] performed soundscape mapping via the ordinary Kriging interpolation technique, while in this article, the inverse distance weighting (IDW) is used, as suggested in the study by Hong and Jeon [17].

In the study by Mascolo *et al.* [18], the soundscape of the campus of Fisciano of the University of Salerno, Italy, was assessed by means of a soundwalk organized by some of the authors, using the recommendation reported in the ISO 12913-2 [19]. This site has been previously used as case study for testing a methodology for noise mapping by means of crowdsourced data in university campus [20]. The results confirmed the expectations that the vibrant areas, as well as the small park in the campus, were the locations with the best soundscape in terms of appropriateness and willingness to return. In the study by Mancini *et al.* [21], the same data have been used for a deeper investigation, including also a circumplex model 2D plane plot, that relates all the soundscape attributes and shows the relations among them.

In this article, the authors propose a soundscape mapping of the campus of Fisciano, University of Salerno, based on pleasantness data recorded with a trained crowdsourcing

technique. The data, in fact, are provided by students of the Engineering Departments, trained by some of the authors to provide reliable sound level measurements and assessment of the soundscape quality [20]. Results are compared with the data collected during the soundwalk activity and presented in studies by Mascolo *et al.* [18] and Mancini *et al.* [21], respectively, to validate the mapping procedure and to highlight strength points and/or possible shortcoming of the proposed methodology. The aim of this work is to provide a methodology useful in similar applications to obtain a detailed mapping of the soundscape over a wide area, with different features and different prevailing sound sources.

2 Materials and methods

In this article a methodology to draw a soundscape map of the campus under study is presented, starting from the sound perception rating provided by the participants to four events at the University of Salerno (Figure 1), named after "NoiseCapture parties."

These parties have been organized by some of the coauthors, under the patronage of the Noise-Planet project team, with the aim of spreading the noise awareness among future engineers (all the participants were students of engineering disciplines) and promoting the tools for environmental noise assessment developed within the project. Among these tools, in fact, the colleagues from Université Gustave Eiffel, CEREMA, UMRAE, France, developed the NoiseCapture app for Android, for measuring the sound levels with the mobile phone's microphone [22]. At the end of each measurement, the user can provide a rating of the pleasantness, on a five-point unipolar continuous-category scale, together with the identification of the predominant sources operating during the measurement (Figure 2). The measurement is embedded with the device identifier and the GPS position and, once stopped, can be uploaded on a cloud that feeds the online and real-time map available at the Noise-Planet project website. The pleasantness rated by the user is assigned to the measurement and averaged with all the pleasantness recorded in the same hexagonal area.

The raw data packages are updated on a daily basis and can be downloaded from a repository, selecting the country, in a compressed folder including points, areas, and trajectories files of the measurements uploaded by the users. Once downloaded, the data can be imported and handled in any GIS software. The idea presented in this article is to use the mean pleasantness recorded by trained users during selected sessions of NoiseCapture measurements, which are the NoiseCapture parties, to draw soundscape maps of the area under study. During a NoiseCapture party the participants are first asked to

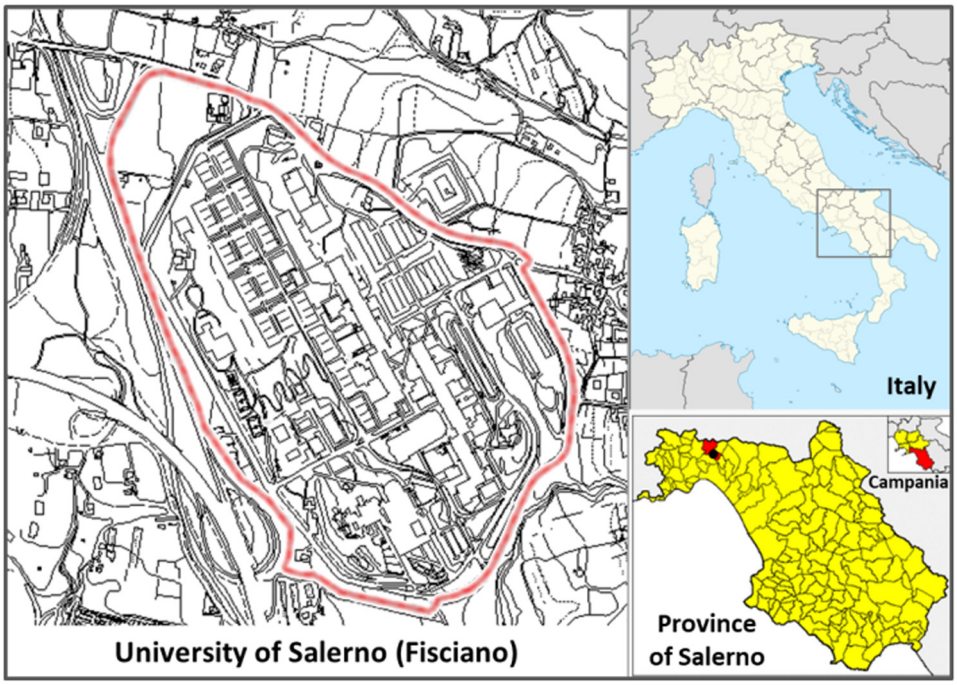


Figure 1: Location of the campus of Fisciano, University of Salerno [21]. Red line in the left plot is the Campus border.

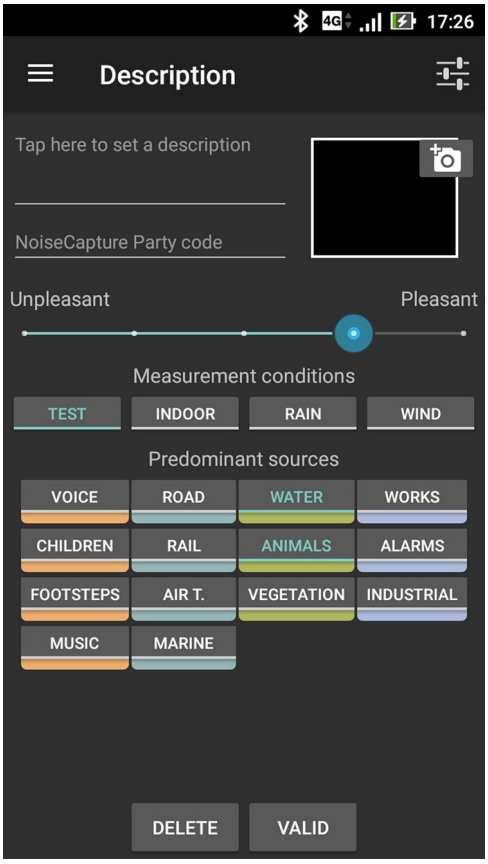


Figure 2: Screen of the app NoiseCapture at the end of measurement, with a five-point unipolar scale to provide pleasantness rating and predominant sources.

calibrate their mobile phone's microphone with one of the several possible techniques listed in the app itself. The NoiseCapture app allows to calibrate smartphones in four ways, namely, with the help of road traffic, by manually calibrating from a reference device or from a calibrator device (in this case, a plug-in external microphone is needed) and by automatic estimating the correction factor from a calibrated smartphone. In the University of Salerno's events, the smartphones of the team members have been calibrated in laboratory by manual comparison with a first-class sound level meter (reference device) and then the participants devices have been calibrated by automatic sharing of the correction factors. The latter operation has been performed in the classroom, measuring the background sound levels (approximately around 60–70 dBA due mostly to Heating, Ventilation and Air Conditioning, HVAC, system and to students chatting) with the two calibrated devices and the smartphones of the students. Via wireless connection, the app provides the correction factors to the smartphones under calibration, considering the levels measured by the calibrated devices.

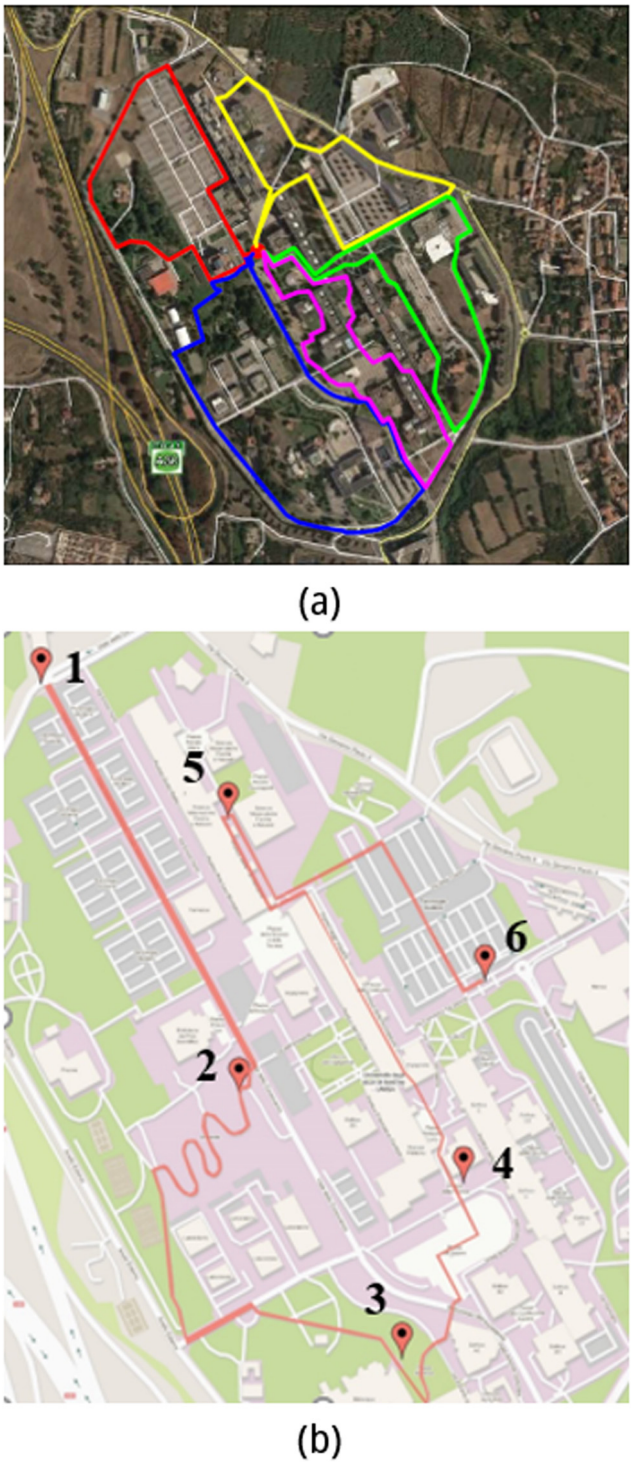


Figure 3: (a) Paths of the NoiseCapture parties (modified from Google Maps©) and (b) route of the soundwalk.

The students have been divided in five teams, each of them including at least three calibrated mobile phones, and they have been asked to walk along the route assigned to each group, as in Figure 3a, measuring the environmental sound level. The students have been asked to stop

the measurement each time a relevant variation of the soundscape occurred, in order to provide homogeneous information about pleasantness and predominant sources. This rule leads to many short measurements that can be handled in a GIS environment and can be used for mapping purposes. In this case, the authors used QGIS (C).

In addition to the NoiseCapture parties, the authors organized a soundwalk, performed following the ISO 12913-2 [19], using questionnaires proposed in method A and method B reported in Annex C3 of the same document [19]. The soundwalk was carried out on March 8, 2019, with the participation of 22 students, most of them attending the Physics class of the first year of the Bachelor in Civil and Environmental Engineering at the University of Salerno. Part of the participants were students working in the Applied Physics Engineering Laboratory for the bachelor or master thesis. All the students were all in the range of 19–26 years and the process selection was made to achieve a gender balance. The participants were asked in anonymous way if they had any hearing impairments, and they were trained before starting the soundwalk, resuming the main concepts of acoustic perception, the soundscape subjective evaluation approach, and the questionnaire structure. The selected students regularly frequented the campus and, thus, have been considered local experts of the area under study. This kind of contribution is crucial to collect and analyze ecologically valid acoustical and perceptual data [19]. The soundwalk was performed following the route and the points reported in Figure 3b. More details about the soundwalk can be found in the study by Mancini *et al.* [21], in which a comprehensive description of the activity is reported, together with a detailed data analysis.

Table 1 presents a summary of the main features of the selected points, as well as the sound continuous equivalent levels measured in each point, with a calibrated class 1 sound level meter (Fusion, 01 dB). The six location points are influenced by different noise sources that characterize them. More specifically, for point 1, the main noise source is the traffic in the internal campus roads network; for point 2, the main source is road traffic flowing in the highway. For points 3 and 6, the main noise source is chatting. In point 3, moreover, noise coming from the temporary work in progress is also affecting the Soundscape. Additional sources for point 4 and point 5 are, respectively, noise coming from water fountain and from plants

Table 1: Description of the six measurement points and L_{eq} results

Location	Description	L_{eq} (dBA)
Point 1	Vehicles entrance and parking lots	55.2
Point 2	Main park, close to the scientific library	53.3
Point 3	Rectorate square, close to the main library	48.3
Point 4	Central square, close to a fountain and a bar	57.0
Point 5	External area, close to HCVA plants	68.2
Point 6	Pedestrian road to the bus station and canteen	55.4

This soundwalk provided robust subjective data about the soundscape of the campus that will be used for comparison with the pleasantness map produced in this article, to validate the methodology proposed. It is worthy to notice that the pleasantness provided by the NoiseCapture data is given in percentage, rating from 0 to 100%, respectively, from unpleasant to pleasant, with steps of 25%. On the other hand, the data collected according to method A of the ISO standard are given in a scale from 5 to 1, from “strongly agree” to “strongly disagree” about how pleasant the soundscape of each point is. The two scales are not directly comparable; thus, the authors converted the 5–1 scale of method A to 100–0%. This was possible because of the availability of the single questionnaire results. As for method B results, since they refer to the soundscape unpleasantness rating, they have been converted into the mean pleasantness by assuming that “non unpleasant” is “pleasant.” This procedure, of course, can lead to a misestimation of the pleasantness, since the subjective rating of how much a location is unpleasant may be affected by the question structure. Asking about the unpleasantness, in fact, may influence the participant and let her/him focus on the negative factors more than on the positive ones, and vice versa. This peculiarity of method B will be confirmed by a general underestimation in the pleasantness results presented in the next section and will lead the authors to use method A results for validation of the mapping, adopting the scale in percentage, as proposed in the NoiseCapture application. The app, in fact, asks to rate the unpleasantness/pleasantness perception in a more neutral way, using a five-point unipolar scale (Figure 2). This approach is also consistent with other studies in the literature, such as in the study by Aletta *et al.* [23]. In this particular research, Aletta *et al.* analyzing the results of Method A and Method B questionnaires during a soundwalk through the Department of Engineering of the University of Roma Tre, observed how choosing a protocol over another one could have an effect on the soundscape data that is being gathered, confirming the necessity of perform a comparison between the two methods.

3 Case study results

The case study presented in this article is the campus of Fisciano of the University of Salerno (UNISA). The authors

Table 2: Details of the NoiseCapture parties@UNISA events

Year	Date	Participants
2018	May 17, morning	25
2019	May 24, morning	29
2022 spring ed	May 16, afternoon	40
2022 fall ed	November 9, afternoon	113

downloaded the data related to Italy and to Salerno province, in which the campus is located. A filter on the date and on the hour has been implemented, to select only the measurements performed during the NoiseCapture party events, celebrated in the dates reported in Table 2. The noise maps resulting from the events and published in the noise-planet.org platform are reported in Figure 4.

This allowed to work with controlled data, recorded by trained users, that are the students involved in the events, thus reducing the probability of corrupted data uploading. Firstly, the mean pleasantness attribute present in each hexagonal area of the campus, with respect to the entire dataset collected during all the NoiseCapture parties described earlier, has been plotted with a colour gradient scale (Figure 5). At this stage, the map does not include any spatial interpolation of the data, but only serves as a "guide for the eye" and represents the database used for the following analysis.

Preliminary comments have been drawn, noting that the areas in which the mean pleasantness is low correspond to those locations in which there is a relevant noise coming from heating/cooling systems or from the nearby roads. On the contrary, the areas with higher pleasantness in the map correspond to locations generally with a better

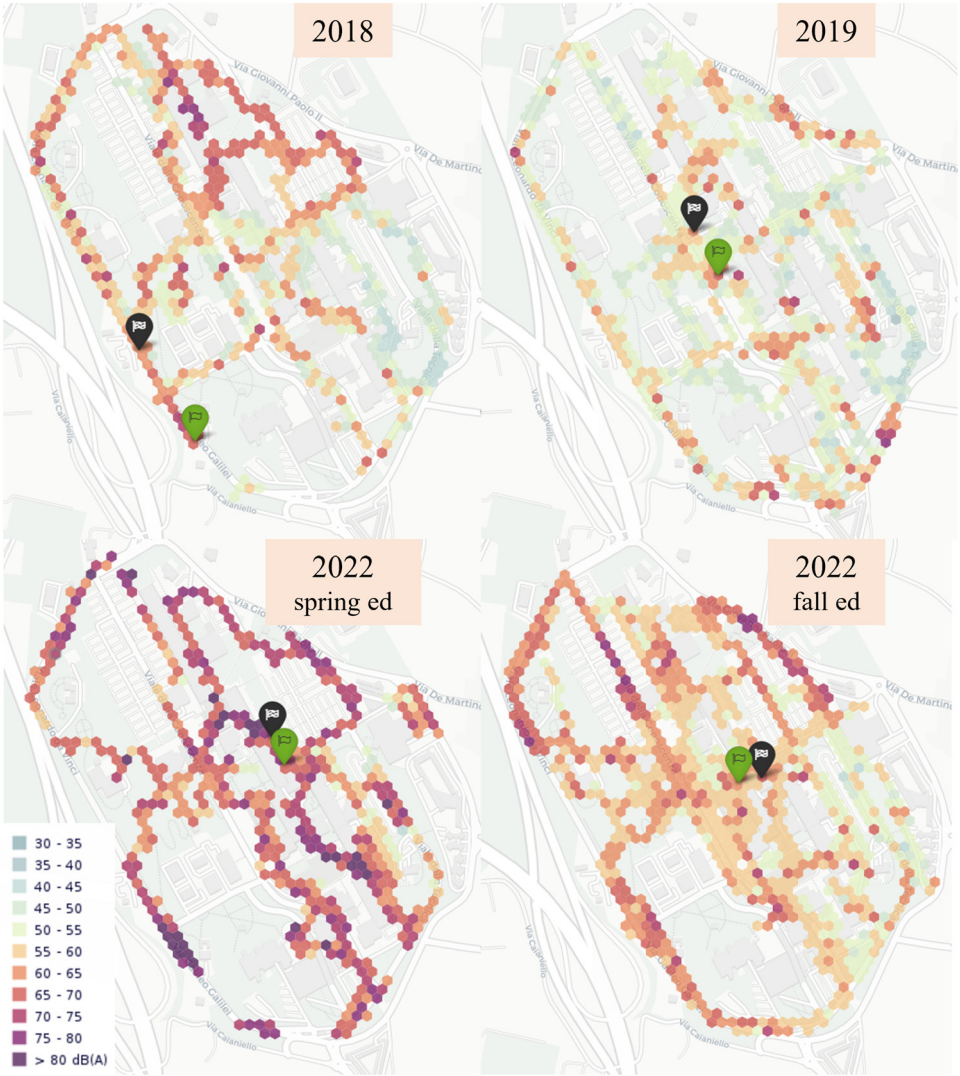


Figure 4: Noise maps obtained during the NoiseCapture parties, published in the Noise-Planet webpage.

soundscape, for instance, the parks and the vibrant areas. Starting from the mean pleasantness recorded during the NoiseCapture parties in each hexagonal area, the authors decided to perform an IDW interpolation to produce a map of the campus pleasantness.

When performing an IDW interpolation, one of the most important parameters is the search radius. This radius influences the amount of data included in the interpolation and, in this specific analysis, from the physical point of view, it expresses the distance among data that can be considered somehow related to an homogeneous soundscape. It is useful to underline that this distance can change according to the areas and the sources occurring within the site under study. Moving inside a big parking lot or along a main road of the campus, such as the path that goes from point 1 to point 2 of the soundwalk performed at UNISA (Figure 3(b)), allows to use a quite large search radius, since this path is approximately 450 m and has a quite homogeneous soundscape. The main sources in fact are vehicles moving along the road and inside the parking lot, as well as people walking out from the parking lot to reach the University buildings. When approaching point 2, the soundscape changes quickly over space, since the path enters the main park of the campus, that is lying below the main campus road level and is characterized by natural sounds. Anyway, the highway in front of the campus is a relevant noise source affecting the appropriateness of the park soundscape. At the conjunction of the two areas (road and park), the search radius should be much lower than before, to consider the sharp variations in the soundscape and the different perception of it by people staying in those areas. To address this issue of nonhomogeneous soundscapes, in the next section, the authors present a sensitivity analysis performed by varying the search radius of the IDW interpolation, to find if an optimal choice for the case under study exists, postponing the possibility of further investigations on variable search radius to a forthcoming article. The first map showed in Figure 6 is obtained by selecting a search radius for the IDW interpolation of 50 m. The classification has been obtained with natural break method.

The map built with the aforementioned procedure has been then compared with the pleasantness recorded during the soundwalk performed by a group of students, as described in Section 2. In particular, the pleasantness measured during the soundwalk, according to method A and method B, has been compared with the results obtained by the IDW interpolation in the six points of the soundwalk. These data are resumed in Table 3 and Figure 7.

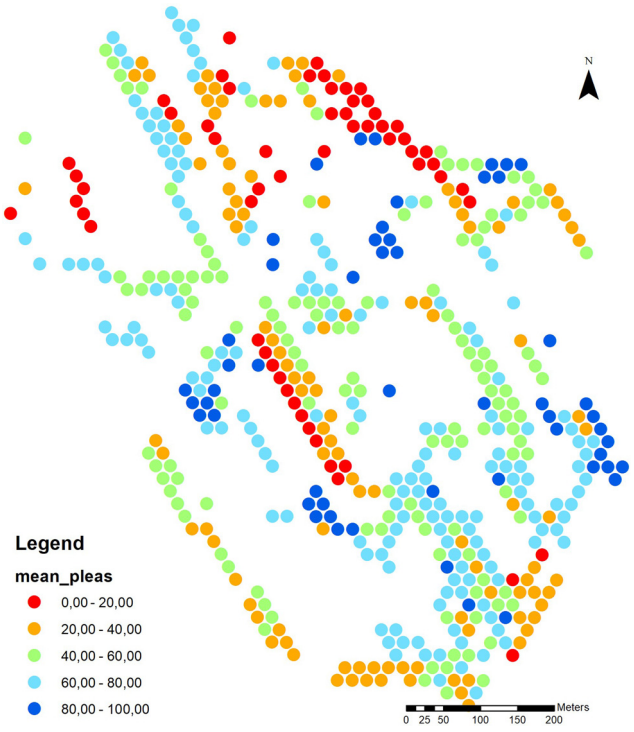


Figure 5: Mean pleasantness measured during the NoiseCapture parties, aggregated on the centroids of the hexagonal grid elements of the OnoMap used for Noise-Planet project.

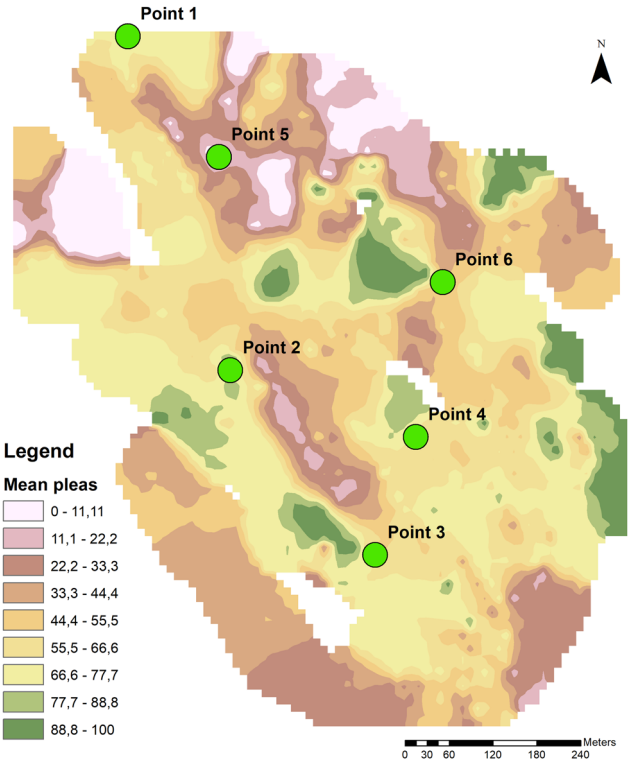


Figure 6: IDW interpolation map of the mean pleasantness in the Campus of Fisciano. The green points are the soundwalk measurement points. The search radius is fixed at 50 m.

Table 3: Mean pleasantness measured with the soundwalk methods and simulated with IDW mapping, with 50 m as search radius

Point	Method A (%)	Method B (%)	IDW map (%)
Point 1	52.3	50.9	75.0
Point 2	72.7	58.6	77.5
Point 3	67.1	57.2	60.3
Point 4	61.4	52.8	61.0
Point 5	2.3	9.0	4.9
Point 6	54.4	46.0	46.6

Table 4: IDW pleasantness in the six considered points with different search radius

Radius (m)	Point					
	1	2	3	4	5	6
50	75.00	77.52	60.28	62.68	4.86	46.59
60	66.95	77.02	60.03	62.91	6.19	52.74
70	68.17	76.26	59.61	62.37	7.17	50.54
80	62.87	75.70	59.85	63.08	8.89	52.91
90	63.03	75.31	59.91	63.26	9.54	51.72
100	60.79	74.99	60.35	63.72	9.94	53.91
150	59.68	74.15	60.24	59.78	11.69	53.62
200	55.65	73.58	59.66	59.34	12.46	53.42
300	53.06	73.06	59.18	59.92	13.43	52.20

3.1 Search radius variation analysis

To investigate how search radius could have effects on the interpolated soundscape map and on its goodness, the procedure described earlier has been repeated, varying the search radius from 50 to 300 m, with smaller steps when closer to the point and larger ones going further from it. In each simulation, the values of the mean pleasantness in the six points under study have been retrieved from the maps and the variations have been evaluated. This has been done to compare the results with the measurements of the soundwalk, considered as benchmark values, with the aim of performing a sensitivity analysis of the search radius parameter. The obtained results are reported in Table 4 and Figure 8, while an example of a different mean pleasantness map, obtained using as a search radius a value of 150 m, is shown in Figure 9.

4 Discussion

The comparison reported in Table 3 highlights that the IDW interpolation is in a quite good agreement with method A in almost all the points, except for point 1. It is important to note that this point is affected by lack of surrounding measured data (Figure 5). The influence of the selected radius, which, when larger, allows to include additional measurements, has been reported in Section 3.1 and will be discussed in details in the following. As already discussed in Section 2, method B is affected by the formulation of the question during the survey, since it asks to rate from 1 to 5 how much unpleasant the location under study is, influencing the participant to focus on the negative factors of the site. Point 2 result is a good example of this comment. It is located in a green park of the campus, full of natural sounds and greenery. Anyway, the soundscape of this point is affected by the highway that runs very close to the campus border, a few hundreds of meters away from the park. For this reason, the same participants gave a high rating in method A questionnaires about

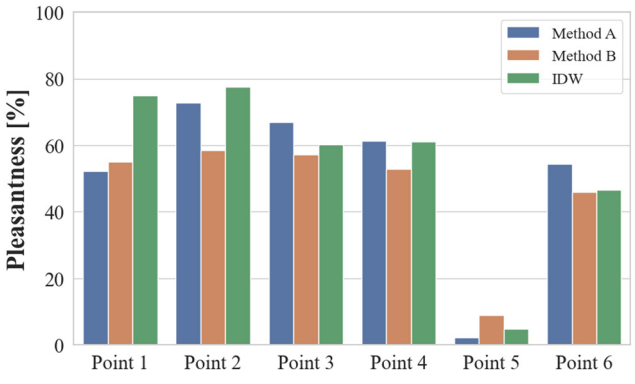


Figure 7: Comparison of mean pleasantness measured with the two methods during the soundwalk and simulated with the IDW interpolation of the NoiseCapture parties data, with 50 m as search radius.

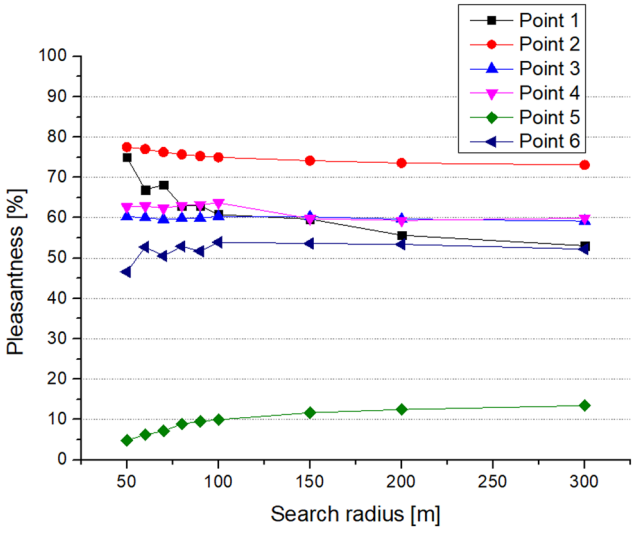


Figure 8: Mean pleasantness values versus IDW search radius.

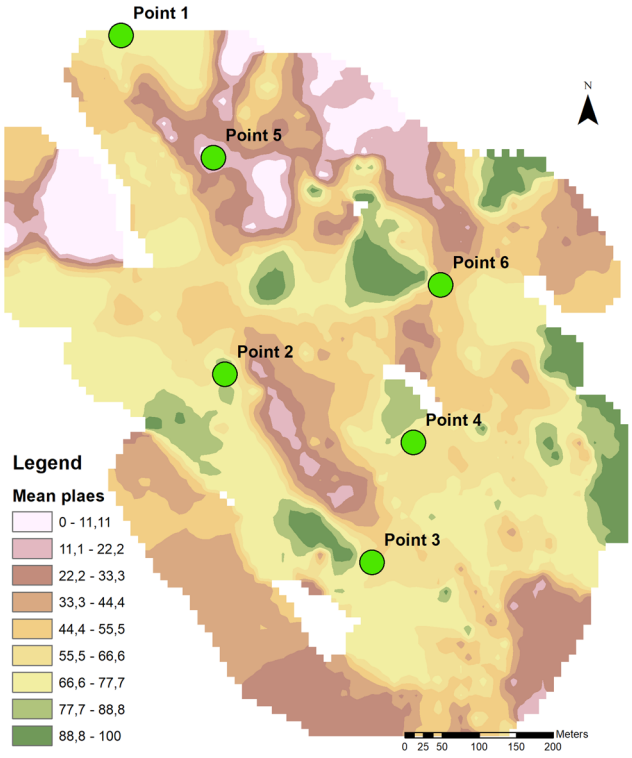


Figure 9: IDW interpolation map of the mean pleasantness in the Campus of Fisciano. The green points are the soundwalk measurement points. The search radius is fixed at 150 m.

how much pleasant this site is, including also the visual factors and the presence of the natural sounds. However, when they concentrated about the unpleasantness, they focused on the presence of the annoying noise coming from the highway and the overall results were worse than the one measured with method A. This effect is not included in the NoiseCapture parties data, in which the question about pleasant-unpleasant soundscape is given in a more neutral way. Despite the comments reported earlier, the agreement between the IDW interpolated map with 50 m as search radius and the results of the soundwalk is reasonable. The mean pleasantness errors, calculated as IDW simulations minus soundwalk measurements, are about 2.5 and 8.5%, respectively, for method A and method B. The general overestimation of the IDW map is influenced by the results in point 1. Excluding this point from the calculation of the error, because of the bad interpolation due to missing measured data, the mean errors are, respectively, −1.5 and 5.3%.

Moving to the search radius analysis discussion, the results reported in Section 3.1 provide several insights that can be underlined. First, looking at Figure 8, it is noticeable that the choice of the radius implies obviously obtaining different values of pleasantness. All the curves present some variations in a closer range (less than 100 m), exhibiting a flat slope increasing the search radius.

Table 5: Difference between IDW simulated values and soundwalk measurements (method A), *i.e.*, pleasantness error

Radius (m)	Point					
	1	2	3	4	5	6
50	22.73	4.79	−6.77	1.32	2.59	−7.82
60	14.68	4.30	−7.02	1.54	3.92	−1.68
70	15.90	3.54	−7.43	1.01	4.90	−3.87
80	10.60	2.98	−7.20	1.72	6.62	−1.50
90	10.76	2.58	−7.13	1.89	7.27	−2.69
100	8.52	2.26	−6.70	2.35	7.66	−0.50
150	7.41	1.43	−6.81	−1.58	9.41	−0.80
200	3.38	0.86	−7.38	−2.03	10.19	−1.00
300	0.79	0.34	−7.87	−1.44	11.15	−2.21

The pleasantness error, calculated as the difference between IDW simulation results and the mean pleasantness obtained during the soundwalk with method-A, considered as a benchmark, is presented in Table 5 and Figure 10.

The error between IDW and the soundwalk values presents different characteristics at the six different measurement points. Point 1 shows the highest variability of the error at varying of the search radius, by diminishing at increasing of the distance. Point 6 also shows a decreasing of the error. Point 5, on the contrary, presents an increasingly higher value of error when increasing the search radius. The other points have smaller oscillation as it can be noticed for point 3 error line, for instance, that is basically flat. These results indicate how the soundscape homogeneity is variable within the area under study and how hard is to find a single values usable for a bigger area, such as the whole campus.

Going more in details, the specific features of each point are relevant to understand the slope of the errors curves. Point 2, for example, is a quite large green area, where people goes for walking and spending free time, and no crowds nor activities are present. Considering the common features of the entire soundscape, the perception of a quiet and pleasant environment is basically maintained through the whole area. As a consequence of that, the mean IDW pleasantness value is quite stable even if considering larger and larger space, leading to a stable error when increasing the search radius. Similar conclusions can be drawn for point 1. Here, a remarkable variation of the pleasantness error is visible, with lower errors as the search radius increases. This is consequential, as in point 2, to the homogeneity of the soundscape under investigation. By taking this homogeneity into account and enlarging the radius used to compute the IDW interpolation, more data were included to estimate and map the

mean perceived pleasantness at this point, enabling a better fit with the results obtained during the soundwalk. However, if point 5 is taken into consideration, the opposite effect can be noticed. This area, as reported earlier, is characterized by its proximity to several very noisy HVAC plants. Such plants affect a very limited area of the campus, being surrounded by buildings that prevent the full propagation of noise to the adjacent areas. The nonhomogeneity of the soundscape in this area can be noticed by examining the values of the errors in it, which increase as the search radius increases. Since larger search radius leads to the inclusion of information that cannot be associated with the actual soundscape under investigation, the error value tends to increase.

Another remark is that the pleasantness error variation is more evident for search radius between 50 and 150 m, but at greater distance, the values remain more or less constant. A crucial output of this analysis is that it is very difficult to find a fixed value for the search radius, that can be considered acceptable in the entire area of the site under study, since the influence distance should be estimated in terms of soundscape homogeneity. Consequently, it is not possible to define a unique search radius that can be used in different contexts because of each site peculiarities.

Nevertheless, the size of the area under study is a relevant parameter. The campus presented in this article has a surface of about 1.200.000 mq, with many facilities and natural areas; thus, it presents a large variability of soundscape and it does not allow to identify a unique search radius. Smaller areas, with homogeneous facilities and activities within, such as for instance urban parks, industrial or residential areas, and areas along main transportation infrastructures, can allow the usage of a single value for the search radius, which will be strictly related to the dimension of the area, as well as to the soundscape features. In the latter case, in fact, an average value of the search radius can be selected, providing robust soundscape maps, consistent with the perceived sound environment, that can be used for multiple applications. For instance, the pleasantness maps provided in this case study can be replicated for other perceptual attributes and can be used for combining multiple attributes, such as in the study by Margaritis and Kang [24]. Margaritis and Kang [24], in fact, provided the maps of perceptual attributes in two UK cities using a 0–10 range scale and combined attributes values in a single map, fixing thresholds for the attributes and highlighting the areas that fulfil these thresholds.

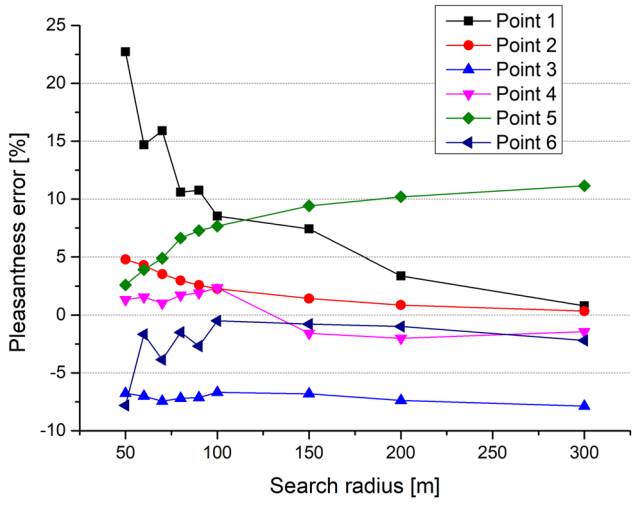


Figure 10: Difference between the pleasantness values obtained with IDW and from soundwalk experience.

5 Conclusions

The need to map soundscape attributes and indices is becoming more and more important. In this article, the authors proposed a methodology to map the pleasantness of a university campus, by using crowdsourced data, provided by the NoiseCapture app during the celebration of “NoiseCapture parties at UNISA,” with a selected group of trained students. These data, averaged in a hexagonal grid, have been used for building a IDW interpolation map. The results of the mapping have been validated on six points included in a soundwalk carried out by some of the authors in the same campus, according to the ISO standards. When considering 50 m as a search radius for the IDW interpolation, the validation showed that the mean pleasantness obtained by the IDW mapping in the six points was comparable with the values measured with method A of the ISO, assumed as benchmark, with a slight overestimation and a mean error of 2.5%.

A further analysis of the IDW mapping, with variable search radius, revealed that a proper tuning of this parameter can indicate how the surroundings of the measurements points can be considered as homogeneous in terms of pleasantness, and which is the spatial limit or “influence radius” until which a sound environmental analysis can be performed being sure the soundscape is not changing. The main outcome of this analysis is that this radius cannot be fixed for the entire site, since it differs greatly from one area to another.

More in general, it can be concluded that the map of the pleasantness obtained with the IDW interpolation of the NoiseCapture parties data is a reliable tool to

provide information about the spatial distribution of the phenomenon.

The main limitation of the study is that results can be affected by the homogeneity of the soundscape of the site, which influences the search radius choice. However, a proper choice of the simulation parameters and the possibility to merge results from nearby points, as well as a knowledge of the area under study main sources, may be useful to finely tune the mapping procedure and to produce even more robust outcomes.

Acknowledgments: The authors are grateful to all the students that took part in the NoiseCapture parties along the years. The authors also acknowledge the contribution of the bachelor and master students that worked on this project during their thesis activity. A special thank goes to the students Antonio Marino, Valentina Pepe, David Vuto, Simone Toscano, and Francesca Castella who voluntarily realized the short videos of the NoiseCapture parties events.

Funding information: This research was partially funded by the Ministery of University and Research, with the PRIN 2022 grant number 2022ZLE8HC.

Author contributions: All authors have accepted responsibility for the entire content of this manuscript and approved its submission.

Conflict of interest: Authors state no conflict of interest.

Data availability statement: The dataset of pleasantness analysed during the current study is available in the NoiseCapture repository, https://noise-planet.org/map_noisecapture/noisecapture_party.html. The dataset regarding the soundwalk generated and analysed during the current study is available from the corresponding author on reasonable request.

References

[1] European Environment Agency. Technical Report, Good practice guide on quiet areas. Copenhagen, Denmark: EEA; 2014.
[2] Yang W, Kang J. Acoustic comfort evaluation in Urban open public spaces. Appl Acoust. 2005;66(2):211–29.
[3] Aletta F, Oberman T, Mitchell A, Erfanian M, Kang J. Soundscape experience of public spaces in different world regions: A comparison between the European and Chinese contexts via a large-scale on-site survey. J Acoust Soc. 2023;154(3):1710–34.
[4] Uebel K, Marselle M, Dean M, Rhodes JR, Bonn A. Urban green space soundscapes and their perceived restorativeness. People Nat. 2021;3(3):756–69.
[5] Liu J, Xiong Y, Wang Y, Luo T. Soundscape effects on visiting experience in city park: A case study in Fuzhou, China. Urban For Urban Green. 2018;31:38–47.
[6] Jeon JY, Jo HI, Lee K. Psycho-physiological restoration with audio-visual interactions through virtual reality simulations of soundscape and landscape experiences in urban, waterfront, and green environments. Sustain Cities Soc. 2023:99;104929.
[7] Chen X, Kang J. Natural sounds can encourage social interactions in urban parks. Landsc Urban Plan. 2023;239:104870.
[8] Masullo M, Ozcevik Bilen A, Toma RA, Akin Guler G, Maffei L, The restorativeness of outdoor historical sites in urban areas: physical and perceptual correlations. Sustainability. 2021;13(10):1–23.
[9] Can A, Gauvreau B. Describing and classifying urban sound environments with a relevant set of physical indicators. J Acoust. 2015;137(1):208–18.
[10] Benocci R, Roman HE, Bisceglie A, Angelini F, Brambilla G, Zambon G. Auto-correlations and long time memory of environment sound: The case of an Urban Park in the city of Milan (Italy). Ecol Indic. 2022;134:108492.
[11] Farina A, Righini R, Fuller S, Li P, Pavan G. Acoustic complexity indices reveal the acoustic communities of the old-growth Mediterranean forest of Sasso Fratino Integral Natural Reserve (Central Italy). Ecol Indic. 2021;120:106927.
[12] Puspagarini DA, Utami SS, Sudarsono AS, Fela RF. Soundscape study of an urban campus park. Proceedings of the 2nd Engineering Physics International Conference EPIC; 2018 31 Oct-2 Nov; Surabaya, Indonesia. AIP Conference Proceedings, 2019.
[13] D'Alessandro F, Evangelisti C, Guattari G, Grazieschi G, Orsini F. Influence of visual aspects and other features on the soundscape assessment of a university external area. Build Acoust. 2018;25(3):199–217.
[14] Indrani HC, Ekasiwi SNN, Arifianto D. Indoor soundscape model: assessing contextual factors in open-plan offices on university campuses in Surabaya, Indonesia. Build Environ. 2023;237:110267.
[15] Aletta F, Lepore F, Kostara-Konstantinou E, Kang J, Astolfi A. An experimental study on the influence of soundscapes on peopleas behaviour in an open public space. Appl Sci. 2016;6(10):276.
[16] Margaritis E, van Herry F. Combining mobile measurements on noise and soundscape evaluation in a University Campus after a renovation plan. Proceedings of the 51st International Congress and Exposition on Noise Control Engineering Inter-Noise; 2022 Aug 21–24; Glasgow, UK. Institute of Noise Control and Engineering, 2022.
[17] Hong JY and Jeon JY. Exploring spatial relationships among soundscape variables in urban areas: A spatial statistical modelling approach. Landsc Urban Plan. 2017;157:352–64.
[18] Mascolo A, Mancini S, Graziuso G, Quartieri J, Guarnaccia C. Comparison between sound pressure levels and perception: a soundscape application in a university campus. J Phys: Conf Ser. 2020;1603:012026.
[19] International Organization for Standardization. ISO/TS 12913-2:2018 acoustics " soundscape" part 2: data collection and reporting requirements. Geneva, Switzerland: ISO; 2018.
[20] Graziuso G, Grimaldi M, Mancini S, Quartieri J, Guarnaccia C. Crowdsourcing data for the elaboration of noise maps: A methodological proposal. J Phys: Conf Ser. 2020;1603:012030
[21] Mancini S, Mascolo A, Graziuso G, Guarnaccia C. Soundwalk, questionnaires and noise measurements in a university campus: A soundscape study. Sustainability. 2021;13(2):841.

[22] Guillaume G, Aumond P, Bocher E, Can A, Écotiére D, Fortin N, et al. NoiseCapture smartphone application as pedagogical support for education and public awareness. J Acoust. 2022;151(5):3255–65.
[23] Aletta F, Guattieri C, Evangelisti L, Asdrubali F, Oberman T, Kang J. Exploring the compatibility of "Method A" and "Method B" data collection protocols reported in the ISO/TS 12913-2: 2018 for urban soundscape via a soundwalk. Appl Acoust. 2019;155:190–203.
[24] Margaritis E, Kang J. Soundscape mapping in environmental noise management and urban planning: case studies in two UK cities. Noise Mapp. 2017;4(1):87–103.

25-29 August 2024
inter.noise
NANTES FRANCE

G

Study of pleasantness maps and perceived predominant sound sources in a university campus soundscape analysis

Aurora Mascolo[1]*
Department of Civil Engineering, University of Salerno
Via Giovanni Paolo II, 132, I-84084 Fisciano, Italy

Domenico Rossi[1]
Department of Civil Engineering, University of Salerno
Via Giovanni Paolo II, 132, I-84084 Fisciano, Italy

Michele Grimaldi[1]
Department of Civil Engineering, University of Salerno
Via Giovanni Paolo II, 132, I-84084 Fisciano, Italy

Claudio Guarnaccia[1]
Department of Civil Engineering, University of Salerno
Via Giovanni Paolo II, 132, I-84084 Fisciano, Italy

ABSTRACT

The soundscape within a University campus is very complex, covering different environments, such as quiet areas to enhance focus during work and study sessions, parking lots, internal road networks, but also vibrant spaces for leisure purposes. These aspects depict University campuses as a perfect example for exploring complex soundscape analyses, and innovative methodologies for its assessment and mapping.

This study presents and explores field data regarding the soundscape in selected points of the Fisciano campus of the University of Salerno (Italy) collected during a soundwalk, as well as pleasantness data obtained in crowdsourcing mode during NoiseCapture parties in the campus area. The soundwalk has been performed according to the ISO 12913, while the crowdsourced data was gathered using the NoiseCapture app. Maps of the soundscape pleasantness have been obtained using an interpolation approach on the crowdsourced data, validated on the soundwalk results and merged with the land use and facility map, to investigate the main role of sound sources in the soundscape's pleasantness rating. The results have been also compared with the predominance rated during the soundwalk. By comparing physical parameters, pleasantness data, and perceptual aspects, this study offers interesting insights on the complex soundscape of the university setting.

1. INTRODUCTION

The number of students enrolling in Europe is notably high: as reported by UNESCO [1], around 235 million students are currently enrolled in universities all around the world. In the last

[1] {amascolo; drossi; migrimaldi; cguarnaccia}@unisa.it

Permission is granted for the reproduction of a fractional part of this paper published in the Proceedings of INTER-NOISE 2024 provided permission is obtained from the author(s) and credit is given to the author(s) and these proceedings.

twenty years, indeed, the number of students pursuing tertiary education globally has more than doubled, with the Gross Enrollment Ratio (GER) doubling from 19% to 40% between 2000 and 2020 [2]. Moreover, by 2040 the number of students enrolled in higher education programs is estimated to reach around 600 million globally [3].

Tertiary studies keep students busy in university activities for most of the day, which is why it is critical to assess and design not only urban environments but also campuses' ones in order to achieve a good quality of life for citizens in every age group. For this reason, several studies in literature aim at analyzing how different aspects and features of campuses actually affect students' lives. Foulkes et al. [4] showed that campus noise has a crucial impact on physical and mental health of undergraduate students living in dormitories. Noise was found to be a source of serious distress: students noted that when noise disrupted their sleep, they experienced feelings of sadness and frustration, which also had an impact on their academic performance [4]. The effects of chronic exposure to high levels of noise on school performances has been largely analyzed for children [5], proving that mainly high cognitive processes such as problem solving and memory development are the most affected by noise exposure. However, similar conclusions can be achieved for college and university students as reported in [6] in which a review of studies regarding the negative effect of noise on students is reported. In particular, the acoustic environments of university campuses are crucial as they directly impact students' learning experiences, communication effectiveness, and overall well-being [4, 7, 8]. Numerous studies have been dedicated to exploring and evaluating the acoustic conditions within these educational settings, carrying out extensive noise measurement campaigns [9-12]. Each of these works has underlined that crucial importance should be attributed to defining and assessing the acoustic environments of campuses, particularly in relation to specific sound sources present in the areas under study, such as honking of trains passing by [10], vendors on the roads surrounding the campus [11] and nearby highways and railway stations [12].

On the other hand, more recently, increasing efforts have been made to analyze the overall auditory experience of users by considering perceptual factors alongside the analysis of sound levels in the area under study, investigating how individuals perceive a given acoustic environment [13]. This approach, that goes under the name of "soundscape approach", is mainly based on designing environments in which audible sounds are identified as desired by people, while unwanted sounds remain mostly not noticed [14, 15]. It has been proven to positively impact human health in various ways. By designing environments that prioritize pleasant and calming sounds while minimizing unwanted noise, indeed, individuals experience reduced stress levels and improved overall well-being [16]. Thus, incorporating the principles of the soundscape approach into urban planning and design can lead to significant benefits for human health and quality of life. For this reason, as reported by Aletta and Kang in [14], more attention should be paid to research on the mechanisms that underlie the perception of environmental sounds within specific contexts and their potential impact on health-related outcomes [15]. Such a target is also in line with the European Environmental Agency (EEA) guidelines [17], which require preserving environmental noise quality where it is good.

Several studies in literature analyzed how the perception of sound is deeply influenced by its source, and different sound sources can evoke varying perceptual consequences, both positive and negative. For instance, green areas such as parks or forests, are characterized by soundscapes filled by natural elements which are typically associated with positive feelings. Research suggests that visual and auditory experiences of natural features compared with urban ones facilitate recovery after psychological stress [18-19]. Moreover, Zhang et al in [20] analyzed how the direct exposure to a green environment helps to restore and relax people's mind, contributing to creating a sense of calm and tranquility and to the overall mental well-being.

Similar conclusions can be drawn for bird sounds which are associated with pleasant stimuli and can evoke feelings of relaxation and tranquility, improving attention restoration and stress recovery, enhancing one's mood and overall well-being as reported by [21-24].

Nevertheless, loud and persistent noises from traffic or construction sites are perceived as negative and annoying leading to a feeling of frustration and to heightened stress levels and irritation, impacting mental and physical health [25]. Recent World Health Organization (WHO) have provided evidence indicating that transportation noise could contribute to high levels of annoyance [26], sleep disturbance [27], and cardio-metabolic disorders [28].

Thus, understanding the influence of different sound sources on human perception is crucial in designing urban environments in order to obtain a higher quality of life for citizens.

In literature, numerous works delve into the assessment of soundscape within university campuses, aiming to analyze their intricate acoustic environments and their impact on students, faculty, and staff. In [29], Ibrahim studied noise effects on students' lives using questionnaires. Goswani et al in [30] delineate the perception of noise and its consequences on community's health using questionnaires in a way to raise awareness about the exposure to transportation noise too. Surveys showed that noise exposure mainly caused headaches, irritability, hearing issues, and trouble concentrating [30]. A study of the Polytechnic Center of the Federal University of Paraná [31, 32] combined the physical approach and the soundscape one aiming to study not only if the noise levels in the campus fall within the regulation limits but also determining if the population involved was sensitive to this kind of pollution. In the work of Lu and Fu [33], the perceived restorative factors of a campus outdoor environment had been investigated and found to be positively correlated with natural features of the area.

Thus, assessing the soundscape of university campuses could provide insights into designing these areas in a manner that promotes positive experiences, enhances learning outcomes, and contributes to the well-being of a significant portion of the global population. Moreover, campuses are very complex and they cover several kinds of environments, such as quiet areas to enhance focus during work and study sessions, parking lots, internal road networks, but also vibrant spaces for leisure purposes. Thus, these aspects depict University campuses as perfect examples for exploring soundscape analyses.

In such a framework, the aim of this paper is to deeply investigate the soundscape of a university campus, using as a case study the Fisciano campus of the University of Salerno (Italy). In particular, soundscape data gathered in selected points of the earlier mentioned campus collected during a soundwalk and pleasantness data obtained in crowdsourcing mode will be used. In addition, soundscape pleasantness maps obtained using an interpolation approach on crowdsourced data and validated on the soundwalk results presented in [34-36] will be analyzed and compared with land use maps in order to compare perceived pleasantness and the presence of specific sound sources. The scope is to compare physical parameters, pleasantness data, and perceptual aspects, offering a detailed analysis of the complex soundscape of the university setting.

2. MATERIALS AND METHODS

In this paper a methodology to compare the pleasantness of a soundscape in a given area and perceived predominant sound sources, within that soundscape, is outlined.

Following the approach reported in [36], in this contribution the authors provide the pleasantness map of the Fisciano Campus of the University of Salerno, drawn using crowdsourced data. Subsequently, the soundscape attribute depicted on the map is classified into five main categories. In order to achieve a better understanding of the relationship between pleasantness and perceived predominant sound sources, this map is then compared with the Campus land use and facility maps with the aim of identifying key sound sources that could affect the overall perception of the acoustic environment. Thereafter, perceptual and

subjective ratings of the predominant sound sources actually perceived by users collected during a soundwalk will also be analysed.

2.1. Soundscape data and assessment of the Campus

As mentioned earlier, the presented research uses as a case study the Fisciano Campus of the University of Salerno, depicted geographically in Figure 1.

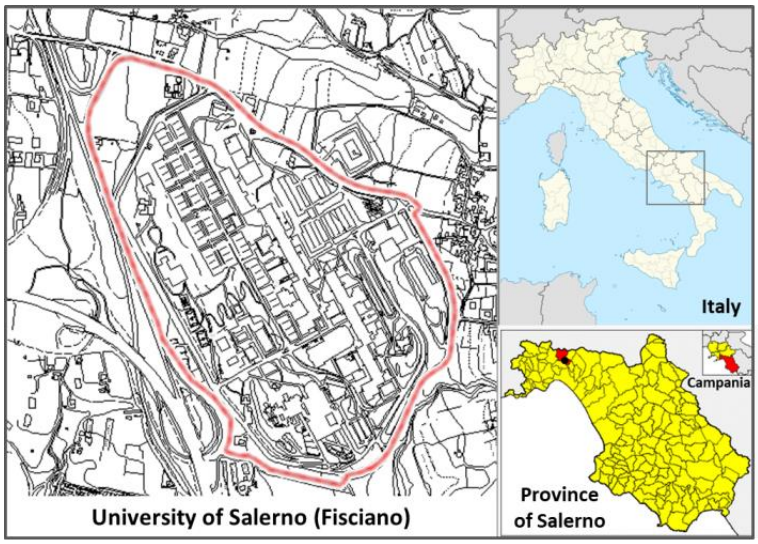


Figure 1: Geographical position of the Fisciano Campus of the University of Salerno. The red line delineates the campus boundary. [34]

Previous researches have already investigated the soundscape of this Campus [34-36]. Due to its size, indeed, it covers a lot of visually and acoustically diverse scenarios within the same area. This rich diversity makes it a particularly compelling case study, with methodologies and insights that have broader applicability beyond just university campuses. This depicts it as a perfect example for exploring complex soundscape analyses, and innovative methodologies for its assessment and mapping.

For instance, some of the coauthors coordinated four events, known as “NoiseCapture parties”, supported by the Noise-Planet project team [37] with the objective of encouraging the use of crowdsourcing noise data collection tools for environmental noise assessment and of raising awareness among future generations of engineers about noise pollution-related issues. Indeed, all participants were engineering students of the University of Salerno. During these events, held between 2018 and 2022, the “NoiseCapture” app for Android (see Figure 2) was used to collect crowdsourcing noise data. The app, developed by researchers from Université Gustave Eiffel, CEREMA, UMRAE (France) allows one to measure sound levels using the mobile phone’s microphone [38]. Clearly, mobile phones must be calibrated before any reliable sound level measurement can be obtained. There are several methods for properly calibrating the mobile phone’s microphone through the app that are not reported here, since sound level measurements were not utilized in the presented research.

Furthermore, and of significant importance for the presented application, users also have the option to rate the pleasantness using a five-point unipolar continuous category scale and to identify predominant perceived sound sources, as shown in Figure 2.

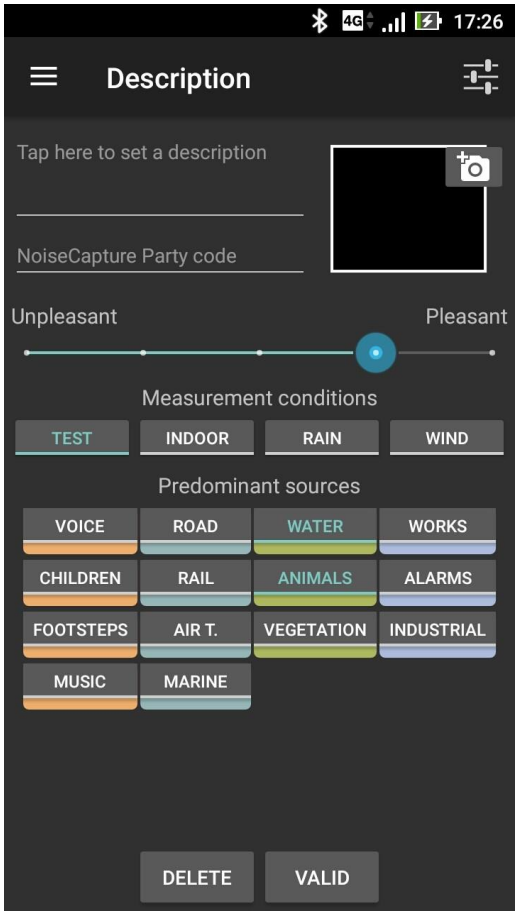
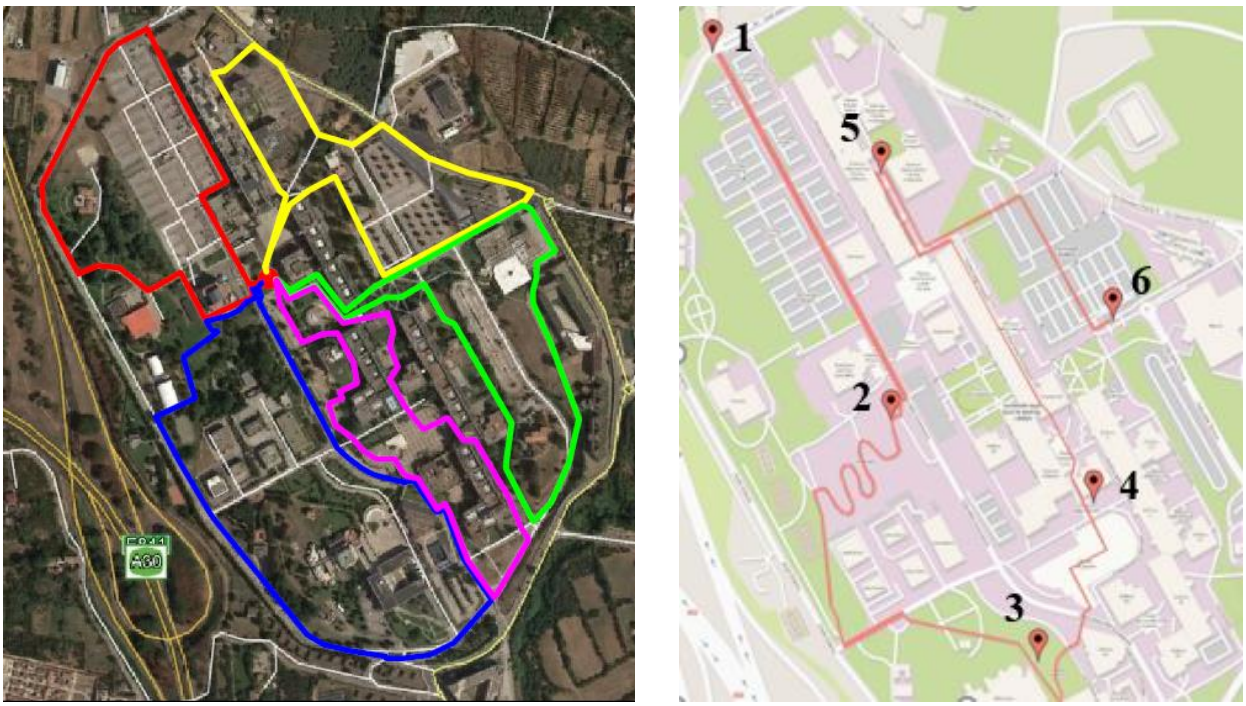


Figure 2: Screenshot from the NoiseCapture app. [37]

The measurements are then labelled with device identifiers and GPS positions and they could also be uploaded to the cloud, where they contributed to an online and real-time map accessible on the Noise-Planet project website. The pleasantness ratings are gathered together with those from all other recordings within the same hexagonal area, and then averaged. In every "edition" of the event, a proper training session on the scope of the events and on the proper use of the app was conducted, after which participating students were divided into five groups and instructed about which route to follow (as shown in Figure 3a). The authors were very clear during the training about the crucial importance of pausing measurements whenever significant changes in the soundscape occurred, ensuring that consistent information on the pleasantness and predominant sources of the soundscape under analysis was obtained.

Additionally, to these events, the authors held a soundwalk in 2019, conducted following the ISO 12913-2 [39] standard, and employing questionnaires from Method A and Method B as outlined in the Annex C3 of the standard itself [39]. The participants, mostly from the Bachelor in Civil and Environmental Engineering programs at the University of Salerno, were trained about fundamentals in acoustics, with specific focus on the soundscape approach and its potential applications and on the proper way to fill the proposed questionnaire. The soundwalk followed the route and the points indicated in Figure 3b; the latter are those at which the participants were invited to stop and fill in the questionnaire concerning the perceived soundscape. Further details about this research activity held in the University of Salerno are available [34, 36], providing a comprehensive explanation of the soundwalk activity.



(a) (b)

Figure 3: (a) Routes followed during the NoiseCapture parties (modified from Google Maps©); (b) Soundwalk path.

2.2 Pleasantness map of the Campus

In [36] a methodology to produce pleasantness maps of a soundscape has been presented. Particularly, the authors generated such maps interpolating perceptual ratings provided by participants during the "NoiseCapture parties" and therefore validated them on data collected during a soundwalk. The soundwalk, indeed, delivered reliable subjective data regarding the Campus soundscape as reported in [34]. In particular, the data collected during the "NoiseCapture parties" was used to perform an IDW (i.e. Inverse Distance Weighting) interpolation to produce the pleasantness map. This procedure can be applied in any GIS environment. In this specific application, the authors utilized QGIS (C).

However, as reported in [36] this mapping procedure heavily relies on soundscape homogeneity and the "influence radius" within which a reliable sound environmental analysis can be conducted without significant soundscape changes. Although the authors in [36] acknowledged that this radius cannot be uniformly fixed across the entire Campus area and for different applications, it was evident that when set at 100 meters, the discrepancy observed during the validation process between the interpolation approach results and the soundwalk's questionnaires answers stabilized itself. For this reason, in the presented application a search radius of 100 meters has been chosen to produce the pleasantness map of the University Campus under analysis.

In order to investigate the obtained map and how it can be related to predominant sound sources within the campus environment, a classification of the pleasantness is performed, using five classes. Such an approach provides a framework for analysing and interpreting the complex auditory landscape of the Campus area. In fact, by dividing the pleasantness into defined classes, deeper insights and a more comprehensive understanding of soundscape can be gained.

2.3 Comparison between pleasantness map and predominant sound sources

Pleasantness maps, along with any other maps depicting soundscape attributes, can be compared with other information depending on the use and purpose of the research. For instance, they can be compared with sound noise levels measurements, interweaving soundscapes information with noise maps of the area to identify potential relationships between physical parameters and perceptual aspects.

In the case presented in this paper, the authors decide to look into how the composition of the acoustic environment contributes to defining the overall pleasantness of a location, mostly investigating the significant role of sound sources. Specifically, the pleasantness map, obtained as discussed in the previous subsections, is overlapped with the Campus land use and facility map to identify significant sound sources that influence the overall perception of the acoustic environment. Furthermore, a comparison is drawn between this data and information on predominant perceived sound sources, information collected during the soundwalk activity.

This additional comparison aims to evaluate the presence of any masking effects or variations in the perception of the acoustic environment, due to the complexity overlapping of numerous and various typologies of possible sound sources present in any area.

A resume of the steps to be followed in the proposed methodology is represented in Figure 4.

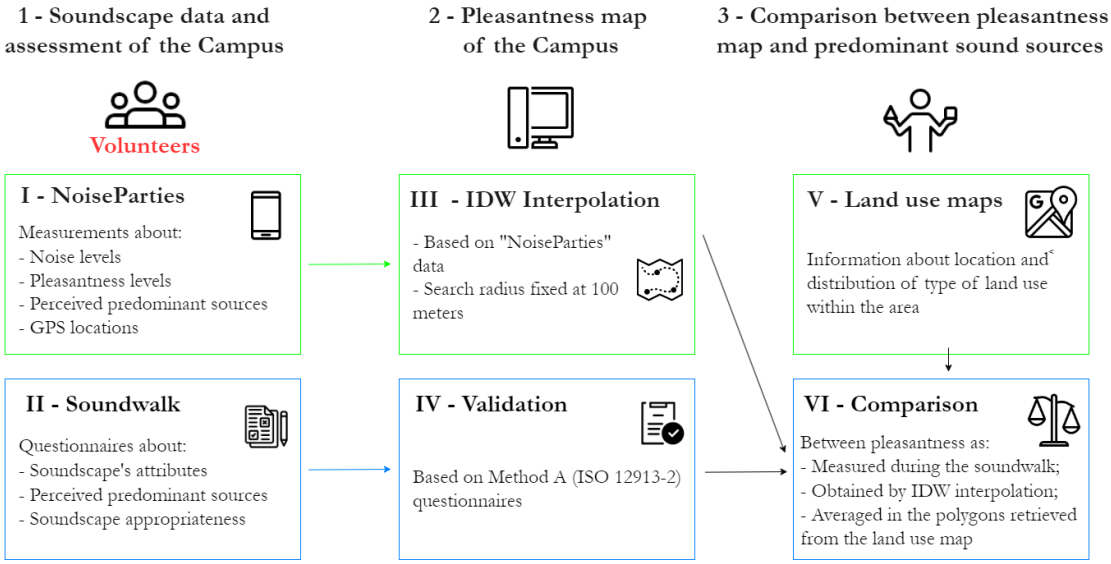


Figure 4: Flowchart resuming the proposed methodology.

3. CASE STUDY AND RESULTS

Following the steps presented in [36], the data regarding the "NoiseCapture parties" performed at the Fisciano Campus of the University of Salerno, has been analysed by the authors. In particular, the information collected during the listed four events has been considered:

- NoiseCapture@Unisa 2018: 17th May 2018
- NoiseCapture@Unisa 2019: 24th May 2019
- NoiseCapture@Unisa 2022: 16th May 2022
- NoiseCapture@Unisa 2022 fall edit.: 9th November 2022

Using the mean pleasantness data collected during these events, the authors performed an IDW interpolation to generate the pleasantness map of the Campus, employing as a search radius a distance of 100 meters. In Figure 5 the obtained map is represented.

Thus, as described in subsection 2.3 a comparison between pleasantness map and predominant sound sources has been pursued. For this purpose, the land use map of the Fisciano Campus has been drawn and it is represented in Figure 6.

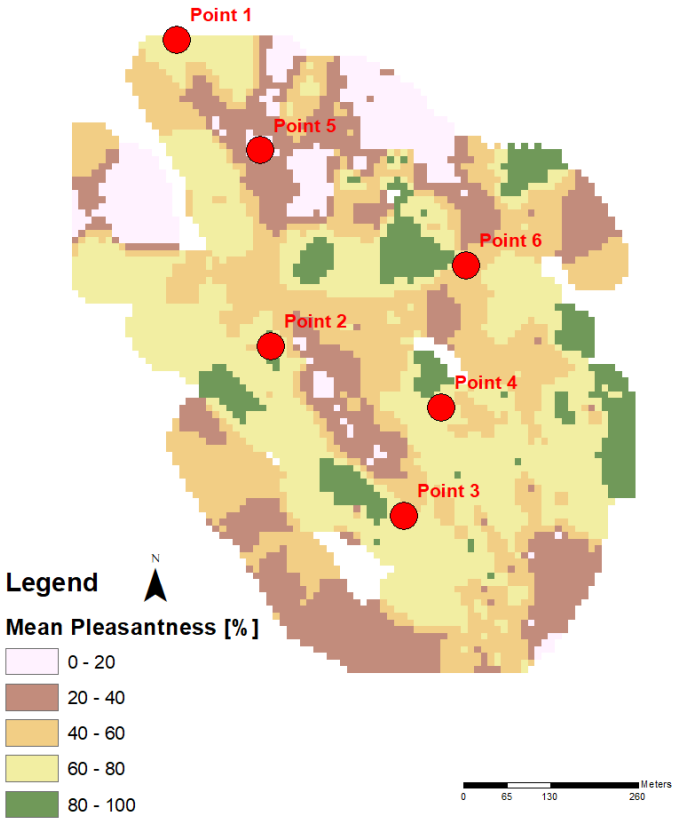


Figure 5: IDW interpolation map of pleasantness across the Fisciano Campus with a fixed search radius of 100 m. The measurement points of the soundwalk activity are shown as red markers.

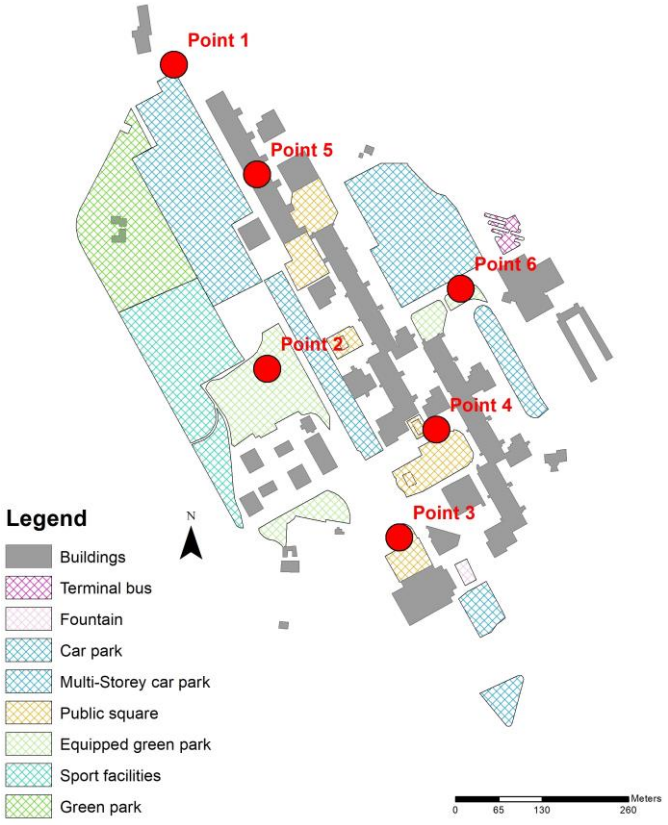


Figure 6: Fisciano Campus facilities and land use map.

Through the overlapping of these two maps, useful insights on the influence of sound sources on human perception of a soundscape could be gained. However, in this phase to obtain a readable map, the authors decided to change the pleasantness map using a grey colour scale from white to black. Figure 7 shows the described map. It is possible to notice that higher pleasantness values are focused mostly in green areas of the campus, where natural sounds are most probably to be heard. Very high values of pleasantness can also be found in vibrant areas, such as in the southern part where squares are located and it is expected to have a lot of people chatting passing by. However, similar values are also present in some portions of the two main parking lots of the Campus: this could be due to the proximity of these portions to other zones characterized by different positive sound sources and features. The parking lot in the North-East part of the Campus exhibits a portion with low pleasantness, close to the main external road and to the terminal bus, and another part with high pleasantness, near the canteen and a small green area. The other parking lot in the North-West area exhibits a similar pattern, with a low pleasantness portion close to a not equipped green area and a high pleasantness region near the main green park. Thus, it can be deduced that road traffic noise is not the predominant sound source in parking lots, but the influence of nearby areas, that are characterized by chatting and natural sounds, contributes to a better perception of such environments.

On the other hand, it seems that lower values of pleasantness are focused on the main road axis of the campus, the central parking lots and on the green area in the North-West part of the Campus. As for the latter, the low values of the pleasantness are probably due to its proximity to the highway located just in front of this area, to the ring road internal at the Campus and to the parking lots. Moreover, in the authors' experience, the green area is not as flattering as that of the nearby equipped park. The visual impact of the highway and of a helicopter parking within the green area, indeed, can be crucial in the soundscape evaluation.

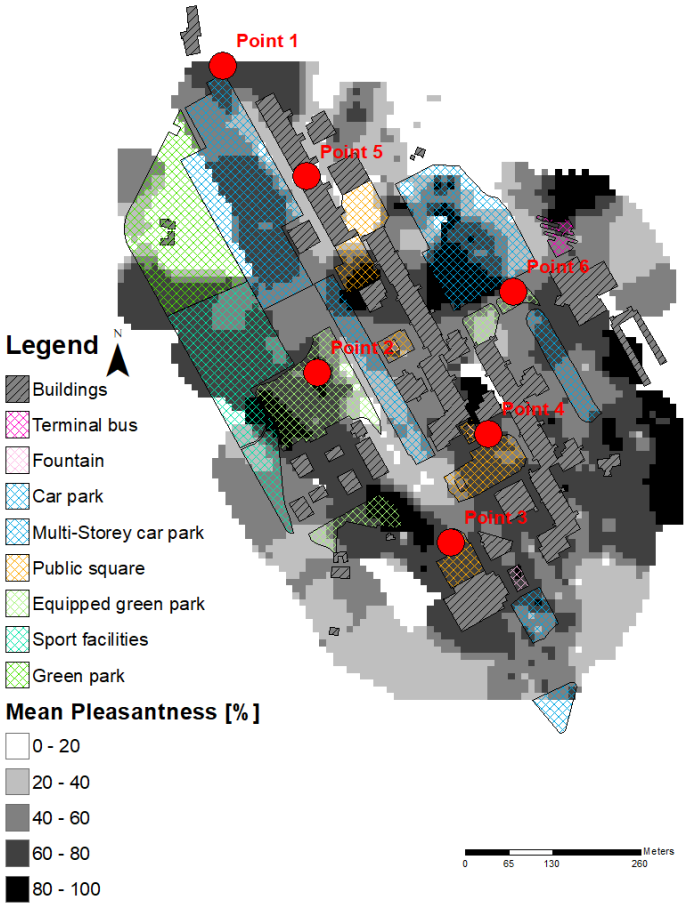


Figure 7: Overlapping of the pleasantness IDW map and the facilities and land use map.

Furthermore, although several academic buildings with classrooms and offices are depicted on the map, it must be emphasised that these insights can only be applied to outdoor spaces, as “NoiseCapture parties” only collected data in outdoor areas. The indoor soundscape has not been analysed in this work, although a similar methodology applied to smaller areas could be used to study the soundscape of academic buildings.

Mean pleasantness values in each polygon of the facilities and land use map has also been computed. Results are represented in Figure 8. It is worth to underline that the colours of the buildings do not refer to the pleasantness indoor, but to the surrounding soundscape.

It can be noticed that most of the areas of the Campus have a pleasantness in a medium-high class. Only the above-mentioned green area in the North-West part of the Campus and the area close to point 5 show a low value of the mean pleasantness. More comments on this result will be reported in the following, when describing the predominant sources in the points of the soundwalk.

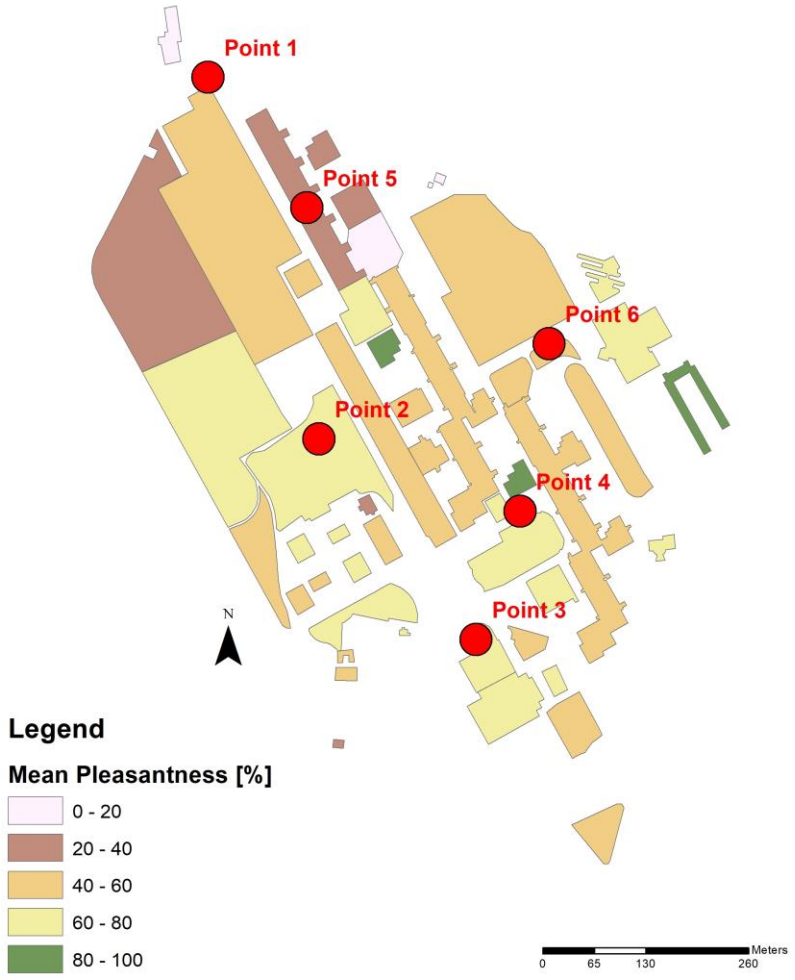


Figure 8: Mean pleasantness in the facilities and land use map’s polygons.

While the intersection between the land use and pleasantness maps helps to provide interesting insights into the relation between the pleasantness and the presence of different sound sources, it is even more significant to identify the link between such soundscape’s attribute and actually perceived sound sources. In this regard, the authors present the analysis of the sound sources detected by the users as predominant during the soundwalk activity in the six selected points. Participants in the soundwalk activity, in each of the six points, gave selected sound sources a score from 0% to 100%, indicating the predominance of each one of them over other sound sources. The selected sound sources to be investigated were: road traffic

noises, other noises (i.e. industrial, construction works, and similar ones), chatting and natural sounds (which includes wind, water, birdsong sounds). Figure 9 shows the perceived predominant sound sources in the six selected points, where scores assigned to each noise source were first averaged and then normalized to 100% so that a comparison between the four sources could be achieved.

Looking at Figure 7, point 1 is located near a parking lot but it shows an intermediate pleasantness value, which agrees with previous comments about its proximity to green areas. This is also confirmed by predominant sources scores obtained by Method-A questionnaires, as shown in Figure 9. Natural sounds, in fact, have been perceived in this point just slightly less predominant than road traffic, demonstrating a positive masking effect.

The same applies to Point 6, which is close to the canteen, in which the proximity to parking lots and roads is not felt as negative, thanks to the predominance of natural sounds and chatting.

Point 2 is in a park, but natural sounds are not perceived as the most predominant, since traffic noise and human voices also influence human perception. However, the pleasantness of this point is not as low as this aspect might suggest. This indicates that the visual aspect has a great influence on how the user perceives the soundscape, suggesting that further analysis could be carried out from this point of view, also considering visual features alongside perceptual and acoustical ones.

Points 3 and 4 are similar in several aspects: human voices and natural sounds are the perceived predominant sound sources and they are located near public squares. The high levels of pleasantness here reported suggest the positive influence of this kind of sounds on human perception of an acoustic environment.

Point 5 is near HVAC machines which explains the high value assigned to the “other sounds”, including industrial source, and the very low pleasantness level.

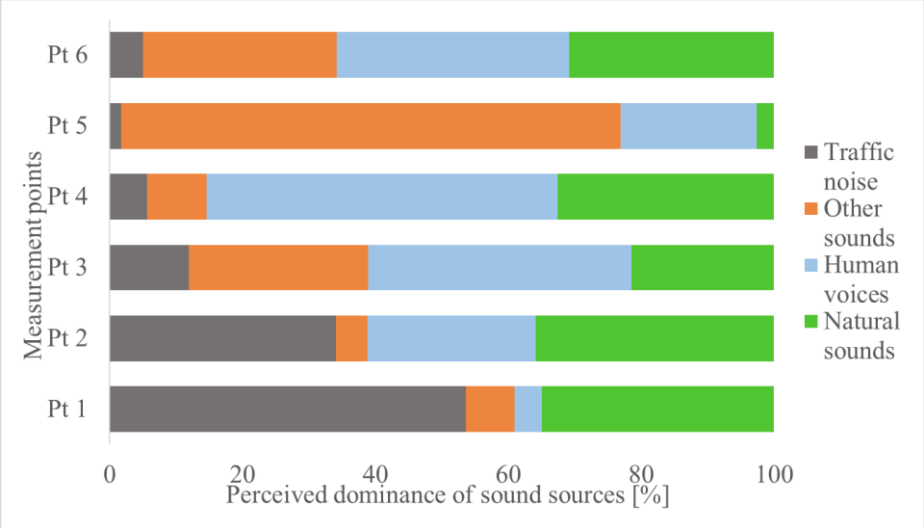


Figure 9: Predominant perceived sound sources in the six selected points of the soundwalk.

A quantitative analysis of the pleasantness in each point, measured during the soundwalk activity, obtained by IDW interpolation map (Figure 5) and averaged in the polygons retrieved from the land use map (Figure 8), is reported in Table 1.

When compared with the pleasantness values measured during the soundwalk activity in the six selected points, the results retrieved by the IDW map, built with a search radius of 100 meters, show a quite good agreement with Method-A questionnaires. Moreover, looking at data in Table 1, it is notable that mean pleasantness values computed in the polygons of the land use map do not describe the soundscape in a whole area properly, since in the selected

points, which belong to the identified polygons, they do not achieve good agreement with soundwalk values. This is mostly due to edge effects and, thus, the proximity between different acoustic environments, that at this stage of the work is not fully considered. Future developments of this methodology aim at analyzing the contribution of each polygon's class to pleasantness maps. Rather than analyzing the mean pleasantness in a single polygon, a further step could be to classify pleasantness as already done in this paper, and then calculate in which percentage the different categories of the land use map contribute to the various pleasantness' classes in the campus.

Table 1: Summary of pleasantness in %, measured through soundwalk activity, computed through IDW interpolation and averaged using polygons from land use map.

Point	Description	Soundwalk pleasantness values [%]	IDW map pleasantness values [%]	Mean pleasantness values in land use map areas [%]
1	Main entrance and parking lots	52.3	60.8	56.7
2	Main park	72.7	75.0	64.1
3	Rectorate square	67.1	60.3	65.7
4	Central square, near a fountain	61.4	63.7	60.2
5	Building area, near HVAC machines	2.3	9.9	32.2
6	Pedestrian road, near canteen and parking	54.4	53.9	50.3

5. CONCLUSIONS

In this contribution, a study of pleasantness and perceived predominant sound sources in a University Campus has been carried out.

A pleasantness map of the Fisciano Campus of the University of Salerno has been drawn using crowdsourcing data collected during "NoiseCapture parties" events. The data was used to perform an IDW (i.e. Inverse Distance Weighting) interpolation to produce the pleasantness map, using a search radius of 100 meters. The map has been also validated comparing it with data collected during a soundwalk activity held in the Campus using Method-A questionnaires of the ISO 12913-2.

In order to investigate the relation between pleasantness and predominant sound sources, a comparison with the Campus land use and facility map has been pursued. In particular, the overlapping of the pleasantness map and of the land use and facility map offers significant insights on the analyzed soundscape and confirms that natural sounds and human voices produce positive effects, contributing to a high level of pleasantness both in parks than in public squares. A masking effect due to both greenery visual impact and natural sounds is also achieved in some green areas which are close to road traffic noise. On the other hand, places near HVAC machines, and thus exposed to "industrial noise", and major roads of the Campus are the areas which generate the lower levels of pleasantness in the Campus itself.

Furthermore, to also take in consideration the human perception of the acoustic environment under study, a comparison between the obtained pleasantness map and

perceived predominant sound sources data collected during a soundwalk activity has been performed. Data collected using Method-A questionnaires has been used.

The mean pleasantness values computed in the polygons retrieved from the land use map has also been reported. However, such indicator is not always providing a comprehensive description of the entire area's soundscape, as in some of the points selected for the soundwalk activity this method fails to accurately align with measured values. When this happens, it probably means that the corresponding land use polygon is not acoustically homogenous, thus resulting in a spatial variation of soundscape features within the polygon.

Future developments could aim at deepening the contribution of each sound source to the pleasantness rate given by users, using land use and facilities map. Instead of analyzing the mean pleasantness within a single polygon, as done in this paper, a supplementary step could be to determine the contribution of the various land use map categories within each pleasantness class across the campus. Moreover, the relevance of buildings presence within the polygons will be considered in future studies, to improve the pleasantness interpolation and, consequently, its spatial classification.

ACKNOWLEDGEMENTS

This study was partially funded by MIUR, with the PRIN 2022 "Nature for sustainable cities: planning cost-effective and just solutions for urban issues" (NatSolis) (grant number 2022ZLE8HC). The authors are also grateful to all the students that took part in the NoiseCapture parties along the years. The authors also acknowledge the contribution of the bachelor and master students that worked on this project during their thesis activity.

REFERENCES

1. UNESCO. Higher education. https://www.unesco.org/en/higher-education . Last accessed 2024-02-16
2. UNESCO, Institute for Statistics. Higher education at a glance, WHEC, 2022.
3. A. Calderon. Massification of higher education revisited, Melburn, Australia, 2018.
4. L. Foulkes, D. McMillan and A.M. Gregory. A bad night's sleep on campus: an interview study of first-year university students with poor sleep quality. *Sleep Health*, **5(3)**, 280-287, 2019.
5. B.M. Shield and J.E. Dockrell. The effects of noise on children at school: A review. *Building acoustics*, **10(2)**, 97-116, 2003.
6. S.A. Ibrahim. Reviewing the effects of noise pollution on students (college and university). *In AIP Conference Proceedings, AIP Publishing LLC.* **2591(1)**, 030056, March, 2023.
7. Y.J. Choi. The intelligibility of speech in university classrooms during lectures. *Applied Acoustics*. **162**, 107211, 2020.
8. Y.J. Choi. Acoustical measurements of masks and the effects on the speech intelligibility in university classrooms. *Applied Acoustics.* **180**, 108145, 2021.
9. B. Phukan and K. Kalita. An experimental study of noise pollution in Gauhati University campus, Guwahati, Assam, India. *International journal of environmental sciences.* **3(5)**, 1776-1784, 2013.
10. V. Kumar, A.V. Ahirwar and A.D. Prasad. Monitoring and mapping noise levels of university campus in central part of India. *Journal of Air Pollution and Health.* 2023.
11. P.M. Jaff and H. Hossieni. Study of Noise pollution at the campus of university of Sulaimani. *Journal of Kirkuk University–Scientific Studies*. **7(1)**, 98-109, 2012.
12. D. Thattai, J.S Sudarsan, R. Sathyanathan and V. Ramasamy. Analysis of noise pollution level in a University campus in South India. *In IOP Conference Series: Earth and Environmental Science, IOP Publishing.* **80(1)**, 012052, 2017.
13. J. Kang and F. Aletta. The impact and outreach of soundscape research. *Environments*. **5(5)**, 58, 2018.
14. F. Aletta and J. Kang. Soundscape approach integrating noise mapping techniques: A case

study in Brighton, UK. *Noise Mapping*. **2(1)**, 2015.
15. F. Aletta and J. Kang. Promoting healthy and supportive acoustic environments: Going beyond the quietness. *International journal of environmental research and public health*. **16(24)**, 4988, 2019.
16. F. Aletta, T. Oberman and J. Kang. Associations between positive health-related effects and soundscapes perceptual constructs: A systematic review. *International journal of environmental research and public health*. **15(11)**, 2392, 2018.
17. European Environment Agency. Good practice guide on quiet areas. *Publications Office of the European Union.* 2014.
18. J.J. Alvarsson, S. Wiens and M.E. Nilsson. Stress recovery during exposure to nature sound and environmental noise. *International journal of environmental research and public health.* **7(3)**, 1036-1046, 2010.
19. L. Tian, D. Winterbottom and J. Liu. Soundscape Optimization Strategies Based on Landscape Elements in Urban Parks: A Case Study of Greenlake Park in Kunming. *Sustainability.* **15(13)**, 10155, 2023.
20. J. Zhang, J, Jin and Y. Liang. The Impact of Green Space on University Students' Mental Health: The Mediating Roles of Solitude Competence and Perceptual Restoration. *Sustainability*. **16(2)**, 707, 2024.
21. J. Liu, J. Kang and H. Behm. Birdsong as an element of the urban sound environment: A case study concerning the area of Warnemünde in Germany. *Acta Acustica united with Acustica*. **100(3)**, 458-466, 2014.
22. E. Ratcliffe, B. Gatersleben and P.T. Sowden. Bird sounds and their contributions to perceived attention restoration and stress recovery. *Journal of Environmental Psychology.* **36**, 221-228, 2013.
23. X.C. Hong, G.Y. Wang, J. Liu, L. Song and E.T. Wu. Modeling the impact of soundscape drivers on perceived birdsongs in urban forests. *Journal of Cleaner Production.* **292**, 125315, 2021.
24. B.J. Park, Furuya K., T. Kasetani, N. Takayama, T. Kagawa and Y. Miyazaki. Relationship between psychological responses and physical environments in forest settings. *Landscape and Urban Planning*. **102(1)**, 24-32, 2011.
25. A. Dzhambov and P. Lercher. Road traffic noise exposure and depression/anxiety: an updated systematic review and meta-analysis. *International journal of environmental research and public health.* **16(21)**, 4134, 2019.
26. R. Guski, D. Schreckenberg and R. Schuemer. WHO environmental noise guidelines for the European region: A systematic review on environmental noise and annoyance. *International journal of environmental research and public health*. **14(12)**, 1539, 2017.
27. M. Basner and S. McGuire. WHO environmental noise guidelines for the European region: a systematic review on environmental noise and effects on sleep. *International journal of environmental research and public health*. **15(3)**, 519, 2018.
28. E. Van Kempen, M. Casas, G. Pershagen and M. Foraster. WHO environmental noise guidelines for the European region: a systematic review on environmental noise and cardiovascular and metabolic effects: a summary. *International journal of environmental research and public health.* **15(2)**, 379, 2018.
29. S.A. Ibrahim. Study noise effects on the students of the faculty of engineering/mustansiriyah university. *Al-Nahrain Journal for Engineering Sciences*. **21(2)**, 178-186, 2018.
30. S. Goswami, S.K. Nayak, A.C. Pradhan and S.K. Dey. A study on traffic noise of two campuses of University, Balasore, India. *Journal of Environmental Biology*. **32(1)**, 105-109, 2011.
31. M.S. Engel, F.H. Ferraz and P.H.T. Zannin. Characterization of environmental noise on a university campus based on noise measurements and interviews. *DAGA 2012–Darmstadt,* 117-118, 2012.
32. P.H.T. Zannin, M.S. Engel, P.E.K. Fiedler and F. Bunn. Characterization of environmental noise based on noise measurements, noise mapping and interviews: A case study at a

university campus in Brazil. *Cities*. **31**, 317-327, 2013.
33. M. Lu and J. Fu. Attention restoration space on a university campus: exploring restorative campus design based on environmental preferences of students. *International journal of Environmental research and public health*. **16(14)**, 2629, 2019.
34. S. Mancini, A. Mascolo, G. Graziuso and C. Guarnaccia. Soundwalk, questionnaires and noise measurements in a university campus: A soundscape study. *Sustainability*. **13(2)**, 841, 2021.
35. A. Mascolo, D. Rossi, M. Grimaldi and C. Guarnaccia. Soundscape indicators assessment and mapping in a university campus. *10th Convention of the European Acoustics Association, Turin, Italy*.
36. A. Mascolo, D. Rossi, M. Grimaldi and C. Guarnaccia. Soundscape maps of pleasantness in a university campus by crowd-sourced measurements interpolation. *Noise Mapping*. **11(1)**, 20220178, 2024.
37. NoiseCapture. https://noise-planet.org/noisecapture.html . Last accessed on 2024-03-14.
38. J. Picaut, N. Fortin, E. Bocher, G. Petit, P. Aumond, G. Guillaume. An open-science crowdsourcing approach for producing community noise maps using smartphones. *Building and Environment*. **148**, 20-33, 2019.
39. International Organization for Standardization. ISO\TS 12913-2: 2017 – Acoustics – Soundscape - Part 2: Data Collection and Reporting Requirements. *Geneva: ISO*; 2017.

DOI: 10.61782/fa.2025.0884

FORUM ACUSTICUM EURONOISE 2025

THE ROLE OF PLEASANTNESS MAPPING IN A UNIVERSITY CAMPUS FOR STUDYING SOUNDSCAPE SUBJECTIVE PERCEPTION IN EVOLVING ENVIRONMENTS

Aurora Mascolo[1*] **Domenico Rossi**[1] **Michele Grimaldi**[1]
Claudio Guarnaccia[1]
[1] Department of Civil Engineering, University of Salerno,
Via Giovanni Paolo II, 132, I-84084 Fisciano, Italy

ABSTRACT

The diversity of acoustic environments within a University campus makes it an ideal case study for exploring soundscape mapping and assessment methodologies. This study focuses on the Fisciano campus of the University of Salerno (Italy), where acoustic and soundscape data have been collected over recent years at different times of the day and across various seasons, offering insights into the temporal evolution of distinct acoustic environments. Soundscape maps were created using spatialization techniques based on perceptual metrics such as pleasantness, while physical sound levels were considered to better understand the acoustic characteristics of the areas. The data were obtained through soundwalks conducted in accordance with ISO 12913 guidelines, as well as crowdsourcing campaigns using the NoiseCapture app. In this work, the maps are used to facilitate an analysis of the campus soundscape's evolution, by comparing results obtained using data collected over the years and considering changes in daily and seasonal activities. This work highlights the potential of soundscape mapping to understand the interplay between acoustic environments and human perception in complex settings that evolve over time, contributing to the development of innovative tools for soundscape analysis and urban planning.

*__Corresponding author__: amascolo@unisa.it.
__Copyright__: ©2025 Mascolo et al. This is an open-access article distributed under the terms of the Creative Commons Attribution 3.0 Unported License, which permits unrestricted use, distribution, and reproduction in any medium, provided the original author and source are credited.

Keywords: *soundscape mapping, campus, pleasantness perception*

1. INTRODUCTION

Globalization, economic growth, and international policies aimed at broadening access to higher education have led to a rise in student enrollment worldwide [1, 2], with projections indicating that the number of students could even exceed 600 million by 2040 [3]. As a consequence, university campuses have become increasingly dense and complex environments, where various factors influence both student well-being and their academic performance. Among these, the acoustic environment plays a crucial role as it directly impacts psychological health and learning outcomes. Numerous studies have shown that noise conditions within campuses can significantly affect students' listening abilities, cognitive performance, and overall mental well-being [4, 5], highlighting the need for careful planning of university spaces. Mealings et al. conducted a scoping review that highlighted a considerable negative relationship between road noise and students' acoustic comfort [6]. Therefore, recent research has shifted toward a more holistic approach, emphasizing not only noise reduction but also the quality of the overall acoustic environment. In this context, the concept of soundscapes within university campuses has gained attention. However, analyzing the soundscape of such areas can be challenging as they are not entirely uniform, presenting various ranges of areas and functions and exhibiting significant variability in their acoustic characteristics. Hence, studying the university's soundscape requires an

approach that accounts for the different acoustic contexts of the various zones across the campus, each influenced by unique configurations and interactions. This is the case of Zhuang and Shang's study, who observed that Linyi campus (China) is characterized by teaching areas and green spaces which generally meet national noise standards, while dormitories, restaurants, sports fields, and the main gate exceed them due to chatting and traffic noise [7]. Similarly, D'Alessandro et al. highlighted how in urban university settings, high traffic and noise pollution can compromise the quality of external spaces [8]. On the other hand, natural sounds can help to enhance soundscape perception. Nevertheless, during high-traffic periods, the masking effect produced by natural sounds and surrounding context may not be enough to minimize such negative sounds [9]. It's then clear that to study the soundscape of a university campus, it's essential to understand how the acoustic environment, its landscape, and all its features evolve and vary.

This variation occurs both spatially, as different sound sources shape the acoustic environment in distinct areas, as stated earlier, and temporally, as the soundscape transforms over time due to daily activity patterns, seasonal changes, and special events that can influence the overall acoustic dynamics. Within this framework, this paper aims to investigate the soundscape of the Fisciano campus of the University of Salerno (Italy) as a case study. The analysis relies on soundscape data collected at specific locations through soundwalks, along with pleasantness data gathered via a crowdsourcing method [10, 11]. Additionally, soundscape pleasantness maps, derived from the interpolation of this crowdsourced data [12–14], will be analyzed, with a particular focus on temporal dynamics. Specifically, the dataset used includes measurements collected over multiple years and across different seasons, enabling a more comprehensive examination of both the spatial distribution and temporal evolution of the campus soundscape. This approach may offer deeper insights into the interplay between physical parameters, perceptual evaluations, and the acoustic environment, shedding light on how these factors interact and transform over time.

2. METHODOLOGY

In this study, the methodology proposed by Mascolo et al. [12,13,15] for generating pleasantness maps of a given area is applied with different time references to analyze the evolution of the campus soundscape over time. The process relies on the collection of sound perception ratings for a specific soundscape attribute to be represented by the maps—in this case, pleasantness.

For this reason, a series of volunteer-based participatory events (i.e., "NoiseCapture parties" [16]) were organized to help with data collection. These events aim at raising awareness regarding noise pollution and promoting the use of tools for environmental noise assessment, particularly those developed within the framework of the NoisePlanet project [17]. Through the use of the "NoiseCapture app", indeed, participants can measure sound levels using their mobile phones' microphones and provide perceptual ratings of the pleasantness of the soundscape on a five-point scale. These measurements constitute the crowdsourced database that has been used to generate the soundscape maps. After completing each measurement, users can also specify the predominant noise sources [15]. The recorded measurements, along with the corresponding pleasantness ratings, can be retrieved from a public repository, allowing users to download point, track, and area datasets. Pleasantness values are available in both the point and area datasets. In the point dataset, these values are assigned to each point along the recorded trajectory, with all the points collectively representing the track followed during the measurement. As for the area dataset, pleasantness values are calculated as the average of all individual point-based ratings that fall within each predefined hexagonal grid cell. By averaging the ratings from all the points within the hexagon, this approach provides a spatially aggregated representation of how users perceive the acoustic environment in that area.

In the authors' previous studies [12, 13, 15], the analysis was pursued on area-based layers and thus with mean values of pleasantness collected throughout the years. Thus, it provided an overview of spatial variations but did not allow for a more detailed temporal analysis. In contrast, the present study aims to examine the soundscape evolution over time by processing point-based data. By doing so, a year-by-year comparison of how the perceived acoustic environment has changed across time could be achieved, generating pleasantness maps for each edition of the NoiseCapture parties. Pleasantness maps have been drawn in a GIS environment through an Inverse Distance Weighted Interpolation method (IDW). To validate the interpolated maps, the authors organized two soundwalk activities across the campus under study to rate the pleasantness in specific locations. The first soundwalk included 6 designated stopping points where participants paused to experience the soundscape and subsequently filled out the questionnaires. The second soundwalk comprised the

same 6 points, plus 3 additional stepovers used to improve the analysis. The pleasantness ratings were obtained following the ISO 12913-2 guidelines [18], using questionnaires from method A, Annex C3, of the Technical Specification.

3. CASE STUDY

The study focuses on the Fisciano campus of the University of Salerno, Italy. The campus hosts a variety of facilities, including lecture halls, laboratories, offices, libraries, the canteen, and sports facilities. The architectural layout integrates pedestrian pathways, vehicular roads, and multiple gathering spaces and green areas.
Figure 1 provides the exact location of the stepovers used during the soundwalk activities, with points from the first soundwalk marked in red and those added during the second one marked in blue.

3.1 Acoustics characteristic of the Campus

The campus' acoustic environment is shaped by the different characteristics and functions of each zone. All areas of the campus, with their predominant sound sources and, thus, the experience users have there, tend to follow a consistent pattern. However, their acoustic environments are not always static and can vary depending on factors such as the time of day, season, and weather conditions.
Certain zones, for example, are characterized by a lot of greenery, with natural sounds like birdsong and wind, offering a tranquil atmosphere. Parks and tree-lined walkways also serve as buffer zones that can mitigate the propagation of near-road traffic, contributing to a more balanced acoustic environment. However, seasonal changes may influence the presence of vegetation and wildlife, while weather conditions, such as wind or rain, may alter sound propagation and overall auditory perception.
The central part of the campus is occupied by buildings, including lecture halls, laboratories, faculty offices, libraries, and the canteen. The acoustic environment in these areas is primarily influenced by human activities, such as conversations, footsteps, and so on. They can be very dynamic environments, changing throughout the day, with peak noise levels during class transitions and breaks and quieter periods during lectures or outside standard working hours. Moreover, in winter, noise from heating systems may be present. Lastly, multiple roadways and parking areas introduce traffic-related noise inside the campus environment. Vehicular movements, particularly during peak hours, for example, right before class hours, affect the surrounding soundscapes. Variations in traffic levels can be observed within different seasons, particularly during course periods or exam sessions. Table 1 shows the main characteristics of the points investigated in the Fisciano Campus of the University of Salerno.

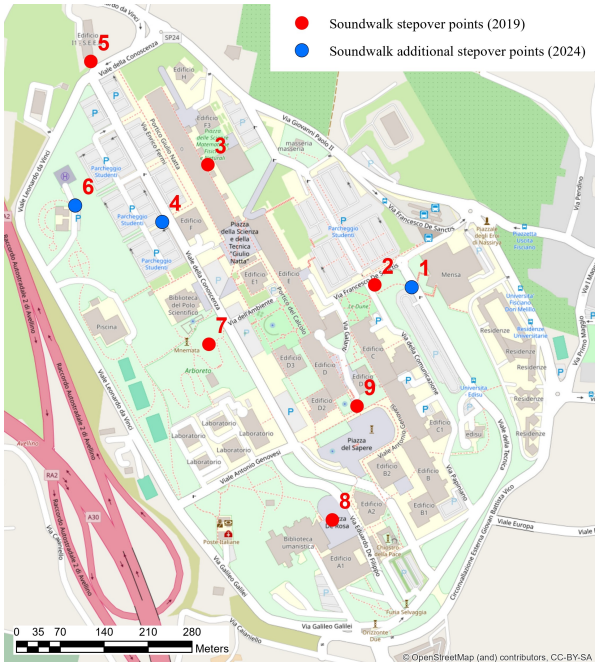


Figure 1. Map of the campus from OSM [19] with soundwalks stepover points: red points are from the first soundwalk, blue points are the additional points from the second soundwalk.

3.2 Data Collection and Analysis

The data analyzed in this study were collected through structured measurement campaigns, including both NoiseCapture parties and soundwalks. As for the NoiseCapture parties, to reduce the risk of erroneous data entries, participants received proper training before each activity. Since measurements are collected while walking, they were instructed to stop recording whenever they perceived a significant change in the soundscape, ensuring that the recorded pleasantness ratings accurately reflected distinct acoustic conditions. However, during the first NoiseCapture party in 2018, the authors were not yet focused on the soundscape approach, resulting in many measurement tracks missing the pleasantness values. Thus, these data were excluded from the present analysis.

Table 1. Soundwalks stepover points characteristics.

Point	Description	Main sound sources
1	Street, near the canteen building	Chatting, road traffic noise
2	Green area, near parking lots and academic buildings	Chatting, road traffic noise, nature
3	Academic building area	Chatting, HVAC implants in winter
4	Academic building area, near parking lots	Chatting, road traffic noise
5	Street, near parking lots and academic buildings	Chatting, road traffic noise, nature
6	Green area	Nature
7	Green area	Nature, road traffic noise
8	Square Area	Chatting
9	Square Area	Chatting

Moreover, to build a reliable dataset, the "*Accuracy*" of each measurement point has also been considered, where "Accuracy" refers to the GPS localization accuracy in meters, i.e., the radius within which there is a 68% probability that the actual location of the measurement point lies. Only points with an accuracy of less than 10 meters have been considered in this study. Moreover, points with missing pleasantness values have been discarded.

As mentioned earlier, soundwalks were also conducted to obtain detailed assessments of the soundscape in specific stepovers [18]. A first soundwalk activity was carried out on March 8, 2019, and a more recent one took place on November 5, 2024. In both soundwalks, a training session was conducted for the participants, and sound continuous equivalent levels were measured at each point with a calibrated class 1 sound level meter (Fusion, 01dB).

The main information for both the NoiseCapture parties (noted as "NC") and the soundwalk activities (noted as "SW") is provided in Table 2. The time of day during which the measurement campaigns took place, the number of participants, and the number of points that make up each year's dataset after the cleaning process are also provided, while for the soundwalks, the number of stepover points is also provided.

4. RESULTS AND DISCUSSION

Following the methodology presented in [12, 13], maps of the pleasantness across the Fisciano Campus of the University of Salerno have been generated for each edition of the NoiseCapture party. For the sake of brevity, the maps will not be reported in this contribution, but only values obtained through the interpolation will be discussed.

To enable a more detailed analysis of the temporal evolution of the campus soundscape features, the first step involved merging all data collected during the various NoiseCapture Party activities into a single dataset to create an overall pleasantness map, consistent with previous studies [12, 13, 15], under the assumption that the campus acoustics characteristics remain relatively stable over time. This served as a baseline for comparison with individual-year pleasantness maps, allowing for the identification of potential temporal variations. For the interpolation process, fixed search radii of 50 and 100 meters were adopted to assess variations at different spatial scales. Table 3 presents a comparative analysis of pleasantness values as measured through the soundwalk activity and estimated via IDW interpolation using both the 2024 dataset and the total cleaned dataset with different search radii. Alongside these, the equivalent continuous sound level $L_{A,eq}$ measured during the 2024 soundwalk edition is also included, offering a direct correlation between the perceptual data and the acoustic measurements at the specified locations.

The pleasantness values obtained through the IDW maps demonstrate relative stability across the different influence radii with both datasets. Moreover, comparing values from the total dataset with those of 2024 shows that some points remained relatively stable over time while others changed significantly. For instance, Point 2 and Point 3 exhibit only minor variations between the IDW-interpolated values from the total dataset and those from the 2024 dataset, suggesting that the acoustic and environmental conditions at these locations have not changed a lot. Specifically, for Point 2, the IDW values for both datasets and search radii remain within a narrow range (approximately 53-58%), and the soundwalk measurement (56.80%) confirms this consistency. Similarly, at Point 3, the IDW values for the total dataset (30.71% for r = 50 m and 30.98% for r = 100 m) are very close to those from the 2024 dataset (24.71% and 26.86%, respectively), while the soundwalk result (21.00%) is just slightly lower, reinforcing the stability of this location.

Conversely, some points show considerable changes over

Table 2. NoiseCapture parties and soundwalk activities main information.

Event	Date	Season	Time of day	Number of participants	Number of points
SW	08/03/2019	Winter	Morning	22	6
NC	24/05/2019	Spring	Morning	39	11766
NC	16/05/2022	Spring	Afternoon	40	4902
NC	09/11/2022	Autumn	Morning	113	24056
NC	26/10/2023	Autumn	Afternoon	78	12560
NC	05/11/2024	Autumn	Afternoon	64	23984
SW	05/11/2024	Autumn	Afternoon	52	9

Table 3. Comparison of pleasantness as measured through soundwalk activity and computed through IDW interpolation with 2024 data and with the total cleaned dataset with different search radius *r*.

Point	$L_{A,eq}$ [dBA]	Pleasantness value [%]				
		IDW map (total, *r=50m*)	IDW map (total, *r=100m*)	IDW map (2024, *r=50m*)	IDW map (2024, *r=100m*)	Soundwalk (2024)
1	61.1	86.30	84.95	33.43	41.14	44.81
2	51.1	53.80	54.00	58.09	56.80	61.00
3	57.8	30.71	30.98	24.71	26.86	21.00
4	51.0	60.69	59.59	35.29	28.80	52.55
5	50.8	47.49	47.67	47.00	-	60.20
6	47.1	-	48.39	-	38.08	77.27
7	44.6	79.60	73.49	70.30	63.34	86.58
8	49.3	62.31	62.92	-	61.37	71.25
9	47.2	53.09	53.88	52.63	53.25	71.15

time, likely due to modifications in their acoustic environment. In Point 1, for example, while the IDW interpolation for the total dataset shows relatively high pleasantness values (86.30% for r = 50 m and 84.95% for r = 100 m), the 2024 dataset reports much lower values (33.43% for r = 50 m and 41.14% for r = 100 m). The soundwalk measurement (44.81%) is closer to the latter, suggesting that recent conditions have negatively influenced perception. This decline may be because 2024 measurements were taken during peak traffic hours, when vehicular noise from the near parking lot was at its highest, as shown by the high $L_{A,eq}$ value. Moreover, ongoing construction work in the canteen building likely masked more pleasant sounds, reducing the perceived pleasantness. Since such works in progress were not present in previous years, the change highlights the dynamic nature of the acoustic environment and the impact of temporary but significant alterations in the soundscape.

Point 4 has undergone a noticeable change. Previously, this location was primarily a parking lot, but a new building has been constructed in recent years, altering both the soundscape and the overall environmental perception. The IDW-interpolated pleasantness values have consequently changed, with a slight decrease compared to the total dataset (from approximately 60% to 35% in the 2024 dataset with r = 50 m). The soundwalk measurement (52.55%) indicates a more moderate perception of pleasantness, possibly influenced by the mixed presence of new infrastructure and residual green areas.

Point 5 is characterized by IDW interpolation values that have remained relatively stable between the total dataset and the 2024 dataset (around 47%). However, the sound-

walk measurement (60.20%) is significantly higher than that, suggesting that direct human perception of pleasantness at this location is more favorable than predicted by the model. Given the noise level ($L_{A,eq}$ = 50.8 dBA), this discrepancy might be explained by additional environmental factors, such as the presence of green spaces and, thus, natural sounds, which enhance the overall experience. The stability of the IDW values suggests that this location has not undergone major transformations, but the difference between the interpolated and measured values underscores the limitations of the IDW method.

Point 6, instead, exhibits a unique pattern due to data limitations. While an IDW-interpolated value was available for the total dataset for r = 100m (48.39%), the absence of a value for r = 50 m suggests a lack of sufficient nearby data points, likely due to fewer participants passing through that area or due to the cleaning process. Consequently, the interpolation may not accurately capture the complexity of local sound conditions, which is instead completely acknowledged during the soundwalk. With influence radii of 100 m, the inclusion of data from more distant points allowed for the generation of estimates. However, these data are predominantly from points near the external road, where perceived pleasantness is likely much lower than in the greener surroundings of the green area in point 6 itself. This aspect underscores the crucial role of the search radius in IDW interpolation, as it defines the spatial extent within which surrounding data affect the estimated values [13].

Another interesting case is Point 7, where pleasantness values have remained high but still show variations between datasets. However, the 2024 dataset shows a slight decrease in interpolated values (70.30% for r = 50 m compared to 79.60% in the total dataset). The soundwalk measurement (86.58%) confirms that the area remains one of the most pleasant locations, but the interpolation discrepancy suggests that the location possesses specific attributes, likely visual or environmental factors, such as greenery, that enhance positive perception when stationary but may not be fully captured by a moving listener.

Points 8 and 9 have a similar trend. While IDW determines relatively stable pleasantness values between the total dataset, the soundwalk measurement tends to be considerably higher, indicating that participants perceived the area as more pleasant than estimated through spatial interpolation. This discrepancy, however, may be influenced by the different times at which participants engaged in the two activities. While both activities started simultaneously, participants in the NoiseCapture Party completed their route more quickly, passing through certain points earlier in the day, when background noise levels were still elevated due to ongoing academic and social activities. In contrast, the soundwalk included scheduled stops and required participants to answer questionnaires, resulting in a longer duration and a later passage through some locations. By that time, the acoustic environment may have been quieter, enhancing the perception of pleasantness. For example, participants in the soundwalk activity passed by Point 8 and 9 around by 6 P.M. when academic activities were almost over and a quite environment was experienced, while the NoiseCapture party participants, passing by during peak hour around 4 P.M., had the full experience of a crowded and chaotic acoustic environment, which may not be perceived as fully pleasant.

4.1 Evolution of the Campus Over the Years

Table 4 provides a comparison of pleasantness values computed through IDW interpolation for each year's dataset with search radius r=100m and measured during the two soundwalks. A clear distinction emerges between areas where the acoustic environment has remained relatively stable and those where it has undergone significant changes. For instance, locations such as Points 2 and 7 exhibit only minor fluctuations, indicating that the environmental and acoustic conditions at these sites have remained mostly unchanged over the years. This stability may be attributed to the consistency of the surrounding areas and the lack of significant alterations to the land use. In contrast, other points of the campus have seen considerable shifts. Several ongoing construction activities have been present lately on the campus, in particular near Points 1, 4, and 5. These modifications in the campus infrastructure have led to an increased auditory presence of disruptive elements, overshadowing the more pleasant sounds that once contributed to the area's positive acoustic perception. For instance, the introduction of a new building near Point 4 appears to have altered the local soundscape, with the IDW interpolation suggesting a drop in pleasantness values in 2024.

4.2 Evolution of the Campus Throughout the Day

While the temporal evolution of the campus over the years reveals broader trends, a closer examination of the daily changes in the soundscape at specific points offers additional insight into the fluctuating nature of the soundscape. Analyzing the data from Table 4 gives a more nuanced understanding of how the soundscape at partic-

Table 4. Comparison of pleasantness computed through IDW interpolation with different datasets and search radius *r=100m*, and measured during soundwalks.

Point	Pleasantness value [%]							
	IDW 2019 *Morning*	**IDW 2022i** *Afternoon*	**IDW 2022ii** *Morning*	**IDW 2023** *Afternoon*	**IDW 2024** *Afternoon*	**IDW Total** -	**SW 2019** *Morning*	**SW 2024** *Afternoon*
1	74.26	38.34	77.56	65.51	41.14	84.95	-	44.81
2	57.02	30.57	59.74	46.51	56.80	54.00	54.40	61.00
3	48.36	25.31	25.43	26.61	26.86	30.98	2.30	21.00
4	73.31	100.00	69.53	41.77	39.13	59.59	-	52.55
5	-	-	-	-	46.77	47.67	52.30	60.20
6	61.00	-	60.85	75.00	38.08	48.39	-	77.27
7	77.42	-	75.94	75.43	63.34	73.49	72.70	86.58
8	66.82	100.00	56.03	76.35	61.37	62.92	67.10	71.25
9	55.65	100.00	49.75	63.68	53.25	53.88	61.40	71.15

ular locations evolves. For instance, Point 1 demonstrates a marked decrease in perceived pleasantness in the first edition of the 2022 and 2024 datasets compared to previous years, likely due to increased vehicular noise from nearby parking facilities during peak hours when such activities took place. Thereafter, Point 7, which is characterized mainly by green spaces and relatively low noise levels, maintains a high perception of pleasantness. However, a slight decrease in pleasantness between the 2024 dataset and the total dataset suggests that time-of-day factors shape the acoustic experience. The timing of the NoiseCapture party activities, which occurred during peak traffic hours, may have contributed to a more intrusive soundscape at this location, probably due to a nearby external road. Similarly, the discrepancies notable in Points 8 and 9 can be attributed to the fact that, while both activities started simultaneously, participants in the NoiseCapture Party completed their route more quickly and passed through these points earlier, when background noise was higher due to ongoing activities, whereas the soundwalk took place later, in quieter conditions, as explained earlier.

5. CONCLUSIONS

This study presented an updated analysis of the soundscape and perceived pleasantness across the Fisciano Campus of the University of Salerno. Using crowdsourced data, a comparison between pleasantness ratings collected over multiple years was performed. Areas with stable pleasantness values and others showing significant shifts over time were identified. Notably, some locations exhibited a marked decrease in pleasantness, potentially related to temporary or permanent changes such as increased traffic during peak hours or construction work. The evolving nature of the campus underscores the utility of continuous monitoring to capture these transformations and maintain an accurate understanding of how soundscapes change over time.

The obtained results highlighted the relevance of a multimethodological approach but also the limitations of the interpolation method in fully reflecting subjective perception, confirming the need for complementary approaches to better capture the complexity of the soundscape.

Nevertheless, the findings support the potential of participatory soundscape mapping as a valuable tool for environmental monitoring. By integrating quantitative acoustic indicators with perceptual data, it is possible to develop a richer understanding of sound environments and their evolution. This integrated perspective can also influence the design and planning of future modifications to campus areas, guiding interventions aimed at enhancing environmental quality and users' well-being.

Future steps may involve combining spatial and temporal analysis to support the identification of emerging trends and critical transitions in campus soundscapes.

6. ACKNOWLEDGMENTS

This study was partially funded by MIUR with the PRIN 2022 "Nature for sustainable cities: planning cost-effective and just solutions for urban issues" (NatSolis) (grant number 2022ZLE8HC). The authors are also grateful to all the students who took part in the NoiseCapture parties over the years.

7. REFERENCES

[1] H. De Wit, "The future of internationalization of higher education in challenging global contexts," *ETD - Educação Temática Digital*, vol. 22, p. 538–545, Aug. 2020. Template.

[2] Indicators OECD, *Education at a Glance 2022*. 2023.

[3] A. Calderon, "Massification of higher education revisited," 2018.

[4] W. Passchier-Vermeer and W. F. Passchier, "Noise exposure and public health.," *Environmental health perspectives*, vol. 108, no. suppl 1, pp. 123–131, 2000.

[5] S. A. Ibrahim, "Reviewing the effects of noise pollution on students (college and university)," in *AIP Conference Proceedings*, vol. 2591, AIP Publishing, 2023.

[6] K. Mealings and J. M. Buchholz, "The effect of classroom acoustics and noise on high school students' listening, learning and well-being: a scoping review," *Facilities*, vol. 42, no. 5/6, pp. 485–503, 2024.

[7] Q. Zhuang and Z. Shang, "Investigation and optimization research of soundscape in linyi university campus, shandong, china," in *Proceedings of the 2nd International Conference on Information, Control and Automation, ICICA 2022, December 2-4, 2022, Chongqing, China*, 2023.

[8] F. D'Alessandro, L. Evangelisti, C. Guattari, G. Grazieschi, and F. Orsini, "Influence of visual aspects and other features on the soundscape assessment of a university external area," *Building Acoustics*, vol. 25, no. 3, pp. 199–217, 2018.

[9] E. M. E. M. Anuar, N. C. Din, and H. Hussein, "Traffic noise influence on soundscape quality at campus landscape area," *Journal of Design and Built Environment*, vol. 17, no. 1, 2017.

[10] A. Mascolo, S. Mancini, G. Graziuso, J. Quartieri, and C. Guarnaccia, "Comparison between sound pressure levels and perception: a soundscape application in a university campus," in *Journal of Physics: Conference Series*, vol. 1603, p. 012026, IOP Publishing, 2020.

[11] S. Mancini, A. Mascolo, G. Graziuso, and C. Guarnaccia, "Soundwalk, questionnaires and noise measurements in a university campus: A soundscape study," *Sustainability*, vol. 13, no. 2, p. 841, 2021.

[12] A. Mascolo, D. Rossi, M. Grimaldi, C. Guarnaccia, *et al.*, "Soundscape indicators assessment and mapping in a university campus," in *10th Convention of the European Acoustics Association, Turin, Italy*, 2023.

[13] A. Mascolo, D. Rossi, M. Grimaldi, and C. Guarnaccia, "Soundscape maps of pleasantness in a university campus by crowd-sourced measurements interpolation," *Noise Mapping*, vol. 11, no. 1, p. 20220178, 2024.

[14] G. Graziuso, M. Grimaldi, S. Mancini, J. Quartieri, and C. Guarnaccia, "Crowdsourcing data for the elaboration of noise maps: A methodological proposal," in *Journal of Physics: Conference Series*, vol. 1603, p. 012030, IOP Publishing, 2020.

[15] A. Mascolo, D. Rossi, M. Grimaldi, and C. Guarnaccia, "Study of pleasantness maps and perceived predominant sound sources in a university campus soundscape analysis," in *INTER-NOISE and NOISE-CON Congress and Conference Proceedings*, vol. 270, pp. 4838–4852, Institute of Noise Control Engineering, 2024.

[16] J. Picaut, N. Fortin, E. Bocher, G. Petit, P. Aumond, and G. Guillaume, "An open-science crowdsourcing approach for producing community noise maps using smartphones," *Building and Environment*, vol. 148, pp. 20–33, 2019.

[17] Noise Planet, "Noise capture," 2025. Accessed: 2025-03-04.

[18] ISO - International Organization for Standardization, "Iso/ts 12913–2:2018 acoustics – soundscape – part 2: Data collection and reporting requirements," tech. rep., ISO, Geneva, 2018.

[19] OpenStreetMap contributors, "Planet dump retrieved from https://planet.osm.org ." `https://www.openstreetmap.org`, 2017.

Bibliography

[1] Gaius Iulius Caesar. *Lex Iulia Municipalis*. Tabula Heracleensis, Corpus Inscriptionum Latinarum. 45 BCE (cited on page 1).

[2] Michael Hewson Crawford and JD Cloud. *Roman statutes*. Vol. 2. Institute of Classical Studies London, 1996 (cited on page 1).

[3] Ernest George Hardy. 'The Table of Heraclea and the Lex Julia Municipalis'. In: *The Journal of Roman Studies* 4 (1914), pp. 65–110 (cited on page 1).

[4] Decimus Iunius Iuvenalis. *Saturae*. Latin literary work, early 2nd century CE. c. 100–127 CE (cited on page 2).

[5] Decimo Giunio Giovenale. *Satire*. Ed. by Giovanni Viansino. Oscar Classici Greci e Latini. Milano: Mondadori, 1990 (cited on page 2).

[6] Publius Vergilius Maro. *Opera [Eclogae, Georgica, Aeneis]*. Latin poetic works, late 1st century BCE. c. 42–19 BCE (cited on page 2).

[7] Wendell Vernon Clausen. *A Commentary on Virgil, Eclogues*. Oxford: Clarendon Press, 1994 (cited on page 2).

[8] Titus Lucretius Carus. *De Rerum Natura*. c. 50–55 BCE (cited on page 2).

[9] Titus Lucretius Carus. *Titi Lucreti Cari De Rerum Natura Libri Sex*. Ed. by Cyril Bailey. Oxford: Clarendon Press, 1947 (cited on page 2).

[10] Emily Cockayne. *Hubbub: Filth, Noise, and Stench in England, 1600–1770*. New Haven: Yale University Press, 2007, pp. 106–120 (cited on page 2).

[11] Charles Dickens. *Nicholas Nickleby*. London: Chapman and Hall, 1839 (cited on page 2).

[12] Giovanni Domenico Mansi. *Sacrorum Conciliorum Nova et Amplissima Collectio*. Vol. 26. Venice: Antonio Zatta, 1784 (cited on page 2).

[13] Joseph Hartzheim and Johann Friedrich Schannat. *Concilia Germaniae: Tomus III*. Cologne: Joannis Wilhelmi Krakamp & haeredum Christiani Simonis, 1760, p. 662 (cited on page 2).

[14] Lane B. Baker. 'The Sound of Sin: Episcopal Noise Regulation in the Later Middle Ages'. In: *Viator* 52.2 (2021), pp. 131–178 (cited on page 2).

[15] Will Steffen et al. 'The trajectory of the Anthropocene: the great acceleration'. In: *The Anthropocene Review* 2.1 (2015), pp. 81–98 (cited on page 2).

[16] Lewis H. Brown and Donald Anderson Laird. *City noise: The report of the commission appointed by Dr. Shirley W. Wynne, Commissioner of Health, to study noise in New York city and to develop means of abating it*. Noise Abatement Commission, Department of Health, City of New York, 1930 (cited on page 2).

[17] Karin Bijsterveld. 'The diabolical symphony of the mechanical age: Technology and symbolism of sound in European and North American noise abatement campaigns, 1900-40'. In: *Social Studies of Science* 31.1 (2001), pp. 37–70 (cited on page 2).

[18] George Rosen. 'A backward glance at noise pollution.' In: *American Journal of public health* 64.5 (1974), pp. 514–517 (cited on page 2).

[19] W. Dixon Ward and James E. Fricke, eds. *Noise as a Public Health Hazard*. American Speech and Hearing Association Reports 4. Washington, D.C.: American Speech and Hearing Association, 1969 (cited on page 2).

[20] Lisa Goines and Louis Hagler. 'Noise pollution: a modem plague'. In: *South Med J* 100.3 (2007), pp. 287–94 (cited on page 2).

[21] U.S. Congress. *Noise Control Act of 1972, Pub. L. No. 92-574, 86 Stat. 1234*. United States Statutes at Large. Available at: https://www.govinfo.gov/content/pkg/STATUTE-86/pdf/STATUTE-86-Pg1234.pdf. Washington, D.C., 1972. (Visited on 02/16/2026) (cited on pages 2, 4).

[22] U.S. Environmental Protection Agency. *Toward a National Strategy for Noise Control*. Report. Washington, D.C.: Office of Noise Abatement and Control, 1972. (Visited on 02/16/2026) (cited on pages 2–4).

[23] Monica S. Hammer, Tracy K. Swinburn, and Richard L. Neitzel. 'Environmental noise pollution in the United States: developing an effective public health response'. In: *Environmental Health Perspectives* 122.2 (2013), p. 115 (cited on page 3).

[24] World Health Organization. *Burden of disease from environmental noise: Quantification of healthy life years lost in Europe*. World Health Organization. Regional Office for Europe, 2011 (cited on pages 3, 12, 37, 107, 109).

[25] European Parliament, Council of the European Union. *Directive 2002/49/EC of the European Parliament and of the Council of 25 June 2002 relating to the assessment and management of environmental noise*. June 2002 (cited on pages 3, 11, 12, 29, 33, 36, 38, 45, 107, 108).

[26] Arline L Bronzaft. 'Impact of noise on health: the divide between policy and science'. In: *Open Journal of Social Sciences* 5.5 (2017), pp. 108–20 (cited on page 3).

[27] European Environment Agency (EEA). *Environmental noise in Europe, 2020*. Publications Office, 2020 (cited on pages 3, 11, 12, 107, 109).

[28] European Environment Agency (EEA). *Environmental noise in Europe, 2025*. Publications Office, 2025 (cited on pages 3, 11, 12, 39, 40, 107–109).

[29] Charlotte World Health Organization: Hurtley. *Night noise guidelines for Europe*. WHO Regional Office Europe, 2009 (cited on pages 3, 5, 12, 107).

[30] Thomas Münzel et al. 'Cardiovascular effects of environmental noise exposure'. In: *European heart journal* 35.13 (2014), pp. 829–836 (cited on pages 3, 4, 108).

[31] World Health Organization. *Environmental noise guidelines for the European region*. World Health Organization. Regional Office for Europe, 2018 (cited on pages 3, 5, 12, 107, 109).

[32] Mathias Basner et al. 'Auditory and non-auditory effects of noise on health'. In: *The lancet* 383.9925 (2014), pp. 1325–1332 (cited on pages 3, 4, 108).

[33] Birgitta World Health Organization: Berglund, Thomas Lindvall, and Dietrich H. Schwela. 'New WHO guidelines for community noise'. In: *Noise & vibration worldwide* 31.4 (2000), pp. 24–29 (cited on pages 3, 12, 107, 109).

[34] Wolfgang Babisch. 'The noise/stress concept, risk assessment and research needs'. In: *Noise and health* 4.16 (2002), pp. 1–11 (cited on pages 4, 108).

[35] Willy Passchier-Vermeer and Wim F. Passchier. 'Noise exposure and public health.' In: *Environmental Health Perspectives* 108 (2000), pp. 123–131 (cited on page 4).

[36] Angel M. Dzhambov and Peter Lercher. 'Road traffic noise exposure and depression/anxiety: an updated systematic review and meta-analysis'. In: *International Journal of Environmental Research and Public Health* 16.21 (2019), p. 4134 (cited on page 4).

[37] Rainer Guski, Dirk Schreckenberg, and Rudolf Schuemer. 'WHO environmental noise guidelines for the European region: a systematic review on environmental noise and annoyance'. In: *International Journal of Environmental Research and Public Health* 14.12 (2017), p. 1539 (cited on pages 4, 5).

[38] Mathias Basner and Sarah McGuire. 'WHO environmental noise guidelines for the European region: a systematic review on environmental noise and effects on sleep'. In: *International Journal of Environmental Research and Public Health* 15.3 (2018), p. 519 (cited on pages 4, 5, 108).

[39] Elise Van Kempen et al. 'WHO environmental noise guidelines for the European region: a systematic review on environmental noise and cardiovascular and metabolic effects: a summary'. In: *International Journal of Environmental Research and Public Health* 15.2 (2018), p. 379 (cited on pages 4, 108).

[40] Alan Lex Brown and Irene Van Kamp. 'WHO environmental noise guidelines for the European region: A systematic review of transport noise interventions and their impacts on health'. In: *International Journal of Environmental Research and Public Health* 14.8 (2017), p. 873 (cited on page 4).

[41] Wolfgang Babisch. 'Stress hormones in the research on cardiovascular effects of noise'. In: *Noise and Health* 5.18 (2003), pp. 1–11 (cited on page 4).

[42] Andreas Daiber et al. 'Oxidative stress and inflammation contribute to traffic noise-induced vascular and cerebral dysfunction via uncoupling of nitric oxide synthases'. In: *Redox Biology* 34 (2020), p. 101506 (cited on page 4).

[43] Ane Arregi et al. 'Road traffic noise exposure and its impact on health: evidence from animal and human studies—chronic stress, inflammation, and oxidative stress as key components of the complex downstream pathway underlying noise-induced non-auditory health effects'. In: *Environmental Science and Pollution Research* 31.34 (2024), pp. 46820–46839 (cited on page 4).

[44] Stephen A. Stansfeld et al. 'Aircraft and road traffic noise and children's cognition and health: a cross-national study'. In: *The Lancet* 365.9475 (2005), pp. 1942–1949 (cited on page 4).

[45] Nicholas Woodward, Caleb E. Finch, and Todd E. Morgan. 'Traffic-related air pollution and brain development'. In: *AIMS Environmental Science* 2.2 (2015), p. 353 (cited on page 4).

[46] Charlotte Clark and Katarina Paunovic. 'WHO environmental noise guidelines for the European region: A systematic review on environmental noise and cognition'. In: *International Journal of Environmental Research and Public Health* 15.2 (2018), p. 285 (cited on page 4).

[47] Yuyan Chen et al. 'Noise exposure-induced the cerebral alterations: From emerging evidence to antioxidant-mediated prevention and treatment'. In: *Ecotoxicology and Environmental Safety* 288 (2024), p. 117411 (cited on page 4).

[48] Zixuan Xue et al. 'Neural Mechanisms of Nonauditory Effects of Noise Exposure on Special Populations'. In: *Noise and Health* 26.121 (2024), pp. 70–81 (cited on page 4).

[49] Charlotte Clark and Katarina Paunovic. 'WHO environmental noise guidelines for the European region: a systematic review on environmental noise and quality of life, wellbeing and mental health'. In: *International Journal of Environmental Research and Public Health* 15.11 (2018), p. 2400 (cited on page 4).

[50] Marin Kuntić et al. 'Crosstalk between oxidative stress and inflammation caused by noise and air pollution—implications for neurodegenerative diseases'. In: *Antioxidants* 13.3 (2024), p. 266 (cited on page 4).

[51] Xiao-jie Dai et al. 'Noise Exposure Promotes Alzheimer's Disease–Like Lesions and DNA Damage'. In: *Noise and Health* 26.122 (2024), pp. 287–293 (cited on page 4).

[52] European Environment Agency. *Unequal exposure and unequal impacts: Social vulnerability to air pollution, noise and extreme temperatures in Europe*. Tech. rep. 22/2018. Publications Office of the European Union, 2018 (cited on page 5).

[53] Stefanie Dreger et al. 'Social inequalities in environmental noise exposure: a review of evidence in the WHO European Region'. In: *International Journal of Environmental Research and Public Health* 16.6 (2019), p. 1011 (cited on page 5).

[54] Cathryn Tonne et al. 'Socioeconomic and ethnic inequalities in exposure to air and noise pollution in London'. In: *Environment International* 115 (2018), pp. 170–179 (cited on page 5).

[55] Laura M. Dale et al. 'Socioeconomic status and environmental noise exposure in Montreal, Canada'. In: *BMC Public Health* 15.1 (2015), p. 205 (cited on page 5).

[56] Mathieu Carrier, Philippe Apparicio, and Anne-Marie Séguin. 'Road traffic noise in Montreal and environmental equity: What is the situation for the most vulnerable population groups?' In: *Journal of Transport Geography* 51 (2016), pp. 1–8 (cited on page 5).

[57] Francesco Aletta et al. 'Exploring the compatibility of "Method A" and "Method B" data collection protocols reported in the ISO/TS 12913-2: 2018 for urban soundscape via a soundwalk'. In: *Applied Acoustics* 155 (2019), pp. 190–203 (cited on pages 5, 110, 129).

[58] Eleanor Ratcliffe. 'Sound and soundscape in restorative natural environments: A narrative literature review'. In: *Frontiers in Psychology* 12 (2021), p. 570563 (cited on pages 5, 6).

[59] Konrad Uebel et al. 'Urban green space soundscapes and their perceived restorativeness'. In: *People and Nature* 3.3 (2021), pp. 756–769 (cited on page 6).

[60] Jesper J. Alvarsson, Stefan Wiens, and Mats E. Nilsson. 'Stress recovery during exposure to nature sound and environmental noise'. In: *International Journal of Environmental Research and Public Health* 7.3 (2010), pp. 1036–1046 (cited on pages 6, 110).

[61] Marc G. Berman, John Jonides, and Stephen Kaplan. 'The cognitive benefits of interacting with nature'. In: *Psychological Science* 19.12 (2008), pp. 1207–1212 (cited on page 6).

[62] Lili Tian, Daniel Winterbottom, and Juanjuan Liu. 'Soundscape optimization strategies based on landscape elements in urban parks: A case study of Greenlake park in Kunming'. In: *Sustainability* 15.13 (2023), p. 10155 (cited on pages 6, 110).

[63] Jun Zhang, Jinghua Jin, and Yimeng Liang. 'The Impact of Green Space on University Students' Mental Health: The Mediating Roles of Solitude Competence and Perceptual Restoration'. In: *Sustainability* 16.2 (2024), p. 707 (cited on pages 6, 110).

[64] Jin Yong Jeon, Hyun In Jo, and Kounseok Lee. 'Psycho-physiological restoration with audio-visual interactions through virtual reality simulations of soundscape and landscape experiences in urban, waterfront, and green environments'. In: *Sustainable Cities and Society* 99 (2023), p. 104929 (cited on page 6).

[65] Xiaochao Chen and Jian Kang. 'Natural sounds can encourage social interactions in urban parks'. In: *Landscape and Urban Planning* 239 (2023), p. 104870 (cited on page 6).

[66] Stephen R. Kellert and Edward O. Wilson. 'The biophilia hypothesis'. In: (1995) (cited on page 6).

[67] Yannick Joye and Andreas De Block. ''Nature and I are two': A critical examination of the biophilia hypothesis'. In: *Environmental Values* 20.2 (2011), pp. 189–215 (cited on page 6).

[68] Edward O. Wilson. *Biophilia*. Harvard University Press, 1986 (cited on page 6).

[69] Stephen Kaplan. 'The restorative benefits of nature: Toward an integrative framework'. In: *Journal of environmental psychology* 15.3 (1995), pp. 169–182 (cited on pages 6, 107, 109).

[70] Avik Basu, Jason Duvall, and Rachel Kaplan. 'Attention restoration theory: Exploring the role of soft fascination and mental bandwidth'. In: *Environment and Behavior* 51.9-10 (2019), pp. 1055–1081 (cited on pages 6, 107, 109, 110).

[71] Susanne Kumpulainen et al. 'Enhancing psychophysiological well-being through nature-based soundscapes: an examination of heart rate variability in a cross-over study'. In: *Psychophysiology* 62.1 (2025), e14760 (cited on page 6).

[72] Jacob A. Benfield et al. 'Natural sound facilitates mood recovery'. In: *Ecopsychology* 6.3 (2014), pp. 183–188 (cited on page 6).

[73] Yuan Zhang, Jian Kang, and Joe Kang. 'Effects of soundscape on the environmental restoration in urban natural environments'. In: *Noise and Health* 19.87 (2017), pp. 65–72 (cited on page 6).

[74] Lauren Abbott, P. Newman, and J. Benfield. 'The influence of natural sounds on attention restoration'. PhD thesis. Pennsylvania State University University Park, PA, USA, 2015 (cited on page 6).

[75] Marcus Hedblom et al. 'Reduction of physiological stress by urban green space in a multisensory virtual experiment'. In: *Scientific Reports* 9.1 (2019), p. 10113 (cited on page 6).

[76] Mercede Erfanian et al. 'The psychophysiological implications of soundscape: A systematic review of empirical literature and a research agenda'. In: *International Journal of Environmental Research and Public Health* 16.19 (2019), p. 3533 (cited on page 6).

[77] Matilda Annerstedt et al. 'Inducing physiological stress recovery with sounds of nature in a virtual reality forest—Results from a pilot study'. In: *Physiology & Behavior* 118 (2013), pp. 240–250 (cited on page 6).

[78] Jiang Liu, Jian Kang, and Holger Behm. 'Birdsong as an element of the urban sound environment: A case study concerning the area of Warnemünde in Germany'. In: *Acta Acustica united with Acustica* 100.3 (2014), pp. 458–466 (cited on page 6).

[79] Eleanor Ratcliffe, Birgitta Gatersleben, and Paul T Sowden. 'Bird sounds and their contributions to perceived attention restoration and stress recovery'. In: *Journal of Environmental Psychology* 36 (2013), pp. 221–228 (cited on page 6).

[80] Xin-Chen Hong et al. 'modelling the impact of soundscape drivers on perceived birdsongs in urban forests'. In: *Journal of Cleaner Production* 292 (2021), p. 125315 (cited on page 6).

[81] Bum-Jin Park et al. 'Relationship between psychological responses and physical environments in forest settings'. In: *Landscape and Urban Planning* 102.1 (2011), pp. 24–32 (cited on page 6).

[82] MaryCarol R. Hunter, Brenda W. Gillespie, and Sophie Yu-Pu Chen. 'Urban nature experiences reduce stress in the context of daily life based on salivary biomarkers'. In: *Frontiers in Psychology* 10 (2019), p. 413490 (cited on page 6).

[83] Michele Antonelli, Grazia Barbieri, and Davide Donelli. 'Effects of forest bathing (shinrin-yoku) on levels of cortisol as a stress biomarker: a systematic review and meta-analysis'. In: *International Journal of Biometeorology* 63.8 (2019), pp. 1117–1134 (cited on page 6).

[84] Weifu Gao et al. 'The effects of environmental sensitivity and noise sensitivity on soundscape evaluation'. In: *Building and Environment* 245 (2023), p. 110945 (cited on page 6).

[85] Injoon Song et al. 'Effects of nature sounds on the attention and physiological and psychological relaxation'. In: *Urban Forestry & Urban Greening* 86 (2023), p. 127987 (cited on page 6).

[86] European Commission - Statistic Explained. *Urban Europe - Statistics on cities, towns and suburbs - 2016 edition*. Publications Office, 2016 (cited on page 11).

[87] European Commission, Knowledge4Policy. *Urbanisation in Europe*. July 2020. URL: https://knowledge4policy.ec.europa.eu/foresight/topic/continuing-urbanisation/urbanisation-europe_en (visited on 11/13/2025) (cited on page 11).

[88] European Commission - Statistic Explained. *Final energy consumption in transport - detailed statistics*. 2024. URL: https://ec.europa.eu/eurostat/statistics-explained/SEPDF/cache/131944.pdf (visited on 11/13/2025) (cited on page 11).

[89] Eurostat. 'Passenger Cars—Per Thousand Inhabitants'. In: (2023) (cited on page 11).

[90] World Health Organization. *Compendium of WHO and other UN guidance in health and environment, 2022 update*. World Health Organization. Regional Office for Europe, 2022 (cited on page 12).

[91] World Health Organization. *Compendium of WHO and other UN guidance in health and environment, 2024 update*. World Health Organization. Regional Office for Europe, 2024 (cited on page 12).

[92] European Commission. 'Pathway to a healthy planet for all. EU action plan: 'Towards zero pollution for air, water and soil''. In: *COM(2021) 400 final* (2021), p. 22. (Visited on 02/16/2026) (cited on page 12).

[93] Stylianos Kephalopoulos, Marco Paviotti, and Fabienne Anfosso-Lédée. *Common noise assessment methods in Europe (CNOSSOS-EU)*. 2012 (cited on pages 12, 29, 34, 49, 51, 52).

[94] European Commission. *Commission Directive (EU) 2015/996 of 19 May 2015 establishing common noise assessment methods according to Directive 2002/49/EC of the European Parliament and of the Council (Text with EEA relevance)*. 2015 (cited on pages 12, 29, 49, 51, 52).

[95] Campbell Steele. 'A critical review of some traffic noise prediction models'. In: *Applied Acoustics* 62.3 (2001), pp. 271–287 (cited on pages 14, 31).

[96] Suman Mann and Gyanendra Singh. 'Traffic noise monitoring and modelling—an overview'. In: *Environmental Science and Pollution Research* 29.37 (2022), pp. 55568–55579 (cited on page 14).

[97] Fidelma Ibili et al. 'Traffic noise models and noise guidelines: a review'. In: *Noise & Vibration Worldwide* 53.1-2 (2022), pp. 65–79 (cited on page 14).

[98] Naveen Garg and Sagar Maji. 'A critical review of principal traffic noise models: Strategies and implications'. In: *Environmental Impact Assessment Review* 46 (2014), pp. 68–81 (cited on page 14).

[99] H.N. Rajakumara and R.M. Mahalinge Gowda. 'Road traffic noise prediction models: a review'. In: *International Journal of Sustainable Development and Planning* 3.3 (2008), pp. 257–271 (cited on page 14).

[100] Guillermo Rey-Gozalo, Juan Miguel Barrigón Morillas, and David Montes González. 'Analysis and Management of Current Road Traffic Noise'. In: *Current Pollution Reports* 8.4 (2022), pp. 315–327 (cited on page 14).

[101] Arnaud Can and Pierre Aumond. 'Estimation of road traffic noise emissions: The influence of speed and acceleration'. In: *Transportation Research Part D: Transport and Environment* 58 (2018), pp. 155–171 (cited on page 14).

[102] Antonio Pascale et al. 'A vehicle noise specific power concept'. In: *2020 Forum on Integrated and Sustainable Transportation Systems (FISTS)*. IEEE. 2020, pp. 170–175 (cited on pages 14, 31).

[103] Antonio Pascale et al. 'A study on vehicle Noise Emission modelling: Correlation with air pollutant emissions, impact of kinematic variables and critical hotspots'. In: *Science of the Total Environment* 787 (2021), p. 147647 (cited on pages 14, 31).

[104] Beranek Bolt et al. *Handbook of Acoustic Noise Control*. Handbook of Acoustic Noise Control v. 1. Wright Air Development Center, Air Research and Development Command, United States Air Force, 1953 (cited on pages 15, 40).

[105] A.F.B Nickson. 'Can community reaction to increased traffic noise be forecast?' In: *Proc. of 5th International Congress on Acoustics*. 1965 (cited on page 15).

[106] D.R. Johnson and E.G. Saunders. 'The evaluation of noise from freely flowing road traffic'. In: *Journal of Sound and Vibration* 7.2 (1968), pp. 287–309 (cited on page 15).

[107] William J. Galloway, Welden E. Clark, and Jean Smalley Kerrick. 'Highway noise measurement, simulation, and mixed reactions'. In: *National Cooperative Highway Research Program (NCHRP) Report* 78 (1969) (cited on page 16).

[108] M.A. Burgess. 'Noise prediction for urban traffic conditions-related to measurements in the Sydney metropiltan area'. In: *Applied Acoustics* 10.1 (1977), pp. 1–7 (cited on page 16).

[109] I.D. Griffiths and Frederick John Langdon. 'Subjective response to road traffic noise'. In: *Journal of Sound and Vibration* 8.1 (1968), pp. 16–32 (cited on page 16).

[110] C. Fagotti and A. Poggi. 'Traffic noise abatement strategies: The analysis of real case not really effective'. In: *Proceedings of 18th International Congress for Noise Abatement*. 1995, pp. 223–233 (cited on page 17).

[111] Centre Scientifique et Technique du Batiment. 'Etude Théorique et Expérimentale de la Propagation Acoustique'. In: *Revue d'Acoustique* 70 (1991) (cited on page 17).

[112] Claudio Guarnaccia. 'Advanced Tools for Traffic Noise modelling and Prediction'. In: *WSEAS Transactions on Systems* 12.2 (2013), pp. 121–130 (cited on page 17).

[113] Domenico Rossi, Aurora Mascolo, and Claudio Guarnaccia. 'Calibration and Validation of a Measurements-Independent Model for Road Traffic Noise Assessment'. In: *Applied Sciences* 13.10 (2023), p. 6168 (cited on pages 18, 46).

[114] Department of Transport, UK Welsh Office. *Calculation of road traffic noise*. 1988 (cited on page 19).

[115] Für Verkehr Bundesministers and Bauund Wohnungswesen. 'Richtlinien für den Lärmschutz an Straßen (RLS 90)'. In: *Verkehrsblatt: Amtsblatt des Bundesministers für Verkehr der Bundesrepublik Deutschland (VkBl.) Nr* 7 (1990) (cited on page 20).

[116] G.B. Cannelli, K Glück, and S Santoboni. 'A mathematical model for evaluation and prediction of the mean energy level of traffic noise in Italian towns'. In: *Acta Acustica united with Acustica* 53.1 (1983), pp. 31–36 (cited on page 20).

[117] A. Cocchi, Angelo Farina, and G Lopes. 'Modelli matematici per la previsione del rumore stradale: verifica ed affinamento del modello CNR in base a rilievi sperimentali nella città di Bologna'. In: *Atti XIX Convegno Nazionale AIA, Napoli*. 1991 (cited on page 20).

[118] Thanaphan Suksaard et al. 'Road traffic noise prediction model in Thailand'. In: *Applied Acoustics* 58.2 (1999), pp. 123–130 (cited on page 21).

[119] Bengang Li et al. 'A GIS based road traffic noise prediction model'. In: *Applied Acoustics* 63.6 (2002), pp. 679–691 (cited on pages 21, 33).

[120] H.L. Nielsen. *Road Traffic Noise: Nordic Prediction Method*. Temanord Series. Stationery Office, 1997 (cited on page 22).

[121] Muhammed Yasin Codur, Ahmet Atalay, and Ahmet Unal. 'Performance evaluation of the ANN and ANFIS models in urban traffic noise prediction'. In: *Fresenius Environment Bulletin* 26 (2017), pp. 4254–4260 (cited on page 23).

[122] Khaled Hamad, Mohamad Ali Khalil, and Abdallah Shanableh. 'Modelling roadway traffic noise in a hot climate using artificial neural networks'. In: *Transportation Research Part D: Transport and Environment* 53 (2017), pp. 161–177 (cited on page 23).

[123] Ali Mansourkhaki et al. 'A neural network noise prediction model for Tehran urban roads'. In: *Journal of Environmental Engineering and Landscape Management* 26.2 (2018), pp. 88–97 (cited on pages 23, 24).

[124] Ibrahim Khalil Umar et al. 'The state-of-the-art in the application of artificial intelligence-based models for traffic noise prediction: a bibliographic overview'. In: *Cogent Engineering* 11.1 (2024), p. 2297508 (cited on page 23).

[125] Paras Kumar, S.P. Nigam, and Narotam Kumar. 'Vehicular traffic noise modelling using artificial neural network approach'. In: *Transportation Research Part C: Emerging Technologies* 40 (2014), pp. 111–122 (cited on page 23).

[126] N. Garg et al. 'Comparison of ANN and analytical models in traffic noise modelling and predictions'. In: *Acoustics Australia* 43 (2015), pp. 179–189 (cited on page 23).

[127] Francis Cirianni and Giovanni Leonardi. 'Artificial neural network for traffic noise modelling'. In: *ARPN Journal of Engineering and Applied Sciences* 10.22 (2015), pp. 10413–10419 (cited on pages 23, 24).

[128] Luis Bravo-Moncayo et al. 'A machine learning approach for traffic-noise annoyance assessment'. In: *Applied Acoustics* 156 (2019), pp. 262–270 (cited on page 24).

[129] Vladimir Nedic et al. 'Comparison of classical statistical methods and artificial neural network in traffic noise prediction'. In: *Environmental Impact Assessment Review* 49 (2014), pp. 24–30 (cited on page 24).

[130] Natalia Genaro et al. 'A neural network based model for urban noise prediction'. In: *The journal of the Acoustical Society of America* 128.4 (2010), pp. 1738–1746 (cited on page 24).

[131] Francis Cirianni and Giovanni Leonardi. 'Road traffic noise prediction models in the metropolitan area of the Strait of Messina'. In: *Proceedings of the Institution of Civil Engineers-Transport*. Vol. 164. 4. Thomas Telford Ltd. 2011, pp. 231–239 (cited on page 24).

[132] Asheesh Sharma et al. 'Adoptive neuro-fuzzy inference system for traffic noise prediction'. In: *International Journal of Computer Applications* 98.13 (2014) (cited on page 24).

[133] Asheesh Sharma et al. 'An adaptive neuro-fuzzy interface system model for traffic classification and noise prediction'. In: *Soft Computing* 22 (2018), pp. 1891–1902 (cited on page 24).

[134] Alejandro Ruiz-Padillo et al. 'Selection of suitable alternatives to reduce the environmental impact of road traffic noise using a fuzzy multi-criteria decision model'. In: *Environmental Impact Assessment Review* 61 (2016), pp. 8–18 (cited on page 24).

[135] Sahar Rahmani, Seyed Mahmoud Mousavi, and M. Jalal Kamali. 'Modelling of road-traffic noise with the use of genetic algorithm'. In: *Applied Soft Computing* 11.1 (2011), pp. 1008–1013 (cited on page 24).

[136] Leila Khouban et al. 'Combination of artificial neural networks and genetic algorithm - gamma test method in prediction of road traffic noise'. In: *Environmental Engineering & Management Journal (EEMJ)* 14.4 (2015) (cited on page 24).

[137] Pushuang Chen et al. 'Research on prediction model of tractor sound quality based on genetic algorithm'. In: *Applied Acoustics* 185 (2022), p. 108411 (cited on page 24).

[138] Joël Lelong. 'Vehicle noise emission: Evaluation of tyre/road and motor-noise contributions'. In: *Proceedings of Internoise 99, Fort Lauderdale, Florida, USA, 6-8 December 1999, Vol. 1*. 1999 (cited on page 25).

[139] Kurt Heutschi. 'SonRoad: New Swiss road traffic noise model'. In: *Acta Acustica united with Acustica* 90.3 (2004), pp. 548–554 (cited on page 26).

[140] G. Watts. *Harmonoise prediction model for road traffic noise*. Transport Research Laboratory, 2005 (cited on page 26).

[141] Gregg G. Fleming, Amanda S. Rapoza, and Cynthia S.Y. Lee. *Development of national reference energy mean emission levels for the FHWA traffic noise model (FHWA TNM), version 1.0*. Tech. rep. United States. Federal Highway Administration, 1995 (cited on page 27).

[142] Office of Natural Environment Federal Highway Admnistritaion. *Technical Manual, Traffic Noise Model 3.1*. U.S. Department of Transportation, 2021 (cited on page 27).

[143] Guillaume Dutilleux et al. 'NMPB-routes-2008: The revision of the french method for road traffic noise prediction'. In: *Acta Acustica united with Acustica* 96.3 (2010), pp. 452–462 (cited on page 28).

[144] Francis Besnard et al. 'Road noise prediction 1-Calculating sound emissions from road traffic'. In: *SETRA, Bagneux* (2009) (cited on page 28).

[145] Jean-Françcois Hamet et al. 'New vehicle noise emission for French traffic noise prediction'. In: *Applied acoustics* 71.9 (2010), pp. 861–869 (cited on page 28).

[146] Official Journal of the European Union Commission Delegated Directive (EU). *21.12.2020 amending, for the purposes of adapting to scientific and technical progress, Annex II to Directive 2002/49/EC of the European Parliament and of the Council as regards common noise assessment methods (CNOSSOS-EU)*. 2021 (cited on pages 29, 49, 51, 52).

[147] A. Kok and A. van Beek. 'Amendments for CNOSSOS-EU: Description of issues and proposed solutions'. In: *Rijksinstituut voor Volksgezondheid en Milieu (RIVM) Letter report* (2019) (cited on page 29).

[148] Marie-Agnès Pallas et al. 'Towards a model for electric vehicle noise emission in the European prediction method CNOSSOS-EU'. In: *Applied Acoustics* 113 (2016), pp. 89–101 (cited on page 30).

[149] Martin Czuka et al. 'Impact of potential and dedicated tyres of electric vehicles on the tyre-road noise and connection to the EU noise label'. In: *Transportation Research Procedia* 14 (2016), pp. 2678–2687 (cited on page 30).

[150] Gaetano Licitra et al. 'CNOSSOS-EU coefficients for electric vehicle noise emission'. In: *Applied Acoustics* 211 (2023), p. 109511 (cited on page 30).

[151] K. Ishii. 'Prediction of road traffic noise (part 1), method of practical calculation'. In: *Journal of the Acoustical Society of Japan* 31 (1975). In japanese, pp. 507–517 (cited on page 30).

[152] K. Ikegaya. 'Mathematical models and estimation for predicting the road traffic noise'. In: *Journal of the Acoustical Society of Japan* 31 (1975). In japanese, pp. 559–565 (cited on page 30).

[153] Shinichi Sakamoto. 'Road traffic noise prediction model "ASJ RTN-Model 2018": Report of the research committee on road traffic noise'. In: *Acoustical Science and Technology* 41.3 (2020), pp. 529–589 (cited on page 30).

[154] Kohei Yamamoto. 'Road traffic noise prediction model "ASJ RTN-Model 2008": report of the research committee on road traffic noise'. In: *Acoustical Science and Technology* 31.1 (2010), pp. 2–55 (cited on page 30).

[155] Bert De Coensel et al. 'Microsimulation based corrections on the road traffic noise emission near intersections'. In: *Acta Acustica United with Acustica* 93.2 (2007), pp. 241–252 (cited on pages 31, 32).

[156] Paulo Fernandes et al. 'Impacts of roundabouts in suburban areas on congestion-specific vehicle speed profiles, pollutant and noise emissions: An empirical analysis'. In: *Sustainable Cities and Society* 62 (2020), p. 102386 (cited on page 31).

[157] Arnaud Can and Dick Botteldooren. 'Towards traffic situation noise emission models'. In: *Acta Acustica United with Acustica* 97.5 (2011), pp. 900–903 (cited on page 31).

[158] Arnaud Can et al. 'Traffic noise spectrum analysis: Dynamic modelling vs. experimental observations'. In: *Applied Acoustics* 71.8 (2010), pp. 764–770 (cited on page 32).

[159] Johan Nygren et al. 'Vehicle-specific noise exposure cost: Noise impact allocation methodology for microscopic traffic simulations'. In: *Transportation Research Part D: Transport and Environment* 118 (2023), p. 103712 (cited on pages 32, 48, 60).

[160] Sacha Baclet et al. 'Near-real-time dynamic noise mapping and exposure assessment using calibrated microscopic traffic simulations'. In: *Transportation Research Part D: Transport and Environment* 124 (2023), p. 103922 (cited on page 32).

[161] Jasso Espadaler-Clapés, Emmanouil Barmpounakis, and Nikolas Geroliminis. 'Traffic congestion and noise emissions with detailed vehicle trajectories from UAVs'. In: *Transportation Research Part D: Transport and Environment* 121 (2023), p. 103822 (cited on page 32).

[162] Arnaud Can et al. 'Accounting for traffic dynamics improves noise assessment: Experimental evidence'. In: *Applied Acoustics* 70.6 (2009), pp. 821–829 (cited on page 32).

[163] Estelle Chevallier et al. 'Improving noise assessment at intersections by modelling traffic dynamics'. In: *Transportation Research Part D: Transport and Environment* 14.2 (2009), pp. 100–110 (cited on page 32).

[164] Laura Estévez-Mauriz and Jens Forssén. 'Dynamic traffic noise assessment tool: A comparative study between a roundabout and a signalised intersection'. In: *Applied Acoustics* 130 (2018), pp. 71–86 (cited on page 32).

[165] Domenico Rossi et al. 'The problem of obtaining vehicles speed input for road traffic noise microscopic models: a comparison between field measurements and a stochastic approach'. In: *INTER-NOISE and NOISE-CON Congress and Conference Proceedings*. Vol. 270. 7. Institute of Noise Control Engineering. 2024, pp. 4979–4988 (cited on page 32).

[166] Claudio Guarnaccia. 'EAgLE: Equivalent acoustic level estimator proposal'. In: *Sensors* 20.3 (2020), p. 701 (cited on pages 32, 34, 46).

[167] Claudio Guarnaccia et al. 'Improvement and Validation of a Smart Road Traffic Noise Model Based on Vehicles Tracking Using Image Recognition: EAgLE 3.0'. In: *Sensors* 25.6 (2025), p. 1750 (cited on pages 32, 34, 46).

[168] Luca Fredianelli et al. 'Traffic flow detection using camera images and machine learning methods in ITS for noise map and action plan optimization'. In: *Sensors* 22.5 (2022), p. 1929 (cited on pages 32, 46).

[169] Ashish Bhaskar, Edward Chung, and Masao Kuwahara. 'Development and implementation of the areawide Dynamic ROad traffic NoisE (DRONE) simulator'. In: *Transportation Research Part D: Transport and Environment* 12.5 (2007), pp. 371–378 (cited on page 32).

[170] Bert De Coensel et al. 'The influence of traffic flow dynamics on urban soundscapes'. In: *Applied Acoustics* 66.2 (2005), pp. 175–194 (cited on page 32).

[171] Valentin Le Bescond et al. 'Open-source modelling chain for the dynamic assessment of road traffic noise exposure'. In: *Transportation Research Part D: Transport and Environment* 94 (2021), p. 102793 (cited on page 32).

[172] Juha Heltimo, Jarkko Niittymäki, and Erkki Björk. 'A microlevel method for road traffic noise prediction'. In: *WIT Transactions on The Built Environment* 60 (2002) (cited on page 32).

[173] Haibo Wang, Zhaolang Wu, and Jincai Chen. 'A Prediction Method for City Traffic Noise Based on Traffic Simulation under a Mixed Distribution Probability'. In: *Sustainability* 16.16 (2024), p. 7065 (cited on page 33).

[174] Mohammed S. Ahmed and Allen R. Cook. *Analysis of freeway traffic time-series data by using Box-Jenkins techniques*. 722. 1979 (cited on page 33).

[175] Claudio Guarnaccia et al. 'Development and application of a time series predictive model to Acoustical noise levels'. In: *WSEAS Transactions on Systems* 13 (2014), pp. 745–756 (cited on page 33).

[176] Claudio Guarnaccia et al. 'Acoustical noise analysis and prediction by means of multiple seasonality time series model'. In: *International Journal of Mathematical Models and Methods in Applied Sciences* 8 (2014), pp. 384–393 (cited on page 33).

[177] Antonio Pascale et al. 'Correlating the effect of Covid-19 lockdown with mobility impacts: a time series study using noise sensors data'. In: *Transportation Research Procedia* 62 (2022), pp. 115–122 (cited on page 33).

[178] N. Garg et al. 'Applications of Autoregressive integrated moving average (ARIMA) approach in time-series prediction of traffic noise pollution'. In: *Noise Control Engineering Journal* 63.2 (2015), pp. 182–194 (cited on page 33).

[179] N. Garg et al. 'Comparison of ARIMA and ANN approaches in time-series predictions of traffic noise'. In: *Noise Control Engineering Journal* 64.4 (2016), pp. 522–531 (cited on page 33).

[180] Shinichi Sakamoto. 'Road traffic noise prediction model "ASJ RTN-Model 2018": Report of the research committee on road traffic noise'. In: *Acoustical Science and Technology* 41.3 (2020), pp. 529–589 (cited on page 34).

[181] Joseph Quartieri, Gerardo Iannone, and Claudio Guarnaccia. 'On the improvement of statistical traffic noise prediction tools'. In: *Proceedings of the 11th WSEAS International Conference on "Acoustics & Music: Theory & Applications"(AMTA'10), Iasi, Romania*. 2010, pp. 201–207 (cited on page 34).

[182] Antonio Pascale et al. 'Road traffic noise monitoring in a Smart City: Sensor and Model-Based approach'. In: *Transportation Research Part D: Transport and Environment* 125 (2023), p. 103979 (cited on pages 34, 46).

[183] Jibran Khan et al. 'Comparison of Road Traffic Noise prediction models: CNOSSOS-EU, Nord2000 and TRANEX'. In: *Environmental Pollution* 270 (2021), p. 116240 (cited on page 35).

[184] Keith Attenborough and Timothy Van Renterghem. *Predicting outdoor sound*. CRC Press, 2021 (cited on page 35).

[185] Timothy Van Renterghem and Dick Botteldooren. 'Landscaping for road traffic noise abatement: Model validation'. In: *Environmental Modelling & Software* 109 (2018), pp. 17–31 (cited on page 35).

[186] David Ecotiere, Cédric Foy, and Guillaume Dutilleux. 'Comparison of engineering models of outdoor sound propagation: NMPB2008 and Harmonoise-Imagine'. In: *Acoustics 2012*. 2012 (cited on page 35).

[187] Carl R. Hart et al. 'Comparisons between physics-based, engineering, and statistical learning models for outdoor sound propagation'. In: *The Journal of the Acoustical Society of America* 139.5 (2016), pp. 2640–2655 (cited on page 35).

[188] Pierre Aumond et al. 'Global sensitivity analysis for road traffic noise modelling'. In: *Applied Acoustics* 176 (2021), p. 107899 (cited on page 35).

[189] A. Prüss-Üstün et al. *Introduction and Methods: Assessing the Environmental Burden of Disease at National and Local Levels*. WHO Environmental Burden of Disease Series 1. Geneva: World Health Organization, 2003 (cited on pages 37, 39, 108).

[190] R. Bos et al. 'Diseases due to unhealthy environments: an updated estimate of the global burden of disease attributable to environmental determinants of health'. In: (2017) (cited on page 37).

[191] WHO Regional Office for Europe. *Health Impact Assessment: Main Concepts and Suggested Approach (Gothenburg Consensus Paper)*. Brussels: European Centre for Health Policy, 1999 (cited on page 37).

[192] Organisation for Economic Co-operation and Development. *Cost-benefit analysis and the environment: further developments and policy use*. OECD Publishing, 2018 (cited on page 37).

[193] Wolfgang Babisch et al. 'Good practice guide on noise exposure and potential health effects'. In: *European Environment Agency, Denmark* 11 (2010) (cited on page 38).

[194] World Bank. *World Development Report 1993: Investing in Health, Volume1*. The World Bank, 1993 (cited on page 39).

[195] Christopher J.L. Murray, Alan D. Lopez, and World Health Organization. *The global burden of disease: a comprehensive assessment of mortality and disability from diseases, injuries, and risk factors in 1990 and projected to 2020: summary*. World Health Organization, 1996 (cited on page 39).

[196] Stephen A. Stansfeld. 'Noise effects on health in the context of air pollution exposure'. In: *International Journal of Environmental Research and Public Health* 12.10 (2015), pp. 12735–12760 (cited on page 40).

[197] Augustinus E.M. de Hollander et al. 'An aggregate public health indicator to represent the impact of multiple environmental exposures'. In: *Epidemiology* (1999), pp. 606–617 (cited on page 40).

[198] Matthias Finger and Teodora Serafimova. *Internalising the external costs of transport*. 2019 (cited on page 40).

[199] European Commission, Directorate-General for Mobility and Transport. *Handbook on the External Costs of Transport. Version 2019 – 1.1*. European Commission, 2019 (cited on page 40).

[200] Johan Nygren et al. 'Agent-specific, activity-based noise impact assessment using noise exposure cost'. In: *Sustainable Cities and Society* (2024), p. 105278 (cited on page 41).

[201] Pierre Hankach et al. 'Individual-level activity-based modelling and indicators for assessing construction sites noise exposure in urban areas'. In: *Sustainable Cities and Society* 101 (2024), p. 105188 (cited on page 41).

[202] Giovanni Nero and John A. Black. 'A critical examination of an airport noise mitigation scheme and an aircraft noise charge: the case of capacity expansion and externalities at Sydney (Kingsford Smith) airport'. In: *Transportation Research Part D: Transport and Environment* 5.6 (2000), pp. 433–461 (cited on page 41).

[203] Judith Tomkins et al. 'Noise versus access: The impact of an airport in an urban property market'. In: *Urban Studies* 35.2 (1998), pp. 243–258 (cited on page 41).

[204] Filiz Ekici et al. 'A policy on the externality problem and solution suggestions in air transportation: The environment and sustainability'. In: *Energy* 258 (2022), p. 124827 (cited on page 41).

[205] Ståle Navrud. 'The economic value of noise within the European union - A review and analysis of studies'. In: *Acta Acustica (Stuttgart)* 89.SUPP. (2003) (cited on page 42).

[206] James E. Larsen and John P. Blair. 'Price effects of surface street traffic on residential property'. In: *International Journal of Housing Markets and Analysis* 7.2 (2014), pp. 189–203 (cited on page 42).

[207] Vincenzo Del Giudice et al. 'The monetary valuation of environmental externalities through the analysis of real estate prices'. In: *Sustainability* 9.2 (2017), p. 229 (cited on page 42).

[208] Mats Wilhelmsson. 'The impact of traffic noise on the values of single-family houses'. In: *Journal of Environmental Planning and Management* 43.6 (2000), pp. 799–815 (cited on page 42).

[209] Benoit Gauvreau. 'Long-term experimental database for environmental acoustics'. In: *Applied Acoustics* 74.7 (2013), pp. 958–967 (cited on pages 46, 59, 60, 62).

[210] Gerardo Iannone. 'PhD Thesis: "Improvements in the acoustical modelling of traffic noise prediction: theoretical and experimental results"'. In: (2011) (cited on pages 46, 48, 60).

[211] Dirk Helbing. 'Derivation and empirical validation of a refined traffic flow model'. In: *Physica A: Statistical mechanics and its applications* 233.1-2 (1996), pp. 253–282 (cited on pages 48, 60).

[212] Dirk Helbing. 'Empirical traffic data and their implications for traffic modelling'. In: *Physical Review E* 55.1 (1997), R25 (cited on pages 48, 60).

[213] Dirk Helbing. 'Fundamentals of traffic flow'. In: *Physical Review E* 55.3 (1997), p. 3735 (cited on pages 48, 60).

[214] Gerardo Iannone, Claudio Guarnaccia, and Joseph Quartieri. 'Speed distribution influence in road traffic noise prediction'. In: *Environmental Engineering And Management Journal* 12.3 (2013), pp. 493–501 (cited on pages 48, 60).

[215] Peter J. Brockwell and Richard A. Davis. *Introduction to time series and forecasting*. Springer, 2002 (cited on page 55).

[216] George E.P. Box et al. *Time series analysis: forecasting and control*. John Wiley & Sons, 2015 (cited on pages 55, 56).

[217] Peter J. Brockwell and Richard A. Davis. *Time series: theory and methods*. Springer Science & Business Media, 2009 (cited on pages 55, 57).

[218] George E.P. Box and Gwilym M. Jenkins. 'Analysis: Forecasting and Control'. In: *San francisco* (1976) (cited on page 56).

[219] Robert H. Shumway and David S. Stoffer. *Time series analysis and its applications: with R examples*. Springer, 2006 (cited on page 57).

[220] *Arrêté du 23 janvier 1995 relatif à l'interdiction de circulation des véhicules de transport de marchandises à certaines périodes*. Version papier numérisée. Paris, France, Jan. 1995 (cited on pages 63, 86, 90).

[221] 'Arrêté du 22 décembre 2003 relatif aux interdictions complémentaires de circulation pour 2004 des véhicules de transport de marchandises et de transport de matières dangereuses'. In: *Journal officiel de la République française. Lois et décrets* 302 (Dec. 2003). Version papier numérisée, p. 22616 (cited on pages 63, 86, 90).

[222] D.M. Murillo Gómez, A. Molina Jaramillo, and J. Ochoa. 'Analysis of the measurement uncertainty and its effects on noise mapping validations'. In: *Journal of Environmental Management* 266 (2020), p. 110606 (cited on page 72).

[223] Rob J. Hyndman and George Athanasopoulos. *Forecasting: principles and practice*. OTexts, 2018 (cited on page 103).

[224] Jian Kang et al. 'Ten questions on the soundscapes of the built environment'. In: *Building and Environment* 108 (2016), pp. 284–294 (cited on pages 107–109).

[225] Nikolaos M Papadakis, Francesco Aletta, and Georgios E Stavroulakis. 'Interrelationships between soundscape attributes and sound categories'. In: *The Journal of the Acoustical Society of America* 158.2 (2025), pp. 878–892 (cited on page 107).

[226] Tjeerd C. Andringa and J. Jolie L. Lanser. 'How pleasant sounds promote and annoying sounds impede health: A cognitive approach'. In: *International Journal of Environmental Research and Public Health* 10.4 (2013), pp. 1439–1461 (cited on pages 107–109).

[227] *Acoustics — Soundscape — Part 1: Definition and conceptual framework*. Geneva, Switzerland: International Organization for Standardisation, 2014 (cited on pages 107, 111, 121, 125).

[228] *Acoustics — Soundscape — Part 2: Data collection and reporting requirements*. Geneva, Switzerland: International Organization for Standardisation, 2018 (cited on pages 107, 112–115, 121, 123, 125, 128, 130, 132, 149, 155).

[229] *Acoustics — Soundscape — Part 3: Data analysis*. Geneva, Switzerland: International Organization for Standardisation, 2019 (cited on pages 107, 112–114, 121, 125, 155).

[230] William Burns and Douglas William Robinson. 'Hearing and noise in industry.' In: (1970) (cited on page 108).

[231] James L. Szalma and Peter A. Hancock. 'Noise effects on human performance: a meta-analytic synthesis.' In: *Psychological Bulletin* 137.4 (2011), p. 682 (cited on page 108).

[232] R.F.S. Job. 'Community response to noise: A review of factors influencing the relationship between noise exposure and reaction'. In: *The Journal of the Acoustical Society of America* 83.3 (1988), pp. 991–1001 (cited on page 108).

[233] Jian Kang. 'Urban sound planning-A soundscape approach'. In: *Acoustics 2019, Sound Decisions: Moving Forward with Acoustics-Proceedings of the Annual Conference of the Australian Acoustical Society*. Australian Acoustical Society. 2019, p. 11 (cited on page 108).

[234] Wei Yang and Jian Kang. 'Acoustic comfort evaluation in urban open public spaces'. In: *Applied Acoustics* 66.2 (2005), pp. 211–229 (cited on page 108).

[235] Wei Yang and Jian Kang. 'Soundscape and sound preferences in urban squares: A case study in Sheffield'. In: *Journal of Urban Design* 10.1 (2005), pp. 61–80 (cited on page 108).

[236] Jian Kang and Francesco Aletta. 'Soundscape design integrating noise mapping techniques: a case study in Brighton, UK'. In: *Noise Mapping* 2.1 (2015), pp. 1–12 (cited on page 108).

[237] Jin You, Pyoung Jik Lee, and Jin Yong Jeon. 'Evaluating water sounds to improve the soundscape of urban areas affected by traffic noise'. In: *Noise Control Engineering Journal* 58.5 (2010), pp. 477–483 (cited on page 109).

[238] Virginia Puyana-Romero et al. 'Sound water masking to match a waterfront soundscape with the users' expectations: the case study of the seafront in Naples, Italy'. In: *Sustainability* 13.1 (2021), p. 371 (cited on pages 109, 112).

[239] Jian Kang. 'On the diversity of urban waterscape'. In: *Acoustics 2012*. 2012 (cited on pages 109, 118).

[240] Tin Oberman et al. 'Using virtual soundwalk approach for assessing sound art soundscape interventions in public spaces'. In: *Applied Sciences* 10.6 (2020), p. 2102 (cited on pages 109, 118).

[241] Lisa R Lavia et al. 'Using a soundscape approach to develop an acoustic ecology plan for a city'. In: *The Journal of the Acoustical Society of America* 130.4_Supplement (2011), pp. 2532–2532 (cited on pages 109, 118).

[242] Aaron Antonovsky. 'Health, stress, and coping'. In: *New Perspectives on Mental and Physical Well-Being* (1979), pp. 12–37 (cited on page 109).

[243] Maurice B. Mittelmark et al. *The handbook of salutogenesis*. Springer Nature, 2022 (cited on page 109).

[244] Eike Von Lindern, Freddie Lymeus, and Terry Hartig. 'The restorative environment and salutogenesis: Complementary concepts revisited'. In: *The Handbook of Salutogenesis* (2022), pp. 371–385 (cited on page 109).

[245] European Environment Agency. *Good practice guide on quiet areas*. Ed. by M. Berg, G. Licitra, and P. Vos. Publications Office, 2014 (cited on page 110).

[246] Andrew Mitchell et al. 'How do we define soundscape?' In: *Proceedings of Forum Acusticum*. European Acoustics Association Forum Acusticum. 2023 (cited on pages 110, 111).

[247] Michael Frank Southworth. 'The sonic environment of cities.' PhD thesis. Massachusetts Institute of Technology, 1967 (cited on page 110).

[248] Raymond Murray Schafer. *The new soundscape: A handbook for the modern music teacher*. BMI Canada Limited Don Mills, 1969 (cited on pages 110, 111).

[249] Raymond Murray Schafer. *The soundscape: Our sonic environment and the tuning of the world*. Simon and Schuster, 1993 (cited on page 110).

[250] Raymond Murray Schafer. *Our sonic environment and the tuning of the world*. Destiny Books, Rochester, Vermont, 1977 (cited on pages 110, 111).

[251] Bernie Krause. 'Bioacoustics, habitat ambience in ecological balance'. In: *Whole Earth Review* 57.472 (1987), pp. 14–18 (cited on page 111).

[252] Jian Kang and Brigitte Schulte-Fortkamp. *Soundscape and the built environment*. Vol. 525. CRC press Boca Raton, FL, USA: 2016 (cited on page 111).

[253] Bryan C Pijanowski et al. 'Soundscape ecology: the science of sound in the landscape'. In: *BioScience* 61.3 (2011), pp. 203–216 (cited on page 111).

[254] Oxford English Dictionary. *"soundscape"*. Accessed by the authors cited: Mar. 2023. Mar. 2023. URL: https://www.oed.com/ (cited on page 111).

[255] Theodore J. Schultz. 'Synthesis of social surveys on noise annoyance'. In: *The Journal of the Acoustical Society of America* 64.2 (1978), pp. 377–405 (cited on page 112).

[256] Rainer Guski, U. Felscher-Suhr, and R. Schuemer. 'The concept of noise annoyance: How international experts see it'. In: *Journal of Sound and Vibration* 223.4 (1999), pp. 513–527 (cited on page 112).

[257] Francesco Aletta, Jian Kang, and Östen Axelsson. 'Soundscape descriptors and a conceptual framework for developing predictive soundscape models'. In: *Landscape and Urban Planning* 149 (2016), pp. 65–74 (cited on page 112).

[258] Östen Axelsson, Mats E Nilsson, and Birgitta Berglund. 'A principal components model of soundscape perception'. In: *The Journal of the Acoustical Society of America* 128.5 (2010), pp. 2836–2846 (cited on page 112).

[259] James A. Russell. 'A circumplex model of affect.' In: *Journal of Personality and Social Psychology* 39.6 (1980), p. 1161 (cited on page 112).

[260] James A. Russell and Jacalyn Snodgrass. 'Emotion and the environment'. In: *Handbook of Environmental Psychology* 1.1 (1987), pp. 245–281 (cited on page 112).

[261] Lawrence M. Ward and James A. Russell. 'The psychological representation of molar physical environments.' In: *Journal of Experimental Psychology: General* 110.2 (1981), p. 121 (cited on page 112).

[262] Francesco Aletta et al. 'Soundscape assessment: Towards a validated translation of perceptual attributes in different languages'. In: *Inter-noise and Noise-con Congress and Conference Proceedings*. Vol. 261. 3. Institute of Noise Control Engineering. 2020, pp. 3137–3146 (cited on page 113).

[263] Francesco Aletta et al. 'Soundscape descriptors in eighteen languages: Translation and validation through listening experiments'. In: *Applied Acoustics* 224 (2024), p. 110109 (cited on page 113).

[264] Francesco Aletta et al. *Soundscape attributes translation: Current projects and challenges*. 2025 (cited on page 113).

[265] Francesco Aletta and Simone Torresin. 'Adoption of ISO/TS 12913-2: 2018 protocols for data collection from individuals in soundscape studies: An overview of the literature'. In: *Current Pollution Reports* 9.4 (2023), pp. 710–723 (cited on pages 115, 116, 129).

[266] Cleopatra Moshona et al. 'What is a soundscape intervention? Exploring definitions and identification criteria and a platform to gather real-world examples'. In: *Inter-noise and Noise-con Congress and Conference Proceedings*. Vol. 265. 7. Institute of Noise Control Engineering. 2023, pp. 854–862 (cited on page 117).

[267] Cleopatra Christina Moshona et al. 'A framework to characterise and classify soundscape design practices based on grounded theory'. In: *Noise Mapping* 11.1 (2024), p. 20240002 (cited on page 117).

[268] The CSI Project Team. *The Catalogue of Soundscape Interventions (CSI)*. June 2023. URL: https://soundscape-intervention.org/ (visited on 01/19/2026) (cited on page 117).

[269] Brigitte Schulte-Fortkamp, Rudi Volz, and Andre Jakob. 'Using the soundscape approach to develop a public space in Berlin-perception and evaluation'. In: *The Journal of the Acoustical Society of America* 123.5_Supplement (2008), pp. 3808–3808 (cited on page 117).

[270] Brigitte Schulte-Fortkamp and Pamela Jordan. 'When soundscape meets architecture'. In: *Noise Mapping* 3.1 (2016) (cited on page 117).

[271] Viviane Acloque and Brigitte Schulte-Fortkamp. 'Validation of the psychoacoustic infrastructure of a public space in Berlin, based on the concept of soundscape'. In: *DAGA, Dusseldorf, Germany* 2 (2011) (cited on page 117).

[272] Cleopatra Moshona et al. 'Deriving a typology of soundscape design interventions'. In: *Proceedings of Forum Acusticum*. European Acoustics Association Forum Acusticum. 2023 (cited on page 118).

[273] Lisa Lavia et al. 'Sounding Brighton: Practical approaches towards better soundscapes'. In: *Inter-noise and Noise-con Congress and Conference Proceedings*. 2012, pp. 436–444 (cited on page 118).

[274] Francesco Aletta, Lisa R Lavia, and Harry J Witchel. 'Urban sound planning in Brighton and Hove'. In: *Proceedings of the Forum Acusticum, Krakow, Poland*. 2014, pp. 7–12 (cited on page 118).

[275] Hastings Rashdall. *The Universities of Europe in the Middle Ages: Salerno. Bologna. Paris*. Vol. 1. Clarendon Press, 1895 (cited on page 119).

[276] Hastings Rashdall. *The universities of Europe in the Middle Ages: in two volumes. II, 2*. Clarendon Press, 1895 (cited on page 119).

[277] Hilde de Ridder-Symoens. *A history of the university in Europe: Volume 1, Universities in the Middle Ages*. Vol. 1. Cambridge University Press, 1991 (cited on page 119).

[278] Hans De Wit. 'The future of internationalization of higher education in challenging global contexts'. In: *ETD Educação Temática Digital* 22.3 (2020), pp. 538–545 (cited on page 119).

[279] UNESCO. *Higher Education*. https://www.unesco.org/en/higher-education. 2026. (Visited on 01/20/2026) (cited on page 119).

[280] OECD Indicators. 'Education at a Glance 2022'. In: (2023) (cited on page 119).

[281] Angel J. Calderon. *Massification of higher education revisited*. 2018 (cited on page 119).

[282] Lucy Foulkes, Dean McMillan, and Alice M. Gregory. 'A bad night's sleep on campus: an interview study of first-year university students with poor sleep quality'. In: *Sleep Health* 5.3 (2019), pp. 280–287 (cited on pages 119, 120).

[283] Bridget M. Shield and Julie E. Dockrell. 'The effects of noise on children at school: A review'. In: *Building Acoustics* 10.2 (2003), pp. 97–116 (cited on page 119).

[284] Shatha A. J. Ibrahim. 'Reviewing the effects of noise pollution on students (college and university)'. In: *AIP Conference Proceedings*. Vol. 2591. 1. AIP Publishing LLC. 2023, p. 030056 (cited on page 119).

[285] Shatha Abduljabbar Ibrahim. 'Study noise effects on the students of the faculty of engineering/mustansiriyah university'. In: *Al-Nahrain Journal for Engineering Sciences* 21.2 (2018), pp. 178–186 (cited on page 119).

[286] Young-Ji Choi. 'The intelligibility of speech in university classrooms during lectures'. In: *Applied Acoustics* 162 (2020), p. 107211 (cited on page 120).

[287] Young-Ji Choi. 'Acoustical measurements of masks and the effects on the speech intelligibility in university classrooms'. In: *Applied Acoustics* 180 (2021), p. 108145 (cited on page 120).

[288] Bhabananda Phukan and Kalyan Kalita. 'An experimental study of noise pollution in Gauhati University campus, Guwahati, Assam, India'. In: *International Journal of Environmental Sciences* 3.5 (2013), pp. 1776–1784 (cited on page 120).

[289] Vishal Kumar, Ajay Vikram Ahirwar, and A.D. Prasad. 'Monitoring and mapping noise levels of university campus in central part of India'. In: *Journal of Air Pollution and Health* (2023) (cited on page 120).

[290] Parekhan M. Jaff and Hossien Hossieni. 'Study of Noise pollution at the campus of university of Sulaimani'. In: *Journal of Kirkuk University: Scientific Studies* 7.1 (2012), pp. 89–109 (cited on page 120).

[291] D. Thattai et al. 'Analysis of noise pollution level in a University campus in South India'. In: *IOP Conference Series: Earth and Environmental Science*. Vol. 80. 1. IOP Publishing. 2017, p. 012053 (cited on page 120).

[292] Margret Sibylle Engel, Fernanda Hariane Ferraz, and Paulo Henrique Trombetta Zannin. 'Characterisation of environmental noise on a university campus based on noise measurements and interviews.' In: *DAGA 2012–Darmstadt* (2012), pp. 117–118 (cited on page 120).

[293] Paulo Henrique Trombetta Zannin et al. 'Characterisation of environmental noise based on noise measurements, noise mapping and interviews: A case study at a university campus in Brazil'. In: *Cities* 31 (2013), pp. 317–327 (cited on page 120).

[294] Dyah Ayu Puspagarini et al. 'Soundscape study of an urban campus park'. In: *AIP Conference Proceedings*. Vol. 2088. 1. AIP Publishing LLC. 2019, p. 050011 (cited on page 120).

[295] Ming Lu and Jingwan Fu. 'Attention restoration space on a university campus: exploring restorative campus design based on environmental preferences of students'. In: *International Journal of Environmental Research and Public Health* 16.14 (2019), p. 2629 (cited on page 120).

[296] Francesco Aletta et al. 'An experimental study on the influence of soundscapes on people's behaviour in an open public space'. In: *Applied Sciences* 6.10 (2016), p. 276 (cited on page 120).

[297] Qianda Zhuang and Zekun Shang. 'Investigation and Optimization Research of Soundscape in Linyi University Campus, Shandong, China'. In: EAI, Mar. 2023 (cited on page 120).

[298] Engku Mastura Engku Mohd Anuar, Nazli Che Din, and Hazreena Hussein. 'Traffic noise influence on soundscape quality at campus landscape area'. In: *Journal of Design and Built Environment* 17.1 (2017) (cited on page 120).

[299] Francesco D'Alessandro et al. 'Influence of visual aspects and other features on the soundscape assessment of a university external area'. In: *Building Acoustics* 25.3 (2018), pp. 199–217 (cited on page 120).

[300] Hedy C. Indrani, Sri Nastiti N. Ekasiwi, and Dhany Arifianto. 'Indoor soundscape model: assessing contextual factors in open-plan offices on university campuses in Surabaya, Indonesia'. In: *Building and Environment* 237 (2023), p. 110267 (cited on page 120).

[301] Audiotopie. *Audiotopie — Expériences sonores immersives*. https://www.audiotopie.com/. 2025. (Visited on 01/20/2026) (cited on page 120).

[302] Valérian Fraisse, Cynthia Tarlao, and Catherine Guastavino. 'Shaping city soundscapes: In situ comparison of four sound installations in an urban public space'. In: *Landscape and Urban Planning* 251 (2024), p. 105173 (cited on page 121).

[303] Hatice Kurukose Cal et al. 'Comparing Teachers' And Students' Perceptions Of School Soundscapes Through A Questionnaire-Based Study'. In: *Proceedings of the 11th Convention of the European Acoustics Association Forum Acusticum/EuroNoise 2025*. European Acoustics Association. 2025, pp. 4889–4895 (cited on page 121).

[304] Università degli Studi di Salerno. *Campus Locations and Maps*. https://web.unisa.it/vivere-il-campus/campus/sedi-e-mappe. 2026. (Visited on 01/22/2026) (cited on page 122).

[305] Aurora Mascolo et al. 'Comparison between sound pressure levels and perception: a soundscape application in a university campus'. In: *Journal of Physics: Conference Series*. Vol. 1603. 1. IOP Publishing. 2020, p. 012026 (cited on page 122).

[306] Simona Mancini et al. 'Soundwalk, questionnaires and noise measurements in a university campus: A soundscape study'. In: *Sustainability* 13.2 (2021), p. 841 (cited on page 122).

[307] Gabriella Graziuso et al. 'Geo-Crowdsourced sound level data in support of the community facilities planning. A Methodological Proposal'. In: *Sustainability* 13.10 (2021), p. 5486 (cited on page 122).

[308] Andrew Mitchell et al. 'Soundscape perception indices (SPIs): Developing context-dependent single value scores of multidimensional soundscape perceptual quality'. In: *The Journal of the Acoustical Society of America* 156.6 (2024), pp. 3694–3706 (cited on page 123).

[309] OpenStreetMap contributors. *OpenStreetMap, Planet dump retrieved from https://planet.osm.org*. https://www.openstreetmap.org. 2026. (Visited on 01/22/2026) (cited on page 124).

[310] Judicaël Picaut et al. 'An open-science crowdsourcing approach for producing community noise maps using smartphones'. In: *Building and Environment* 148 (2019), pp. 20–33 (cited on page 125).

[311] Noise-Planet. *NoiseCapture*. https://noise-planet.org/noisecapture.html. 2026. (Visited on 01/26/2026) (cited on pages 125–127).

[312] Gwenaël Guillaume et al. 'NoiseCapture smartphone application as pedagogical support for education and public awareness'. In: *The Journal of the Acoustical Society of America* 151.5 (2022), pp. 3255–3265 (cited on page 126).

[313] Efstathios Margaritis and Ferry van Kann. 'Combining mobile measurements on noise and soundscape evaluation in a University Campus after a renovation plan.' In: *Inter-noise and Noise-con Congress and Conference Proceedings*. Vol. 265. 3. Institute of Noise Control Engineering. 2023, pp. 4882–4890 (cited on page 127).

[314] George Y. Lu and David W. Wong. 'An adaptive inverse-distance weighting spatial interpolation technique'. In: *Computers & geosciences* 34.9 (2008), pp. 1044–1055 (cited on page 128).

[315] QGIS Development Team. *QGIS Geographic Information System*. QGIS Association. 2026 (cited on pages 128, 140, 146).

[316] Esri. *IDW (Geostatistical Analyst)*. URL: https://pro.arcgis.com/en/pro-app/latest/tool-reference/geostatistical-analyst/idw.htm (visited on 01/27/2026) (cited on page 128).